

Program subject to change until 12/16/2019.



105[™] Scientific Assembly and Annual Meeting December 1–6 | McCormick Place, Chicago







BR101-ED-X

Demystifying Breast MRI: A Pictorial Review of the ACR BI-RADS MRI Lexicon and Reporting

All Day Room: BR Community, Learning Center Digital Education Exhibit

Participants

Andra Perja, MD, Cluj-Napoca, Romania (*Abstract Co-Author*) Nothing to Disclose Angelica R. Chiorean, MD, PhD, Cluj Napoca, Romania (*Presenter*) Nothing to Disclose Madalina B. Szep, MD, Cluj-Napoca, Romania (*Abstract Co-Author*) Nothing to Disclose Roxana Pintican, MD, Cluj-Napoca, Romania (*Abstract Co-Author*) Nothing to Disclose Maria M. Duma, MD, Cluj-Napoca, Romania (*Abstract Co-Author*) Nothing to Disclose Calin Pop, Cluj, Romania (*Abstract Co-Author*) Nothing to Disclose Diana S. Feier, MD, Cluj-Napoca, Romania (*Abstract Co-Author*) Nothing to Disclose Bogdan Fetica, Cluj-Napoca, Romania (*Abstract Co-Author*) Nothing to Disclose Liliana Rogojan, Cluj Napoca, Romania (*Abstract Co-Author*) Nothing to Disclose Calin Schiau, MD, Sebes, Romania (*Abstract Co-Author*) Nothing to Disclose Tudor Safirescu, Cluj-Napoca, Romania (*Abstract Co-Author*) Nothing to Disclose Dan Eniu, Cluj-Napoca, Romania (*Abstract Co-Author*) Nothing to Disclose

For information about this presentation, contact:

andra.dumitru_bv@yahoo.com

TEACHING POINTS

The purposes of this exhibit are: 1. To review and to illustrate the ACR BI-RADS MRI lexicon. 2. To clarify breast MRI interpreting and to provide radiologists with a systematic approach of standardized reporting.

TABLE OF CONTENTS/OUTLINE

1. Clinical information and aquisition parameters 2. BI-RADS MRI lexicon a. Amount of fibroglandular tissue b. Background parenchymal enhancement c. Focus d. Masses e. Non-masses f. Intramammary lymph node g. Skin lesion h. Non-enhancing findings i. Associated features j. Fat containing lesions k. Location of lesions l. Kinetic curve assessment m. Implants 3. Assessment categories and management





BR121-ED-X

Problem Solving with Breast MRI

All Day Room: BR Community, Learning Center Digital Education Exhibit

Participants

Jordan M. Burner, MD, Winston Salem, NC (*Presenter*) Nothing to Disclose Kelly A. Brozzetti-Cronin, MD, Winston Salem, NC (*Abstract Co-Author*) Nothing to Disclose Margaret A. Yacobozzi, MD, Winston-Salem, NC (*Abstract Co-Author*) Nothing to Disclose

TEACHING POINTS

Following review of this educational exhibit, the reader will better: • Understand clinical scenarios in which breast MRI is an an effective diagnostic problem solving tool, beyond screening and new diagnosis of breast cancer • Recognize imaging findings and limitations of breast MRI in the setting of neoadjuvant therapy • Differentiate benign and malignant findings following lumpectomy

TABLE OF CONTENTS/OUTLINE

Current Indications for Breast MRI beyond screening and new diagnosis • Assess for residual disease after lumpectomy with positive margins -Expected postoperative findings versus suspicious findings • Surveillance of lumpectomy sight • Evaluating response to neoadjuvant chemotherapy -Potential pitfalls • Axillary metastasis with unknown primary (occult breast cancer detection) • Paget disease • Evaluation of silicone implants







BR130-ED-X

False Negative Lesions of Breast Cancer: The Variable Features in Previous MRI

All Day Room: BR Community, Learning Center Digital Education Exhibit

Participants

Young-eun Kim, MD, Seoul, Korea, Republic Of (*Presenter*) Nothing to Disclose Joo Hee Cha, MD, Seoul, Korea, Republic Of (*Abstract Co-Author*) Nothing to Disclose Hak Hee Kim, MD, Seoul, Korea, Republic Of (*Abstract Co-Author*) Nothing to Disclose Hee Jung Shin, MD, Seoul, Korea, Republic Of (*Abstract Co-Author*) Grant, General Electric Company Eun Young Chae, Seoul, Korea, Republic Of (*Abstract Co-Author*) Nothing to Disclose Woo Jung Choi, MD, Seoul, Korea, Republic Of (*Abstract Co-Author*) Nothing to Disclose

For information about this presentation, contact:

happyfreekye@daum.net

TEACHING POINTS

Despite the excellent contribution of contrast enhanced breast MRI, there are variable MRI-false negative cases. The purpose of this exhibit is to familiarize the reader with a variety of false negative findings of breast cancer on previous MRI and help readers in making an accurate diagnosis. Also, we emphasize that careful and strict application of BI-RADS is necessary as well as an appropriate biopsy.

TABLE OF CONTENTS/OUTLINE

1. Introduction of false negative breast cancer on MRI. 2. Inclusion criteria. 3. Characteristics of missed cancer. 4. Presentation of the missed cancers on previous MRI compared with current MRI. 5. Analyzing the reasons of misinterpretation. 6. Presenting some tips reducing misinterpretation.







BR131-ED-X

Breast Edema Terminology: To Standardize the Language of T2WI Breast MRI

All Day Room: BR Community, Learning Center Digital Education Exhibit

FDA Discussions may include off-label uses

Participants

Taiyo L. Harada, Tokyo, Japan (*Presenter*) Nothing to Disclose Kazuaki Nakashima, MD, Shizuoka, Japan (*Abstract Co-Author*) Nothing to Disclose Takayoshi Uematsu, MD, PhD, Nagaizumi, Japan (*Abstract Co-Author*) Nothing to Disclose

For information about this presentation, contact:

t.uematsu@scchr.jp

TEACHING POINTS

Breast edema on T2WI breast MRI is one of important breast MRI findings because recent studies reported that breast edema can contribute breast cancer diagnosis and it is a prognostic biomarker of breast cancer. However, ACR BI-RADS MRI lexicon does not include breast edema terminology now and this situation can cause confusion to use the terminology. To accurately use breast edema terminology is important to standardize the language of T2WI breast MRI for research and clinical setting. We will: 1. Review published research about breast edema on T2WI breast MRI and organize breast edema terminology to standardize the language of T2WI breast MRI. 2. Discuss most effective usage of breast edema terminology based on each pathological finding.

TABLE OF CONTENTS/OUTLINE

1. Introduction: the definition of breast edema 2. Review of breast edema terminology of T2WI breast MRI 3. Diffuse breast edema and focal breast edema 4. 3 types of focal breast edema 5. Relation between breast edema and neoadjuvant chemotherapy efficacy 6. Summary





BR132-ED-X

Contrast Enhanced Mammography versus Dynamic Contrast-Enhanced MRI: Which is Right for Who?

All Day Room: BR Community, Learning Center Digital Education Exhibit

Awards Certificate of Merit

Participants

Rasha M. Kamal, MD, Cairo, Egypt (*Presenter*) Nothing to Disclose Mennat-Allah M. Hanafy IV, MA, Cairo, Egypt (*Abstract Co-Author*) Nothing to Disclose Abeer Alsharawy IV, Cairo, Egypt (*Abstract Co-Author*) Nothing to Disclose Hebatallah M. Azzam, Cairo, Egypt (*Abstract Co-Author*) Nothing to Disclose Lamia Bassam, Cairo, Egypt (*Abstract Co-Author*) Nothing to Disclose Mona E. Marey, BA, Cairo, Egypt (*Abstract Co-Author*) Nothing to Disclose Radwa Essam, MBBCh, MBBS, Cairo, Egypt (*Abstract Co-Author*) Nothing to Disclose Amr F. Moustafa, MD, Cairo, Egypt (*Abstract Co-Author*) Nothing to Disclose Mohammed M. Gomaa, MD, Cairo, Egypt (*Abstract Co-Author*) Nothing to Disclose

For information about this presentation, contact:

rashaakamal@hotmail.com

TEACHING POINTS

Both CESM and MRI have features in common. They both use contrast material to enhance morphology assessment and provide some functional information with comparable sensitivity and specificity. The oververlap between the advantages, limitations and indications of both modalities poses a diagnostic challenge. Therefore, we aim to clarify which modality is more appropriate to be used in four different clinical scenarios namely: detection, diagnosis, local staging and follow up of patients after adequate management. This review would help breast imaging radiologists to understand when to ask for contrast imaging of the breast and how to choose the optimum modality to be able to make the most appropriate diagnosis.

TABLE OF CONTENTS/OUTLINE

1. Technique of CESM and DCE-MRI. 2. Indications of CESM and DCE-MRI. 3. Advantages and limitations of CESM and DCE-MRI. 4. Discuss 4 clinical scenarios: Detection, diagnosis, local staging and follow-up 5. Emphasize which of the two imaging modalities is more appropriate to be used. in each scenario.







BR141-ED-X

Will You Pass the Test? A Diagnostic Strategy for Breast MRI Interpretation

All Day Room: BR Community, Learning Center Digital Education Exhibit

Participants

Lucia I. Beccar Varela, MD, Vicente Lopez, Argentina (*Presenter*) Nothing to Disclose Maria Soledad Nocetti, MD, Vicente Lopez, Argentina (*Abstract Co-Author*) Nothing to Disclose Veronica E. Grondona, MD, Buenos Aires, Argentina (*Abstract Co-Author*) Nothing to Disclose Florencia Melendez, MD, Buenos Aires, Argentina (*Abstract Co-Author*) Nothing to Disclose Flavia B. Sarquis, MD, Villa Ballester, Argentina (*Abstract Co-Author*) Nothing to Disclose

For information about this presentation, contact:

lu,beccar.varela@gmail.com

TEACHING POINTS

• Provide tips for interpretation of a Breast MRI exam for beginners. • Learn through clinical cases to use the information provided by the different MRI sequences to achieve a correct diagnosis and accurate report using the BIRADS lexicon. • Expose the diagnostic challenge that some patients constitute in everyday practice.

TABLE OF CONTENTS/OUTLINE

Breast MRI currently has an established and definite role as a clinically useful imaging tool. As the role of breast MRI expands, many more radiologists, currently involved in breast imaging but not necessarily experienced in MRI, will become involved with the technique. The purpose of this exhibit is to offer a comprehensive pictorial guide to breast MRI for radiologists in training. Through clinical cases, illustrations and figures, we aim to provide tips and tricks that are potential pitfalls associated with the interpretation of the breast MRI examination. At the end we will expose readers to a series of challenging cases in order to improve their diagnostic accuracy and clinical acumen.







BR142-ED-X

Assessment of Extent of Disease with Breast MRI Pitfalls for Residents

All Day Room: BR Community, Learning Center Digital Education Exhibit

Participants

Lucia I. Beccar Varela, MD, Vicente Lopez, Argentina (*Presenter*) Nothing to Disclose Maria Soledad Nocetti, MD, Vicente Lopez, Argentina (*Abstract Co-Author*) Nothing to Disclose Veronica E. Grondona, MD, Buenos Aires, Argentina (*Abstract Co-Author*) Nothing to Disclose Diego Gangi, Vicente Lopez, Argentina (*Abstract Co-Author*) Nothing to Disclose Flavia B. Sarquis, MD, Villa Ballester, Argentina (*Abstract Co-Author*) Nothing to Disclose

For information about this presentation, contact:

lu.beccar.varela@gmail.com

TEACHING POINTS

• Understand the importance of Breast MRI as an accurate and sensitive diagnostic method for assessment of extent of breast cancer. • Learn a diagnostic algorithm when examining women with breast cancer to give all the information needed for a correct pre-operative planning.

TABLE OF CONTENTS/OUTLINE

Assessment of extent of disease is one of the most important indications for use of breast MRI preoperatively. Of all breast imaging techniques, breast MRI has the greatest sensitivity for the detection of breast cancer. It is for this reason that MR mammography is especially suited to give additional preoperative information about the tumor size and extent, the presence of an extensive intraductal component (EIC), posible multifocality or multicentricity, the presence of contralateral breast cancer and lymph node involvement. This work is a resident primer on, through diferent clinical cases, learning what the surgeon needs to know for preoperative staging for the effective planning of the appropriate stage-dependent treatment strategy.





BR143-ED-X

The New Era for Breast Cancer Screening: Abbreviated Breast Magnetic Resonance Imaging

All Day Room: BR Community, Learning Center Digital Education Exhibit

Participants

Maria Jose Chico, Buenos Aires, Argentina (*Presenter*) Nothing to Disclose Karina Pesce, Capital Federal, Argentina (*Abstract Co-Author*) Nothing to Disclose Maria P. Swiecicki, MD, Buenos Aires, Argentina (*Abstract Co-Author*) Nothing to Disclose

For information about this presentation, contact:

mariajchico@gmail.com

TEACHING POINTS

To review the technical aspects of Abbreviated Breast MRI. To describe on Abbreviated Breast MRI Protocols. To comment on current and future directions on this subject matter

TABLE OF CONTENTS/OUTLINE

Introduction and review of current literature. Description of MRI indications for Breast Cancer Screening. Interpretation algorithms. Illustration with cases from our institution. Conclusions.







BR147-ED-X

To Scan or Not to Scan, That is the Question: Role of Breast MRI in Cancer Staging

All Day Room: BR Community, Learning Center Digital Education Exhibit

Participants

Maria Jose Chico, Buenos Aires, Argentina (*Presenter*) Nothing to Disclose Maria P. Swiecicki, MD, Buenos Aires, Argentina (*Abstract Co-Author*) Nothing to Disclose Karina Pesce, Capital Federal, Argentina (*Abstract Co-Author*) Nothing to Disclose Maria B. Orruma, MD, Hudson, Argentina (*Abstract Co-Author*) Nothing to Disclose

For information about this presentation, contact:

mariajchico@gmail.com

TEACHING POINTS

Describe the advantages and disadvantages of breast cancer staging with MRI. Discuss the surgical outcome after breast cancer staging with MRI, and consider whether the treatment plan was modified based on the MRI findings. Depict histological types of breast cancer that have been proven to benefit from breast MRI staging.

TABLE OF CONTENTS/OUTLINE

Introduction and review of current literature. Description of breast MRI indications for cancer staging. Illustration with typical and atypical teaching cases. Discussion of benefits and potential pitfalls of breast MRI in cancer staging.





BR152-ED-X

Diffusion-Weighted Imaging (DWI) and ADC Features of Triple Negative Breast Cancer (TNBC) Pre and Post Neoadjuvant Chemotherapy

All Day Room: BR Community, Learning Center Digital Education Exhibit

Participants

Patricia A. Baron Rodiz, MD, Madrid, Spain (*Presenter*) Nothing to Disclose Paul M. Aguilar Angulo, MD, Toledo, Spain (*Abstract Co-Author*) Nothing to Disclose Ruben Giovanetti Gonzalez, MD, Toledo, Spain (*Abstract Co-Author*) Nothing to Disclose Lina Marcela CRUZ HERNANDEZ, Toledo, Spain (*Abstract Co-Author*) Nothing to Disclose Pilar Sanchez Camacho, Toledo, Spain (*Abstract Co-Author*) Nothing to Disclose Cristina Romero, MD, Toledo, Spain (*Abstract Co-Author*) Nothing to Disclose

For information about this presentation, contact:

patriciabaronrodiz8@hotmail.com

TEACHING POINTS

- To review the MRI features of triple negative breast cancer. - To provide the DWI and ADC features of TNBC pre and post neoadjuvant chemotherapy. - To provide a systematic approach for the diagnosis of TNBC with MRI. - To assess the role of DWI and ADC for neoadjuvant chemotherapy (NAC) follow-up.

TABLE OF CONTENTS/OUTLINE

TNBC accounts for 10%-20% of all breast cancers and is a clinical challenge because of its aggressive nature and poor prognosis. At present, cytotoxic chemotherapy is the standard treatment option for these patients. Pathologic complete response (PCR) rates after neoadjuvant chemotherapy have been shown to be higher in triple-negative breast cancers compared with estrogen receptor-positive breast cancers. MRI consistently demonstrates the presence of all TNBC with a higher level of accuracy compared with other tumors sub-types, and provides a reliable baseline for neoadjuvant chemotherapy (NAC) follow-up. Preliminary studies also suggest that MRI may predict complete NAC response in TNBC more sensitively than other methods. We present a collection of cases of TNBC that were diagnosed by US or stereotactic-guided biopsy showing the DWI and ADC features pre and post neoadjuvant chemotherapy.

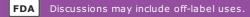




BR154-ED-X

Clinical and Radiological Approach to Different Causes of Mastitis

All Day Room: BR Community, Learning Center Digital Education Exhibit



Participants

Youstina G. Ebrahim, MD, Giza, Egypt (*Abstract Co-Author*) Nothing to Disclose Mariam R. Louis, MD, Cairo, Egypt (*Presenter*) Nothing to Disclose

For information about this presentation, contact:

youstina_youanna@yahoo.com

TEACHING POINTS

1. This exihibit shows an algohythm which can help in reaching the cause of mastitis based on the sono-mammography and MRI imaging. 2. The exihibit shows how MRI can help to differentiate the causes of masitis.

TABLE OF CONTENTS/OUTLINE

Different causes of mastitis. How to approach a case with mastitis. Role of MRI in differentiation of the benign and malignant mastitis. Illustrative cases.







BR155-ED-X

Non-Contrast-Enhanced Breast MR Screening for Women with Dense Breasts

All Day Room: BR Community, Learning Center Digital Education Exhibit

FDA Discussions may include off-label uses.

Participants

Takayoshi Uematsu, MD, PhD, Nagaizumi, Japan (*Presenter*) Nothing to Disclose Kazuaki Nakashima, MD, Shizuoka, Japan (*Abstract Co-Author*) Nothing to Disclose Taiyo L. Harada, Tokyo, Japan (*Abstract Co-Author*) Nothing to Disclose

For information about this presentation, contact:

t.uematsu@scchr.jp

TEACHING POINTS

The sensitivity of dense breast mammograms could be about half the near 100% sensitivity of fatty breast mammograms. The current reports show that contrast-enhanced breast MRI (CE MRI) outperforms mammography and ultrasound in all women with any breast cancer risk. Nowadays, abbreviated breast MRI protocols are developed, it is shorter and less costly than CE MRI. However, it still needs an intravenous contrast agent. It is costly, painful, time-consuming, and health concerns. Recent studies reported non-contrast-enhanced breast MRI screening using diffusion-weighted imaging (DWI) and STIR/T2WI might be useful as a supplemental breast cancer screening modality. We will: 1. Review the current status and clinical pathways regarding non-contrast-enhanced breast MRI screening using DWI and STIR/T2WI 2. Discuss and propose non-contrast-enhanced breast MR screening for women with dense breasts.

TABLE OF CONTENTS/OUTLINE

1. Introduction 2. Overview of non-contrast-enhanced breast MRI using DWI and STIR/T2WI 3. Detection, diagnosis, and characterization using non-contrast-enhanced breast MRI using DWI and STIR/T2WI 4. Assessment criteria for non-contrast-enhanced breast MR screening 5. Illustrate findings of non-contrast-enhanced breast MRI using DWI and STIR/T2WI with pathological findings 6. Summary





BR160-ED-X

Dreadful Tuberculosis Affecting the Mammary Tissue

All Day Room: BR Community, Learning Center Digital Education Exhibit

FDA Discussions may include off-label uses

Participants

Palak Thakrar, Mumbai, India (*Presenter*) Nothing to Disclose Mitusha Verma, MBBS, Mumbai, India (*Abstract Co-Author*) Nothing to Disclose Saumya C. Rao, MBBS, Mumbai, India (*Abstract Co-Author*) Nothing to Disclose Deepak Patkar, MD, Mumbai, India (*Abstract Co-Author*) Nothing to Disclose

For information about this presentation, contact:

drpalakt@gmail.com

TEACHING POINTS

Breast tuberculosis can clinically and radiologically mimic carcinoma. MRI helps to differentiate based on the associated features and enhancement pattern.

TABLE OF CONTENTS/OUTLINE

It is rare to have tuberculosis involving the breast, even in the countries which are endemic for tuberculosis with a high number of pulmonary and non-pulmonary cases. Having atypical clinical features, the true diagnosis of the disease remains obscure and is often mistaken for inflammatory carcinoma. MRI aids to differentiate tuberculous mastitis and abscess from inflammatory carcinoma, although there may be a clinical overlap of the symptoms. We observed the absence of diffuse skin thickening, skin oedema, no satellite lesions, no extra-parenchymal spread of disease such as pectoralis infiltration. Most importantly the kinetics showed typically Type I pattern of progressive enhancement with a continuous increase in signal intensity on each successive contrast-enhanced image in tuberculosis, unlike inflammatory carcinoma which typically shows initial rapid enhancement with washout or plateau curves. Our cases had primary breast tuberculosis. The findings were confirmed on histopathology by image-guided biopsy which stated granulomatous disease and positive Acid-Fast bacilli on Ziehl-Neelsen staining.





BR180-ED-X

Breast MRI: Identification of Malignancy in the Lactating Patient

All Day Room: BR Community, Learning Center Digital Education Exhibit

Awards Certificate of Merit

Participants

Sophia R. O'Brien, MD, Philadelphia, PA (*Presenter*) Nothing to Disclose Samantha P. Zuckerman, MD, Philadelphia, PA (*Abstract Co-Author*) Nothing to Disclose Katrina Korhonen, MD, Philadelphia, PA (*Abstract Co-Author*) Nothing to Disclose Susan Domchek, MD, Philadelphia, PA (*Abstract Co-Author*) Nothing to Disclose Emily F. Conant, MD, Philadelphia, PA (*Abstract Co-Author*) Grant, Hologic, Inc; Consultant, Hologic, Inc; Grant, iCAD, Inc; Consultant, Advisory Panel, iCAD, Inc; Speaker, iiCME

For information about this presentation, contact:

sophia.obrien@pennmedicine.upenn.edu

TEACHING POINTS

The purpose of this exhibit is to: 1. Review the controversy over the use of breast MRI during lactation: a. There is widespread belief that breast MRI is limited by lactational changes b. Multiple studies have in fact shown that malignancy can be distinguished from lactational changes on breast MRI 2. Review the breast MRI findings of normal lactational changes 3. Describe the unique imaging characteristics of breast cancer in relation to normal lactational changes on breast MRI

TABLE OF CONTENTS/OUTLINE

- Briefly review the imaging characteristics of normal lactational changes seen on breast MRI - Imaging cases demonstrating normal lactational changes on breast MRI with corresponding mammography - Review the literature for the perceived limitations of breast MRI during lactation - Review studies which have demonstrated breast MRI's utility in the lactating patient - Describe the imaging features that allow malignancy to be distinguished from normal lactational changes - Imaging cases of malignancy identified in the lactating breast. Each case will have mammographic and sonographic correlations as well as non-lactating breast MRI in the same patient when available.







BR187-ED-X

Not Blind Enough: What Radiologists Need to Know to Avoid Over-Reporting Implant Failures Magnetic Resonance Imaging

All Day Room: BR Community, Learning Center Digital Education Exhibit

Participants

Chitrangada Singh, MD, Mumbai, India (*Presenter*) Nothing to Disclose Urszula Wegner, MD, Norwich, United Kingdom (*Abstract Co-Author*) Nothing to Disclose

For information about this presentation, contact:

chitrangada.singh@gmail.com

TEACHING POINTS

A dozen of educational articles are available describing breast implant failures and complications. However we realised the need to emphasises on the -a) Limits of normalcy when imaging breast implants in the clinics. b)Substantial and balanced guidelines to prevent over-diagnosis as well as missing grave complications like Implant associated B-Cell lymphomas

TABLE OF CONTENTS/OUTLINE

-Introduction to Breast Implants MRI- (including a small table for MRI Breast Reporting tips) - A brief description of the various types of implant failures and normal conditions that can mimic them.-Assessment protocol and flowchart to avoid over-diagnosis of the same -Summary





HP104-ED-X

Mentorship, Sponsorship, and Coaching: Key Faculty and Resident Development Concepts and a Guide for Successful Implementation in the Radiology Department

All Day Room: HP Community, Learning Center Digital Education Exhibit

Participants

Sofya Kalantarova, MD, Mineola, NY (*Presenter*) Nothing to Disclose Ragni Jindal, MD, Mineola, NY (*Abstract Co-Author*) Nothing to Disclose Jonathan Minkin, Mineola, NY (*Abstract Co-Author*) Nothing to Disclose Christopher M. Foresto, MD, Jericho, NY (*Abstract Co-Author*) Nothing to Disclose Douglas S. Katz, MD, Mineola, NY (*Abstract Co-Author*) Nothing to Disclose Jason C. Hoffmann, MD, Garden City, NY (*Abstract Co-Author*) Speakers Bureau, Merit Medical Systems, Inc; ; Miltiadis Tembelis, Mineola, NY (*Abstract Co-Author*) Nothing to Disclose

For information about this presentation, contact:

Jason.Hoffmann@nyulangone.org

TEACHING POINTS

1. While mentorship, coaching, and sponsorship are used interchangeably by some people, they are three very different concepts and approaches to professional development.2. An understanding of the key differences between mentorship, sponsorship, and coaching will allow administrators and leaders to more effectively design and implement faculty and resident development programming at their institution.

TABLE OF CONTENTS/OUTLINE

Define mentorship, coaching, and sponsorship.Review similarities and differences between these employee development concepts.Highlight the use of these three approaches in the business world, medicine, and specifically in radiology.Detail how each of these may be used in unique situations, depending on the needs of the trainee.Review the current status of mentorship, coaching, and sponsorship programs in radiology training.Provide a guide for use of these professional development tools within radiology training.Suggest unique uses and/or combinations of these tools to maximize resident and faculty development in the radiology department.





HP118-ED-X

Optimizing the Mentor-Mentee Relationship: A Guide for Mentees

All Day Room: HP Community, Learning Center Digital Education Exhibit

Participants

Monica M. Sheth, MD, Manhasset, NY (*Presenter*) Nothing to Disclose Tara M. Catanzano, MD, Springfield, MA (*Abstract Co-Author*) Nothing to Disclose Jordana Phillips, MD, Newton Center, MA (*Abstract Co-Author*) Research Grant, General Electric Company Consultant, General Electric Company Georgeann McGuinness, MD, New York, NY (*Abstract Co-Author*) Nothing to Disclose

For information about this presentation, contact:

monica.sheth@nyulangone.org

TEACHING POINTS

1. Before you can find a mentor, you must determine your personal and professional needs. 2. Mentors can help you navigate your organization and provide guidance, support, and encouragement to help you reach your goals. 3. Sometimes you need a sponsor, a more senior person who can openly advocate on your behalf and connect you to career opportunities. 4. It is important to have multiple mentors, both male and female, in varying professional stages. 5. Mentees should 'manage-up' and be active participants in the mentor-mentee relationship.

TABLE OF CONTENTS/OUTLINE

1. Discuss the value of mentorship in career growth 2. Discuss the difference between mentors, sponsors, and career coaches and when each would be needed 3. Review the importance of understanding yourself, your core values and goals in order to find the appropriate type of mentor 2. Review how to be a SMART goal writer & provide a personal evaluation worksheet example 5. Recognize characteristics of high-quality mentors and where to find them 6. Identify methods for mentees to promote effective mentor relationships





VI107-ED-X

Evaluation of Peripheral Vascular Disease Using CT and MR Angiography

All Day Room: VI Community, Learning Center Digital Education Exhibit

Participants

Hye-Young Choi, Seoul, Korea, Republic Of (*Presenter*) Nothing to Disclose Hyun Jung Koo, MD, Seoul, Korea, Republic Of (*Abstract Co-Author*) Nothing to Disclose Joon-Won Kang, MD, Seoul, Korea, Republic Of (*Abstract Co-Author*) Nothing to Disclose Dong Hyun Yang, MD, Seoul, Korea, Republic Of (*Abstract Co-Author*) Nothing to Disclose

For information about this presentation, contact:

radkoo@amc.seoul.kr

TEACHING POINTS

1. Review the imaging modalities for peripheral vascular disease 2. Describe the strengths and limitations of CT angiography, enhanced MR angiography and non-enhanced MR angiography 3. Demonstrate various CT and MR images of peripheral vascular disease

TABLE OF CONTENTS/OUTLINE

1. Introduction - Disease entities of peripheral vascular disease - The use of CT and MR angiography - Needs of non-enhanced MR angiography 2. Imaging Modalities 1) CT angiography protocol 2) MR angiography protocol - Contrast enhanced MR angiography - Non-enhanced MR angiography (sequences such as REACT, TOF, ASL, BOLD) 3. Various Cases - Traumatic injury (for flap operation) - Critical limb ischemia including diabetes foot - Peripheral arteriovenous malformation





VI124-ED-X

Comparison of Non-Contrast MR Angiography to CT Angiography to Evaluate the Access Route of Transfemoral Transcatheter Aortic Valve Replacement

All Day Room: VI Community, Learning Center Digital Education Exhibit

Participants

Naoki Hosoda, Tokyo, Japan (Presenter) Nothing to Disclose

For information about this presentation, contact:

hosoda121@gmail.com

TEACHING POINTS

1) To describe the assessment method for access route of transfemoral Transcatheter Aortic Valve Replacement (TAVR). 2) To describe the scan parameters of Non-contrast MR Angiography (NC-MRA). 3) To describe the usefulness of NC-MRA to evaluate the access route of transfemoral TAVR, using the data compared NC-MRA and CT Angiography (CTA).

TABLE OF CONTENTS/OUTLINE

Assessment points and images of access route of transfemoral TAVR: diameter, tortuousness, presence or absence of calcification, cross sectional images, volume rendering. Advantages and limitations of NC-MRA: non-contrast, respiratory gating, short time scan, signal void of calcification. It was suggested that the assessment of access route of transfemoral TAVR using NC-MRA is useful by comparison of measurement results (n=560). Since NC-MRA can be performed without using contrast media, it can be applied to patients with renal dysfunction or contrast allergy. This method uses respiratory gating and can be used for arrhythmia patients. The scan time is about 4 minutes, comparable to CTA. Since calcification is difficult to recognize in MRI, evaluation of calcification requires plain CT.







SPAI11

RSNA AI Deep Learning Lab: Beginner Class: Classification Task (Intro)

Sunday, Dec. 1 10:30AM - 12:00PM Room: AI Showcase, North Building, Level 2, Booth 10342



Participants

Bradley J. Erickson, MD, PhD, Rochester, MN (Presenter) Board of Directors and Stockholder, VoiceIt Technologies, LLC; Board of Directors, FlowSigma, LLC; Officer, FlowSigma, LLC; Stockholder, FlowSigma, LLC;

Special Information

In order to get the best experience for this session, it is highly recommended that attendees bring a laptop with a keyboard and decent-sized screen. Having a Gmail account will be helpful. Here are instructions for creating and deleting a Gmail account.

ABSTRACT

This class will focus on basic concepts of convolutional neural networks (CNNs) and walk the attendee through a working example. A popular training example is the MNIST data set which consists of hand-written digits. This course will use a data set we created, that we call 'MedNIST', and consists of images of 6 different classes: Chest X-ray, Chest CT, Abdomen CT, Head CT, Head MR and Breast MRI. The task is to identify the image class. This will be used to train attendees on the basic principles and some pitfalls in training a CNN. • Intro to CNNs • Data preparation: DICOM to jpeg, intensity normalization, train vs test • How do we choose the labels? Inconsistencies... Use Fast.AI routines to classify; Validation of results: Are the performance metrics reliable?; 'Extra Credit': if there is time, explore data augmentation options, effect of batch size, training set size.





SPCT10

Best Clinical Trials @ RSNA 2019

Sunday, Dec. 1 10:45AM - 12:15PM Room: E352



AMA PRA Category 1 Credits ™: 1.50 ARRT Category A+ Credit: 1.75

Participants

Udo Hoffmann, MD, Boston, MA (*Moderator*) Research Grant, Kowa Company, Ltd ; Research Grant, Abbott Laboratories; Research Grant, HeartFlow, Inc; Research Grant, AstraZeneca PLC;

David A. Mankoff, MD, PhD, Philadelphia, PA (*Moderator*) Speaker, Koninklijke Philips NV Consultant, General Electric Company Advisory Board, RefleXion Medical Inc Consultant, Blue Earth Diagnostics Ltd Research Funded, Siemens AG Advisory Board, ImaginAb, Inc Spouse, Owner, Trevarx

Ruth C. Carlos, MD, MS, Ann Arbor, MI (*Moderator*) Editor, Journal of the American College of Radiology; Support, Harvey L. Neiman Health Policy Institute; In-kind support, Reed Elsevier;

Sub-Events

SPCT10A MRI in Addition to Mammography Screening in Women with Extremely Dense Breasts: Primary Outcome of the Randomized DENSE Trial

Participants

Marije F. Bakker, PhD, Utrecht, Netherlands (*Abstract Co-Author*) Grant, Bayer AG; Software support, Volpara Health Technologies Limited

Stephanie V. de Lange, Utrecht, Netherlands (*Presenter*) Research Grant, Bayer AG; Software support, Volpara Health Technologies Limited

Rudolf M. Pijnappel, MD, PhD, Haren, Netherlands (Abstract Co-Author) Research Grant, Bayer AG

Ritse M. Mann, MD, PhD, Nijmegen, Netherlands (*Abstract Co-Author*) Researcher, Siemens AG; Researcher, Seno Medical Instruments, Inc; Researcher, Identification Solutions, Inc; Researcher, Micrima Limited; Researcher, Medtronic plc; Scientific Advisor, ScreenPoint Medical BV; Scientific Advisor, Transonic Imaging, Inc; Stockholder, Transonic Imaging, Inc Claudette E. Loo, MD, Amsterdam, Netherlands (*Abstract Co-Author*) Nothing to Disclose Bob Bisschops, Dordrecht, Netherlands (*Abstract Co-Author*) Nothing to Disclose

Marc Lobbes, MD, Maastricht, Netherlands (Abstract Co-Author) Nothing to Disclose

Mathijn D. De Jong, MD, 's-Hertogenbosch, Netherlands (Abstract Co-Author) Nothing to Disclose

Katya M Duvivier, MD, Amsterdam, Netherlands (*Abstract Co-Author*) Nothing to Disclose

Jeroen Veltman, MD, Hengelo, Netherlands (*Abstract Co-Author*) Nothing to Disclose

Wouter B. Veldhuis, MD, PhD, Utrecht, Netherlands (*Abstract Co-Author*) Nothing to Disclose

Carla H. van Gils, PhD, Utrecht, Netherlands (Abstract Co-Author) Software support, Volpara Health Technologies Limited

ABSTRACT

PURPOSE To evaluate the effect of supplemental MRI for women with extremely dense breasts within a population-based screening program. METHOD AND MATERIALS Between 2011-2015, we randomized 40,373 screening participants (aged 50-75) with a negative screening mammography and extremely dense breasts (ACR category 4 by Volpara software) to (an invitation for) supplemental 3.0-T MRI at 8 sites (intervention arm; n=8,061) or mammography screening only (control arm; n=32,312). The difference in interval cancers after the first (prevalent) screening round, during the two-year screening interval, was investigated by intentionto-treat (ITT) analysis, and by complier-average causal effect (CACE) analysis to account for noncompliance. The performance of the incident screening rounds was investigated as well. RESULTS In the intervention arm, 4,783 (59%) underwent MRI examination. Cancer detection rate was 16.5/1000 screens [95%CI:13.3-20.5]. For this, 9.5% of women were recalled (6.3% with biopsy). Positive predictive values are 17.4% [95%CI:14.2%-21.2%] (recall) and 26.3% [95%CI:21.7%-31.6%] (biopsy). In the intervention arm, cancers were more frequently stage 0-I than in the control arm (82.8% vs 41.6%, p<0.001). With ITT analysis, the interval cancer rate was 4.98/1000 women in the control arm and 2.48/1000 women in the intervention arm, leading to a reduction of 2.50/1000 women [95%CI:0.98-3.71]; p<0.001. With CACE analysis, this reduction was 4.22/1000 women [95%CI:2.01-6.43]. Preliminary results of the incident screening rounds showed that 3,548 women had again undergone (at least one) mammographic screening with a negative result. Supplemental cancer detection rate was 5.3/1000 screens [95%CI:3.4-7.7]. For this, 2.8% [95%CI:2.4%-3.4%] of women were recalled for further diagnostic work-up. At the meeting, results on cost-effectiveness will be presented as well. CONCLUSION Supplemental MRI screening in women with extremely dense breasts results in statistically significantly fewer interval cancers. In subsequent rounds, both the cancer detection rate and the false-positive rate decrease. CLINICAL RELEVANCE/APPLICATION There is a heated debate on the value of supplemental screening in women with dense breasts. The DENSE trial is the first randomized trial on supplemental MRI screening that has been performed in women with dense breasts.

SPCT10B Disscussant for MRI In Addition to Mammography Screening

Participants

Christopher E. Comstock, MD, New York, NY (Presenter) Nothing to Disclose

SPCT10C 18F-FDG PET-MR Enterography in Predicting Histological Active Disease in Ulcerative Colitis: A Randomized Controlled Trial Using Nancy Index

Participants Yan Li, Essen, Germany (*Presenter*) Nothing to Disclose Benedikt M. Schaarschmidt, MD, Essen, Germany (*Abstract Co-Author*) Nothing to Disclose Lale Umutlu, MD, Essen, Germany (*Abstract Co-Author*) Consultant, Bayer AG Michael Forsting, MD, Essen, Germany (*Abstract Co-Author*) Nothing to Disclose Aydin Demircioglu, Essen, Germany (*Abstract Co-Author*) Nothing to Disclose Anna K. Koch, Essen, Germany (*Abstract Co-Author*) Nothing to Disclose Ole Martin, Duesseldorf, Germany (*Abstract Co-Author*) Nothing to Disclose Ken Herrmann, Essen, Germany (*Abstract Co-Author*) Nothing to Disclose Biosciences Consultant, Ipsen SA Consultant, Siemens AG Research Grant, Advanced Accelerator Applications SA Research Grant, Ipsen SA

Hendrik Juette, Bochum, Germany (*Abstract Co-Author*) Nothing to Disclose Andrea Tannapfel, Bochum, Germany (*Abstract Co-Author*) Nothing to Disclose Jost Langhorst, Essen, Germany (*Abstract Co-Author*) Nothing to Disclose

ABSTRACT

PURPOSE To evaluate the diagnostic performance of PET-MR enterography in detecting histological active inflammation in patients with ulcerative colitis and the impact of bowel purgation on diagnostic accuracies of PET-MR parameters. METHOD AND MATERIALS Fifty patients were enrolled in this randomized controlled trial (clinicaltrials.gov [NCT03781284]). 40 patients were randomized in two study arms, in which bowel purgation was performed either before or after PET-MR enterography. All patients underwent ileocolonoscopy with mucosal biopsies after PET-MR within 24h. Diagnostic performance of MR morphological parameters (MRmorph), diffusion-weighted imaging (DWI) and PET in detecting histological inflammation determined by Nancy index was compared with each other and between study arms. Correlation between PET and histological inflammatory severity was calculated. RESULTS In study arm without previous bowel purgation, SUVmax ratio of bowel segment (relative to SUVmax of the liver) facilitated the highest specificity and diagnostic accuracy compared to MRmorph and DWI. Bowel cleansing led to markedly increased metabolic activity of bowel segments, resulting in significantly reduced specificity of PET compared to study arm without purgation (0.808 vs. 0.966, p = 0.007, respectively). Inter-observer concordance for assessing MRmorph was clearly increased after bowel cleansing (Cohen's K: 0.847 vs. 0.665, p = 0.013, respectively), though diagnostic performance of MRmorph was not significantly improved. Our findings suggested that the change of metabolic status was mainly associated with the grade of neutrophil infiltrate and less dependent on chronic infiltrate. CONCLUSION PET-MR enterography was an excellent non-invasive diagnostic method in the assessment of ulcerative colitis without the need of previous bowel purgation. CLINICAL RELEVANCE/APPLICATION SUVmaxRatio was a reliable parameter facilitating best diagnostic operating characteristics in predicting histological active disease in patients with ulcerative colitis and no previous bowel purgation was needed for PET-MR.

SPCT10D Discussant for 18F-FDG PET-MR Enterography

Participants

Joel G. Fletcher, MD, Rochester, MN (*Presenter*) Grant, Siemens AG; Consultant, Medtronic plc; Consultant, Takeda Pharmaceutical Company Limited; Grant, Takeda Pharmaceutical Company Limited; ;

SPCT10E Clinical and Cost-Effectiveness Implications of Utilizing Immediate Acute Magnetic Resonance Imaging (MRI) in the Management of Patients with Suspected Scaphoid Fracture and Negative Initial Radiographs: Results from a Randomized Clinical Trial

Participants

Tiago Rua, BSC,MSc, London, United Kingdom (*Abstract Co-Author*) Nothing to Disclose Sanjay Vijayanathan, MBBS, Harrow, United Kingdom (*Abstract Co-Author*) Nothing to Disclose Davina Mak, MBBS, BSC, Middlesex, United Kingdom (*Presenter*) Nothing to Disclose Alireza Zavareh, MD, FRCR, Bristol, United Kingdom (*Abstract Co-Author*) Nothing to Disclose Amanda Isaac, MBChB, FRCR, Rickmansworth, United Kingdom (*Abstract Co-Author*) Nothing to Disclose Bharti Malhotra, MBA, London, United Kingdom (*Abstract Co-Author*) Nothing to Disclose Laura Hunter, London, United Kingdom (*Abstract Co-Author*) Nothing to Disclose Janet Peacock, PhD, London, United Kingdom (*Abstract Co-Author*) Nothing to Disclose James Shearer, PhD, London, United Kingdom (*Abstract Co-Author*) Nothing to Disclose Vicky J. Goh, MBBCh, Chalfont St Giles, United Kingdom (*Abstract Co-Author*) Research Grant, Siemens AG ; Speaker Bureau, Siemens AG Paul McCrone, London, United Kingdom (*Abstract Co-Author*) Nothing to Disclose Sam Gidwani, London, United Kingdom (*Abstract Co-Author*) Nothing to Disclose

ABSTRACT

PURPOSE Given the limited accuracy of radiographs on presentation to the Emergency Department (ED), the management of suspected scaphoid fractures remains clinically challenging and an economic burden to healthcare systems. This trial evaluated the clinical and cost-effectiveness implications of using immediate Magnetic Resonance Imaging (MRI) as an add-on test during the ED attendance for patients with negative findings on the initial radiographs. METHOD AND MATERIALS A pragmatic, randomized, singlecenter trial compared the use of immediate MRI for patients presenting to the ED with suspected scaphoid fractures against standard care with radiographs only. Participants' use of health services was estimated from primary care and secondary care databases and questionnaires at baseline, 3 and 6 months post-recruitment. Costs were compared using generalized linear models and combined with quality-adjusted life years (QALYs) to estimate cost-effectiveness. RESULTS A total of 136 participants were recruited based on 1:1 ratio, block randomization methods (mean age 37 years; 57% male; 79% full-time employed). 6.2% (4/65, control group) and 10% (7/67, intervention group) of participants sustained scaphoid fractures (p=0.37). 7.7% (5/65, control group) and 22% (15/67, intervention group) of participants had other fractures diagnosed (p=0.019). The use of MRI increased the diagnostic accuracy both in the diagnosis of scaphoid fracture (100.0% vs 93.8%) and any other fracture (98.5% vs 84.6%). Mean (SD) cost per participant up to 3 months post-recruitment was £542.4 (£855.2) for the control group and £368.4 (£338.6) for the intervention, leading to a cost difference of £174 (95% CI -£30 to £378, p=0.094). The cost difference per participant at 6 months increased to £266 (95% CI £3.3 to £528, p=0.047). The MRI intervention dominated standard care costing less and achieving more QALY gains, presenting a probability of 96% and 100% of being cost-effective at month 3 and 6 considering traditional willingnessto-pay thresholds. CONCLUSION The use of immediate MRI in the management of participants with suspected scaphoid fracture and negative radiographs led to significant cost-savings whilst improving and expediting the pathway's diagnostic accuracy. CLINICAL RELEVANCE/APPLICATION The immediate use of MRI in the management of suspected scaphoid fractures should be included as part of standard of care as an add-on test for patients with negative radiographs.

SPCT10F Discussant for Clinical and Cost-Effectiveness Implications

Garry E. Gold, MD, Stanford, CA (Presenter) Research support, General Electric Company

SPCT10G Imaging-guided Target Volume Reduction in Radiotherapy of Lung Cancer: The Prospective Randomized Multinational PET-Plan Trial

Participants

Tanja Schimek-Jasch, MD, Freiburg, Germany (Abstract Co-Author) Nothing to Disclose Ursula Nestle, MD, PhD, Monchengladbach, Germany (Presenter) Nothing to Disclose Stephanie Kremp, DIPLPHYS, Homburg, Germany (Abstract Co-Author) Nothing to Disclose Andrea Schaefer, PhD, Homburg, Germany (Abstract Co-Author) Nothing to Disclose Andreas Kusters, MD, Krefeld, Germany (Abstract Co-Author) Nothing to Disclose Marco Tosch, MD, Wuppertal, Germany (Abstract Co-Author) Nothing to Disclose Thomas Hehr, MD, PhD, Stuttgart, Germany (Abstract Co-Author) Nothing to Disclose Martina Eschmann, Stuttgart, Germany (Abstract Co-Author) Nothing to Disclose Yves-Pierre Bultel, Trier, Germany (Abstract Co-Author) Nothing to Disclose Peter Hass, Magdeburg, Germany (Abstract Co-Author) Nothing to Disclose Jochen Fleckenstein, Homburg, Germany (Abstract Co-Author) Nothing to Disclose Alexander Thieme, Berlin, Germany (Abstract Co-Author) Nothing to Disclose Marcus Stockinger, Mainz, Germany (Abstract Co-Author) Nothing to Disclose Matthias Miederer, Mainz, Germany (Abstract Co-Author) Nothing to Disclose Gabriele Holl, Berlin, Germany (Abstract Co-Author) Nothing to Disclose Christian Rischke, MD, Kirchzarten, Germany (Abstract Co-Author) Nothing to Disclose Sonja Adebahr, MD, Freiburg, Germany (Abstract Co-Author) Nothing to Disclose Eleni Gkika, Freiburg, Germany (Abstract Co-Author) Nothing to Disclose Jochem Koenig, Mainz, Germany (Abstract Co-Author) Nothing to Disclose Anca-Ligia Grosu, Freiburg, Germany (Abstract Co-Author) Nothing to Disclose

ABSTRACT

PURPOSE Advanced medical imaging offers a chance for target volume reduction in modern radiotherapy, which may lead to more effective local treatments with reduced toxicity and offer the protection of draining lymph nodes and large vessels, possibly of importance for the upcoming combination of radiotherapy and immunotherapy. Locally advanced non-small cell lung cancer (NSCLC) with improvable local control and high toxicity is an excellent model to investigate this topic. METHOD AND MATERIALS In the prospective randomised controlled PET-Plan trial (NCT00697333), patients with inoperable stage II/III NSCLC and an indication for radiochemotherapy were randomized at a 1:1 ratio. In conventional arm A target volumes were informed by FDG-PET and CT plus elective nodal irradiation and in experimental arm B they were solely informed by FDG-PET. In both arms, quality assured isotoxically dose-escalated IMRT or 3D-CRT (60 - 74Gy, 2Gy per fraction) was planned and applied to the respective target volumes along with simultaneous platinum-based chemotherapy. The primary objective was time to locoregional progression (LRP) in terms of noninferiority of experimental arm B. RESULTS 311 patients were recruited, 205 patients included in the intent to treat (ITT) (A: n=99, B: n=106) and 172 patients in the per protocol (PP) analysis (A: n=84, B: n=88). Median FU time in the PP set was 16 months. Non-inferiority of experimental arm B was confirmed for the pre-specified non-inferiority margin. The risk of LRP was lower in the experimental arm B (2y-LRP 0.20 vs. 0.39; HR=0.57; 95% CI: 0.30-1.06; p=0.039) with no difference between study arms concerning survival (2y-OS 0.57 vs. 0.54), out-field recurrence and toxicity. CONCLUSION In radiochemotherapy for locally advanced NSCLC, PET-Imaging based reduction of radiotherapy target volumes is feasible and may improve local control without increasing toxicity. CLINICAL RELEVANCE/APPLICATION The procedures established in this clinical trial provide a radiotherapy standard for future NSCLC trials including immunotherapy and may furthermore inspire trials on imaging based target volume reduction for other tumor types.

SPCT10H Discussant for Imaging-guided Target Volume Reduction

Participants

Daniel Pryma, MD, Philadelphia, PA (*Presenter*) Research Grant, Siemens AG; Research Grant, 511 Pharma; Research Grant, Progenics Pharmaceuticals, Inc; Research Consultant, Progenics Pharmaceuticals, Inc; Research Consultant, 511 Pharma; Research Consultant, Actinium Pharmaceuticals, Inc; Research Consultant, Nordic Nanovector ASA





SSA02

Breast Imaging (MRI Diagnostics)

Sunday, Dec. 1 10:45AM - 12:15PM Room: S402AB



AMA PRA Category 1 Credits ™: 1.50 ARRT Category A+ Credit: 1.75

FDA Discussions may include off-label uses.

Participants

Mami Iima, MD, PhD, Kyoto, Japan (Moderator) Nothing to Disclose

Thomas H. Helbich, MD, Vienna, Austria (*Moderator*) Research Grant, Medicor, Inc Research Grant, Siemens AG Research Grant, C. R. Bard, Inc

Sub-Events

SSA02-01 High-Risk Lesions Detected by MRI-Guided Core Biopsy: Upgrade Rates at Surgical Excision and Implications for Management

Sunday, Dec. 1 10:45AM - 10:55AM Room: S402AB

Participants

Aya Michaels, MD, New York, NY (*Presenter*) Nothing to Disclose Genevieve N. Abbey, MD, New York, NY (*Abstract Co-Author*) Nothing to Disclose Paula Ginter, New York, NY (*Abstract Co-Author*) Nothing to Disclose Katerina Dodelzon, MD, New York, NY (*Abstract Co-Author*) Nothing to Disclose

For information about this presentation, contact:

aym9010@med.cornell.edu

PURPOSE

To assess clinical and imaging characteristics of high-risk lesions detected by MRI-guided core biopsy and to evaluate upgrade rates to carcinoma at surgical excision

METHOD AND MATERIALS

A retrospective review was performed for all women presenting to an academic breast radiology center for MRI-guided biopsy from January 2015 - November 2018. Histopathological results from each biopsy were extracted, and high-risk lesions [atypical ductal hyperplasia (ADH), lobular carcinoma in situ (LCIS), atypical lobular hyperplasia (ALH), radial scar, papilloma, flat epithelial atypia (FEA), and benign vascular lesion] were included for analysis. Clinical history, imaging characteristics, surgical outcome following excision, and follow-up data were also recorded. If the lesion was excised in a mastectomy specimen or a lumpectomy specimen with a known cancer, then upgrade status was deemed indeterminate and not included in the upgrade rate calculation. Rigorous radiologic pathologic correlation was performed of upgraded lesions to determine whether biopsy results were concordant and the lesion was adequately sampled.

RESULTS

Of 810 MRI-guided biopsies, 189 biopsies (23.3%) met inclusion criteria as high-risk lesions. Excluded were 151 (18.6%) malignant and 470 (58.0%) benign lesions. Mean patient age of the included patients was 58.4 years (range 30-83). Upgrade rate was indeterminate in 41 (21.7%) of high-risk lesions. Surgical upgrade rates were high for ADH 32.4% (12/37) and FEA 100.0% (2/2); moderate for LCIS 7.0% (3/43); and low for ALH 0.0% (0/10), radial scar 0.0% (0/24), papilloma 0.0% (0/29), and benign vascular lesions 0.0% (0/3). Of the upgraded lesions, 82.4% (14/17) had concurrent breast carcinoma (7 contralateral and 7 ipsilateral), and 76.5% (13/17) were upgraded to DCIS or well-differentiated carcinoma. ADH was significantly more likely to be upgraded than non-ADH lesions (p<0.0001).

CONCLUSION

ADH obtained on MRI-guided core biopsy warrants surgical excision. Other high-risk lesions, however, may be candidates for imaging follow-up rather than surgical excision, especially in the setting of no concurrent breast carcinoma, and after meticulous radiologic-pathologic correlation.

CLINICAL RELEVANCE/APPLICATION

Identifying subsets of high-risk lesions biopsied under MRI-guidance that are rarely upgraded to carcinoma at surgical excision can safely prevent many women from undergoing surgery.

SSA02-02 Tumor Necrosis at Baseline Dynamic Contrast Enhanced (DCE) MRI for Prediction of Neoadjuvant Chemotherapy Treatment (NACT) Response in Triple Negative Breast Cancer (TNBC) Patients

Sunday, Dec. 1 10:55AM - 11:05AM Room: S402AB

Beatriz E. Adrada, MD, Houston, TX (Abstract Co-Author) Nothing to Disclose Benjamin Musall, BS, Houston, TX (Abstract Co-Author) Nothing to Disclose Jingfei Ma, PhD, Houston, TX (Abstract Co-Author) Royalties, Siemens AG; Royalties, General Electric Company; Consultant, C4 Imaging Rosalind P. Candelaria, MD, Houston, TX (Abstract Co-Author) Nothing to Disclose Wei T. Yang, MD, Houston, TX (Abstract Co-Author) Consultant, General Electric Company; Medical Advisory Board, Seno Medical Instruments, Inc Kenneth Hess, PhD, Houston, TX (Abstract Co-Author) Nothing to Disclose Lumarie Santiago, MD, Houston, TX (Abstract Co-Author) Nothing to Disclose Gary J. Whitman, MD, Houston, TX (Abstract Co-Author) Nothing to Disclose H. Carisa Le-Petross, MD, FRCPC, Houston, TX (*Abstract Co-Author*) Nothing to Disclose Tanya W. Moseley, MD, Houston, TX (*Abstract Co-Author*) Consultant, Hologic, Inc Elsa M. Arribas, MD, Houston, TX (Abstract Co-Author) Scientific Advisory Board, Volumetric Biotechnologies, Inc; Stockholder, Volumetric Biotechnologies, Inc Deanna L. Lane, MD, Houston, TX (Abstract Co-Author) Nothing to Disclose Marion E. Scoggins, MD, Houston, TX (Abstract Co-Author) Institutional Research Grant, General Electric Company Jessica W. Leung, MD, Houston, TX (Abstract Co-Author) Scientific Advisory Board, Subtle Medical Mark D. Pagel, PhD, Houston, TX (Abstract Co-Author) Nothing to Disclose Ken-Pin Hwang, PHD, Houston, TX (Abstract Co-Author) Nothing to Disclose Jong Bum Son, PhD, Houston, TX (Abstract Co-Author) Nothing to Disclose Jennifer Litton, Houston, TX (Abstract Co-Author) Nothing to Disclose Senthil Damodaran, Houston, TX (Abstract Co-Author) Nothing to Disclose Bora Lim, MD, Houston , TX (Abstract Co-Author) Nothing to Disclose Jason White, Houston, TX (Abstract Co-Author) Nothing to Disclose Hagar S. Mahmoud, MBBCh, Alexandria, Egypt (Abstract Co-Author) Nothing to Disclose Vicente Valero, MD, Houston, TX (Abstract Co-Author) Nothing to Disclose Alastair Thompson, Houston, TX (Abstract Co-Author) Nothing to Disclose Stacy Moulder, MD, Houston, TX (Abstract Co-Author) Research funded, AstraZeneca PLC Research funded, F. Hoffmann-La Roche Ltd Research funded, Oncothyreon Research funded, Novartis AG Research funded, Merck KGaA Gaiane M. Rauch, MD, PhD, Houston, TX (Abstract Co-Author) Nothing to Disclose

For information about this presentation, contact:

abeerhamed2009@gmail.com

PURPOSE

To determine the predictive value of tumor necrosis at baseline DCE-MRI on treatment response to NACT in TNBC patients.

METHOD AND MATERIALS

This IRB-approved study includes 85 patients with stage I-III TNBC, who had baseline MRI, underwent NACT followed by definitive surgery. Tumors were segmented on the early phase subtraction of DCE-MRI. Necrosis was identified as non-enhancing intratumoral tissue on DCE with high T2 signal and shine through on the Apparent Diffusion Coefficient (ADC). Necrotic tumors were segmented with and without inclusion of necrotic regions. The longest dimension of the tumors, volume and percent of necrosis were calculated from contours. Metrics of necrosis were compared with pathologic complete response (pCR) or non-pCR in tissue evaluated after surgical resection, T stage of the tumor, and regional lymph node (LN) involvement at staging and at surgery (positive vs negative). Receiver operating characteristic (ROC) curves, Wilcoxon rank sum tests, and odds ratios (OR) were used for analysis.

RESULTS

Necrosis was seen in 31 pts (36.5 %), median volume was 4.8 cm3 (range 0.7-945 cm3), median percent was 22.8 % (range 4.6-86 %). pCR occurred in 37 pts (43.5%). There was no significant association between pCR and presence of necrosis (OR = 1.4, 95% CI (0.6, 3.3), P=0.49). The volume and percent of necrosis were not significantly different between pts with pCR and non-pCR [AUROCC = 0.52, 95% CI (0.40, 0.65); p=0.69; AUROCC = 0.54, 95% CI (0.41, 0.66) p = 0.52, respectively]. No significant association between T stage of the TNBC and presence of necrosis [OR = 2.3, 95% CI (0.6, 8.8) p = 0.23] was found. Necrotic lesions were seen in 21% (3/14) T1 lesions, 39% (17/44) T2 and 37% (10/27) T3-T4 lesions. There was no significant association between baseline necrosis and LN involvement at staging or at surgery [OR = 0.9, 95% CI = (0.4, 2.1), p = 0.73; OR = 0.5, 95% CI = (0.1, 1.4), p=0.16 respectively]. Tumor necrosis was seen in 38% (15/39) LN+ and in 35% (16/46) LN- pts at staging; 41% (26/64) LN+ and 24% (5/21) LN- pts at surgery.

CONCLUSION

Tumor necrosis at baseline in TNBC patients was not associated with pCR or nodal involvement and was not a predictor of response to NACT.

CLINICAL RELEVANCE/APPLICATION

Our study found that tumor necrosis at baseline imaging in TNBC patients had no association with their treatment response and therefore should not affect their treatment planning.

SSA02-03 Feasibility of Supine MRI-Navigated Ultrasound in Breast Cancer Patients

Sunday, Dec. 1 11:05AM - 11:15AM Room: S402AB

Participants

Ga Young Yoon, MD, Gangwon-do, Korea, Republic Of (*Abstract Co-Author*) Nothing to Disclose Hye J. Eom, MD, Seoul, Korea, Republic Of (*Abstract Co-Author*) Nothing to Disclose Woo Jung Choi, MD, Seoul, Korea, Republic Of (*Abstract Co-Author*) Nothing to Disclose Eun Young Chae, Seoul, Korea, Republic Of (*Abstract Co-Author*) Nothing to Disclose Joo Hee Cha, MD, Seoul, Korea, Republic Of (*Abstract Co-Author*) Nothing to Disclose Hee Jung Shin, MD, Seoul, Korea, Republic Of (*Abstract Co-Author*) Nothing to Disclose Hak Hee Kim, MD, Seoul, Korea, Republic Of (*Abstract Co-Author*) Grant, General Electric Company Hak Hee Kim, MD, Seoul, Korea, Republic Of (*Presenter*) Nothing to Disclose

PURPOSE

To evaluate the feasibility of image fusion between ultrasound (US) and supine magnetic resonance (MR) in breast cancer patients and to evaluate the differences in tumor location between prone and supine positions.

METHOD AND MATERIALS

This prospective study was approved by our institutional review board, and informed consent was obtained. Between May 2016 and December 2017, 88 patients who were undergoing additional supine MR (MRsup) following routine prone MR (MRpro) for breast cancer were included. Clockwise location of the tumor and discrepancies in the distances from nipple to lesion (NLD), skin to lesion (SLD), and lesion to chest wall (CLD) were evaluated between MRpro and MRsup (MRpro-sup), MRpro and MRsup navigated US (MRpro-USnav) and MRsup and USnav (MRsup-USnav). Associations between breast thickness and measurement discrepancies were analyzed using Pearson's correlation.

RESULTS

Total 91 index lesions were evaluated in 88 patients. The intraclass correlation coefficients (ICCs) for the clockwise location of MRpro and MRsup compared with USnav were 0.994 (range: 0.990-0.996) and 0.998 (range: 0.996-0.998), respectively. The mean MRpro-sup and MRpro-USnav measurement discrepancies were greater than those of MRsup-USnav. NLD showed the smallest mean MRsup-USnav measurement discrepancy. Most outer locations showed greater mean measurement discrepancies than inner locations, and each NLD, SLD, and CLD mean measurement discrepancy showed different tendencies according to location and lesion depth. High breast thickness showed significantly greater mean measurement discrepancies than low breast thickness (cutoff: median thickness of 74 mm). Breast thickness showed moderate and strong correlations with MRpro-sup (r=0.583, p<0.001) and MRpro-USnav (r=0.634, p<0.001) CLD discrepancies, and weak correlations with MRpro-sup (r=0.347, p=0.001) and MRpro-USnav (r=0.343, p=0.001) NLD discrepancies.

CONCLUSION

Image fusion between US and supine MR is feasible in breast cancer patients, although there is a considerable difference in tumor location measurements between prone and supine positions, especially with thicker breasts.

CLINICAL RELEVANCE/APPLICATION

Supine MRI-navigated US is feasible, and the error range between supine and prone position is predictable and may be helpful for estimating breast cancer location and surgical planning.

SSA02-04 Usefulness of MRI Projection Mapping System for Conserving Surgery of Breast Cancer: Comparison with Conventional Method and Pathohistological Findings

Sunday, Dec. 1 11:15AM - 11:25AM Room: S402AB

Participants

Maki Amano, MD, Tokyo, Japan (*Presenter*) Nothing to Disclose Toshiaki Kitabatake, MD, Tokyo, Japan (*Abstract Co-Author*) Nothing to Disclose Yuko Ichikawa, Tokyo, Japan (*Abstract Co-Author*) Nothing to Disclose Reiko Inaba, RT, Tokyo, Japan (*Abstract Co-Author*) Nothing to Disclose Otoichi Nakata, Ebina, Japan (*Abstract Co-Author*) Nothing to Disclose Yutaka Ozaki, MD, PhD, Tokyo, Japan (*Abstract Co-Author*) Nothing to Disclose Kuniaki Kojima, MD, Tokyo, Japan (*Abstract Co-Author*) Nothing to Disclose Kazuyuki Ito, RT, Tokyo, Japan (*Abstract Co-Author*) Nothing to Disclose Chie Kurokawa, PhD, Tokyo, Japan (*Abstract Co-Author*) Nothing to Disclose Shigeki Aoki, MD, PhD, Tokyo, Japan (*Abstract Co-Author*) Nothing to Disclose Shigeki Aoki, MD, PhD, Tokyo, Japan (*Abstract Co-Author*) GE, Toshiba/Canon, Fuji, Fuji RI, Eisai, Daiichi-Sankyo, Mediphysics, Siemens, Bayer, Guerbet, Bracco-Eisai Ryohei Kuwatsuru, MD, Tokyo, Japan (*Abstract Co-Author*) Nothing to Disclose

For information about this presentation, contact:

ma-amano@mbj.nifty.com

PURPOSE

Conserving surgery of breast cancer is conventionally performed by referring MRI acquired in the prone position owing to its accurate detection of the tumor extent. However, the shapes of breast and cancer during MRI scan differ from those under surgery, because the surgery is performed in the supine position. The aim of this study was to evaluate usefulness of MRI projection mapping system (PMS), which we have developed as a prototype, for determining the tumor extent and surgical line in patients who underwent conserving surgery of breast cancer.

METHOD AND MATERIALS

Eleven patients with invasive breast cancer were enrolled. Contrast-enhanced breast MRI in the prone and supine positions was performed separately using a 1.5 T. Conserving surgery of breast cancer was performed based on the conventional method: its extent was determined by palpation, ultrasonography (US) and prone MRI. Immediately before the surgery, maximum intensity projection (MIP) image generated from supine MRI was projected onto the breast surface using structured light method by the MRI-PMS, which consisted of projector-camera system and personal computer. We compared the tumor location and associated intraductal component between the conventional method, MRI-PMS and pathohistological findings.

RESULTS

MRI projection mapping was successfully completed in 9 of the 11 patients; an operational failure occurred in 2 patients. The discrepancy of tumor location ranged from 3 to 9 mm (mean, 4.5 mm) between the conventional method and MRI-PMS. The 5 patients had intraductal component.. The intraductal component was visualized more clearly and perceived more easily by MRI-PMS than by the conventional method in the 4 of them. The total tumor extent defined by MRI -PMS corresponded to that by pathohistological findings in these patients.

CONCLUSION

MRI-PMS visualizes the breast cancer. especially that with intraductal component. Thus. MRI-PMS can be recommended for

conserving surgery of breast cancer.

CLINICAL RELEVANCE/APPLICATION

MRI projection mapping system is useful for conserving surgery of breast cancer because it visualizes the breast cancer well, especially that with intraductal component.

SSA02-05 Accelerating Acquisition of RESOLVE-DWI with Simultaneous Multi-slice (SMS) Technique in Diagnosing Breast Lesions

Sunday, Dec. 1 11:25AM - 11:35AM Room: S402AB

Participants

Tao Ai, MD, Wuhan, China (*Presenter*) Nothing to Disclose Yiqi Hu, Wuhan, China (*Abstract Co-Author*) Nothing to Disclose Chenao Zhan, Wuhan, China (*Abstract Co-Author*) Nothing to Disclose Liming Xia, MD, Wuhan, China (*Abstract Co-Author*) Nothing to Disclose Xu Yan, Shanghai, China (*Abstract Co-Author*) Nothing to Disclose Xiaoyong Zhang, Shenzhen, China (*Abstract Co-Author*) Nothing to Disclose Huiting Zhang, Wuhan, China (*Abstract Co-Author*) Nothing to Disclose Wei Liu, Shenzhen, China (*Abstract Co-Author*) Nothing to Disclose Baiyun Liu, PhD, Shanghai, China (*Abstract Co-Author*) Employee, Infervision

For information about this presentation, contact:

aitao007@hotmail.com

PURPOSE

To investigate the feasibility and effectiveness of diffusion weighted imaging (DWI) using Simultaneous Multi-slice readoutsegmented echo planar imaging (rs-EPI) to diagnose breast lesions.

METHOD AND MATERIALS

The IRB approved study was performed on a 3T scanner with a dedicated 16-channel phased-array breast coil (MAGNETOM Skyra, Siemens Healthcare, Erlangen, Germany). 46 female patients (average age of 42.3 years; range of 26-57 years) with 48 lesions (41 malignant and 7 benign) were enrolled in this study. Patients underwent bilateral breast MRI using a prototypical SMS rs-EPI sequence and a conventional rs-EPI sequence. T1-weighted MRI, T2-weighted MRI, and dynamic contrast-enhanced (DCE-MRI) were also conducted as references. The details of imaging parameters of both DWI sequences were listed in Figure 1. ADC, MK, MD values were quantitatively calculated for each lesion on both sequences. In addition, all images were qualitatively analyzed by a blinded read using a 5-point scale (1 = poor, 5 = excellent). The difference and correlation of both quantitative and qualitative parameters between conventional rs-EPI and SMS rs-EPI data were statistically analyzed.

RESULTS

Compared to conventional rs-EPI, The acquisition time of SMS rs-EPI was markedly reduced (2:17 vs4:27 minutes). The Pearson's correlation showed a excellent linear relationship for each parameter between SMS rs-EPI and conventional rs-EPI (r = 0.935, 0.914 and 0.965 for MK, MD and ADC respectively; P<0.01 for all, Fig.2). Furthermore, the ROC analysis demonstrated SMS rs-EPI had better diagnostic performance than conventional rs-EPI, however the values didn't differ significantly (Fig.3). In blinded read, SMS rs-EPI showed comparable imaging quality with conventional rs-EPI (Fig.4&5), with moderate to good inter-rater reliability (ICC = 0.63-0.83).

CONCLUSION

Compared to conventional rs-EPI technique, SMS rs-EPI can markedly reduce the acquisition time and yield similar diagnostic accuracy and comparable image quality, which may be useful to expand the scope of its clinical application in breast imaging, and increase the patient throughout.

CLINICAL RELEVANCE/APPLICATION

SMS RESOLVE allows for rapid realization of breast MR imaging, which may serve as a superior alternative for the diagnosis of breast lesions.

SSA02-06 Quantitative Tumor Volumes by Fast Dynamic Contrast Enhanced (DCE) MRI Predict Pathologic Complete Response (pCR) to Neoadjuvant Chemotherapy (NACT) in Triple Negative Breast Cancer (TNBC)

Sunday, Dec. 1 11:35AM - 11:45AM Room: S402AB

Participants

Benjamin Musall, BS, Houston, TX (*Presenter*) Nothing to Disclose Jingfei Ma, PhD, Houston, TX (*Abstract Co-Author*) Royalties, Siemens AG; Royalties, General Electric Company; Consultant, C4 Imaging Beatriz E. Adrada, MD, Houston, TX (*Abstract Co-Author*) Nothing to Disclose Abeer H. Abdel Hameed, MBChB, Houston, TX (*Abstract Co-Author*) Nothing to Disclose Rosalind P. Candelaria, MD, Houston, TX (*Abstract Co-Author*) Nothing to Disclose Wei T. Yang, MD, Houston, TX (*Abstract Co-Author*) Nothing to Disclose Wei T. Yang, MD, Houston, TX (*Abstract Co-Author*) Consultant, General Electric Company; Medical Advisory Board, Seno Medical Instruments, Inc Kenneth Hess, PhD, Houston, TX (*Abstract Co-Author*) Nothing to Disclose Lumarie Santiago, MD, Houston, TX (*Abstract Co-Author*) Nothing to Disclose H. Carisa Le-Petross, MD, FRCPC, Houston, TX (*Abstract Co-Author*) Nothing to Disclose Tanya W. Moseley, MD, Houston, TX (*Abstract Co-Author*) Consultant, Hologic, Inc Elsa M. Arribas, MD, Houston, TX (*Abstract Co-Author*) Scientific Advisory Board, Volumetric Biotechnologies, Inc; Stockholder, Volumetric Biotechnologies, Inc

Deanna L. Lane, MD, Houston, TX (Abstract Co-Author) Nothing to Disclose Jessica W. Leung, MD, Houston, TX (Abstract Co-Author) Scientific Advisory Board, Subtle Medical Marion E. Scoggins, MD, Houston, TX (Abstract Co-Author) Institutional Research Grant, General Electric Company Mark D. Pagel, PhD, Houston, TX (Abstract Co-Author) Nothing to Disclose Ken-Pin Hwang, PHD, Houston, TX (Abstract Co-Author) Nothing to Disclose Jong Bum Son, PhD, Houston, TX (Abstract Co-Author) Nothing to Disclose Jason White, Houston, TX (Abstract Co-Author) Nothing to Disclose Jennifer Litton, Houston, TX (Abstract Co-Author) Nothing to Disclose Senthil Damodaran, Houston, TX (Abstract Co-Author) Nothing to Disclose Bora Lim, MD, Houston , TX (*Abstract Co-Author*) Nothing to Disclose Brandy J. Willis, MBA,RT, Houston, TX (*Abstract Co-Author*) Nothing to Disclose Hagar S. Mahmoud, MBBCh, Alexandria, Egypt (Abstract Co-Author) Nothing to Disclose Ayah A. Megahed, MBBCh, Cairo, Egypt (Abstract Co-Author) Nothing to Disclose Alastair Thompson, Houston, TX (Abstract Co-Author) Nothing to Disclose Stacy Moulder, MD, Houston, TX (Abstract Co-Author) Research funded, AstraZeneca PLC Research funded, F. Hoffmann-La Roche Ltd Research funded, Oncothyreon Research funded, Novartis AG Research funded, Merck KGaA Gaiane M. Rauch, MD, PhD, Houston, TX (Abstract Co-Author) Nothing to Disclose

For information about this presentation, contact:

bcmusall@mdanderson.org

PURPOSE

In TNBC, non-pCR has high risk of recurrence. We evaluated the dependence of the quantitative tumor volumes for predicting pCR status in TNBC on the temporal resolution of DCE MRI.

METHOD AND MATERIALS

In the ARTEMIS trial (NCT02276443), TNBC pts receive 4 cycles of Adriamycin-based chemo (C4AC) followed by taxane-based NACT. 35 pts underwent fast DCE-MRI with range of temporal resolution 8-49 s at baseline (BL) and after C4AC. A retrospective cohort (RC) of 50 TNBC pts who had NACT and BL standard DCE-MRI (temporal resolution 90-120 s) was compared. For all pts pCR was assessed at surgery. 3-dimensional tumor measurements were obtained and tumor volume was contoured by a breast radiologist on the early subtraction phase. Clinical tumor volume (CTV) was calculated using 3 tumor dimensions. Enhanced tumor volume (ETV) was extracted as volume of the contoured voxels, and functional tumor volume (FTV) was extracted as the subset of ETV with voxels below preset signal enhancement ratio (SER). CTV, ETV, FTV, and their changes between BL and C4AC scans were compared between pCR and non-pCR using Receiver Operator Characteristic (ROC) curve and Wilcoxon rank sum test.

RESULTS

An optimal SER of 0.45 was found to maximize AUC of pCR vs non-pCR in ARTEMIS group. In ARTEMIS pts, CTV, ETV, and FTV at BL were able to discriminate pCR and non-pCR, with the pCR pts having significantly smaller tumor volumes (AUC = 0.75, 0.74, 0.74 and p=0.0096, 0.022, 0.022, respectively). CTV, ETV, and FTV at C4AC were significantly different between pCR and non-pCR (AUC = 0.71, 0.74, 0.75 and p=0.041, 0.017, 0.019, respectively). The changes in CTV, ETV, and FTV from BL to C4 were significantly different between pCR and non-pCR (AUC = 0.70, 0.73, 0.71 and p=0.044, 0.026, 0.038). In contrast, CTV, ETV, and FTV in the RC at BL were not significantly different between pCR and non-pCR and non-pCR pts (AUC=0.62, 0.54, 0.53 and p=0.16, 0.66, 0.74 respectively). Tumor volumes measured in ARTEMIS pts were smaller than in the RC (p=0.061).

CONCLUSION

Quantitative tumor volumes measured by fast DCE may serve as an early predictor of treatment response in TNBC. Standard DCE MRI with lower temporal resolution may overestimate the tumor volumes.

CLINICAL RELEVANCE/APPLICATION

Tumor volumes measured with fast DCE MRI improve prediction of treatment response to NACT in TNBC in comparison with standard DCE MRI and may be useful imaging biomarkers of treatment response.

SSA02-07 Efficacy of 3-D Diffusion Weighted Imaging with Background Suppression (DWIBS) in Detection of Breast Carcinoma Compare to Dynamic Contrast Enhanced MRI

Sunday, Dec. 1 11:45AM - 11:55AM Room: S402AB

Participants

Pratiksha Yadav, Pune, India (*Presenter*) Nothing to Disclose Yashraj Patil, Pune, India (*Abstract Co-Author*) Nothing to Disclose Amarjit Singh, MD, DMRD, Pune, India (*Abstract Co-Author*) Nothing to Disclose Saumya Harit, Manipal, India (*Abstract Co-Author*) Nothing to Disclose

For information about this presentation, contact:

yadavpratiksha@hotmail.com

PURPOSE

Aim is to evaluate the efficacy 3-D Diffusion weighted imaging with background suppression in detection of breast carcinoma. To evaluate efficacy of DWIBS in differentiation of malignant and benign breast lesions and it's comparison with CEMR. To evaluate ADC values of benign and malignant breast lesions.

METHOD AND MATERIALS

Study IRB and IEC approved.Study included 103 breast lesions which were detected on mammography and breast ultrasound. All the cases underwent breast MRI on 1.5 Tesla machine using dedicated breast coil. Multiplaner localizer applied with 3mm slice thickness. T1WI, T2WI and STIR in axial, STIR coronal, & sagittal plane. Axial DWI was done with b value 1500 sec/mm2. Pre contrast fat-suppressed T1W gradient echo images were obtained followed by intravenous contrast injection. Post processing was done by digitally subtracting the pre-contrast.ADC calculations obtained.All the cases were correlated histopathologically.

RESULTS

Study included 103 lesions.Lesions which showed diffusion restriction considered positive whereas lesions did not show restriction were considered as benign lesions. DWI with increase b value demonstrates lesions better with background suppression. Total 52(50.5%) lesions were benign and 51(49.5%) were malignant on Histopathology. Sensitivity of DWI was 90.2% (95% CI= 84.5,95.9), specificity was 94.2% (95% CI =89.7,98.7), PPV 93.9% 95% CI =89.3,98.5) and NPV 90.7% (95% CI =85.1,96.3). Mean ADCs of malignant lesions was $0.933 \pm 0.21 \times 103$ mm 2/s. and benign lesions was $1.847 \pm 0.51 \times 103$ mm2/s. Area under curve was 0.97. with P value <0.001(significant).Cut off ADC value was 1.08×103 mm2. Sensitivity for the CEMR was 94.3 %(95% CI= 88.7-99.8), specificity 96.9% (95% CI = 92.7-100.0) PPV 97.1 95% CI =93,100) and NPV 93.9 95% CI =82.2,99.6).

CONCLUSION

DWIBS is an excellent non contrast investigation which can detect breast carcinoma and differentiate benign and malignant breast lesions and the result was comparable to CEMR technique. It can diagnose skin changes and nipple areolar changes as well.

CLINICAL RELEVANCE/APPLICATION

DWIBS can be use as non invasive, non radiation, non contrast method for differentiation in benign and malignant pathology and number of biopsy can be reduced in the clear benign pathologies . This method can be use in the screening of the high risk and dense breast parenchyma, younger population.

SSA02-08 Power of Time-dependent Diffusion MRI as a Prognostic Biomarker in the Breast

Sunday, Dec. 1 11:55AM - 12:05PM Room: S402AB

Participants

Mami İima, MD, PhD, Kyoto, Japan (*Presenter*) Nothing to Disclose Masako Y. Kataoka, MD, PhD, Kyoto, Japan (*Abstract Co-Author*) Nothing to Disclose Maya Honda, Kyoto, Japan (*Abstract Co-Author*) Nothing to Disclose Akane Ohashi, Kyoto-hu, Japan (*Abstract Co-Author*) Nothing to Disclose Ayami Ohno Kishimoto, MD, Kyoto, Japan (*Abstract Co-Author*) Nothing to Disclose Rie Ota, MD, Kyoto, Japan (*Abstract Co-Author*) Nothing to Disclose Kanae K. Miyake, MD, PhD, Kyoto, Japan (*Abstract Co-Author*) Nothing to Disclose Yuta Urushibata, Tokyo, Japan (*Abstract Co-Author*) Employee, Siemens AG Thorsten Feiweier, Erlangen, Germany (*Abstract Co-Author*) Employee, Siemens AG Stockholder, Siemens AG Patent holder, Siemens AG

Masakazu Toi, Kyoto, Japan (*Abstract Co-Author*) Nothing to Disclose Kaori Togashi, MD, PhD, Kyoto, Japan (*Abstract Co-Author*) Research Grant, Bayer AG Research Grant, DAIICHI SANKYO Group Research Grant, Eisai Co, Ltd Research Grant, FUJIFILM Holdings Corporation Research Grant, Nihon Medi-Physics Co, Ltd Research Grant, Canon Medical Systems Corporation

For information about this presentation, contact:

mamiiima@kuhp.kyoto-u.ac.jp

PURPOSE

To investigate the utility of ADC values obtained with the different diffusion times (including short diffusion time recently available on clinical scanners) for differentiation of benign and malignant breast tumors as well as their prognostic biomarkers.

METHOD AND MATERIALS

200 cases were prospectively enrolled to this IRB-approved study and 149 breast lesions (86 malignant, 63 benign) were analyzed. DWI scans with prototype sequences using different diffusion times (effective diffusion time Deff = 5.1 ms and 96.6 ms) were performed, with b-values of 0 and 700 s/mm2 and acquisition time of 2.5 min for each on a 3T MRI. ADC change was calculated; (ADCshort - ADClong) / ADCshort x 100 (%), where ADC short and ADC long are ADC values with Deff = 5.1 ms and 96.6 ms. ADC values and ADC changes were compared between malignant and benign breast tumors, as well as between positivity and negativity in expression of their prognostic biomarkers.

RESULTS

Significantly smaller ADCshort and ADClong values were found in malignant compared than benign lesions (P < 0.0001 and < 0.0001). ADClong had significantly lower values than ADCshort, both in malignant and benign lesions (P < 0.0001 and < 0.0001, respectively). ADC changes were significantly larger in malignant compared with benign lesions (P < 0.0001). PgR-positive breast cancers had significantly lower ADCshort and ADClong values than PgR negative (P < 0.01 and < 0.05). Both ADCshort and ADClong values than PgR negative (P < 0.05 and < 0.05). Both ADCshort and ADClong values were significantly lower in ER-positive than ER-negative breast cancers (P < 0.05 and < 0.05). Significantly larger ADC change was observed in Ki-67 positive compared to Ki-67 negative cancers (P < 0.01). ADC decrease with diffusion times was remarkable in the peripheral region of typical invasive ductal carcinoma, while center had almost no ADC change, suggesting of central necrosis.

CONCLUSION

ADC values significantly changed depending on tumor types or prognostic factors of breast cancers. Time-dependent diffusion MRI might be a useful prognostic and predictive biomarker, allowing more accurate diagnosis and a safe promising approach to personalized therapy of breast cancer. Our results also underline the importance of checking diffusion times in the interpretation of breast DWI.

CLINICAL RELEVANCE/APPLICATION

The diffusion time dependence of ADC values can be a prognostic marker, potentially allowing to tailor treatment plans of breast cancers without the need of contrast agents

SSA02-09 Feasibility Study of Applying Simultaneous Multi-slice Technique in Diffusion-weighted Imaging of Breast Lesions

Participants Fei Wang, Anqing, China (*Presenter*) Nothing to Disclose Juan Zhu, Anqing, China (*Abstract Co-Author*) Nothing to Disclose Qing H. Yang, MD,MSc, Anqing, China (*Abstract Co-Author*) Nothing to Disclose Mengxiao Liu, Shanghai, China (*Abstract Co-Author*) Nothing to Disclose Chunyan Liu, Changchun, China (*Abstract Co-Author*) Nothing to Disclose

For information about this presentation, contact:

bbyxywf@163.com

PURPOSE

To evaluate the feasibility of applying simultaneous multi-slice (SMS) single-shot echo planar imaging (EPI) to accelerate MR diffusion imaging for breast lesions.

METHOD AND MATERIALS

60 patients (30 breast carcinoma,17 fibroadenoma of breast and 13 normal breast) who underwent breast MRI (3T,MAGNETOM Skyra,Siemens Healthcare) were collected.The following three different diffusion weighted imaging (DWI) scan protocols were applied.The first sequence(A) is the conventional single-shot echo planar DWI (EPI-DWI):TR/TE 5200ms/72ms,FOV 360mm×227.4mm,Slice thickness 5mm,Distance factor 1mm,Slices 30,Bandwidth 1644Hz/pix,Voxel size 0.9×0.9×5mm3,GRAPPA factor 2,b-values(averages) 50s/mm2(2) and 800s/mm2(6) with 3-scan trace mode,Scan time 2:31min.For the second(B) and the third(C) DWI protocols,a SMS factor of two and three were applied, respectively.In order to compare the image quality with those acquired by sequence A,all the sequence parameters were kept the as described above, except for changing the TR of sequence B to 2600ms(scan time 75s) and the TR of sequence C to 1800ms(scan time 55s).For all sequences,image quality is evaluated by two radiologists blinded to the acquisition schemes on a five-point scale.The quantitative analysis for the three sequences included image signal-to-noise ratio (SNR),ADC values of normal breast parenchyma and breast lesions.Paired t-test was used to compare the differences of SNR and ADC values between A and B,A and C.Inter-reader reliability was analyzed by calculating the intra-class correlation coefficient (ICC).

RESULTS

Compared with protocol A, the image quality of protocol C was significant reduced (ICC=0.4), while that of protocol B was stable (ICC= 0.9). The image SNR of A, B and C scan protocols were 21.2 \pm 3.0, 19.8 \pm 3.3 and 15.3 \pm 3.7, respectively. There was no significant difference between protocol B and A (p=0.162) of the image SNR. The SNR of protocol C were significant lower than those of protocol A(p<0.001). The ADC values (×10-3mm2/s) of normal breast parenchyma, breast carcinoma lesions and fibroadenoma of breast were 2.01 \pm 0.35, 0.98 \pm 0.25, 1.78 \pm 0.36, respectively. With SMS factor of 2, the ADC values of those three parts were 1.98 \pm 0.39,1.02 \pm 0.21,1.82 \pm 0.33. The ADC value of 3×SMS were 1.83 \pm 0.27,0.87 \pm 0.31, 1.87 \pm 0.27,respectively. There was no significant difference in ADC values between protocol B and A,C and A in normal breast parenchyma and lesions (all p > 0.05).

CONCLUSION

By applying SMS technique with a factor of 2, the acquisition time of breast DWI can be significantly reduced without sacrificing the image quality. However, if the SMS factor increases to 3, the image SNR decreases which affects clinical diagnosis.

CLINICAL RELEVANCE/APPLICATION

Comparing with conventional EPI-DWI, the SMS markedly Reduces the diffusion scan time and the image SNR still shows a good quality. Thus, SMS technique is recommended for DWI of the MR breast study.







SSA04

Cardiac (Myocardial Ischemia and Viability (MRI))

Sunday, Dec. 1 10:45AM - 12:15PM Room: S102CD



AMA PRA Category 1 Credits ™: 1.50 ARRT Category A+ Credit: 1.75

FDA Discussions may include off-label uses.

Participants

Susan K. Hobbs, MD, PhD, Pittsford, NY (Moderator) Nothing to Disclose

Sub-Events

SSA04-01 Intracoronary Compared with Intravenous Bolus tirofiban on No-Reflow Phenomenon in Patients with ST-Segment Elevation Myocardial Infarction Undergoing Primary Percutaneous Coronary Intervention: A Cardiac Magnetic Resonance Study

Sunday, Dec. 1 10:45AM - 10:55AM Room: S102CD

Participants

Quanmei Ma, Shenyang, China (*Presenter*) Nothing to Disclose Yang Hou, MD, Shenyang, China (*Abstract Co-Author*) Nothing to Disclose Yue Ma, Shenyang, China (*Abstract Co-Author*) Nothing to Disclose Xiaonan Wang, Shenyang, China (*Abstract Co-Author*) Nothing to Disclose Tongtong Yu, Shenyang, China (*Abstract Co-Author*) Nothing to Disclose

PURPOSE

The aim of the study was to investigate potential effect of intracoronary administration of glycoprotein IIb/IIIa inhibitor tirofiban on no-reflow phenomenon (NR) assessed by CMR compared to intravenous routine in patients with ST-segment elevated myocardial infarction undergoing primary percutaneous coronary intervention (PCI).

METHOD AND MATERIALS

120 patients were randomized into 2 groups (Tirofiban i.c. Versus i.v.). CMR was completed within 3-7 days after ST-segment elevation myocardial infarction. CMR was also performed in 3 to 6 months follow up after discharge. Left ventricular function, volumes, infarct size, microvascular obstruction, hemorrhage, myocardial salvage, myocardial perfusion index and tissue tracking strain were performed on CMR analysis.

RESULTS

The microvascular obstruction (32/52 versus 24/68, p < 0.05) showed significantly difference between the intravenous and the intracoronary tirofiban groups. The area at risk (34.4% [interquartile range: 9.0% to 62.4%] versus 33.5% [interquartile range: 8.9% to 50.5%], p > 0.05) and infarct size (17.8% [interquartile range: 9.3% to 25.5%] versus 16.8% [interquartile range: 8.8% to 24.3%], p > 0.52) did not differ significantly between the two groups. The myocardial salvage index was similar (22.4% [interquartile range: 8% to 43%] versus 21.6% [interquartile range: 7% to 42%], p > 0.05). No significantly difference was found in myocardial perfusion index, myocardial strain between the two groups. The intracoronary tirofiban group was associated with higher % Δ LVEDV compared with intravenous group (-9.41% [interquartile range: -13.5% to -2.41%] versus -0.09% [interquartile range: -7.7% to 7.37%], p<0.01).

CONCLUSION

This CMR study in ST-segment elevation myocardial infarction patients showed benefit of decreasing MVO for intracoronary tirofiban administration compared to intravenous in patients undergoing PICC. Intracoronary tirofiban administration showed improvement in left ventricular remodeling. No benefit was found with respect to infarct size, myocardial perfusion index and myocardial strain 3-6 months after infarction.

CLINICAL RELEVANCE/APPLICATION

Intracoronary tirofiban administration could be potentially applied to reduce MVO incidence compared to intravenous in STEMI patients undergoing PICC.

SSA04-02 Assessment of Early Left Ventricle Myocardial Strain with Cardiovascular Magnetic Resonance Feature Tracking: A Prospective Study in Patient of Acute ST-elevated Myocardial Infarction

Sunday, Dec. 1 10:55AM - 11:05AM Room: S102CD

Participants

Jinsen Zou, MD, Shenzhen, China (*Presenter*) Nothing to Disclose Genwen Hu, MD, Shenzhen, China (*Abstract Co-Author*) Nothing to Disclose Suihao Zhang, MD,MD, Shenzhen, China (*Abstract Co-Author*) Nothing to Disclose Qin Qin, MMed, Shenzhen, China (*Abstract Co-Author*) Nothing to Disclose Xiaoting Wei, MD,MD, Shenzhen, China (*Abstract Co-Author*) Nothing to Disclose Yangyang Zhou, Shenzhen, China (*Abstract Co-Author*) Nothing to Disclose Jianmin Xu, Shenzhen, China (*Abstract Co-Author*) Nothing to Disclose

For information about this presentation, contact:

zouzousen@icloud.com

PURPOSE

To investigate the diagnostic performances of early left ventricular (LV) strain, using a cardiovascular magnetic resonance feature tracking (CMR-FT) technology, in patients with acute ST-elevation myocardial infarction (STEMI) after primary percutaneous coronary intervention (PPCI).

METHOD AND MATERIALS

Seventy-eight patients of acute STEMI underwent CMR imaging at 2-6 days after successful PPCI. The imaging protocol included conventional cine imaging, for assessing LV regional radial (RS), circumferential (CS), longitudinal (LS) strains as well as function, and late gadolinium enhancement for assessing LV infarct size, transmurality and microvascular obstruction (MVO). LV strain were analyzed in a 16-segment model.

RESULTS

Hyperenhancement was detected in 495 (40%) of 1248 segments, including 423 (85%) transmural hyperenhancement, and was accompanied by MVO in 173 (35%) of hyperenhancement segments. Regional radial (RS) and circumferential strain (CS) were significantly diminished in segments with hyperenhancement and decreased even further if MVO was also present (p<0.001). CS surpassed RS in its ability to differentiate between transmural and non-transmural infarct (p<0.001 and p=0.002, respectively). Furthermore, CS was superior to RS in discriminating infarcted segments with MVO from infarcted segments without MVO (all p<0.001).

CONCLUSION

Regional strain analysis performs ability in differentiating between non-infarcted myocardium, infarcted myocardium with and without MVO, transmural and non-transmural infarcted myocardium. Peak circumferential strain is the most accurate marker of regional function.

CLINICAL RELEVANCE/APPLICATION

Strain shows great potential in noninvasive diagnosis of early LV regional infarct, transmurality, and MVO in patient of acute STEMI. CMR-FT may provide a useful tool in early assessment of myocardial strain.

SSA04-03 Impact of Ischemia Time on Cardiac Functional and Structural Parameters: CMR Assessment and Histological Correlation in a Porcine Model of Myocardial Infarction

Sunday, Dec. 1 11:05AM - 11:15AM Room: S102CD

Awards

Trainee Research Prize - Fellow

Participants

Monika Arzanauskaite, MMedSc, Liverpool, United Kingdom (*Presenter*) Nothing to Disclose Manuel Gutierrez, Barcelona, Spain (*Abstract Co-Author*) Nothing to Disclose Laura Casani, Barcelona, Spain (*Abstract Co-Author*) Nothing to Disclose Soumaya Soumaya Ben-Aicha, Barcelona, Spain (*Abstract Co-Author*) Nothing to Disclose Guiomar Mendieta, Barcelona, Spain (*Abstract Co-Author*) Nothing to Disclose Alberto Hidalgo, MD, Barcelona, Spain (*Abstract Co-Author*) Nothing to Disclose Teresa Padro, Barcelona, Spain (*Abstract Co-Author*) Nothing to Disclose Gemma Vilahur, Barcelona, Spain (*Abstract Co-Author*) Nothing to Disclose Lina Badimon, Barcelona, Spain (*Abstract Co-Author*) Nothing to Disclose

For information about this presentation, contact:

arzanauskaite@gmail.com

PURPOSE

The pig model of myocardial infarction (MI) is considered the gold standard for the analysis of cardioprotective/regenerative strategies before moving towards the clinical setting. However, there is no systematic study investigating cardiac structural and functional outcomes in relation to the duration of the ischemic insult. We have evaluated the impact of time of ischemia in cardiac damage and performance over time by CMR.

METHOD AND MATERIALS

Pigs (N=32) underwent MI by closed chest balloon occlusion of the mid-left anterior descending (LAD) coronary artery. Animals were randomized into four groups differing in the duration of ischemia (30, 60, 90, and 120min) and then reperfused. A sham-operated group was performed (N=8). The impact of ischemia was assessed by serial CMR at days 3 and 42 post-MI. The following parameters were determined: global and regional function, wall edema, necrosis, and microvascular obstruction. Molecular markers of fibrosis and myocyte hypertrophy were determined in the ischemic myocardium.

RESULTS

At day3, CMR revealed that cardiac damage and function was similar in sham and pigs subjected to 30min ischemia. In contrast, edema and necrosis significantly increased from 60min onwards with a progressive trend over time. Microvascular obstruction was most extensively seen in animals with >=90min of ischemia. These structural alterations associated to a significant and comparable drop in systolic function in pigs subjected to >=60min ischemia (p=60min of ischemia (p=60min of ischemia (p=60min ischemia (p=60min ischemia (p=60min of ischemia (p=60min of ischemia (p=60min ischemia (p

the infarcted myocardium of pigs subjected to 60min or longer ischemia (P<0.05 vs 30min). The same was true for myocyte surface and volume extension.

CONCLUSION

Mid-LAD coronary occlusion for 60min suffices to induce cardiac structural and functional alterations amenable to therapeutic interventions.

CLINICAL RELEVANCE/APPLICATION

There is a need to standardize methodological approaches of MI-induction in human-like animal models to successfully translate preclinical benefits into the clinical arena.

SSA04-04 Early Detection of Myocardial Fibrosis by CMR Quantitation Extracellular Volume Fraction in a Hypertensive Swine Model

Sunday, Dec. 1 11:15AM - 11:25AM Room: S102CD

Participants

Baiyan Zhuang, Beijing, China (*Presenter*) Nothing to Disclose Chen Cui, MSc, Beijing, China (*Abstract Co-Author*) Nothing to Disclose Arlene Sirajuddin, MD, Bethesda, MD (*Abstract Co-Author*) Nothing to Disclose Minjie Lu, MD, PhD, Beijing, China (*Abstract Co-Author*) Nothing to Disclose

For information about this presentation, contact:

zbyan10@163.com

PURPOSE

Our study aims to determine whether ECV and Native T1 quantified by cardiac magnetic resonance (CMR) can demonstrate left ventricle (LV) extracellular interstitial fibrosis in a hypertensive (HTN) swine model and quantitatively evaluate the dynamic change over time.

METHOD AND MATERIALS

Twenty-five adult male Chinese miniature pigs aged 6-12 months underwent cardiac MR imaging at three time points: pre- and 1 month-, 3 months- post induction of hypertension. Native T1 value and ECV fraction was prospectively performed at all imaging time points. The left ventricle (LV) systolic function was calculated using the cine images. Individual and segmental native T1 value and ECV fraction were compared to the late gadolinium enhancement (LGE) images. Animals were euthanized after the last examination of MRI. Histopathologic examinations of heart were performed later.

RESULTS

The systolic/diastolic pressure was gradually increased. There was no obvious abnormal performance in the triphenyl tetrazolium chloride (TTC) stain and no obvious increased signal intensity in the LGE in all stages of hypertension. However, the ECV fraction and Native T1 value increased with modelling time (p < 0.001). The results were demonstrated by pathological results where fibrous tissues were observed increasing gradually in the HE, Masson and Picrosirius stain.

CONCLUSION

T1 and ECV derived from CMR may be a non-invasive method in the early detection of myocardial interstitial fibrosis in hypertensive heart disease prior LGE detectable by conventional CMR. T1 and ECV can also reflect the severity of myocardial involvement in the progress of hypertension. For detection of myocardial fibrosis, combined both advantages of native T1(higher sensitivity) and ECV(higher specificity) can make a more accurate evaluation of myocardial fibrosis.

CLINICAL RELEVANCE/APPLICATION

The presence of diffuse fibrosis may be a potential mechanism for increasing cardiovascular risk in HTN patients. Early detection and taking methods to reduce diffuse fibrosis can reduce the incidence of such risk.

SSA04-05 The Relationship between Systolic and Diastolic Strains Measured from Tissue Tracking Cardiovascular Magnetic Resonance and Adverse Remodeling in Post-STEMI Patients

Sunday, Dec. 1 11:25AM - 11:35AM Room: S102CD

Participants Kaiyue Diao, Chengdu , China (*Presenter*) Nothing to Disclose Rui Shi, Chengdu, China (*Abstract Co-Author*) Nothing to Disclose Shan Huang, Chengdu, China (*Abstract Co-Author*) Nothing to Disclose Zhigang Yang, MD, Chengdu, China (*Abstract Co-Author*) Nothing to Disclose

For information about this presentation, contact:

kaiyuediao@qq.com

PURPOSE

Adverse left ventricle (LV) remodeling was supposed to be the main culprits of ST-segment elevation myocardial infarction (STEMI) patients' poor life quality. This study aimed to determine associations between the diastolic strains rate and adverse LV remodeling in post-STEMI patients.

METHOD AND MATERIALS

A number of 52 (M/F: 46/6, age: 54.27 yrs) STEMI patients who underwent coronary intervention three months ago were prospectively recruited from 2016 to 2017. Follow-up was done until 2018. The primary end points were the symptoms of heart failure (NYHA II-IV). Consent was acquired from each patient and 3.0 T MRI was arranged. Adverse LV remodeling defined by a 12%

increase in LV end diastolic volume (LVEDV). The early (EDSR) and late (LDSR) peak diastolic strain rates were derived from the two peak points on the corresponding curve of time-to-SR curve in the diastole (Figure 1). t-test was performed when comparing between groups. Logistic regression test was done for statistical analysis and P < 0.05 was considered as significant.

RESULTS

Myocardial infarction size, all the peak strains, systolic peak strain rates and the early diastolic strain rates were significantly correlated with Adverse LV remodeling. None of the parameters was independent determinant. 23/52 (44.2%) patients complained of heart failure symptoms at the one-year follow-up. Multivariate Logistic regression test showed that only the ratio between the EDSR and LDSR in the radial direction on the short axis (DSRR-SR) was the independent predictor of the heart failure symptoms (6.59; range, 6.71-3.68; P=0.026).

CONCLUSION

Both systolic and diastolic strains were correlated with Adverse LV remodeling at short-time follow-up for STEMI patients, while only the DSRR-SR could independently predict heart failure at the long-time follow-up. The quantitative measurement of diastolic function through myocardium strains might help with better clinical management for STEMI patients.

CLINICAL RELEVANCE/APPLICATION

This study gave clues that myocardium deformation was associated with adverse LV remodeling at the early stage for post-STEMI patients. Furthermore, the diastolic strain rates could potentially provide unique prognostic information for STEMI patients to predict heart failure.

SSA04-06 Ectopic Fat Deposition in Obese Patients with Type 2 Diabetes: Correlation with Left Ventricle Function and Microcirculation

Sunday, Dec. 1 11:35AM - 11:45AM Room: S102CD

Participants

Yue Gao, Chengdu, China (*Presenter*) Nothing to Disclose Zhigang Yang, MD, Chengdu, China (*Abstract Co-Author*) Nothing to Disclose Yingkun Guo, Chengdu, China (*Abstract Co-Author*) Nothing to Disclose Li Jiang, Chengdu, China (*Abstract Co-Author*) Nothing to Disclose Rui Shi, Chengdu, China (*Abstract Co-Author*) Nothing to Disclose Meng-ting Shen, Chengdu , China (*Abstract Co-Author*) Nothing to Disclose Pei-lun Han, Chengdu , China (*Abstract Co-Author*) Nothing to Disclose

PURPOSE

To investigate the relationship between microvascular dysfunction and ectopic fat deposition in type 2 diabetes mellitus (T2DM) patients with preserved ejection fraction.

METHOD AND MATERIALS

Forty-eight T2DM patients (23 males, age 56.23±10.65) and fifteen healthy volunteers were prospectively enrolled. All of them were underwent CMR (3.0-T, Siemens Medical Solutions, Erlangen, Germany). Patients with LVEF< 55% were excluded, and all the patients were divided into obesity group (BMI>=24) and non-obesity group(BMI<24). All CMR parameters were measured using the cine sequence and perfusion imaging. Single-voxel H-magnetic resonance spectroscopy was performed to detect the triglyceride content of myocardial (Interventricular septum), liver(segment VII) and muscle(The erector spinae of the same level as the liver), which was calculated as a percentage relative to the signal of myocardial water by the post-processing software (jMRUI, version 6.0).

RESULTS

All patients remained normal LV function and LV global stress compared with normal controls(P>0.05). Myocardial triglyceride content was significantly higher in T2DM patients compared with healthy volunteers ($1.41\pm0.65\%$ vs. $0.61\pm0.22\%$, P<0.001). Compared with non-obesity group, triglyceride content of heart and liver were increased in obese group (all P<0.05). Myocardial triglyceride content was correlated with left ventricle mass (r=0.52), Upslope (r=-0.53) and TimeMax (r=0.49), and liver triglyceride content was correlated with Upslope (r=-0.33) and TimeMax (r=0.43). ROC analysis revealed that sensitivity and specificity were obtained for predicting the occurrence of TimeMax with the Myocardial triglyceride content (AUC=0.83) and myocardial triglyceride content (AUC=0.63).

CONCLUSION

T2DM with obesity are more prone to fatty ectopic deposits. Although the patient's myocardial function and global strain did not show be damaged, ectopic fat may cause myocardial microcirculation disturbance. At the same time, we found in addition to myocardium, excessive deposition of liver fat may also lead to myocardial microcirculation.

CLINICAL RELEVANCE/APPLICATION

Although the patient's myocardial function and global strain did not show be damaged, ectopic fat may cause myocardial microcirculation disturbance.

SSA04-07 Relationship between Myocardial Microvascular Dysfunction and Myocardial Triglyceride Content in Preserved Ejection Fraction Type 2 Diabetes Mellitus: Assessment with 1H-Magnetic Resonance Spectroscopy

Sunday, Dec. 1 11:45AM - 11:55AM Room: S102CD

Participants Yue Gao, Chengdu, China (*Presenter*) Nothing to Disclose Zhigang Yang, MD, Chengdu, China (*Abstract Co-Author*) Nothing to Disclose Yingkun Guo, Chengdu, China (*Abstract Co-Author*) Nothing to Disclose Li Jiang, Chengdu, China (*Abstract Co-Author*) Nothing to Disclose Rui Shi, Chengdu, China (*Abstract Co-Author*) Nothing to Disclose

For information about this presentation, contact:

304789161@qq.com

PURPOSE

Cardiac lipid over-storage and lipotoxic injury to cardiomyocytes have been considered as one of the important mechanisms of cardiac dysfunction coursed by metabolic abnormalities. For patients with early diabetic cardiomyopathy, the presence of myocardial microvascular dysfunction requires greater attention. The purpose of this study was to assess the effects of myocardial triglyceride content on left ventricle myocardial microvascular dysfunction in type 2 diabetes mellitus with Preserved left ventricle ejection fraction (LVEF).

METHOD AND MATERIALS

forty-eight type 2 diabetes patients (23 males, age 56.23±10.65) and fifteen healthy volunteers were prospectively enrolled. All of them were underwent CMR (3.0-T, Siemens Medical Solutions, Erlangen, Germany). We excluded patients with LVEF <55%. All cardiac function parameters were measured using the cine sequence. Myocardial perfusion parameters included upslope, time to maximum signal intensity (TTM) and max signal intensity (MaxSI), which were calculated by the signal-time curve of the first-pass myocardial perfusion imaging. Single-voxel 1H-magnetic resonance spectroscopy was performed to detect the myocardial triglyceride content, which was calculated as a percentage relative to the signal of myocardial water by the post-processing software (jMRUI, version 6.0).

RESULTS

Myocardial triglyceride content was significantly higher in T2DM patients compared with healthy volunteers (1.46±0.705% vs. 0.61±0.22%, p< 0.001). Systolic and diastolic function did not significantly differ between patients and healthy. The Pearson analysis showed the myocardial triglyceride content was associated with LVEDV (r=0.32, p<0.05), LVESV (r=0.31, p<0.05), upslope (r=-0.34, p<0.05) and TTM (r=0.37, p<0.05). Multivariable analysis indicated that myocardial triglyceride content was associated with TTM ($\beta=0.51$, p<0.05, 95%CI:2.24-20.74), independently of diabetic duration, age, sex, BMI, blood pressure and LV functional parameters.

CONCLUSION

Myocardial triglyceride content is increased in preserved ejection fraction T2DM and is associated with myocardial microvascular dysfunction, independently of diabetic duration and Individual basic characteristics.

CLINICAL RELEVANCE/APPLICATION

For diabetic with preserved ejection fraction, myocardial triglyceride content is increased than normal, and is associated with myocardial microvascular dysfunction

SSA04-08 Novel Short Inversion Time 3D LGE Imaging in Ischaemic Scars

Sunday, Dec. 1 11:55AM - 12:05PM Room: S102CD

Participants

Malgorzata Polacin, MD, Zurich, Switzerland (*Presenter*) Nothing to Disclose Mareike Gastl, MD, Zurich, Switzerland (*Abstract Co-Author*) Nothing to Disclose Ioannis Kapos, Zurich, Switzerland (*Abstract Co-Author*) Nothing to Disclose Alexander Gotschy, Zurich, Switzerland (*Abstract Co-Author*) Nothing to Disclose Jochen Von Spiczak, MD, Zurich, Switzerland (*Abstract Co-Author*) Nothing to Disclose Hatem Alkadhi, MD, Zurich, Switzerland (*Abstract Co-Author*) Nothing to Disclose Robert Manka, Zurich, Switzerland (*Abstract Co-Author*) Nothing to Disclose

For information about this presentation, contact:

Malgorzata.Polacin@usz.ch

PURPOSE

Late gadolinium enhancement (LGE) visualizes myocardial scar and fibrosis. After myocardial infarction (MI), subendocardial infarcts can be missed due to poor contrast between the blood pool and the subendocardium. The aim of this study was to evaluate the benefit of 3D LGE imaging using a single breath-hold inversion recovery sequence with a fixed, short inversion time (TI =100 ms) (short3D LGE) in comparison to standard 3D LGE imaging with an adjusted TI (3D LGE).

METHOD AND MATERIALS

3D LGE and short3D LGE (both sequences with the same spatial resolution of $1.2 \times 1.2 \text{ mm}^2$ and slice-thickness of 8 mm; field of view, 350 x 350 mm², single breath-hold) were acquired in 40 patients with MI (12 female, mean age 61.1 ± 14 years) at 1.5T (Achieva, Philips, Best, Netherlands). Two independent, blinded readers evaluated 680 segments (AHA 17-segment model) using a 5-point Likert scale in terms of scar visibility. Contrast-to-noise ratio (CNR) between scar and blood pool and between normal myocardium and blood pool was calculated in both datasets.

RESULTS

3D LGE showed 131 infarcted segments out of 680 (19.2%), short3D LGE revealed 141 segments (20.7%). Short3D LGE demonstrated better scar visibility (4.3 vs 2.9, p < 0.01) and excellent CNR between scar and blood pool (824.3 \pm 249 vs. 221 \pm 156, p < 0.01), but weak CNR between remote myocardium and blood pool (247.5 \pm 241 vs. 1246.6 \pm 363, p < 0.01) compared to 3D LGE. Agreement between the readers was moderate for 3D LGE and substantial for short3D LGE (weighted κ = 0.55 vs. 0.76).

CONCLUSION

Short3D LGE provided very good scar visualization and revealed even more infarcted segments in comparison to standard 3D LGE. Although not suitable to replace standard 3D LGE imaging due to insufficient contrast between remote myocardium and blood pool, this novel single breath-hold sequence could be used additionally to standard 3D LGE imaging, especially in patients with subendocardial scars and suboptimal nulling of the myocardium.

CLINICAL RELEVANCE/APPLICATION

Short3D LGE with fixed inversion time makes scar detection easier especially in subtle subendocardial infarcts and when myocardial nulling is difficult.

SSA04-09 The Relationship between Circulating miR-1 Change and Ischemia-Reperfusion Injury in Patients with ST-Segment-Elevation Myocardial Infarction: A Cardiovascular Magnetic Resonance Study

Sunday, Dec. 1 12:05PM - 12:15PM Room: S102CD

Participants Quanmei Ma, Shenyang, China (*Presenter*) Nothing to Disclose Yang Hou, MD, Shenyang, China (*Abstract Co-Author*) Nothing to Disclose Yue Ma, Shenyang, China (*Abstract Co-Author*) Nothing to Disclose Xiaonan Wang, Shenyang, China (*Abstract Co-Author*) Nothing to Disclose Tongtong Yu, Shenyang, China (*Abstract Co-Author*) Nothing to Disclose

PURPOSE

This study aimed to evaluate the relationship between circulating microRNAs (miRNAs) and ischemia-reperfusion injury using cardiovascular magnetic resonance (CMR).

METHOD AND MATERIALS

Sixty patients with a first STEMI treated with primary percutaneous coronary intervention(PCI) who underwent CMR imaging at 1 week and 3-6 months after STEMI were evaluated. miR-1 was measured using PCR-based technologies in plasma samples collected at admission and 3 days after PCI. The difference of miR-1 (Δ miR-1) was calculated. The relationship between Δ miR-1 and Microvascular obstruction (MVO) was estimated. The association between Δ miR-1 and the changes of LV diastolic volumes(Δ LVEDV), and ejection fraction(Δ LVEF) at follow up were estimated.

RESULTS

The miR-1 at admission showed no difference between MVO positive group and MVO negative group (P >0.05). miR-1 at admission exhibited positive associated with &LVEDV at 3-6 months (r=0.378, P < 0.05). No significant difference was found between miR-1 at admission and changes of LVEF during follow-up (P = 0.43). The expression different of miR-1 showed difference in the MVO positive group and MVO negative group, 5.46 ± 15.32 vs. -5.45 ± 12.37, respectively,p<0.01. The area under the curve of receiver operator curve analysis for Δ miR-1 was 0.81,and when the cut off valve of Δ miR-1 was 1.54,the sensitivity and specificity were 0.64,0.91, respectively. No significant difference was found between Δ miR-1 at admission and &LVEDV, and &LVEF.

CONCLUSION

Plasma Δ miRNA-1 was associated with ischemia-reperfusion injury in STEMI patients undergoing PCI. miRNA-1 at admission was a predictor of LV remodeling at 3-6 months after STEMI.

CLINICAL RELEVANCE/APPLICATION

Plasma ΔmiRNA-1 could potentially be applied to estimate ischemia-reperfusion injury extent in STEMI patients undergoing PCI.

Printed on: 01/07/20







SSA07

Gastrointestinal (LIRADS)

Sunday, Dec. 1 10:45AM - 12:15PM Room: S103AB



AMA PRA Category 1 Credits ™: 1.50 ARRT Category A+ Credit: 1.75

Participants

Khaled M. Elsayes, MD, Pearland, TX (*Moderator*) Nothing to Disclose Kathryn J. Fowler, MD, San Diego, CA (*Moderator*) Consultant, 12 Sigma Technologies; Researcher, Nuance Communications, Inc; Contractor, Midamerica Transplant Services; ; Alexa G. Ortiz Escobar I, MD, Mexico City, Mexico (*Moderator*) Nothing to Disclose

Sub-Events

SSA07-01 Accuracy of Liver Imaging Reporting and Data System Category 4 or 5 for Diagnosing Hepatocellular Carcinoma: A Systematic Review and Meta-Analysis

Sunday, Dec. 1 10:45AM - 10:55AM Room: S103AB

Participants

Dong Hwan Kim, MD, Seoul, Korea, Republic Of (*Presenter*) Nothing to Disclose Sang Hyun Choi, Seoul, Korea, Republic Of (*Abstract Co-Author*) Nothing to Disclose Seong Ho Park, MD, Seoul, Korea, Republic Of (*Abstract Co-Author*) Research Grant, Central Medical Service Co, Ltd Kyung Won Kim, MD, Seoul, Korea, Republic Of (*Abstract Co-Author*) Nothing to Disclose Jae Ho Byun, MD, Seoul, Korea, Republic Of (*Abstract Co-Author*) Nothing to Disclose So Yeon Kim, Seoul, Korea, Republic Of (*Abstract Co-Author*) Nothing to Disclose So Yeon Kim, Seoul, Korea, Republic Of (*Abstract Co-Author*) Nothing to Disclose Seung Soo Lee, MD, Seoul, Korea, Republic Of (*Abstract Co-Author*) Nothing to Disclose Yong Moon Shin, Seoul, Korea, Republic Of (*Abstract Co-Author*) Nothing to Disclose Hyung Jin Won, MD, Seoul, Korea, Republic Of (*Abstract Co-Author*) Nothing to Disclose Pyo Nyun Kim, MD, Seoul, Korea, Republic Of (*Abstract Co-Author*) Nothing to Disclose

For information about this presentation, contact:

edwardchoi83@gmail.com

PURPOSE

We aimed to systematically determine the accuracy of Liver Imaging Reporting and Data System (LI-RADS) for magnetic resonance imaging (MRI) diagnosis of hepatocellular carcinoma (HCC) and to determine the sources of heterogeneity between reported results.

METHOD AND MATERIALS

Original studies that reported the diagnostic accuracy of LI-RADS for HCC using MRI were identified in MEDLINE and EMBASE up to October 25, 2018. Study quality was assessed using QUADAS-2. We categorized studies into two groups, LR-5, and LR-4 or LR-5, criteria, and obtained the meta-analytic summary sensitivity and specificity of both criteria with a bivariate random-effects model. Subgroup analyses and meta-regression analysis were performed to further explore study heterogeneity.

RESULTS

Among the 157 articles screened, 18 studies covered LR-5 (3651 lesions), and 16 studies covered LR-4 or LR-5 (3182 lesions). For the LR-5 criterion, the meta-analytic summary sensitivity and specificity were 62.1% (95% CI [confidence interval], 53.9-69.7%; *I*2=91.6%) and 92.8% (95% CI, 89.9-94.9%; *I*2=66.8%), respectively (Fig. 1A). For the LR-4 or LR-5 criterion, the meta-analytic summary sensitivity and specificity were 88.4% (95% CI, 82.7-92.5%; *I*2=89.2%) and 81.7% (95% CI, 73.5-87.8%; *I*2=88.3%), respectively (Fig. 1B). For the LR-5 criterion, the three factors of subject enrollment, MRI scanner field strength, and type of reference standard were significantly associated with study heterogeneity ($P \le 0.04$). For the LR-4 or LR-5 criterion, the study heterogeneity (P <= 0.03).

CONCLUSION

The LR-5 criterion was highly specific, but showed suboptimal sensitivity for diagnosing HCC in patients at risk of HCC. In comparison with the LR-5 criterion, the sensitivity of the LR-4 or LR-5 criterion increased, but the specificity decreased. Substantial study heterogeneity was noted, and four significant factors were identified: subject enrollment, the type of reference standard, MRI scanner field strength, and contrast agent type.

CLINICAL RELEVANCE/APPLICATION

The LR-5 criterion was highly specific, but had suboptimal sensitivity for diagnosing HCC. Substantial study heterogeneity was noted, and further randomized controlled studies are needed to validate the diagnostic performance of LI-RADS.

SSA07-02 Using Ancillary Features to Update Liver Imaging Reporting and Data System version 2018 on Gadobenate Dimeglumine-Enhanced MRI

Participants Yao Zhang, Guangzhou, China (*Abstract Co-Author*) Nothing to Disclose Jingbiao Chen, Guangzhou, China (*Abstract Co-Author*) Nothing to Disclose Sichi Kuang, Guangzhou, China (*Abstract Co-Author*) Nothing to Disclose Bingjun He, Guangzhou, China (*Abstract Co-Author*) Nothing to Disclose Kathryn J. Fowler, MD, San Diego, CA (*Abstract Co-Author*) Consultant, 12 Sigma Technologies; Researcher, Nuance Communications, Inc; Contractor, Midamerica Transplant Services; ; Claude B. Sirlin, MD, San Diego, CA (*Abstract Co-Author*) Research Grant, Gilead Sciences, Inc; Research Grant, General Electric Company; Research Grant, Siemens AG; Research Grant, Bayer AG; Research Grant, Koninklijke Philips NV; Consultant, AMRA AB; Consultant, Fulcrum; Consultant, IBM Corporation; Consultant, Exact Sciences Corporation; Consultant, Boehringer Ingelheim GmbH; Consultant, Arterys Inc; Consultant, Epigenomics; Author, Medscape, LLC; Lab service agreement, Gilead Sciences, Inc; Lab service agreement, ICON plc; Lab service agreement, Intercept Pharmaceuticals, Inc; Lab service agreement, Shire plc; Lab service agreement, Enanta; Lab service agreement, Takeda Pharmaceutical Company Limited; Lab service agreement, Alexion Pharmaceuticals, Inc; Lab service agreement, NuSirt Biopharma, Inc Jin Wang, MD, Guangzhou, China (*Presenter*) Nothing to Disclose

For information about this presentation, contact:

569874016@qq.com

PURPOSE

To evaluate whether ancillary features on gadobenate dimeglumine-enhanced MRI can be used to upgrade LI-RADS categories from LR-4 to LR-5.

METHOD AND MATERIALS

260 patients with chronic liver disease at high risk for HCC were retrospectively included. Hepatobiliary phase (HBP) was obtained 2 hours after gadobenate dimeglumine injection at 3.0T scanner, and all HBP images can be used to evaluate liver observations according to LI-RADS criteria. Blinded to the clinical and pathological data, two abdominal radiologists evaluated LI-RADS v2018 major and ancillary features for the largest observation in each patient on MR images in consensus. Observations were categorized according to LI-RADS version 2018 as well as various modifications to LI-RADS, in which LR-4 could be upgraded to LR-5 by the presence of ancillary features as listed in Table 1. Diagnostic sensitivity, specificity, accuracy, false negative rate (FNR), false positive rate (FPR), positive predictive value (PPV), negative predictive value (NPV) of category LR- 5 were calculated for LI-RADS v2018 and for each modified LI-RADS. Receiver operating characteristic (ROC) curves were generated and areas under the ROC curve (AUC) were computed.

RESULTS

Final diagnoses for the 260 observations included 216 HCCs, 5 intrahepatic cholangiocarcinomas, 5 combined hepatocellularcholangiocarcinomas, 2 metastatic tumors, 2 focal nodular hyperplasias, 7 arterio-portal shunts, 20 hemangiomas, 1 abscess, 1 cyst, and 1 dysplastic nodule. Overall, 0% LR-1(0/2) and LR-2 (0/28), 90% (10/11) LR-3, 86% LR-4 (19/22), and 99% LR-5 (174/175) were HCCs according to LI-RADS v2018. The final LI-RADS categories, as well as the sensitivity, specificity, accuracy, FNR, FPR, PPV, NPV and AUC of LR-5 using v2018 and each modified LI-RADS are listed in table 1. Modified LI-RADS I (in which HBP hypointensity can be used to upgrade LR-4 to LR-5) showed higher sensitivity (94.4 vs 80.6%) and accuracy (93.5 vs 83.5%) than LI-RADS v2018 without significantly reducing specificity (88.6 vs 97.7%), PPV (97.6 vs 99.4%), or AUC (0.915 vs 0.891).

CONCLUSION

Modified LI-RADS I may improve sensitivity and accuracy for diagnosing HCC without impairing specificity or positive predictive value.

CLINICAL RELEVANCE/APPLICATION

HBP hypointensity may be used to upgrade LR-4 to LR-5 without impairing specificity or positive predictive value for a diagnosis of HCC on gadobenate dimeglumine-enhanced MRI in Chinese patients.

SSA07-03 Effect of Upgrading LR-4 Lesions to LR-5 Using HCC Favoring Ancillary Features on Diagnostic Performance of HCC

Sunday, Dec. 1 11:05AM - 11:15AM Room: S103AB

Participants

Jae Hyon Park, MD, Seoul, Korea, Republic Of (*Presenter*) Nothing to Disclose Yong Eun Chung, MD, PhD, Seoul, Korea, Republic Of (*Abstract Co-Author*) Nothing to Disclose Jin-Young Choi, Seoul, Korea, Republic Of (*Abstract Co-Author*) Nothing to Disclose Mi-Suk Park, MD, Seoul, Korea, Republic Of (*Abstract Co-Author*) Nothing to Disclose Myeong-Jin Kim, MD, PhD, Seoul, Korea, Republic Of (*Abstract Co-Author*) Nothing to Disclose

For information about this presentation, contact:

YELV@yuhs.ac

PURPOSE

To determine whether upgrading LR-4 lesion to LR-5 using ancillary features (AF) favoring HCC in LI-RADS version 2018 increases the diagnostic performance of HCC.

METHOD AND MATERIALS

112 patients with chronic B-, C- viral hepatitis or cirrhosis and surgically proven primary hepatic malignancy (98 HCC, 11 cHCC-CCC, 2 IHCC, 1 dysplastic nodule) were evaluated with gadoxetate-enhanced MRI in 2013. Two board-certified radiologists retrospectively assessed the presence of major features of HCC, imaging features of LR-M criteria, and HCC favoring ancillary features according to LI-RADS v2018 and assigned an LI-RADS category for each nodule in consensus. The diagnostic accuracy of each LI-RADS category was described by sensitivity, specificity and positive and negative predictive values with 95% confidence

interval. LR-4 lesions were then upgraded to LR-5 if (1) at least one HCC favoring AF was present and (2) lesion was not previously upgrade from LR-3 to LR-4. Diagnostic accuracy of this upgraded LR-5 was compared to initial LR-5 using McNemar X2-test. 5-year overall survival (OS) was evaluated via Kaplan-Meier method, log rank test and Cox proportional hazard model.

RESULTS

All three out of three LR-3 lesions, 18 (85%) out of 21 LR-4 lesions, 70 (98%) out of 71 LR-5 lesions and 7 (41%) out of 17 LR-M lesions were HCCs. As for non-HCC malignancy, except for 3 (27%) out of 11 cHCC-CCCs and 1 dysplastic nodule, all non-HCC malignancy were assigned as LR-M. 9 (42%) out of 21 initial LR-4 lesions were upgraded to LR-5 due to more than one HCC favoring AF. For HCC, initial LR-5 showed sensitivity and specificity of 71.4% and 92.8%, while HCC favoring AF-upgraded LR-5 showed sensitivity and specificity of r9.6% and 85.7%. Accuracy of upgraded LR-5 was 80.4% compared to 74.1% of initial LR-5. In McNemar X2-test, specificity of initial LR-5 was not significantly different from specificity of upgraded LR5 (P=0.317).

CONCLUSION

Upgrading LR-4 lesions to LR-5 increases accuracy without significantly decreasing HCC specificity; thus HCC favoring AF can be used to upgrade LR-4 to LR-5.

CLINICAL RELEVANCE/APPLICATION

Contrary to LI-RADS v2018, HCC favoring ancillary features should be used to upgrade LR-4 lesions to LR-5 because it increases accuracy of HCC without significantly decreasing HCC specificity.

SSA07-04 Assessing Accuracy of the LI-RADS v2017 Treatment Response Algorithm in Evaluating Ablated Hepatocellular Carcinoma

Sunday, Dec. 1 11:15AM - 11:25AM Room: S103AB

Participants

Mohammad Chaudhry, MBBS, Durham, NC (*Presenter*) Nothing to Disclose Katrina A. McGinty, MD, Chapel Hill, NC (*Abstract Co-Author*) Nothing to Disclose Benjamin Mervak, MD, Chapel Hill, NC (*Abstract Co-Author*) Nothing to Disclose Erin Shropshire, MD, Durham, NC (*Abstract Co-Author*) Nothing to Disclose James S. Ronald, MD, PhD, Durham, NC (*Abstract Co-Author*) Nothing to Disclose Leah Commander, Chapel Hill, NC (*Abstract Co-Author*) Nothing to Disclose Johann Hertel, MD, Chapel Hill, NC (*Abstract Co-Author*) Nothing to Disclose Reginald Lerebours, MA, Durham, NC (*Abstract Co-Author*) Nothing to Disclose Cai Li, PhD, Durham, NC (*Abstract Co-Author*) Nothing to Disclose Sheng Luo, PhD, Durham, NC (*Abstract Co-Author*) Nothing to Disclose Mustafa R. Bashir, MD, Cary, NC (*Abstract Co-Author*) Nothing to Disclose Grant, Pinnacle Clinical Research; Research Grant, ProSciento Inc; Research Consultant, RadMD Lauren M. Burke, MD, Chapel Hill, NC (*Abstract Co-Author*) Nothing to Disclose

For information about this presentation, contact:

mohammad.b.waseem@gmail.com

PURPOSE

To assess the performance of the LI-RADS v2017 Treatment Response Algorithm (TRA) in identifying viability of ablated hepatocellular carcinoma (HCC).

METHOD AND MATERIALS

This was an Institutional Review Board approved and HIPAA compliant retrospective study. Patients who underwent ablation of HCC prior to liver transplantation between January 1, 2011, and December 31, 2015, at a single tertiary care center were identified. All patients underwent pretreatment abdominal MRI within 90 days of treatment and post-treatment MRI within 90 days of transplant. Based on transplant histopathology colocalized with imaging, lesions were categorized as completely (100%) or incompletely (<=99%) necrotic. Three radiologists classified each nodule into an LR-TR category (Viable/Non-Viable) according to imaging features. Final LR-TR categories were compared with histopathology and the correlation was calculated. Inter-reader agreement was assessed using Fleiss' Kappa.

RESULTS

36 patients with 53 lesions were included. 58% (31/53) of lesions were ablated using microwave ablation, and the remaining 42% (22/53) with radiofrequency ablation. TRA accuracy for predicting complete tumor necrosis at the time of transplant ranged from 0.75-0.78, with a negative predictive value ranging from 0.77-0.80. Accuracy for predicting incomplete tumor necrosis at the time of transplant ranged from 0.61-0.78, with a positive predictive value ranging from 0.68-0.89. 11% (6/53) of treated lesions were LR-TR Equivocal by consensus, with most (5/6) incompletely necrotic on histopathology. Inter-reader agreement for pre-treatment LI-RADS category was k=0.44 (95% CI 0.16-0.62), lower than agreement for TRA category, k=0.68 (95% CI 0.57-0.78).

CONCLUSION

The TRA is accurate in predicting viable or non-viable HCC after ablation. Of the ablated lesions rated as LR-TR Equivocal, many were incompletely necrotic nodules.

CLINICAL RELEVANCE/APPLICATION

The LI-RADS TRA's performance for predicting histopathological necrosis in HCC lesions following locoregional therapy has not been extensively assessed, and in this work is shown to be accurate.

SSA07-05 Ancillary Features in LI-RADS Version 2018: A Strategy to Improve Diagnostic Performance for HCC on Gadoxetate Disodium-enhanced MRI

Participants Ji Hun Kang, Seoul, Korea, Republic Of (*Presenter*) Nothing to Disclose Sang Hyun Choi, Seoul, Korea, Republic Of (*Abstract Co-Author*) Nothing to Disclose Jae Ho Byun, MD, Seoul, Korea, Republic Of (*Abstract Co-Author*) Nothing to Disclose Dong Hwan Kim, MD, Seoul, Korea, Republic Of (*Abstract Co-Author*) Nothing to Disclose So Jung Lee, Seoul, Korea, Republic Of (*Abstract Co-Author*) Nothing to Disclose So Yeon Kim, MD, Seoul, Korea, Republic Of (*Abstract Co-Author*) Nothing to Disclose Hyung Jin Won, MD, Seoul, Korea, Republic Of (*Abstract Co-Author*) Nothing to Disclose Yong Moon Shin, Seoul, Korea, Republic Of (*Abstract Co-Author*) Nothing to Disclose Pyo Nyun Kim, MD, Seoul, Korea, Republic Of (*Abstract Co-Author*) Nothing to Disclose

For information about this presentation, contact:

jhbyun@amc.seoul.kr

PURPOSE

To determine the frequency of occurrence and strength of association with hepatocellular carcinoma (HCC) of each ancillary feature (AF) in the Liver Imaging Reporting and Data System (LI-RADS) version 2018, and to develop an appropriate strategy for applying the AFs to improve diagnostic performance on gadoxetate disodium-enhanced MRI.

METHOD AND MATERIALS

A total of 385 nodules (283 HCCs, 18 non-HCC malignancies, 84 benign nodules) of 3.0 cm or smaller in 266 patients at risk for HCC who underwent gadoxetate disodium-enhanced MRI in 2016 were retrospectively evaluated. Two radiologists independently assigned a LI-RADS category to each nodule. The frequency and diagnostic odds ratio of each AF were assessed. To improve the diagnostic performance for HCC, various criteria were developed based on the number of AFs detected favoring malignancy in general or HCC in particular. Generalized estimating equation models were used to compare the diagnostic performance of each criterion with that of the major features (MFs) only.

RESULTS

The AFs showing a significantly different frequency between HCC and non-HCC lesions were restricted diffusion, mild-moderate T2 hyperintensity, transitional-phase hypointensity, hepatobiliary-phase hypointensity, and hepatobiliary-phase isointensity. Of these AFs, hepatobiliary-phase hypointensity had the highest frequency and strongest association with HCC. When we applied AFs in addition to MFs, the new criterion (with a number of AFs >=4) had significantly higher sensitivity (80.6% vs. 70.0%; P<.001) than MFs only, without a significant lowering of specificity (85.3% vs. 90.2%; P=.060).

CONCLUSION

The AFs varied in the frequencies of occurrence and strengths of association with HCC. To improve the diagnostic performance for HCC, a new criterion of four or more AFs in addition to the MFs might be the best option.

CLINICAL RELEVANCE/APPLICATION

A criterion of four or more AFs in addition to MFs may be the best strategy to improve the diagnostic performance for HCC on gadoxetate disodium-enhanced MRI using LI-RADS, and is recommended in the evaluation of suspected HCC in patients at risk.

SSA07-06 LI-RADS v2018: Value of Quantitative Assessment of Arterial Phase Hyperenhancement and Washout with Extracellular MRI Contrast Agent

Sunday, Dec. 1 11:35AM - 11:45AM Room: S103AB

Participants

Daniel Stocker, MD, Zurich, Switzerland (*Presenter*) Nothing to Disclose Anton S. Becker, MD,PhD, New York, NY (*Abstract Co-Author*) Nothing to Disclose Borna Barth, Zurich, Switzerland (*Abstract Co-Author*) Nothing to Disclose Stephan M. Skawran, MD, Zurich, Switzerland (*Abstract Co-Author*) Nothing to Disclose Malwina Kaniewska, MD, Baden, Switzerland (*Abstract Co-Author*) Nothing to Disclose Michael A. Fischer, MD, Zurich, Switzerland (*Abstract Co-Author*) Nothing to Disclose Olivio Donati, MD, Zurich, Switzerland (*Abstract Co-Author*) Nothing to Disclose Caecilia S. Reiner, MD, Durham, NC (*Abstract Co-Author*) Nothing to Disclose

For information about this presentation, contact:

daniel.stocker@usz.ch

PURPOSE

To assess the influence of quantitative arterial phase hyperenhancement (APHE) and washout (WO) of contrast enhanced MRI on LI-RADS v2018 categorization and compare the quantitative LI-RADS score with conventional qualitative reading.

METHOD AND MATERIALS

60 patients (19 female; mean age 56y) at risk for HCC with 71 liver lesions (28 hepatocellular carcinoma (HCC), 43 benign lesions) who underwent MRI with extracellular contrast agent were included in this HIPPA-compliant retrospective study. Four blinded radiologists independently reviewed all MRI and assigned a LI-RADS score per lesion. Two other radiologists drew regions of interests within the lesion and the adjacent liver parenchyma on pre- and post-contrast MR images. The percentage of arterial enhancement and the liver-to-lesion contrast ratio were calculated for quantification of APHE and WO. The presence or absence of APHE, WO or both was recorded according to the quantitative measurements. Using these quantitative parameters, a quantitative LI-RADS score was assigned in lesions classified as LR-3-5. The diagnostic accuracy was assessed with receiver-operating-characteristics (ROC) analysis and the DeLong test to compare for significant differences between the area under the curve (AUC).

RESULTS

The ROC analysis for the qualitative LI-RADS score showed an AUC of 0.869, 0.946, 0.940 and 0.919 for reader 1, 2, 3, and 4,

respectively. The quantitative LI-RADS score where only APHE/WO/or both were replaced showed an AUC of 0.875/0.849/0.874, 0.942/0.924/0.914, 0.933/0.917/0.878 and 0.902/0.852/0.843 for readers 1, 2, 3 and 4, respectively. The AUC of the quantitative LI-RADS score was significantly lower than of the qualitative score only for reader 4 when quantitative WO (p=0.012) and both, quantitative APHE and WO (p=0.047) were used.

CONCLUSION

The qualitative LI-RADS score showed similar or higher diagnostic accuracy compared to the quantitative LI-RADS score. Therefore, qualitative visual assessment appears to be the better approach to scoring liver lesions according to LI-RADS v2018.

CLINICAL RELEVANCE/APPLICATION

A quantitative approach for LI-RADS scoring does not increase diagnostic accuracy; hence, visual assessment should be maintained to score liver lesions according to LI-RADS v2018.

SSA07-07 Hepatocellular Carcinoma Detection by Abbreviated-Protocol Dynamic Contrast-enhanced MRI in Patients with Cirrhosis Using LI-RADS v2018

Sunday, Dec. 1 11:45AM - 11:55AM Room: S103AB

Participants

Takeshi Yokoo, MD, PhD, Dallas, TX (*Presenter*) Nothing to Disclose Lakshmi Ananthakrishnan, MD, Irving, TX (*Abstract Co-Author*) Nothing to Disclose Alberto Diaz de Leon, MD, Dallas, TX (*Abstract Co-Author*) Nothing to Disclose David T. Fetzer, MD, Dallas, TX (*Abstract Co-Author*) Researcher, Koninklijke Philips NV; Researcher, Siemens AG; Consultant, Koninklijke Philips NV; Speakers Bureau, Koninklijke Philips NV; Speakers Bureau, Siemens AG; ; John R. Leyendecker, MD, Dallas, TX (*Abstract Co-Author*) Nothing to Disclose Ivan Pedrosa, MD, Dallas, TX (*Abstract Co-Author*) Nothing to Disclose Gaurav Khatri, MD, Irving, TX (*Abstract Co-Author*) Nothing to Disclose

PURPOSE

Determine the accuracy of abbreviated-protocol dynamic contrast enhanced MRI and complete-protocol MRI for detection of hepatocellular carcinoma (HCC) in cirrhosis patients

METHOD AND MATERIALS

In this IRB-approved HIPAA-compliant retrospective cohort study, 100 consecutive cirrhosis patients underwent standard complete-protocol MRI (cMRI) at 1.5T or 3T for workup for suspected HCC, using extracellular gadolinium contrast. Images of abbreviated-protocol MRI (aMRI; coronal T2-weighted and axial dynamic contrast-enhanced T1-weighted sequences) were extracted from cMRI (aMRI sequences + unenhanced axial T2-, T1-, and diffusion-weighted sequences). Both aMRI and cMRI images were independently read by 4 blinded fellowship-trained abdominal radiologists using Liver Imaging and Reporting Data System (LI-RADS) v2018. Each review (aMRI, cMRI) was scored as positive if any liver observation of LR-4, 5, or M was present, or negative otherwise. Each patient was followed from the time of index cMRI until final HCC status was determined using a composite reference standard of histopathlogy <=6 months, consensus expert panel review of index cMRI or followup-CT/MRI <=6 months (by two different senior abdominal radiologists), and clinic followup at >12 months (in those with negative index cMRI only). Patient-level HCC detection sensitivity and specificity were calculated for aMRI and cMRI with 95% confidence intervals, and compared by McNemar's test at a=0.05.

RESULTS

Mean age of the study cohort was 57.7 years (range 23-77). 14 patients were excluded due to non-diagnostic exam (5), prior HCC treatment (1), use of hepatobiliary contrast agent (1), loss to followup (3), and unable to determine final HCC diagnosis (4). Perreader detection accuracy of aMRI and cMRI in remaining 86 cirrhosis patients are shown in Figure. No statistically significant differences were found by McNemar's test (p>0.05) between aMRI and cMRI, in sensitivity or specificity.

CONCLUSION

Abbreviated-protocol dynamic contrast enhanced MRI has sensitivity 89.3-96.4% and specificity 84.5-89.7% for HCC detection; no statistically significant difference was found compared to complete-protocol MRI. Further validation is needed in an asymptomatic cirrhosis population to support its use as a screening test.

CLINICAL RELEVANCE/APPLICATION

Abbreviated-protocol dynamic contrast enhanced MRI (a 15-min exam) offers high sensitivity and specificity for hepatocellular carcinoma (HCC) detection and has a potential as a screening test in cirrhosis patients at risk for HCC.

SSA07-08 Inter-reader Reproducibility and Overall Survival Predictability of LI-RADS Tumor Response Algorithm after Drug-eluting-Beads Transarterial Chemoembolization as an Initial Treatment Hepatocellular Carcinoma

Sunday, Dec. 1 11:55AM - 12:05PM Room: S103AB

Participants

Ali Pirasteh, MD, Dallas, TX (*Abstract Co-Author*) Nothing to Disclose Endel A. Sorra II, MD, Dallas, TX (*Abstract Co-Author*) Nothing to Disclose Hector J. Marquez, MD, Dallas, TX (*Abstract Co-Author*) Nothing to Disclose Robert C. Sibley III, MD, Irving, TX (*Abstract Co-Author*) Nothing to Disclose Takeshi Yokoo, MD, PhD, Dallas, TX (*Presenter*) Nothing to Disclose

PURPOSE

LI-RADS (Liver Imaging and Reporting Data System) Tumor Response (LR-TR) algorithm standardizes the assessment of tumor response to locoregional therapy in hepatocellular carcinoma (HCC). This study evaluated the inter-reader reproducibility of LR-TR categories (nonviable, equivocal, viable), and whether LR-TR categories predict survival in patients with HCC after first-time drugeluting-beads transarterial chemoembolization (DEB-TACE).

METHOD AND MATERIALS

All DEB-TACE procedures from 2011 to 2015 at two hospitals affiliated with a liver transplant center were reviewed. Key exclusion criteria were prior HCC-related treatment and lack of pre- and post-treatment multiphasic abdominal MRI or CT within 3 months of DEB-TACE. Four readers (2 radiology residents and 2 fellowship-trained abdominal radiologists) independently reviewed the pre- and post-treatment exams, assigned LR-TR categories to up to two treated tumors per patient, and measured the size of the pre-treatment and the enhancing component of the treated tumor. Inter-reader agreement for LR-TR categories and tumor size were respectively assessed by Fleiss' kappa and intra-class correlation coefficient (ICC). Kaplan-Meier/Cox survival analysis for patient-level LR-TR category (the mode of all lesion LR-TR categories by all readers in a patient) was performed, before and after adjusting for Barcelona Clinic for Liver Cancer stage (BCLC A vs. >=B) and Child-Pugh-Turcott class (CPT A vs. >=B).

RESULTS

75 patients were included, yielding 108 lesions. Inter-reader agreement was moderate for the three LR-TR categories (κ =0.56 [0.55,0.58]). Inter-reader reproducibility for tumor size was excellent for untreated tumors (ICC=0.94 [0.92,0.95]) and good for treated tumors (ICC=0.83 [0.78,0.87]). No significant difference was detected in overall survival between LR-TR nonviable and viable groups (Fig. 1) before or after adjustment for BCLC stage/CPT class, respectively p=0.96 and 0.78.

CONCLUSION

LI-RADS tumor response algorithm for HCC after first-time DEB-TACE has moderate inter-reader reproducibility but may not predict overall survival. Further reader education/training is needed to improve reproducibility. Further research is needed to better translate LR-TR assessment to predict patient survival/guide therapy.

CLINICAL RELEVANCE/APPLICATION

LI-RADS tumor response algorithm for HCC requires reader education and may not predict survival in patients undergoing first-time DEB-TACE.

SSA07-09 Clinical Validation of CEUS LI-RADS in Prospective Multi-Center Study: Preliminary Results

Sunday, Dec. 1 12:05PM - 12:15PM Room: S103AB

Participants

Andrej Lyshchik, MD, PhD, Philadelphia, PA (*Presenter*) Research support, Bracco Group; Advisory Board, Bracco Group; Research support, General Electric Company; Research support, Siemens AG; Research support, Canon Medical Systems Corporation; Speaker, SonoScape Co, Ltd

Yuko Kono, MD, PhD, San Diego, CA (*Abstract Co-Author*) Equipment support, Canon Medical Systems Corporation Equipment support, General Electric Company Contrast agent support, Lantheus Medical Imaging, Inc Contrast agent support, Bracco Group Fabio Piscaglia, Bologna, Italy (*Abstract Co-Author*) Research support, Esaote SpA; Speaker, Bayer AG; Speaker, Bracco Group; Speaker, Bristol-Myers Squibb Company; Speaker, Eisai Co, Ltd; Advisory Board, AstraZeneca PLC; Advisory Board, Bayer AG; Advisory Board, Eisai Co, Ltd; Advisory Board, General Electric Company; Advisory Board, Siemens AG; Advisory Board, Tiziana Life Sciences;

Shuchi K. Rodgers, MD, Philadelphia, PA (Abstract Co-Author) Nothing to Disclose

Geoffrey E. Wile, MD, Nashville, TN (Abstract Co-Author) Nothing to Disclose

Aya Kamaya, MD, Stanford, CA (*Abstract Co-Author*) Royalties, Reed Elsevier; Researcher, Koninklijke Philips NV; Researcher, Siemens AG

Alexandra Medellin, MD, Calgary, AB (Abstract Co-Author) Nothing to Disclose

Lisa Finch, Seattle, WA (Abstract Co-Author) Nothing to Disclose

Stephanie R. Wilson, MD, Calgary, AB (*Abstract Co-Author*) Equipment support, Koninklijke Philips NV; Equipment support, Siemens AG; Equipment support, Samsung Electronics Co, Ltd; Research support, LANDAUER, Inc; Research support, Samsung Electronics Co, Ltd; Speakers Bureau, Koninklijke Philips NV

PURPOSE

The American College of Radiology Contrast-Enhanced Ultrasound Liver Imaging Reporting and Data System (CEUS LI-RADS) is developed to classify focal liver observations in patients at risk of HCC. The aim of this prospective multicenter study is to validate the CEUS LI-RADS.

METHOD AND MATERIALS

A total of 273 nodules from 255 patients at risk of HCC are included in this ongoing study conducted at 8 centers (6 in the USA, 1 in Canada and 1 in Italy). Focal liver observations are classified as LR-5, (definitely HCC) if greater than 1 cm with arterial phase hyperenhancement, and late, mild washout. Rim enhancement and/or early washout and/or marked washout qualify as LR-M (malignant, but not specific for HCC). Other observations are classified as definitely benign (LR-1); probably benign (LR-2), intermediate malignancy probability (LR-3); probably HCC (LR-4). Tumor-in-Vein is characterized as LR-TIV. Definite HCC diagnosis on MRI, imaging follow-up or histology for MRI-indeterminate observations were used as reference standard.

RESULTS

The median focal liver observation size is 2.4cm. Of 273 nodules, 162 (59%) have confirmed diagnosis while 111 (41%) nodules remain indeterminate, currently undergoing imaging surveillance or awaiting histological confirmation. Of 162 confirmed nodules, 136 are HCC (82%), 6 (4%) other malignancies (2 ICC, 1 combined hepatocellular-cholangiocarcinoma, 3 metastasis) and 22 (14%) are benign. A total of 84 confirmed observations are characterized as LR-5 and 100% of them are HCC. The sensitivity of LR-5 for HCC is 63%. All 14 LR-1 and LR-2 observations are benign. All 11 LR-M observations are malignant (5 HCC, 4 metastasis, 2 ICC). 67% (14/21) of LR-3 observations and 92% (24/26) of LR-4 observations are HCC. 5% of nodules are not characterized on CEUS (LR-NC)

CONCLUSION

The CEUS LR-5 classification is 100% specific for HCC, confirming high clinical value of CEUS for noninvasive HCC diagnosis.

CLINICAL RELEVANCE/APPLICATION

Contrast-enhanced ultrasound is a reliable method of focal liver observations classification in patients at risk for HCC







SSA08

Gastrointestinal (Radiomics)

Sunday, Dec. 1 10:45AM - 12:15PM Room: S104A



AMA PRA Category 1 Credits ™: 1.50 ARRT Category A+ Credit: 1.75

Participants

Bachir Taouli, MD, New York, NY (*Moderator*) Research Grant, Bayer AG Aliya Qayyum, MD, MBBS, Houston, TX (*Moderator*) Nothing to Disclose Achille Mileto, MD, Seattle, WA (*Moderator*) Research support, General Electric Company;

For information about this presentation, contact:

aqayyum@mdanderson.org

Sub-Events

SSA08-01 MRI Radiomics Features Predict Immuno-oncological Characteristics and Recurrence of Hepatocellular Carcinoma

Sunday, Dec. 1 10:45AM - 10:55AM Room: S104A

Participants

Stefanie Hectors, PhD, New York, NY (Presenter) Nothing to Disclose Sara Lewis, MD, New York, NY (Abstract Co-Author) Nothing to Disclose Cecilia Besa, MD, Santiago, Chile (Abstract Co-Author) Nothing to Disclose Michael J. King, MD, New York, NY (Abstract Co-Author) Nothing to Disclose Daniela Said, MD, New York, NY (Abstract Co-Author) Nothing to Disclose Juan Putra, New York, NY (Abstract Co-Author) Nothing to Disclose Stephen Ward, MD, New York, NY (Abstract Co-Author) Nothing to Disclose Takaaki Higashi, New York, NY (Abstract Co-Author) Nothing to Disclose Swan Thung, New York, NY (Abstract Co-Author) Nothing to Disclose Shen Yao, New York, NY (Abstract Co-Author) Nothing to Disclose Ilaria Laface, New York, NY (Abstract Co-Author) Nothing to Disclose Myron Schwartz, New York, NY (Abstract Co-Author) Advisory Board, Bayer AG Advisory Board, Onyx Pharmaceuticals, Inc Sacha Gnjatic, New York, NY (Abstract Co-Author) Nothing to Disclose Miriam Merad, New York, NY (Abstract Co-Author) Nothing to Disclose Yujin Hoshida, New York, NY (Abstract Co-Author) Nothing to Disclose Bachir Taouli, MD, New York, NY (Abstract Co-Author) Research Grant, Bayer AG

PURPOSE

To assess the value of qualitative and quantitative radiomics features measured with MRI for noninvasive prediction of histopathologic and genomics characteristics, as well as outcomes of hepatocellular carcinoma (HCC).

METHOD AND MATERIALS

This retrospective study was IRB-approved and the requirement of informed consent was waived. Forty-eight patients with HCC (M/F 35/13, mean age 60y) who underwent hepatic resection or transplant within 4 months of abdominal MRI were included. Qualitative imaging traits, quantitative non-texture related and texture features were assessed in index lesions on contrast-enhanced T1-weighted and diffusion-weighted images. Advanced histopathological analysis was performed using multiplex immunohistochemistry. Gene expression analysis was performed on paraffin-embedded tissue blocks of the index HCC lesions. The association of imaging features with histopathologic and genomics features was assessed using binary logistic regression analysis was also employed to analyze the association of radiomics, histopathologic and genomics features with radiological recurrence of HCC at 12 months.

RESULTS

Qualitative (correlation coefficient r=-0.41-0.40, P<0.042) and quantitative (r=-0.52-0.45, P<0.049) radiomics features correlated with immunohistochemical cell type markers for T-cells (CD3), macrophages (CD68), and endothelial cells (CD31). MRI radiomics features also correlated with expression of immunotherapy targets PD-L1 at protein level (r=0.41-0.47, P<0.029) as well as PD1 and CTLA4 at mRNA expression level (r=-0.48-0.47, P<0.037). Follow-up imaging data up to at least 1 year after surgery was available for 43 patients, of whom 10 patients showed HCC recurrence within 1 year after surgery. Several radiomics features showed significant association with HCC recurrence (highest AUC =0.80, odds ratio=5.51, P<0.028), while histopathologic and genomics features did not (P>0.098).

CONCLUSION

We observed significant associations of MRI radiomics features with HCC histopathological and genomics characteristics and recurrence. We are currently validating these results in a prospective study.

Our results suggest that MRI radiomics features may serve as noninvasive predictors of HCC biological properties and recurrence, providing potentially valuable information for treatment planning.

SSA08-02 Multi-Institutional Study using Radiomics and Machine Learning Model to Differentiate Benign and Malignant Focal Hepatic Lesions on Dual-Energy CT

Sunday, Dec. 1 10:55AM - 11:05AM Room: S104A

Participants

Ramandeep Singh, MBBS, Boston, MA (Presenter) Nothing to Disclose Dinesh Manoharan, MD, MBBS, Chennai, India (Abstract Co-Author) Nothing to Disclose Sanjay Sharma, MD, FRCR, New Delhi, India (Abstract Co-Author) Nothing to Disclose Madhusudhan Kumble Seetharama, MD, FRCR, New Delhi, India (Abstract Co-Author) Nothing to Disclose Arjunlokesh Netaji, MBBS, New Delhi, India (Abstract Co-Author) Nothing to Disclose Mannudeep K. Kalra, MD, Lexington, MA (Abstract Co-Author) Research Grant, Siemens AG; Research Grant, Riverain Technologies, IIC: Subba R. Digumarthy, MD, Boston, MA (Abstract Co-Author) Researcher, Siemens AG; Contract, Merck & Co, Inc; Contract, Pfizer Inc; Contract, Bristol-Myers Squibb Company; Contract, Novartis AG; Contract, F. Hoffmann-La Roche Ltd; Contract, Polaris; Contract, Cascadian; Contract, AbbVie Inc; Contract, Consulting Medical Associates, Inc; Contract, Bayer AG; Contract, Zai Laboratries; ; Fatemeh Homayounieh, MD, Boston, MA (Abstract Co-Author) Nothing to Disclose Felix Lades, Forchheim, Germany (Abstract Co-Author) Employee, Siemens AG Martin U. Sedlmair, MS, Forchheim, Germany (Abstract Co-Author) Employee, Siemens AG Sanjay Saini, MD, Boston, MA (Abstract Co-Author) Nothing to Disclose PURPOSE

To assess the application of a machine learning (ML) model-based approach for differentiating benign and malignant focal hepatic lesions on post-contrast dual energy CT (DECT) using tumor analysis and radiomics prototypes (eXamine, Siemens Healthineers).

METHOD AND MATERIALS

Our included 174 adults from the US (Site-A: 103, 65 ± 15 years, 53M:50F) and India (Site-B=71, 48 ± 17 years, 46M:25F) with benign (Site-A=60;Site-B=35) or malignant (Site-A=43;SiteB=36) focal hepatic lesions on post-contrast dual source, DECT (Site-A: Siemens Force or Flash; Site-B: Siemens Flash). Most malignant lesions had histology; benign lesions had characteristic imaging features or were stable on follow-up CT. Low and high kV images in arterial phase (2-3mm) were de-identified, exported, and processed with the TA prototype to derive iodine concentrations and uptakes as well as 585 radiomic features within each lesion's volume and rim. ML model based statistical evaluation (Site-A: Training; Site-B: Test) was performed with the radiomics prototype. Random Forest Classifier was used to calculate the accuracy (AUC) for differentiating benign and malignant hepatic lesions.

RESULTS

Multivariate logistic regression demonstrated that 31 radiomic features enabled distinction between benign and malignant lesions (AUC 0.7-0.8; p=0.0002-0.03; gldm, glszm, glrlm, glszm, first order-kurtosis). With ML model based random forest classifier 12 inner rim radiomic features enabled lesion characterization (AUC=0.82, p<0.0001) with high specificity (97%) and positive predictive value (94%). Only 1/35 benign (flash-filling hemangioma) lesions was classified as malignant lesion (false positive). Compared to radiomics, accuracy was lower for normalized and total iodine uptake (AUC= 0.7; p-0.003; outer lesion rim).

CONCLUSION

With a ML model, the DECT based tumor analysis and radiomics prototypes enable accurate differentiation of benign and malignant hepatic lesions.

CLINICAL RELEVANCE/APPLICATION

Trained ML based predictive models can be generated and integrated with clinical workflow to characterize and classify focal hepatic lesions seen on dual-energy CT.

SSA08-03 Application of Radiomic MRI Features in Differentiation of Combined Hepatocellular Cholangiocarcinoma, Cholangiocarcinoma, and Hepatocellular Carcinoma Using Machine Learning

```
Sunday, Dec. 1 11:05AM - 11:15AM Room: S104A
```

Participants

Xiaoyang Liu, MD, PhD, Toronto , ON (*Presenter*) Nothing to Disclose Farzad Khalvati, PhD,MSc, Toronto, ON (*Abstract Co-Author*) Nothing to Disclose Khashayar Namdar, MSc,MENG, Toronto, ON (*Abstract Co-Author*) Nothing to Disclose Sandra Fischer, MD, Toronto, ON (*Abstract Co-Author*) Nothing to Disclose Masoom A. Haider, MD, Toronto, ON (*Abstract Co-Author*) Nothing to Disclose Kartik S. Jhaveri, MD, Mississauga, ON (*Abstract Co-Author*) Nething to Disclose Sander, Siemens AG; Speaker, Bayer AG Sara Lewis, MD, New York, NY (*Abstract Co-Author*) Nothing to Disclose Bachir Taouli, MD, New York, NY (*Abstract Co-Author*) Research Grant, Bayer AG

PURPOSE

Definitive morphological imaging features of combined hepatocellular-cholangiocarcinoma (cHCC-CC) have not been established. We aim to use radiomic features to predict diagnosis of cHCC-CC, cholangiocarcinoma (CC) and hepatocellular carcinoma (HCC) with machine learning.

METHOD AND MATERIALS

We conducted a retrospective review of pre-treatment gadolinium or gadoxetate disodium enhanced liver MRI performed between 2004 and 2018 in our institute for 86 patients with pathology proven cHCC-CC (n=38), CC (n=24) and HCC (n=24). Precontrast, arterial, portal venous, hepatic venous and 5 minutes delayed phases were included. Regions of interest (ROIs) were drawn around

the largest diameter of the tumors, avoiding nearby normal tissues. 1370 radiomic features were extracted by standard library (PyRadiomics 2.1.2). Using Principle Component Analysis, they were fused to 20 first principle components that explain the majority of variance. These components were used in a 4-fold cross-validation by a Support Vector Machine (SVM) classifier to evaluate the performance of the predictive model for each MRI sequence using pathology diagnosis as endpoints.

RESULTS

We tested two endpoints predictions: 1. cHCC-CC vs. non cHCC-CC with the expectation of differentiating cHCC-CC from HCC and CC, given its unique pathology; 2. HCC vs. non HCC, due to the difference in management. For differentiation of cHCC-CC from HCC and CC, fused radiomic features from hepatic venous and precontrast phases demonstrated higher prediction value than other sequences, with AUC of 0.77 and 0.64 respectively. For the differentiation of HCC from cHCC-CC and CC, arterial, 5 min delayed, portal venous, and hepatic venous phases demonstrated highest prediction values, with AUC of 0.81, 0.80, 0.79, and 0.79 respectively.

CONCLUSION

cHCC-CC is a unique histological entity with treatment implications including liver transplantation due to poorer prognosis than either HCC or CC. Our results demonstrated fused MRI radiomic features in hepatic venous and precontrast phases are promising in differentiating cHCC-CC from HCC and CC. MRI of arterial and 5 min delayed phases have good predictive value to differentiate cHCC-CC and CC from HCC.

CLINICAL RELEVANCE/APPLICATION

The promising predicative value of radiomic MRI features in the differentiation of cHCC-CC, HCC and CC will help with improved preoperative imaging diagnosis and treatment planning including liver transplantation.

SSA08-04 A Radiomics Model Based on Preoperative Gadoxetic Acid-Enhanced MR Imaging for Predicting Liver Failure after Major Hepatectomy

Sunday, Dec. 1 11:15AM - 11:25AM Room: S104A

Participants

Wangshu Zhu, Guangzhou, China (*Presenter*) Nothing to Disclose Siya Shi, Guangzhou, China (*Abstract Co-Author*) Nothing to Disclose Zehong Yang, Guangzhou, China (*Abstract Co-Author*) Nothing to Disclose Chao Song, Guangzhou, China (*Abstract Co-Author*) Nothing to Disclose Jun Shen, MD, Guagnzhou, China (*Abstract Co-Author*) Nothing to Disclose

For information about this presentation, contact:

zhuwsh5@mail2.sysu.edu.cn

PURPOSE

The clinical indexes are not sufficiently accurate in predicting the outcome of remnant liver function after surgery. The purpose of this study was to determine a radiomics model based on preoperative gadoxetic acid-enhanced MR imaging for predicting liver failure (LF) after major hepatectomy in cirrhotic patients with hepatocellular carcinoma (HCC).

METHOD AND MATERIALS

For this retrospective study, a radiomics-based model was developed based on 101 patients with HCC, with major liver resection between June 2012 and June 2018. Radiomic features were obtained from hepatobiliary phase of gadoxetic acid-enhanced MR images. The radiomics signature was built by using the least absolute shrinkage and selection operator method and multivariable logistic regression model was adopted to establish a radiomics nomogram. Nomogram performance for predicting liver failure was determined using its receiver operating characteristics curve, calibration curve and decision curve.

RESULTS

The radiomics signature, with radiomics score calculated consisting of 5 radiomics features, achieved favorable performance for predicting LF. The radiomics nomogram, which incorporated the radiomics signature and indocyanine green clearance rate at 15 minutes (ICG-R15), showed the highest performance for predicting liver failure (area under the curve [AUC], 0.894; 95% confidence intervals [CI], 0.823-0.964). The integrated discrimination improvement (IDI) analysis showed a significant improvement in the accuracy of LF prediction, especially when radiomics signature was added to the clinical prediction model (IDI = 0.117, P = 0.002).

CONCLUSION

A radiomics-based model of preoperative gadoxetic acid-enhanced MR images can be used for liver failure in cirrhotic patients with HCC after major liver resection.

CLINICAL RELEVANCE/APPLICATION

A radiomics-based model in predicting liver failure after major hepatectomy

SSA08-05 Radiomic Analysis for Preoperative T-Staging in Patients with Rectal Cancer

Sunday, Dec. 1 11:25AM - 11:35AM Room: S104A

Participants

Wei Lu, Ningbo, China (*Presenter*) Nothing to Disclose Pengfei Yang, Hangzhou, China (*Abstract Co-Author*) Nothing to Disclose Hailan Zheng, Taizhou, China (*Abstract Co-Author*) Nothing to Disclose Jihong Sun, MD, PhD, Hangzhou, China (*Abstract Co-Author*) Nothing to Disclose Tianye Niu, PhD, Hangzhou, China (*Abstract Co-Author*) Nothing to Disclose Yinhua Jin, Ningbo, China (*Abstract Co-Author*) Nothing to Disclose

For information about this presentation, contact:

PURPOSE

The accurate preoperative assessment of tumor stage is critical for treatment and prognosis of rectal cancer. This study was aimed at constructing a radiomic prediction model to preoperatively assess the primary tumor (T) stage accurately in patients with rectal cancer.

METHOD AND MATERIALS

The magnetic resonance imaging (MRI) data of 349 patients with rectal cancer were collected from February 2011 to October 2017 in this study (T1, n=49; T2, n=79; T3, n=157; T4, n=64). The patients were divided randomly into training cohort (n=240) and validation cohort (n=109). The radiomic features were extracted from high-resolution T2-weighted imaging (HR-T2WI) and diffusion-weighted imaging (DWI) data, then selected to compose radiomic signatures. Incorporating the radiomic signatures and clinical independent risk factors, we constructed a radiomic assessment model by artificial neural network (ANN). The calibration, discrimination, and clinical utility of the radiomic models were assessed by independent validation.

RESULTS

The radiomic signature was significantly related to T stage of rectal cancer (p<0.01), and showed good preoperatively T-staging performance. The area under the curve (AUC) was 0.822, 0.733 and 0.779 in discriminating between early stages (T1 and T2 stage, T1/2) and advanced stages (T3 and T4 stage, T3/4), between T1 and T2 stages, and between T3 and T4 stages, respectively. Moreover, with combination of the raidomic signature and clinical independent risk factors, the raidiomic assessment models showed improved performance. The AUC was 0.858, 0.801 and 0.815 discriminating between T1/2 and T3/4 stages, between T1 and T2 stages, and between T3 and T4 stages, respectively. And the performance was confirmed in an independent validation cohort (AUC, 0.842, 0.773 and 0.730).

CONCLUSION

The radiomic model has an excellent performance in preoperative assessment of T stage of rectal cancer. It can improve the accuracy of T staging in patients with rectal cancer.

CLINICAL RELEVANCE/APPLICATION

The radiomic prediction model can improve the accuracy of T-staging assessment in patients with rectal cancer.

SSA08-06 Radiomics Signature on Multiparametric MRI: Association with Disease-free Survival in Patients with Locally Advanced Rectal Cancer

Sunday, Dec. 1 11:35AM - 11:45AM Room: S104A

Participants

Yanfen Cui, Taiyuan, China (*Presenter*) Nothing to Disclose Xiaotang Yang, Taiyuan, China (*Abstract Co-Author*) Nothing to Disclose

For information about this presentation, contact:

yanfen210@126.com

PURPOSE

To develop a radiomics signature based on pre-treatment multiparameter MRI features to estimate disease-free survival (DFS) in patients with locally advanced rectal cancer (LARC) after receiving neoadjuvant chemoradiotherapy (CRT) and to establish a radiomics nomogram incorporating the radiomics signature and clinicopathological findings.

METHOD AND MATERIALS

142 consecutive patients with LARC (training: validation cohorts = 71:71) were enrolled in our retrospective study. 1188 imaging features were extracted from pre-CRT T2WI, contrast enhanced T1WI, and ADC images for each patient. Least absolute shrinkage and selection operator (LASSO) Cox regression was performed to select key features and build a radiomics signature in the training set, and the cutoff point of the radiomics signature to divide the patients into high- and low-risk groups was determined using ROC curve analysis. Kaplan-Meier analysis was used to determine the association of the radiomics signature and DFS. Combining clinicopathological factors, a radiomics nomogram was constructed to validate the radiomic signatures for individualized DFS estimation. Nomogram discrimination and calibration were evaluated.

RESULTS

Higher Rad-scores were significantly associated with worse DFS in both the training and validation cohorts (both P< 0.05). The radiomics nomogram, incorporating the radiomics signature and ypN, tumor differentiation, and MRF, estimated DFS (C-index, 0.715; 95% confidence interval [CI], 0.67-0.79) better than the clinicopathological or Rad-score-only nomograms.

CONCLUSION

This study demonstrated that the radiomics signature is an independent biomarker for the estimation of DFS in patients with LARC. Combining the radiomics nomogram improved individualized DFS estimation.

CLINICAL RELEVANCE/APPLICATION

radiomics signature is an independent biomarker for the estimation of DFS in patients with LARC

SSA08-07 Reproducibility of Radiomics Features Using Single-Energy Dual-Source CT: Influence of Radiation Dose and CT Reconstruction Settings Within the Same Patient

Sunday, Dec. 1 11:45AM - 11:55AM Room: S104A

Participants

Federica Vernuccio, MD, Palermo, Italy (Abstract Co-Author) Nothing to Disclose

Rendon C. Nelson, MD, Durham, NC (Abstract Co-Author) Consultant, VoxelMetrix, LLC; Co-owner, VoxelMetrix, LLC; Advisory Board, Bracco Group; Advisory Board, Guerbet SA; Speakers Bureau, Bracco Group; Royalties, Wolters Kluwer nv

Juan Carlos Ramirez-Giraldo, PhD, Cary, NC (*Abstract Co-Author*) Employee, Siemens AG Justin B. Solomon, PhD, Durham, NC (*Abstract Co-Author*) License agreement, Sun Nuclear Corporation License agreement, 12 Sigma Technologies

Bhavik N. Patel, MD, Fremont, CA (*Abstract Co-Author*) Speakers Bureau, General Electric Company; Research Grant, General Electric Company

Ehsan Samei, PhD, Durham, NC (*Abstract Co-Author*) Research Grant, General Electric Company Research Grant, Siemens AG Advisory Board, medInt Holdings, LLC License agreement, 12 Sigma Technologies License agreement, Gammex, Inc Daniele Marin, MD, Durham, NC (*Abstract Co-Author*) Research support, Siemens AG

PURPOSE

To investigate the impact of radiation dose and reconstruction CT settings on the reproducibility of radiomic features within the same patient, as well as to identify correction factors for mitigating these sources of variability.

METHOD AND MATERIALS

This is a retrospective study of 78 patients (33 women [mean age, 61 years; age range, 28-74 years] and 55 men [mean age, 60 years; age range, 34-81 years] with 151 metastatic liver lesions who underwent a single-energy dual-source contrast-enhanced dose split staging CT. By using the imaging raw datasets technique parameters were altered, resulting in 28 different CT datasets per patient which included different dose level, section thickness, kernel and reconstruction algorithms settings. Using a training dataset, reproducible intensity, shape and texture RFs (r2>0.95) were selected and correction factors were calculated by using a linear model to convert each RF to its estimated value under the reference technique. Using a test dataset, reproducibility of hierarchical clustering based on RFs measured under different CT techniques was assessed.

RESULTS

The percentage of RFs deemed reproducible for any variation of the different technical parameters was 11% (12/106). RFs in the shape category were the least likely to be affected by variability due to changes in technical parameters (87.5% [14/16]). Of all technical parameters, reconstructed section thickness had the largest impact on the reproducibility of RFs (12.3% [13/106]). The results of the hierarchical cluster analysis, showed improved clustering reproducibility when reproducible RFs without and with dedicated correction factors (Prob=0.62-1.0) where used.

CONCLUSION

Our patient study confirmed that many RFs are highly affected by CT acquisition and reconstruction settings to the point of being non-reproducible. By selecting reproducible RFs along with dedicated correction factors a significant improvement in the clustering reproducibility of RFs could be achieved.

CLINICAL RELEVANCE/APPLICATION

Radiomic features of databases with heterogenous CT radiation dose and reconstruction settings are largely non-reproduceable and thus, may be limited in their use for prognostic clinical studies.

SSA08-08 Prediction and Measurement of Treatment Response in Metastatic Liver Disease with Machine Learning Radiomics

Sunday, Dec. 1 11:55AM - 12:05PM Room: S104A

Participants

Leila Mostafavi, MD, MBA, Boston, MA (Presenter) Nothing to Disclose

Fatemeh Homayounieh, MD, Boston, MA (Abstract Co-Author) Nothing to Disclose

Subba R. Digumarthy, MD, Boston, MA (*Abstract Co-Author*) Researcher, Siemens AG; Contract, Merck & Co, Inc; Contract, Pfizer Inc; Contract, Bristol-Myers Squibb Company; Contract, Novartis AG; Contract, F. Hoffmann-La Roche Ltd; Contract, Polaris; Contract, Cascadian; Contract, AbbVie Inc; Contract, Consulting Medical Associates, Inc; Contract, Bayer AG; Contract, Zai Laboratries; ;

Felix Lades, Forchheim, Germany (Abstract Co-Author) Employee, Siemens AG

Gina Basinsky, BS, Boston, MA (Abstract Co-Author) Nothing to Disclose

Gordon J. Harris, PhD, Boston, MA (*Abstract Co-Author*) Medical Advisory Board, Fovia, Inc; Member, IQ Medical Imaging LLC; Member, Novometrics, LLC; ;

Mannudeep K. Kalra, MD, Lexington, MA (*Abstract Co-Author*) Research Grant, Siemens AG; Research Grant, Riverain Technologies, LLC;

For information about this presentation, contact:

lmostafavi@mgh.harvard.edu

PURPOSE

To assess if machine learning (ML) based-radiomics can predict and measure treatment response in patients with metastatic liver disease in patients with breast cancer.

METHOD AND MATERIALS

Our IRB approved study included 98 adult women (mean age 54±11 years) with metastatic liver disease from breast cancer. All patients underwent contrast abdomen-pelvis CT in portal venous phase at two timepoints - baseline (BL: pre-treatment) and follow-up (FU: between 3-12 months following treatment). Patients were subcategorized into three subgroups based on RECIST 1.1. criteria (Response Evaluation Criteria in Solid Tumors version 1.1): 32 with stable disease (SD), 32 with partial response (PR) and 34 with progressive disease (PD) on follow up CT. CT images from BL and FU were deidentified and exported to radiomics prototype (eXamine, Siemens Healthineers). The prototype enabled semiautomatic segmentation of the target liver lesions for extraction of first and high order radiomics. Statistical analyses with logistic regression and random forest classifiers was performed with the prototype to assess how well BL radiomics predicts treatment response, and whether radiomics can differentiate SD from PD and PR on the two timepoints.

RESULTS

BL radiomics differentiated SD from PR (AUC 0.718) and also SD from PD (AUC 0.797). There was no significant difference between the radiomics on BL and FU CT images of patients with SD (P=0.998). Busyness (an NGTDM feature) and surface volume ratio (a shape feature) were the most powerful predictors of PD between the BL and FU exams (AUC 0.892). BL and FU radiomics were strong measures of PR (AUC 0.938; p=0.026 with multivariate logistic regression) and random forest classification (AUC 0.78).

CONCLUSION

Radiomics can predict and measure treatment response in patients with metastatic liver disease.

CLINICAL RELEVANCE/APPLICATION

Machine-learning based radiomics has promise to help predict and differentiate stable metastatic liver disease from progressive disease and partial response to treatment.

SSA08-09 Preoperative Prediction of Early Recurrence in Advanced Gastric Cancer: A Radiomic Model Using Computed Tomography

Sunday, Dec. 1 12:05PM - 12:15PM Room: S104A

Participants

Wenjuan Zhang, Lanzhou, China (*Presenter*) Nothing to Disclose Mengjie Fang, Beijing, China (*Abstract Co-Author*) Nothing to Disclose Junlin Zhou, Lanzhou, China (*Abstract Co-Author*) Nothing to Disclose

For information about this presentation, contact:

hxzhangwj121@163.com

PURPOSE

In the clinical management of advanced gastric cancer (AGC), preoperative identification of early recurrence after curative resection is essential. Thus, we aimed to create a Radiomic Model Using Computed Tomography to predict early recurrence in AGC patients preoperatively.

METHOD AND MATERIALS

Ethical approval was obtained for this retrospective analysis, and the informed consent requirement was waived. This study enrolled 521 consecutive patients (302 in the training set and 219 in the test set) with clinicopathologically confirmed AGC from our center. Radiomic features were extracted from preoperative diagnostic CT images. Machine learning methods were applied to shrink feature size and build a predictive radiomic signature. We incorporated the radiomic signature and clinical risk factors into a nomogram using multivariable logistic regression analysis. The area under the curve (AUC) of operating characteristics (ROC) and accuracy were assessed to evaluate the nomogram's performance in discriminating early recurrence.

RESULTS

A radiomic signature, including two hand crafted features and one deep learning feature, was significantly associated with early recurrence (p-value<0.0001 for both sets). The radiomic signature showed a good performance for discriminating early recurrence with AUCs of 0.820 (95% CI, 0.772-0.869) in the training set and 0.799 (95% CI, 0.741-0.857) in the test set. In addition, clinical N stage, clinical T stage, and carcinoembryonic antigen levels were considered independent predictors for early recurrence. The nomogram, combining all these predictors, showed powerful prognostic ability in both the training and test sets with AUCs of 0.851 (95% CI, 0.807-0.895) and 0.842 (95% CI, 0.791-0.894), respectively. The predicted risk yielded good agreement with the observed recurrence probability.

CONCLUSION

By incorporating a radiomic signature and clinical risk factors, we created a radiomic nomogram to predict early recurrence in patients with AGC, preoperatively, which may serve as a potential tool to guide personalized treatment.

CLINICAL RELEVANCE/APPLICATION

radiomic nomogram may improve risk stratification and serve as a potential biomarker for guiding individual care in patients with AGC.

Printed on: 01/07/20





SSA09

Gastrointestinal (Rectal Cancer)

Sunday, Dec. 1 10:45AM - 12:15PM Room: S103CD



AMA PRA Category 1 Credits ™: 1.50 ARRT Category A+ Credit: 1.75

FDA Discussions may include off-label uses.

Participants

David D. Bates, MD, Hastings On Hudson, NY (*Moderator*) Research support, General Electric Company Viktoriya Paroder, MD,PhD, Bronx, NY (*Moderator*) Nothing to Disclose Andrea Laghi, MD, Rome, Italy (*Moderator*) Speaker, General Electric Company; Speaker, Guerbet SA; Speaker, Bayer AG; Speaker, Bracco Group; Speaker, Merck & Co, Inc Myles T. Taffel, MD, New York City, NY (*Moderator*) Nothing to Disclose

Sub-Events

SSA09-02 Radiomic Shape Descriptors of Rectal Wall and Lumen on MRI are Associated with Low and High Pathologic Tumor Stages After Chemoradiation for Rectal Cancer

Sunday, Dec. 1 10:55AM - 11:05AM Room: S103CD

Participants

Charlems Alvarez-Jimenez, MSc, Cleveland, OH (Abstract Co-Author) Nothing to Disclose Jacob T. Antunes, Cleveland, OH (Abstract Co-Author) Nothing to Disclose Amrish Selvam, Naperville, IL (Abstract Co-Author) Nothing to Disclose Kaustav Bera, MBBS, Cleveland, OH (Abstract Co-Author) Nothing to Disclose Justin T. Brady, MD, Cleveland, OH (Abstract Co-Author) Nothing to Disclose Sharon Stein, Cleveland, OH (Abstract Co-Author) Nothing to Disclose Kenneth Friedman, Cleveland, OH (Abstract Co-Author) Nothing to Disclose Eduardo Romero, MD, PhD, Bogota, Colombia (Abstract Co-Author) Nothing to Disclose Anant Madabhushi, PhD, Cleveland, OH (Abstract Co-Author) Stockholder, Elucid Bioimaging Inc; Stockholder, Inspirata Inc; Consultant, Inspirata Inc; Scientific Advisory Board, Inspirata Inc; Scientific Advisory Board, AstraZeneca PLC; Scientific Advisory Board, Merck & Co, Inc; Researcher, Koninklijke Philips NV; Researcher, Inspirata Inc; License agreement, Elucid Bioimaging Inc; License agreement, Inspirata Inc; Grant, PathCore Inc; Grant, Inspirata Inc Jaykrishna Gollamudi, MD, Beechwood, OH (Abstract Co-Author) Nothing to Disclose Rajmohan Paspulati, MD, Cleveland, OH (Abstract Co-Author) Nothing to Disclose Andrei S. Purysko, MD, Westlake, OH (Abstract Co-Author) Nothing to Disclose Satish Viswanath, Cleveland, OH (Presenter) Scientific Advisory Board, Virbio Inc

For information about this presentation, contact:

cxa220@case.edu

PURPOSE

The relatively poor expert restaging accuracy of MRI in rectal cancer after chemoradiation (sensitivity \sim 53%) may be due to difficulties in visual assessment of residual tumor. However, both the rectal wall and lumen may distort in shape due to tumor impact. While previous studies have examined radiomic appearance (texture) of rectal tumors on MRI, we evaluated whether radiomic shape features of the entire rectal wall and the lumen are associated with pathologic tumor stage after chemoradiation therapy (CRT).

METHOD AND MATERIALS

60 patients were retrospectively identified across 2 sites, from whom an axial 3T T2W MRI was available after standard-of-care chemoradiation but prior to excision surgery. The entire rectal wall (ERW) and the lumen were annotated by an expert radiologist on all MRIs. 96 shape descriptors (2D and 3D) were extracted from each of lumen and ERW separately, for each patient. Top 2 ranked radiomic shape features associated with pathologic tumor stage (evaluated on excised specimens) were identified via cross-validation on a training subset from Site 1 (n=33). These were evaluated using discriminant analysis on a hold-out validation set of 27 patients (n=13 from Site 1, n=14 from Site 2).

RESULTS

Top-ranked radiomic shape descriptors for distinguishing low (ypT0-2) and high (ypT3-4) stages after CRT were 2D shape change in ERW across rectal volume (p=0.0004) and 3D volumetric roundness of the lumen (p=0.0014). These features resulted in an AUC of 0.82 in the training set (n=33), and an AUC of 0.82 on hold-out validation (n=27, 2 sites). By contrast, ERW volume (p=0.0357) and lumen volume (p=0.8431) were not significantly different or discriminatory between pathologic stages in either cohort.

CONCLUSION

Radiomic shape features of the entire rectal wall and lumen are highly relevant for discriminating patients with low and high tumor stage after chemoradiation, likely capturing implicit effects of residual tumor expanding or contracting the rectum.

CLINICAL RELEVANCE/APPLICATION

First study of radiomic shape features of rectal structures on post-chemoradiation MRI reveal physiologically intuitive differences in low and high pathologic tumor stages, and could enable better evaluation of rectal cancer response to neoadjuvant CRT.

SSA09-03 Diagnostic Accuracy of Magnetic Resonance Tumor Regression Grade for Pathological Complete Response in Rectal Cancer Treated with Neoadjuvant Chemoradiotherapy: A Systematic Review and Meta-Analysis

Sunday, Dec. 1 11:05AM - 11:15AM Room: S103CD

Participants

Jong Keon Jang, MD, Seoul, Korea, Republic Of (*Presenter*) Nothing to Disclose Sang Hyun Choi, Seoul, Korea, Republic Of (*Abstract Co-Author*) Nothing to Disclose Seong Ho Park, MD, Seoul, Korea, Republic Of (*Abstract Co-Author*) Research Grant, Central Medical Service Co, Ltd Kyung Won Kim, MD, Seoul, Korea, Republic Of (*Abstract Co-Author*) Nothing to Disclose Hyun Jin Kim, MD, Seoul, Korea, Republic Of (*Abstract Co-Author*) Nothing to Disclose Ah Young Kim, MD, Seoul, Korea, Republic Of (*Abstract Co-Author*) Nothing to Disclose

For information about this presentation, contact:

edwardchoi83@gmail.com

PURPOSE

We aimed to systematically evaluate and determine the diagnostic accuracy of the magnetic resonance tumor regression grade (mrTRG) for diagnosing pathological complete response (pCR) and pathological T1 or lower than T1 stage (<=ypT1) in rectal cancer patients treated with neoadjuvant chemoradiotherapy (CRT), with a focus on the selection of candidates for less aggressive treatments such as local excision or watch and wait approaches.

METHOD AND MATERIALS

Original studies that investigated the correlation of mrTRG with pathological tumor regression grade and pathological T stage were identified in MEDLINE and EMBASE up until August 31, 2018 according to PRISMA guidelines. The search terms included colorectal cancer, chemoradiation therapy, magnetic resonance imaging, and response or regression. A bivariate random effects model was used to for statistical analysis.

RESULTS

Six studies with 916 patients were included. The meta-analytic summary sensitivity and specificity of mrTRG 1 for pCR were 32.3% (95% CI, 18.2-50.6%) and 93.5% (95% CI, 91.5-95.1%) (Fig. 1A), while for \leq ppT1 they were 31.8% (95% CI, 16.2-53.0%) and 94.7% (95% CI, 91.9-96.5%) (Fig.1B). On the contrary, sensitivity and specificity of mrTRG 1 or 2 for pCR were 69.9% (95% CI, 60.2-78.1%) and 62.2% (95% CI, 56.2-67.8%), while those for \leq ppT1 were 71.4% (95% CI, 61.6-79.6%) and 67.7% (95% CI, 59.8-74.7%).

CONCLUSION

mrTRG 1 showed high specificity for pCR and <=ypT1, but suboptimal sensitivity. mrTRG 1 or 2 showed higher sensitivity for pCR and <=ypT1, but lower specificity. Because of the suboptimal sensitivity of mrTRG 1, it might be limited as a criterion for organ preservation after CRT.

CLINICAL RELEVANCE/APPLICATION

Good response of mrTRGs may be a limited criterion for diagnosing pCR or selecting patients for local excision or watch and wait approaches.

SSA09-04 Locally Advanced Rectal Cancer: The Value of Intravoxel Incoherent Motion Imaging and Diffusion Kurtosis Imaging in Evaluating Pathological Complete Response to Neoadjuvant Chemoradiotherapy

Sunday, Dec. 1 11:15AM - 11:25AM Room: S103CD

Participants

Lanqing Yang, Chengdu, China (*Presenter*) Nothing to Disclose Bing Wu, MD, Chengdu, China (*Abstract Co-Author*) Nothing to Disclose Xiaoxin Liu, Yinchuan, China (*Abstract Co-Author*) Nothing to Disclose

For information about this presentation, contact:

lqyang95@163.com

PURPOSE

To investigate the role of intravoxel incoherent motion diffusion-weighted imaging (IVIM) and diffusion kurtosis imaging (DKI) in evaluating pathological complete response (pCR) to neoadjuvant chemoradiotherapy (CRT) in locally advanced rectal cancer (LARC).

METHOD AND MATERIALS

42 LARC patients (cT3/4 or N+) were consecutively enrolled in this prospective study, and underwent pre- and post-CRT rectal MRI on a 3.0 T MRI scanner, including IVIM and DKI sequences with 12 b values. They all received neoadjuvant CRT and subsequent surgery. Pathological tumor regression grade (TRG) of the surgical specimen served as the reference standard. Patients were divided into pCR (TRG0) and non-pCR group (TRG1-3). Slow diffusion coefficient (D) (.10-3 mm2/s), fast diffusion coefficient (D*) (.10-3 mm2/s), perfusion-related diffusion fraction (f), mean kurtosis (MK), mean diffusion (MD) (.10-3 mm2/s) and monoexponential ADC value (.10-3 mm2/s) were calculated by manually drawing ROIs on three representative slices of primary and residual tumor on pre- and post-CRT b=800 s/mm2 images. ROIs were then copied to images of IVIM and DKI parameters. Independent t test, Mann-Whitney U test, and ROC curves were used for statistical analyses.

RESULTS

The pCR group (n=7) had a significant higher post-CRT f (P=0.012), $D^*(P=0.027)$, MD (P=0.005) and ADC value (P=0.016) than non-pCR group (n=35). Also the percentage changes of f (P=0.034), MD (P=0.043) and ADC value (P=0.030) after CRT were significant higher in the pCR group. ROC curves showed that post-CRT f, D^* , MD and ADC value presented AUCs of 0.739, 0.722, 0.788, and 0.767 in selecting pCR, and the post-CRT MD had a higher sensitivity (82.9% vs. 77.1%) and similar specificity (both 85.7%) than ADC value. Besides, percentage changes of f, MD, and ADC value after treatment presented AUCs of 0.755, 0.747, and 0.735 in identifying pCR, and the percentage f had a higher specificity (85.7% vs. 71.4%) and lower sensitivity(71.4% vs. 80%) than ADC value.

CONCLUSION

IVIM and DKI parameters, especially MD and f could help to differentiate pCR from non-pCR after nCRT in LARC.

CLINICAL RELEVANCE/APPLICATION

IVIM and DKI could help to more reliably select pCR in patients with LARC after CRT, thus could help individualized treatment in clinical. Complere responders may receive non-operative treatment instead of radical resection with reduced surgery related morbidities and improved life quality.

SSA09-05 The Additional Value of Post-nCRT MRI Characteristics for Predicting Locally Advanced Rectal Cancer Patients 3-year DFS

Sunday, Dec. 1 11:25AM - 11:35AM Room: S103CD

Participants

Yankai Meng, Beijing , China (*Presenter*) Nothing to Disclose Chen Wang, MMed, Xuzhou, China (*Abstract Co-Author*) Nothing to Disclose Pei P. Dou, Xuzhou , China (*Abstract Co-Author*) Nothing to Disclose Hongmei Zhang, MD, Beijing, China (*Abstract Co-Author*) Nothing to Disclose Kai Xu, MD, PhD, Xuzhou, China (*Abstract Co-Author*) Nothing to Disclose Chunwu Zhou, MD, Beijing, China (*Abstract Co-Author*) Nothing to Disclose

For information about this presentation, contact:

mengyankai@126.com

PURPOSE

The aim of this study was to investigate the additional value of post-nCRT MRI characteristics for predicting locally advanced rectal cancer patients 3-year DFS.

METHOD AND MATERIALS

In this retrospective study, pre- and post-neoadjuvant chemoradiotherapy (nCRT) MRI morphologic (e.g. pre-nCRT MRI-detected extramural venous invasion) and clinicopathologic variabilities (e.g. pathological complete response) were evaluated in all patients. 3-year DFS was estimated using Kaplan-Meier product-limit method, and Cox proportional hazards models were used to determine associations between morphologic or clinicopathologic variabilities and survival outcomes.

RESULTS

A total of 171 patients (median age of 55 years; age range, 27-82 years) were included in the study. 137 (80.1%) patients performed both pre- and post-nCRT MRI examination, while 34 (19.9%) patients did not perform post-nCRT MRI. Pathological type of tumor was an independent predictor for 3-year survival on pathologic variables. In univariate and multivariate analysis, non-adenocarcinoma was a significant factor for worse long-term survival outcomes with the DFS of 38.0 months (95% CI 25.1-51.0 months, P=0.022) in univariate and with the HR of 3.155 (95% CI 1.160-8.586) in multivariate analysis (P=0.024). Other pathologic characteristics subgroup (vascular tumor thrombus, dentate line involvement, CRM involvement and KRAS gene mutation) showed worse DFS compared to reference subgroup in Kaplan-Meier univariate analysis, but the difference were not significant in COX analysis. The 3-year DFS of patients with positive mrEMVI were 52.6 months in univariate analysis, while the negative patients were 65.1 months (P=0.003). Multivariate analysis result was not significantly different (P=0.563), but the HR in mrEMVI positivity patients was 1.270. In univariate analysis, mrTRG was the independent predictor for 3-year survival on post-nCRT MRI variables (P=0.011). Partial response patients showed worse DFS compared to those with complete response (HR=2.809, 95% CI 0.451-17.496), but the difference was not significant (P=0.268).

CONCLUSION

Pathological type was the independent risk factor for long-term outcomes in LARC patients; while the other morphologic and clinicopathologic characteristics were not significantly related to survival.

CLINICAL RELEVANCE/APPLICATION

Pre- and post-nCRT MRI characteristics provide more individualieze predicting information for LARC patients outcomes.

SSA09-06 MRI in Restaging Locally Advanced Rectal Cancer: Detailed Reasons of Discrepancy when Taking Pathology as Standard of Reference

Sunday, Dec. 1 11:35AM - 11:45AM Room: S103CD

Participants

Xiaoxuan Jia, MA, Beijing, China (*Presenter*) Nothing to Disclose Yinli Zhang, Beijing, China (*Abstract Co-Author*) Nothing to Disclose Yi Wang, MD, Beijing, China (*Abstract Co-Author*) Nothing to Disclose Caizhen Feng, MBChB, Beijing, China (*Abstract Co-Author*) Nothing to Disclose Danhua Shen, Beijing, China (*Abstract Co-Author*) Nothing to Disclose Yingjiang Ye, Beijing, China (*Abstract Co-Author*) Nothing to Disclose Nan Hong, MD, Beijing, China (*Abstract Co-Author*) Nothing to Disclose

For information about this presentation, contact:

jiaxiaoxuanfs@163.com

PURPOSE

To analyze the detailed reasons of discrepancy between restaging MRI and pathology in comprehensive morphologic indicators of tumor response

METHOD AND MATERIALS

The MRI and pathological data of 57 consecutive patients who received neoadjuvant treatment and curative surgery from August 2015 to July 2018 were prospectively collected and retrospectively analyzed. The sensitivity and specificity of restaging MRI in detecting tumor regression grade (TRG), T, N stage, circumferential resection margin (CRM), extramural vascular invasion (EMVI) were calculated when taking pathology as reference. One-by-one comparison between restaging MRI and pathology was conducted to analyze the detailed reasons of discrepancy.

RESULTS

The sensitivity of restaging MRI in detecting TRG3-5, T3-4, N+, CRM involvement and EMVI was 77.1%, 100.0%, 75.0%, 87.5% and 91.7%, respectively. Whereas the specificity was 72.7%, 62.5%, 70.7%, 85.7% and 64.4%, respectively. Perirectal irregular spiculation of fibrosis caused overstaging of T2 disease. Extramural infiltration depth of residual tumor in fibrotic area was not accurately identified, therefore accurate T3 staging was not obtained. Massive fibrosis mixed with tumor-like signal could stretch mesorectal fasica or adjacent organs, and be evaluated as persistent CRM involvement or T4b disease. Fibrosis could manifest as similar shape and signal intensity to invaded vessels shrinked after treatment, resulted in the overstaging of EMVI. Inflammatory cell infiltration in fibrotic area could demonstrate as high signal intensity on DWI, which was similar to residual tumor and resulted in the omission of pCR. Acellular mucin scattered in massive fibrosis could manifest as residual tumor. Edematous mucosa and submucosa, and muscularis propria could also be mistaken as residual tumor for the intermediate signal intensity on T2 weighted images.

CONCLUSION

MRI was prone to overstage the residual tumor. The discrepancy between MRI and pathology was mostly caused by the misinterpretation of fibrosis. Inflammation cell infiltration, acellular mucin, edematous mucosa and submucosa, and muscularis propria could also be mistaken as residual tumor.

CLINICAL RELEVANCE/APPLICATION

Preoperative prediction of tumor response is essential for treatment decision. Identification of what MRI features lead to misinterpretation could help improve selection of good responders.

SSA09-07 CT-derived Radiogenomic Signatures Predicting BRAF/KRAS Mutations and Overall Survival in Primary Colorectal Carcinoma Patients

Sunday, Dec. 1 11:45AM - 11:55AM Room: S103CD

Participants

Amy D. Metry, MD, Cairo, Egypt (*Presenter*) Nothing to Disclose Tagwa Idris, MD, Houston, TX (*Abstract Co-Author*) Nothing to Disclose Nabil A. Elshafeey, MD, Houston, TX (*Abstract Co-Author*) Nothing to Disclose Ly Nguyen, Houston, TX (*Abstract Co-Author*) Nothing to Disclose Ganiraju Manyam, Houston, TX (*Abstract Co-Author*) Nothing to Disclose Meiyue Hong, Houston, TX (*Abstract Co-Author*) Nothing to Disclose Jeniffer S. Davis, PhD, Houston, TX (*Abstract Co-Author*) Nothing to Disclose Zhiqin Jiang, Houston, TX (*Abstract Co-Author*) Nothing to Disclose David Menter, Houston, TX (*Abstract Co-Author*) Nothing to Disclose Jeffrey Morris, Houston, TX (*Abstract Co-Author*) Nothing to Disclose David Hong, Houston, TX (*Abstract Co-Author*) Nothing to Disclose Scott Kopetz, MD, Houston, TX (*Abstract Co-Author*) Nothing to Disclose Rivka R. Colen, MD, Houston, TX (*Abstract Co-Author*) Nothing to Disclose

For information about this presentation, contact:

rrcolen@gmail.com

PURPOSE

To determine the ability of CT-derived radiogenomic signatures/models to predict between key mutation (BRAF/KRAS/other wild-type {WT}) of primary colorectal carcinoma (CRC) patients and their overall survival (OS).

METHOD AND MATERIALS

In this retrospective study, we evaluated 134 histopathological proven CRC patients with known genomic data, and available treatment naïve contrast-enhanced CT scans. Using 3D slicer, the entire primary tumor was semi-automatically segmented on the porto-venous phase, and the volume of interest (VOI) was extracted; subsequently, the VOI was imported into our in-house pipeline radiomic analysis to obtain 610 radiomic features per volume. For feature selection, classification model and validation, the least absolute shrinkage selection operator regression (LASSO), Xgboost, and leave-one-out-cross-validation were used, respectively.

RESULTS

Of 134 patients (male, 66; female, 68; average age, 57.9 years) with BRAF (N=47), KRAS (N=46), and WT (N=41); for mutation status, top 55 LASSO features were able to stratify the CRC patients, with an accuracy (99.3%), area under the curve (99.88%-100%), and *P*-value (2.2e-16). For overall survival 40 LASSO features were able to predict good versus poor OS (30 months), with sensitivity, specificity, and *P*-value of 100%, 97%, and 2e-16 respectively. Additional subgroup analysis revealed the ability of only 10 LASSO features to predict OS for BRAF, KRAS and WT with *P*-value of 3.049e-9, 9.19e-11, and 2.87e-7.

Our radiogenomic signatures were able robustly to stratify the CRC patients based on their molecular data, and to predict their OS status using pre-treatment CT scans.

CLINICAL RELEVANCE/APPLICATION

Radiogenomics is an emerging field that lends a non-invasive tool for quick CRC patients stratification based on their genomic/molecular profiles.

SSA09-08 Building of Comprehensive Prognostic Scoring System for Recurrence After Rectal Cancer Surgery: Based on Radiologic and Clinicopathologic Evaluation

Sunday, Dec. 1 11:55AM - 12:05PM Room: S103CD

Participants

Seo Yeon Youn, Seoul, Korea, Republic Of (*Presenter*) Nothing to Disclose Soon Nam Oh, MD, Seoul, Korea, Republic Of (*Abstract Co-Author*) Nothing to Disclose Moon Hyung Choi, MD, Seoul, Korea, Republic Of (*Abstract Co-Author*) Nothing to Disclose Dong Myung Yeo, Daejeon, Korea, Republic Of (*Abstract Co-Author*) Nothing to Disclose Seong-Taek Oh, Uijeongbu, Korea, Republic Of (*Abstract Co-Author*) Nothing to Disclose Sung Eun Rha, MD, Seoul, Korea, Republic Of (*Abstract Co-Author*) Nothing to Disclose

PURPOSE

To evaluate risk factors of rectal cancer and develop prognostic scoring system for individual recurrence risk assessment.

METHOD AND MATERIALS

Total 489 rectal cancer patients who underwent surgery from 2009 to 2013 were included in the study. Univariate and multivariate Cox proportional hazard model were used to determinate significant prognostic factors among clinical (age, sex, clinical stage, CEA level, anastomotic leak), radiological (anal verge, tumor length, peritoneal reflection, T-, N-stage, lateral LN involvement, threatened circumferential resection margin (CRM), T3 subclassification, extramural venous invasion (EMVI), mean apparent diffusion coefficient (ADC), diffusion volumetry), and pathologic variables (pCRM, lymphatic/venous/perineural invasion, pathologic subtype, immunohistochemistry markers, T-, N-stage). Individual prognostic scores were calculated from selected significant prognostic factors. Patients were divided into low, moderate, and high risk groups according to the prognostic scores. Recurrence rates of each risk groups were obtained. Recurrence free survivals were analyzed by Kaplan-Meier method with the log-rank test.

RESULTS

Distance from anal verge, presence of EMVI on MRI; perineural invasion, N stage on pathology were selected as significant prognostic factors in multivariate analysis. Pathologic T-stage was added to these factors to build prognostic scoring system. Risk coefficient of each 5 factor was assigned as 2, 3, 3, 3, 1, respectively, according to the beta coefficient ($\beta = 0.52$, 0.65, 0.8, 0.31, 0.89). Total 489 patients were classified as low (score 0-1, n=172), intermediate (score 2-3, n=123), and high (score 4-11, n=194) risk groups, according to individual prognostic scores (0-11). Recurrence rates of low, intermediate, and high risk groups were 7.6%, 15.5%, 36.6%, respectively (p<0.001). The Kaplan-Meier curve for recurrence free survival showed the prognostic differences between the 3 risk groups.

CONCLUSION

Multifactorial prognostic scoring system based on radiologic and clinicopathologic variables correlated well with recurrence rate after rectal cancer surgery and could be a comprehensive approach to evaluate the prognosis of individuals.

CLINICAL RELEVANCE/APPLICATION

New prognostic scoring system, based on radiologic, and clinicopathologic factors, is useful for comprehensive assessment of individual recurrence risk in the post-operative rectal cancer patients.

SSA09-09 Scan Time Reduction in Rectal Diffusion-Weighted Imaging: Evaluation of the Simultaneous Multislice Acceleration Technique

```
Sunday, Dec. 1 12:05PM - 12:15PM Room: S103CD
```

Participants

Jae Hyon Park, MD, Seoul, Korea, Republic Of (*Presenter*) Nothing to Disclose Nieun Seo, MD, Seoul, Korea, Republic Of (*Abstract Co-Author*) Nothing to Disclose Joonseok Lim, MD, Seoul, Korea, Republic Of (*Abstract Co-Author*) Nothing to Disclose Jongmoon Hahm, Seoul, Korea, Republic Of (*Abstract Co-Author*) Nothing to Disclose Myeong-Jin Kim, MD, PhD, Seoul, Korea, Republic Of (*Abstract Co-Author*) Nothing to Disclose

For information about this presentation, contact:

sldmsdl@yuhs.ac

PURPOSE

To assess the feasibility of simultaneous multislice-accelerated diffusion-weighted imaging (SMS-DWI) of the rectum compared to conventional DWI (C-DWI) for rectal cancer patients.

METHOD AND MATERIALS

DWI of the rectum was performed for 65 patients with initially diagnosed rectal cancer. All patients underwent C-DWI and SMS-DWI with acceleration factors of 2 and 3 (SMS2-DWI and SMS3-DWI, respectively) using a 3 T machine. Acquisition times of three DWI sequences were measured. Image quality among the three DWI sequences was reviewed by two independent radiologists using a 4-point Likert scale and subsequently compared using the Friedman test. Apparent diffusion coefficient (ADC) values for rectal cancer and normal rectal wall were compared among the three sequences using repeated measures analysis of variance.

RESULTS

Acquisition times using SMS2-DWI and SMS3-DWI were 38.2% and 55.5%, respectively, shorter than those with C-DWI. For all image quality ratings other than distortion (image sharpness, artifact, lesion conspicuity, and overall image quality), C-DWI and SMS2-DWI produced better image qualities than did SMS3-DWI (P < 0.001), with no significant differences observed between C-DWI and SMS2-DWI (P >= 0.054). ADC values of rectal cancer (P = 0.943) and normal rectal wall (P = 0.360) were not significantly different among C-DWI, SMS2-DWI.

CONCLUSION

SMS-DWI using an acceleration factor of 2 is feasible for rectal MRI, resulting in substantial reductions in acquisition time while maintaining diagnostic image quality and ADC values similar to those with C-DWI.

CLINICAL RELEVANCE/APPLICATION

SMS-DWI using an acceleration factor of 2 can be incorporated into routine rectal MRI protocol, with shorter scan time and similar image quality compared to conventional DWI.

Printed on: 01/07/20







SSA10

Science Session with Keynote: Genitourinary (Benign Gynecologic Disease)

Sunday, Dec. 1 10:45AM - 12:15PM Room: N228



AMA PRA Category 1 Credits ™: 1.50 ARRT Category A+ Credit: 1.75

Participants

Jean-Yves Meuwly, MD, Lausanne, Switzerland (*Moderator*) Nothing to Disclose David D. Childs, MD, Clemmons, NC (*Moderator*) Nothing to Disclose Elaine M. Caoili, MD, MS, Ann Arbor, MI (*Moderator*) Nothing to Disclose

Sub-Events

SSA10-01 Genitourinary Keynote Speaker: New Frontier in Imaging the Benign Female Pelvis

Sunday, Dec. 1 10:45AM - 10:55AM Room: N228

Participants Nicole M. Hindman, MD, New York, NY (*Presenter*) Nothing to Disclose

For information about this presentation, contact:

Nicole.Hindman@nyulangone.org

SSA10-02 The Additional Value of Expertise and Structured Reporting in Pelvic MRI Assessment of Endometriosis: A Comparison of Three Review Methods for Diagnosis and Staging

Sunday, Dec. 1 10:55AM - 11:05AM Room: N228

Participants Adrian M. Jaramillo-Cardoso, MD, Boston, MA (*Presenter*) Nothing to Disclose Anuradha S. Shenoy-Bhangle, MD, Lexington, MA (*Abstract Co-Author*) Nothing to Disclose Koenraad J. Mortele, MD, Boston, MA (*Abstract Co-Author*) Nothing to Disclose

For information about this presentation, contact:

amarceljc@gmail.com

PURPOSE

To compare the diagnostic characteristics of Routine-Read, Structured-Reported read, and Structured Expert-Read pelvic MRI for the diagnosis and staging of pelvic endometriosis in a tertiary care academic medical center.

METHOD AND MATERIALS

530 patients with pathological confirmation of endometriosis were found from 2013-2018; 59/530 (11.1%) had surgical staging and adequate preoperative pelvic MRIs for review. Reports on file were considered routine-read (RR); MRI studies were independently reassessed with a structured-reporting template (SR) and by an structured expert reader (SER). Involvement was recorded by compartment [anterior (AC), middle (MC), posterior (PC), adnexal (AX), and other compartments (OC)]. Using surgical-pathologic staging as the gold standard, diagnostic discrepancy between the RR, SR and SER was assessed with the McNemar's test for paired nominal data. Agreement between SR and SER was assessed using Cohen's unweighted kappa.

RESULTS

295 compartments were assessed in 59 women (mean age= 38.8 y; range= 20-69) and 147/295 (49.8%) were involved surgically/pathologically. Diagnostic comparison results: (1) sensitivity: RR=42.9%; SR=86.4%; SER=74.2%. SR's increased sensitivity was significant for the PC, MC, AC (all, p=0.001) and AX (p=0.038) but not OC (p>0.05). Higher sensitivity by SER was significant for the PC and AC (p<0.001), and MC (p=0.004), but not AX or OC (p>0.05); (2) overall specificity: RR=95.3%; SR=45.9%; SER=81.8%. Neither SR nor SER found different results for specificity in OC (p>0.5) when compared to RR. RR sensitivity relied heavily on detection of AX involvement whereas SR and SER showed additional sites of disease (mainly in the PC, MC and AC), while maintaining a comparable specificity for SER. Agreement between SR and SER was fair at k=0.342 (95% CI: 0.25, 0.44).

CONCLUSION

Even at a tertiary care academic center, SER outperforms both SR and RR in the assessment of pelvic endometriosis. Although lack of expertise may reduce specificity, the use of a structured reporting template can significantly increase sensitivity the detection and staging of endometriosis; especially in the posterior, middle and anterior compartments.

CLINICAL RELEVANCE/APPLICATION

Structured reporting in conjunction with expertise can assist in surgical planning and counseling of patients living with endometriosis. MRI can play a vital role in surgical candidacy determination and surgeon selection.

SSA10-03 Vaginal and Rectal Gel Filling Improves the Diagnostic Performance of Endometriosis MRI in Detecting

Deep Infiltrating Peritoneal and Rectal Endometriosis

Sunday, Dec. 1 11:05AM - 11:15AM Room: N228

Participants Kirsi H. Harma, MD, Ch-3010 Bern, Switzerland (*Presenter*) Nothing to Disclose Aleksandra Binda, CH-3010 Bern, Switzerland (*Abstract Co-Author*) Nothing to Disclose Franziska Siegenthaler, CH-3010 Bern, Switzerland (*Abstract Co-Author*) Nothing to Disclose Michael Mueller, CH-3010 Bern, Switzerland (*Abstract Co-Author*) Nothing to Disclose Sara Imboden, CH-3010 Bern, Switzerland (*Abstract Co-Author*) Nothing to Disclose Johannes T. Heverhagen, MD, PhD, Bern, Switzerland (*Abstract Co-Author*) Research Grant, Bracco Group Research Grant, Guerbet SA Research Grant, Siemens AG Speaker, Bayer AG

For information about this presentation, contact:

kirsihannele.haermae@insel.ch

PURPOSE

No consensus exists in the literature on the value of vaginal and rectal filling in the pre-operative MRI diagnostics of DIE. The aim of our study was to investigate this.

METHOD AND MATERIALS

103 patients, operated 2015-2017 with preoperative 1,5 T and 3 T pelvic MRI with or without vaginal and rectal gel opacification blinded to intraoperative findings were analyzed retrospectively by a specialized gynecologic radiologist and then compared to intraoperative findings by looking at the operation report, postoperative diagnosis and intraoperative images and videos. All lesions were histopathological proven (except bowel lesions not being resected). Statistical analysis was performed with SPSS (Vers 25.0) with ANOVA and Excel (Crosstabs, confusion matrix, correlation coefficient, T-test).

RESULTS

103 patients were analyzed, 45% with, 55% without gel filling. Mean age was 33,2 years (18-46), mean BMI 23.0 (16.1-36.8) and the women had a mean of 1,4 previous surgery. The prevalence of endometriosis in the study population was 0.80. 32.6% of the patients had a rASF °I and° II endometriosis, 55.9% °III and °IV. The detection accuracy of DIE improved significantly when proceeding MRI with vaginal and rectal gel filling (filling / non-filling group: Sens. 0.92/0.82, Spec. 0.56/0.41, PPV 0.89/0.84, NPV 0.63/0.38, Acc. 0.85/0.74). 22% of the patients underwent a bowel resection. The overall detection of rectal endometriosis (serosal, musc. propria, mucosal) was higher in the filling group (Correl. 0.68 vs. 0.46) and clearly superior in the detection of deeper rectal endometriosis (musc. propria and mucosal layers) : filling-group: Sens. 100%, NPP 100% / non-filling-group: Sens. 13%, NPP 53%. Sigma endometriosis was observed in 17/103 patients (17%), 9 of them underwent bowel resection.

CONCLUSION

Adapted MRI protocols with vaginal and rectal gel opacification lead to better preoperative diagnostic in peritoneal deep infiltrating endometriosis and in evaluation the depth of the intra-intestinal endometriosis. The feasibility of this so called 'MRI-jelly method' was high.

CLINICAL RELEVANCE/APPLICATION

For planning surgery and weighing the indication to bowel resection accurate pre-operative diagnostic of DIE is crucial. Adapted MRI protocol with vaginal and rectal gel application is recommendable non-invasive method.

SSA10-04 Uterine Junctional Zone Thickness in Patients with Intrauterine Device (IUD): Is There a Difference from the General Female Population?

Sunday, Dec. 1 11:15AM - 11:25AM Room: N228

Participants

Leticia M. Nunes, MD, Sao Paulo, Brazil (*Presenter*) Nothing to Disclose Barbara B. Zanoni, Sao Paulo, Brazil (*Abstract Co-Author*) Nothing to Disclose Fernando I. Yamauchi, MD, Sao Paulo, Brazil (*Abstract Co-Author*) Nothing to Disclose Caroline D. Amoedo, MD, Sao Paulo, Brazil (*Abstract Co-Author*) Nothing to Disclose Ronaldo H. Baroni, MD, Sao Paulo, Brazil (*Abstract Co-Author*) Nothing to Disclose

For information about this presentation, contact:

leticia.ma.on@gmail.com

PURPOSE

Our purpose is to evaluate the thickness of the uterine junctional zone in patients with IUD and compare with literature values for the general female population.

METHOD AND MATERIALS

This is an observational retrospective IRB approved study. From the period of January 2016 until March 2018, 292 pelvic MRI of women of reproductive age (between 17 and 50 years old) and with IUD were evaluated. Exclusion criteria were direct signs of adenomyosis (periendometric cysts, adenomyomas and asymmetric thickening of the junctional zone). The thickness of the junctional zone was measured in the sagittal T2-weighted TSE sequences without fat suppression. In addition, the relationship between the thickness of the junctional zone and the thickness of the entire myometrium was measured at the same location.

RESULTS

The mean thickness of the junctional zone was 8 mm (range: 2 to 27 mm). The mean ratio of junctional zone thickness to myometrium thickness was 0.47 (range: 0 to 1.55). The junctional zone of 135 patients (46.2%) showed normal value thickness (< 7 mm). Moderate thickening (between 7 and 12 mm) of the junctional zone was seen in 136 women (46.6%). Exuberant thickening (> 12 mm) was seen in 21 patients (7.2%), with no other findings of adenomyosis. The relation between junctional zone thickness

and myometrium were 0.4 or less in 106 patients (36.3%) - within normal range based on the literature - and greater than 0.4 in 186 women (63.7%). When we compared our findings with normal values of the literature (normal up to 7 mm), the results showed to be statistically significant (p<0.001), suggesting that junctional zone of --patients with IUD is thicker).

CONCLUSION

IUD is associated with thickening of the uterine junctional zone beyond normal values, a finding that should not be mistaken for adenomyosis.

CLINICAL RELEVANCE/APPLICATION

The knowledge of new values --considered normal for the uterine junction zone thickness in patients with IUD helps to avoid the misdiagnosis of adenomyosis based on this indirect sign alone.

SSA10-05 Multi-parametric MR Relaxometry of Adenomyosis: Assessment of Symptom and Prediction of Response to Gonadotropin Releasing Hormone Analogue

Sunday, Dec. 1 11:25AM - 11:35AM Room: N228

Participants

Chengyu Lin, Beijing, China (*Presenter*) Nothing to Disclose Yonglan He, MD, Beijing, China (*Abstract Co-Author*) Nothing to Disclose Yafei Qi I, MD, Beijing, China (*Abstract Co-Author*) Nothing to Disclose Xiaoqi Wang, Beijing, China (*Abstract Co-Author*) Nothing to Disclose Hailong Zhou, Beijing, China (*Abstract Co-Author*) Nothing to Disclose Huadan Xue, MD, Beijing, China (*Abstract Co-Author*) Nothing to Disclose Zhengyu Jin, Beijing, China (*Abstract Co-Author*) Nothing to Disclose

For information about this presentation, contact:

allenwithyou@foxmail.com

PURPOSE

To investigate whether MR relaxometry can evaluate symptoms of adenomyosis including dysmenorrhea and abnormal uterine bleeding, and to explore whether MR relaxometry can further predict the therapeutic response to gonadotropin releasing hormone analogue (GnRHa) in patients with adenomyosis.

METHOD AND MATERIALS

Between Nov 2017 and Aug 2018, 52 patients clinically diagnosed as adenomyosis underwent multi-parameter uterine MR examinations including T1, T2 and T2* relaxometry on a 3T MR scanner (Ingenia CX, Philips Healthcare, the Netherlands) during peri-ovulatory period. Visual analogue scale (VAS) of dysmenorrhea and blood hemoglobin level were collected before GnRHa injections and 6 months after. T1, T2, and T2* relaxation times of lesions were measured blindly by two radiologists via Intellispace Portal (version 10.1.0.64190, Philips Healthcare, the Netherlands) on slices showing maximum lesion area, as well as maximum diameters of lesions on sagittal T2W images. Spearman rank correlation coefficients were calculated to determine the relationship between relaxation times and VAS. Student t tests were performed to compare the difference of lesions' features between patients with different therapeutic responses. A p value <0.05 was considered statistically significant.

RESULTS

A moderate, negative correlation was found between T2* relaxation time of lesions and VAS (r=-0.4808, p=0.0004). Twenty-three patients received GnRHa injection, and 14 of them achieved complete response (CR, VAS=0 and normal Hgb) after 6 months, while 9 patients with partial response (PR, VAS>0 or anemia). T2* relaxation times of lesions were shorter in patients with CR than those with PR (43.73 \pm 2.019 ms vs. 55.43 \pm 5.465 ms, p=0.0295). Differences were found regarding T2 relaxation times and lesion maximum diameters but they were not statistically significant (63.12 \pm 1.913 ms vs. 71.07 \pm 3.685ms, p=0.0501, and 61.46 \pm 6.899 mm vs. 41.69 \pm 5.721 mm, respectively).

CONCLUSION

T2* relaxation time of lesions can quantitatively assess dysmenorrhea severity in patients with adenomyosis. Furthemore, T2* relaxometry showed potential as a quantitative imaging marker to predict GnRHa therapeutic response in patients with adenomyosis.

CLINICAL RELEVANCE/APPLICATION

T2* relaxometry can make both assessment and prediction as a non-invasive method, and guide different patients to GnRHa or other therapeutic plans based on different findings.

SSA10-06 Uterine Fibroid Embolization: MRI Texture Analysis as a Predictor of Radiological Outcome

Sunday, Dec. 1 11:35AM - 11:45AM Room: N228

Participants

Anass Benomar, MD, Montreal, QC (*Presenter*) Nothing to Disclose Amit Shrivstava, Montreal, QC (*Abstract Co-Author*) Nothing to Disclose David A. Valenti, MD, Montreal, QC (*Abstract Co-Author*) Nothing to Disclose Louis-Martin N. Boucher, MD, PhD, Montreal, QC (*Abstract Co-Author*) Nothing to Disclose Peter Savadjiev, Montreal, QC (*Abstract Co-Author*) Nothing to Disclose Reza Forghani, MD,PhD, Cote Saint-Luc, QC (*Abstract Co-Author*) Stockholder, Real-Time Medical, Inc Founder, 4 Intel Inc Stockholder, 4 Intel Inc Consultant, General Electric Company Speaker, General Electric Company Caroline Reinhold, MD, MSc, Montreal, QC (*Abstract Co-Author*) Nothing to Disclose

PURPOSE

To assess the association of morphologic and texture features on pre-embolization contrast-enhanced MRI with the radiological response of uterine artery embolization (UAE) for uterine fibroids

METHOD AND MATERIALS

This retrospective study analysed the pre-embolization pelvic MRI studies of 80 patients that underwent UAE in our tertiary care centre. Cases were chosen to have good representation of two types of post MRI embolization response: 1) good - > 70% fibroid necrosis (48 cases) and 2) poor < 70% fibroid necrosis (32 cases). Quantitative differences of multiple texture parameters between the two groups were assessed on the venous phase of the pre-embolization MRI. The dominant fibroid on the venous phase was delineated in 3D with semi-automatic in-house software. Volume and six histogram-derived texture features (mean, variance, skewness, kurtosis, entropy, uniformity) were computed for each region of interest. Univariate t-tests were computed to test for statistical difference between the two outcome-based groups. Accounting for Bonferroni correction for multiple comparisons, features with p<(0.05/7)=0.0071 were selected and univariate diagnostic models were built separately for each selected feature. 95% confidence intervals were estimated using 1000 bootstrap iterations.

RESULTS

Three features with p<0.0071 were found, with the following diagnostic performance (95% confidence interval shown in parentheses): The AUC, Sensitivity and Specificity for Volume 0.86 (0.71, 0.92) 0.88 (0.74, 1.0) 0.79 (0.48, 0.86) Mean 0.75 (0.63, 0.85) 0.78 (0.53, 0.94) 0.70 (0.29, 0.78) Skewness 0.73 (0.59, 0.82) 0.44 (0.27, 0.55) 0.76 (0.73, 1.0) respectively.

CONCLUSION

Among the three selected features, volume appears to be the single best feature and outperformed other histogram-based texture features. In future work, we will collect an independent testing dataset, at which time machine learning techniques will be used to optimize a predictive model.

CLINICAL RELEVANCE/APPLICATION

Volume and regional texture features (mean, skewness) can help predict radiological outcomes of UAE and such studies may eventually allow better patient selection for UAE

SSA10-07 A Retrospective Study of the Ultrasound Characteristics of Surgically-proven Ovarian Torsion

Sunday, Dec. 1 11:45AM - 11:55AM Room: N228

Participants Suehyb G. Alkhatib, MD, Fort Washington, MD (*Presenter*) Nothing to Disclose Michael Cousar, MD, Philadelphia, PA (*Abstract Co-Author*) Nothing to Disclose Jonathan D. Dorff, MD, Wynnewood, PA (*Abstract Co-Author*) Nothing to Disclose

PURPOSE

Ovarian torsion can be a challenging diagnosis to confirm or exclude with ultrasound. In this 5-year retrospective study, we aimed to evaluate the ultrasound characteristics of the ovaries in women who underwent surgery for the presumed diagnosis of ovarian torsion.

METHOD AND MATERIALS

We queried our institution's electronic medical record system for all women who were admitted or discharged from two hospitals in our healthcare system between November 2012 and November 2017 and had an ICD-9 or ICD-10 code diagnosis of ovarian torsion. All patients who underwent surgery for the treatment of ovarian torsion were included in the study. The pre-surgical ultrasound studies were then reviewed by an attending radiologist and two radiology residents to determine ovarian volumes, ovarian parenchymal echotexture, ovarian color and spectral flow patterns, ovary location, ascites, presence of an adnexal mass, and presence of the whirlpool sign. We then reviewed the operative notes and corresponding pathology reports to determine which patients had confirmed ovarian torsion. Statistical analysis was performed using SAS.

RESULTS

A total of 64 patients were admitted or discharged with a diagnosis of ovarian torsion. Of these, 55 patients underwent surgery and were included in the analysis. The average patient age was 30 years old. At surgery, 39 patients had confirmed ovarian torsion (71%) and 16 did not (29%). The average volume of torsed ovaries was 202 ml (CI 125 - 279 ml) and for non-torsed ovaries 135 ml (CI 58 - 212 ml). The distribution of ovarian volumes was positively skewed, and no significant difference was found between the torsed ovaries and non-torsed ovaries (P = 0.12). The positive predictive values (PPV) were 86% for absent flow on color doppler, 79% for absent arterial flow on spectral doppler, and 75% for absent venous flow. PPV for the presence of heterogenous stroma was 74%, peripheral follicles 88%, presence of a mass 73%, moderate or large volume of ascites 80%, and for the whirlpool sign was 90%.

CONCLUSION

False positive rates remain high (29%), and no single sonographic finding is specific to ovarian torsion. Positive predictive values for common findings ranged from 75% for absent venous flow to 90% for whirlpool sign, which was only seen in 10 patients.

CLINICAL RELEVANCE/APPLICATION

Our results suggest evaluation of the vascular pedicle for whirlpool sign may be of utility when looking for ovarian torsion.

SSA10-08 Differentiation Between Ovarian Ischemia and Hemorrhagic Infarction by MRI in Cases of Adnexal Torsion

Sunday, Dec. 1 11:55AM - 12:05PM Room: N228

Participants

Yasser Ragab, MD, PhD, Cairo, Egypt (*Presenter*) Nothing to Disclose Hoda Khier II, MD, Cairo, Egypt (*Abstract Co-Author*) Nothing to Disclose Hosny M. Hamza, MD, FRCR, Bromley, United Kingdom (*Abstract Co-Author*) Nothing to Disclose Sherif Abolyazid, Jeddah, Saudi Arabia (*Abstract Co-Author*) Nothing to Disclose Mohamed Khalil IV, MD, Stockholm, Sweden (*Abstract Co-Author*) Nothing to Disclose

For information about this presentation, contact:

yragab61@gmail.com

PURPOSE

To demonstrate the role of magnetic resonance (MR) imaging findings, in differentiating between ovarian infarction and ischaemia and consequently the rate of ovarian salvage in cases of adnexal torsion.

METHOD AND MATERIALS

25 patients with surgically proven ovarian torsion were evaluated by two radiologists regarding the following MR findings: Ovarian enlargement, ovarian parenchymal hypointensity on T2-weighted images (WI), Hyperintensity on T1 (WI) with fat saturation, Recognition of twisted pedicle, Diffusion restriction and Ovarian parenchymal enhancement. Also Pelvic fluid collection, and Uterine deviation These MR findings were statistically correlated with the operative findings and histopathological results (for cases of ovarian infarction).

RESULTS

Pathologically, ovarian haemorrhagic infarction was confirmed in 6 out of 25 cases. Ovarian hyposignal on T2 WI was seen in all cases with infarction 6/6. Ovarian hyperintensity (compared to the contralateral sides) was observed in 4/6 and 5/6 cases with infarction on T1WI and DWI, respectively Ovarian enlargement, fluid collections, uterine deviation and twisted pedicle were detected in most cases with or without haemorrhagic infarction. Poor parenchymal contrast enhancement was observed in all cases without or with necrosis

CONCLUSION

Detection of ovarian infarction is of prognostic importance in cases of torsion to assess salvageability, and thus may affect the surgical decision. Swollen hypointense ovarian parenchyma on T2 WI with lack of contrast uptake are the most reliable MRI signs, followed by hypersignal on T1 WI fat sat and DWI.

CLINICAL RELEVANCE/APPLICATION

MRI is not commonly employed as a first-line imaging study in suspected torsion, but can be very helpful in pregnant patients with an inconclusive US or as a problem solver in equivocal cases. It is important to assess salvageablity of the torsed ovary preoperatively.

SSA10-09 Prevalence of Pathologies in Infertile Women Identified by MR Virtual Hysterosalpingography

Sunday, Dec. 1 12:05PM - 12:15PM Room: N228

Participants

Patricia M. Carrascosa, MD, Buenos Aires, Argentina (*Presenter*) Research Consultant, General Electric Company Carlos Capunay, MD, Buenos Aires, Argentina (*Abstract Co-Author*) Nothing to Disclose Jimena B. Carpio, MD, Buenos Aires, Argentina (*Abstract Co-Author*) Nothing to Disclose Mariano Baronio, Buenos Aires, Argentina (*Abstract Co-Author*) Nothing to Disclose

For information about this presentation, contact:

patriciacarrascosa@diagnosticomaipu.com.ar

PURPOSE

CT Virtual Hysterosalpingography (CT-VHSG) emerged as a good non-invasive modality to evaluate the gynecologist system using very low radiation dose. Recently MR-Virtual Hysterosalpingography (MR-VHSG) appears with the advantage of lacking of ionizing radiation. The objective of this paper is to evaluate the usefulness of MR-VHSG in infertility versus CT-VHSG, and determine the prevalence of disease in each anatomic region of the gynecologist system.

METHOD AND MATERIALS

Patients were studied by CT-VHSG and MR-VHSG. CT studies were performed in a 128-slice CT scanner (Discovery CT750 HD, GE Healthcare) and MR studies in a high filed 3T scanner (Discovery HXT, GE Healthcare). Findings in each modality were reported by two different radiologists in a blinded fashion according to different anatomic regions: cervix, uterine wall, uterine cavity and fallopian tubes. Sensitivity (S), Specificity (SP), Positive Predictive Value (PPV) and Negative predictive Value (NPV) were determined by the exact binomial method for each region.

RESULTS

Fifty two infertile women were studied. In the cervix, 21 patients presented pathological findings: 6 polyps, 6 C-section scars, 3 stenosis,1 sinequiae, 7 hypertrophic folds, 5 glandular dilatation. Prevalence of disease: 9,77 %. Per patient S, Sp, PPV and NPV were: 96%, 95%, 96% and 95%. Per lesion S, Sp, PPV and NPV were 89%, 95%, 92%, 98%. In the uterine wall, 6 patients presented anomalies (1 septate, 3 unicorn, 2 arcuate uterus). S, Sp, PPV and NPV 100%. In uterine cavity, 13 patients presented pathology (6 polyps,1 submucosal myoma, 5 sinequiae,1 hyperplasic folds). Disease prevalence 5.24 %. Per patient S, Sp, PPV and NPV were 100%, 94%, 85%, 100%. Per lesion S, Sp, PPV and NPV were 92%, 98%, 80%, 99%. In the fallopian tubes 8 patients presented pathology: tubal occlusion, dilatation, hidrosalpinx and negative Cotte. Per patient, S, Sp, PPV and NPV were 82%, 92%, 72%, 97%. Disease prevalence 17,65%. Per lesion S, Sp, PPV and NPV were 88%, 99%, 88%, 99%.

CONCLUSION

MR-VHSG showed very good results in the evaluation of the gynecological system. These promising results should be validated in a larger number of patients so as to determine its the role in clinical work.

CLINICAL RELEVANCE/APPLICATION

MR-VHSG is a promising, ionizing radiation-free examination for the evaluation of the infertile woman.

Printed on: 01/07/20





SSA13

Science Session with Keynote: Molecular Imaging (Neuroimaging)

Sunday, Dec. 1 10:45AM - 12:15PM Room: S503AB



AMA PRA Category 1 Credits ™: 1.50 ARRT Category A+ Credit: 1.75

FDA Discussions may include off-label uses.

Participants

Peter Herscovitch, MD, Bethesda, MD (*Moderator*) Nothing to Disclose Karina Mosci, MD, Brasilia, Brazil (*Moderator*) Nothing to Disclose

Sub-Events

SSA13-01 Molecular Imaging Keynote Speaker: Artificial Intelligence in Neuroimaging

Sunday, Dec. 1 10:45AM - 11:05AM Room: S503AB

Participants

Satoshi Minoshima, MD, PhD, Salt Lake City, UT (*Presenter*) Consultant, Hamamatsu Photonics KK; Research Grant, Hitachi, Ltd; Research Grant, Nihon Medi-Physics Co, Ltd;

SSA13-03 Clinical-Radiological Features of Methotrexate Induced Sub-Acute Leukoencephalopathy in Patients with Acute Lymphoblastic Leukemia: "Panda Eye Sign" on DW-MR Imaging

Sunday, Dec. 1 11:05AM - 11:15AM Room: S503AB

Participants

Abhishek Mahajan, MBBS, MD, Mumbai, India (*Presenter*) Nothing to Disclose Hasmukh Jain, Mumbai, India (*Abstract Co-Author*) Nothing to Disclose Tanvi Vaidya, Mumbai, India (*Abstract Co-Author*) Nothing to Disclose Santhosh K. G V, MD, Bangalore, India (*Abstract Co-Author*) Nothing to Disclose Anurag Gupta, MD, Mumbai, India (*Abstract Co-Author*) Nothing to Disclose Manju Sengar, MD, Mumbai, India (*Abstract Co-Author*) Nothing to Disclose

For information about this presentation, contact:

drabhishek.mahajan@yahoo.in

PURPOSE

Subacute leukoencephalopathy in ALL is a rare complication after high dose methotrexate (HDMTX) administration and recognizing this self-remitting entity has important therapeutic implications. We did a retrospective study to evaluate the role of MR imaging in diagnosing this entity and assess the incremental value of Qualitative and Quantitative diffusion weighted MR (DW-MRI).

METHOD AND MATERIALS

A retrospective review of database was performed for adolescent and adult ALL (Aged>14 years) patients who were treated at our center with the modified Berlin-Frankfurt-Münster (BFM)-90 protocol (BFM-90 protocol). 438 patients were screened from year 2014-2015, of which 239 patients were eligible for the BFM-90 protocol. All patients were treated with high dose methotrexate (>1g/m2) and presented with new onset of neurological disturbances were identified. Eleven patients of ALL aged >14 years who developed acute onset of neurological symptoms within two weeks (14 days) after administration of high dose methotrexate and underwent CT and MR imaging with diffusion weighted MR imaging (with 48 hours of presentation) were analyzed. The mean mADC values (10-3 cm2/sec) were calculated on a voxel-by-voxel basis using ADW 4.4 software provided with the MR imaging unit.

RESULTS

Eleven patients were identified from a cohort of 239 patients (~5%). They presented with focal neurological deficits within ~14 days after HDMTX that resolved completely with conservative measures. The CT scans were normal in all these patients. A consistent finding seen in all these cases was the occurrence of restricted diffusion in the region of the centrum semiovale on DW-MRI. On diffusion maps, symmetrical areas of hyperintensity resembled 'Panda eyes' and mADC cut-off of our series was 0.000453 x $10-3 + - 0.000120 \text{ cm}^2/\text{sec}$.

CONCLUSION

CT brain and Conventional MR imaging have no significant role to play in diagnosing this entity however restricted in the centrum semiovale is a consistent imaging finding and the "panda eye sign" as seen on DW imaging can be considered diagnostic for methotrexate induced subacute leukoencephalopathy and this sign can help in timely establishment of the diagnosis and appropriate management.

CLINICAL RELEVANCE/APPLICATION

The literature is limited on incremental of colored diffusion maps and mean apparent diffusion co-efficient (mADC) values and their role in diagnosing MIN.

SSA13-04 Biotin-Conjugated Upconversion Nanoparticles for Metabolic MR Imaging of Invasive Margin of Glioma

Sunday, Dec. 1 11:15AM - 11:25AM Room: S503AB

Participants

Hua Zhang, Shanghai, China (Presenter) Nothing to Disclose

PURPOSE

To prepare one stable biotinylated/polyethylene glycolylated upconversion nanoprobes (biotin/PEG-UCNPs) to study the expression level of biotin receptor in GL261 glioma and its feasibility for detection invasive margin of glioma

METHOD AND MATERIALS

Hydrophobic multifunctional upconversion nanoparticles (UCNPs) were synthesized by solvothermal method. TEM, XRD ,fluorolog-3 modular fluorescence spectrometer and other instruments were used to analyze the surface features such as uniformity and dispersion of nanoprobes. Cell counting kit-8 (CCK-8) analyzed the effect of bion-UCNPs on the activity of RAW264.7 and BCECs. CLSM was used to observe the endocytosis efficiency of GL261 glioma cells for biotinylated and non-biotinylated nanoprobes, then the distribution of nanoprobes in glioma tissues compared with pathology. GE Discovery 3.0T MR analyzed the relaxation rate of biotinylated nanoprobes and the relative signal intensity (rSI) of biotinylated nanoprobes in gliomas at different time points. HE staining of cortical, striatum, hippocampal and hematological parameters of normal C57BL/6 mice were evaluated the potential toxicity of biotinylated nanoprobes to living organisms.

RESULTS

Biotinylated nanoprobes with similar particle size (particle size of about 25 nm) possessed good dispersibility, low toxicity and single-band UCL spectrum centered at 660 nm. The relaxation rate reached 6.124 mM-1S-1. Under CLSM, the glioma cells significantly endocytosed biotinylated nanoprobes rather than the non-biotinylated nanoprobes. After biotin receptor presaturation, the glioma cell endocytosis was significantly reduced. T1 signal generated by the biotinylated nanoprobes in the glioma region could still be observed in 24 hours, and the tumor developing area was expanding. The body boundary of biotinylated nanoprobes well corresponded to the HE-stained glioma border, but the tumor cells were scattered around the boundary. No obvious adverse reactions were observed in the cortical, striatum, hippocampal.

CONCLUSION

GL261 gliomas highly express biotin receptors. Biotinylated UCNPs are able to efficiently target glioma via biotin receptors, and show a significant contrast effect on the edge of glioma invasion.

CLINICAL RELEVANCE/APPLICATION

(dealing with invasive margin of glioma) Biotin-UCNPs can explicitly demonstrate the glioma cells scattered around the boundary via biotin receptor

SSA13-05 Dynamic Contrast-Enhanced Magnetic Resonance Imaging for Monitoring the Anti-angiogenesis Efficacy in a C6 Glioma Rat Model

Sunday, Dec. 1 11:25AM - 11:35AM Room: S503AB

Participants

Weishu Hou, Hefei, China (*Presenter*) Nothing to Disclose Xiaohu Li, MD, Hefei, China (*Abstract Co-Author*) Nothing to Disclose Hongli Pan, Hefei, China (*Abstract Co-Author*) Nothing to Disclose Man Xu, Hefei, China (*Abstract Co-Author*) Nothing to Disclose Yinfeng Qian, Hefei, China (*Abstract Co-Author*) Nothing to Disclose Yongqiang Yu, MD, Hefei, China (*Abstract Co-Author*) Nothing to Disclose

For information about this presentation, contact:

biyuntian33@163.com

PURPOSE

To observe the changes of dynamic contrast-enhanced magnetic resonance imaging (DCE-MRI) parameters in monitoring the early effects of antiangiogenic therapy in a C6 glioma rat model.

METHOD AND MATERIALS

Twenty-six rats were used to establish a C6 glioma model and were randomly divided into a treated group (n = 13) and a control group (n = 13). Rats in the treated group were administered with bevacizumab (Bev) for 7 days, while rats in the control group were administered with vehicle at the same dose. Conventional MRI and DCE-MRI scans were obtained, respectively, on days 0, 1, 3, 5, and 7 after treatment; tumor volume and MRI parameters were dynamically observed. Hematoxylin and eosin (HE) and immunohistochemical (IHC) examination including MVD and proliferating cell nuclear antigen (PCNA) were performed on day 7. Oneway ANOVA was used to compare intra-group differences in each group and t-test was used to compare inter-group differences of MRI parameters between the two groups. Correlations between MRI quantitative parameters and IHC scores were analyzed.

RESULTS

The tumor volume and relative change of tumor volume in the treated group were significantly lower than that of control group on day 7 after treatment with Bev. Ktrans and Kep decreased in the treated group while they increased in the control group; Ve increased in the treated group while it decreased in the control group. A significant difference in MRI parameters between the two groups was observed on days 5 and 7 after treatment. Ktrans and Kep showed positive correlations with MVD, while Ve showed negative correlation with PCNA.

CONCLUSION

DCE-MRI dynamically and accurately assessed the early effects of anti-angiogenic therapy against tumors and may be used as a

therapeutic strategy.

CLINICAL RELEVANCE/APPLICATION

DCE-MRI can assessed effects of anti-angiogenic therapy of glioma.

SSA13-06 The Correlation Analysis of MR Diffusion Tensor Imaging: MR Perfusion Weighted Imaging and Fluorine-18-deoxyglucose Positron Emission Tomography in Patients with Malignant Brain Tumors

Sunday, Dec. 1 11:35AM - 11:45AM Room: S503AB

Participants Xiang Liu, MD, Rochester, NY (*Presenter*) Nothing to Disclose Wei Tian, MD, PhD, Rochester, NY (*Abstract Co-Author*) Nothing to Disclose Henry Z. Wang, MD, PhD, Pittsford, NY (*Abstract Co-Author*) Nothing to Disclose

For information about this presentation, contact:

Xiang_LIu@URMC>Rochester.edu

PURPOSE

MR diffusion tensor imaging (DTI), MR dynamic susceptibility contrast perfusion weighted imaging (DSC-PWI), and fluorine-18deoxyglucose (FDG) positron emission tomography (PET) are major clinical advanced imaging techniques for malignant brain tumors. The purpose of this study is to evaluate the correlation between MR DTI and PWI parameters and FDG-PET changes in patients with malignant brain tumors.

METHOD AND MATERIALS

75 paired MR DTI, DSC-PWI and FDG-PET examinations in 62 patients with malignant brain tumors, including high grade gliomas, brain metastases and cerebral lymphomas, were enrolled in this study. The interval between MR (DTI and DSC-PWI) and FDG-PET examinations ranged from 0 to 13 days in 66 paired MR DSC-PWI and FDG-PET examinations, another 6 paired stable post-surgical scans were acquired within 28 days. The ADC, FA and rCBV maximal rCBV ratio without and with contrast leakage correction were measured using FDA-approved GE BrainStat and NordicICE programs. The tumor versus normal tissue count ratio (TNR) in the "hot" ROIs were calculated for comparison. The correlations between minimal ADC, maximal FA and maximal rCBV ratio of rCBV without and with contrast leakage correction and TNR were evaluated with Spearman Rank correlation analysis.

RESULTS

There was no significant correlation between ADC and FA and TNR derived from FDG-PET (p>0.05). The mean maximal rCBV ratio of rCBV with contrast leakage correction (1.88 ± 1.41) were higher than rCBV without contrast leakage correction (1.19 ± 0.77 , p<0.05). The rCBV with contrast leakage correction has better correlation with FDG-PET-TNR than rCBV without contrast leakage correction, p<0.001. Figure 1.

CONCLUSION

The rCBV with contrast leakage correction shows better correlation with FDG-PET-TNR. Combination of MR DTI, MR-DSC-PWI and FDG-PET parameters could provide comprehensive information of tumor microstructure, hemodynamic and metabolic abnormality.

CLINICAL RELEVANCE/APPLICATION

Combination of MR DTI, MR-DSC-PWI and FDG-PET parameters could provide comprehensive information of tumor microstructure, hemodynamic and metabolic abnormality.

SSA13-07 Radiomic Classification of Tumors Based on Tumor-Associated Macrophage Burden

Sunday, Dec. 1 11:45AM - 11:55AM Room: S503AB

Participants

Zbigniew Starosolski, PhD, Houston, TX (*Abstract Co-Author*) Stockholder, Alzeca Biosciences, LLC Amy Courtney, Houston, TX (*Abstract Co-Author*) Nothing to Disclose Igor Stupin, Houston, TX (*Abstract Co-Author*) Nothing to Disclose Linjie Guo, Houston, TX (*Abstract Co-Author*) Nothing to Disclose Ananth Annapragada, PhD, Houston, TX (*Abstract Co-Author*) Stockholder, Alzeca Biosciences, LLC; Stockholder, Sensulin, LLC; Stockholder, Abbott Laboratories; Stockholder, Johnson & Johnson; Research Grant, Alzeca Biosciences, LLC Leonid Metelitsa, MD,PhD, Houston, TX (*Abstract Co-Author*) Nothing to Disclose Ketan B. Ghaghada, PhD, Houston, TX (*Presenter*) Research Consultant, Alzeca Biosciences, LLC

For information about this presentation, contact:

kbghagha@texaschildrens.org

PURPOSE

A high burden of tumor-associated macrophages (TAMs) has been correlated with an aggressive disease phenotype and poor prognosis in several cancer types. Non-invasive imaging techniques for stratifying tumors based on TAM burden could help in treatment planning and monitoring response to immune-directed therapies. In this pre-clinical study, we investigated a radiomics approach for the stratification of solid tumors based on TAM burden.

METHOD AND MATERIALS

Studies were performed in transgenic mouse models of neuroblastoma (NB) with low and high TAM burden. The SV40-induced NB mouse model, which develops spontaneous adrenal tumors (NB-Tag), was used as a model of low TAM burden (n=5). Knock-out NB-Tag mouse models lacking Ja18 (Ja18-/-) (n=6) or CD1d (CD1d-/-) (n=4) were used as models of high TAM burden. The high TAM burden in knock-out models was confirmed by flow cytometry. Contrast-enhanced CT (CECT) imaging was performed four days after administration of a liposomal-iodine (Lip-I) nanoparticle contrast agent. Tumors were segmented in CT images and quantitative radiomic analysis was performed using an open-source software (PyRadiomics). A Wilcoxon statistical test was used for

selection of radiomic features.

RESULTS

Average tumor CT signal did not differ significantly between tumors in low and high TAM burden groups. However, radiomic analysis identified 49 features that differentiated (p<0.05) low TAM tumors from high TAM *CD1d-/-* tumors, and 31 features that differentiated (p<0.05) low TAM tumors from high TAM *Ja18-/-* tumors. Subsequently, tumors in two high TAM burden groups (*CD1d-/-* and *Ja18-/-*) were pooled together and compared against tumors in low TAM NB-Tag group to determine if radiomic analysis differentiated tumors based on TAM burden but independent of knock out model. Analysis yielded 26 features that separated (p<0.05) low TAM tumors from high TAM tumors. Radiomic features based on first order statistics and gray level size zone matrix represented the dominant set of features that enabled separation of tumors based on TAM burden, suggesting markedly different tumor texture in CECT images in low and high TAM burden tumors.

CONCLUSION

Radiomic analysis identified texture-based features that stratified tumors based on macrophage burden.

CLINICAL RELEVANCE/APPLICATION

Radiomics may enable surveillance of immune cell burden in solid tumors.

SSA13-08 Long-Duration MRI Imaging of Single-Cell In-Vivo and In-Vitro via Magnetic Vortex Nanorings

Sunday, Dec. 1 11:55AM - 12:05PM Room: S503AB

Participants

Ran Sun, Chengdu, China (*Presenter*) Nothing to Disclose Liu Hanrui, Chengdu, China (*Abstract Co-Author*) Nothing to Disclose Yingkun Guo, Chengdu, China (*Abstract Co-Author*) Nothing to Disclose Haiming Fan, Xian, China (*Abstract Co-Author*) Nothing to Disclose

For information about this presentation, contact:

2806467300@qq.com

PURPOSE

To develop an ultra-high sensitive MRI contrast agent for long-term in vivo and in vitro single-cell tracking, which can escape early lysosomes into cytoplasm, especially under the disturbance of alternating magnetic field.

METHOD AND MATERIALS

Bone marrow mesenchymal stem cells (BMSCs) of SD rats were labeled with 50 µg/ml Fe ferrimagnetism vortex magnetic nanorings (FVIOs). In vitro MRI was performed on three groups with number of 1, 5 and 10 labeled BMSCS. For in vivo imaging, 10, 100 and 1000 labeled BMSCs were injected into SD rats' brain via stereotaxis technology and scanned at 7T SWI (susceptibility weighted imaging). After 1h of co-culture of BMSCs and nanorings, alternating magnetic field (AMF) were added for minutes of continuous interference. Another 23h co-culture was performed, then BMSCs were stained and lysosomal escape effect was detected under confocal microscope. GFP-transfected BMSCs were co-cultured with FVIOs by the same method and transplanted into the striatum of SD rats according to the number of cells for long-term magnetic resonance detection.

RESULTS

From the in vitro 7T MRI images, the signals of single FVIOs labeled BMSCs could be clearly detected compared with contract groups. And the in vivo results shows that at least 10 transplanted BMSCs in SD rats' brain could be detected by strong MRI signal. Confocal results also shows that AFM disturbance could successfully facilitate FVIOs to escape from lysosomes into cytoplasm in 10 minutes at early period of co-culture of BMSCs and FVIOs. The same FVIOs labeled GFP-MSCs were transplanted into rats' brain and also could be detected for more than 8 weeks at 7T MRI. Immunofluorescence histochemical analysis showed that some transplanted cells were still alive and corresponding to the signal position detected by MRI.

CONCLUSION

The FVIOs we reported had ultra-high MRI sensitivity to accurately track single cell both in vitro and in vivo, as well as succeed in escaping the lysosome under the interference of alternating magnetic field.

CLINICAL RELEVANCE/APPLICATION

Ferrimagnetism vortex magnetic nanorings has a broad prospect of clinical application because of its low toxicity, low dose and high sensitivity. Its high safety and efficiency surpasses the contrast agents currently used in clinic. In addition, it provides a robust tracer technology support in the further treatment of stem cells and promote stem cell treatment to the clinic faster and better.

SSA13-09 Quantification of Blood Spinal Cord Barrier Opening After Application of Magnetic Resonance Guided Focused Ultrasound

Sunday, Dec. 1 12:05PM - 12:15PM Room: S503AB

Awards

Trainee Research Prize - Medical Student

Participants

Chloe G. Cross, BSC, Salt Lake City, UT (*Presenter*) Nothing to Disclose Allison Payne, PhD, Salt Lake City, UT (*Abstract Co-Author*) Nothing to Disclose Gregory W. Hawryluk, Salt Lake City, UT (*Abstract Co-Author*) Nothing to Disclose Riley Haag-Roeger, Salt Lake City, UT (*Abstract Co-Author*) Nothing to Disclose Rahul Cheeniyil, Salt Lake City, UT (*Abstract Co-Author*) Nothing to Disclose Henrik Odeen, PhD, Salt Lake City, UT (*Abstract Co-Author*) Nothing to Disclose Satoshi Minoshima, MD, PhD, Salt Lake City, UT (*Abstract Co-Author*) Nothing to Disclose Satoshi Minoshima, MD, PhD, Salt Lake City, UT (*Abstract Co-Author*) Consultant, Hamamatsu Photonics KK; Research Grant, Hitachi, Ltd; Research Grant, Nihon Medi-Physics Co, Ltd;

For information about this presentation, contact:

chloegcross@gmail.com

PURPOSE

To develop observer-independent MRI quantification of blood spinal cord barrier (BSCB) permeability after magnetic resonance guided focused ultrasound (MRgFUS) in spinal cord injury (SCI).

METHOD AND MATERIALS

Rats (n=21) underwent T8-T10 laminectomy and extradural compression of the spinal cord (23g weighted aneurysm-type clip, 1 min). High-resolution T1w MR images (3T Siemens, 3D VIBE, FOV=162 mm162 mm×45 mm, res=0.4 mm×0.4 mm×0.8 mm interpolated to 0.2 mm×0.4 mm, TR/TE=6.21/2.94 ms, FA=10°) were obtained pre-MRgFUS without contrast, pre-MRgFUS half-dose contrast, and post-MRgFUS full-dose contrast (Gadoteridol, 0.25 mL/kg, 0.1 mL saline). Rats (n=11) were placed on a MRgFUS system (256-element phased-array transducer, f=940 kHz, focal depth=10cm, intensity FWHM=1.8×2.5×10.9 mm3), injected Optison microbubbles (0.2 mL/kg, 0.1 mL saline) and received 3 doses in 4 locations, 2 mm apart (25 ms bursts, 1 Hz pulses for 3 min, 1.0-2.1 MPa peak pressure). Shams (n=10) received equivalent procedures with no sonications. Spinal cords were segmented manually or semi-automatically using the Spinal Cord Toolbox. SCI rats post-MRgFUS average ROI intensity were normalized to pre-MRgFUS half-contrast. Non-injured rats (n=3) were administered Evans Blue post-MRgFUS and spinals cords were sectioned into 5 mm x 7 samples. Absorbance was measured by spectrophotometry at 655 nm per mg tissue and correlated to post-MRgFUS ROIs normalized to pre-MRgFUS.

RESULTS

Semi-automatic segmentation reduced time by 95% and showed no difference to the manual method (Pearson = 0.92, p=.0001, n=71 regions). Evans Blue absorbance correlated to image intensity in MRgFUS and control ROI (Pearson = 0.82, p=.02, n=6). Increase in signal intensity in MRgFUS ROI relative to control was seen in all SCI MRgFUS rats ($10.65\pm12.4\%$, range: 0.96-43.9%, n=11). SCI sham MRgFUS revealed no change ($0.63\pm0.52\%$, range: 0.15-1.63%, n=10). This result was significant between both groups (p=.003).

CONCLUSION

Semi-automatic segmentation of the rat spinal cord was successful. Evans Blue absorbance was correlated to image intensity values in non-injured rats. Quantitative methods are sensitive for detection of BSCB opening induced by MRgFUS in the SCI animal model.

CLINICAL RELEVANCE/APPLICATION

Most potential therapeutics for SCI require invasive (surgery) or semi-invasive (intrathecal) delivery. The use of MRgFUS to open the BSCB and deliver therapeutics will facilitate recovery from SCI.

Printed on: 01/07/20





SSA18

Neuroradiology (Brain Tumors 1)

Sunday, Dec. 1 10:45AM - 12:15PM Room: S401CD



AMA PRA Category 1 Credits ™: 1.50 ARRT Category A+ Credit: 1.75

FDA Discussions may include off-label uses.

Participants

Leo J. Wolansky, MD, Farmington, CT (*Moderator*) Institutional Grant, Guerbet SA Ramon F. Barajas JR, MD, Portland, OR (*Moderator*) Nothing to Disclose Rajan Jain, MD, Hartsdale, NY (*Moderator*) Consultant, Cancer Panels; Royalties, Thieme Medical Publishers, Inc

Sub-Events

SSA18-01 Glioma Grading Using Microstructural MRI: A Comparison of Diffusion Tensor, Diffusion Kurtosis, and Neurite Orientation Dispersion and Density Imaging

Sunday, Dec. 1 10:45AM - 10:55AM Room: S401CD

Participants

Laura Mancini, London, United Kingdom (*Abstract Co-Author*) Nothing to Disclose Francesco Carletti, MD,PhD, London, United Kingdom (*Presenter*) Nothing to Disclose Sebastian Brandner, London, United Kingdom (*Abstract Co-Author*) Nothing to Disclose Lewis Thorne, London, United Kingdom (*Abstract Co-Author*) Nothing to Disclose Anna Miserocchi, London, United Kingdom (*Abstract Co-Author*) Nothing to Disclose Andrew McEvoy, MD, London, United Kingdom (*Abstract Co-Author*) Nothing to Disclose George George Samandouras, London, United Kingdom (*Abstract Co-Author*) Nothing to Disclose Steffi Thust, London, United Kingdom (*Abstract Co-Author*) Nothing to Disclose Jeremy Rees, London, United Kingdom (*Abstract Co-Author*) Nothing to Disclose Ses Sanverdi, London, United Kingdom (*Abstract Co-Author*) Nothing to Disclose Sotirios Bisdas, MD, London, United Kingdom (*Abstract Co-Author*) Nothing to Disclose

For information about this presentation, contact:

francesco.carletti@nhs.net

PURPOSE

To evaluate the diagnostic performance of diffusion tensor imaging (DTI), diffusion kurtosis imaging (DKI) and neurite orientation dispersion and density imaging (NODDI) for in-vivo grading of gliomas according to the histomolecular integrated 2016 WHO classification.

METHOD AND MATERIALS

41 patients with histopathologically confirmed primary, treatment-naive gliomas (23 grade 2 and 18 grade 3-4 tumours; 10 IDH wildtype (IDHwt), 17 IDH mutant (IDHmut) 1p/19q retained and 14 IDHmut 1p/19q codeleted; 33 non-oligodendroglial and 8 oligodendroglial tumours) prospectively underwent a multi-shell diffusion-weighted protocol to assess the DTI, DKI, and NODDIderived tumour features. Data were analysed with DKE, FSL and the NODDI Matlab Toolbox. Metric values were extracted from whole tumour segmentations and analysed by descriptive statistics and linear regression (Stata software).

RESULTS

Statistically significant differences were found for the average tumour mean kurtosis (MK) and apparent diffusion coefficient (ADC) between the IDHmut and IDHwt gliomas (p-value<=0.02); for the average MK, intra-cellular volume fraction (ficvf) and ADC between IDHmut 1p/19q retained and IDHwt gliomas (p-value<=0.04). The area under curve (AUC) was moderate (0.72-0.75) for all metrics. NODDI-derived parameters, inclunding CSF volume fraction (fiso) and ficvf showed weak significance for differentiating the IDHmut from the IDHwt gliomas (p-value 0.05-0.07) but significant differences between 1p/19q retained and codeleted gliomas (p-value 0.002).

CONCLUSION

Microstructural imaging provided satisfactory diagnostic value to differentiate IDHwt from 1p/19q retained IDHmut gliomas but only NODDI parameters could reliably probe the 1p/19q codeletion effect on the tumour microstructure in the IDHmut tumours.

CLINICAL RELEVANCE/APPLICATION

Microstructural DWI-based techniques offer complementary information for the non-invasive histomolecular WHO staging of gliomas and their combined use showed encouraging results in this pilot study.

SSA18-02 Prediction of Core Signaling Pathway using Physiologic MR Imaging Phenotypes in IDH Wild Type Glioblastoma

Participants Minjae Kim, Seoul, Korea, Republic Of (*Presenter*) Nothing to Disclose Ji Eun Park, Seoul, Korea, Republic Of (*Abstract Co-Author*) Nothing to Disclose Ho Sung Kim, MD, Seoul, Korea, Republic Of (*Abstract Co-Author*) Nothing to Disclose Seo Young Park, Seoul, Korea, Republic Of (*Abstract Co-Author*) Nothing to Disclose Youngheun Jo, Seoul, Korea, Republic Of (*Abstract Co-Author*) Nothing to Disclose Jeong Hoon Kim, Seoul, Korea, Republic Of (*Abstract Co-Author*) Nothing to Disclose

For information about this presentation, contact:

jieunp@gmail.com

PURPOSE

Radiogenomic analysis in gliomas informs multiple associations between genomic alteration and imaging phenotypes, but clinical implication for therapeutic options has been limited. This study aims to predict core signaling pathways in IDH-wild type glioblastoma for targeted therapy by exploring associations between MR imaging phenotypes and next generation sequencing (NGS).

METHOD AND MATERIALS

Genetic alterations were detected with NGS for 120 pathologically proven glioma patients who underwent multi-parametric MRI. First step found significant radiomics features for each genomic mutation using t-test with false discovery rate and lasso penalization. Second step predicted receptor tyrosine kinase (RTK), P53, and Rb pathways, with each pathway contains at least 1 relevant genetic mutation, by using radiogenomic features, age, sex, and locations using random forest and logistic regression classifier. The performance of radiogenomic modeling was tested in the independent validation set of IDH-wild type glioblastoma (n = 35) in prospective registry (NCT02619890) using area under the receiver-operating-characteristics curve (AUC).

RESULTS

First step found in 23, 19, and 29 features for EGFR, PI3KCA, and PTEN mutation in RTK pathway, 6 and 11 features for MDM2 and TP53 mutation in P53 pathway, and 3, 6, and 26 features for CDK4, CDKN2A, and Rb1 mutation in Rb pathway. The performance of core signaling pathway was AUC 0.875 (95% CI 0.743 - 1) for RTK pathway, AUC 0.757 (95% CI 0.592 - 0.921) for P53 pathway, and AUC 0.807 (95% CI 0.641 - 0.972) for Rb pathway in IDH-wild type glioblastoma. Age become significant predictor for RTK pathway.

CONCLUSION

Multiparametric MR imaging phenotypes can help characterize core signaling pathway and offers potential guidance to targeted therapy noninvasively for IDH-wild type glioblastoma.

CLINICAL RELEVANCE/APPLICATION

In this study, we included copy number variation, single nucleotide variation, and insertion/deletion to account the full width of genetic alterations causing alteration of core signaling pathway in gliomagenesis. The machine-learning based model provides individual probability of patients among three major signal pathways, including receptor tyrosine kinase (RTK), p53, and Rb pathway and allows more precise prediction to the patient-tailored targeted therapy.

SSA18-03 Lipid Fraction as a Novel Biomarker for Predicting Survival Outcome of Glioma

Sunday, Dec. 1 11:05AM - 11:15AM Room: S401CD

Participants

Norlisah Mohd Ramli, FRCR, Kuala Lumpur, Malaysia (*Presenter*) Nothing to Disclose Pohchoo Seow, Kuala Lumpur, Malaysia (*Abstract Co-Author*) Nothing to Disclose Vairavan Narayanan, MD, Kuala Lumpur, Malaysia (*Abstract Co-Author*) Nothing to Disclose Ronie Romelean, Kuala Lumpur, Malaysia (*Abstract Co-Author*) Nothing to Disclose Jeannie H. Wong, PhD, Kuala Lumpur, Malaysia (*Abstract Co-Author*) Nothing to Disclose Hari Chandran, Kuala Lumpur, Malaysia (*Abstract Co-Author*) Nothing to Disclose Kartini Rahmat, MBBS,FRCR, Kuala Lumpur, Malaysia (*Abstract Co-Author*) Nothing to Disclose

For information about this presentation, contact:

norlisah@ummc.edu.my

PURPOSE

We evaluated the capability of MRI in-and opposed-phase (IOP) derived lipid fraction as a novel prognostic biomarker of survival outcome in glioma.

METHOD AND MATERIALS

The medical records and MRI images of forty-six histologically proven glioma (WHO Grade II to IV) patients using standard 3T MRI brain tumor protocol and IOP sequence were evaluated. Lipid fraction was derived from the IOP sequence signal-loss ratio. The lipid fraction of solid non-enhancing region of glioma was analyzed, using a three-group analysis approach based on volume under surface (VUS) of receiver operating characteristics to stratify the prognostic factors into three groups of low, medium, and high lipid fraction. The survival analysis was performed, using Kaplan-Meier survival analysis and Cox regression model.

RESULTS

Significant differences were demonstrated between the three groups (low, medium, and high lipid fraction groups) stratified by the optimal cut-off point (OCP) for overall survival (OS) (p=<0.01) and time to progression (p=<0.01). The OS plot stratified by lipid fraction also had a strong correlation with OS plot stratified by WHO grade (R=0.61, p<0.01).

CONCLUSION

The lipid fraction of solid non-enhancing region showed potential for prognostication of glioma. This method will be a useful adjunct

in imaging protocol for treatment stratification and as a prognostic tool in glioma patients.

CLINICAL RELEVANCE/APPLICATION

The addition of lipid fraction analysis to standard tumor protocol assessment has the potential to augment pre-treatment planning, especially focusing on intervention for the high-risk group. Future lipidomics anaylysis possible with a reliable bomarkers using IOP sequence

SSA18-04 Using Advanced DWI-MRI Parameters from Multi- B Values Acquisition and a Histogram Approach for Assessment of Early Therapeutic Response in Glioblastoma

Sunday, Dec. 1 11:15AM - 11:25AM Room: S401CD

Participants

Shahriar Islam, MBBS, London, United Kingdom (*Presenter*) Nothing to Disclose Melanie Morrison, PhD, London, United Kingdom (*Abstract Co-Author*) Nothing to Disclose Matthew R. Orton, MENG, PhD, Sutton, United Kingdom (*Abstract Co-Author*) Nothing to Disclose Matthew Grech-Sollars, PhD, London, United Kingdom (*Abstract Co-Author*) Nothing to Disclose Steffi Thust, London, United Kingdom (*Abstract Co-Author*) Nothing to Disclose Eric Aboagye, London, United Kingdom (*Abstract Co-Author*) Nothing to Disclose Gerry Thompson, Edinburgh, United Kingdom (*Abstract Co-Author*) Nothing to Disclose Adam D. Waldman, MBChB, London, United Kingdom (*Abstract Co-Author*) Nothing to Disclose

For information about this presentation, contact:

s.islam@imperial.ac.uk

PURPOSE

To assess the utility of advanced quantitative diffusion MRI derived from multi b value acquisitions in the assessment of treatment response, using a spatially-independent approach.

METHOD AND MATERIALS

13 patients (7M,6F; mean age 56) were prospectively enrolled into our multicentre study. All patients had biopsy confirmed GBM and completed RT with adjuvant TMZ. Imaging was performed using a Siemens Verio (3T); pre-RT and mid RT. The MRI protocol included a 'low b value' acquisition (b= 0s/mm, 50s/mm, 150s/mm, 200s/mm, 500s/mm, 1000s/mm) from which monoexponential diffusion indices ADC and biexponential indices, IVIM parameters D*, D and f were calculated. A 'high b value' acquisition (b=0 s/mm, 500s/mm, 200s/mm, 3000s/mm, 3500s/mm, 4000s/mm) was acquired to allow stretched exponential diffusion indices, DDC and alpha to be derived. FLAIR sequences were used to define ROI and clinical assessment of mid-treatment and end-treatment response using RANO criteria.Histograms were generated from voxels located within manually segmented ROIs defined by increased signal on T2 FLAIR images. Changes in histogram percentile profiles were evaluated across the two timepoints and compared with RANO assessment at the mid treatment and end treatment timepoints.

RESULTS

Following completion of treatment, 5 patients had PD, 4 SD and 4 CR. Patients with PD showed a histogram shift to the left across all diffusion models, in keeping with increasing diffusion restriction and implying increased cellularity. Patients with SD or CR showed little or no shift in the histogram.DDC and f are the most predictive of progression against RANO assessment, and appear superior to routine ADC. Reduction in 75th centile (f) and 95th centile (DDC) are the most sensitive histogram metrics for predicting early progressive disease.

CONCLUSION

Preliminary results suggest association between early changes in specific diffusion components and subsequent treatment response. Spatially-independent diffusion parameter comparisons provide unbiased sampling of tumour heterogeneity and abrogate the confound of voxel-to-voxel misregistration due to tumour growth/shrinkage.

CLINICAL RELEVANCE/APPLICATION

This is the first study to use advanced diffusion histogram analysis as a marker of early treatment response and can potentially identify patients who need to be switched to second line therapies earlier.

SSA18-05 Relationships between Shear Stiffness Measured by Magnetic Resonance Elastography and Perfusion Parameters Measured by Perfusion Computed Tomography of Meningiomas

Sunday, Dec. 1 11:25AM - 11:35AM Room: S401CD

Participants

Tomohiro Takamura, Chuo, Japan (*Presenter*) Nothing to Disclose Utaroh Motosugi, MD, Chuo, Japan (*Abstract Co-Author*) Nothing to Disclose Masakazu Ogiwara, Chuo-shi , Japan (*Abstract Co-Author*) Nothing to Disclose Yu Sasaki, Chuo-shi , Japan (*Abstract Co-Author*) Nothing to Disclose Kevin J. Glaser, Rochester, MN (*Abstract Co-Author*) Intellectual property, Magnetic Resonance Elastography Technology Stockholder, Resoundant, Inc Richard L. Ehman, MD, Rochester, MN (*Abstract Co-Author*) CEO, Resoundant, Inc; Stockholder, Resoundant, Inc; Hiroyuki Kinouchi, Chuo-shi , Japan (*Abstract Co-Author*) Nothing to Disclose Hiroshi Onishi, MD, Yamanashi, Japan (*Abstract Co-Author*) Nothing to Disclose

For information about this presentation, contact:

ttakamura@yamanashi.ac.jp

PURPOSE

To examine the relationships between stiffness measured by magnetic resonance elastography (MRE) and perfusion parameters.

METHOD AND MATERIALS

Twelve patients with meningiomas underwent 3D brain MRE and PCT examination before surgery. MRE was performed using a superconducting magnet operating at 3.0 T. PCT was performed on a 320-row multidetector CT scanner with rapid injection of nonionic iodine contrast media. Normalized ratios (normalized to normal white matter) of perfusion maps of cerebral blood flow (CBF), cerebral blood volume (CBV), and mean transit time (MTT) (defined as nCBF, nCBV, and nMTT, respectively) were generated. ROIs were manually drawn on the T1-weighted image coregistered into the MRE-space for stiffness map and on the enhanced-CT image for perfusion map, including the entire lesion of the meningioma. Mean values of tumor stiffness and perfusion parameters were compared by Pearson correlation. ROC analysis was used to investigate the predictive ability of perfusion parameters for firm tumors (>2.7 kPa).

RESULTS

The mean stiffness values, nCBF, nCBV, and nMTT for 12 meningiomas were 2.6 ± 3.0 kPa, 6.1 ± 3.5 , 8.1 ± 5.5 , and 1.2 ± 0.2 , respectively. All perfusion parameters were significantly inversely correlated with stiffness values (r=-0.6385 to -0.7380, p<0.0254). The correlation between tumor stiffness and nCBV was the most marked (r=-0.7380, p=0.0061). Regarding stiffness measurement, 5 meningiomas were firm (>2.7 kPa) and 7 were non-firm. ROC analysis revealed that nCBV was a good predictor of firm tumors, with area under the ROC curve of 0.94. Using a cutoff value of >6.4, nCBV showed 100% sensitivity (5/5) and 85.7% specificity (6/7) for predicting firm tumors (fig. 1). Color-coded stiffness and nCBV maps of meningiomas in two patients are shown (Fig. 2). A firm meningioma with stiffness of 2.8 kPa in a 62-year-old woman has lower nCBV (3.4) compared with a non-firm tumor with stiffness of 2.4 kPa in a 75-year-old woman (nCBF=8.0).

CONCLUSION

We found a significant correlation between stiffness and perfusion parameters in meningiomas. In particular, CBV was a useful method for predicting a firm meningioma.

CLINICAL RELEVANCE/APPLICATION

There was a significant correlation between stiffness and perfusion parameters in meningiomas. In particular, CBV was a useful method for predicting a hard meningioma.

SSA18-06 Static and Dynamic Gallium-68-DOTATATE PET/MRI in the Diagnosis and Management of Recurrent and Progressive Intracranial Meningiomas

Sunday, Dec. 1 11:35AM - 11:45AM Room: S401CD

Participants

Jana Ivanidze, MD, PhD, New York, NY (*Presenter*) Research Grant, General Electric Company; Spouse, Consultant, F. Hoffmann-La Roche Ltd; Spouse, Advisory Board, F. Hoffmann-La Roche Ltd; Myrto Skafida, MD, New York, NY (*Abstract Co-Author*) Nothing to Disclose Eaton Lin, MD, New York, NY (*Abstract Co-Author*) Nothing to Disclose Michelle Roytman, MD, New York, NY (*Abstract Co-Author*) Nothing to Disclose Benjamin Liechty, MD, NYC, NY (*Abstract Co-Author*) Nothing to Disclose Theodore H. Schwartz, New York, NY (*Abstract Co-Author*) Nothing to Disclose Susan C. Pannullo, MD, NYC, NY (*Abstract Co-Author*) Nothing to Disclose Joseph R. Osborne, MD, New York, NY (*Abstract Co-Author*) Nothing to Disclose Nicolas A. Karakatsanis, PhD, New York, NY (*Abstract Co-Author*) Nothing to Disclose

For information about this presentation, contact:

jai9018@med.cornell.edu

PURPOSE

Meningiomas are the most common primary intracranial tumors. Contrast enhanced MRI is the gold standard for diagnosis and treatment planning, however MRI can have limited accuracy in distinguishing recurrence from treatment effect in the postsurgical and post-radiation setting. [68]Ga-DOTATATE is a PET radiotracer targeting somatostatin receptor 2 (SSTR2) with high affinity. Meningiomas express high levels of SSTR2. The purpose of our study was to evaluate [68]Ga-DOTATATE PET/MRI in a prospective clinical cohort of patients with meningioma.

METHOD AND MATERIALS

20 patients with clinically-suspected or pathology proven meningioma were imaged over a time period of 6 months. [68]Ga-DOTATATE-PET/MRI was acquired in 3D list mode over 50 minutes, beginning 5-15 minutes post injection. SUVmax values in meningiomas and suspected post treatment change were obtained, as well as the pituitary gland (positive reference) and superior sagittal sinus (SSS, background reference). In a subset of 11 patients we generated dynamic time-activity curves binned into 5minute frames, and analyzed time-activity and time-SUVmean curves in target lesions including meningioma, post-treatment change, pituitary glands, and SSS individually as well as across the cohort.

RESULTS

A total of 50 meningiomas were identified based on PET (median: 2 per patient, range 0-14). In 17 patients PET confirmed recurrence, while in 3 patients low avidity favored a diagnosis of post-treatment change. [68]Ga-DOTATATE PET provided improved extent of disease visualization and confirmed parenchymal and osseus invasion. Dynamic PET data demonstrated unique kinetic uptake patterns for meningiomas, pituitary glands and post treatment change across the cohort.

CONCLUSION

[68]Ga-DOTATATE PET/MRI is a promising tool in the assessment of meningiomas, particularly in the post-surgical and postradiation setting, allowing improved diagnosis and extent of disease evaluation without increasing acquisition time. Incorporating dynamic PET data acquisition and analysis can provide additional valuable information in differentiating recurrence from post treatment change, and inform future prospective clinical trials.

CLINICAL RELEVANCE/APPLICATION

In this consecutive series of 20 cases, we report a novel clinical application of combined static and dynamic [68Ga]-DOTATATE

PET/MRI in diagnosis and treatment response assessment in recurrent and progressive meningioma.

SSA18-07 Outcomes of Treatment Induced Pseudoprogression and Correlation with MGMT Methylation Status in GBM Patients

Sunday, Dec. 1 11:45AM - 11:55AM Room: S401CD

Participants

Lisa Morris, Columbia, MO (*Abstract Co-Author*) Nothing to Disclose Ayman Nada, MD, PhD, Cairo, MO (*Presenter*) Nothing to Disclose Joseph P. Cousins, MD,PhD, Columbia, MO (*Abstract Co-Author*) Nothing to Disclose Tolga Tuncer, Columbia, MO (*Abstract Co-Author*) Nothing to Disclose Gregory Biedermann, MD, Columbia, MO (*Abstract Co-Author*) Nothing to Disclose

For information about this presentation, contact:

anvrx@health.missouri.edu

PURPOSE

A challenge in the management of glioblastoma is distinguishing true progression from pseudoprogression (PsP), which may have improved survival. MGMT methylation has been shown to correlate with PsP. This study aims to evaluate the rates of PsP and its outcomes, and correlate to MGMT status.

METHOD AND MATERIALS

An IRB-approved retrospective study included patients with histologically confirmed glioblastoma between 2010 and 2018. All patients underwent surgical resection followed by temozolomide and radiation. Baseline pre- and post-radiation MRIs were reviewed to assess the treatment response according to RANO criteria. Maximum dimensions and volumetric evaluations were performed. Patients were graded as partial response (PR), progressive disease (PD) or stable disease (SD). Those with initial PD who had subsequent improvement without intervention were classified as PsP. We evaluated overall survival (OS) and time to progression (TTP) from the time of diagnosis, with TTP based on subsequent MRI images and clinical response, and this was correlated with the MGMT.

RESULTS

Of 101 patients diagnosed with glioblastoma, 45 had at least 9 months follow-up. The MGMT status was methylated in 7, indeterminate in 2, unmethylated in 11, and not evaluable in 22. The response was recorded as PsP in 16, PD in 12, SD in 2, PR in 12. Patients with PsP had an excellent mean TTP and OS of 327 and 545 days. The mean TTP and OS for those with PD was 250 and 450 days, and for those with PR was 446 and 676 days. Those with MGMT methylation and PsP had TTP and OS of 437 and 560 days which was similar to those with PR. Those with PsP and unmethylated MGMT had a worse mean TTP and OS of 198 and 438 days.

CONCLUSION

Patients with PsP have improved outcomes compared to those with PD or SD, with a mean TTP and OS that is between those seen with PR/CR and PD/SD. These outcomes are further improved with MGMT promoter methylation. This data substantiates prior studies' conclusions that MGMT status may significantly influence response, and patients with PsP have improved survival compared to PD/SD.

CLINICAL RELEVANCE/APPLICATION

Pseuodprogression may predict a better overall response, and recognizing it in an earlier fashion may prevent initiation of unnecessary salvage therapies that can be reserved for later in the treatment course. Interestingly, MGMT methylation has been shown to correlate with pseudoprogression and increased survival.

SSA18-08 A Single Institution Review of Primary and Secondary Imaging Characteristics of Hypophysitis in Adult Oncologic Patients Undergoing Immune Checkpoint Inhibitor Therapy

Sunday, Dec. 1 11:55AM - 12:05PM Room: S401CD

Participants

Robert R. Devita, MD, Cleveland, OH (*Presenter*) Nothing to Disclose Daniel A. Smith, MD, Cleveland, OH (*Abstract Co-Author*) Nothing to Disclose Ethan Radzinsky, Cleveland, OH (*Abstract Co-Author*) Nothing to Disclose Sreeharsha Tirumani, MBBS, MD, Beachwood, OH (*Abstract Co-Author*) Nothing to Disclose Christopher Hoimes, DO, Cleveland, OH (*Abstract Co-Author*) Nothing to Disclose Nikhil H. Ramaiya, MD, Shaker Heights, OH (*Abstract Co-Author*) Nothing to Disclose

For information about this presentation, contact:

robert.devita@uhhospitals.org

PURPOSE

Immune checkpoint inhibitor (ICI) therapy is becoming more prevalent in the treatment of a diverse array of malignancies. With the increasing use of ICI therapy, numerous treatment related complications, termed "immune related adverse events" (irAEs), have emerged. Hypophysitis is a rare and potentially fatal toxicity requiring prompt recognition and early treatment. The purpose of this study was to identify the primary and secondary imaging characteristics of hypophysitis in patients undergoing treatment with ICIs.

METHOD AND MATERIALS

A retrospective chart review was performed of 228 adult oncology patients undergoing treatment with ipilimumab or ipilimumab and nivolumab at a single institution from 2010-2018. Primary and secondary imaging characteristics (adrenal, thyroid, uterine/ovarian atrophy) of hypophysitis were evaluated. The patients' key clinical features, labs, and patient outcomes were assessed from the medical records.

RESULTS

Hypophysitis was diagnosed in 15 (7%) of the 228 patients reviewed with a mean-onset time of 11.2 weeks (range 5-19 weeks) after initiation of ICI therapy. The mean age of diagnosis was 61 ± 16 years with 80% of the patients being male. Sixty percent of patients were treated with ipilimumab alone, and 40% with a combination of ipilimumab and nivolumab. Most patients (14) were treated for melanoma and one was treated for chondosarcoma. Imaging indications included fatigue (85%), headache (77%), and nausea (54%). Brain imaging was performed in 13 patients during and after ICI therapy. Nine patients demonstrated diffuse pituitary enlargement. Of the 9 patients, 5 demonstrated homogenous pituitary enhancement and 3 had heterogeneous enhancement on T1 post-gadolinium images). The patients were subsequently treated with steroids with a mean of 79 days until resolution of imaging findings. All patients developed adrenal atrophy and 2 (13%) had thyroid atrophy on follow up imaging.

CONCLUSION

The expanding role of ICI therapy has resulted in the increased prevalence of irAEs such as hypophysitis. The key radiological findings in hypophysitis are often subtle, but include diffuse pituitary enlargement and adrenal and thyroid atrophy.

CLINICAL RELEVANCE/APPLICATION

Hypophysitis is a rare but potentially fatal complication in oncologic patients undergoing ICI therapy. Imaging, in conjunction with clinical findings, can aid in the rapid diagnosis of the condition.

SSA18-09 Potential Imaging Biomarkers for Assessment of Treatment Response of Metastatic Brain Lesions in Patients with Small Cell Lung Cancer Using Conventional and Diffusion Weighted MR Sequences

Sunday, Dec. 1 12:05PM - 12:15PM Room: S401CD

Participants

Tyler Richards, MD, Cleveland, OH (*Presenter*) Nothing to Disclose Sreeharsha Tirumani, MBBS, MD, Beachwood, OH (*Abstract Co-Author*) Nothing to Disclose Robert R. Devita, MD, Cleveland, OH (*Abstract Co-Author*) Nothing to Disclose Elias Kikano, MD, Cleveland, OH (*Abstract Co-Author*) Nothing to Disclose Afshin Dowlati, MD, Cleveland, OH (*Abstract Co-Author*) Nothing to Disclose Nikhil H. Ramaiya, MD, Shaker Heights, OH (*Abstract Co-Author*) Nothing to Disclose

For information about this presentation, contact:

tyler.richards@uhhospitals.org

PURPOSE

The purpose of the study is to evaluate changes in MR characteristics of individual small cell lung cancer (SCLC) brain metastases (BMs) pre and post initial treatment following the diagnosis of BMs. The impact of these changes on CNS progression free survival (PFS) and overall survival (OS) will be assessed in an attempt to identify MR imaging biomarkers to assess response to therapy.

METHOD AND MATERIALS

In this observational study, MR characteristics of individual SCLC BMs (n=57) were evaluated pre and post treatment in 20 patients. The MRI characteristics analyzed included lesion size, T1 and T2 weighted signal, surrounding edema, hemorrhage, and diffusivity. Initial and interval changes in imaging characteristics were correlated with OS and CNS PFS. For statistical analysis, patients undergoing systemic chemotherapy only were grouped with patients receiving chemotherapy and whole brain radiation therapy (WBRT), which together (n=11) were compared to the group that received WBRT only (n=9) following the diagnosis of BMs.

RESULTS

There was statistically significant difference between the pre and post treatment means of lesion size (p<0.0001, Wilcoxon Signed Rank) and ADC (p=0.0017, Wilcoxon Signed Rank) but there was no difference across the treatment groups within pairs or among pairs. Parametric Survival analysis for OS showed statistically significant survival difference in terms of treatment type (p<0.001). Analysis of the MRI features of the BMs revealed that the percent increase of ADC (p=0.0001) was correlated with increased OS. Survival analysis showed difference between treatment groups in terms of OS (p=0.0122, Wilcoxon Test) but not in terms of CNS PFS (p=0.1371, Wilcoxon Test). There was no difference between the treatment groups in terms of percentage change in lesions size (p=0.9405, Kruskal-Wallis test) and percentage change in ADC (p=0.5635, Kruskal-Wallis test). Regarding other MRI features, there was no difference in signal characteristics including T1 signal, T2 signal and edema before and after treatment.

CONCLUSION

Changes in diffusivity from pre to post systemic chemotherapy and/or WBRT may be a useful biomarker to assess treatment response in patients with SCLC and BMs.

CLINICAL RELEVANCE/APPLICATION

The percentage change of ADC of small cell lung cancer brain metastases pre to post treatment is correlated with increased overall survival (p=0.0001).

Printed on: 01/07/20





SSA22

Physics (MRI - New Techniques and Image Quality)

Sunday, Dec. 1 10:45AM - 12:15PM Room: E353A



AMA PRA Category 1 Credits ™: 1.50 ARRT Category A+ Credit: 1.75

FDA Discussions may include off-label uses.

Participants

Konstantinos Arfanakis, PhD, Chicago, IL (*Moderator*) Nothing to Disclose Baowei Fei, PhD, Cleveland, OH (*Moderator*) Nothing to Disclose R. Jason Stafford, PhD, Houston, TX (*Moderator*) Nothing to Disclose

Sub-Events

SSA22-01 Hybrid MR-OR Siting and Safety

Sunday, Dec. 1 10:45AM - 10:55AM Room: E353A

Participants

Anshuman Panda, PhD, Indianapolis, IN (*Presenter*) Nothing to Disclose Yuxiang Zhou, PhD, Phoenix, AZ (*Abstract Co-Author*) Nothing to Disclose William F. Sensakovic, PhD, Scottsdale, AZ (*Abstract Co-Author*) Founder, Telerad Physics Teaching, LLC Robert G. Paden, MS, Phoenix, AZ (*Abstract Co-Author*) Nothing to Disclose William Pavlicek, PhD, Scottsdale, AZ (*Abstract Co-Author*) Nothing to Disclose

CONCLUSION

The hybrid MR-OR environment provides many clinical advantages but is not free of a certain degree of risk. The risk is further compounded with lack of consistent safety standards. Engineering MR safety into the practice design and strict adherence to MRI safety checklists, policy enforcement and regular personnel training is critical to maintaining MR safety in this complex multidisciplinary procedural environment.

Background

Hybrid MR-OR for interventional and intraoperative procedures has emerged from its infancy to a standard setup at major academic medical centers. The American College of Radiology (ACR) white paper on MR Safety is a primary reference used by most sites for designing MR safety best practices; unfortunately, it is lacking specific guidance on hybrid MR-OR siting and safety. We attempt to provide a template for hybrid MR-OR siting and safety that builds on the ACR white paper terminology and covers unique considerations regarding design, layout, access, training, screening, infection control and procedural considerations when developing hybrid MR-OR siting and safety practices.

Evaluation

A key challenge of hybrid MR-OR environment is its multidisciplinary, interdepartmental nature, and as such requiring a strong collaborative approach in the design of the hybrid environment and implementation of education and safety protocols. Safety not only has to be forefront in awareness, but also engineered into the workflow. We highlight three key elements of engineering safety into the practice design through 1) siting considerations 2) workflow and training considerations and 3) procedural safety considerations.

Discussion

Siting considerations should include architectural layout, scanner choice (on rails vs stationary), zone designs, and screening equipment. Workflow and training consideration should include staff training (with emphasis on hands-on training), access control, and patient/staff movement. Procedural safety considerations should include level 2 personnel staffing, patient screening, procedural pause, surgical equipment screening, and infection control. Ongoing evaluation of procedural process is critical as new procedures are added.

SSA22-02 Lower Risk of Hearing Loss Without Sacrificing Image Quality in Fetal MR Imaging: A Feasibility Study Using Acoustic Reduction Technique

Sunday, Dec. 1 10:55AM - 11:05AM Room: E353A

Participants

Le Cao, Xian, China (*Presenter*) Nothing to Disclose Jianxin Guo, Xian, China (*Abstract Co-Author*) Nothing to Disclose Xiang Liu, Xian, China (*Abstract Co-Author*) Nothing to Disclose Xiaocheng Wei, Beijing, China (*Abstract Co-Author*) Employee, General Electric Company Yun Shen, PhD, Beijing, China (*Abstract Co-Author*) Employee, General Electric Company Researcher, General Electric Company Jian Yang, Xian, China (*Abstract Co-Author*) Nothing to Disclose

For information about this presentation, contact:

PURPOSE

The purpose of this study was to evaluate whether ART is reliable and applicable in fetus brain imaging.

METHOD AND MATERIALS

We collected from September 2017 to October 2018 using 3.0T MR scannerfor fetal head exams. 10 subjects underwent ART sequences (group A), the matched 10 subjects underwent traditional sequences (group B). The protocol of tradition sequences includes T2 single short fast spin echo (SSFSE) (axial, sagittal, coronal); while the ART sequences contains ART T2 SSFSE (axial, sagittal, coronal) (Table1). A quantitative assessment by the ROI of 1 mm was manually placed on the different layers of the brain (Fig 1A). A qualitative evaluation including eight criteria (1. Delineation of germinal zone and gray matter, 2. Delineation of white matter, 3. Delineation of internal and external CSF spaces, 4. Delineation of amniotic fluid adjacent to the skull, 5.Delineation of brain stem, 6. Delineation of cerebellum, 7. Severity of motion artifacts, 8. Overall image quality) were evaluated on an ordinal scale regarding signal characteristics, potential dysmorphism and developmental anomalies (5= optimal diagnostic quality; 4= very good image quality;3= diagnostic image quality, 2= image quality below diagnostic standards; 1= image quality too poor to correctly identify anatomy.

RESULTS

The maximum differences of peak and equivalent sound pressure between the two groups are 18.1dBA and 16.1dBA respectively, indicating the ART sequences have lower noise than traditional sequences. Comparative ratios calculated between germinal matrix/air, periventricular layer/air, subplate layer/air, and cortical layer/air for group A $(33.97\pm17.52, 42.45\pm16.65, 46.37\pm22.46, 43.03\pm20.89)$ were lower than that of group B $(52.54\pm25.61, 33.39\pm12.91, 69.17\pm35.21, 64.76\pm32.53)$, but with no significant difference (P=0.09,0.20, 0.12, 0.11). The qualitative results showed that the image quality of group B and group A scored 4.42 + 0.37 and 4.36 + 0.49 respectively. There was no significant difference in image quality score between the two groups.

CONCLUSION

Acoustic reduction sequence can acquire high quality images in 3.0T scanner, meanwhile decrease hearing loss risk in fetal head examinations compared with the conventional method.

CLINICAL RELEVANCE/APPLICATION

Acoustic reduction sequence can acquire high quality images in 3.0T scanner, meanwhile decrease hearing loss risk in fetal head examinations compared with the conventional method.

SSA22-03 Multi-Site, Multi-Vendor, and Multi-Platform Assessment of Accuracy of Quantitative Proton-Density Fat Fraction (PDFF) at 1.5 and 3 Tesla with a Standardized Spherical Phantom: Results from a Study by the RSNA QIBA PDFF Committee

Sunday, Dec. 1 11:05AM - 11:15AM Room: E353A

Participants

Houchun H. Hu, PhD, Columbus, OH (Presenter) Nothing to Disclose

Takeshi Yokoo, MD, PhD, Dallas, TX (Abstract Co-Author) Nothing to Disclose

Scott B. Reeder, MD, PhD, Madison, WI (Abstract Co-Author) Nothing to Disclose

Mustafa R. Bashir, MD, Cary, NC (*Abstract Co-Author*) Research Grant, Siemens AG; Research Grant, General Electric Company; Research Grant, NGM Biopharmaceuticals; Research Grant, Madrigal Pharmaceuticals, Inc; Research Grant, Metacrine, Inc; Research Grant, Pinnacle Clinical Research; Research Grant, ProSciento Inc; Research Consultant, RadMD

Claude B. Sirlin, MD, San Diego, CA (*Abstract Co-Author*) Research Grant, Gilead Sciences, Inc; Research Grant, General Electric Company; Research Grant, Siemens AG; Research Grant, Bayer AG; Research Grant, Koninklijke Philips NV; Consultant, AMRA AB; Consultant, Fulcrum; Consultant, IBM Corporation; Consultant, Exact Sciences Corporation; Consultant, Boehringer Ingelheim GmbH; Consultant, Arterys Inc; Consultant, Epigenomics; Author, Medscape, LLC; Lab service agreement, Gilead Sciences, Inc; Lab service agreement, ICON plc; Lab service agreement, Intercept Pharmaceuticals, Inc; Lab service agreement, Shire plc; Lab service agreement, Enanta; Lab service agreement, Takeda Pharmaceutical Company Limited; Lab service agreement, Alexion Pharmaceuticals, Inc; Lab service agreement, NuSirt Biopharma, Inc

Diego Hernando, PhD, Madison, WI (Abstract Co-Author) Co-founder, Calimetrix, LLC

Walter Henderson, La Jolla, CA (Abstract Co-Author) Nothing to Disclose

Suraj D. Serai, PhD, Philadelphia, PA (Abstract Co-Author) Nothing to Disclose

Dariya Malyarenko, PhD, Ann Arbor, MI (Abstract Co-Author) Nothing to Disclose

Thomas L. Chenevert, PhD, Ann Arbor, MI (Abstract Co-Author) Consultant, Koninklijke Philips NV

Gavin Hamilton, PhD, San Diego, CA (Abstract Co-Author) Nothing to Disclose

Michael S. Middleton, MD,PhD, San Diego, CA (*Abstract Co-Author*) Institutional research contract, Alexion Pharmaceuticals, Inc; Institutional research contract, AstraZeneca PLC; Institutional research contract, BioClinica, Inc; Institutional research contract, Biomedical Systems; Consultant, Bracco Group; Institutional research contract, Bristol-Myers Squibb Company; Institutional research contract, Enanta; Institutional research contract, Galmed Pharmaceuticals Ltd; Institutional consultant contract, F. Hoffmann-La Roche Ltd; Institutional research contract, General Electric Company; Institutional research contract, Inc; Institutional research contract, Guerbet SA; Institutional research contract, ICON plc; Institutional research contract, Intercept Pharmaceuticals, Inc; Consultant, Kowa Company, Ltd; Consultant, MEDIAN Technologies; Consultant, IBM Corporation; Consultant, Novo Nordisk AS; Institutional research contract, Pfizer Inc; Stockholder, Pfizer Inc; Institutional research contract, Prosciento; Consultant, Quantitative Insights, Inc; Institutional research contract, F. Hoffmann-La Roche Ltd; Institutional research contract, Synageva; Institutional research contract, Siemens AG; Institutional research contract, VirtualScopics, Inc

Yunhong Shu, PhD, Rochester, MN (Abstract Co-Author) Nothing to Disclose

Mark A. Smith, MS, ARRT, Columbus, OH (Abstract Co-Author) Nothing to Disclose

Jean Shaffer, Durham, NC (Abstract Co-Author) Nothing to Disclose

Jean A. Tkach, PhD, Cincinnati, OH (Abstract Co-Author) Nothing to Disclose

Andrew T. Trout, MD, Cincinnati, OH (*Abstract Co-Author*) Author, Reed Elsevier; Author, Wolters Kluwer nv; Research Grant, Canon Medical Systems Corporation; Board Member, Joint Review Committee on Educational Programs in Nuclear Medicine Technology; Speakers Bureau, Reed Elsevier; Speakers Bureau, iiCME

Jean H. Brittain, PhD, Madison, WI (Abstract Co-Author) Co-founder, Calimetrix, LLC;

PURPOSE

Proton Density Fat Fraction (PDFF) is a popular MRI/S biomarker of hepatic steatosis. The QIBA PDFF Committee was formed in 2015. In this work, the committee conducted a multi-center and multi-vendor phantom study. The objective was to characterize the accuracy of PDFF as a robust biomarker, as measured by various SPGR chemical-shift-encoded sequences against a standardized phantom with known PDFF values.

METHOD AND MATERIALS

9 sites with multiple commercial 1.5T and 3T systems were invikved. The phantom contained 12 vials of known PDFF. Sites were asked to test several protocols, to their best capability. P1: a vendor-sourced 'out-of-the-box' liver PDFF protocol. Each site ran P1 'as is', using default parameters for GE's IDEAL-IQ, Siemens' LiverLab, and Philips' mDIXON-Quant. P2: a complex-based QIBA recommended protocol. P3: a magnitude-based Liver Imaging of Phase-interference signal Oscillation and Quantification protocol. Each site acquired P1-P3 data, which were reviewed by an independent reader. For P1 and P2, each vendor's online multi-fat-peak complex-based data reconstruction algorithm and software was used for PDFF generation, with no modifications to reconstruction parameters. No work-in-progress software was used. For P3, data were sent to an additional independent site for multi-fat-peak magnitude-based reconstruction. A single analyst made all PDFF measurements. Linear regression was performed against reference values.

RESULTS

149 scans of the phantom were performed, 45 on 1.5T (15xP1, 12xP2, 18xP3), and 104 on 3T (33xP1, 24xP2, and 47xP3). Pooled P1 data for 1.5T: (slope=0.97, bias=0.15, r2=0.99), for 3T: (slope=0.99, bias=-0.69, r2=0.99); pooled P2 data for 1.5T: (slope=0.99, bias=-0.35, r2=1.0), for 3T: (slope=1.0, bias=-1.01, r2=0.99); pooled P3 data for 1.5T: (slope=0.96, bias=-0.25, r2=1.0), for 3T: (slope=0.97, bias=-0.02, r2=0.99). Lin's concordance correlation coefficient for all 1.5T data was 0.9973 and 0.9972 for all 3T data.

CONCLUSION

Quantitative PDFF data collected in a standardized phantom are accurate using vendor-source and QIBA-recommended complexbased water-fat separation protocols and an independent magnitude-based protocol.

CLINICAL RELEVANCE/APPLICATION

The PDFF from MRI and MRS is a robust and accurate quantitative imaging biomarker of hepatic steatosis across different magnet field strengths, imager manufacturers, and reconstruction methods.

SSA22-04 Effect of Post Labelling Delay on Arterial Spin Labelling

Sunday, Dec. 1 11:15AM - 11:25AM Room: E353A

Participants

Chiu Fung Cheung, BEng,BSC, Hong Kong, Hong Kong (*Abstract Co-Author*) Nothing to Disclose Anson Cm Chau, Hong Kong, Hong Kong (*Abstract Co-Author*) Nothing to Disclose Victor S. Chan, FRCR, MBBS, Hong Kong, Hong Kong (*Presenter*) Nothing to Disclose Yi Wah Eva Cheung, MSc,CMD, Hong Kong, Hong Kong (*Abstract Co-Author*) Nothing to Disclose Henry K. Mak, MBChB, Hong Kong, Hong Kong (*Abstract Co-Author*) Nothing to Disclose

For information about this presentation, contact:

makkf@hku.hk

CONCLUSION

Single PLD ASL is a robust technique in obtaining CBF values but the accuracy is still confounded by the PLD settings. This study showed that CBF values at different PLD could be significantly different. 2000ms was the most appropriate settings (27/29 cases) which agreed well with the white paper. We also noticed that ATA signs could present after 2000ms. Radiographers should take up the role in real time image interpretation. If ATA were spotted, repeated examination with a longer PLD would be necessary.

Background

Arterial Spin Labelling (ASL) is a MRI perfusion technique utilizing magnetically labelled blood as endogenous tracers. Post Labelling Delay (PLD) is applied to ensure an equilibrium state is reached. However, a short PLD could not ensure an equilibrium state while a long PLD could lead to reduced SNR. Failure to account for could compromise the accuracy.

Evaluation

29 dementia patients in December 2018 were prospectively recruited. Pseudo-continuous ASL was acquired in a 3T scanner (Achieva, Philips Healthcare) with 3 PLD settings (TR=4000ms, TE=11ms, labeling-duration=1600ms, PLD=1800/2000/2500ms). Data analysis were done by MRIcloud online.

Discussion

Recommended single compartment model should give the same CBF values regardless of the PLD settings but our data showed that CBF values at each PLD were significantly different (Repeated measures ANOVA, p=0.000). After referencing with the buxton's kinetic model, 5 conditions were recognized and summarized in the figure. 2 cases showed 'steady state' in which CBF values were similar at each PLD. 10 cases showed 'ATA effects' in which equilibrium was reached after 2000ms. CBF values at 1800ms was erroneous as it violated the model assumption. 9 cases showed 'SNR penalty' in which there might be measurement errors due to reduced SNR at 2500ms leading to abnormally low CBF values. CBF values could not converge in the remaining 8 cases.'Mixed effects' (n=6) might be due to a combination of 'ATA effects' and 'SNR penalty' where 2000ms, theoretically, would be the acceptable setting. In 'severe ATA effects' (n=2), CBF values at 2000ms were abnormally high due to an incorrect model inversion. 2500ms would be the appropriate choice.

SSA22-05 Using Water-In-Oil Emulsions in Phantom for Quality Control of Diffusion-Weighted Magnetic

Resonance Imaging

Sunday, Dec. 1 11:25AM - 11:35AM Room: E353A

Participants Kristina Sergunova, Moscow, Russia (*Presenter*) Nothing to Disclose Ekaterina S. Ahmad, Moscow, Russian Federation (*Abstract Co-Author*) Nothing to Disclose Alexey Petryaikin, MD,PhD, Moscow, Russian Federation (*Abstract Co-Author*) Nothing to Disclose Stanislav A. Kivasev, Moscow, Russian Federation (*Abstract Co-Author*) Nothing to Disclose Nikolay V. Anisimov, Moscow, Russian Federation (*Abstract Co-Author*) Nothing to Disclose Dmitriy S. Semenov, Moscow, Russian Federation (*Abstract Co-Author*) Nothing to Disclose Iurii Vasilev, MD, Saint Petersburg, Russia (*Abstract Co-Author*) Nothing to Disclose Anton V. Vladzymyrskyy, MD,PhD, Moscow, Russia (*Abstract Co-Author*) Nothing to Disclose Sergey Morozov, MD,MPH, Moscow, Russia (*Abstract Co-Author*) Clinical Advisory Board, Agfa-Gevaert Group Clinical Advisory Board, Bayer AG

For information about this presentation, contact:

ska@rpcmr.org.ru

sergunova@npcmr.ru

CONCLUSION

We developed a phantom containing control substances with predefined apparent diffusion coefficients ranging from normal tissue to benign and malignant lesions. The use of W/O emulsions as a part of the phantom allowed modeling a restricted diffusion represented in the image by a high-intensity signal in a wide range of the b-value. The proposed substances also allow evaluating the effectiveness of fat suppression.

Background

To control the quality of diffusion-weighted magnetic resonance imaging (DWI), phantoms with control substances (with stable physical characteristics and known diffusion coefficients) are used. According to literature, aqueous solutions of polymer are used to achieve different diffusion coefficients. These materials model only hindered diffusion, while the diffusion of water molecule inside the cell is restricted. In this work we give results of combination water-in-oil (W/O) emulsions and polymer solutions to model not only restricted, but also hindered diffusion.

Evaluation

As a hindered diffusion model, we used aqueous solutions of polyvinylpyrrolidone (PVP) with concentrations of 0-50%. We created W/O emulsions to simulate a restricted diffusion based on substances with high time T2 - siloxanes: cyclomethicone (Cycl) and caprylyl methicone (Cap). We chose emulsions with equal proportions of water/fatty phases: 1:1 Cap:Water and 1:1 Cycl:Water. According to the dispersion analysis, the size of micelles in the emulsions was $4.8\pm1.8 \mu$ m. The apparent diffusion coefficient (ADC) of emulsion depends on the true diffusion coefficient inside micelles and the time interval between diffusion gradients Δ . We also included silicon oil in phantom to control fat suppression. To estimate the effectiveness of phantom, we scanned it on different MR scanners.

Discussion

With the increase of Δ from 44.4 ms to 60 ms, we restated the decrease of ADC of emulsion by 0.02 μ m2/ms, whereas this effect wasn't observed for water and Cap. True diffusion coefficients of material were determined with the accuracy of 4%. When comparing the ADC results of different MR scanners, the mean variation reached 5.1%, and the relative error was 9.3%. The use of correction factor allow decreasing the error to 2.5 %.

SSA22-06 Improvement of Late Gadolinium Enhancement Image Quality Using a Novel, Deep Learning Based, Reconstruction Algorithm and Its Influence on Myocardial Scar Quantification

Sunday, Dec. 1 11:35AM - 11:45AM Room: E353A

Participants

Nikki van der Velde, MD, Rotterdam, Netherlands (*Presenter*) Nothing to Disclose Brendan Bakker, Rotterdam, Netherlands (*Abstract Co-Author*) Nothing to Disclose Carlijne Hassing, MD,PhD, Rotterdam, Netherlands (*Abstract Co-Author*) Nothing to Disclose Piotr A. Wielopolski, PhD, Rotterdam, Netherlands (*Abstract Co-Author*) Nothing to Disclose R. Marc Lebel, Calgary, AB (*Abstract Co-Author*) Employee, General Electric Company Martin A. Janich, PhD, Munich, Germany (*Abstract Co-Author*) Employee, General Electric Company; Stockholder, General Electric Company Ricardo P. Budde, MD,PhD, Rotterdam, Netherlands (*Abstract Co-Author*) Nothing to Disclose

A. Hirsch, MD,PhD, Rotterdam, Netherlands (Abstract Co-Author) Research Grant, General Electric Company

For information about this presentation, contact:

n.vandervelde.1@erasmusmc.nl

PURPOSE

The aim of this study was 1) to evaluate myocardial late gadolinium enhancement (LGE) image quality using a deep learning (DL) based magnetic resonance image reconstruction algorithm and 2) to assess its effect on the quantification of myocardial scar.

METHOD AND MATERIALS

Thirty-five patients (46±17y, 51% male) with suspected ischemic or non-ischemic cardiomyopathy underwent cardiovascular magnetic resonance imaging (CMR) with gadolinium contrast (0.15 to 0.2 mmol/kg; Gadovist) on a 1.5T scanner (SIGNA Artist, GE Healthcare). Short axis 2D LGE images were reconstructed twice: once with the vendor standard reconstruction, and once with vendor supplied DLRecon prototype. The DL reconstruction is based on a deep convolutional residual encoder network trained from a database of over 10.000 images to reconstruct images with high signal-to-noise ratio (SNR) and high spatial resolution. The

network offered tunable noise reduction (NR) factors from 0-100% to accommodate user preference. Two observers scored image quality and myocardial nulling of both original images and reconstructed images with 75% NR level using a 5 point scale (1=poor to 5=excellent). SNR and contrast-to-noise ratio (CNR) were measured. In 20 patients with LGE, scar size was quantified using thresholding by 2, 4, and 6 standard deviation (SD) above remote myocardium, and using full width at half maximum (FWHM) technique in images with 25%, 50%, 75% and 100% NR levels.

RESULTS

Both image quality and myocardial nulling improved by DLRecon method $(3.3\pm0.6 \text{ vs. } 3.7\pm0.6, p<0.001 \text{ and } 3.3\pm0.6 \text{ vs. } 3.4\pm0.6, p=0.03)$. SNRscar and CNRscar-remote increased significantly with 150% and 158%, respectively at a NR level of 75% (both p<0.001). Due to reduction in noise, scar size increased significantly with increasing NR levels using SD methods, however with the FWHM method no difference in scar size was found (figure).

CONCLUSION

Using a novel, deep learning based, reconstruction algorithm myocardial LGE image quality improved significantly. However, these algorithms have important impact on scar size quantification depending on technique used. The FWHM method is preferred because it is independent of the level of noise.

CLINICAL RELEVANCE/APPLICATION

LGE by CMR is the gold-standard technique for assessing myocardial scar and by using a novel, deep learning based, image reconstruction algorithm image quality can be improved.

SSA22-07 Comparison Between Readout Segmented Diffusion Weighted Imaging and Single Shot Echo Planar Imaging in Image Quality

Sunday, Dec. 1 11:45AM - 11:55AM Room: E353A

Participants

Chuangbo Yang, MMed, Xianyang City, China (*Presenter*) Nothing to Disclose Yongjun Jia, MMed, Xianyang, China (*Abstract Co-Author*) Nothing to Disclose Shan Dang, Xianyang, China (*Abstract Co-Author*) Nothing to Disclose Qi Yang, Xianyang, China (*Abstract Co-Author*) Nothing to Disclose Guangming Ma, Xianyang, China (*Abstract Co-Author*) Nothing to Disclose Jun Wang, Xianyang, China (*Abstract Co-Author*) Nothing to Disclose Zhou Xiaorong Z. Zhou Xiaorong I, ARRT, ARRT, Xianyang, China (*Abstract Co-Author*) Nothing to Disclose Shutong Liu, Xianyang, China (*Abstract Co-Author*) Nothing to Disclose Lanxin Zhang, Xianyang, China (*Abstract Co-Author*) Nothing to Disclose

PURPOSE

To compare difference of readout segmented diffusion weighted imaging (RS-EPI) and single shot echo planar imaging (SS-EPI) on image quality with ultra-high b value for prostate cancer detection.

METHOD AND MATERIALS

37 patients with prostate disease who underwent both RS-EPI and SS-EPI were enrolled in this study. All data were collected on a 3T MR scanner (MAGNETOM Skyra, Siemens Healthcare, Erlangen, Germany) with the b value of 0, 1000,2000, 3000s/mm2. The image quality including lesions clarity, anatomical distortion, image sharpness, detail display based on diffusion weighted imaging (DWI) were classified according to Likert score into 1 to 5 grade.(Grade 1 : cannot be used for diagnosis; Grade 2: poor; Grade 3: acceptable; Grade 4: good; Grade 5: very good.) All the images were analyzed by two experienced radiologists blinded to any clinical information as well as MR sequence type. The classification was provided from two radiologists separately. The signal-tonoise ratio (SNR), and contrast ratio, and contrast to noise ratio (CNR) were also measured on workstations by the radiologist.

RESULTS

The scores concluded by the two radiologists have good consistency, Kappa value>0.80. The image quality including lesions clarity, anatomical distortion, image sharpness, detail display obtained from RS-EPI sequences were higher than those obtained from SS-EPI regardless of 1000, 2000, 3000s/mm2 (P<0.001). The signal-to-noise ratio (SNR), and contrast ratio, and contrast to noise ratio (CNR) measured on RS-EPI sequences were also higher than those measured on SS-EPI (P<0.001) (table1).

CONCLUSION

Compared with the SS-EPI sequence, ultra-high b value RS-EPI sequence significantly improves the image quality, which is more conducive to the detection of prostate lesions.

CLINICAL RELEVANCE/APPLICATION

Compared with the SS-EPI sequence, ultra-high b value RS-EPI sequence significantly improves the image quality, which is more conducive to the detection of prostate lesions.

SSA22-08 Radiologic Technologists' Decision-Making for Protocol Repetition in Whole-Body MR Imaging and the Potential for Automated Image Quality Assessment: A Large Population-Based Cohort Study

Sunday, Dec. 1 11:55AM - 12:05PM Room: E353A

Participants

Ricarda V. von Kruchten, MD, Heidelberg, Germany (*Presenter*) Nothing to Disclose Christopher Schuppert, MD, Heidelberg, Germany (*Abstract Co-Author*) Nothing to Disclose Jochen Hirsch, Bremen, Germany (*Abstract Co-Author*) Nothing to Disclose Daniel Hoinkiss, Bremen, Germany (*Abstract Co-Author*) Nothing to Disclose Sonja Selder, Munich, Germany (*Abstract Co-Author*) Nothing to Disclose Oyunaa von Stackelberg, Heidelberg, Germany (*Abstract Co-Author*) Nothing to Disclose Hans-Ulrich Kauczor, MD, Heidelberg, Germany (*Abstract Co-Author*) Nothing to Disclose Fabian Bamberg, MD, Tuebingen, Germany (*Abstract Co-Author*) Speakers Bureau, Bayer AG; Speakers Bureau, Siemens AG;

PURPOSE

Cost-effectiveness in health care delivery and diagnostic medical imaging have become increasingly important. Such considerations are relevant when repeating protocols in Whole-Body MR imaging, especially when conducting large cohort studies. We studied the frequency of protocol repetition by radiologic technologists who performed whole-body MR imaging protocols in the multi-center German National Cohort (GNC), and the impact of automation on the need for protocol repetition, considering the local, staffing, and technical factors involved. Additionally, we studied its impact on scan time, automated image quality assessment, and protocol repetition.

METHOD AND MATERIALS

A total of 11,347 subjects underwent whole-body MRI as part of the MR sub-study of the GNC cohort (2014-2016). Whole-body imaging was conducted at five sites using a uniform set of twelve protocols. Image acquisitions were independently conducted by radiologic technologists (RT), whose decisions for protocol repetition was compared with image quality parameters that were automatically derived.

RESULTS

At least one repeat protocol by the RT occurred in 12% (n=1,365) of subjects. The frequency of repetition differed across protocols (p<0.0001), and across sites (range: 5.28%-24.34%, p<0.0001), and varied over time (p<0.0001). Mean total scan time of 62.6min increased by 4.8min (95%CI: 4.5-5.2min) in subjects needing protocol repetition. The automatically-derived image quality parameters that retrospectively predicted the need for protocol repetition included image sharpness and signal-to-noise ratio. However, their predictive value was not uniform across all protocols.

CONCLUSION

The need to repeat MR protocols, even in highly standardized settings such as population study cohorts, is highly prevalent. Our findings indicate that automated image quality assessment has predictive value, and reduces the need for protocol repetition, thereby improving workflow efficiency and cost-effectiveness in the conduct of such studies.

CLINICAL RELEVANCE/APPLICATION

Patients find MRI studies daunting, hence MRI protocol repetition by radiologic technologists increase not only costs, but also patient discomfort. Automation of MRI image workflow has the potential to improve both.

SSA22-09 An Experimental Study of MRI Induced Heating in Conductive Loops

Sunday, Dec. 1 12:05PM - 12:15PM Room: E353A

Participants

Wing-Chi E. Kwok, PhD, Rochester, NY (*Presenter*) Nothing to Disclose William Badger, Rochester, NY (*Abstract Co-Author*) Nothing to Disclose

For information about this presentation, contact:

edmund_kwok@urmc.rochester.edu

edmund_kwok@urmc.rochester.edu

CONCLUSION

This work indicates that size and presence of a gap are factors to consider in the risk assessment of piercings. It has important implication for dermal piercings since there may be unknown gap in the piercing under the skin.

Background

Patients who are unable or reluctant to remove metallic piercings before MRI are at risk of injuries due to magnetic force and radiofrequency (RF) heating. While magnetic force risk can be reduced by screening with a ferromagnetic detector, it is harder to assess the risk of RF burn from piercing. The purpose of this investigation is to conduct experiments to evaluate the relationship of RF heating with the size and configuration of conductive loops to provide a better understanding of the factors related to RF heating in piercings.

Evaluation

The study was conducted on a GE 3T MR system. Circular loops of diameter 5cm, 8cm and 11cm with an air gap of 0, 0.3mm or 2.5mm for each diameter were constructed from copper wire (gauge 10). They were placed one at a time horizontally in a container with the loop touching the skin of a pig knuckle specimen at the loop gap position. The setup was mounted on top of a 27cm spherical phantom and scanned using a fast spin echo sequence for 10:33 minutes. Temperature at the contact point between each loop and the specimen skin was measured with a Philips patient monitor temperature sensor. The results show temperature rise of 1.4 and 1.8 deg C in the 8cm loops with a gap of 0.3mm and 2.5mm respectively, and temperature rise of 5.0 and 5.2 deg C in the 11cm loops with a gap of 0.3mm and 2.5mm respectively. There was no measured temperature increase in all loops with zero gap and in the 5cm loops with a gap.

Discussion

This study shows that RF heating risk increases with the size of conducting loops and with the presence of a gap. The result indicates high induced electric field at the gap of the larger loops causes current to flow in the skin with high resistance leading to the heating. However, this study does not imply MRI safety for piercings smaller than a certain size or without a gap since RF heating depends also on other factors and settings not covered in this study.







AI12

AI Theater: Japan's Startup Unlocking the Power of AI: Presented by LPIXEL, Inc.

Sunday, Dec. 1 11:00AM - 11:20AM Room: AI Showcase, North Building, Level 2, Booth 10724

Participants

Mariko Takahashi, DDS, Tokyo, Japan (Presenter) Nothing to Disclose

Program Information

LPIXEL is a University of Tokyo spin-off that hones its expertise in AI and medical imaging analytics. As the leading medical AI startup in Japan, LPIXEL has made significant progress in delivering its AI-driven medical image diagnostic technology, 'EIRL,' to hospitals and medical institutions across Japan and overseas. This session will touch on LPIXEL's key highlights of this year, which will include the most up to date information of its AI-powered diagnostic algorithms which focus on brain MRA/MRI, chest X-ray and CT, breast mammography, colonoscopy and more. Other highlights include participating in the Japan Medical Image Database (JMID) project for the development and implementation of the AI annotation tool, and receiving marketing certification in Japan for its diagnostic algorithms which target brain MR images. Join LPIXEL for even more, and how AI in medical imaging is leading the new generation of healthcare. For a personal demonstration of our algorithm, please visit our booth #11703.





AI16

AI Theater: Comparing Acceleration of MRI Brain Scans: Compressed Sensing and AI-assisted Image Processing Technologies: Presented by Medic Vision

Sunday, Dec. 1 1:00PM - 1:20PM Room: AI Showcase, North Building, Level 2, Booth 10724

Participants

Lawrence N. Tanenbaum, MD, Riverside, CT (*Presenter*) Speaker, General Electric Company; Speaker, Siemens AG; Speaker, Guerbet SA; Speaker, Koninklijke Philips NV; Consultant, Enlitic, Inc; Consultant, icoMetrix NV; Consultant, Subtle Medical; Consultant, Arterys Inc

Program Information

Reducing MR scan time allows significant benefits, including fewer repeating scans due to patient's movement, increased efficiency and productivity. However, MR constitutes an inherent trade-off between scan time and image quality. Hence, when scan time is reduced, image resolution, contrast, signal-to-noise ratio (SNR), and appearance of artifacts, among other characteristics, can be adversely affected. Thus, the distinct need for a solution that can enable faster MRI scans without affecting the image quality. Consequently, in the past decades, there has been a concerted effort to develop fast imaging techniques, while maintaining diagnostic image guality. During the past few years, new approaches have become available, the latest being Compressed Sensing (CS), a new under-sampling technique, in which only the information required for reconstruction is collected, facilitating significant reduction in acquisition time. Currently available CS-based functions include Philips Compressed SENSE, GE HyperSense and Siemens Compressed Sensing. Iterative image reconstruction (IIR) technology has been used for more than 10 years to allow dose reduction in CT scanners. In MRI, IIR presents a new approach to scan time reduction. In IIR, less data is acquired during the scan, resulting in a faster acquisition time, but producing poor-quality and noisy images. These non-diagnostic images are then post-processed by strong image reconstruction and enhancement algorithms, aimed to produce high-quality diagnostic-worthy images. This presentation showcases a comparison case report on CS and AI - assisted IIR, in the ability to reduce MR scan time while maintaining image quality. Specifically, Philips Compressed SENSE, GE HyperSense (CS technology), and Medic Vision iQMR (AIassisted IIR technology) are compared and evaluated. The case report compared complete brain exams that were acquired by the site's routine scan (11 minutes 50 seconds) and by accelerated acquisition (5 minutes 50 seconds, 50% scan time reduction). Acquired images were processed and reviewed blindly by acknowledged neuroradiologists. The results demonstrate definite preference towards AI- assisted IIR-processed fast MR scans, for all evaluation characteristics.

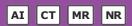




SPAI12

RSNA AI Deep Learning Lab: Segmentation

Sunday, Dec. 1 1:00PM - 2:30PM Room: AI Showcase, North Building, Level 2, Booth 10342



AMA PRA Category 1 Credits ™: 1.50 ARRT Category A+ Credit: 1.75

Participants

George L. Shih, MD, New York, NY (*Presenter*) Consultant, Image Safely, Inc; Stockholder, Image Safely, Inc; Consultant, MD.ai, Inc; Stockholder, MD.ai, Inc;

Special Information

In order to get the best experience for this session, it is highly recommended that attendees bring a laptop with a keyboard, a decent-sized screen, and the latest version of Google Chrome. Additionally, it is recommended that attendees have a basic knowledge of deep learning programming and some experience running a Google CoLab notebook. Having a Gmail account is also helpful. Here are instructions for creating and deleting a Gmail account.

ABSTRACT

This session will focus on the use of deep learning methods for image segmentation, applied to the challenge of CT or MR brain segmentation. While focused on this particular problem, the concepts should generalize to other organs and image types.







VW14

A Practical Approach to Breast Magnetic Resonance Imaging (MRI) Interpretation: Presented by Siemens Healthineers

Sunday, Dec. 1 1:05PM - 2:15PM Room: North Building, Booth 8563

Participants

Susan Weinstein, MD, Philadelphia, PA (Presenter) Nothing to Disclose

Program Information

This interactive session will include both didactic and hands-on case review at workstations equipped with *syngo*. MR Brevis. A practical approach to breast MRI interpretation will be discussed as well as utilizing the available sequences and techniques to improve interpretive skills. *RSVP is required; adding this session to your agenda does not secure your seat in this session. Click the link below to RSVP.*

RSVP

https://www.fairorg.de/Siemens-Healthineers/portal/workshop.cfm/rsna19/







Advanced Muscle Imaging: State of the Art

Sunday, Dec. 1 2:00PM - 3:30PM Room: E450A



AMA PRA Category 1 Credits ™: 1.50 ARRT Category A+ Credit: 1.75

Participants

Robert D. Boutin, MD, Davis, CA (Director) Nothing to Disclose

LEARNING OBJECTIVES

1) Assess state-of-the-art imaging techniques for diagnosis of acute and chronic muscle derangements, with an emphasis on MRI, CT, and sonography.

Sub-Events

RC104A Acute Muscle Injuries: MRI Protocol, Classification, and Prognosis

Participants James M. Linklater, MBBS, St Leonards , Australia (*Presenter*) Nothing to Disclose

For information about this presentation, contact:

JamesLinklater@casimaging.com

LEARNING OBJECTIVES

1) Define the musculo-tendinous anatomy of the hamstring, quadriceps, adductor and gastrocnemius-soleus muscle groups. 2) Define efficient, sensitive MRI protocols to assess for acute muscle injuries in the lower extremities. 3) Identify on imaging and classify patterns of injury to the hamstring, quadriceps, adductor and gastrocnemius-soleus muscle groups. 4) Understand classification and grading systems used in the evaluation of acute muscle injuries in the lower extremities and their potential value in determining prognosis regarding return to sport.

Active Handout: James MacPherson Linklater

http://abstract.rsna.org/uploads/2019/19000728/Active RC104A.pdf

RC104B Chronic Muscle Conditions: A Practical Approach

Participants Robert D. Boutin, MD, Davis, CA (*Presenter*) Nothing to Disclose

LEARNING OBJECTIVES

1) Review chronic muscle derangements and apply knowledge using a case-based approach, with an emphasis on practical differential diagnostic patterns.

RC104C MRI versus Ultrasound of Muscle: Choosing When and How

Participants Kambiz Motamedi, MD, Los Angeles, CA (*Presenter*) Nothing to Disclose

For information about this presentation, contact:

kmotamedi@mednet.ucla.edu

LEARNING OBJECTIVES

1) Identify the appropriate diagnostic imaging modality for common muscle pathologies. 2) Describe normal and abnormal ultrasound appearance of muscle. 3) Compare imaging characteristics of muscle pathology on MRI versus ultrasound.

Active Handout:Kambiz Motamedi

http://abstract.rsna.org/uploads/2019/19000731/Active RC104C.pdf

Active Handout:Kambiz Motamedi

http://abstract.rsna.org/uploads/2019/19000731/Active RC104C.pdf

RC104D Muscle Ischemia, Infarction, and Compartment Syndrome

Participants

Michael D. Ringler, MD, Rochester, MN (Presenter) Nothing to Disclose

LEARNING OBJECTIVES

4) Recorded for discussion data a contract of the contract of the contract for the contract of the books of the contract of th

1) Recognize imaging findings associated with common clinical syndromes involving muscle ischemia, including compartment syndrome. 2) Differentiate appearance of irreversible myonecrosis from treatable ischemia. 3) Design an MR protocol for Chronic Exertional Compartment Syndrome.

RC104E Imaging of Muscle Quality: Myosteatosis Revisited

Participants Leon Lenchik, MD, Winston-Salem, NC (*Presenter*) Nothing to Disclose

For information about this presentation, contact:

llenchik@wakehealth.edu

LEARNING OBJECTIVES

1) Discuss the imaging diagnosis of myosteatosis and its relation to muscle quality.







Abbreviated/Faster MRI Abdominal Pelvic Protocols

Sunday, Dec. 1 2:00PM - 3:30PM Room: E450B



AMA PRA Category 1 Credits ™: 1.50 ARRT Category A+ Credit: 1.75

Participants

Claude B. Sirlin, MD, San Diego, CA (*Moderator*) Research Grant, Gilead Sciences, Inc; Research Grant, General Electric Company; Research Grant, Siemens AG; Research Grant, Bayer AG; Research Grant, Koninklijke Philips NV; Consultant, AMRA AB; Consultant, Fulcrum; Consultant, IBM Corporation; Consultant, Exact Sciences Corporation; Consultant, Boehringer Ingelheim GmbH; Consultant, Arterys Inc; Consultant, Epigenomics; Author, Medscape, LLC; Lab service agreement, Gilead Sciences, Inc; Lab service agreement, ICON plc; Lab service agreement, Intercept Pharmaceuticals, Inc; Lab service agreement, Shire plc; Lab service agreement, Enanta; Lab service agreement, Takeda Pharmaceutical Company Limited; Lab service agreement, Alexion Pharmaceuticals, Inc; Lab service agreement, NuSirt Biopharma, Inc

Sub-Events

RC109A Hepatocellular Carcinoma Screening

Participants

Claude B. Sirlin, MD, San Diego, CA (*Presenter*) Research Grant, Gilead Sciences, Inc; Research Grant, General Electric Company; Research Grant, Siemens AG; Research Grant, Bayer AG; Research Grant, Koninklijke Philips NV; Consultant, AMRA AB; Consultant, Fulcrum; Consultant, IBM Corporation; Consultant, Exact Sciences Corporation; Consultant, Boehringer Ingelheim GmbH; Consultant, Arterys Inc; Consultant, Epigenomics; Author, Medscape, LLC; Lab service agreement, Gilead Sciences, Inc; Lab service agreement, ICON plc; Lab service agreement, Intercept Pharmaceuticals, Inc; Lab service agreement, Shire plc; Lab service agreement, Enanta; Lab service agreement, Takeda Pharmaceutical Company Limited; Lab service agreement, Alexion Pharmaceuticals, Inc; Lab service agreement, NuSirt Biopharma, Inc

For information about this presentation, contact:

csirlin@ucsd.edu

LEARNING OBJECTIVES

1) Explain the need for HCC screening in adults with cirrhosis. 2) Explain the limitations of ultrasound for HCC screening in adults with cirrhosis, in particular adults with overweight or obesity. 3) Explain one approach for abbreviated MRI for HCC screening as a potential alternative to ultrasound.

RC109B Pancreatic Tumor Evaluation and Follow-up

Participants Kumaresan Sandrasegaran, MD, Phoenix, AZ (*Presenter*) Nothing to Disclose

For information about this presentation, contact:

sandrasegaran.kumaresan@mayo.edu

LEARNING OBJECTIVES

1) Understand pitfalls in diagnosing, staging and post-therapy assessment of pancreatic ductal adenocarcinoma (PDAC). 2) Understand what the surgeon and oncologist want from a staging CT/MRI report. 3) Learn to use standardized reporting template for staging PDAC.

ABSTRACT

This presentation covers the diagnosis and staging of pancreas cancer (pancreatic ductal adenocarcinoma). There are multiple pitfalls in the diagnosis of pancreas cancer and these are highlighted. The staging of pancreas cancer has changed in recent years because of advances in surgical and oncologic therapy. Radiologists need to be aware of these developments, so that accurate information may be reported. The value of standardized reporting is discussed.

RC109C Faster MR Enterography

Participants Michael S. Gee, MD, PhD, Boston, MA (*Presenter*) Nothing to Disclose

LEARNING OBJECTIVES

1) To comprehend the indications for MR enterography. 2) To apply structured interpretation and reporting of MR enterography studies. 3) To apply new techniques for decreasing MR enterography scan time.

ABSTRACT

None.

RC109D Raticipation Staging

Michael H. Rosenthal, MD, PhD, Boston, MA (Presenter) Nothing to Disclose

LEARNING OBJECTIVES

1. Understand best practices for MR imaging of rectal cancer at diagnosis. 2. Learn and apply diagnostic criteria to accurately stage rectal adenocarcinomas using MRI. 3. Understand common pitfalls in the interpretation of rectal MRI.





Peripheral Artery Disease: CTA and MRA (Interactive Session)

Sunday, Dec. 1 2:00PM - 3:30PM Room: S404CD



AMA PRA Category 1 Credits ™: 1.50 ARRT Category A+ Credit: 1.75

FDA Discussions may include off-label uses.

Participants

Constantino S. Pena, MD, Key Biscayne, FL (*Moderator*) Speakers Bureau, Cook Group Incorporated; Speakers Bureau, Medtronic plc; Speakers Bureau, W. L. Gore & Associates, Inc; Speakers Bureau, Penumbra, Inc; Speakers Bureau, Terumo Corporation; Speakers Bureau, Merit Medical Systems, Inc; Advisory Board, C. R. Bard, Inc; Advisory Board, Boston Scientific Corporation; Stephan Clasen, MD, Tuebingen, Germany (*Moderator*) Nothing to Disclose

For information about this presentation, contact:

stephan.clasen@med.uni-tuebingen.de

Special Information

This interactive session will use RSNA Diagnosis Live[™]. Please bring your charged mobile wireless device (phone, tablet or laptop) to participate.

LEARNING OBJECTIVES

1) Describe techniques for acquisition, reconstruction, and image interpretation of peripheral CTA and MRA. 2) Discuss available data and evidence-based results for peripheral CTA and MRA, and expected impact on patient care. 3) Compare advantages and drawbacks of lower extremity CTA and MRA.

Sub-Events

RC112A Interventional Procedure Planning: Role for CTA and MRA

Participants

Constantino S. Pena, MD, Key Biscayne, FL (*Presenter*) Speakers Bureau, Cook Group Incorporated; Speakers Bureau, Medtronic plc ; Speakers Bureau, W. L. Gore & Associates, Inc; Speakers Bureau, Penumbra, Inc; Speakers Bureau, Terumo Corporation; Speakers Bureau, Merit Medical Systems, Inc; Advisory Board, C. R. Bard, Inc; Advisory Board, Boston Scientific Corporation;

LEARNING OBJECTIVES

1) Understand the value of peripheral CTA and MRA. 2) Discuss the benefits of CTA in comparison to MRA in the treatment of PAD. 3) Comprehend the importance of MRA sequences to highlight particular details in peripheral MRA. 4) Understand the importance of image reconstruction for peripheral CTA and MRA.

RC112B Peripheral CTA

Participants Stephan Clasen, MD, Tuebingen, Germany (Presenter) Nothing to Disclose

For information about this presentation, contact:

stephan.clasen@med.uni-tuebingen.de

LEARNING OBJECTIVES

1) Describe techniques for acquisition, reconstruction, and image interpretation of peripheral CTA. 2) Discuss available data and evidence-based results for peripheral CTA, and expected impact on patient care. 3) Compare advantages and drawbacks of lower extremity CTA in comparison to other imaging modalities and diagnostic tools for arterial occlusive disease.

ABSTRACT

Peripheral arterial disease (PAD) is a common cause of morbidity and mortality in developed countries. Traditionally, imaging for risk stratification and therapeutic planning involved catheter angiography. In recent years, cross-sectional imaging by CTA and MRA has proven a robust technique for non-invasive PAD assessment. Given ubiquity of CT scanning technology, CTA is widely available. High resolution datasets can be acquired rapidly, which facilitates assessment of clinically labile or trauma patients. To be optimally effective, CTA techniques require particular attention to contrast medium and scan protocol. With appropriate protocol design, data acquisition requires limited operator dependence. The acquired 3D dataset is rich with information, but requires careful scrutiny by the interpreting physician. Volumetric review of these datasets produces the most accurate results. Extensive small vessel calcification remains a potential barrier to full assessment of pedal vessels by CTA. Recent published data validates the clinical effectiveness of CTA for diagnosis of PAD and for the direction of treatment planning. Ongoing research aims to exploit the newest generation of CT scanners to acquire additional information, including dual energy data, time-resolved information, and radiation dose savings.

Participants

James C. Carr, MD, Chicago, IL (*Presenter*) Research Grant, Siemens AG; Advisory Board, Siemens AG; Travel support, Siemens AG; Advisory Board, General Electric Company; Speaker, General Electric Company; Research Grant, Bayer AG; Advisory Board, Bayer AG; Travel support, Bayer AG; Speaker, Bayer AG; Research Grant, Guerbet SA; Advisory Board, Guerbet SA; Travel support, Guerbet SA; Consultant, Circle; Speaker, Circle

RC112D Interventional Complications: Role for CTA and MRA

Participants

Charles Y. Kim, MD, Raleigh, NC (Presenter) Consultant, Medtronic plc; Consultant, Humacyte; Consultant, Galvani

For information about this presentation, contact:

charles.kim@duke.edu

LEARNING OBJECTIVES

1) Understand decision making for assessment of stent patency with CTA vs MRA 2) Describe endovascular aneurysm repair with endografts as well as types of endoleaks and associated implications. 3) Discuss current methods for optimal detection endoleaks with CTA and MRA, with understanding of advantages and disadvantages.

ABSTRACT

Stents are used ubiquitously for the management of atherosclerotic lesions in peripheral arterial disease. While symptomology is an important metric, noninvasive imaging is also a crucial tool for more detailed assessment. Both CTA and MRA have been validated for the assessment of stent patency, although there are nuances for both modalities, and in certain circumstances, one may outperform the other. Imaging of endoleaks has evolved over the past two decades, to include a multitude of techniques with CTA and MRA. While national guidelines for post-EVAR surveillance are relatively unidimensional, it is important for the practicing radiologist to understand the spectrum of available CT and MR techniques for detection of endoleaks, along with the advantages and disadvantages to each approach.





Advanced MRI Applications

Sunday, Dec. 1 2:00PM - 3:30PM Room: E353C



AMA PRA Category 1 Credits ™: 1.50 ARRT Category A+ Credit: 1.75

Participants

Christopher E. Comstock, MD, New York, NY (Moderator) Nothing to Disclose

For information about this presentation, contact:

zuleyml@upmc.edu

Sub-Events

RC115A AB-MRI

Participants Christopher E. Comstock, MD, New York, NY (*Presenter*) Nothing to Disclose

For information about this presentation, contact:

comstocc@mskcc.org

LEARNING OBJECTIVES

1) Describe the concept of Abbreviated Breast MRI (AB-MR) in screening average risk women with dense breasts. 2) Review the current data on the performance of AB-MR compared to DBT and WBUS. 3) Appropriately characterize lesions found on AB-MR and improve interpretation accuracy.

RC115B Ultrafast MRI

Participants

Ritse M. Mann, MD, PhD, Nijmegen, Netherlands (*Presenter*) Researcher, Siemens AG ; Researcher, Seno Medical Instruments, Inc; Researcher, Identification Solutions, Inc; Researcher, Micrima Limited; Researcher, Medtronic plc; Scientific Advisor, ScreenPoint Medical BV; Scientific Advisor, Transonic Imaging, Inc; Stockholder, Transonic Imaging, Inc

LEARNING OBJECTIVES

1) To design a breast MRI protocol incorporating ultrafast breast MRI. 2) To learn how to interpret ultrafast breast MRI. 3) To understand the clinical value of ultrafast breast MRI in lesion detection and classification.

RC115C DWI and Multiple Parametric Imaging

Participants

Katja Pinker-Domenig, MD, New York, NY (Presenter) Nothing to Disclose

For information about this presentation, contact:

pinkerdk@mskcc.org

LEARNING OBJECTIVES

1) Describe the principle of DWI of the breast. 2) Define the basic requirements for the clinical application of DWI in breast imaging. 3) Understand the role of DWI as an essential part of a multiparametric breast MRI protocol. 4) Use multiparametric breast MRI in clinical practice.

ABSTRACT

Magnetic resonance imaging (MRI) of the breast is undisputedly the most sensitive imaging method to detect cancer, with a higher detection rate than mammography, digital breast tomosynthesis, and ultrasound. To overcome limitations of dynamic contrastenhanced (DCE) MRI in specificity, additional functional MRI parameters have been explored, with diffusion-weighted imaging (DWI) emerging as the most robust and reliable. In DWI, the random movement of water molecules in body tissue can be visualized and quantified by calculating the apparent diffusion coefficient (ADC). Malignancies typically show restricted water molecule diffusivity with higher signal on DWI images and lower signal on ADC maps due to increased cell density, which leads to compression of extracellular space and microstructural changes. Breast DWI can be easily combined with DCE-MRI in every breast MRI protocol without substantially increasing the total scan time, an approach defined as multiparametric MRI. Several studies have demonstrated that multiparametric MRI of the breast biopsies in benign breast tumors. It is therefore increasingly being implemented in clinical routine for an improved cancer detection, characterization and treatment response assessment. Other functional MRI parameters are currently under investigation for the clinical implementation in a multiparametric MRI of the breast in the clinical setting.





Emerging Technology: Imaging of Dementias and Movement Disorders Update 2019

Sunday, Dec. 1 2:00PM - 3:30PM Room: S504CD



AMA PRA Category 1 Credits ™: 1.50 ARRT Category A+ Credit: 1.75

Participants

Rathan M. Subramaniam, MD, PhD, Dunedin, New Zealand (Moderator) Nothing to Disclose

For information about this presentation, contact:

rathan.subramaniam@utsouthwestern.edu

LEARNING OBJECTIVES

1) To review the value of FDG and amyloid PET/CT in diagnosis of dementia. 2) To review the value of MR imaging in diagnosis of dementia. 3) To review the value of tau PET/CT in diagnosis of dementia.

ABSTRACT

This session will review the importance and value of FDG PET, Amyloid PET, MRI and Tau PET imaging in diagnosis of dementia.

Sub-Events

RC117A Imaging Dementias: FDG and Amyloid PET/CT

Participants

Rathan M. Subramaniam, MD, PhD, Dunedin, New Zealand (Presenter) Nothing to Disclose

LEARNING OBJECTIVES

1) Understand which FDA approved MR techniques are currently available for improving differential diagnosis in patients with dementia. 2) Improve basic knowledge of how MR results correspond to clinical dementia phenotypes. 3) Discuss recent technological advances including applications of dynamic susceptibility contrast (DSC) MR, arterial spin labelling (ASL) and resting state functional connectivity MRI (rs-fcMRI) in the setting of patients with dementia.

RC117B Imaging Dementias - Tau PET/CT: Update 2019

Participants

Val J. Lowe, MD, Rochester, MN (*Presenter*) Research Grant, General Electric Company; Research Grant, Siemens AG; Research Grant, Eli Lilly and Company; Advisory Board, Merck & Co, Inc

LEARNING OBJECTIVES

1) Describe the basic science principles behind tau PET/CT imaging. 2) Understand the utility of tau PET/CT imaging in neurodegenerative disease. 3) Identify the findings of a positive tau PET/CT scan.

RC117C Imaging of Movement Disorders: Update 2019

Participants Kevin P. Banks, MD, Joint Base San Antonio , TX (*Presenter*) Nothing to Disclose

For information about this presentation, contact:

kevin.p.banks.civ@mail.mil

LEARNING OBJECTIVES

1) Understand the Parkinsonian Syndrome entities and their clinical features. 2) Analyze the role and efficacy of I-123 Ioflupane Brain SPECT in the diagnosis and management of PS. 3) Learn the essential steps of proper exam preparation and acquisition. 4) Comprehend the interpretation criteria for I-123 Ioflupane Brain SPECT and potential pitfalls.





Interactive Game: Cases in Body Oncologic Imaging that I Have Learned the Most From (Interactive Session)

Sunday, Dec. 1 2:00PM - 3:30PM Room: S102CD

CT MR OI US

AMA PRA Category 1 Credits ™: 1.50 ARRT Category A+ Credit: 1.75

FDA Discussions may include off-label uses.

Participants

Deborah J. Rubens, MD, Rochester, NY (Moderator) Nothing to Disclose

For information about this presentation, contact:

Deborah_rubens@urmc.rochester.edu

Special Information

This interactive session will use RSNA Diagnosis Live[™]. Please bring your charged mobile wireless device (phone, tablet or laptop) to participate.

Sub-Events

RC118A Ultrasound

Participants Deborah J. Rubens, MD, Rochester, NY (*Presenter*) Nothing to Disclose

For information about this presentation, contact:

deborah_rubens@urmc.rochester.edu

LEARNING OBJECTIVES

1) Review some commonly performed examinations where US leads to oncologic diagnosis. 2) Identify those technical parameters which are critical to accurate ultrasound performance, especially color and spectral Doppler, as exemplified by pitfalls and 'missed' cases. 3) Explore the role of US in management of oncologic patients, including contrast enhanced ultrasound.

RC118B Computed Tomography

Participants

Christine O. Menias, MD, Chicago, IL (Presenter) Nothing to Disclose

For information about this presentation, contact:

menias.christine@mayo.edu

LEARNING OBJECTIVES

1) Review CT imaging features of challenging abdominal and pelvic oncologic cases encountered in clinical practice using casebased examples. 2) Highlight the imaging pearls and pitfalls that may impact diagnosis and treatment. 3) Discuss potential differential diagnoses and mimics of oncologic abdominal and pelvic cases.

RC118C Magnetic Resonance Imaging

Participants

Richard Kinh Gian Do, MD, PhD, New York, NY (*Presenter*) Consultant, Bayer AG; Author, Reed Elsevier; Spouse, Author, Wolters Kluwer nv; Spouse, Data Monitoring Committee, Alk Abello

For information about this presentation, contact:

dok@mskcc.org

LEARNING OBJECTIVES

1) Assess the role of diffusion weighted imaging in oncology. 2) Explain the presence of susceptibility artifacts on different MRI sequences. 3) Compare the use of extracellular and hepatobiliary contrast agents for liver MRI.

RC118D PET/CT

Participants Luigi Aloj, MD, Cambridge, United Kingdom (*Presenter*) Nothing to Disclose

For information about this presentation, contact:

la398@cam.ac.uk

LEARNING OBJECTIVES

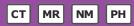
1) Biochemical characterisation of cancer through PET imaging.2) How combinations of radiopharmaceuticals may be relevant to diagnosis.3) Tumour heterogeneity as detected by PET and implications for patient management.4) The role of PET/CT in theragnostics





Innovations in Hybrid Imaging

Sunday, Dec. 1 2:00PM - 3:30PM Room: E351



AMA PRA Category 1 Credits ™: 1.50 ARRT Category A+ Credit: 1.75

Participants

Osama R. Mawlawi, PhD, Houston, TX (Coordinator) Research Grant, General Electric Company Research Grant, Siemens AG

For information about this presentation, contact:

omawlawi@mdanderson.org

LEARNING OBJECTIVES

1) Become more proficient with the latest innovations in PET/CT imaging and their impact of scanner performance. 2) Learn about the challenges and opportunities in PET/MR image quantification and potential clinical applications. 3) Understand the various corrections necessary to generate a quantifiable SPECT image.

ABSTRACT

This sesion will cover the latest innovations in hybrid immaging. The session will have three speakers covering 3 different topics. The first talk will cover the latest in PET/CT imaging including silicon photomultiplier tubes, larger axial fields of view and the effects these innovations have on scanner performance. The second talk will focus on PET/MR imaging and disuss the challenges and opportunities of PET/MR image quantification and potential clinical applications. Finally, the third talk will focus on SPECT/CT image quantification while discussing the various correction factors and processes needed to to generate a quantifiable SPECT image.

Sub-Events

RC121A Innovations in PET/CT

Participants

Osama R. Mawlawi, PhD, Houston, TX (Presenter) Research Grant, General Electric Company Research Grant, Siemens AG

For information about this presentation, contact:

omawlawi@mdanderson.org

LEARNING OBJECTIVES

1) List the latest advances in PET/CT imaging. 2) Understand the impact of these innovations on scanner performance and image quality.b3) Recognize the differences between commercial PET/CT systems with respect to these innovations.

ABSTRACT

This talk will focus on the latest innovations in PET/CT imaging. Topics covered will include silicon photomultiplier (SiPM) tubes, large axial PET scanners, data driven gating, and the impact these innovations have on scanner performance and image quality.

RC121B Opportunities in PET/MR

Participants

Thomas Beyer, PhD, Vienna, Austria (Presenter) Co-founder cmi-experts GmbH; Co-founder Dedicaid GmbH

For information about this presentation, contact:

thomas.beyer@meduniwien.ac.at

LEARNING OBJECTIVES

1) Appreciate benefits and challenges of quantification in PET. 2) Be made aware of the basic principles of fully-integrated PET/MR imaging systems. 3) Understand the fundamental challenges and potential of MR-guided PET quantification. 4) Be pointed to potential applications of fully-integrated PET/MR in clinical research, and possibly routine.

ABSTRACT

PET is a non-invasive imaging technique that provides reproducible and fully-quantitative information on preselected metabolic/signaling pathways. PET is highly sensitive, thus, requiring only small amounts of biomarkers to be used for visualization and quantification purposes. By comparison to high-resolution anatomical images PET images appear blurred, which is attributed to the positron range effects and the limited detector size of the PET ring systems.Today, clinical PET imaging systems are offered almost exclusively in combination with CT and MR systems. Combined PET/MR, in particular, offers a number of intrinsic methodological advantages over PET only. These include, the use of MR imaging (e.g., by means of MR navigators) to estimate involuntary patient motion as a pre-requisite for motion compensation, and, thus, subsequent improvement of PET image quality and quantification. Following appropriate motion compensation, PET data can be improved in quality and accuracy through the use of MR-guided partial volume corrections and image reconstruction. In this presentation we will highlight the most important advances of PET instrumentation and data processing that help facilitate fully-integrated PET/MR in the first place, and draw a

benefit from this integration for the PET data. This includes a brief discussion of the effect of the static MR field on positron range effects, in particular for higher-energetic positron emitters. Overall, increase volume sensitivity helps reduce the amount of radiotracer injected into patients or shorten the emission scan time, in combination with increased signal-to-noise in the emission images (thanks to the use of time-of-flight, a concept different from TOF-MR) it helps increase sensitivity and reader accuracy of PET images. Lastly, advances in image reconstruction have brought the level of PET, and the appearance of the PET images, closer to the common understanding of radiologically useful images.

RC121C SPECT/CT Quantitation

Participants

Srinivas C. Kappadath, PhD, Houston, TX (*Presenter*) Research Grant, General Electric Company; Research Grant, BTG International Ltd; Consultant, BTG International Ltd; Consultant, ABK Biomedical Inc; Consultant, Terumo Corporation

For information about this presentation, contact:

skappadath@mdanderson.org

LEARNING OBJECTIVES

1) Identify the various correction factors applied to SPECT. 2) Understand the processes used for quantification of SPECT. 3) Describe the various approaches used commercially for SPECT quantitation.







MRI O-RADS (Interactive Session)

Sunday, Dec. 1 2:00PM - 3:30PM Room: N227B



AMA PRA Category 1 Credits ™: 1.50 ARRT Category A+ Credit: 1.75

Sub-Events

RC129A Overview and O-RADS 0-1

Participants Caroline Reinhold, MD, MSc, Montreal, QC (*Presenter*) Nothing to Disclose

LEARNING OBJECTIVES

1) To introduce MRI O-RADS (Ovarian-Adnexal Reporting and Data Systems) 2) To review the MRI O-RADS governing concepts. 3) To know the main terms for O-RADS MRI scores 0 and 1. 4) To understand the application of O-RADS MRI scores 0 and 1 to adnexal masses and the associated risk of malignancy. 5) To recognize O-RADS MRI score 1 lesions by review of cases.

RC129B O-RADS 2

Participants

Evan S. Siegelman, MD, Media, PA (*Presenter*) Advisory Board, Spreemo Health; Consultant, BioClinica, Inc; Consultant, ICON plc; Consultant, inviCRO, LLC

For information about this presentation, contact:

evan.siegelman@uphs.upenn.edu

LEARNING OBJECTIVES

1) Describe the MR terms that characterize adnexal lesions that are almost certainly benign (O-RADS 2). 2) Identify those MR imaging features that would upgrade an adnexal lesion to a higher O-RADS category. 3) Illustrate MR imaging examples of O-RADS 2 lesion such as endometrioma, cystadenoma, mature cystic teratoma, hydrosalpinx and peritoneal inclusion cyst.

RC129C O-RADS 3

Participants

Isabelle Thomassin-Naggara, MD, Paris, France (*Presenter*) Researcher, General Electric Company; Research funded, General Electric Company; Researcher, Canon Medical Systems Corporation; Research funded, Canon Medical Systems Corporation; Research funded, Hologic, Inc; Research funded, Siemens AG; Research funded, Guerbet SA

For information about this presentation, contact:

isabelle.thomassin@aphp.fr

LEARNING OBJECTIVES

1) To combine all useful MR features to characterize indeterminate adnexal masses. 2) To describe how to perform DCE MR analysis on solid tissue. 3) To identify how lesions should be classified O-RADS 3. 4) To specify which adnexal lesions will be rated O-RADS 3

RC129D O-RADS 4-5

Participants

Andrea G. Rockall, FRCR, MRCP, London, United Kingdom (Presenter) Speaker and Chairman, Guerbet SA

LEARNING OBJECTIVES

1) To know the main terms for O-RADS MR score 4 and 5. 2) To be familiar with the application of O-RADS MR score 4 and 5 to adnexal masses. 3) To recognise O-RADS MR score 4 and 5 lesions by review of cases.

ABSTRACT

The preponderant contribution of MRI in adnexal mass evaluation is its specificity because it provides confident diagnosis of many benign adnexal lesions A standardization of the MR reporting may allow a tailored, patient-centered approach, allowing avoidance of over-extensive surgery and/or fertility preservation where appropriate, whilst ensuring early detection of lesions with high likelihood of malignancy. O-RADS classification is accurate and based on 5 categories related to the rik of malignancy. An adnexal lesion with a solid tissue that enhances according a time intensity curve type 2 or 3 or which is associated with peritoneal implants should be categorized O-RADS 4 or 5. A lesion classified O-RADS 5 has a risk of malignangy higher than 95% and must be referred to a gynecological oncologist

RC129E Case Review

Participants Elizabeth A. Sadowski, MD, Madison, WI (*Presenter*) Nothing to Disclose

For information about this presentation, contact:

esadowski@uwhealth.org

LEARNING OBJECTIVES

1) Understand the basic sequences necessary for characterizing adnexal lesions. 2) Classify adnexal masses using the ACR ORADS MRI system, based on their signal characteristics and enhancement patterns. 3) Assign an ACR ORAD MRI risk score based on the MRI appearance of an adnexal lesion and clinical information.





MR Imaging-guided Breast Biopsy (Hands-on)

Sunday, Dec. 1 2:00PM - 3:30PM Room: E260



AMA PRA Category 1 Credits ™: 1.50 ARRT Category A+ Credit: 1.75

Participants

Amy L. Kerger, DO, Plain City, OH (Presenter) Nothing to Disclose Kirti M. Kulkarni, MD, Chicago, IL (Presenter) Nothing to Disclose Wendi A. Owen, MD, Saint Louis, MO (Presenter) Nothing to Disclose Gary J. Whitman, MD, Houston, TX (Presenter) Nothing to Disclose Mai A. Elezaby, MD, Madison, WI (Presenter) Research Grant, Exact Sciences Corporation Amado B. del Rosario, DO, Mesa , AZ (Presenter) Nothing to Disclose Mitra Noroozian, MD, Ann Arbor, MI (Presenter) Institutional Grant, General Electric Company; Investigator, General Electric Company Anika N. Watson, MD, Atlanta, GA (Presenter) Nothing to Disclose Lara D. Richmond, MD, Toronto, ON (Presenter) Nothing to Disclose Nikki S. Ariaratnam, MD, Moorestown, NJ (Presenter) Consultant, Cleerly, Inc Clayton R. Taylor, MD, Upper Arlington, OH (Presenter) Nothing to Disclose Rifat A. Wahab, DO, Cincinnati, OH (Presenter) Nothing to Disclose Laurie R. Margolies, MD, New York, NY (Presenter) Research Consultant, FUJIFILM Holdings Corporation; Research Consultant, Imago Corporation Vandana M. Dialani, MD, Boston, MA (Presenter) Nothing to Disclose Esther N. Udoji, MD, Birmingham, AL (Presenter) Nothing to Disclose Jill J. Schieda, MD, Avon Lake, OH (Presenter) Nothing to Disclose Su-Ju Lee, MD, Cincinnati, OH (Presenter) Spouse, Stockholder, General Electric Company; Spouse, Stockholder, Siemens AG Elsa M. Arribas, MD, Houston, TX (Presenter) Scientific Advisory Board, Volumetric Biotechnologies, Inc; Stockholder, Volumetric Biotechnologies, Inc Karen A. Lee, MD, New York, NY (Presenter) Nothing to Disclose Ami D. Shah, MD, New York, NY (Presenter) Nothing to Disclose Katharine D. Maglione, MD, New York, NY (Presenter) Nothing to Disclose Wade C. Hedegard, MD, Brighton, NY (Presenter) Nothing to Disclose Manisha Bahl, MD, MPH, Boston, MA (Presenter) Nothing to Disclose For information about this presentation, contact: laurie.margolies@mountsinai.org

nariaratnam@sjra.com

karen.lee2@mountsinai.org

mbahl1@mgh.harvard.edu

LEARNING OBJECTIVES

1) Explain why MR-guided breast biopsy is needed for patient care. 2) Identify relative and absolute contraindications to MR-guided breast biopsy. 3) Describe criteria for MR-guided breast biopsy patient selection. 4) Debate risks and benefits of pre-biopsy targeted ultrasound for suspicious MRI findings. 5) Understand the basic MR-guided biopsy procedure, protocol and requirements for appropriate coil, needle and approach selection. 6) Manage patients before, during and after MR-guided breast biopsy. 7) Define the benefits and limitations of MR-guided vacuum assisted breast biopsy. 8) How to problem shoot complicated cases due to lesion location, patient anatomy, etc.

ABSTRACT

This course is intended to provide basic didactic instruction and hands-on experience for MR-guided breast biopsy. Because of the established role of breast MRI in the evaluation of breast cancer through screening and staging, there is a proven need for MR-guided biopsy of the abnormalities that can only be identified at MRI. This course will be devoted to the understanding and identification of: 1) appropriate patient selection 2) optimal positioning for biopsy 3) target selection and confirmation 4) various biopsy technologies and techniques 5) potential problems and pitfalls and 6) practice audits. Participants will spend 30 minutes in didactic instruction followed by 60 minutes practicing MR-guided biopsy using provided phantoms. Various combinations of full size state-of-the-art breast MRI coils, biopsy localization equipment and needles from multiple different vendors will be available for hands-on practice. Some stations will have monitors loaded with targeting software. Expert breast imagers from around the world will be at each of 10 stations to provide live coaching, tips, techniques and advice.

Active Handout: Amy L. Kerger

http://abstract.rsna.org/uploads/2019/6005779/Active RC150.pdf







CS23

Density "Inform" and Insurance Legislation Update: Presented by Bayer

Monday, Dec. 2 8:30AM - 9:30AM Room: S105D

Participants

JoAnn Pushkin, Deerpark, NY (Presenter) Nothing to Disclose

PROGRAM INFORMATION

Existing density "inform" laws vary widely; will the soon-to-be-made public FDA national reporting requirement rectify that? This presentation will provide an update on state inform and insurance laws, explain the federal legislative and regulatory processes for a national standard, and share available patient and provider information on the topic of breast density.

CME

This program does not offer CME credit.





MSMI21

Molecular Imaging Symposium: Basics of Molecular Imaging

Monday, Dec. 2 8:30AM - 10:00AM Room: S405AB



AMA PRA Category 1 Credits ™: 1.50 ARRT Category A+ Credit: 1.75

Participants

Zaver M. Bhujwalla, PhD, Baltimore, MD (*Moderator*) Nothing to Disclose Jan Grimm, MD,PhD, New York, NY (*Moderator*) Nothing to Disclose

For information about this presentation, contact:

Grimmj@mskcc.org

Sub-Events

MSMI21A Molecular Imaging using Radioactive Tracers

Participants

Jan Grimm, MD, PhD, New York, NY (Presenter) Nothing to Disclose

LEARNING OBJECTIVES

1) Discuss the various radio tracers and their applications in Molecular Imaging studies. 2) Understand in which situations to use which radio tracers, what to consider when developing the imaging construct and what controls to obtain for nuclear imaging studies. 3) Examples will contain imaging with small molecules, with antibodies and nanoparticles as well as with cells in order to provide the participants with examples how o correctly perform their imaging studies. 4) Most of the examples will be from the oncology field but their underlying principles are universally applicable to other areas as well.

MSMI21B Molecular Imaging with MRI and MRS

Participants Zaver M. Bhujwalla, PhD, Baltimore, MD (*Presenter*) Nothing to Disclose

LEARNING OBJECTIVES

1) To list the basic principles of magnetic resonance (MR) molecular imaging. 2) To describe the uses of noninvasive multi-nuclear MRI and magnetic resonance spectroscopic imaging (MRSI) for molecular imaging applications that provide spatial and temporal information on vasculature, metabolism and physiology. 3) To identify the applications of targeted MR contrast agents to detect receptor and gene expression. 4) To describe strategies that combine detection with therapy for theranostic imaging and for metabolotheranostics. 5) To provide examples of translational applications of molecular imaging and theranostics.

ABSTRACT

Noninvasive multi-nuclear magnetic resonance (MR) imaging and spectroscopic imaging (MRSI) provide a wealth of spatial and temporal information on vasculature, metabolism and physiology. Novel targeted contrast agents have widened the scope of MR techniques for molecular imaging applications to detect receptor and gene expression. In cancer, molecular imaging can be applied to identify targets specific to cancer with imaging, design agents against these targets to visualize their delivery, and monitor response to treatment, with the overall purpose of minimizing collateral damage. Genomic and proteomic profiling can provide an extensive 'fingerprint' of each tumor. With this cancer fingerprint, theranostic agents can be designed to personalize treatment for precision medicine of cancer, and minimize damage to normal tissue.

MSMI21C Molecular Imaging with Nanoparticles

Participants Heike E. Daldrup-Link, MD, Palo Alto, CA (*Presenter*) Nothing to Disclose

LEARNING OBJECTIVES

1) To understand important safety aspects of ultrasmall superparamagnetic iron oxide nanoparticles (USPIO). 2) To understand the biodistribution of ferumoxytol nanoparticles and implications for imaging diagnoses. 3) To recognize the value of ferumoxytol nanoparticles for cancer MR imaging and PET/MR imaging.

ABSTRACT

Gadolinium chelates as contrast agents for MRI have been associated with mounting concerns about nephrogenic sclerosis and gadolinium deposition in the brain. Therefore, a search for safe alternatives is currently underway. In North America, the iron supplement ferumoxytol has gained considerable interest as an MR contrast agent. In Europe, ferumoxtran-10 is re-entering clinical trials. Both ferumoxytol and ferumoxtran-10 provide long-lasting blood pool enhancement, which can be used for MR imaging exams that require detailed and/or long-lasting vessel delineation for MR angiographies, tissue perfusion studies, and whole body tumor staging. Iron oxide nanoparticles are slowly phagocytosed by macrophages in the reticuloendothelial system, making them ideal for MR imaging detection of tumors in the liver, spleen, lymph nodes, and bone marrow. Similarly, iron oxide nanoparticles are slowly phagocytosed by tumor-associated inflammation and monitor the efficacy of new cancer immunotherapies. This presentation provides an introduction to the use of iron oxide

nanoparticles for clinical MR and PET/MR imaging, including safety data acquired in children thus far, recent insights and mechanisms of rare, but potentially severe adverse reactions, applications that impact patient care and comparisons with gadolinium chelates. New developments for image guided therapy and theranostics are under way.

MSMI21D Ultrasound Molecular Imaging with Targeted Bubbles

Participants

Alexander L. Klibanov, PhD, Charlottesville, VA (*Presenter*) Co-founder, Targeson, Inc, now dissolved; Shareholder, Targeson, Inc, now dissolved; Institutional research collaboration, AstraZeneca PLC; NIH Grant subcontract to UVA lab, SoundPipe Therapeutics;

LEARNING OBJECTIVES

1) Understand the principles of microbubble design-how to prepare fully biocompatible and safe ultrasound contrast agent particles that are clinically translatable, stable on storage, provide strong acoustic response and high sensitivity of detection by clinical ultrasound imaging systems, and could be targetable. 2) Understand the principles of selection of disease-specific targeting ligands usable for contrast ultrasound imaging, based on receptor levels in the vasculature in the disease issues, as well as vascular biomechanics. 3) Assess the results of early stage clinical trials performed with targeted microbubbles, and opportunities for clinical translation in diagnostic imaging and image-guided interventions.

ABSTRACT

Ultrasound is the most widespread clinical imaging modality. Therefore, enabling molecular imaging potential in an ultrasound setting will lead to the expanded and improved clinical diagnostic benefit. Ultrasound contrast microbubbles are already used in clinic as blood pool contrast agents, with excellent detection sensitivity: single particles with sub-picogram mass can be observed with clinical imaging systems in real time, at a depth of several cm. To achieve biomarker-selective molecular imaging, microbubble shell surface is decorated with targeting ligand molecules (antibodies, peptides, carbohydrates) that assure selective binding and retention in the areas of disease. Clinical microbubbles are typically 1-3 um in diameter; they do not extravasate, so target biomarker receptors should be located on the luminal surface of vessel wall, e.g., vascular endothelium. Microbubbles are targeted to the biomarkers in the areas of inflammation and ischemia-reperfusion injury (P- and E-selectin, VCAM-1, ICAM-1) or to tumor neovasculature (VEGFR2). The latter, a heterodimeric peptide-targeted contrast microbubble from industry, has successfully completed Phase 1-2 clinical trials for imaging of ovarian, breast and prostate cancer lesions. Overall, targeted microbubbles empower molecular ultrasound imaging; they could also be used in conjunction with image-guided interventions, such as targeted biopsy and therapy.

MSMI21E Quantitative Imaging Biomarkers and Radiogenomics

Participants

Lawrence H. Schwartz, MD, New York, NY (Presenter) Nothing to Disclose





Musculoskeletal Series: MRI of Ankle and Foot

Monday, Dec. 2 8:30AM - 12:00PM Room: E451B



AMA PRA Category 1 Credits ™: 3.00 ARRT Category A+ Credits: 3.50

Participants

William E. Palmer, MD, Boston, MA (*Moderator*) Nothing to Disclose Corrie M. Yablon, MD, Ann Arbor, MI (*Moderator*) Nothing to Disclose Yulia Melenevsky, MD, Vestavia, AL (*Moderator*) Nothing to Disclose Hilary R. Umans, MD, Ardsley, NY (*Moderator*) Nothing to Disclose

Sub-Events

RC204-01 MRI of Anatomic Variants of the Foot and Ankle and Their Significance

Monday, Dec. 2 8:30AM - 8:50AM Room: E451B

Participants Yulia Melenevsky, MD, Vestavia, AL (*Presenter*) Nothing to Disclose

For information about this presentation, contact:

yuliavm@gmail.com

LEARNING OBJECTIVES

1) List common anatomic variants of foot and ankle. 2) Recognize and describe MRI appearances of foot and ankle anatomic variants. 3) Determine clinical significance based on imaging appearance and clinical presentation.

RC204-02 MRI of Ankle Instability

Monday, Dec. 2 8:50AM - 9:10AM Room: E451B

Participants William E. Palmer, MD, Boston, MA (*Presenter*) Nothing to Disclose

For information about this presentation, contact:

wpalmer@mgh.harvard.edu

LEARNING OBJECTIVES

1) Describe MRI signs of ankle instability. 2) Differentiate primary and secondary signs of instability. 3) Identify MRI findings in lateral and medial instability.

RC204-03 MRI Patterns of Acute Distal Tibiofibular Syndesmotic Injuries in the Pediatric Population

```
Monday, Dec. 2 9:10AM - 9:20AM Room: E451B
```

Participants

William Walter, MD, New York, NY (*Presenter*) Nothing to Disclose Zehava S. Rosenberg, MD, Hoboken, NJ (*Abstract Co-Author*) Nothing to Disclose

For information about this presentation, contact:

william.walter@nyulangone.org

PURPOSE

To compare pediatric MRI patterns of acute distal tibiofibular syndesmotic ligamentous injuries to those of adults. To the best of our knowledge, this has not been previously described.

METHOD AND MATERIALS

3 cohorts of patients with ankle MRIs were retrospectively identified via PACS database search: 1) pediatric patients (<=16 years) with normal distal tibiofibular syndesmosis based on non-traumatic indications and no MRI findings of acute or chronic trauma, 2) pediatric patients and 3) adult patients (>=17 years) with unequivocal MRI evidence of acute tears of the syndesmotic ligaments (anterior, posterior inferior tibiofibular and/or interosseous ligaments/membrane), based on previously established literature criteria. Studies were reviewed in consensus by 2 MSK radiologists with 3 and 25 years of experience, respectively, for MRI appearance of normal and torn syndesmotic ligaments, presence of avulsion fractures, and periosteal tearing. Pertinent electronic medical record data were also reviewed.

RESULTS

68 anble MDIs were identified from a total of 371 MDIs (25 natiatis nations with average are 13 0 years standard deviation

(SD)=2.2 years) with normal syndesmosis, and 20 pediatric (13.3 years, SD=1.7 years) and 23 adult (53.2, SD=12.1 years) cases with syndesmotic injuries). -Fibrous and cambrial periosteal layers were identified in all normal pediatric cases; normal ligaments were attached to tibial and fibular fibrous periosteum prior to full bony ossification. MRIs with syndesmotic ligamentous injury depicted stripping of tibial periosteum in 8/20 (40.0%) of pediatric and 1/23 (4.0%) of adult cases. 1/20 (5%) pediatric and 4/23 (17.4%) of adult cases with syndesmotic injuries demonstrated avulsion fractures.

CONCLUSION

There is a spectrum of MRI appearances of distal tibiofibular syndesmotic injuries among pediatric and adult patients. Osseous avulsions appear to be more common in adults whereas periosteal stripping, which should not be mistaken for a tibial fracture, is seen almost exclusively in pediatric patients. This may be due to the syndesmotic ligaments' insertion to periosteum rather than to bone.

CLINICAL RELEVANCE/APPLICATION

Tibial periosteal stripping in children, in the setting of acute distal tibiofibular syndesmotic ligamentous injuries, should not be misinterpreted as tibial fractures but rather be recognized as part of MRI patterns of ligamentous injuries in this population.

RC204-04 Calcaneofibular Ligament Anatomy Under Different Ankle Positions

Monday, Dec. 2 9:20AM - 9:30AM Room: E451B

Participants

Yoshihiro Akatsuka, RT, Sapporo, Japan (*Presenter*) Nothing to Disclose Atsushi Teramoto, MD,PhD, Sapporo, Japan (*Abstract Co-Author*) Nothing to Disclose Hiroyuki Takashima, PhD, Sapporo, Japan (*Abstract Co-Author*) Nothing to Disclose Rui Imamura, Sapporo, Japan (*Abstract Co-Author*) Nothing to Disclose Tomoyuki Suzuki, MD, Sapporo, Japan (*Abstract Co-Author*) Nothing to Disclose Kota Watanabe, MD,PhD, Sapporo, Japan (*Abstract Co-Author*) Nothing to Disclose Toshihiko Yamashita, MD, PhD, Sapporo, Japan (*Abstract Co-Author*) Nothing to Disclose

For information about this presentation, contact:

akatsuka.y@sapmed.ac.jp

PURPOSE

To investigate the anatomical changes of the calcaneofibular ligament (CFL) under different ankle positions and obtain basic data to use in functional CFL assessments, injury diagnoses, and determination of treatment effects.

METHOD AND MATERIALS

We enrolled 10 healthy volunteers (10 ankles) with a mean age of 27.8 years and no history of ankle disease. We took ankle images (neutral position, maximum dorsiflexion, and maximum plantar flexion) using a 3-T MRI and 3-dimensional fast imaging employing steady-state acquisition cycled phases (3D FIESTA-C). We processed the 3D images of the CFL, peroneal muscle tendons, fibula, and calcaneus at a workstation, and measured CFL variables.

RESULTS

In all positions, the CFLs showed a gently curving course with the peroneal muscle tendons as a fulcrum. The tortuosity angle was significantly smaller in plantar flexion $(30.0^{\circ} \pm 7.4^{\circ})$ than in the neutral position $(41.7^{\circ} \pm 8.3^{\circ})$.

CONCLUSION

Our 3D MRI images showed that, in all positions, the CFLs were curved due to the influence of the peroneal muscle tendons. With maximum plantar flexion, the CFL tortuosity angles were small, which is probably due to CFL tension. This should be considered when diagnosing CFL injuries and evaluating treatment outcomes.

CLINICAL RELEVANCE/APPLICATION

Clarification of the normal CFL functional anatomy will aid to diagnose CFL injuries and may facilitate accurate evaluations of treatment outcomes.

RC204-05 MRI of Ankle Impingement

Monday, Dec. 2 9:30AM - 9:50AM Room: E451B

Participants Corrie M. Yablon, MD, Ann Arbor, MI (*Presenter*) Nothing to Disclose

For information about this presentation, contact:

cyablon@med.umich.edu

LEARNING OBJECTIVES

1) List the causes of ankle impingement. 2) Describe the MR imaging findings of ankle impingement. 3) Discuss common potential sites of ankle impingement.

RC204-06 MRI of the Midfoot

Monday, Dec. 2 10:20AM - 10:40AM Room: E451B

Participants Hilary R. Umans, MD, Ardsley, NY (*Presenter*) Nothing to Disclose

LEARNING OBJECTIVES

1) Describe the normal MRI anatomy of the midfoot. 2) Discuss osseous abnormalities of the Chopart joint and Lisfranc joint complex. 3) Identify tendinous pathology of the midfoot.

Active Handout:Hilary Ruth Umans

http://abstract.rsna.org/uploads/2019/19000740/Active RC204-06.pdf

RC204-07 Dynamic-Imaging of the Lisfranc Joint by Utilizing a Novel: MRI Compatible Stress Device

Monday, Dec. 2 10:40AM - 10:50AM Room: E451B

Participants

Drew Gunio, MD, MS, New York, NY (*Presenter*) Nothing to Disclose Carlos L. Benitez, MD, New York, NY (*Abstract Co-Author*) Nothing to Disclose

For information about this presentation, contact:

drew.gunio@gmail.com

PURPOSE

To evaluate the applicability of a novel, MRI-stress device in the evaluation of Lisfranc joint injury

METHOD AND MATERIALS

This is a prospective study that evaluated Lisfranc joint injury by utilizing a joint specific, MRI-compatible stress device. The MRIstress device applies a multidimensional load to the foot to simulate weight bearing. We obtained non-stressed and stressed MR images of the injured and non-injured (control) feet and measured changes in ligament morphology and joint alignment between stressed and non-stressed images. Patient recruitment occurred over a three-year period.

RESULTS

We recruited 10 patients with Lisfranc joint injuries, 8 males and 2 females (mean age 35.5 years). 9 patients reported an axialloading mechanism of injury with 1 midfoot crush injury. Time from injury to imaging was 3 to 42 days. Interosseous Lisfranc ligament (ILL), plantar capsular ligament (PCL), and dorsal capsular ligament (DCL) injuries ranged from Grade 1 sprains to complete tears. All morphologically normal ligaments on standard MR imaging lacked stress-induced ligament lengthening and laxity, whereas all ligaments with abnormal signal or morphology demonstrated measurable, stress-induced ligament laxity. Abnormal morphology and inducible laxity were most prominent in the PCL, followed by the ILL; suggesting a plantar to dorsal propagation of force and ligament tearing during injury. 5 patients demonstrated dorsal subluxation of the tarsometatarsal joint, requiring high-grade tearing of both the ILL and PCL and at least mild partial tearing of the DCL for stress-induced subluxation to occur. Comitant, moderate tearing of the ILL and PCL alone did not result in stress-induced dorsal subluxation. Higher grade injuries revealed more prominent stress-induced, morphological changes. Interrogation of lower grade injuries allowed the Orthopedic surgeons to pursue conservative management.

CONCLUSION

Our MRI stress device provides physiologic evaluation of the Lisfranc joint beyond that of traditional, static MRI examinations and may allow Orthopaedic surgeons to better determine patient management and surgical candidacy.

CLINICAL RELEVANCE/APPLICATION

Dynamic MR imaging allows high resolution imaging under reproducible and physiologic conditions, ultimately allowing the Radiologist to provide a more thorough evaluation of joint pathology and degree of injury.

RC204-08 Tricomponent T2* Analyses Performed on Ultrashort Echo Time (UTE) MRI Images Correlate Significantly with Mechanical Properties of Cortical Bone

Monday, Dec. 2 10:50AM - 11:00AM Room: E451B

Participants

Saeed Jerban, PhD, San Diego, CA (*Presenter*) Nothing to Disclose Xing Lu, San Diego, CA (*Abstract Co-Author*) Nothing to Disclose Erik W. Dorthe, La Jolla, CA (*Abstract Co-Author*) Nothing to Disclose Salem Alenezi, Riyadh, Saudi Arabia (*Abstract Co-Author*) Nothing to Disclose Yajun Ma, San Diego, CA (*Abstract Co-Author*) Nothing to Disclose Lena Kakos, San Diego , CA (*Abstract Co-Author*) Nothing to Disclose Hyungseok Jang, La Jolla, CA (*Abstract Co-Author*) Nothing to Disclose Robert Sah, La Jolla, CA (*Abstract Co-Author*) Nothing to Disclose Eric Y. Chang, MD, San Diego, CA (*Abstract Co-Author*) Nothing to Disclose Darryl D'Lima, MD, PhD, La Jolla, CA (*Abstract Co-Author*) Research funded, Stryker Corporation; Consultant, Advanced Mechanical Technology, Inc; Research funded, ConforMIS, Inc; Consultant, Ossur HF; Officer and Stockholder, XpandOrtho, Inc Jiang Du, PhD, San Diego , CA (*Abstract Co-Author*) Nothing to Disclose

PURPOSE

To investigate the relationship between human cortical bone mechanical properties and bone bound and pore water fractions estimated with tricomponent ultrashort echo time (UTE) MRI T2* fitting.

METHOD AND MATERIALS

135 cortical bone strips (\sim 4×2×40 mm3) were harvested from the tibial and femoral midshafts of 37 donors (61±24 yo). Specimens were scanned using a 1-inch diameter T/R birdcage coil on a 3T clinical scanner (MR750, GE). Ten sets of dual-echo 3D-UTE-Cones sequences with different echo time from 0.032ms to 24.0ms (TR=28ms, flip angle=10°, and 26 µs rectangular RF pulse) were performed for T2* bicomponent (2-com) and tricomponent (3-com) decay analyses. Other imaging parameters included: field of view=40×40mm2, matrix=160×160, slice-thickness=2mm, bandwidth=±62.5kHz. Specimens were later scanned using a Skyscan 1076 (Kontich, Belgium) µCT at 9 µm3 voxel size to measure bone porosity and bone mineral density (BMD). Finally, mechanical

properties of the bone specimens (Young's modulus, yield stress, ultimate stress, and failure energy) were estimated using 4-point bending tests. Pearson's correlation coefficients were calculated between water fractions-estimated with 3-com and 2-com UTE-MRI T2* analyses-and μ CT measures of porosity and BMD, as well as mechanical properties.

RESULTS

Fig.1a shows a representative UTE-MRI image at the middle of a cortical bone specimen. Figs. 1c,d depict 2-com and 3-com fitting for the selected specimen, respectively. From 2-com fitting, bound water fraction (FracBW) and pore water fraction (FracPW) showed significant (p<0.01) moderate correlations with bone porosity and BMD (R=0.61-0.65), as well as with mechanical properties (R=0.52-0.54). From 3-com fitting, FracBW showed significant strong correlations with porosity and BMD (R=0.70-0.73). It also demonstrated significant moderate correlation with mechanical properties (R=0.58-0.62) at a level higher than the correlations presented by 2-com analysis. Figs. 1e-j show the scatter plots and linear regressions of porosity, yield stress, and ultimate stress on FracBW from both 2-com and 3-com T2* fittings, respectively.

CONCLUSION

Consideration of the fat signal contribution in UTE-MRI using the 3-com T2* fitting model can improve the correlations between estimated bound and pore water fractions and bone mechanics.

CLINICAL RELEVANCE/APPLICATION

An MRI technique that improves water quantifications in cortical bone may help diagnose bone diseases.

RC204-09 Non-Invasive Measurements of Microstructural and Mechanical Properties from the Achilles Tendon (AT) in Healthy Humans Using UTE MRI and Shear Wave US Elastography

Monday, Dec. 2 11:00AM - 11:10AM Room: E451B

Participants

Felix Gonzalez, MD, Atlanta, GA (*Presenter*) Nothing to Disclose Adam D. Singer, MD, Atlanta, GA (*Abstract Co-Author*) Nothing to Disclose Zahra Hosseini, Atlanta, GA (*Abstract Co-Author*) Employee, Siemens AG Monica B. Umpierrez, MD, Atlanta, GA (*Abstract Co-Author*) Nothing to Disclose David Reiter, Atlanta, GA (*Abstract Co-Author*) Nothing to Disclose

PURPOSE

Bicomponent UTE T2* MRI relaxation parameters show sensitivity to distinct microstructural tissue compartments in tendon. Shear wave US elastograms provide tissue mechanical properties like elastic modulus (E) and wave speed (v) that relate to function and load bearing capacity. The purpose is to compare these modalities in healthy adult AT.

METHOD AND MATERIALS

Healthy volunteers were recruited for this study (N=9, 4 females, ave+/-SD 39+/-13.2 yrs) under the approval of an institutional IRB. MR imaging was performed using a 3T Siemens Prisma with a flexible 4-ch coil wrapped around the left ankle. UTE images (Fig1a) were acquired in the sagittal plane with 4mm slice thickness, 0.625mm in plane resolution, and 16 non-linearly spaced echoes between 60µs and 30ms. Region of interest analysis was performed for biexponential modeling of relaxation (i.e. fs, T2*s, and T2*l) at the mid-substance of the AT. Ultrasound analysis was performed on the left AT using a 2D SWE GE Logiq s8 ultrasound machine (Fig1b,c). Measurements were performed in neutral-relaxed (NR) and under voluntary active maximum dorsiflexion (VAMD). E and v were determined in both the long axis and short axis planes relative to the AT.

RESULTS

T2*s was positively associated with age (p=.0006) and T2*I showed a weak negative trend (n.s.) with age (Fig1d,e). NR SWEderived E and v showed weak trends (n.s.) with age. VAMD SWE-derived E and v showed modest trends with age with short axis v showing a significant association (p=.04), suggesting an increase in stiffness (Fig1f). T2*s and T2*I showed no association with NR SWE values. T2*s and T2*I showed weak (n.s.) trends with short axis v (ρ =.52 and -.47, resp).

CONCLUSION

Changes in bicomponent relaxation parameters, surrogates for collagen fibril and interstitial microstructure, are consistent with agerelated disorganization of collagen fibril structure and desiccation of interstium; these changes are consistent with observed SWEderived increase in mechanical stiffness. These preliminary data from this ongoing study show emerging relationships between tendon microstructure and mechanical propeties in healthy individuals. This approach could provide non-invasive characterization of tendon pathology.

CLINICAL RELEVANCE/APPLICATION

Non-invasive measures of tendon microstructural and mechanical properties can provide information specific to tissue function that could be used to evaluate pathology and therapeutic intervention.

RC204-10 Elastosonography Evaluation after ESWT (Extracorporeal Shock Wave Therapy) Treatment in Plantar Fasciopathy

Monday, Dec. 2 11:10AM - 11:20AM Room: E451B

Participants

Giuseppe Schillizzi, Roma, Italy (*Presenter*) Nothing to Disclose Daniela Elia, Roma, Italy (*Abstract Co-Author*) Nothing to Disclose Daniele Fresilli, Roma, Italy (*Abstract Co-Author*) Nothing to Disclose Carlo Catalano, MD, Rome, Italy (*Abstract Co-Author*) Nothing to Disclose Ferdinando D'Ambrosio, Rome, Italy (*Abstract Co-Author*) Nothing to Disclose Vito Cantisani, MD, Roma, Italy (*Abstract Co-Author*) Speaker, Canon Medical Systems Corporation; Speaker, Bracco Group; Speaker, Samsung Electronics Co, Ltd; Antonello Rubini, MD, Roma, Italy (*Abstract Co-Author*) Nothing to Disclose Marzia Russomando, Rome , Italy (*Abstract Co-Author*) Nothing to Disclose Eriselda Kutrolli, JD, Rome, Italy (*Abstract Co-Author*) Nothing to Disclose Federica Alviti, Rome, Italy (*Abstract Co-Author*) Nothing to Disclose

PURPOSE

To evaluate the clinical role of elastosonography to assess plantar fascia elasticity features and variation in patients with diagnosis of plantar fasciitis before and after ESWT treatment.

METHOD AND MATERIALS

20 Patients with diagnosis of plantar fasciitis with the following criteria were enrolled in this study: (1) plantar fascia thickness > 4mm, (2) pain assessed through VAS scale > 4 out of 10 and (3) more than 3 months of heel pain non responsive to previous noninvasive conservative treatment with nonsteroidal anti-inflammatory medication. Clinical and ultrasound evaluation (including Swear Wave Elastography and Compression Elastography) were performed at baseline (T0), when patients underwent the first ESWT treatment, 1 month (T1) and 3 months (T2) after treatment ended. Patients were treated with 3 session, once a week of ESWT.

RESULTS

At baseline, (T0) statistically significant differences were found in SWE velocity between the affected side and healthy side with higher value in healthy side with value equal to 3.8 (1.5; 5.1) ms-1 and 4.7 (4.07;7.04) ms-1 respectively (p=0,006; z=2,758), while no significant differences were found for strain ratio (p=0.656; z=0.445). One month after ESWT treatment (T1) the strain ratio of the affected side increased, with median value equal to 0.89 (0.3-1.5) at baseline to 1.16 (0.3-1.6) at 1 month and decreased at three months (T2) with median value equal to 0.82 (0.38-1.12). No statistically significant differences were found. Significant differences were found in shear wave velocity over time, with an increase of SWE velocity after shock-wave treatment (p=0.04; χ 2=11.167), results showed significant differences from T0 to T2 with median value varying from 3.8 (1.5-5.1) ms-1 at baseline and 5.23 (4.55-6.74) ms-1 a three months after treatment ended respectively (p=0.003).

CONCLUSION

Shear Wave Elastography seems to be more accurate to assess soft tissue stiffness, it provides more objective results and less technical variation than compression elastography. SWE seems effective tool to assess ESWT treatments efficacy.

CLINICAL RELEVANCE/APPLICATION

US-elastography especially with shear wave may increase ultrasound accuracy for plantar fasciitis diagnosis and can be an important additional tool to evaluate ESWT efficacy.

RC204-11 MRI of Achilles and Plantar Fascia

Monday, Dec. 2 11:20AM - 11:40AM Room: E451B

Participants

Roar Pedersen, Tonsberg, Norway (*Presenter*) Nothing to Disclose

For information about this presentation, contact:

pedersen70@gmail.com

LEARNING OBJECTIVES

1) Identify the normal anatomy and variants of the Achilles tendon and the plantar fascia. 2) Describe pathology of the Achilles tendon and its insertion. 3) Describe pathology of the plantar fascia. 4) Consider differential diagnoses of the heel not related to the tendon and fascia.

RC204-12 MRI of the Nerves in the Foot and Ankle

Monday, Dec. 2 11:40AM - 12:00PM Room: E451B

Participants Michel O. De Maeseneer, MD, PhD, Jette , Belgium (*Presenter*) Nothing to Disclose

For information about this presentation, contact:

michel.demaeseneer@uzbrussel.be

LEARNING OBJECTIVES

1) Define the different nerves about the foot and ankle and discuss the aspect on anatomy and MRI. 2) Identify common pathological conditions of the nerves. 3) Classify pathologies affecting the webspaces (Bursitis, Plantar plate tear, Morton's neuroma).





Body Imaging Expert Panel: CTA or MRA?

Monday, Dec. 2 8:<u>30AM - 10:00AM Room: S104A</u>



AMA PRA Category 1 Credits ™: 1.50 ARRT Category A+ Credit: 1.75

Participants

Martin R. Prince, MD,PhD, New York, NY (*Moderator*) Patent agreement, General Electric Company; Patent agreement, Hitachi, Ltd; Patent agreement, Siemens AG; Patent agreement, Koninklijke Philips NV; Patent agreement, Nemoto Kyorindo Co, Ltd; Patent agreement, Bayer AG; Patent agreement, Lantheus Medical Imaging, Inc; Patent agreement, Bracco Group; Patent agreement, Mallinckrodt plc; Patent agreement, Guerbet SA; Patent agreement, Toshiba Corporation

Sub-Events

RC212A MRA

Participants J. Paul Finn, MD, Los Angeles, CA (*Presenter*) Nothing to Disclose Scott B. Reeder, MD,PhD, Madison, WI (*Presenter*) Nothing to Disclose Robert R. Edelman, MD, Evanston, IL (*Presenter*) Research support, Siemens AG; Royalties, Siemens AG

LEARNING OBJECTIVES

1) Discuss CTA and MRA methods and techniques for optimized vascular imaging in clinical practice. 2) Debate the advantages and disadvantages of CTA and MRA in clinical practice. 3) Recommend the application of CTA or MRA for common challenging clinical scenarios.

RC212B CTA

Participants

Elliot K. Fishman, MD, Owings Mills, MD (*Presenter*) Institutional Grant support, Siemens AG; Institutional Grant support, General Electric Company; Co-founder, HipGraphics, Inc

W. Dennis Foley, MD, Milwaukee, WI (Presenter) Nothing to Disclose

Geoffrey D. Rubin, MD, Durham, NC (*Presenter*) Consultant, Fovia, Inc; Advisor, HeartFlow, Inc; Consultant, General Electric Company; Advisor, Boehringer Ingelheim GmbH; Advisor, Siemens AG;

For information about this presentation, contact:

dfoley@mcw.edu

efishman@jhmi.edu

grubin@duke.edu

LEARNING OBJECTIVES

1) Discuss CTA and MRA methods and techniques for optimised vascular imaging in clinical practice. 2) Debate the advantages and disadvantages of CTA and MRA in clinical practice. 3) Recommend the application of CTA or MRA for common challenging clinical scenarios.





Breast Series: MRI

Monday, Dec. 2 8:30AM - 12:00PM Room: Arie Crown Theater



AMA PRA Category 1 Credits ™: 3.25 ARRT Category A+ Credits: 3.75

Participants

Wendy B. Demartini, MD, Stanford, CA (Moderator) Nothing to Disclose

Thomas H. Helbich, MD, Vienna, Austria (*Moderator*) Research Grant, Medicor, Inc Research Grant, Siemens AG Research Grant, C. R. Bard, Inc

Hiroyuki Abe, MD, Chicago, IL (Moderator) Nothing to Disclose

Colleen H. Neal, MD, Ann Arbor, MI (*Moderator*) Institutional Research Grant, General Electric Company; Investigator, General Electric Company

For information about this presentation, contact:

zuleyml@upmc.edu

Sub-Events RC215-01 MRI: Part 1

RC215-02 How Genetics Will Fit Into Your Practice

Monday, Dec. 2 8:30AM - 8:55AM Room: Arie Crown Theater

Participants

Elizabeth A. Morris, MD, New York, NY (Presenter) Nothing to Disclose

For information about this presentation, contact:

morrise@mskcc.org

LEARNING OBJECTIVES

1) Understand the impact that genetics will have on the future of screening. 2) Understand the different methods of assessing risk for breast cancer. 3) Assess different algorithms for screening beyond mammography.

RC215-03 MRI in Addition to Mammography Screening in Women with Extremely Dense Breasts: Primary Outcome of the Randomized DENSE Trial

Monday, Dec. 2 8:55AM - 9:05AM Room: Arie Crown Theater

Participants

Marije F. Bakker, PhD, Utrecht, Netherlands (*Presenter*) Grant, Bayer AG; Software support, Volpara Health Technologies Limited Stephanie V. de Lange, Utrecht, Netherlands (*Abstract Co-Author*) Research Grant, Bayer AG; Software support, Volpara Health Technologies Limited

Rudolf M. Pijnappel, MD, PhD, Haren, Netherlands (Abstract Co-Author) Research Grant, Bayer AG

Ritse M. Mann, MD, PhD, Nijmegen, Netherlands (*Abstract Co-Author*) Researcher, Siemens AG; Researcher, Seno Medical Instruments, Inc; Researcher, Identification Solutions, Inc; Researcher, Micrima Limited; Researcher, Medtronic plc; Scientific Advisor, ScreenPoint Medical BV; Scientific Advisor, Transonic Imaging, Inc; Stockholder, Transonic Imaging, Inc Claudette E. Loo, MD, Amsterdam, Netherlands (*Abstract Co-Author*) Nothing to Disclose

Bob Bisschops, Dordrecht, Netherlands (*Abstract Co-Author*) Nothing to Disclose

Marc Lobbes, MD, Maastricht, Netherlands (Abstract Co-Author) Nothing to Disclose

Mathijn D. De Jong, MD, 's-Hertogenbosch, Netherlands (Abstract Co-Author) Nothing to Disclose

Katya M Duvivier, MD, Amsterdam, Netherlands (Abstract Co-Author) Nothing to Disclose

Jeroen Veltman, MD, Hengelo, Netherlands (Abstract Co-Author) Nothing to Disclose

Wouter B. Veldhuis, MD, PhD, Utrecht, Netherlands (Abstract Co-Author) Nothing to Disclose

Carla H. van Gils, PhD, Utrecht, Netherlands (Abstract Co-Author) Software support, Volpara Health Technologies Limited

PURPOSE

To evaluatue the effect of supplemental MRI for women with extremely dense breasts within a population-based screening program.

METHOD AND MATERIALS

Between 2011-2015, we randomized 40,373 screening participants (aged 50-75) with a negative screening mammography and extremely dense breasts (ACR category 4 by Volpara software) to (an invitation for) supplemental 3.0-T MRI at 8 sites (intervention arm; n=8,061) or mammography screening only (control arm; n=32,312). The difference in interval cancers after the first (prevalent) screening round, during the two-year screening interval, was investigated by intention-to-treat (ITT) analysis, and by complier-average causal effect (CACE) analysis to account for noncompliance. The performance of the incident screening rounds was investigated as well.

In the intervention arm, 4,783 (59%) underwent MRI examination. Cancer detection rate was 16.5/1000 screens [95%CI:13.3-20.5]. For this, 9.5% of women were recalled (6.3% with biopsy). Positive predictive values are 17.4% [95%CI:14.2%-21.2%] (recall) and 26.3% [95%CI:21.7%-31.6%] (biopsy). In the intervention arm, cancers were more frequently stage 0-I than in the control arm (82.8% vs 41.6%, p<0.001). With ITT analysis, the interval cancer rate was 4.98/1000 women in the control arm and 2.48/1000 women in the intervention arm, leading to a reduction of 2.50/1000 women [95%CI:0.98-3.71]; p<0.001. With CACE analysis, this reduction was 4.22/1000 women [95%CI:2.01-6.43]. Preliminary results of the incident screening rounds showed that 3,548 women had again undergone (at least one) mammographic screening with a negative result. Supplemental cancer detection rate was 5.3/1000 screens [95%CI:3.4-7.7]. For this, 2.8% [95%CI:2.4%-3.4%] of women were recalled for further diagnostic work-up. At the meeting, results on cost-effectiveness will be presented as well.

CONCLUSION

Supplemental MRI screening in women with extremely dense breasts results in statistically significantly fewer interval cancers. In subsequent rounds, both the cancer detection rate and the false-positive rate decrease.

CLINICAL RELEVANCE/APPLICATION

There is a heated debate on the value of supplemental screening in women with dense breasts. The DENSE trial is the first randomized trial on supplemental MRI screening that has been performed in women with dense breasts.

RC215-04 Abbreviated Screening Breast MRI Protocol: Impact on Cancer Detection and Biopsy Rates

Monday, Dec. 2 9:05AM - 9:15AM Room: Arie Crown Theater

Participants

Andrew J. Lukaszewicz, MD, Brampton, ON (*Abstract Co-Author*) Nothing to Disclose Leslie Lamb, MD, Boston, MA (*Abstract Co-Author*) Nothing to Disclose Paul Healey, Ottawa, ON (*Abstract Co-Author*) Nothing to Disclose Ellen Alie, Ottawa, ON (*Abstract Co-Author*) Nothing to Disclose Jean M. Seely, MD, Ottawa, ON (*Presenter*) Nothing to Disclose

For information about this presentation, contact:

jeseely@toh.ca

PURPOSE

To assess patient outcomes with the implementation of an abbreviated breast magnetic resonance imaging (MRI) protocol for highrisk breast screening.

METHOD AND MATERIALS

In this IRB-approved study performed at a large academic institution, an abbreviated breast MRI protocol (AP) was implemented for high-risk patients (IBIS lifetime risk \geq 25%) in a population-based high-risk screening program (pre and two post-contrast T1 and T2 sequences). The protocol was evaluated prospectively for 10 months. It was compared to a standard protocol (SP) in the same population during the 12 previous months. MRI scanning times, BI-RADS assessment categories, positive predictive values (PPV3) and cancer detection rates (CDR) were evaluated.

RESULTS

A total of 1539 patients during the 22-month study period were included. 658 patients underwent 658 AP screening MRIs. Of those, 135 (20.5%) were baseline exams and 523 (79.5%) were prevalent exams. 881 patients underwent 881 SP screening MRIs during the comparison study period. Of those, 230 (26.1%) were baseline exams and 651 (73.9%) were prevalent exams. The AP scanning time was an average of 16.3 minutes (range 12-25), compared to 27 minutes (range 25-30) in the SP. Abnormal interpretation rate with the AP was 12.5% (82/658) compared to 19.1% (168/881) with the SP (p<0.001). The BI-RADS 3 rate for the AP was 6.9% (45/658) compared to 7.2% (63/881) with the SP (p=0.81). Breast biopsies were performed in fewer patients with the AP [8.4% (55/658)] than with the SP [13.7% (121/881) (p=0.001). PPV3 for the AP was 20.0% (11/55) compared to 12.4% (15/121) for the SP (p =0.19). The CDR was 16.7/1000 (11/658) with the AP and 17.0/1000 (15/881) with the SP (p=0.96).

CONCLUSION

Using an abbreviated breast screening MRI protocol in high-risk patients led to fewer false positives, and was associated with 5% fewer benign biopsies, while a similar cancer detection rate was maintained.

CLINICAL RELEVANCE/APPLICATION

Abbreviated breast MRI screening protocols may lead to increased tolerability and MRI capacity while optimizing quality indicators. Further study is required to determine long-term outcomes.

RC215-05 Radiomics for Prediction of Breast Cancer Prognosis Using Dynamic Contrast-Enhanced Magnetic Resonance Imaging (DCE-MRI)

Monday, Dec. 2 9:15AM - 9:25AM Room: Arie Crown Theater

Participants

Seri Kang, Iksan , Korea, Republic Of (*Abstract Co-Author*) Nothing to Disclose Hye-won Kim, MD,PhD, Iksan, Korea, Republic Of (*Presenter*) Nothing to Disclose

For information about this presentation, contact:

kangseli21@naver.com

PURPOSE

To evaluate the value of dynamic contrast enhanced magnetic resonance imaging (DCE-MRI) parameters as an imaging biomarker for predicting prognosis in the breast cancer, we analyzed the association with the histopathologic factors of the tumor.

METHOD AND MATERIALS

A total of 122 invasive ductal carcinomas (IDCs) in 105 women who underwent preoperative breast DCE-MRI on a 3T scanner between November 2017 and December 2018 were enrolled. Twenty-fifth, 50th, 75th percentile and coefficient of variation (CV) of each perfusion parameter (Ktrans, Kep, Ve and Vp) were calculated within each tumor. Histopathologic factors such as estrogen receptor (ER), progesterone receptor (PR), human epidermal growth factor receptor 2 (HER2), Ki-67, p53, epidermal growth factor receptor (EGFR), CK 5/6, histologic grade and lymphovascular space invasion (LVSI) status were assessed. The student's t-test or Mann-Whitney U test were used for comparison of two groups and ANOVA or Kruskal-Wallis test for multiple groups.

RESULTS

Triple negative breast cancers exhibited higher Ktransmedian, Ktrans75, Kepmedian and Kep75 than luminal cancers (p<.05). ERnegative tumors showed higher Ktransmean, Ktransmedian and Ktrans75 than ER-positive tumors (p<.05). PR-negative tumors presented higher Ve25, Vemean, Vemedian and Ve75 than PR-positive tumors (p<.05). Tumors with higher Ki-67 showed higher Kep25, Kepmean and Kepmedian than tumors with lower Ki-67 (p<.05). P53-positive tumors exhibited higher Ktrans25, Ktransmean, Ktransmedian, Ktrans75, Kepmean, Kepmedian and Kep75 than p53-negative tumors (p<.05). Higher histologic grade tumors (grade II/III) presented higher Ktrans25, Ktransmean, Ktransmedian, Ktrans75, Kep25, Kepmean, Kepmedian, Kep75, Vp25, Vpmean and Vpmedian (p<.04) than grade I tumor. Tumors with LVSI presented higher Ktrans25, Ktransmedian, Ktrans75, Kepmean, Kepmedian and Kep75 than tumors without LVSI (p<.05). On the other hand, EGFR, CK 5/6 showed no significant correlation.

CONCLUSION

We identified breast cancer presenting higher Ktrans and Kep on DCE-MRI was associated with poor prognostic factors. Therefore, DCE-MRI perfusion parameters can be useful imaging biomarkers for prediction of tumor prognosis.

CLINICAL RELEVANCE/APPLICATION

DCE-MRI may be helpful to predict prognosis of breast cancer through analysis of perfusion parameters.

RC215-06 Prognostic Factors Associated with Survival in Breast Cancer Patients: Magnetic Resonance Imaging and Clinico-Pathologic Factors Associated with Disease Recurrence

Monday, Dec. 2 9:25AM - 9:35AM Room: Arie Crown Theater

Participants

Eunjin Lee, Suwon, Korea, Republic Of (*Presenter*) Nothing to Disclose Jeong Min Lee, Seoul, Korea, Republic Of (*Abstract Co-Author*) Nothing to Disclose Sung-Hun Kim, MD, Seoul, Korea, Republic Of (*Abstract Co-Author*) Nothing to Disclose Bong Joo Kang, Seoul, Korea, Republic Of (*Abstract Co-Author*) Nothing to Disclose Heerin Lee, Seoul, Korea, Republic Of (*Abstract Co-Author*) Nothing to Disclose

PURPOSE

To investigate prognostic factors predicting recurrence of breast cancer, focusing on imaging factors including advanced MR techniques and clinico-pathologic factors.

METHOD AND MATERIALS

This retrospective study was approved by our institutional review board, and the requirement to obtain informed consent was waived. A total of 267 patients with breast cancer who underwent dynamic contrast-enhanced magnetic resonance imaging (MRI) before surgery from February 2014 to June 2016 was included in the study sample. Imaging parameters of MRI, including morphologic information, perfusion parameters, and texture analysis, were retrospectively reviewed by two breast expert radiologists. Patient clinical pathologic information was also reviewed. Univariable and multivariable Cox proportional hazards regression analyses were used to identify factors associated with cancer recurrence. Using Kaplan-Meier survival analysis, disease-free survival was compared between patients who experienced recurrence and those who did not.

RESULTS

At a median follow up of 26 months, 23 patients (8%) showed disease: five cases of ipsilateral breast or axilla recurrence, one case of contralateral breast recurrence, 15 cases of distant metastasis, and one case of both ipsilateral breast recurrence and distant metastasis. Increased ipsilateral vascularity, entropy and kurtosis from texture analysis, and multiple perfusion parameters showed significant association with disease recurrence. The Ve 25th percentile value of perfusion parameters had the highest hazard ratio of 4.37 [95% confidence interval (CI): 1.80-11.18]. Pathologic stage, especially if higher than stage II, also showed significant association with disease recurrence, independent of multiple MRI parameters. In addition, higher entropy, higher Kep 25th percentile, higher Ve 25th percentile value, and increased ipsilateral vascularity were associated with short interval time to disease recurrence by Kaplan-Meier survival analysis.

CONCLUSION

Higher pathologic stage and MRI parameters of texture parameters, perfusion parameters, and increased ipsilateral vascularity are predictors of breast cancer recurrence and may also be predictors of poor survival.

CLINICAL RELEVANCE/APPLICATION

Multiple parameters of breast MRI including perfusion and texture analysis can predict breast cancer recurrence in addition to the clinico-pathologic factors.

RC215-07 Diffusion with Very High b-Value in Breast MRI: End of the Contrast Injection?

Monday, Dec. 2 9:35AM - 9:45AM Room: Arie Crown Theater

Participants Hajar Hamri, MD, Paris , France (*Presenter*) Nothing to Disclose Zoe Jolibois, Paris, France (*Abstract Co-Author*) Nothing to Disclose Elisabeth Weiland, Erlangen, Germany (*Abstract Co-Author*) Nothing to Disclose Cedric M. De Bazelaire, MD, PhD, Paris , France (*Abstract Co-Author*) Nothing to Disclose

PURPOSE

To evaluate diagnostic yield of diffusion weighted imaging (DWI) with very high b-value combined with T2 weighted sequence in breast MRI.

METHOD AND MATERIALS

130 patients were included consecutively in this retrospective study approved by our IRB.All patients underwent breast MRI (MAGNETOM Aera, Siemens 1.5T, 18-channel breast antenna) with a 2D-SS-EPI-SPAIR diffusion sequence (TR / TE: 5200 / 67ms, b 2500s / mm²) in addition to the standard protocol with 2D-T1-FSE, 3D-T2-SPAIR and 3D-T1-VIBE-SPAIR -DCE. 2 independent readings were performed by 2 radiologists in consensus: 1) combined analysis of the DWI and T2W sequences and 2) analysis of the standard protocol according to BIRADS lexicon. All findings with hypersignal DWI and low T2 signal were considered as suspicious. All suspicious lesions were biopsied. BIRADS 1-3 lesions had at least 2years follow-up or histological proof. Diagnostic yields were compared using ROC curves.

RESULTS

A total of 180 lesions were analyzed of wich 27% were malignant. Similar sensitivity but higher specificity were found with the combined analysis of DWI and T2W sequences compared with T1W, T2W and DCE sequences (92%, 92% vs 96%, 82% respectively). However, the comparison of ROC curves showed no significant difference (AUC= 0.92 vs 0.89 respectively, p= 0,364).

CONCLUSION

Combined analysis of DWI with a b-value of 2500s / mm² and T2W sequences could be a reliable alternative to gadolinium injection, particularly for screening in women at high risk of breast cancer.

CLINICAL RELEVANCE/APPLICATION

Diagnosis of breast cancer is possible with combined analysis of DWI with a b-value of 2500s/mm² and T2W sequences, even in non-contrast MR imaging.

RC215-08 Updates on the Use of Breast MRI in Women with Higher than Average Risk

Monday, Dec. 2 9:45AM - 10:10AM Room: Arie Crown Theater

Participants Debra L. Monticciolo, MD, Temple, TX (*Presenter*) Nothing to Disclose

LEARNING OBJECTIVES

1) To understand which populations at higher than average risk for breast cancer that may benefit from supplemental screening with MRI. 2) To provide an update of the latest ACR recommendations for the use of breast MRI in women of higher risk. 3) To understand the reasoning and data supporting the newest recommendations for high risk women.

RC215-09 MRI: Part 2

RC215-10 MRI Biomarkers

Monday, Dec. 2 10:30AM - 10:55AM Room: Arie Crown Theater

Participants Julia Camps Herrero, MD, Alzira, Spain (*Presenter*) Nothing to Disclose

For information about this presentation, contact:

juliacamps@gmail.com

LEARNING OBJECTIVES

1) To learn about the pathway of an imaging biomarker in its different stages: proof of concept, proof of mechanism, proof of principle and proof of efficacy and effectiveness. 2) To know the different types of MR-derived imaging biomarkers and their current clinical use. 3) To understand how the quantitative MR-phenotypes can be integrated into clinical practice as well as the challenges we face in this implementation.

ABSTRACT

Breast MRI is the most sensitive modality for high-risk screening and for the diagnosis and characterization of breast lesions. Both qualitative and quantitative imaging biomarkers can be derived from breast MRI that can be associated with a patient's risk to develop a breast cancer, the prognosis of a known breast cancer through data mining of MR-phenotypes or a prediction of response evaluation to neoadjuvant therapies.BM of breast cancer risk that can be analyzed through breast MRI are breast density and background parenchymal enhancementBC is a heterogeneous disease and the different molecular subtypes that have been described in the last decade have had a tremendous impact on the personalized treatment of the disease. These subtypes have been shown to be predictive of disease free survival and overall survival. Computer extraction or analysis of quantitative imaging features also known as radiomics has been applied to MRI data (tumor morphology, texture and enhancement kinetics) in order to build predictive or prognostic models and correlate MR features with BC molecular subtypes. The correlation of imaging phenotypes assays. These MR-phenotypes can serve as surrogate markers of tumor behaviour and survival and speed up drug development as well as personalized therapies. The process of imaging biomarker validation is not easy nor simple, standardisation of imaging processing and analysis and measurement of the MR features is still a challenge.

RC215-11 Comparison of Four Radiomics-Based Classification Methods in Diagnosis of Breast Lesions with Multi-b Diffusion-Weighted MR Imaging

Monday, Dec. 2 10:55AM - 11:05AM Room: Arie Crown Theater

Participants

Kun Sun, Shanghai, China (*Presenter*) Nothing to Disclose Zhicheng Jiao, Chapel Hill, NC (*Abstract Co-Author*) Nothing to Disclose Xu Yan, Shanghai, China (*Abstract Co-Author*) Employee, Siemens AG Han Zhang, Chapel Hill, NC (*Abstract Co-Author*) Nothing to Disclose Jie-Zhi Cheng, BEng,PhD, Shanghai, China (*Abstract Co-Author*) Employee, Shanghai United Imaging Healthcare Co, Ltd Fuhua Yan, MS, Shanghai, China (*Abstract Co-Author*) Nothing to Disclose Dinggang Shen, Chapel Hill, NC (*Abstract Co-Author*) Nothing to Disclose

PURPOSE

To compare the diagnostic performance of four radiomics-based classification methods in differentiation between benign and malignant breast lesions with multi-b diffusion-weighted MR imaging.

METHOD AND MATERIALS

Totally, 542 lesions in 542 patients with multi-b diffusion-weighted-images (b values: 0-2500 s/mm2) were acquired, where 100 radiomic features (by using Pyradiomics toolbox) were computed with multi-b diffusion-weighted-imaging, as well as monoexponential (ME) with ME-ADC0-1000 and ME-ADCall-b, bi-exponential (BE) with BE-D, BE-D*, and BE-f, stretched-exponential (SE) with SE-DDC and SE-a, and diffusion kurtosis imaging (DKI) with DKI-D and DKI-K. Radiomics-based analysis was performed by using four classification methods, including random forest (RF), principal component analysis (PCA), L1 regularization (L1R), and support vector machine (SVM). The dataset is randomly split into the training and testing sets for 100 times to evaluate the performance of all the classification models. The training and testing sets were randomly split into 50% and 50%. The radiomics-based diagnosis was compared to the pathological results. AUCs were used to compare performances of the four classification models.

RESULTS

The AUCs of RF in the differential diagnosis of breast lesions ranged from 0.80 (BE-D*) to 0.85 (BE-D), whereas the AUCs of PCA ranged from 0.53 (SE-DDC) to 0.79 (b1500). The AUCs of L1R and SVM ranged from 0.53 (SE-DDC) to 0.83 (ME-ADC0-1000) and from 0.51 (SE-DDC) to 0.82 (b2500), respectively. The top 5 sequences with the highest AUCs by the RF are BE-D (0.85), ME-ADCall-b (0.84), DKI-K (0.84), ME-ADC0-1000 (0.83) and b2500 (0.83). The top 5 sequences with the highest mean AUCs are b2500 (0.82), b2000 (0.81), ME-ADC0-1000 (0.81), b1500 (0.81), and BE-D (0.81). RF attained higher AUCs than L1R, PCA and SVM. However, there was no significant difference among these four classification methods in the top 5 sequences with the highest mean AUCs (all P > 0.002).

CONCLUSION

Radiomics-based analysis with RF model was recommended for the classification of breast lesions. BE-D with the highest AUC by RF model and b2500 with the highest mean AUC were recommended for the diffusion-related radiomic analysis in breast cancer evaluation.

CLINICAL RELEVANCE/APPLICATION

For radiomic analysis of multi-b diffusion-weighted imaging in the evaluation of breast lesions, RF model is provided to be a reliable classification technique.

RC215-12 Radiomic Features Derived from Contrast-Enhanced Magnetic Resonance and Diffusion Weighted Imaging for the Assessment of Breast Cancer Molecular Subtypes

Monday, Dec. 2 11:05AM - 11:15AM Room: Arie Crown Theater

Participants

Doris Leithner, MD, Frankfurt Am Main, Germany (*Presenter*) Nothing to Disclose Marius E. Mayerhoefer, MD,PhD, Vienna, Austria (*Abstract Co-Author*) Speaker, Siemens AG; Research support, Siemens AG Blanca Bernard-Davila, MPH,MS, New York, NY (*Abstract Co-Author*) Nothing to Disclose Maxine S. Jochelson, MD, New York, NY (*Abstract Co-Author*) Speaker, General Electric Company Joao V. Horvat, MD, New York, NY (*Abstract Co-Author*) Nothing to Disclose Maria Adele Marino, MD, Messina, Italy (*Abstract Co-Author*) Nothing to Disclose Daly B. Avendano, MD, Monterrey, Mexico (*Abstract Co-Author*) Nothing to Disclose Danny F. Martinez, BSC,MSc, New York, NY (*Abstract Co-Author*) Nothing to Disclose Sunitha Thakur, PhD, MS, New York, NY (*Abstract Co-Author*) Nothing to Disclose Christophe Arendt, MD, Frankfurt am Main, Germany (*Abstract Co-Author*) Nothing to Disclose Elizabeth A. Morris, MD, New York, NY (*Abstract Co-Author*) Nothing to Disclose Katja Pinker-Domeniq, MD, New York, NY (*Abstract Co-Author*) Nothing to Disclose

For information about this presentation, contact:

doris.leithner@gmail.com

PURPOSE

To evaluate the performance of combined radiomic features extracted from contrast-enhanced magnetic resonance imaging (CE-MRI) and diffusion-weighted imaging (DWI) for the assessment of breast cancer receptor status and molecular subtypes.

METHOD AND MATERIALS

Ninety-one patients with biopsy-proven breast cancer (luminal A, n=49; luminal B, n=8; HER2-enriched, n=11; triple negative (TN), n=23) who underwent 3T CE-MRI and DWI were included in this IRB-approved HIPAA-compliant retrospective study. Radiomic features (co-occurrence and run-length matrix, absolute gradient, autoregressive model, Haar wavelet transform and lesion geometry) were extracted from manually defined ROIs (total number of features per lesion, n=704) on early CE-MR images and ADC maps. The five best features for the differentiation of molecular subtypes were selected, separately for each technique (i.e. CE-

MRI and ADC) using probability of error and average correlation coefficients. A multi-layer perceptron feed-forward artificial neural network (MLP-ANN) was used for radiomics-based classification, with histopathology serving as reference standard. 70% of the cases were used for training, and 30% for validation. The analysis was performed five times each.

RESULTS

MLP-ANN yielded an overall median area under the receiver-operating-characteristic curve (AUC) of of 0.86 (0.77-0.92) for separation of TN from all other cancers, with median accuracies of 85.9% in the training and 85.2% in the validation datasets. The separation of luminal A and triple negative cancers yielded an overall median AUC of 0.8 (0.75-0.83), with median accuracies of 74% in the training, and 68.2% in the validation dataset. All other AUCs were below 0.8.

CONCLUSION

Combination of radiomic features extracted from CE-MRI and DWI may be useful to differentiate triple negative and luminal A breast cancers from other subtypes.

CLINICAL RELEVANCE/APPLICATION

Combined CE-MRI and DWI radiomic features may potentially provide prognostic indicators derived from the entire tumor, which may be used for tumor monitoring during treatment.

RC215-13 Change in Contralateral Parenchymal Enhancement during Neoadjuvant Endocrine Treatment is Associated with Tumor Response in Unilateral ER+/HER2- Breast Cancer Patients

Monday, Dec. 2 11:15AM - 11:25AM Room: Arie Crown Theater

Participants

Max Ragusi, MD, Utrecht, Netherlands (*Presenter*) Nothing to Disclose Claudette E. Loo, MD, Amsterdam, Netherlands (*Abstract Co-Author*) Nothing to Disclose Bas H. van der Velden, MSc, Utrecht, Netherlands (*Abstract Co-Author*) Nothing to Disclose Jelle Wesseling, Amsterdam, Netherlands (*Abstract Co-Author*) Nothing to Disclose Regina G. Beets-Tan, MD, PhD, New York, NY (*Abstract Co-Author*) Nothing to Disclose Sjoerd G. Elias, MD, PhD, Utrecht, Netherlands (*Abstract Co-Author*) Nothing to Disclose Kenneth G. Gilhuijs, PhD, Amsterdam, Netherlands (*Abstract Co-Author*) Nothing to Disclose

For information about this presentation, contact:

m.a.a.ragusi-2@umcutrecht.nl

PURPOSE

To investigate whether contralateral parenchymal enhancement (CPE), a quantitative measure of parenchymal enhancement, is associated with tumor response during neoadjuvant endocrine treatment (NET) of unilateral ER+/HER2- breast cancer.

METHOD AND MATERIALS

Retrospective single center cohort study of unilateral ER+/HER2- breast cancer patients treated with NET between Jan 2013 and Dec 2017. Pretreatment and response DCE-MRIs (3 and 6 months) were acquired using 1.5T or 3T MRI. The early contrastenhanced images were acquired after 90s post-contrast injection and the late images after 360-450s. CPE is defined as the mean of the top-10% relative parenchymal enhancement between early and late post-contrast images of the contralateral breast. Tumor response was expressed by the preoperative endocrine prognostic index (PEPI), which identifies three distinct groups based on post-treatment pT, pN, Ki-67 and ER-status. A high PEPI-group is associated with increased risks of relapse and death. We used a linear mixed model to assess log(CPE) during NET in relation to tumor response, using patient-level random intercepts to account for clustered data.

RESULTS

A total of 39 patients with 79 CPE measurements were available (patients with unavailable PEPI-score [n=2] or MRIs with motion artifacts [n=2] were excluded). Mean age was 61 (\pm 11) years. Mean treatment duration was 7.2 (\pm 1.4) months. After NET, 12 patients had PEPI-1 score, 15 PEPI-2, and 12 PEPI-3. Pretreatment CPE did not differ between PEPI-groups: difference of 7.8% in PEPI-1 vs 2 (P=.593), 29.9% in PEPI-1 vs 3 (P=.091), and 20.5% in PEPI-2 vs 3 (P=.209). Change in CPE over time depended on tumor response (Pinteractiontime*PEPI=.005). CPE increased in PEPI-1 by 5.0% (95% CI= 0.8-9.4%, P=.025) per month, and decreased in the less favorable groups by 2.4% (95% CI= -1.4-6.0%, P=.224) for PEPI-2 and 5.8% (95% CI= -0.1-11.3%, P=.058) for PEPI-3 per month. The difference in CPE over time was significant for PEPI-1 vs 2 (P=.014) and PEPI-1 vs 3 (P=.005), but not for PEPI-2 vs 3 (P=.327).

CONCLUSION

Change in CPE during NET is associated with tumor response: an increase in CPE over time was associated with a favorable tumor response.

CLINICAL RELEVANCE/APPLICATION

Contralateral parenchymal enhancement has potential as a prognostic biomarker in breast cancer patients to assess tumor response during neoadjuvant endocrine treatment.

RC215-14 DCE-MRI Biomarkers of Changes in Peri-Tumoral and Intra-Tumoral Heterogeneity for Improving Early Prediction of Survival after Neoadjuvant Chemotherapy for Breast Cancer

Monday, Dec. 2 11:25AM - 11:35AM Room: Arie Crown Theater

Participants Nariman Jahani, Philadelphia, PA (*Presenter*) Nothing to Disclose Eric A. Cohen, Philadelphia, PA (*Abstract Co-Author*) Nothing to Disclose Susan Weinstein, MD, Philadelphia, PA (*Abstract Co-Author*) Nothing to Disclose Nola M. Hylton, PhD, San Francisco, CA (*Abstract Co-Author*) Research support, General Electric Company David Newitt, PhD, San Francisco, CA (*Abstract Co-Author*) Nothing to Disclose Christos Davatzikos, PhD, Philadelphia, PA (*Abstract Co-Author*) Nothing to Disclose Despina Kontos, PhD, Philadelphia, PA (*Abstract Co-Author*) Nothing to Disclose

For information about this presentation, contact:

nariman.jahani@uphs.upenn.edu

PURPOSE

To evaluate changes in peri- and intra-tumoral DCE-MRI heterogeneity as a biomarker for early prediction of recurrence-free survival (RFS) after neoadjuvant chemotherapy (NAC) for breast cancer.

METHOD AND MATERIALS

We analyzed DCE-MRI scans of 132 women from the I-SPY1 TRIAL acquired before and after the first cycle of NAC. A deformable registration technique was applied to quantify voxel-wise changes during NAC. From that, two groups of feature maps were extracted within peri- and intra-tumoral regions: 1) four features representing deformations in shapes and volumes and 2) four kinetic features indicating changes in enhancement patterns. Also, eight additional features were computed to indicate relative changes between peri- and intra-tumoral heterogeneity. Thus, a total of 24 imaging features were extracted and evaluated in three models: 1) using combinations of peri- and intra-tumor features 2) using only intra-tumoral features 3) using only peri-tumoral features. For a proper comparison, the same number of features (top six RFS-associated features) were selected for each model by Cox regression via five-fold cross-validation. Functional tumor volume (FTV) and established covariates of age, race, and hormone receptor status were considered. The C-statistic was evaluated over the cross-validation loops and the likelihood ratio test was used to compare nested models.

RESULTS

Significant improvement was achieved when using both peri- and intra-tumoral features (c-statistic=0.77, p<0.05) compared to models using only peri- or intra-tumoral features (c-statistics =0.70 and 0.73, respectively). For the combined model, all selected features including three of relative changes, two intra-tumoral, and one peri-tumoral features had strong associations with RFS (p<0.01). Performance of the combined model was improved further by adding FTV and the established histopathologic and demographic covariates (c-statistic=0.79, pLikelihood-Ratio<0.001).

CONCLUSION

Analysis of changes in peri-tumoral heterogeneity features and their relative changes with respect to intra-tumoral heterogeneity may reveal markers from the surrounding tumor tissues that could improve early assessment of RFS for breast cancer NAC.

CLINICAL RELEVANCE/APPLICATION

Quantification of changes in peri- and intra-tumoral heterogeneity may improve early prediction of patient survival after NAC providing better guidance for personalized cancer treatment.

RC215-15 Background Parenchymal Enhancement

Monday, Dec. 2 11:35AM - 12:00PM Room: Arie Crown Theater

Participants

Christoph I. Lee, MD, Mercer Island, WA (*Presenter*) Royalites, The McGraw-Hill Companies; Royalties, Oxford University Press; Royalties, Wolters Kluwer nv;

LEARNING OBJECTIVES

1) Provide an overview of reporting standards for breast parenchymal enhancement observed on breast MRI. 2) Describe the current evidence regarding breast parenchymal enhancement and associated breast cancer risk. 3) Identify future directions for incorporating breast parenchymal enhancement in cancer risk assessment.







RC217

Emerging Technology: 3D Joint MR Imaging



Participants

Avneesh Chhabra, MD, Flowermound, TX (*Moderator*) Consultant, ICON plc; Consultant, Treace Medical Inc; Author with royalties, Wolters Kluwer nv; Author with royalties, Jaypee Brothers Medical Publishers Ltd

For information about this presentation, contact:

Avneesh.chhabra@utsouthwestern.edu

LEARNING OBJECTIVES

1) Gain knowledge of techniques of optimal 3D isotropic MRI technique for joint and bone evaluation. 2) Learn how to create meniscus, cruciate and ankle ligament, and rotator cuff specific reconstructions using 3D MRI. 3) Learn 3D evaluation of internal joint derangements and their arthroscopy correlations. 4) Explain the advantages and drawbacks of 3D MSK MRI. 5) Describe new techniques to accelerate 3D MSK MRI. 6) Gain knowledge of the optimal 3D isotropic MRI technique for knee meniscus and bone evaluation. 7) Learn how to create meniscus and cruciate specific reconstructions using 3D MRI. 8) Learn how to evaluate meniscus tears and describe their longitudinal extent with arthroscopy correlations. 9) To apply current techniques and acquisition strategies for isotropic 3D MRI of the ankle joint. 10) To review the diagnostic performance and comparative accuracy of 3D MRI of the ankle joint. 11) To illustrate the strengths and limitations of 3D MRI of the ankle. 12) Define technical elements that allow acquisition of high resolution 3D MRI and conventional MR sequences to referring clinicians. 15) Discuss accuracy of 3D MRI of the hip as compared to conventional MR sequences and MR arthrogram. 16) List pitfalls and list measures to minimize artifacts in using high resolution 3D Sequences of the hip. 17) Review the imaging and post-processing techniques used to create 3D MRI shoulder models. 18) Discuss the use of 3D MRI bone models in the evaluation of anterior shoulder instability patients. 19) Discuss the use of 3D MRI bone models in the evaluation of anterior shoulder instability patients. 19) Discuss

Sub-Events

RC217A Fast 3D Imaging: Emerging Techniques to Accelerate 3D Acquisitions

Participants

Naveen Subhas, MD, Shaker Heights, OH (Presenter) Research support, Siemens AG

LEARNING OBJECTIVES

1) Explain the advantages and drawbacks of 3D MSK MRI. 2) Describe new techniques to accelerate 3D MSK MRI.

RC217B 3D MR Imaging of Knee Joint

Participants

Avneesh Chhabra, MD, Flowermound, TX (*Presenter*) Consultant, ICON plc; Consultant, Treace Medical Inc; Author with royalties, Wolters Kluwer nv; Author with royalties, Jaypee Brothers Medical Publishers Ltd

For information about this presentation, contact:

Avneesh.chhabra@utsouthwestern.edu

LEARNING OBJECTIVES

1) Gain knowledge of the optimal 3D isotropic MRI technique for knee meniscus and bone evaluation. 2) Learn how to create meniscus and cruciate specific reconstructions using 3D MRI. 3) Learn how to evaluate meniscus tears and describe their longitudinal extent with arthroscopy correlations.

RC217C 3D MR Imaging of Ankle Joint

Participants

Jan Fritz, MD, Baltimore, MD (*Presenter*) Institutional research support, Siemens AG; Institutional research support, Johnson & Johnson; Institutional research support, Zimmer Biomet Holdings, Inc; Institutional research support, Microsoft Corporation; Institutional research support, BTG International Ltd; Scientific Advisor, Siemens AG; Scientific Advisor, General Electric Company; Scientific Advisor, BTG International Ltd; Speaker, Siemens AG; Patent agreement, Siemens AG

For information about this presentation, contact:

janfritz777@gmail.com

LEARNING OBJECTIVES

1) To apply current techniques and acquisition strategies for isotropic 3D MRI of the ankle ioint. 2) To review the diagnostic

performance and comparative accuracy of 3D MRI of the ankle joint. 3) To illustrate the strengths and limitations of 3D MRI of the ankle.

RC217D 3D MR Imaging of Hip Joint

Participants Oganes Ashikyan, MD, Dallas, TX (*Presenter*) Nothing to Disclose

For information about this presentation, contact:

oganes.ashikyan@utsouthwestern.edu

LEARNING OBJECTIVES

1) Define technical elements that allow acquisition of high resolution 3D MR images of the hip. 2) List common clinical indications for 3D MR imaging of the hip. 3) Explain differences between high resolution 3D MRI and conventional MR sequences to referring clinicians. 4) Discuss accuracy of 3D MRI of the hip as compared to conventional MR sequences and MR arthrogram. 5) List pitfalls and list measures to minimize artifacts in using high resolution 3D sequences of the hip.

RC217E 3D MR Imaging of Shoulder Joint

Participants Soterios Gyftopoulos, MD, Scarsdale, NY (*Presenter*) Nothing to Disclose

For information about this presentation, contact:

Soterios.Gyftopoulos@nyumc.org

LEARNING OBJECTIVES

1) Review the imaging and post-processing techniques used to create 3D MRI shoulder models. 2) Discuss the use of 3D MRI bone models in the evaluation of anterior shoulder instability patients. 3) Discuss the use of 3D MRI soft tissue models in the evaluation of rotator cuff tendon tears.

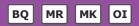




RC218

Whole Body MRI for Precision Oncology in Malignant Bone Disease

Monday, Dec. 2 8:30AM - 10:00AM Room: S103AB



AMA PRA Category 1 Credits ™: 1.50 ARRT Category A+ Credit: 1.75

FDA Discussions may include off-label uses.

Participants

Evis Sala, MD, PhD, Cambridge, United Kingdom (Moderator) Nothing to Disclose

LEARNING OBJECTIVES

1) Describe the limitations of current imaging modalities in evaluation of metastatic bone disease. 2) Learn the added value of whole body MRI in evaluation of metastatic bone disease in various malignancies including prostate cancer and multiple myeloma. 3) Understand the role of quantitative whole body MRI in delivering precision medicine in oncology.

Sub-Events

RC218A Imaging of Metastatic Bone Disease: Current Limitations

Participants

Hebert Alberto Vargas, MD, Cambridge, United Kingdom (Presenter) Nothing to Disclose

LEARNING OBJECTIVES

1) Discuss the challenges associated with the diagnosis and interpretation of bone findings in patients with metastatic disease.

ABSTRACT

Conventional imaging of metastatic disease to the bone is notoriously difficult. Unlike soft tissue metastases, significant cortical disruption is required before a bone metastases is visible on CT, and bone scan demonstrates the effect of the metastases on bone, rather than the metastases themselves. MR partially overcomes these limitations, as early bone metastases can be detected. However, even after bone metastases are apparent on imaging, it is difficult to assess their evolution with regards to therapy response.

RC218B WB-MRI of Multiple Myeloma: My-RADS

Participants

Christina Messiou, MD, BMBS, London, United Kingdom (Presenter) Nothing to Disclose

For information about this presentation, contact:

Christina.Messiou@icr.ac.uk

LEARNING OBJECTIVES

1) List indications for WB-MRI in multiple myeloma. 2) Describe the core and comprehensive protocols for WB-MRI in multiple myeloma. 3) Apply a systematic approach to reporting WB-MRI in multiple myeloma as outlined in MY-RADS. 4) Review the MY-RADS criteria for assessing disease phenotype, burden and response assessment with case examples.

ABSTRACT

Acknowledging the increasingly important role of WB-MRI for directing myeloma patient care, a multidisciplinary international expert panel of radiologists, medical physicists and haematologists convened to discuss the performance standards, merits and limitations of WB-MRI in myeloma. The MY-RADS imaging recommendations are designed to promote standardization and diminish variations in the acquisition, interpretation, and reporting of WB-MRI in myeloma both in the clinical setting and within clinical trials. MY-RADS comprehensive disease classification requires validation within clinical trials including assessments of reproducibility.

Active Handout:Christina Messiou

http://abstract.rsna.org/uploads/2019/18001096/Messiou Final RSNA 2019 WB MRI in multiple myeloma.pdf

RC218C WB-MRI of Metastatic Bone: MET-RADS

Participants

Anwar R. Padhani, MD,FRCR, Northwood, United Kingdom (*Presenter*) Advisory Board, Siemens AG; Speakers Bureau, Siemens AG; Speakers Bureau, sanofi-aventis Group; Speakers Bureau, Johnson & Johnson; Speakers Bureau, Astellas Group

For information about this presentation, contact:

anwar.padhani@stricklandscanner.org.uk

LEARNING OBJECTIVES

1) MET-RADS measurement protocols distinguishing between tumor detection (core) and response (comprehensive) assessments.

2) To highlight and review the MET-RADS response assessment criteria and their application. 3) To illustrate MET-RADS usage with case examples and to provide efficacy data on MET-RADS use in clinical practise. 4) Outline development steps for MET-RADS.

ABSTRACT

MET-RADS provides the minimum standards for whole body MRI with DWI regarding image acquisitions, interpretation, and reporting of both baseline and follow-up monitoring examinations of patients with advanced, metastatic cancers. MET-RADS is suitable for guiding patient care in practice (using the regional and overall assessment criteria), but can also be incorporated into clinical trials when accurate lesion size and ADC measurements become more important (the recording of measurements is not mandated for clinical practice). MET-RADS enables the evaluation of the benefits of continuing therapy to be assessed, when there are signs that the disease is progressing (discordant responses). MET-RAD requires validation within clinical trials initially in studies that assess the effects of known efficacious treatments. METRADS measures should be correlated to other tumor response biomarkers, quality of life measures, rates of skeletal events, radiographic progression free survival and overall survival. The latter will be needed for the introduction of WB-MRI into longer term follow-up studies, that will allow objective assessments of whether WB-MRI is effective in supporting patient care

RC218D Quantitative WB-MRI for Promoting Precision Oncology

Participants

Dow-Mu Koh, MD, FRCR, Sutton, United Kingdom (Presenter) Nothing to Disclose

LEARNING OBJECTIVES

1) To review the quantitative parameters that can be derived from WB-MRI studies. 2) To understand the evolving role of quantitative WB-MRI for the evaluation of metastatic bone disease. 3) To appreciate the application of quantitative WB-MRI for precision oncology in assessing tumour treatment response and disease heterogeneity.





RC229

Abbreviated Liver MRI

Monday, Dec. 2 8<u>:30AM</u> - 10:00AM Room: <u>N228</u>



AMA PRA Category 1 Credits ™: 1.50 ARRT Category A+ Credit: 1.75

FDA Discussions may include off-label uses.

LEARNING OBJECTIVES

1) To define the objective of abbreviated MRI protocols from a cost-effectiveness standpoint. 2) To outline a conceptual framework for evaluating the cost-effectiveness of an abbreviated liver MRI protocol. 3) To project how different factors related to the test performance and cost of an abbreviated liver MRI protocol are likely to shape its downstream value. 4) Select patients in whom abbreviated MRI is indicated for quantitative evaluation of diffuse liver disease. 5) Build an abbreviated MRI examination protocol for diffuse liver disease evaluation. 6) Interpret quantitative imaging biomarker maps (fat, iron, and fibrosis) of the liver and generate a clinical report. 7) Explain the essential sequences required within an abbreviated protocol for the detection of liver metastases. 8) Compare the diagnostic performance of an abbreviated protocol versus standard multiparametric liver protocol for the assessment of colorectal liver metastases. 9) Identify pitfalls / challenges for the abbreviated liver protocol. 10) Review current guidelines for liver cancer screening. 11) Review the current options for abbreviated MRI protocol and early results for liver cancer screening.

Sub-Events

RC229A Cost Evaluation of Abbreviated Liver MRI Protocols

Participants

Pari V. Pandharipande, MD, MPH, Chestnut Hill, MA (Presenter) Research Grant, Medical Imaging & Technology Alliance

For information about this presentation, contact:

pari@mgh-ita.org

LEARNING OBJECTIVES

1) To define the objective of abbreviated MRI protocols from a cost-effectiveness standpoint. 2) To outline a conceptual framework for evaluating the cost-effectiveness of an abbreviated liver MRI protocol. 3) To project how different factors related to the test performance and cost of an abbreviated liver MRI protocol are likely to shape its downstream value.

RC229B Abbreviated Liver Protocol in Diffuse Liver Disease

Participants

Takeshi Yokoo, MD, PhD, Dallas, TX (Presenter) Nothing to Disclose

For information about this presentation, contact:

Takeshi.Yokoo@UTSouthwestern.EDU

LEARNING OBJECTIVES

1) Select patients in whom abbreviated MRI is indicated for quantitative evaluation of diffuse liver disease. 2) Build an abbreviated MRI examination protocol for diffuse liver disease evaluation. 3) Interpret quantitative imaging biomarker maps (fat, iron, and fibrosis) of the liver and generate a clinical report.

RC229C Abbreviated Liver Protocol in Metastatic Disease

Participants

Angela M. Riddell, MBBS, London, United Kingdom (Presenter) Nothing to Disclose

LEARNING OBJECTIVES

1) Explain the essential sequences required within an abbreviated protocol for the detection of liver metastases. 2) Compare the diagnostic performance of an abbreviated protocol versus standard multiparametric liver protocol for the assessment of colorectal liver metastases. 3) Identify pitfalls / challenges for the abbreviated liver protocol.

RC229D Abbreviated Liver Protocol for HCC Screening and Surveillance

Participants

Bachir Taouli, MD, New York, NY (Presenter) Research Grant, Bayer AG

For information about this presentation, contact:

bachir.taouli@mountsinai.org

LEARNING OBJECTIVES

1) Review current guidelines for liver cancer screening. 2) Review the current options for abbreviated MRI protocol and early results

for liver cancer screening.

ABSTRACT

Hepatocellular carcinoma (HCC) is the 2nd leading cause of cancer-related death worldwide, and the fastest growing cause of cancer death in the USA. The most important risk factor for HCC is cirrhosis. In this presentation, we will discuss the performance of ultrasound for HCC screening and surveillance and we will review recent developments in the use of abbreviated MRI protocols for HCC screening and surveillance.

RC229E Round Table Discussion

Participants

Pari V. Pandharipande, MD, MPH, Chestnut Hill, MA (*Presenter*) Research Grant, Medical Imaging & Technology Alliance Takeshi Yokoo, MD, PhD, Dallas, TX (*Presenter*) Nothing to Disclose Angela M. Riddell, MBBS, London, United Kingdom (*Presenter*) Nothing to Disclose Bachir Taouli, MD, New York, NY (*Presenter*) Research Grant, Bayer AG





CS21

Hot Topics in Contrast-Enhanced MRI: Presented by Northwest Imaging Forums, educational grant provided by Bracco Diagnostics, Inc.

Monday, Dec. 2 9:00AM - 10:30AM Room: S101AB

Participants

David S. Enterline, MD, Durham, NC (*Presenter*) Consultant, Bracco Group Speakers Bureau, Bracco Group Consultant, General Electric Company Research support, Siemens AG Research support, Koninklijke Philips Electronics NV Emanuel Kanal, MD, Pittsburgh, PA (*Presenter*) Consultant, Medtronic plc; Consultant, Bracco Group; Consultant, General Electric Company;

Matthew J. Kuhn, MD, Peoria, IL (Presenter) Chief Medical Officer, AI Analysis, Inc

PROGRAM INFORMATION

In an effort to provide Physicians and other Health Care professionals with current information and data to make informed decisions in their clinical settings, this symposium will focus on differentiating characteristics of each GBCA, the impact of Artificial Intelligence and how special populations are affected.

СМЕ

Yes, CME credit is available through a third-party provider: click here to claim credit

RSVP Link

https://nwifinvite.com/events/hot-topics-in-contrast-enhanced-mri/

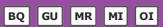




MSMI22

Molecular Imaging Symposium: Oncologic MI Applications

Monday, Dec. 2 10:30AM - 12:00PM Room: S405AB



AMA PRA Category 1 Credits ™: 1.50 ARRT Category A+ Credit: 1.75

FDA Discussions may include off-label uses.

Participants

Peter L. Choyke, MD, Rockville, MD (*Moderator*) Nothing to Disclose Vikas Kundra, MD, PhD, Houston, TX (*Moderator*) Institutional license agreement, Introgen Therapeutics, Inc; Research Grant, General Electric Company

For information about this presentation, contact:

pchoyke@mail.nih.gov

vkundra@mdanderson.org

LEARNING OBJECTIVES

1) To understand current advances in PET molecular imaging and clinical applications. 2) To understand new applications of advanced MRI techniques. 3) To improve understanding of theranostic agents based on targeted imaging agents. 4) To improve understanding of imaging delivered gene expression.

Sub-Events

MSMI22A Hyperpolarized MRI of Cancer

Participants

Daniel B. Vigneron, PhD, San Francisco, CA (Presenter) Research Grant, General Electric Company;

For information about this presentation, contact:

dan.vigneron@ucsf.edu

MSMI22B Imaging of Delivered Gene Expression

Participants Vikas Kundra, MD, PhD, Houston, TX (*Presenter*) Institutional license agreement, Introgen Therapeutics, Inc; Research Grant, General Electric Company

For information about this presentation, contact:

vkundra@mdanderson.org

LEARNING OBJECTIVES

1) To improve understanding of imaging of delivered gene expression. 2) Multiple modalities and reporter systems will be discussed.

MSMI22C PSMA Imaging in Prostate Cancer

Participants Peter L. Choyke, MD, Rockville, MD (*Presenter*) Nothing to Disclose

For information about this presentation, contact:

pchoyke@mail.nih.gov

LEARNING OBJECTIVES

1) To understand the basic biology of PSMA and its role in prostate cancer. 2) To describe the sensitivity of PSMA PET with regard to other PET agents for prostate cancer. 3) To demonstrate potential pitfalls and unexpected findings with PSMA PET imaging.

ABSTRACT

PSMA PET imaging is a highly sensitive method of detecting prostate cancer. It can be used in the initial diagnosis and staging, for recurrence and to assess metastatic disease. PSMA is expressed in aggressive cancers but not in low grade or highly undifferentiated cancers. It is superior to all other PET agents in terms of sensitivity especially in the recurrence setting. It can be used to determine if lesions seen on CT or MRI are related to prostate cancer. Pitfalls include false negatives in highly aggressive disease, the diagnosis of additional malignancies and false positives in the cisterna chyli and fibrous dysplasia. PSMA PET will have a profound impact on the management of prostate cancer.

MSMI22D Gastrin Releasing Peptide Receptors: When in the Course of Prostate Cancer Will They Be Useful?

Participants

Andrei Iagaru, MD, Emerald Hills, CA (*Presenter*) Research Grant, General Electric Company; Research Grant, Progenics Pharmaceuticals, Inc; Research Grant, Advanced Accelerator Applications SA

LEARNING OBJECTIVES

1) List some of the radiopharmaceuticals targeting gastrin-releasing peptide receptors that are used in prostate cancer. 2) Understand underlying biology and mechanism of action for the radiopharmaceuticals targeting gastrin-releasing peptide receptors in prostate cancer. 3) Discuss patterns of prostate cancer appearance when using the radiopharmaceuticals targeting gastrinreleasing peptide receptors.

ABSTRACT

Various radiopharmaceuticals targeting different molecules have been studied in prostate cancer (PC). One recent class of tracers are the gastrin releasing peptide (GRP) analogs. Bombesin (BBN) is analog to the mammalian GRP, and it binds with high affinity to its transmembrane receptors, the GRP receptors (GRPR). Preclinical evaluation in PC cells and animal models have reported encouraging results; therefore, they are currently investigated as targets both for PC imaging and therapy. Increases in GRPR expression have been shown in 63-100% of intraprostatic PC, and 50-80% of nodal and osseous metastases. High density expression of GRPR has been reported in primary PC in contrast to surrounding healthy tissues and hyperplastic prostate, allowing for detection of early neoplastic events in the prostate with high specificity.

MSMI22E Iron Oxide Enhanced MR Imaging in GU Malignancies

Participants

Baris Turkbey, MD, Bethesda, MD (*Presenter*) Research support, Koninklijke Philips NV; Royalties, Invivo Corporation; Investigator, NVIDIA Corporation

For information about this presentation, contact:

turkbeyi@mail.nih.gov

LEARNING OBJECTIVES

1) Understand mechanism of iron-oxide enhanced MRI. 2) Understand imaging findings of iron-oxide enhanced MRI. 3) Understand pitfalls and limitations of iron-oxide enhanced MRI.

ABSTRACT

n/a







SPAI21

RSNA AI Deep Learning Lab: Beginner Class: Classification Task (Intro)

Monday, Dec. 2 10:30AM - 12:00PM Room: AI Showcase, North Building, Level 2, Booth 10342



Participants

Bradley J. Erickson, MD, PhD, Rochester, MN (Presenter) Board of Directors and Stockholder, VoiceIt Technologies, LLC; Board of Directors, FlowSigma, LLC; Officer, FlowSigma, LLC; Stockholder, FlowSigma, LLC;

Special Information

In order to get the best experience for this session, it is highly recommended that attendees bring a laptop with a keyboard and decent-sized screen. Having a Gmail account will be helpful. Here are instructions for creating and deleting a Gmail account. Here are instructions for creating and deleting a Gmail account.

ABSTRACT

This class will focus on basic concepts of convolutional neural networks (CNNs) and walk the attendee through a working example. A popular training example is the MNIST data set which consists of hand-written digits. This course will use a data set we created, that we call 'MedNIST', and consists of images of 6 different classes: Chest X-ray, Chest CT, Abdomen CT, Head CT, Head MR and Breast MRI. The task is to identify the image class. This will be used to train attendees on the basic principles and some pitfalls in training a CNN. • Intro to CNNs • Data preparation: DICOM to jpeg, intensity normalization, train vs test • How do we choose the labels? Inconsistencies... Use Fast.AI routines to classify; Validation of results: Are the performance metrics reliable? 'Extra Credit': if there is time, explore data augmentation options, effect of batch size, training set size.





SSC02

Cardiac (Nonischemic Cardiomyopathies)

Monday, Dec. 2 10:30AM - 12:00PM Room: S401CD



AMA PRA Category 1 Credits ™: 1.50 ARRT Category A+ Credit: 1.75

FDA Discussions may include off-label uses.

Participants

Karen G. Ordovas, MD, San Francisco, CA (*Moderator*) Advisor, Arterys Inc; Research Grant, General Electric Company Mayil S. Krishnam, MBBS, MRCP, Orange, CA (*Moderator*) Nothing to Disclose

Sub-Events

SSC02-01 The Left Ventricular Flow Patterns and Trabecular Complexity in Hypertrophic Cardiomyopathy: Assessment with Multi-Modality Cardiac Magnetic Resonance

Monday, Dec. 2 10:30AM - 10:40AM Room: S401CD

Participants

Xin Zhang, Nanchang City, China (*Abstract Co-Author*) Nothing to Disclose Lianggeng Gong, Nanchang, China (*Abstract Co-Author*) Nothing to Disclose Tian Zheng, Nanchang, China (*Abstract Co-Author*) Nothing to Disclose Shuli Zhou, Nanchang, China (*Abstract Co-Author*) Nothing to Disclose Xiaoxin Liu, Yinchuan, China (*Presenter*) Nothing to Disclose

For information about this presentation, contact:

zx930324@163.com

PURPOSE

This paper aims to assess left ventricular flow patterns and trabecular complexity of obstructive hypertrophic cardiomyopathy (HOCM) and non-obstructive hypertrophic cardiomyopathy (NOHCM) patients using multi-modality cardiac magnetic resonance (CMR) including 4D Flow, fractal analysis and feature tracking.

METHOD AND MATERIALS

CMR was performed in 76 HCM patients stratified into HOCM (22-65 years; males, n=25) and NOHCM group (26-59 years; males, n=24) based on LV outflow tract obstruction (>=30 mmHg) and 30 healthy subjects (21-65 years; males, n=18). Fast imaging employing steady state acquisition (FIESTA) images and 4D flow were acquired at 3.0T MRI. All data was evaluated by the postprocessing software (cvi42, Circle Cardiovascular Imaging, v. 5.6, Calgary, AB, Canada). The LV blood flow path lines were separated into four different components: Direct Flow, Retained Inflow, Delayed Ejection Flow and Residual Volume. The degree of LV trabeculation was assessed by fractal dimension (FD), a dimensionless measure of trabeculation complexity. Myocardial deformation was evaluated by feature tracking.

RESULTS

The Retained Inflow, Delayed Ejection Flow and Residual Volume of LV showed significant differences between the HOCM group and the NOHCM group (18.48 ± 8.37 VS. 9.59 ± 4.68 , P = 0.038; 14.39 ± 6.63 VS. 28.30 ± 10.23 , P = 0.021; 57.11 ± 7.26 VS. 46.65 ± 8.84 , P = 0.047). Mean global FD of the left ventricle was higher in the HOCM and the NOHCM group than in the healthy group (1.304 ± 0.038 VS. 1.292 ± 0.039 VS. 1.236 ± 0.024 , P = 0.433, P<0.001, P<0.001). Max apical FD was higher in the HOCM group than the NOHCM group (1.400 ± 0.077 VS. 1.338 ± 0.067 , P = 0.001). Myocardial deformation analysis showed that increased global FD was associated with changed myocardial deformation across global strain value (circumferential: r =0.567, P<0.001; radial: r =-0.622, P<0.001; and longitudinal: r =?0.535, P<0.001).

CONCLUSION

Our results demonstrate that LV retained blood remains more in HOCM patients, and the degree of the apical trabecular complexity is increased compared with NOHCM.

CLINICAL RELEVANCE/APPLICATION

The trabecular complexity and retained blood flow in the left ventricular are promising to be remarkable risk factors for assessment in sudden cardiac death, and guide the clinical management for hypertrophic cardiomyopathy.

SSC02-02 Magnetic Resonance Fingerprinting for Multiparametric Quantitative Assessment in Hypertrophic Cardiomyopathy: Comparison with Conventional Cardiac Relaxometry

Monday, Dec. 2 10:40AM - 10:50AM Room: S401CD

Participants Christian P. Houbois, MD, Toronto, ON (*Presenter*) Nothing to Disclose Marshall S. Sussman, PhD, Toronto, ON (*Abstract Co-Author*) Nothing to Disclose Kate Hanneman, MD, FRCPC, Toronto, ON (*Abstract Co-Author*) Nothing to Disclose Yuchi Liu, Cleveland, OH (*Abstract Co-Author*) Nothing to Disclose Nicole Seiberlich, PhD, Cleveland, OH (*Abstract Co-Author*) Research Grant, Siemens AG Jesse Hamilton, Cleveland, OH (*Abstract Co-Author*) Nothing to Disclose Bernd J. Wintersperger, MD, Toronto, ON (*Abstract Co-Author*) Speaker, Siemens AG Research support, Siemens AG Institutional research agreement, Siemens AG Speaker, Bayer AG

For information about this presentation, contact:

christian.houbois@uhn.ca

PURPOSE

The objective of this study is to evaluate cardiac magnetic resonance fingerprinting (MRF) in the assessment of myocardial relaxation times compared to standard relaxometry.

METHOD AND MATERIALS

64 Pts (55m,56+/-12.3y) with suspicion/known HCM underwent CMR at 3T. Midventricular SAX T1/T2 values were evaluated with pre-(5(3)3) and post-contrast (4(1)3(1)2) modified Look-Locker inversion recovery (MOLLI) and T2-prep fast low-angle shot (FLASH) techniques. MRF was performed at identical SAX slice position pre-/post-contrast (15 heartbeats). Post-contrast imaging was done >10min after injection of Gadobutrol (0.15mmol/kg). Inline motion correction with pixel-wise fitting was performed for MOLLI/T2-prep FLASH based T1/T2 maps. Acquired MRF raw data was reconstructed off-line for creation of T1/T2 maps. All maps were visually assessed for general image quality using a 5-point Likert scale (1=non-diagnostic/5=excellent). Quantitative Map evaluation was performed using dedicated software and extracellular volume fraction (ECV) calculated with patients' hematocrit. Statistical analysis was performed including Wilcoxon rank-sum test and Spearman's correlation. Data presented as median and IQR.

RESULTS

Image quality of MOLLI T1 was superior to MRF T1 in pre- (5 vs. 4;p=.0029) and post-contrast data (5 vs. 4;p=.0004). T2 FLASH showed better image quality than MRF T2 (5 vs 4;p<.0001). MRF T1 values were significantly longer than MOLLI T1 in pre-contrast (1385ms [IQR:1336/1437ms] vs. 1250ms [IQR:1220/1290ms];p<.0001) and post-contrast (514ms [IQR:458/542ms] vs. 485ms [IQR:435/523ms];p<.0001) settings. MOLLI T1 based ECV values (23% [IQR:21/27%]) were significantly lower than MRF T1 based data (27% [IQR:23/31%]) (p<.0001). MRF T2 values were significant different to T2 FLASH data (32.5ms [IQR:30.2/35.2ms] vs. 39.9ms [IQR:38.6/41.8ms];p<.0001). Significant correlations between MRF and standard cardiac relaxometry were found for all evaluated parameters (figure).

CONCLUSION

Single breath-hold MRF allows for simple and faster quantitative multiparametric evaluation of the myocardium than conventional fitting based relaxometry with significant correlations. Automatic co-registration of MRF maps may provide further benefits.

CLINICAL RELEVANCE/APPLICATION

MRF allows robust single breath-hold multiparametric mapping with intrinsic co-registration. Thus, it may allow improved distinction/differential diagnosis of various cardiomyopathies including HCM.

SSC02-03 Antimalarial-Induced Cardiomyopathy Resembles Fabry Disease on Cardiac MRI

Monday, Dec. 2 10:50AM - 11:00AM Room: S401CD

Participants Kate Hanneman, MD, FRCPC, Toronto, ON (*Presenter*) Nothing to Disclose Hugo A. Vidal, MD, Toronto, ON (*Abstract Co-Author*) Nothing to Disclose Kostantinos Tselios, Toronto, ON (*Abstract Co-Author*) Nothing to Disclose Dinesh Thavendiranathan, MD, Toronto, ON (*Abstract Co-Author*) Nothing to Disclose Murray Urowitz, Toronto, ON (*Abstract Co-Author*) Nothing to Disclose Paula Harvey, Toronto, ON (*Abstract Co-Author*) Nothing to Disclose

PURPOSE

Antimalarials (AM) are frequently used in the treatment of patients with systemic lupus erythematosus (SLE). AM-induced cardiomyopathy (AMIC) is associated with high mortality and is likely under-recognized in clinical practice. The purpose of this study was to evaluate cardiac magnetic resonance imaging (MRI) findings in AIMC.

METHOD AND MATERIALS

Cardiac MRI studies were compared between 11 SLE patients with AMIC (63.0 ± 7.8 years, 90.9% female) and 32 SLE patients without AMIC (42.8 ± 16.5 years, 90.3% female). The diagnosis of AMIC was confirmed by endomyocardial biopsy and/or autopsy in 4 patients and presumed based on concordant history and abnormal cardiac biomarker levels that improved after AM cessation in 7 patients.

RESULTS

Patients with AMIC were significantly older (p<0.001) and had longer AM treatment duration (26.1±11.7 years vs. 5.4±6.9 years, p<0.001) compared to those without. There were no significant differences in left ventricular (LV) end-diastolic volumes and ejection fraction between groups (p=0.515 and p=0.489, respectively). However, indexed LV mass was significantly higher and concentric LVH was more common in patients with AMIC compared to those without (68.9±17.4 g/m2 vs. 52.3±11.0 g/m2, p=0.001 and 80.0% vs. 26.7%, p=0.007, respectively). Late gadolinium enhancement (LGE) was present in all 10 patients with AMIC who had undergone LGE imaging (vs. 22.6% of those without AMIC, p<0.001). In patients with AMIC, the pattern of LGE was most commonly mid-wall located at the basal to mid inferior lateral segment (90.0%). Native T1 values outside areas of LGE were low in patients with AMIC who had undergone T1 mapping (1062 ms at 3T and 997 ms at 1.5T).

CONCLUSION

To our knowledge this is the largest cardiac MRI study in AMIC to date. Typical cardiac MRI findings in AMIC include concentric LVH, LGE at the basal to mid inferior lateral segment and low native T1 values. This cardiac MRI appearance is similar to Fabry

disease (a lysosomal storage disease). The resemblance is striking given previously described histopathological similarities between AMIC and Fabry disease and supports the hypothesis that AMIC may be caused by reversible inhibition of myocyte lysosomal activity.

CLINICAL RELEVANCE/APPLICATION

These results may allow for earlier detection of AMIC, and support the necessity for future larger studies to evaluate the prognostic significance of MRI findings and correlation with histopathology.

SSC02-04 Role of Cardiac MRI in Identification of Myocardial Fibrosis in Patients of Non-Ischemic Dilated Cardiomyopathy

Monday, Dec. 2 11:00AM - 11:10AM Room: S401CD

Participants

Anita K. Meena, MD, Delhi , India (*Presenter*) Nothing to Disclose Sanjeev Kumar, MBBS, MD, Delhi, India (*Abstract Co-Author*) Nothing to Disclose Sanjiv Sharma, MBBS, MD, New Delhi, India (*Abstract Co-Author*) Nothing to Disclose Nitish Naik, Delhi, India (*Abstract Co-Author*) Nothing to Disclose Ambuj Roy, Delhi , India (*Abstract Co-Author*) Nothing to Disclose Arun K. Gupta, MBBS, MD, New Delhi, India (*Abstract Co-Author*) Nothing to Disclose

For information about this presentation, contact:

anita.lhmc@gmail.com

PURPOSE

To study the prevalence of myocardial scar and its quantification on Cardiac MRI (CMRI) and its utility in predicting clinical outcomes in patients of non-ischemic dilated cardiomyopathy (NIDCM)

METHOD AND MATERIALS

In this prospective observational study we enrolled 88 consecutive patients of clinically diagnosed NIDCM. Routine CMR sequences was done including black blood imaging T1W and T2W, Steady state free precession Cine images, first pass perfusion images at rest and post contrast (10-15 minutes) 2D segmented inversion recovery gradient recalled echo (GRE) imaging during diastole, inversion time set to null normal myocardium. Myocardial scar was defined as late gadolinium enhancement (LGE) and it's extent was quantified using visual scoring method. Patients were followed-up for major adverse cardiac events (MACE), including cardiovascular death, aborted sudden death and heart failure for a mean period of 12 months. ROC curve was generated to know the accuracy of LGE extent in predicting MACE.

RESULTS

Of 88 patients (median age: 42 years, 66% male), mainly presenting with congestive heart failure symptoms (79%) and palpitations (16%). On CMR 50% of patients showed LGE of variable pattern out of which mid myocardial enhancement was most frequent. The percentage of LGE in these patients ranged from 1.4% to 88%, with a median of 25%. With LGE cut off of 26%, MACE can be predicted with 70% sensitivity and 73.5% specificity (AUROC=0.75). During 12 months follow-up, 16 patients developed MACE,out of which 10 were LGE+ and 6 were LGE-ve.The higher event rate was observed in patients with LGE volume of >26% compared to LGE <26% (43.6% vs 10.7%).

CONCLUSION

In NIDCM, presenting with heart failure or ventricular arrhythmias, presence of myocardial scar and its extent gives additional prognostic information compared to left ventricular ejection fraction (LVEF) and other traditional risk factors. Even though the final diagnosis is uncertain in NIDCM, extensive amount of LGE should be considered as a sign of poor prognosis.

CLINICAL RELEVANCE/APPLICATION

Risk stratification depending solely on LVEF in NIDCM patients may be fallacious, as most patients who experience sudden cardiac death (SCD) did not have severely reduced LVEF. Identification and quantification of myocardial fibrosis could be used as an adjunct for more accurate risk stratification in these patients.

SSC02-05 Chemotherapy Induces Left Ventricular Hypertrophy and Increases T1 Relaxation Times in Female Patients with Breast Cancer

Monday, Dec. 2 11:10AM - 11:20AM Room: S401CD

Participants

Enver G. Tahir, MD, Hamburg, Germany (Presenter) Nothing to Disclose Manuella Azar, Hamburg, Germany (Abstract Co-Author) Nothing to Disclose Sahar Shihada, Hamburg, Germany (Abstract Co-Author) Nothing to Disclose Jitka Starekova, Hamburg, Germany (Abstract Co-Author) Nothing to Disclose Malte L. Warncke, MD, Hamburg, Germany (Abstract Co-Author) Nothing to Disclose Katharina Seiffert, Hamburg, Germany (Abstract Co-Author) Nothing to Disclose Volkmer Muller, Hamburg, Germany (Abstract Co-Author) Nothing to Disclose Isabell Witzel, Hamburg, Germany (Abstract Co-Author) Nothing to Disclose Yvonne Goy, Hamburg, Germany (Abstract Co-Author) Nothing to Disclose Cordula L. Petersen, Dresden, Germany (Abstract Co-Author) Nothing to Disclose Ulf K. Radunski, Hamburg, Germany (Abstract Co-Author) Nothing to Disclose Sebastian Bohnen, Hamburg, Germany (Abstract Co-Author) Nothing to Disclose Jan Schneider, Hamburg, Germany (Abstract Co-Author) Nothing to Disclose Kai Muellerleile, Hamburg, Germany (Abstract Co-Author) Nothing to Disclose Gerhard B. Adam, MD, Hamburg, Germany (Abstract Co-Author) Nothing to Disclose Gunnar K. Lund, MD, Hamburg, Germany (Abstract Co-Author) Nothing to Disclose

For information about this presentation, contact:

e.tahir@uke.de

PURPOSE

To detect and monitor cardiomyopathy by cardiac magnetic resonance (CMR) in female patients with first-time radiochemotherapy treatment of breast cancer.

METHOD AND MATERIALS

39 female patients (51 ±11 years) with newly diagnosed breast cancer underwent serial 3 Tesla CMR (Ingenia, Philips Medical Systems). Baseline (BL) CMR was performed 10 ±9 days before the start of therapy. First follow-up (FU1) CMR was 13 ±12 days and second follow-up (FU2) 8 ±2 months after completion of chemotherapy. SSFP cine sequences were performed to determine cardiac volumes and function. T1 mapping CMR was performed using a 5s(3s)3s MOLLI sequence. CMR data were analyzed using the commercially available software cmr42 (Circle Cardiovascular Imaging Inc., Calgary, Alberta, Canada). LV end-diastolic and end-systolic volumes were obtained from cine-CMR short-axes to calculate LV stroke volumes (LVSV) as well as LV ejection fraction (LVEF).

RESULTS

The mean dose of chemotherapeutic agents used was as follows: epirubicin 663 ±60 mg/m2, cyclophosphamid 4421 ±398 mg/m2 and paclitaxel 1646 ±275 mg/m2. High sensitive Troponin T increased on FU1 (5 ±4 vs. 8 ±4 pg/ml, P<0.05) and remained high at FU2 (8 ±11 pg/ml, P=0.845). Creatine kinase remained unchanged at FU1 (68 ±29 vs. 78 ±51 pg/ml, P=0.189) and increased at FU2 (97 ±33 pg/ml.) NT-proBNP remained unchanged throughout the observation period. LVEF was constant between FU1 (61 ±5 vs. 62 ±6%, P=0.712) and FU2 (60 ±6%, P=0.094). LV mass increased at FU1 (48 ±5 vs. 52 ±7%, P<0.01) and remained high at FU2 (52 ±7%, P<0.01). T1 relaxation times were increased at FU1 (1258 ±31 vs. 1283 ±44 ms, P<0.01) and declined at FU2 (1269 ±26 ms, P=0.123). ECV did not show any differences between BL and FU2 (28 ±2 vs. 29 ±2%, P=0.519).

CONCLUSION

Chemotherapy treatment in breast cancer patients can lead to myocardial hypertrophy, which is stable on a 8 month follow-up. Increase in T1 relaxation times of LV myocardium can be detected immediately after completion of radiochemotherapy, but subside on a 8 month follow-up.

CLINICAL RELEVANCE/APPLICATION

Increase in LV mass and T1 relaxation times of myocardium might be used as early indicators of subclinical cardiomyopathy in asymptomatic patients with breast cancer undergoing chemotherapy.

SSC02-06 Correlation Between Quantitative Left Ventricular Myocardial Scar Volume and Left Ventricular Ejection Fraction in Cardiac Sarcoidosis

Monday, Dec. 2 11:20AM - 11:30AM Room: S401CD

Participants Hemant Desai, MD, Morrisville, NC (*Presenter*) Nothing to Disclose Joseph G. Mammarappallil, MD,PhD, Durham, NC (*Abstract Co-Author*) Nothing to Disclose Arya M. Iranmanesh, MD, Cary, NC (*Abstract Co-Author*) Nothing to Disclose Hamid Chalian, MD, Durham, NC (*Abstract Co-Author*) Nothing to Disclose

For information about this presentation, contact:

hamid.chalian@duke.edu

PURPOSE

The purpose of this study was to utilize cardiac MRI (cMRI) to determine if there is an association between quantitative left ventricular myocardial scar volume and left ventricular function, as measured by left ventricular ejection fraction (LVEF), in patients with suspected cardiac sarcoidosis.

METHOD AND MATERIALS

IRB approval was obtained for this HIPAA compliant study. cMRIs of 355 cases with a clinical suspicion for cardiac sarcoidosis were reviewed by 2 cardiothoracic imaging trained radiologists. cMRI based LVEF, and quantitative myocardial scar volume were calculated for all cases and compared between patients with and without cMRI findings suggestive of cardiac sarcoidosis. Correlation between LVEF and myocardial scar volume was assessed with Pearson Correlation Coefficient test. Significance was set at P value=0.05.

RESULTS

A total of 355 patients with a clinical suspicion of cardiac sarcoidosis were included in this study (mean age 58.0 +/- 12.2). Ninety (25.4%) patients demonstrated cMRI imaging findings suggestive of cardiac sarcoidosis (mean age 60.0 +/- 12.6; 26.7% female, 73.3% male; 47% African American, 50% Caucasian). Myocardial scar volume determined by cMRI was significantly higher in sarcoid positive cases (11.9% +/-10.8% vs. 2.7%+/-6.7%, P<0.001) vs sarcoid negative cases. LVEF was significantly lower in the sarcoid positive group when compared to the sarcoid negative group (46.7%+/-16.1 vs. 54.8+/-13.4, P<0.001). Additionally, in those with cMRI findings suggestive of cardiac sarcoidosis, myocardial scar mass volume was significantly correlated (P<0.001) to the left ventricular ejection fraction with Pearson Correlation Coefficient of R= -0.630. In those with cMRI findings suggestive of cardiac sarcoidosis, African Americans demonstrated larger quantitative scar volumes and greater reduction in MRI LVEF than Caucasians (14.1% vs. 9.95; 41.7% vs. 51.4%).

CONCLUSION

In patients with cMRI findings of sarcoidosis, left ventricular myocardial quantitative scar volume was negatively correlated with left ventricular ejection fraction. In patients with cMRI findings of sarcoidosis, African Americans demonstrated a greater scar volume and a higher decline in ejection fraction when compared to Caucasians.

CLINICAL RELEVANCE/APPLICATION

Ouantitative muse and a car volume may be a useful quantitative parameter for prediction of IVEE in patients with suspected

Quantitative myocardial scar volume may be a userul quantitative parameter for prediction of LVEF in patients with suspected myocardial sarcoidosis.

SSC02-07 The Effects of Left Ventricular Remodeling, Myocardial Perfusion and Tissue Characteristic on Cardiac Motion in Diabetic Cardiomyopathy: A Multimodal Cardiac Magnetic Resonance Study

Monday, Dec. 2 11:30AM - 11:40AM Room: S401CD

Participants

Li Jiang, Chengdu, China (*Presenter*) Nothing to Disclose Zhigang Yang, MD, Chengdu, China (*Abstract Co-Author*) Nothing to Disclose Yingkun Guo, Chengdu, China (*Abstract Co-Author*) Nothing to Disclose Yue Gao, Chengdu, China (*Abstract Co-Author*) Nothing to Disclose Biyue Hu, MD, Chengdu, China (*Abstract Co-Author*) Nothing to Disclose

For information about this presentation, contact:

jianglifs@163.com

PURPOSE

This study was to determine the effects of left ventricular(LV) remodeling, myocardial perfusion and tissue characteristic on cardiac motion in type 2 diabetes mellitus(T2DM), and to explore the risk factors affecting systolic and diastolic functions, based on a multimodal cardiovascular magnetic resonance (CMR) study.

METHOD AND MATERIALS

A total of 85 clinically diagnosed T2DM patients and 39 healthy controls underwent CMR examination. The CMR parameters including morphological structure (LV mass and remodeling index), motion (peak strain(PS), peak systolic strain rate, and peak diastolic strain rate), perfusion (upslope, MaxSI, TTM, and perfusion-index), T1 mapping and T2 mapping were analyzed and compared between controls and T2DM patients. The univariable and multivariable analysis was performed to identify the imaging and clinical variables affecting motion functions.

RESULTS

Compared with controls, T2DM patients presented significantly decreased motion function in radial, circumferential and longitudinal direction (PS radial, 32.16±8.80 vs. 39.32 ± 9.51 , p=0.001; PS circumferential, -19.67 ± 3.83 vs. -21.00 ± 3.35 , p=0.036; and PS longitudinal, -11.93 ± 3.50 vs. -15.85 ± 3.79 , p=0.000), decreased perfusion function (perfusion index, 0.11 ± 0.04 vs. 0.13 ± 0.03 , p=0.010), increased myocardial fibrosis (extracellular volume fraction, 31.36 ± 7.83 vs. 27.52 ± 3.05 , p=0.000), increased myocardial edema(41.88 ± 5.12 vs. 40.34 ± 2.67 , p=0.044) and increased LV mass(59.46 ± 17.49 vs. 42.57 ± 10.38 , p=0.000). With univariable and multivariable analysis, myocardial perfusion function is related to both systolic and diastolic motion, while LV remodeling, myocardial fibrosis and edema significantly affected diastolic motion.

CONCLUSION

The cardiac motion, perfusion, tissue characteristic and remodeling of T2DM patients are impaired. Both systolic and diastolic motion were related to myocardial perfusion function, while diastolic dysfunction is more susceptible to LV remodeling and myocardial fibrosis and edema.

CLINICAL RELEVANCE/APPLICATION

Cardiac motional disorder is the final path of all cardiac pathophysiological changes and is the driving factor of heart failure. Diabetes mellitus and its associated risk factors contribute to cardiac motional disorder by causing damage to different pathophysiological processes in the heart. However, the relationship between cardiac pathophysiological changes and cardiac motion has rarely been studied.

SSC02-08 Relation of Regional Myocardial Perfusion and Systolic Strain in Hypertrophic Cardiomyopathy and Cardiac Amyloidosis: A Cardiovascular Magnetic Resonance Analysis

Monday, Dec. 2 11:40AM - 11:50AM Room: S401CD

Participants

Shan Huang, Chengdu, China (*Abstract Co-Author*) Nothing to Disclose Zhigang Yang, MD, Chengdu, China (*Abstract Co-Author*) Nothing to Disclose Kaiyue Diao, Chengdu, China (*Presenter*) Nothing to Disclose Ke Shi, Chengdu, China (*Abstract Co-Author*) Nothing to Disclose Yue Gao, Chengdu, China (*Abstract Co-Author*) Nothing to Disclose Yi Zhang, MS, Chengdu, China (*Abstract Co-Author*) Nothing to Disclose Meng-ting Shen, Chengdu, China (*Abstract Co-Author*) Nothing to Disclose Yingkun Guo, Chengdu, China (*Abstract Co-Author*) Nothing to Disclose Pei-lun Han, Chengdu, China (*Abstract Co-Author*) Nothing to Disclose Rui Shi, Chengdu, China (*Abstract Co-Author*) Nothing to Disclose

For information about this presentation, contact:

huangshan82833@163.com

PURPOSE

To investigate the microvascular dysfunction and its relation with myocardial strains in cardiac amyloidosis (CA) and hypertrophic cardiomyopathy (HCM) with increased wall thickness.

METHOD AND MATERIALS

We included 25 biopsy-proven CA (65.4 ± 10.7 years, 54% female) and 35 patients with HCM (65.4 ± 10.7 years, 59% female). Segments with a wall thickness (WT) >12mm were considered thickened. Perfusion parameters including slope, time to maximum signal intensity (TTM) and time to 50% maximum signal intensity (50%TTM) were obtained from the myocardial signal intensity-time curve. Myocardial strain indices including circumferential (CS) and longitudinal (LS) strain were derived from the tissue tracking model on cine images. The AHA 16-segment model was used for regional perfusion and strain analyses.

RESULTS

In total, 169 thickened segments in CA and 228 in HCM with WT >12mm (WT 14.7 \pm 2.2 mm in CA vs. 16.4 \pm 3.9 mm in HCM, p<0.05) were evaluated. Thickened CA segments demonstrated more impaired myocardial strain and microvascular function compared with HCM segments. Multivariable linear regression analysis showed that CS had association with slope [beta 0.8, 95% confidence interval (CI) 0.3-1.3; P<0.001], wall thickness and hypertrophic phenotype (HCM or CA) (P<0.001 for both). The ROC analyses demonstrated that 50%TTM performed best in differentiating CA from HCM (AUC 0.92, sensitivity 81.7%, and specificity 91.7%, cut-off value 22.3).

CONCLUSION

Our results demonstrated that amyloid infiltration impairs the regional microvascular system and systolic function more seriously than HCM characterized with cellular hypertrophy. Regional myocardial mechanics are significantly influenced by microvascular function.

CLINICAL RELEVANCE/APPLICATION

Amyloid infiltration causes more severe myocardial perfusion disorder and systolic dysfunction. Myocardial perfusion parameters have great performance in differentiating cardiac amyloidosis from hypertrophic cardiomyopathy.

SSC02-09 Diagnostic Value of Quantitative Tissue-Tracking Cardiac Magnetic Resonance of Myocardium Deformation in Hypertrophic Cardiomyopathy

Monday, Dec. 2 11:50AM - 12:00PM Room: S401CD

Participants

Yi Zhu, Shenzhen , China (*Presenter*) Nothing to Disclose Guanxun Cheng, Shenzhen, China (*Abstract Co-Author*) Nothing to Disclose Lingbo Deng, Shenzhen, China (*Abstract Co-Author*) Nothing to Disclose

For information about this presentation, contact:

yanyinoein@163.com

PURPOSE

To explore the diagnostic value of quantitative tissue-tracking cardiac magnetic resonance (CMR) of left ventricular global myocardium deformation in hypertrophic cardiomyopathy (HCM).

METHOD AND MATERIALS

18 cases of essential HCM (HCM group,13 males, 5 females, aged 25~72 years with a mean of 40.89±15.13) and 19 cases of normal subjects (control group, 16 males, 3 females, aged 21~71 years with a mean of 39.58±13.57) were enrolled. All patients were subjected to CMR. The CMR bright blood cine sequences were including short-axis, long-axis and four-chamber of left ventricle(Balance turbo field echo, B-TFE). All DICOM images were performed with the Circle Cardiovascular software(cvi42 version 5.10.1, Calgary, Alberta, Canada) to get left ventricular muscle mass (LVMM), left ventricular end-diastolic volume(LVEDV), left ventricular end-systolic volume (LVESV), stroke volume(SV),cardiac output (CO) and left ventricular ejection fractions(LVEF) in the Short 3D modular, get left atrial minimal volume (LAVmin)and left atrial maximal volume (LAVmax) in the Biplanar LAX modular, and get global peak radial strain (GPSR), global peak circumferential strain (GPSC) and global peak long strain(GPSL) of left ventricle in the Tissue Tracking modular.

RESULTS

1. There were no significant differences in the clinical profiles (gender, age) between the HCM group and control group (P>0.05).2. LVMM in the HCM group were significantly greater than in the control group [(193.74 ± 44.68)g, 125.18 ± 29.34]g, P=0.00)]. LAVmin and LAVmax in the HCM group were significantly greater than in the control group. [(40.25 ± 20.64)ml,(18.63 ± 8.65)ml, P=0.00 and (71.66 ± 27.98)ml, (47.69 ± 12.53)ml, P0.05).3. In correlation analysis in HCM group, LVMM did not correlate significantly with GPSR, GPSC and GPSL.4.The area under ROC curve of GPSR, GPSC and GPSL in diagnosis of HCM were 0.199, 0.807 and 0.857, and the area under ROC curve of GPSL was the largest.

CONCLUSION

CMR feature tracking technology can quantitatively evaluate cardiomyopathy deformation of HCM. The ventricular diastolic dysfunction of HCM is earlier than that of systolic dysfunction. Left ventricular myocardial mass is not significantly correlated with myocardial deformation. GPSC and GPSL have favorable effective functions for the diagnosis in HCM.

CLINICAL RELEVANCE/APPLICATION

CMR feature tracking technology can quantitatively evaluate cardiomyopathy deformation of HCM.

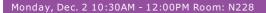






SSC05

Gastrointestinal (Hepatocellular Carcinoma)





AMA PRA Category 1 Credits ™: 1.50 ARRT Category A+ Credit: 1.75

Participants

Mustafa R. Bashir, MD, Cary, NC (*Moderator*) Research Grant, Siemens AG; Research Grant, General Electric Company; Research Grant, NGM Biopharmaceuticals; Research Grant, Madrigal Pharmaceuticals, Inc; Research Grant, Metacrine, Inc; Research Grant, Pinnacle Clinical Research; Research Grant, ProSciento Inc; Research Consultant, RadMD Kristin K. Porter, MD, PhD, Baltimore, MD (*Moderator*) Nothing to Disclose Mishal Mendiratta-Lala, MD, Ann Arbor, MI (*Moderator*) Nothing to Disclose

Sub-Events

SSC05-01 How Frequently Does HCC Develop in At-Risk Patients with a Negative Liver MRI Examination?

Monday, Dec. 2 10:30AM - 10:40AM Room: N228

Participants

Islam H. Zaki, MBBCh, Durham, NC (*Presenter*) Nothing to Disclose Erin Shropshire, MD, Durham, NC (*Abstract Co-Author*) Nothing to Disclose Shuaiqi H. Zhang, Durham, NC (*Abstract Co-Author*) Nothing to Disclose Benjamin Wildman-Tobriner, MD, Durham, NC (*Abstract Co-Author*) Nothing to Disclose Daniele Marin, MD, Durham, NC (*Abstract Co-Author*) Research support, Siemens AG Rajan T. Gupta, MD, Durham, NC (*Abstract Co-Author*) Consultant, Bayer AG; Speakers Bureau, Bayer AG; Consultant, Invivo Corporation; Consultant, C. R. Bard, Inc Alaattin H. Erkanli, PhD, Durham, NC (*Abstract Co-Author*) Nothing to Disclose Rendon C. Nelson, MD, Durham, NC (*Abstract Co-Author*) Nothing to Disclose Rendon C. Nelson, MD, Durham, NC (*Abstract Co-Author*) Consultant, VoxelMetrix, LLC; Co-owner, VoxelMetrix, LLC; Advisory Board, Bracco Group; Advisory Board, Guerbet SA; Speakers Bureau, Bracco Group; Royalties, Wolters Kluwer nv Mustafa R. Bashir, MD, Cary, NC (*Abstract Co-Author*) Research Grant, Siemens AG; Research Grant, General Electric Company; Research Grant, NGM Biopharmaceuticals; Research Grant, Madrigal Pharmaceuticals, Inc; Research Grant, Metacrine, Inc; Research Grant, Pinnacle Clinical Research; Research Grant, ProSciento Inc; Research Consultant, RadMD

For information about this presentation, contact:

Islam.Zaki@duke.edu

PURPOSE

Guidelines for hepatocellular carcinoma (HCC) screening typically recommend imaging surveillance at 6 month intervals. For patients who undergo US screening and have a liver MRI for other reasons, or are screened with MRI due to poor quality US (obesity or hepatic steatosis), a longer interval after may be appropriate. The purpose of this study was to determine the rate of development of significant liver lesions after a negative MRI in a screening population.

METHOD AND MATERIALS

This retrospective study included patients from 2013 at risk of developing HCC, who underwent MRI surveillance, with follow up CTs or MRIs for at least 12 months read using the Liver Imaging and Reporting Data System (LI-RADS)[3]. Patients with baseline focal liver lesions categorized not LR-1, history of primary liver cancer, prior treatment of a liver lesion, or liver transplant were excluded. All available CTs and MRIs that were compliant with the LI-RADS technical guidelines were included in the follow-up assessment. Follow-up examinations were classified as negative (no lesions or only LR-1 lesions) or positive (at least one observation of any category other than LR-1). Time to first positive examination and observation types were recorded.

RESULTS

204 patients (mean age 58 ± 11 years, 128 women, 168 patients with cirrhosis, most with non-alcoholic steatohepatitis (n=117), were included. Median follow up duration was 28 (range 12-60) months. 5.9% (12/204) of patients developed a lesion at follow-up ("became positive"). At 6-9 months, one patient (0.5%, 1/204) became positive, with new LR-3 nodules measuring up to 11 mm. At 12±3 months, three additional patients (cumulative 2%, 4/204) became positive: a 12 mm LR-3 nodule, a 10 mm LR-4 nodule, and a 29 mm LR-M nodule. By two years, two additional patients became positive with LR-3 nodules.

CONCLUSION

Clinically significant (LR-4, LR-5, LR-M) liver nodules develop in a minority (1%) of patients in the first year following negative MRI. While ongoing surveillance is necessary, after a negative MRI it may be reasonable to perform the screening imaging at 1 year.

CLINICAL RELEVANCE/APPLICATION

In patients at risk for HCC with a negative MRI, the next imaging surveillance for HCC could be delayed until one year after the MRI

SSC05-02 Hepatobiliary Phase Hypointense Nodule without Arterial Phase Hyperenhancement on Gadoxetic Acid-Enhanced MRI: Risk of HCC Intrahepatic Distant Recurrence after Radiofrequency Ablation or Hepatectomy: A Systematic Review and Meta-Analysis

Participants

Tae-Hyung Kim, MD, Seoul, Korea, Republic Of (*Presenter*) Nothing to Disclose Sungmin Woo, MD, Seoul, Korea, Republic Of (*Abstract Co-Author*) Nothing to Disclose Sangwon Han, Seoul, Korea, Republic Of (*Abstract Co-Author*) Nothing to Disclose Chong Hyun Suh, MD, Seoul, Korea, Republic Of (*Abstract Co-Author*) Nothing to Disclose Dong Ho Lee, MD, Seoul, Korea, Republic Of (*Abstract Co-Author*) Nothing to Disclose Jeong Min Lee, MD, Seoul, Korea, Republic Of (*Abstract Co-Author*) Nothing to Disclose Jeong Min Lee, MD, Seoul, Korea, Republic Of (*Abstract Co-Author*) Grant, Bayer AG Grant, General Electric Company Grant, Koninklijke Philips NV Grant, STARmed Co, Ltd Grant, RF Medical Co, Ltd Grant, Samsung Electronics Co, Ltd Grant, Guerbet SA

For information about this presentation, contact:

kth1205@gmail.com

PURPOSE

To perform a systematic review and meta-analysis to determine intrahepatic distant recurrence (IDR) risk of hepatobiliary phase (HBP) hypointense nodules without arterial phase hyperenhancement (APHE) on pretreatment gadoxetic-acid enhanced MRI in patients with hepatocellular carcinoma (HCC) treated with either hepatectomy or radiofrequency ablation (RFA).

METHOD AND MATERIALS

Pubmed and EMBASE databases were searched up to April 6th 2019. We included studies that evaluated HBP hypointense nodules without APHE as risk factors for IDR in HCC patients treated with either hepatectomy or RFA. Hazard ratios (HR) were metaanalytically pooled using random-effects model. Subgroup analyses stratified to clinicopathologic variables were performed to explore heterogeneity. Methodological quality of included studies was assessed using Quality in Prognostic Studies (QUIPS) tool.

RESULTS

Eight studies with 842 patients were analyzed. The overall pooled HR for IDR was 2.44 (95% CI, 1.99-2.98) and were (2.14 (95% CI, 1.66-2.76) and 3.07 (95% CI, 2.19-4.31) for patients that underwent hepatectomy and RFA, respectively. No significant heterogeneity was present (I2 = 0%). The presence of these nodules was consistently shown to be significant factors for IDR in other subgroups (HR = 1.74-3.07). Study quality was generally moderate.

CONCLUSION

HBP hypointense nodules without APHE are risk factors for IDR in HCC patients treated with either RFA or hepatectomy. Stratification of patient management with regard to performing additional tests or treatment for these nodules and modification of proper follow-up strategies may be required in patients with HCC who have these nodules on pretreatment gadoxetic acidenhanced MRI.

CLINICAL RELEVANCE/APPLICATION

HBP nodules without APHE in pretreatment gadoxetic acid-MR should be recognized as a significant risk factor for increased IDR after curative treatment for HCCs and therefore, it may require stratification of patient management with regard to deciding whether to perform additional pathologic test or treatment to these nodules and modification of proper follow-up strategies after curative treatment for HCCs in patients who harbor these nodules.

SSC05-03 Prospective Intraindividual Comparison of CT, MRI with Extracellular Contrast and Gadoxetic Acid for Diagnosis of HCC

Monday, Dec. 2 10:50AM - 11:00AM Room: N228

Participants

Ji Hye Min, MD, PhD, Seoul, Korea, Republic Of (*Presenter*) Nothing to Disclose Young Kon Kim, MD, PhD, Seoul, Korea, Republic Of (*Abstract Co-Author*) Nothing to Disclose Jeong Eun Lee, Daejeon, Korea, Republic Of (*Abstract Co-Author*) Nothing to Disclose Kyung-Sook Shin, MD, Daejeon, Korea, Republic Of (*Abstract Co-Author*) Nothing to Disclose Yeun-Yoon Kim, MD, Seoul, Korea, Republic Of (*Abstract Co-Author*) Nothing to Disclose Dong Ik Cha, MD, Seoul, Korea, Republic Of (*Abstract Co-Author*) Nothing to Disclose

For information about this presentation, contact:

minjh1123@gmail.com

PURPOSE

We prospectively evaluated the diagnostic performance of computed tomography (CT), magnetic resonance imaging (MRI) with extracellular contrast agents (ECA-MRI), and MRI with hepatobiliary agents (HBA-MRI) for the diagnosis of hepatocellular carcinoma (HCC) using the Liver Imaging Reporting and Data System (LI-RADS) with pathological confirmation.

METHOD AND MATERIALS

Between November 2016 and February 2019, we enrolled 125 patients with chronic liver disease who underwent CT, ECA-MRI, and HBA-MRI within one month before surgery for initial hepatic nodules detected via ultrasound. Two radiologists evaluated the presence of major and ancillary HCC features and assigned LI-RADS categories (v2018) based on CT and MRI. We then compared the diagnostic performance for LR-5 for each modality alone and in combination.

RESULTS

In total, 163 observations (124 HCCs, 13 non-HCC malignancies, and 26 benign lesions; mean size, 20.7 mm) were identified. ECA-MRI showed a higher rate of identifying arterial phase hyperenhancement (16.1% and 8.1%), washout (5.6% and 6.5%), and enhancing capsule (51.6% and 44.4%) compared with CT and HBA-MRI, respectively. ECA-MRI showed better sensitivity and accuracy (83.1% and 86.5%) than either CT (63.7% and 71.8%) or HBA-MRI (69.4% and 76.1%), while all imaging modalities achieved 97.4% specificity. When combining CT with ECA-MRI or HBA-MRI, sensitivity (89.5% and 83.1%) and accuracy (91.4%

and 86.5%) were increased compared with CT alone.

CONCLUSION

ECA-MRI showed better sensitivity and accuracy than CT or HBA-MRI for the diagnosis of HCC with LI-RADS. We achieved better diagnostic performance when applying CT in combination with one of the two MRI compared with CT alone.

CLINICAL RELEVANCE/APPLICATION

Our study confirms that significant discrepancy of HCC imaging features across the imaging modality, and clinicians need to select the appropriate imaging modality for their preferred sensitivity/specificity trade off.

SSC05-04 Long-Term Evolution of Hepatocellular Adenomas at MR Imaging Follow-Up

Monday, Dec. 2 11:00AM - 11:10AM Room: N228

Awards

Trainee Research Prize - Fellow

Participants

Federica Vernuccio, MD, Palermo, Italy (*Presenter*) Nothing to Disclose Maxime Ronot, MD, Clichy, France (*Abstract Co-Author*) Nothing to Disclose Marco Dioguardi Burgio, MD, Paris, France (*Abstract Co-Author*) Nothing to Disclose Francois Cauchy, Clichy, France (*Abstract Co-Author*) Nothing to Disclose Dominique-Charles Valla, Clichy, France (*Abstract Co-Author*) Liver Safety Committee, Agomelatine Safi Dokmak, Clichy, France (*Abstract Co-Author*) Nothing to Disclose Jessica Zucman-Rossi, Paris, France (*Abstract Co-Author*) Nothing to Disclose Valerie Paradis, MD, Clichy, France (*Abstract Co-Author*) Nothing to Disclose Valerie Vilgrain, MD, Paris, France (*Abstract Co-Author*) Nothing to Disclose

For information about this presentation, contact:

federicavernuccio@gmail.com

PURPOSE

Hepatocellular adenomas (HCAs) are rare benign liver tumors. Guidelines recommend continued surveillance for patients diagnosed with HCAs, but these recommendations are mainly based on uncontrolled studies or experts' opinion. The aims of this study were to analyze the long-term course of evolution of HCAs including solitary and multiple lesions, and to identify predictive features of progression.

METHOD AND MATERIALS

In a retrospective cohort study performed at a tertiary care hospital, we included 118 patients (mean 40 \pm 10 years old) with HCAs proven at biopsy or surgery: 41 patients had solitary HCAs and 77 patients had multiple HCAs. Imaging follow-up with MR was analyzed and tumor evolution was evaluated using the Response Evaluation Criteria in Solid Tumors (RECISTv1.1) thresholds.

RESULTS

Median follow-up of the entire study population was 5.0 years. Overall, 37/41 (90%) solitary HCAs and 55/77 (71%) patients with multiple HCAs showed stable or regressive disease (i.e. >30% size decrease). After resection of solitary HCAs, new lesions appeared only in 2/29 (7%) patients, both with HCAs at-risk of malignancy. In the multiple HCAs cohort, HNF-1A inactivated HCAs showed a higher rate of progression compared to inflammatory HCAs (11/26 [42.3%] vs. 7/37 [18.9%], p = 0.043), lower use of oral contraceptives (28/32 [87.5%] vs. 45/45 (100%), p = 0.027) and lesser duration of oral contraception intake (mean 12.0 years ± 7.5 vs. 19.2 years ± 9.2, p = 0.001).

CONCLUSION

Seventy-eight percent of HCAs showed long-term stability or size regression. After resection of solitary HCAs, tumor progression occurred only in HCAs at-risk of malignancy. Patients with multiple HCAs were more likely to show progressive disease, with HNF-1 A inactivated HCAs being the most common subtype showing progression.

CLINICAL RELEVANCE/APPLICATION

This is the first study demonstrating the long-term evolution of hepatocellular adenomas (HCAs). In patients with resected solitary HCAs, surveillance may be potentially discontinued after resection, except in case of β -catenin mutated HCAs or foci of malignancy within the tumor. In patients with multiple HCAs, progressive disease may occur in up to 31% of cases, and, therefore, continued surveillance is suggested regardless of surgery.

SSC05-05 Clinical Outcomes of Patients with Elevated Alpha-Fetoprotein Level but Negative CT or MRI Findings in the Post-Treatment Surveillance After Curative-Intent Surgery or Radiofrequency Ablation for Hepatocellular Carcinoma

Monday, Dec. 2 11:10AM - 11:20AM Room: N228

Participants

Jihyuk Lee, MD, Seoul, Korea, Republic Of (Presenter) Nothing to Disclose

Ijin Joo, MD, Seoul, Korea, Republic Of (Abstract Co-Author) Nothing to Disclose

Dong Ho Lee, MD, Seoul, Korea, Republic Of (Abstract Co-Author) Nothing to Disclose

Jeong Min Lee, MD, Seoul, Korea, Republic Of (*Abstract Co-Author*) Grant, Bayer AG Grant, General Electric Company Grant, Koninklijke Philips NV Grant, STARmed Co, Ltd Grant, RF Medical Co, Ltd Grant, Samsung Electronics Co, Ltd Grant, Guerbet SA

PURPOSE

To evaluate the outcomes of patients with elevated alpha-fetoprotein (AFP) but negative CT or MRI findings in the post-treatment surveillance after curative-intent surgery or radiofrequency ablation (RFA) for hepatocellular carcinoma (HCC) and to determine predictive factors for subsequent detectable recurrence.

METHOD AND MATERIALS

This single-center retrospective study analyzed 76 patients who presented elevated AFP (>=20 ng/mL) without detectable recurrence on concurrent CT or MRI during surveillance after receiving curative-intent surgery or RFA. Time to imaging progression (development of detectable recurrence) after initial event of AFP elevation was estimated by the Kaplan-Meier method and was compared using univariate Cox regression analysis according to following parameters: surgery versus RFA, AFP elevation >50 ng/mL, prior post-treatment AFP <20 ng/mL, and negative imaging results on CT versus MRI.

RESULTS

In patients with post-treatment AFP elevation but without detectable recurrence on concurrent CT or MRI, the median time to imaging progression was 7.0 months (95% confidence interval: $6.0 \sim 9.0$ months). Of the 76 patients enrolled, 57 patients (75.0%) developed either intra-hepatic (n=55) or extra-hepatic (n=2) recurrence detected on the average 2.6th follow-up CT or MRI studies after a mean of 7.9 months, whereas the other 19 patients (25.0%) did not develop any recurrence during average 4.4th CT or MRI studies for a mean follow of 15.9 months. Patients with prior post-treatment AFP <20 ng/mL showed significantly shorter time to imaging progression than those without (median 6.0 versus 16.0 months, P=0.001), while no significant differences were found according to prior treatment options, AFP elevation degrees, and imaging modalities showing negative results (Ps>0.05).

CONCLUSION

Elevated AFP (>=20 ng/mL) but negative CT or MRI findings in the post-treatment surveillance for HCC was frequently associated with subsequent imaging detectable recurrence in a short-term period. In addition, interval increment of post-treatment AFP from <20 to >=20 ng/mL was a significant risk factor for early recurrence.

CLINICAL RELEVANCE/APPLICATION

Elevated AFP after HCC treatment requires intensive follow-up to timely detect tumor recurrence, even if imaging studies show negative results at the time of initial AFP elevation.

SSC05-06 Intra Individual Prospective Comparison of Extracellular and Hepatobiliary MR Contrast Agent for the Diagnosis of HCC

Monday, Dec. 2 11:20AM - 11:30AM Room: N228

Participants

Anita Paisant, Angers, France (*Presenter*) Nothing to Disclose Maxime Ronot, MD, Clichy, France (*Presenter*) Nothing to Disclose Frederic Oberti, MD,PhD, Angers, France (*Abstract Co-Author*) Nothing to Disclose Jerome Lebigot, MD, Angers, France (*Abstract Co-Author*) Nothing to Disclose Valerie Vilgrain, MD, Paris, France (*Abstract Co-Author*) Nothing to Disclose Christophe Aube, MD, PhD, Angers, France (*Abstract Co-Author*) Nothing to Disclose

PURPOSE

Hepato-biliary (HB) contrast agent became part of international guidelines for the non-invasive diagnostic of hepatocellular carcinoma (HCC). The aim of this study was to compare performances of MRI with extra-cellular contrast agent (ECA-MRI) to HB contrast agent (HBA-MRI) for the diagnostic of small HCCs in a face to face comparison.

METHOD AND MATERIALS

All patients gave written informed content and this prospective study was approved by IRB. Between August 2014 and October 2017, 172 patients with cirrhosis, each 1 to 3 nodules from 1 to 3 cm large, were included in 8 centers. All patients had both ECA-MRI and HBA-MRI within a month. The non-invasive diagnostic of HCC was made when nodule was hyper-vascularized at arterial phase (HA) with wash-out at portal phase (PP) and/or delayed phase for ECA-MRI, or PP and/or HB phase (HBP) for HBA-MRI. The Gold Standard was defined by a composite algorithm previously published (CHIC study).

RESULTS

225 nodules, among them 153 HCCs and 72 not HCCs, were included. Both MRI sensitivities were similar (71.2%). Specificity was 83.3% for ECA-MRI and 68.1% for HBA-MRI. Concerning HCCs: on ECA-MRI, 138 were HA, 84 had wash-out at PP and 104 at DP; on HBA-MRI, 120 were HA, 79 had wash-out at PP and 105 at HBP. For nodules from 2 to 3 cm, sensitivity and specificity were similar with respectively 70.9% and 75.0%. For nodules from 1 to 2 cm, specificity drop down to 66.1% for HBA-MRI vs 85.7% for ECA-MRI.

CONCLUSION

HBA-MRI specificity is lower than HCA-MRI for the diagnostic of small HCC on cirrhotic patients. These results must question about the proper use of HBA-MRI in algorithm for the non-invasive diagnostic of small HCCs.

CLINICAL RELEVANCE/APPLICATION

The use of HBA-MRI in international guidelines for the non-invasive diagnostic of HCC should be used with caution.

SSC05-07 Can Baseline MR Imaging Biomarkers Enhance Survival Prediction of Hepatocellular Carcinoma (HCC) Patients?

Monday, Dec. 2 11:30AM - 11:40AM Room: N228

Participants

Mounes Aliyari Ghasabeh, MD, Baltimore, MD (*Abstract Co-Author*) Nothing to Disclose Ankur Pandey, MD, Baltimore, MD (*Abstract Co-Author*) Nothing to Disclose Mohammadreza Shaghaghi, MD, Baltimore, MD (*Abstract Co-Author*) Nothing to Disclose Sanaz Ameli, MD, Baltimore, MD (*Abstract Co-Author*) Nothing to Disclose Bita Hazhirkarzar, MD, Baltimore, MD (*Abstract Co-Author*) Nothing to Disclose Roya Rezvani Habibabadi, Baltimore, MD (*Abstract Co-Author*) Nothing to Disclose Pallavi Pandey, MD, Baltimore, MD (*Abstract Co-Author*) Nothing to Disclose Robert Grimm, Erlangen, Germany (*Abstract Co-Author*) Employee, Siemens AG Stockholder, Siemens AG Patent holder, Siemens AG Pegah Khoshpouri, MD, Baltimore, MD (*Abstract Co-Author*) Nothing to Disclose Maryam Ghadimi, MD, Baltimore, MD (*Presenter*) Nothing to Disclose Li Pan, Baltimore, MD (*Abstract Co-Author*) Nothing to Disclose Ihab R. Kamel, MD, PhD, Baltimore, MD (*Abstract Co-Author*) Research Grant, Siemens AG

For information about this presentation, contact:

maliyar1@jhmi.edu

PURPOSE

To evaluate role of baseline ADC and tumor margin as independent predictors of overall survival (OS) in HCC patients and assess how incorporating these variables to current staging systems may enhance survival prediction in these group of patients.

METHOD AND MATERIALS

In a retrospective IRB approved study clinical, laboratory and imaging parameters of 273 randomly selected HCC patients were collected. Cox regression model was utilized to identify parameters that were significantly related to survival. Patients were stratified based on BCLC and CLIP. Recursive partitioning test were applied on a test set of patients (70%) to identify the optimal cutoff of ADC in stratifying patient based on difference is survival. The estimated cutoff was validated on the validation set of patients. Binary ADC value (above or below the cutoff) and tumor margin were integrated in to BCLC and CLIP. Kaplan- Myer curves were drown and overall survival was measured for patients based on BCLC, CLIP, combined model of BCLC + ADC + margin and CLIP + ADC + margin. Predictive performance of each model was measured and compared using C statistical analysis.

RESULTS

At baseline, patients with Low tumor ADC and well- defined tumor margin (favorable imaging biomarkers) had longer survival compared with those with high ADC and ill-defined tumor margin (unfavorable imaging biomarkers) (median OS of 63 months and 6 months, respectively). Tumor ADC and tumor margin remained as the two strong independent predictors of survival in HCC patients after adjustment for other clinical variables. Incorporating ADC (at cutoff of 1390×106 mm/s) and tumor margin into BCLC and CLIP improved performance of survival prediction by 10% in BCLC group (0.63 Vs 0.73; p<0.001) and 7% in CLIP group (0.68 vs 0.75; p<0.001), Table 1. Regardless of BCLC and CLIP stage patients with unfavorable ADC and TM had significantly shorter OS compared to patients with both favorable ADC and TM (p<0.001), Figure 1.

CONCLUSION

Incorporating ADC and tumor margin to currently used staging systems for HCC significantly improve prediction performance of these criteria. Also, it could potentially change prediction of OS regardless of patient clinical status.

CLINICAL RELEVANCE/APPLICATION

ADC and tumor margin are two imaging biomarkers that can improve prediction performance of current staging systems, help to better stratify patients at baseline and define optimized treatment plan for them

SSC05-08 Comparison of the Diagnostic Performance of Imaging Criteria for Early-Stage Hepatocellular Carcinoma on Gadoxetate Disodium-Enhanced MRI

Monday, Dec. 2 11:40AM - 11:50AM Room: N228

Participants

Jieun Byun, MD, Seoul, Korea, Republic Of (*Presenter*) Nothing to Disclose Sang Hyun Choi, Seoul, Korea, Republic Of (*Abstract Co-Author*) Nothing to Disclose Jae Ho Byun, MD, Seoul, Korea, Republic Of (*Abstract Co-Author*) Nothing to Disclose So Jung Lee, Seoul, Korea, Republic Of (*Abstract Co-Author*) Nothing to Disclose So Yeon Kim, MD, Seoul, Korea, Republic Of (*Abstract Co-Author*) Nothing to Disclose Hyung Jin Won, MD, Seoul, Korea, Republic Of (*Abstract Co-Author*) Nothing to Disclose Yong Moon Shin, Seoul, Korea, Republic Of (*Abstract Co-Author*) Nothing to Disclose Pyo Nyun Kim, MD, Seoul, Korea, Republic Of (*Abstract Co-Author*) Nothing to Disclose

PURPOSE

We aimed to compare the diagnostic performance of imaging criteria for early-stage hepatocellular carcinoma (HCC) on gadoxetate disodium-enhanced MRI.

METHOD AND MATERIALS

We retrospectively evaluated 570 nodules (440 HCCs, 25 other malignancies, 105 benign nodules) of 3.0 cm or smaller from 418 patients at risk for HCC who underwent gadoxetate disodium-enhanced MRI from July 2015 to December 2016. Final diagnosis was assessed histopathologically or clinically (marginal recurrence after treatment or change in lesion size on follow-up imaging). We compared the sensitivity and specificity for diagnosing HCC among the latest versions of four imaging criteria, including Liver Imaging Reporting and Data System (LI-RADS), European Association for the Study of the Liver (EASL), Asian Pacific Association for the Study of the Liver (APASL), and Korean Liver Cancer Association-National Cancer Center (KLCA-NCC), using the generalized estimating equations.

RESULTS

For >=10 mm nodules, APASL showed the highest sensitivity (85.0%), significantly higher than LI-RADS category 4 or 5 (75.9%), LI-RADS category 5 (64.2%), and EASL (63.4%) (P <= .001). Regarding the specificity, LI-RADS category 5 was highest (94.7%), significantly higher than KLCA-NCC (83.0%) and APASL (78.7%) (P < .001). For <10 mm nodules, the sensitivity and specificity of LI-RADS category 4 or 5 were 17.1% and 97.2%, respectively, and those of APASL were 73.2% and 83.3%, respectively (P < .001 for sensitivity, and P = .1 for specificity). For histopathologically confirmed lesions, the results of subgroup analysis were similar to those of all lesions.

CONCLUSION

Of the four international imaging criteria, APASL had the highest sensitivity and LI-RADS category 5 showed the highest specificity

for diagnosing early-stage HCC in high-risk patients on gadoxetate disodium-enhanced MRI.

CLINICAL RELEVANCE/APPLICATION

To improve diagnostic performance of gadoxetate disodium-enhanced MRI for early-stage HCC, it is important to understand the differences of various imaging criteria for HCC.

SSC05-09 Hepatobiliary Phase Hypointensity as Predictor of Progression to Hepatocellular Carcinoma for Intermediate-High Risk Lesions

Monday, Dec. 2 11:50AM - 12:00PM Room: N228

Participants

Federica Vernuccio, MD, Palermo, Italy (*Presenter*) Nothing to Disclose Roberto Cannella, MD, Palermo, Italy (*Abstract Co-Author*) Nothing to Disclose Mathias Meyer, Mannheim, Germany (*Abstract Co-Author*) Researcher, Siemens AG; Researcher, Bracco Group Kingshuk Choudhury, PhD, Durham, NC (*Abstract Co-Author*) Nothing to Disclose Alessandro Furlan, MD, Pittsburgh, PA (*Abstract Co-Author*) Book contract, Reed Elsevier; Royalties, Reed Elsevier Daniele Marin, MD, Durham, NC (*Abstract Co-Author*) Research support, Siemens AG

For information about this presentation, contact:

federicavernuccio@gmail.com

PURPOSE

To determine the prognostic performance of hepatobiliary phase hypointensity, and Liver Imaging Reporting and Data System (LI-RADS) major imaging features in the prediction of progression to hepatocellular carcinoma (HCC) in LR-3 and LR-4 hepatic lesions with arterial phase hyperenhancement (APHE) measuring \geq 10 mm in patients at high risk of HCC.

METHOD AND MATERIALS

This retrospective dual-institution study included 160 LR-3 and 26 LR-4 lesions measuring more than 10 mm and having APHE in 136 consecutive patients (mean age(SD), 57 (11) years old; mean lesion size (SD), 14 (4) mm). A composite reference standard of pathologic analysis and imaging follow-up was used. The prognostic performance (sensitivity and specificity) of hepatobiliary phase hypointensity and LI-RADS version 2018 major imaging features other than APHE for the prediction of probability of progression to HCC and time to progression to HCC was assessed and compared by means of Log-rank test, Cox-regression and Kaplan-Meier curves.

RESULTS

Hepatobiliary phase hypointensity was a predictor of progression to HCC at univariate (p<0.0001) and multivariate (p<0.0001) analysis, with an odds ratio of 20.6. Median time to progression to HCC was 284 days [95%CI: 266-363). In LR-3 and LR-4 lesions >= 10 mm with APHE that progressed to HCC, the presence of hepatobiliary phase hypointensity, nonperipheral washout or enhancing capsule did not predict time to progression to HCC.

CONCLUSION

Hepatobiliary phase hypointensity is an independent predictor of progression to HCC in intermediate-high risk lesions measuring \geq 10 mm and having APHE in patients at risk for HCC.

CLINICAL RELEVANCE/APPLICATION

Intermediate and high risk lesions not fulfilling definitive imaging criteria for HCC account for about 40% of observations during interpretation of CT and MR imaging studies. Natural history of these lesions may be extremely variable. The prognostic information provided by hepatobiliary phase hypointensity in terms of prediction of progression to HCC allows for more tailored management.





SSC07

Science Session with Keynote: Genitourinary (Prostate MRI in Biopsy, Therapy, and Surveillance)

Monday, Dec. 2 10:30AM - 12:00PM Room: E260



AMA PRA Category 1 Credits ™: 1.50 ARRT Category A+ Credit: 1.75

FDA Discussions may include off-label uses.

Participants

Aytekin Oto, MD, Chicago, IL (*Moderator*) Research Grant, Koninklijke Philips NV; Research Grant, Guerbet SA; Research Grant, Profound Medical Inc; Medical Advisory Board, Profound Medical Inc; Consultant, AbbVie Inc; ; ;

Vinay A. Duddalwar, MD, FRCR, Los Angeles, CA (*Moderator*) ; Research Grant, Samsung Electronics Co, Ltd; Advisory Board, DeepTek; Consultant, Radmetrix

Ronaldo H. Baroni, MD, Sao Paulo, Brazil (Moderator) Nothing to Disclose

Sub-Events

SSC07-01 Genitourinary Keynote Speaker: Next Generation Prostate Imaging

Monday, Dec. 2 10:30AM - 10:40AM Room: E260

Participants

Daniel J. Margolis, MD, New York, NY (Presenter) Consultant, Blue Earth Diagnostics Ltd

PURPOSE

Prostate imaging has transformed over the past decade, with the advent of iterations on multiparametric MRI in addition to smallmolecule PET agents targeting the extracellular domain of prostate specific membrane antigen (PSMA) and high-resolution ultrasound. These innovative magnetic resonance imaging techniques both facilitate new treatment methods, and more importantly, allow for assessment of the efficacy of these new treatments. From MRI-ultrasound image fusion targeted biopsy and ablation to quantitative assessment of treatment response of medical and ablative therapies, the field of prostate imaging is rife with novel applications. These techniques individualize patient care through more accurate identification of the location and stage of prostate cancer so that only significant cancers receive treatment, and then monitor the response to directed therapies. Perhaps most intriguing is the application of artificial intelligence, which augments the radiologist's acumen, improving the value we deliver to our patients. We stand on the cusp of the age of radiologist-driven prostate cancer management.

SSC07-02 MR-US Fusion Prostate Biopsy: The Added Value of Systematic Core Biopsy to MR-Targeted Cores for Prostate Cancer Grading

Monday, Dec. 2 10:40AM - 10:50AM Room: E260

Participants

Sohrab Afshari Mirak, MD, Los Angeles, CA (*Presenter*) Nothing to Disclose Amirhossein Mohammadian Bajgiran, MD, Los Angeles, CA (*Abstract Co-Author*) Nothing to Disclose Anthony Sisk, DO, Los Angeles, CA (*Abstract Co-Author*) Nothing to Disclose Steven S. Raman, MD, Santa Monica, CA (*Abstract Co-Author*) Consultant, Johnson & Johnson; Consultant, Bayer AG; Consultant, Merck & Co, Inc; Consultant, Amgen Inc; Consultant, Profound Medical Inc

For information about this presentation, contact:

safsharimirak@mednet.ucla.edu

PURPOSE

To investigate the value of the systematic core biopsy (S-Bx) to MR-US fusion targeted core biopsy (MR-F Bx) for detection and grading of prostate cancer (PCa) using whole mount histopathology (WMHP) as reference.

METHOD AND MATERIALS

This IRB approved, HIPAA compliant observational study cohort comprises 295 patients with 716 pathology PCa lesions, who underwent MR-F bx prior to radical prostatectomy, between 7/2010-2/2019. All patients had MR-F Bx and S-Bx. The pathology reports of all of the cores were evaluated and the characteristics of patients with higher reported Gleason score (GS) for S-Bx as compared to MR-F bx were assessed.

RESULTS

Mean patient age and PSA were 62.9±6.3 years and 8.9±10.5 ng/ml, respectively. Mean PCa lesion number on WMHP was 2.4 (1-6). Mean S-Bx and MR-F bx cores were 11.4 (6-16) and 5.3 (1-10), respectively. Mean positive cores for S-Bx was 3 (0-12) and for MR-F Bx was 3.3 (0-10). The per-patient performance of S-Bx and MR-F Bx for PCa detection were 82.4% (243/295) and 95.6% (282/295), respectively. Overall, 37.6% (111/295), 48.8% (144/295) and 13.6% (40/295) of cases had similar GS in S-Bx and MR-F Bx, higher GS in MR-F Bx and higher GS in the S-Bx, respectively. In 4.1% (12/295) of all cases, S-Bx cores upgraded PCa from GS 6 to GS>6. Among cases with higher GS in S-Bx, 32.5% (13/40) cases had benign findings on MR-F bx. 82.5% (33/40) of the higher GS cases in S-Bx were taken from the same lesion as MR-F Bx as a result of wider sampling and the characteristics of these lesions were as follows: 51.5% (17/33) PIRADSv2 score 3, 33.3% (11/33) score 4 and 15.2% (5/33) score 5; 14.5% (15/33) in apex, 33.3% (11/33) in midgland and 21.2% (7/33) in base; 42.4% (14/33) in a different sextant for the same lesion in contralateral side (3/14) or a different level (11/14). In 22.5% (9/40) of all cases with higher GS in S-Bx and in 8.3% (1/12) of upgraded cases from GS 6 to >6 in S-Bx, the report of the higher GS was false considering WMHP.

CONCLUSION

Although S-Bx at the time of MR-F Bx can slightly improve PCa grading, however, in almost one quarter of the cases, we found false upgrading. The true rate of upgrading with S-Bx is minimal and significant portion of the upgraded lesions are ipsilateral to the target.

CLINICAL RELEVANCE/APPLICATION

PCa treatment selection depends on the results of the prostate biopsy. S-Bx improves diagnostic yield only slightly for clinically significant disease over MR-F Bx.

SSC07-03 Manual Adjustment in mpMRI-Guided Prostate Biopsy Significantly Improves the Detection Rate of Prostate Cancer: Experience in 400 Patients

Monday, Dec. 2 10:50AM - 11:00AM Room: E260

Participants

Sarah Alessi, MD, Milano, Italy (*Presenter*) Nothing to Disclose Paola Pricolo, MD, Milano, Italy (*Abstract Co-Author*) Nothing to Disclose Paul E. Summers, Milan, Italy (*Abstract Co-Author*) Stockholder, QMRI Tech iSrl Giuseppe Renne, Milan, Italy (*Abstract Co-Author*) Nothing to Disclose Gennaro Musi, Milano, Italy (*Abstract Co-Author*) Nothing to Disclose Roberto Bianchi, Milano, Italy (*Abstract Co-Author*) Nothing to Disclose Barbara Jereczek-Fossa, MD, Milan, Italy (*Abstract Co-Author*) Nothing to Disclose Massimo Bellomi, MD, Milan, Italy (*Abstract Co-Author*) Nothing to Disclose Ottavio de Cobelli, Milano , Italy (*Abstract Co-Author*) Nothing to Disclose Giuseppe Petralia, MD, Milano, Italy (*Abstract Co-Author*) Nothing to Disclose

PURPOSE

to compare the results of software-guided sampling with those obtained after manual adjustment in multiparametric MRI-guided prostate biopsy (mpMRI-PB) and to evaluate whether manual adjustment improves the detection rate of prostate cancer (PCa).

METHOD AND MATERIALS

We enrolled 400 consecutive patients between November 2014 and February 2018, who underwent mpMRI-PB of the target lesion visible on previous mpMRI (average 11.6 mm, range 4-40mm). All mpMRI-PBs were performed on a 1.5T MR scanner (Magnetom Avanto, Siemens Healthineers, Germany) using a commercially available MR transrectal biopsy device (DynaTRIM, Invivo, USA). After calibration of the biopsy device, the first sample was obtained using the coordinates provided by the device software to guide the needle along a trajectory to the target lesion. The trajectory was then manually adjusted to improve localization to the target lesion for further biopsy samples.

RESULTS

225 out of 400 patients were positive for PCa after mpMRI-PB, with PCa diagnosed in 55/62 PI-RADS 5 (88.7%), 136/188 PI-RADS 4 (72.3%), 33/127 PI-RADS 3 (25.9%) and 1/23 PIRADS 2 lesions (4.3%). The first sample was positive for PCa in just 117 cases. After manual adjustment, an additional 108 positive biopsies were obtained, corresponding to an increase in the detection rate of 92.3% (p < 0.0001; McNemar's Test). The core involvement averaged 50.3% (range 1-100%). To date, 101 of the 225 PCa patients have undergone surgery, with an average lesion diameter in the surgical specimen of 15.7 mm (range 5-40mm).

CONCLUSION

Manual adjustment of needle trajectory significantly improves the detection rate of PCa when performing mpMRI-PB.

CLINICAL RELEVANCE/APPLICATION

mpMRI guided prostate biopsy is associated with an improvement of detection rate of prostate cancer after manual adjustment of needle trajectory.

SSC07-04 Deep Learning-Based Automated Segmentation of Prostate Cancer on Multiparametric MRI: Comparison with Experienced Uroradiologists

Monday, Dec. 2 11:00AM - 11:10AM Room: E260

Participants

Wonmo Jung, Seoul, Korea, Republic Of (*Presenter*) Nothing to Disclose Sung Il Hwang, MD, Seongnam, Korea, Republic Of (*Abstract Co-Author*) Nothing to Disclose Sejin Park, MS, Seoul, Korea, Republic Of (*Abstract Co-Author*) Nothing to Disclose Jin-Kyeong Sung, MD, Seoul, Korea, Republic Of (*Abstract Co-Author*) Employee, VUNO Inc Kyu-Hwan Jung, PhD, Seoul, Korea, Republic Of (*Abstract Co-Author*) Employee, VUNO Inc Hyungwoo Ahn, MD, Seongnam, Korea, Republic Of (*Abstract Co-Author*) Nothing to Disclose Hak Jong Lee, MD, PhD, Seongnam, Korea, Republic Of (*Abstract Co-Author*) Nothing to Disclose Sang Youn Kim, Seoul, Korea, Republic Of (*Abstract Co-Author*) Nothing to Disclose Myoung Seok Lee, MD, Seoul, Korea, Republic Of (*Abstract Co-Author*) Nothing to Disclose Younggi Kim, Seongnam, Korea, Republic Of (*Abstract Co-Author*) Nothing to Disclose

For information about this presentation, contact:

wm.jung@vuno.co

PURPOSE

To compare the performance of deep learning based prostate cancer (PCa) segmentation with manual segmentation of experienced uroradiologists.

METHOD AND MATERIALS

From 2011 Jan to 2018 Apr, 350 patients who underwent prostatectomy for prostate cancer were enrolled retrospectively. To collect histopathological ground truth, pathologic slides of whole resected prostate were scanned and PCa lesions were drawn by a uropathologist with 25 years' experience. With reference to the histopathological lesion, radiological ground truth of PCa was drawn on the T2 weighted image by a uroradiologist with 19 years' experience. A U-Net type deep neural network, in which the encoder part has more convolution blocks than the decoder, was trained for segmentation. Four different MR sequences including T2 weighted images, diffusion weighted images (b = 0, 1000), and apparent diffusion coefficient (ADC) images, were used as input images after affine registration. Besides the automatic segmentation by the deep neural network, two experienced uroradiologists marked suspected sectors of PCa among 39 sectors provided by PIRADS-v2 after reviewing same images of four MR sequences. The manual segmentation performance of uroradiologists was measured using the number of sectors that coincided with the ground truth PCa lesion.

RESULTS

The dice coefficient scores (DCSs) achieved by two uroradiologists were 0.490 and 0.310 respectively. The DCS was calculated based on the number of sectors. The DCS of automatic segmentation by a deep neural network was 0.558 (calculated by the number of pixels) which is slightly better than the average (0.40) DCSs of uroradiologists.

CONCLUSION

Automated segmentation of PCa on multiparametric MR based on histopathologically confirmed lesion label achieved comparable performance with experienced uroradiologist.

CLINICAL RELEVANCE/APPLICATION

The automated segmentation of prostate cancer using a deep neural network not only reduce time consuming work but also provide reliable location and size information required for treatment decision.

SSC07-05 Multiparametric MRI Can Exclude Prostate Cancer Progression in Patients Under Active Surveillance

Monday, Dec. 2 11:10AM - 11:20AM Room: E260

Participants

Lars Schimmoeller, MD, Dusseldorf, Germany (*Abstract Co-Author*) Nothing to Disclose Tim Ullrich, Duesseldorf, Germany (*Presenter*) Nothing to Disclose Fabian Mones, Dusseldorf, Germany (*Abstract Co-Author*) Nothing to Disclose Christian Arsov, MD, Duesseldorf, Germany (*Abstract Co-Author*) Nothing to Disclose Robert Rabenalt, Duesseldorf, Germany (*Abstract Co-Author*) Nothing to Disclose Gerald Antoch, MD, Dusseldorf, Germany (*Abstract Co-Author*) Nothing to Disclose

For information about this presentation, contact:

Lars.schimmoeller@med.uni-duesseldorf.de

PURPOSE

To assess the ability of multiparametric MRI (mp-MRI) of the prostate to exclude prostate cancer (PCa) progression in patients under active surveillance.

METHOD AND MATERIALS

One hundred and forty-seven consecutive patients under active surveillance with known PCa with a Gleason score of 3+3=6 or 3+4=7a were initially enrolled and received mp-MRI (T2WI, DWI, DCE-MRI) of the prostate at 3T. Of these patients, fifty-five received follow-up MRI after a minimum interval of 12 months with subsequent targeted MR/US fusion-guided (FUS-GB) plus systematic transrectal ultrasound-guided (TRUS-GB) biopsy. Primary endpoint was negative predictive value (NPV) of the follow-up mp-MRI to exclude tumor progression. Secondary endpoints were positive predictive value (PPV), sensitivity, specificity, and cancer upgrade after initial mp-MRI.

RESULTS

Of 55 patients 28 (51%) had a Gleason score upgrade in the re-biopsy. All of the 28 patients showed findings in the follow-up mp-MRI that were suspicious of tumor progress. 16 of 55 patients (29%) showed signs of tumor progress in the follow-up MRI but had a stable re-biopsy. 11 of 55 patients (20%) showed no signs of progress in follow-up MRI and none of these patients had a Gleason score upgrade in the re-biopsy. NPV was 100%. PPV was 64%. Sensitivity was 100% and specificity 59%.

CONCLUSION

MP-MRI can reliably exclude PCa progression in patients under active surveillance. Over 60% of the patients with signs of tumor progress in follow-up mp-MRI had a Gleason score upgrade in repeat biopsy.

CLINICAL RELEVANCE/APPLICATION

Patients under active surveillance should receive follow-up MRI to monitor tumor progress. Standard re-biopsy protocols might be waived if follow-up mp-MRI is stable.

SSC07-06 Post-ablation Prostate Imaging Reporting and Data System (PAPI-RADS): Preliminary Results at 12 Months After Whole-Gland MRI-Guided Transurethral Ultrasound Ablation (TULSA)

Monday, Dec. 2 11:20AM - 11:30AM Room: E260

Steven S. Raman, MD, Santa Monica, CA (Abstract Co-Author) Consultant, Johnson & Johnson; Consultant, Bayer AG; Consultant, Merck & Co, Inc; Consultant, Amgen Inc; Consultant, Profound Medical Inc Sandeep S. Arora, MBBS, Nashville, TN (Abstract Co-Author) Speaker, Profound Medical Inc Researcher, Profound Medical Inc Derek W. Cool, MD, PhD, London, ON (Abstract Co-Author) Nothing to Disclose Andrei S. Purysko, MD, Westlake, OH (Abstract Co-Author) Nothing to Disclose Daniel N. Costa, MD, Dallas, TX (Abstract Co-Author) Nothing to Disclose Joyce G. Bomers, Arnhem, Netherlands (Abstract Co-Author) Nothing to Disclose Jurgen J. Futterer, MD, PhD, Nijmegen, Netherlands (Abstract Co-Author) Research Grant, Siemens AG Carlos Nicolau, MD, Barcelona, Spain (Abstract Co-Author) Nothing to Disclose Thorsten Persigehl, MD, Koeln, Germany (Abstract Co-Author) Nothing to Disclose Kiran R. Nandalur, MD, Bloomfield Hills, MI (Abstract Co-Author) Nothing to Disclose Robert Staruch, Mississauga, ON (Abstract Co-Author) Employee, Profound Medical Inc Mathieu Burtnyk, DIPLPHYS, Toronto, ON (Abstract Co-Author) Employee, Profound Medical Inc David Bonekamp, MD, PhD, Heidelberg, Germany (Abstract Co-Author) Speaker, Profound Medical Inc Masoom A. Haider, MD, Toronto, ON (Abstract Co-Author) Nothing to Disclose Katarzyna J. Macura, MD, PhD, Catonsville , MD (Abstract Co-Author) Author with royalties, Reed Elsevier; Research Grant, Profound Medical Inc; Research Grant, GlaxoSmithKline plc; Research Grant, Siemens AG Aytekin Oto, MD, Chicago, IL (Abstract Co-Author) Research Grant, Koninklijke Philips NV; Research Grant, Guerbet SA; Research Grant, Profound Medical Inc; Medical Advisory Board, Profound Medical Inc; Consultant, AbbVie Inc; ; ;

For information about this presentation, contact:

atirkes@iu.edu

PURPOSE

PI-RADS v2 criteria do not specifically address evaluation of the prostate gland after non-surgical treatment. We present a modified scoring system for MRI detection of prostate cancer (PCa) in the post-ablation setting (PAPI-RADS), comparing the preliminary diagnostic performance of PAPI-RADS and PI-RADS v2 against histopathology.

METHOD AND MATERIALS

PAPI-RADS was defined by consensus among radiologists participating in an IRB-approved, HIPAA-compliant 13-center pivotal trial of whole-gland MRI-guided transurethral ultrasound ablation (TULSA) in 115 men with PCa. The proposed system uses a 5-point likelihood score for residual/recurrent PCa, with the same MRI acquisition parameters recommended by PI-RADS v2. PAPI-RADS criteria give emphasis to focal early enhancement on dynamic contrast-enhanced images, over abnormal T2-weighted hypointensity or diffusion restriction. We present the interpretation by 13 on-site radiologists, in addition to a separate blinded central radiologist who scored all 12-month MRIs according to PI-RADS v2 and PAPI-RADS. Diagnostic accuracy was assessed against histopathology obtained at 12-month post-ablation 10-core biopsy.

RESULTS

At time of this submission, local PI-RADS v2 was available for 111/111 men with 12-month MRI and biopsy, central PI-RADS v2 for 76/111. At 12 months, local and central radiologists identified PI-RADS v2 score >=3 and >=4 lesions in 28/111 (25%) and 13/111 (12%) men, vs. 23/76 (30%) and 15/76 (20%) men, respectively. Local and central PAPI-RADS was available for 55/111 and 29/55 men, with score >=3 and >=4 lesions identified in 12/55 (22%) and 9/55 (16%) of men, vs. 7/29 (24%) and 5/29 (17%). Preliminary diagnostic performance of both criteria against 10-core biopsy (median sampling density 1.0 cores/cc) are listed in Table 1, with higher negative predictive values for PAPI-RADS (local: 96% vs. 89% for score >=4, central: 92% vs. 90%). Results from all patients will be available in December.

CONCLUSION

Preliminary results of 12-month post-ablation mpMRI with the proposed PAPI-RADS scoring system provided improved diagnostic performance for detection of prostate cancer over PI-RADS v2.

CLINICAL RELEVANCE/APPLICATION

PI-RADS v2 was designed for treatment-naïve prostates. The proposed modified post-ablation MRI criteria improves accuracy by addressing prostate tissue changes following ablative therapy for PCa.

SSC07-07 Pivotal Trial of MRI-Guided Transurethral Ultrasound Ablation (TULSA) in Patients with Localized Prostate Cancer

Monday, Dec. 2 11:30AM - 11:40AM Room: E260

Participants

Steven S. Raman, MD, Santa Monica, CA (Presenter) Consultant, Johnson & Johnson; Consultant, Bayer AG; Consultant, Merck & Co, Inc; Consultant, Amgen Inc; Consultant, Profound Medical Inc Aytekin Oto, MD, Chicago, IL (Abstract Co-Author) Research Grant, Koninklijke Philips NV; Research Grant, Guerbet SA; Research Grant, Profound Medical Inc; Medical Advisory Board, Profound Medical Inc; Consultant, AbbVie Inc; ; ; Katarzyna J. Macura, MD, PhD, Catonsville, MD (Abstract Co-Author) Author with royalties, Reed Elsevier; Research Grant, Profound Medical Inc; Research Grant, GlaxoSmithKline plc; Research Grant, Siemens AG Sandeep S. Arora, MBBS, Nashville, TN (Abstract Co-Author) Speaker, Profound Medical Inc Researcher, Profound Medical Inc Temel Tirkes, MD, Indianapolis, IN (Abstract Co-Author) Nothing to Disclose Jurgen J. Futterer, MD, PhD, Nijmegen, Netherlands (Abstract Co-Author) Research Grant, Siemens AG Daniel N. Costa, MD, Dallas, TX (Abstract Co-Author) Nothing to Disclose David Bonekamp, MD, PhD, Heidelberg, Germany (Abstract Co-Author) Speaker, Profound Medical Inc Masoom A. Haider, MD, Toronto, ON (Abstract Co-Author) Nothing to Disclose Derek W. Cool, MD, PhD, London, ON (Abstract Co-Author) Nothing to Disclose Carlos Nicolau, MD, Barcelona, Spain (Abstract Co-Author) Nothing to Disclose Thorsten Persigehl, MD, Koeln, Germany (Abstract Co-Author) Nothing to Disclose Kiran R. Nandalur, MD, Bloomfield Hills, MI (Abstract Co-Author) Nothing to Disclose Robert Staruch, Mississauga, ON (Abstract Co-Author) Employee, Profound Medical Inc Mathieu Burtnyk, DIPLPHYS, Toronto, ON (Abstract Co-Author) Employee, Profound Medical Inc Marc Serrallach, Barcelona, Spain (Abstract Co-Author) Nothing to Disclose

Gregory Zagaja, Chicago, IL (*Abstract Co-Author*) Nothing to Disclose Gencay Hatiboglu, Heidelberg, Germany (*Abstract Co-Author*) Nothing to Disclose James D. Relle, MD, West Bloomfield, MI (*Abstract Co-Author*) Nothing to Disclose Allan Pantuck, MD, Los Angeles, CA (*Abstract Co-Author*) Nothing to Disclose Yair Lotan, MD, Dallas, TX (*Abstract Co-Author*) Nothing to Disclose Axel Heidenreich, Cologne, Germany (*Abstract Co-Author*) Nothing to Disclose Michiel Sedelaar, MD, PhD, Nijmegen, Netherlands (*Abstract Co-Author*) Nothing to Disclose Joseph Chin, MD, London, ON (*Abstract Co-Author*) Nothing to Disclose Michael Koch, Bloomington, IN (*Abstract Co-Author*) Nothing to Disclose Christian Pavlovich, MD, Baltimore, MD (*Abstract Co-Author*) Nothing to Disclose David Penson, MD, Nashville, TN (*Abstract Co-Author*) Nothing to Disclose Laurence Klotz, Toronto, ON (*Abstract Co-Author*) Nothing to Disclose

For information about this presentation, contact:

SRaman@mednet.ucla.edu

PURPOSE

MRI-guided transurethral ultrasound ablation (TULSA) is an incision-free method for customized prostate ablation using directional ultrasound under MRI thermometry feedback control. We report 12-month (12mo) outcomes from the TULSA-PRO Ablation Clinical Trial (TACT) Pivotal study.

METHOD AND MATERIALS

TACT enrolled 115 men with localized prostate cancer at 13 sites. Treatment intent was whole-gland ablation sparing the urethra and urinary sphincter. Primary endpoints were adverse events and proportion of men with PSA reduction >=75%. Secondary endpoints included 12mo 10-core biopsy, mpMRI, prostate volume reduction, and quality of life.

RESULTS

Median (IQR) age was 65 (59-69) years and PSA 6.3 (4.6-7.9) ng/ml. Pre-treatment, 72/115 (63%) men had Grade Group 2 (GG2) disease. PI-RADSv2 score >=3 lesions were present in 98/115 (85%) men, >=4 in 77 (67%). Ablation times were 51 (39-66) min for targeted prostate volumes of 40 (32-50) cc. MRI thermometry during treatment indicated 98% (95-99%) thermal coverage with ablation precision of ± 1.4 mm, confirmed qualitatively by post-treatment CE-MRI. Grade 3 adverse events occurred in 8% of men (all resolved), with no rectal injuries or Grade >=4 events. At 12mo, 1% of men were incontinent (>1 pad/day), and 69/92 (75%) maintained erections sufficient for penetration (IIEF Q2 >=2). PSA reduction >=75% was achieved in 110/115 (96%), with median reduction of 95% and nadir of 0.34 ng/ml. Median perfused prostate volume decreased from 41 to 4 cc at 12mo MRI. Of 68 men with baseline GG2 disease, 54 (79%) were free of GG2 on 12mo biopsy. Overall, 72/111 (65%) had no evidence of any cancer. Of 98 men with PI-RADSv2 >=3 at baseline, 26 had MRI lesions at 12mo, 11/26 with biopsy-confirmed GG2 (negative predictive value, NPV 93%). Multivariate predictors of residual GG2 included intraprostatic calcifications at screening, MRI thermal coverage of target volume, and PI-RADSv2 >=3 at 12mo (p<0.05).

CONCLUSION

The TACT Pivotal study of MRI-guided TULSA for whole-gland ablation in men with localized prostate cancer met its primary PSA endpoint in 96% of patients, with low rates of severe toxicity and residual GG2 disease. MRI at 12mo detected residual disease with NPV of 93%.

CLINICAL RELEVANCE/APPLICATION

Whole-gland ablation using MRI-guided TULSA achieves predictable PSA and prostate volume reduction. Multiparametric MRI is promising for post-TULSA follow-up.

SSC07-08 Early Diffusion and Perfusion Changes of Prostate Cancer on IVIM MR Imaging after ADT Therapy

Monday, Dec. 2 11:40AM - 11:50AM Room: E260

Participants

Yu Guo, Tianjin, China (*Abstract Co-Author*) Nothing to Disclose Hui Li, Tianjin, China (*Presenter*) Nothing to Disclose Penghui Wang, Tianjin, China (*Abstract Co-Author*) Nothing to Disclose Yu Zhang, Beijing, China (*Abstract Co-Author*) Nothing to Disclose Zhaoyang Fan, West Hollywood, CA (*Abstract Co-Author*) Nothing to Disclose Wen Shen, Tianjin, China (*Abstract Co-Author*) Nothing to Disclose

For information about this presentation, contact:

shenwen66happy@163.comzhaoyang.fan@csmc.edu

PURPOSE

To investigate the usefulness of intravoxel incoherent motion (IVIM) MR in early detection of therapeutic changes from androgen deprivation therapy (ADT) in prostate cancer patients.

METHOD AND MATERIALS

MR examinations in 22 patients with advanced prostate cancer were performed before and three months after ADT treatment, using a 3.0T system (Ingenia, Philips Healthcare) equipped with a 16-channel body coil. The imaging protocol included axial T1WI ,axial T2WI , coronal T2WI and axial IVIM. The IVIM was performed at 11 b values of 0, 10, 20, 30, 50, 75, 100, 250, 500, 750 and 1000s/mm2. T2WI and IVIM images were qualitatively reviewed by an experienced radiologist. The prostate-specific antigen (PSA) levels were also assessed. The diffusion coefficients (D), perfusion fractions (f) and the perfusion-related diffusion Coefficient (D*) values were quantitatively measured in the prostate cancer area and bone metastasis. Changes in these IVIM measurements between pre- and post-treatment timepoints were evaluated using a paired Student t test. P<0.05 indicated a significant difference.

RESULTS

Prostate and tumor volume of the patients showed different degrees of reduction after ADT therapy except for 3 patients. T2weighted images signal was diffusely reduced after therapy. The signal intensities of most cancerous and non-cancer areas were visually similar. The mean PSA level was significantly reduced. At 3 months after treatment, the D value of cancer area $((0.902\pm0.118)\times10-3mm2/s)$ was significantly increased as compared with the pretreatment value $((0.585\pm0.142)\times10-3 mm2/s)$, (p < 0.001). The f value of cancer area (0.299 ± 0.074) was significantly increased compared with the pretreatment one (0.254 ± 0.064) (P < 0.05). The D and f value of bone metastases was significantly increased after treatment (P < 0.05). D* showed no significant changes before and after treatment.

CONCLUSION

T2WI images after ADT therapy are of little value for determining the location and boundary of the tumor. The IVIM MR allows noninvasive quantitative characterization of biological changes (both diffusion and perfusion fraction) of prostate cancer after treatment. This technique may potentially be useful for the evaluation of therapeutic effect and risk for recurrence.

CLINICAL RELEVANCE/APPLICATION

It may have potential technique in the evaluation of therapeutic effect and early prediction of efficacy.

SSC07-09 Baseline Multiparametric MRI Characteristics of Exceptional Pathologic Response to Neoadjuvant Enzalutamide for High-Risk, Localized Prostate Cancer

Monday, Dec. 2 11:50AM - 12:00PM Room: E260

Participants

Stephanie A. Harmon, PhD , Bethesda, MD (Presenter) Research funded, NCI Scott Wilkinson, PhD, Bethesda, MD (Abstract Co-Author) Nothing to Disclose Huihui Ye, MD, Boston , MA (Abstract Co-Author) Nothing to Disclose Fatima Karzai, MD, Bethesda, MD (Abstract Co-Author) Nothing to Disclose Nicole L. Carrabba, Bethesda, MD (Abstract Co-Author) Nothing to Disclose Nicholas L. Terrigino, Bethesda, MD (Abstract Co-Author) Nothing to Disclose Rayann Atway, Bethesda, MD (Abstract Co-Author) Nothing to Disclose John Bright, Bethesda, MD (Abstract Co-Author) Nothing to Disclose Stephanie M. Walker, Bethesda, MD (Abstract Co-Author) Nothing to Disclose Lake L. Ross, Bethesda, MD (Abstract Co-Author) Nothing to Disclose David J. Vanderweele, MD, PhD, Bethesda , MD (Abstract Co-Author) Nothing to Disclose Peter L. Choyke, MD, Rockville, MD (Abstract Co-Author) Nothing to Disclose Peter Pinto, Bethesda, MD (Abstract Co-Author) Nothing to Disclose William Dahut, Bethesda, MD (Abstract Co-Author) Nothing to Disclose Adam G. Sowalsky, PhD, Bethesda, MD (Abstract Co-Author) Nothing to Disclose Baris Turkbey, MD, Bethesda, MD (Abstract Co-Author) Research support, Koninklijke Philips NV; Royalties, Invivo Corporation; Investigator, NVIDIA Corporation

PURPOSE

To assess multiparametric MRI (mpMRI) characteristics of high-risk prostate cancer patients demonstrating minimal residual disease (MRD) at radical prostatectomy (RP) after neoadjuvant androgen deprivation therapy (ADT) + enzalutamide.

METHOD AND MATERIALS

Patients with untreated high risk prostate cancer enrolled on a clinical trial evaluating neoadjuvant ADT + enzalutamide (160mg/day), receiving mpMRIat baseline and 6-months post-treatment followed by RP. RP specimens were sectioned in same plane as MR using a patient-specific 3D printed mold. Fixed tissue sections of baseline biopsy and tumor on RP specimens were stained, laser capture microdissected, and analyzed using whole exome sequencing to define clonally independent tumors. Non-responding tumors were pathologically defined by residual tumor burden >0.05 cc, measured by an expert GU pathologist. All mpMRI imaging was interpreted by a single expert radiologist. Regions encompassing suspected lesions were contoured at baseline and follow-up. Quantitative characteristics including volume, Apparent Diffusion Coefficients (ADC), and perfusion (Ktrans; calculated using a two compartment Tofts model with standardized arterial input function) were collected. Association between metrics and residual disease was evaluated using appropriate nonparametric statistical testing.

RESULTS

31 patients completed all imaging and RP, with 49 lesions detected on baseline mpMRI, of which 39 remained measurable at 6-mo. follow-up imaging. Two patients had at least 2 clonally independent lesions distinguishable on baseline imaging showing differential response at RP assessment. Lesion burden at both mpMRI timepoints was strongly associated with residual cancer (N=16) on pathology (p=0.002 vs p=0.003, respectively). Baseline summary diffusion (ADC) and perfusion (Ktrans) characteristics showed modest association to residual disease, further enhanced when assessing heterogeneity of signal intensity (ADCentropy 0.003, Ktrans, entropy 0.056).

CONCLUSION

While quantitative mpMRI metrics have shown correlation to Gleason grading and disease burden in untreated cases, distinct features also correlate with likelihood of residual cancer burden after intensive neoadjuvant therapy.

CLINICAL RELEVANCE/APPLICATION

Selection of patients based on these parameters may improve overall responses to treatment in subsequent clinical trials.





SSC10

Neuroradiology (Diffusion/Perfusion)

Monday, Dec. 2 10:30AM - 12:00PM Room: S502AB



AMA PRA Category 1 Credits ™: 1.50 ARRT Category A+ Credit: 1.75

FDA Discussions may include off-label uses.

Participants

Kei Yamada, MD, Kyoto, Japan (Moderator) Nothing to Disclose

Joshua S. Shimony, MD, PhD, Saint Louis, MO (Moderator) Nothing to Disclose

Jochen B. Fiebach, MD, Heidelberg, Germany (*Moderator*) Consultant, BioClinica, Inc; Speaker, BioClinica, Inc; Advisory Board, BioClinica, Inc; Consultant, Cerevast; Speaker, Cerevast; Advisory Board, Cerevast; Consultant, Artemida; Speaker, Artemida; Advisory Board, Artemida; Consultant, Brainomix; Speaker, Brainomix; Advisory Board, Brainomix; Consultant, Biogen Idec Inc; Speaker, Biogen Idec Inc; Advisory Board, Biogen Idec Inc; Consultant, Bristol-Myers Squibb Company; Speaker, Bristol-Myers Squibb Company; Advisory Board, Bristol-Myers Squibb Company; Consultant, Eisai Co, Ltd; Speaker, Eisai Co, Ltd; Advisory Board, Eisai Co, Ltd

Sub-Events

SSC10-01 Super-Resolution Reconstruction from Orthogonal Slice-Undersampled Diffusion MRI Data

Monday, Dec. 2 10:30AM - 10:40AM Room: S502AB

Participants

Yoonmi Hong, PhD, Chapel Hill, NC (*Presenter*) Nothing to Disclose Geng Chen, Chapel Hill, NC (*Abstract Co-Author*) Nothing to Disclose Pew-Thian Yap, PhD, Chapel Hill, NC (*Abstract Co-Author*) Nothing to Disclose Dinggang Shen, Chapel Hill, NC (*Abstract Co-Author*) Nothing to Disclose

PURPOSE

Diffusion MRI (dMRI) is a powerful imaging technique for characterizing the brain white matter tissue microstructure. However, dMRI requires longer acquisition times for sufficient coverage of the *q*-space. Each point in *q*-space corresponds to a diffusion-weighted image (DWI), and a sufficient number of DWIs are required for accurate characterization of the microstructure. To accelerate acquisition, we introduce a super-resolution (SR) reconstruction that only requires a subsample of slices for each DWI, instead of scanning full DWIs. Each DWI is subsampled with a different slice offset and imaging plane, so that the volume captures complementary information that can be used to improve the reconstruction of other DWIs.

METHOD AND MATERIALS

We selected 16 subjects from the HCP database and performed 4-fold cross-validation with 12 subjects for training and 4 subjects for testing. For each subject, 90 DWIs with b=2000 s/mm2 were used for evaluation. DWIs were retrospectively undersampled by factors R=3, 4 and 5. The mapping from the undersampled to the full DWIs is learned using a graph convolutional neural network (GCNN). We fully exploit the relationships of neighboring sampling points in the spatial domain and *q*-space in the form of a graph. To learn the target with better perceptual quality, we employ the GCNN as the generator in a generative adversarial network.

RESULTS

We compared our SR method with two conventional methods: Bicubic interpolation and 3D U-Net. Representative reconstruction results for GFA at R=4, shown in the figure, indicate that the proposed SR recovers more structural details compared with the two conventional methods which exploit only spatial correlation. We measure the reconstruction accuracy of the reconstructed dMRI by mean absolute error (MAE), peak signal-to-noise ratio (PSNR), and structural similarity index (SSIM). The quantitative results are summarized in the figure.

CONCLUSION

We have proposed to employ slice-undersampling for acceleration of dMRI. The non-linear mapping from undersampled DWI to the full DWIs is learned using GCNN. The spatio-angular relationship is jointly considered when constructing the graph. The experimental results demonstrate that the proposed SR outperforms the conventional interpolation and a 3D U-Net based SR.

CLINICAL RELEVANCE/APPLICATION

The proposed method can efficiently accelerate the acquisition of dMRI data and reconstruct DW images with minimal information loss.

SSC10-02 Prediction of Multi-Shell Diffusion MRI Data Using Deep Neural Networks with Diffusion Loss

Monday, Dec. 2 10:40AM - 10:50AM Room: S502AB

Participants Geng Chen, Chapel Hill, NC (*Presenter*) Nothing to Disclose Yoonmi Hong, PhD, Chapel Hill, NC (*Abstract Co-Author*) Nothing to Disclose Khoi M. Huynh, Chapel Hill, NC (*Abstract Co-Author*) Nothing to Disclose Weili Lin, PhD, Chapel Hill, NC (*Abstract Co-Author*) Nothing to Disclose Dinggang Shen, Chapel Hill, NC (*Abstract Co-Author*) Nothing to Disclose Pew-Thian Yap, PhD, Chapel Hill, NC (*Abstract Co-Author*) Nothing to Disclose

PURPOSE

Acquisition of multi-shell (MS) diffusion MRI (dMRI) data requires longer acquisition time, beyond what is typical in clinical settings. Deep learning can be used to reduce scan time by predicting MS data from data with fewer shells. Existing deep learning methods utilize an I1 loss function as the network optimization target. This is effective in constraining the prediction to match the target MS data but may not ensure the quality of microstructure indices estimated from the predicted data. To overcome this limitation, we propose a novel loss function, called diffusion loss, to explicitly take into account microstructural properties in dMRI prediction. The diffusion loss consists of two parts, including an I1 loss for the predicted dMRI data and another I1 loss for microstructure indices.

METHOD AND MATERIALS

An overview of our network is shown in Fig. 1. Overall, the network consists of two parts, including a sub-network for MS dMRI data prediction and another sub-network for microstructure estimation. We aim to learn a non-linear function fP for predicting the expected MS dMRI data, SMS from the input dMRI data SIn. The microstructure estimator fE predicts microstructure indices from the dMRI data. We demonstrate the effectiveness of diffusion loss using data from the Baby Connectome Project. Our dataset consists of 13 subjects. We utilize 5 of them for training, 5 for testing, and another 3 for validation. All the data were acquired using a Siemens MR scanner with two imaging protocols, including (i) a 2-shell protocol with 74 gradient directions and (ii) a 6-shell protocol with 144 gradient directions.

RESULTS

In this work, we aim to predict the 6-shell data from their 2-shell counterpart. The data predictor, trained without the microstructure estimator, was utilized as the comparison baseline. The results, shown in Fig. 2, indicate that the diffusion loss reduces the mean square error value of not only the predicted dMRI data but also a variety of microstructure indices. Furthermore, the results, shown in Fig. 3, indicate that the diffusion loss reduces GFA errors significantly.

CONCLUSION

We have proposed a novel loss function specifically designed for predicting MS dMRI data. The experimental results demonstrate the effectiveness of our method.

CLINICAL RELEVANCE/APPLICATION

The proposed method predicts high-quality MS data from the dMRI data with fewer shells, allowing analysis with advanced microstructure models.

ssc10-03 White Matter Changes Near to and Distant from Chronic Black Holes in Multiple Sclerosis

Monday, Dec. 2 10:50AM - 11:00AM Room: S502AB

Participants

Dhairya Lakhani, MD, Nashville, TN (*Presenter*) Nothing to Disclose Giulia Franco, Nashville, TN (*Abstract Co-Author*) Nothing to Disclose Aneri Balar, Nashville, TN (*Abstract Co-Author*) Nothing to Disclose Seth A. Smith, PhD, Nashville, TN (*Abstract Co-Author*) Nothing to Disclose Junzhong Xu, Nashville, TN (*Abstract Co-Author*) Nothing to Disclose Richard Dortch, PhD, Nashville, TN (*Abstract Co-Author*) Nothing to Disclose Francesca Bagnato, MD, Nashville, TN (*Abstract Co-Author*) Nothing to Disclose

For information about this presentation, contact:

Dhairya.Lakhani@gmail.com

PURPOSE

Histopathological evidence show that anterograde and retrograde degeneration follows focal axonal transection in brains of persons with multiple sclerosis (MS). However, quantifying and characterizing this damage in vivo is challenging due to lack of imaging techniques sensitive to axonal and myelin injury. We propose to use quantitative magnetization transfer imaging (qMT), Spherical Mean Technique (SMT) and Neurite Orientation Dispersion and Density Imaging (NODDI) to identify and characterize myelin and axonal injuries following focal lesional transection, in vivo.

METHOD AND MATERIALS

In this prospective case-control study 18 persons with MS and nine age-and-sex-matched healthy controls (HCs) were included. T2-lesions with and without an associated chronic black hole (cBH) were identified. Region of interests (ROIs) on T2-lesions and cBHs as well as on adjacent normal appearing white matter (NAWM) referred as border zone hereafter and contra-lateral NAWM were drawn. ROIs were then co-registered on SIR-qMT, SMT and NODDI maps. Differences between tissues types were measured using paired t-tests as appropriate.

RESULTS

Preliminary results indicate differences in PSR (p<0.001) and Vax (p<0.001) between NAWM adjacent to cBHs compared to contralateral anatomically matched NAWM ROIs.(Fig1) No significant associations were seen between PSR and Vax values within each tissue type.

CONCLUSION

Our preliminary findings suggest that border zones adjacent to cBHs have reduced values of PSR and Vax. Which confirms the ability of MRI metrics to capture anterograde and retrograde degeneration following a focal MS lesion. However, no correlation was observed with PSR and Vax in each tissue subtypes. In border zones and NAWM in general typically myelin loss is secondary to axonal degeneration thus an association between the two measures should be expected. We postulate that different scales of the two metrics may contribute to our finding. It is also conceivable that longitudinal, rather than cross-sectional measurements may

better capture such an association. Last, it may be plausible that the degree of axonal and myelin loss seen in NAWM are not sufficient to result into significant associations between the two.

CLINICAL RELEVANCE/APPLICATION

NAWM near cBHs has a different composition as compared to NAWM. Targeting border zones disease may serve as measure of outcome during clinical trials exploring reparative effects of experimental molecules.

SSC10-04 Visualization and Microstructural Investigation of the Vestibulocochlear Nerve and Central Hearing Pathways Using MR Diffusion Tensor Imaging

Monday, Dec. 2 11:00AM - 11:10AM Room: S502AB

Participants

Arthur P. Wunderlich, PhD, Ulm, Germany (*Presenter*) Nothing to Disclose Thomas Hoffmann, Ulm, Germany (*Abstract Co-Author*) Nothing to Disclose Meinrad J. Beer, MD, Ulm, Germany (*Abstract Co-Author*) Nothing to Disclose Wiebke Schloetzer, Ulm, Germany (*Abstract Co-Author*) Nothing to Disclose Eva Goldberg-Bockhorn, Ulm, Germany (*Abstract Co-Author*) Nothing to Disclose Martha Shenton, PhD, Boston, MA (*Abstract Co-Author*) Nothing to Disclose Sylvain Bouix, Boston, MA (*Abstract Co-Author*) Nothing to Disclose Marlene C. Wigand, Ulm, Germany (*Abstract Co-Author*) Nothing to Disclose

For information about this presentation, contact:

arthur.wunderlich@uni-ulm.de

PURPOSE

Diffusion Tensor Imaging (DTI) is an MRI based method for non-invasive visualization and characterization of nerve tracts. It allows to study the microstructure of white matter pathways and to analyze changes related to different pathologies. While it has had great impact in the field of neuroradiology and psychiatry, there are only few studies involving DTI in otorhinolaryngology. This study was performed to investigate whether DTI is feasible in the vestibulocochlear nerve (VN) and auditory pathways.

METHOD AND MATERIALS

We investigated fourteen healthy, normal hearing volunteers on a 3 T MRI scanner (Magnetom Skyra, Siemens Healthcare, Erlangen, Germany). Diffusion weighted images at an isotropic resolution of 1.5 mm, 96 slices covering the whole brain, and with 30 diffusion directions were acquired. A special diffusion sequence using readout segmentation of long variable echo-trains (RESOLVE) was used which reduces distortion and signal loss in regions with field inhomogeneity. Acquisition time was 76 min. After manually defining and applying regions of interest, two-tensor tractography was used to identify the VN, arcuate fasciculus and the interhemispheric auditory pathway of the corpus callosum. Subsequently, diffusion parameters, namely fractional anisotropy (FA), trace, axial, and radial diffusivity, were calculated. Parameters were statistically tested for side and gender differences.

RESULTS

The desired auditory pathways could be isolated from the datasets in all subjects and were visualized. For the left VN, we found a gender difference: men showed significantly lower FA values than women [mean FA = $.32 \pm .5$ vs. $.38 \pm .04$; F(1,12) = 7.989, p < 0.05]. The right VN did not show a significant gender difference: group mean values of FA were $.33 \pm .05$ in men and $.36 \pm .05$ in women.

CONCLUSION

Despite its small size and challenging location, we were able to visualize and characterize the vestibulocochlear nerve (VN). Moreover, the arcuate fasciculus and the interhemispheric auditory pathway were displayed. Surprisingly, significant gender differences were found for FA in the left VN of normal-hearing subjects.

CLINICAL RELEVANCE/APPLICATION

DTI is a promising new tool for microstructural analysis of vestibulocochlear nerve and central hearing pathways and might provide new insights for the investigation of different hearing impairments.

SSC10-05 Mapping the Cortical Connections of the Ventral Intermediate Nucleus (VIM) with Tractography in Patients Undergoing MRI-Guided High Intensity Focused Ultrasound (HIFU) Thalamotomy

Monday, Dec. 2 11:10AM - 11:20AM Room: S502AB

Participants

Ana Ezponda, MD, Pamplona, Spain (*Presenter*) Nothing to Disclose Marta Calvo-Imirizaldu, MD, Pamplona, Spain (*Abstract Co-Author*) Nothing to Disclose Patricia Malmierca, Pamplona, Spain (*Abstract Co-Author*) Nothing to Disclose Reyes M. Garcia-Eulate, Pamplona, Spain (*Abstract Co-Author*) Nothing to Disclose Jose Luis Zubieta, Pamplona, Spain (*Abstract Co-Author*) Nothing to Disclose Iciar Aviles, Pamplona, Spain (*Abstract Co-Author*) Nothing to Disclose Maria Cruz Rodriguez Oroz, Pamplona, Spain (*Abstract Co-Author*) Nothing to Disclose Jorge Guridi, Pamplona, Spain (*Abstract Co-Author*) Nothing to Disclose Miguel Fernandez, Pamplona, Spain (*Abstract Co-Author*) Nothing to Disclose Pablo Dominguez Echavarri, MD, Pamplona, Spain (*Abstract Co-Author*) Nothing to Disclose

For information about this presentation, contact:

aezponda@unav.es

PURPOSE

MRI-guided high-intensity focused ultrasound (HIFU) is an effective therapeutic approach for the ablation of the ventral

intermediate nucleus (VIM) of the thalamus in drug refractory tremor. Cortical connections of VIM might differ from person to person. For treatment planning best seeds points at cortex are not defined. The aim of this study was to assess the cortical connections of VIM nucleus using diffusion tensor Imaging (DTI)-based tractography that overlap with the lesion location.

METHOD AND MATERIALS

Twenty-two consecutive patients (20 right-handed) with medication-refractory ET (n=17) or PD (n=5) were recruited. All of them underwent VIM ablations contralateral to the patient's hand dominance using HIFU equipment compatible with the 3-T MR scanner. Pre-treatment and immediately after treatment structural and DTI MRI data were acquired. Pre-treatment DTI was co-registered with the post-treatment 3D T2WI sequences. The treatment-induced VIM lesion was used as seed for the DTI-based tractography. Topography of the VIM lesions and cortical connections were registered. Distance to the mid-sagittal plane was quantified at the juxtacortical white matter on axial T2WI.

RESULTS

Overall, HIFU was effective for immediate tremor control, awaiting for a longer follow-up. Mean size of the focused-sonography lesions was 6.3 ± 2.7 mm on axial 3D-T2WI. Mean distances to the midline and lateral wall of the third ventricle were 14.7 ± 1.1 and 10.5 ± 0.6 mm, respectively. Lesions were 1.6 ± 1.4 mm above the intercommissural plane and 6.8 ± 1.2 anterior to the posterior commissure. According to the cortical connections of the VIM nucleus, patients were allocated in 4 groups: medial aspect of the primary motor cortex (mM, n=7); intermediate region of the primary motor cortex (between m-M and hand-knob, iM, n=10); hand-knob region of the primary motor cortex (hM, n=2) and medial premotor area (preM, n=3). Mean distance from mid-sagittal plane at these sites were 10.7 ± 1 (mM), 17.9 ± 3.4 (iM), 21.9 ± 4.5 (hM) and 8.6 ± 3.1 (preM) mm.

CONCLUSION

Seeding of the VIM lesions on pre-treatment DTI shows connections predominantly to the primary motor cortex, usually medial to the hand-knob region.

CLINICAL RELEVANCE/APPLICATION

DTI tractography defines the topography of juxtacortical white matter projections of the VIM. For treatment planning, cortical seeds should more frequently be placed at the primary motor cortex, medial to the hand-knob region.

SSC10-06 Comparison between Readout-Segmented EPI and Single-Shot Turbo Spin Echo Diffusion-Weighted Imaging for Cholesteatoma Diagnostics

Monday, Dec. 2 11:20AM - 11:30AM Room: S502AB

Participants

Wolfgang Wust, MD, Erlangen, Germany (*Abstract Co-Author*) Speakers Bureau, Siemens AG Rafael Heiss, Erlangen, Germany (*Abstract Co-Author*) Speakers Bureau, Siemens AG Christoph Treutlein, Erlangen, Germany (*Abstract Co-Author*) Nothing to Disclose Michael Uder, MD, Erlangen, Germany (*Abstract Co-Author*) Nothing to Disclose Frederik B. Laun, Erlangen, Germany (*Abstract Co-Author*) Nothing to Disclose Matthias S. May, MD, Erlangen, Germany (*Abstract Co-Author*) Speakers Bureau, Siemens AG Marco Wiesmueller, MD, Erlangen, Germany (*Presenter*) Speakers Bureau, Siemens AG

For information about this presentation, contact:

wolfgang.wuest@uk-erlangen.de

PURPOSE

Comparison of the diagnostic value of readout-segmented diffusion-weighted imaging (rsDWI) and single-shot turbo spin echo diffusion-weighted imaging (tseDWI) for cholesteatoma diagnostics.

METHOD AND MATERIALS

30 patients with clinically suspected cholesteatoma were examined with a protocol including a rsDWI and a single-shot tseDWI sequence at 1.5 T. Acquisition parameters of both diffusion-weighted sequences were: $b = 1000 \text{ s/mm}^2$, axial and coronal slice orientation, slice thickness 3 mm. Image quality was evaluated by two readers on a 5-point Likert scale with respect to subjective image resolution, lesion conspicuity, and for the presence of artifacts mimicking cholesteatomas. Sensitivity and specificity were calculated using histology results as the gold standard.

RESULTS

30 patients with clinically suspected cholesteatoma were examined with a protocol including a rsDWI and a single-shot tseDWI sequence at 1.5 T. Acquisition parameters of both diffusion-weighted sequences were: $b = 1000 \text{ s/mm}^2$, axial and coronal slice orientation, slice thickness 3 mm. Image quality was evaluated by two readers on a 5-point Likert scale with respect to lesion conspicuity, for the presence of artifacts mimicking cholesteatomas and overall subjective image quality. Sensitivity and specificity were calculated using histology results as the gold standard.

CONCLUSION

Our data indicate that the use of tseDWI is advisable for cholesteatoma diagnostics in comparison to rsDWI.

CLINICAL RELEVANCE/APPLICATION

In cholesteatoma diagnostics, the use of single-shot turbo spin echo DWI is recommended over readout-segmented DWI.

SSC10-07 Machine Learning for Definition of Optimal Timing and Duration of CT Perfusion Scanning: Recommendations Based on Evaluation of 1400 Patients

Monday, Dec. 2 11:30AM - 11:40AM Room: S502AB

Kristine A. Blackham, MD, Basel, Switzerland (Abstract Co-Author) Nothing to Disclose

PURPOSE

CT Perfusion used in imaging of patients suspected for an ischemic stroke is a dose intensive examination as it involves numerous scans in order to enable a complete acquisition of the first pass of iodinated contrast medium through brain tissue, nevertheless, the radiation exposure should be limited to abide by the ALARA principle. We present a proposal for optimal timing and scan duration based on evaluation of more than 1400 examinations.

METHOD AND MATERIALS

More than 1400 examinations performed with our standard CT Perfusion protocol consisting of 28 scans were included. 54 seconds of scanning was started with a fixed delay of 6 seconds after beginning of injection of iodinated contrast medium (50 ml, flow of 5 ml/s). Syngo.Via (Siemens) was used for depiction of vessel attenuation changes. Retrospective analysis using machine learning was performed.

RESULTS

Statistical analysis revealed that in the majority of the patients the attenuation values at first time point stayed at the baseline and thus could be omitted without affecting arterial time-attenuation curve. The venous time attenuation-curve on the other hand was truncated in 5% of the patients. Machine learning with a "nearest-neighbour analysis" determined that a 60 second scan duration would allow for full coverage of venous output of this subgroup.

CONCLUSION

A scan time of 54 seconds allows for acquisition of attenuation changes of arterial input function but based on analysis of our data, the start of CTP scanning could be initiated with a longer delay after contract injection (7,5 seconds) or the initial scans could be acquired with a lower sampling rate (resulting in lower radiation exposure). Conversely, using this length of scan time results in truncation of venous output function curve in some patients and this in turn might lead to over/underestimation of infarct core and penumbra volume, depending on CT perfusion parameters used for its calculation; therefore, an additional 2 scans at the end, with a temporal resolution of 1 scan every 3 seconds, should be considered.

CLINICAL RELEVANCE/APPLICATION

Acquisition of complete arterial input and venous output is necessary for proper calculation of CT perfusion maps. Failure to do so might lead to over/underestimation of infarct core and penumbra. At the same time limiting the number of scans leads to lower radiation exposure of patients.

SSC10-08 Diagnostic Value of Multiple Post-Labeling Delay Arterial Spin Labeling for Cerebrovascular Reactivity in Steal Phenomenon

Monday, Dec. 2 11:40AM - 11:50AM Room: S502AB

Participants

Hye Jeong Choi, Seongnam, Korea, Republic Of (*Presenter*) Nothing to Disclose Chul-Ho Sohn, MD, Seoul, Korea, Republic Of (*Abstract Co-Author*) Nothing to Disclose Tae Jin Yun, MD, Seoul, Korea, Republic Of (*Abstract Co-Author*) Nothing to Disclose Seung Hong Choi, MD, PhD, Seoul, Korea, Republic Of (*Abstract Co-Author*) Nothing to Disclose Ji-hoon Kim, MD, PhD, Seoul, Korea, Republic Of (*Abstract Co-Author*) Nothing to Disclose Koung Mi Kang, MD, Seoul, Korea, Republic Of (*Abstract Co-Author*) Nothing to Disclose

PURPOSE

Cerebrovascular reactivity is a physiological characteristic of the brain that is related to the intrinsic ability of arteries to alter their diameters in response to a vasoactive stimulus, and this parameter is important in cerebrovascular disease. Steal is one of the impairment of CVR which refers a paradoxic flow reduction in response to a vasodilatory stress. In the present study, we evaluated the arterial transit time (ATT) in addition to the time corrected CBF (TCF) from the multiple post-labeling delay ASL as compared with basal/acetazolamide stress Technetium99-hexamethylpropylene amineoxime (99mTc-HMPAO) SPECT in prediction of the cerebrovascular reactivity, especially in steal phenomenon.

METHOD AND MATERIALS

TCF maps and ATT maps were acquired in 30 consecutive patients with unilateral ICA or MCA steno-occlusive disease (severe stenosis or occlusion). Internal carotid artery territory-based ROIs were applied to both perfusion maps. Additionally, impairments in the CVR were evaluated according to both qualitative and quantitative analyses of the ROIs on basal/acetazolamide stress 99mTc-HMPAO SPECT using a previously described method. The ROIs were divided into four groups; group A included normal basal CBF and normal reactivity on acetazolamide challenge, group B included decreased CBF and impaired reactivity on acetazolamide challenge, group C included normal CBF and impaired reactivity on acetazolamide (Figure 1). ANOVA test was performed to compare the ATT and TCF among four groups. Diagnostic decision tree was developed to differentiate among four groups.

RESULTS

ATT is significantly prolonged in group C (1848.0 [1644.0; 1980.0] [ms], compared with other groups (Figure.2). In the diagnostic tree, a cut off value of ATT as 1816 [ms] and TCF as 26 [ml/100 g/min], the four groups were differentiated 83.82% of accuracy (Figure 3).

CONCLUSION

Our results demonstrate that the ATT with TCF based on multiple postlabeling delay ASL perfusion MRI can be useful in prediction of the cerebrovascular reactivity, especially in steal phenomenon.

CLINICAL RELEVANCE/APPLICATION

ATT and TCF from multiple postlabeling delay ASL is useful in detecting cerebrovascular reactivity (CVR), especially in steal phenomenon, and is recommended in evaluation of CVR, instead of acetazolamide stress test.

SSC10-09 Predicting PET Cerebrovascular Reserve with Deep Learning from Baseline MRI: Towards a "Drug-Free" Brain Stress Test

Monday, Dec. 2 11:50AM - 12:00PM Room: S502AB

Participants David Y. Chen, MD, New Taipei City, Taiwan (*Presenter*) Nothing to Disclose Yosuke Ishii, Tokyo, Japan (*Abstract Co-Author*) Nothing to Disclose Audrey Fan, Stanford, CA (*Abstract Co-Author*) Nothing to Disclose Greg Zaharchuk, MD, PhD, Stanford, CA (*Abstract Co-Author*) Research Grant, General Electric Company; Research Grant, Bayer AG; Stockholder, Subtle Medical

For information about this presentation, contact:

b91401019@ntu.edu.tw

PURPOSE

To predict the cerebrovascular reserve (CVR) in Moyamoya patients using deep learning on PET/MRI images without the need for pharmacological vasodilation.

METHOD AND MATERIALS

Simultaneous [150]-water PET/MRI including arterial spin labeling (ASL) MRI was acquired to assess cerebral blood flow (CBF) in 20 Moyamoya patients and 10 healthy controls before and after a vasodilator (acetazolamide, ACZ) injection. A deep convolutional neural network (dCNN) was used to predict the absolute change in perfusion (Δ CBF) due to vasodilation from only baseline MRI. The dCNN structure was a U-Net, with multiple baseline MR inputs, including perfusion images (CBF, arterial transit time on ASL), structural scans (T2 FLAIR, T1) and brain template coordinate, to predict the voxelwise synthesized Δ CBF (syn- Δ CBF). The dCNN was trained on the ground truth (PET- Δ CBF) and tested on the 30 studies with 5-fold cross-validation. Image quality was evaluated with peak signal-to-noise ratio (PSNR) and normalized root mean squared error (NRMSE). Mean Δ CBF was calculated in ASPECTS ROIs. Syn- Δ CBF and ASL- Δ CBF were compared to the PET reference with correlation and Bland-Altman analyses. The accuracy for identifying vascular territories with impaired PET- Δ CBF (<75% Δ CBF in cerebellum) was evaluated.

RESULTS

Syn- Δ CBF had significantly higher PSNR (20.4±1.2 vs. 14.3±4.7, p<0.001) and lower NRMSE (0.36±0.07 vs. 0.87±0.67, p<0.001) than ASL- Δ CBF. Quantitatively, syn- Δ CBF yielded similar ROI values compared to PET- Δ CBF (0.90±0.20 vs. 0.91±0.24, p=0.77), while ASL- Δ CBF significantly overestimated Δ CBF (0.99±0.52, p<0.001). Both syn- Δ CBF and ASL- Δ CBF showed significant correlation with PET- Δ CBF (β =0.51, r =0.68 vs. β =1.28, r =0.57). However, on Bland-Altman plots, syn- Δ CBF showed less bias and reduced variance than ASL- Δ CBF, which showed overestimation errors for larger Δ CBF values. The sensitivity/specificity for identifying impaired PET- Δ CBF was 81%/95% for syn- Δ CBF and 76%/85% for ASL- Δ CBF.

CONCLUSION

The dCNN combines multi-contrast from baseline ASL and structural MRI to predict PET- Δ CBF, with higher image quality and quantification accuracy than ASL- Δ CBF. The prediction of PET-based CVR using only MRI and without injecting ACZ enables accurate CVR measurements in routine MRI settings.

CLINICAL RELEVANCE/APPLICATION

The ability to assess PET-CVR without the need for pharmacological vasodilation and radiotracers is of high value to the clinical evaluation in chronic cerebrovascular patients.





3D22

3D + AV Theater: Overcoming Funding Challenges to Scale 3DP at the Point-of-Care. Lessons from an Innovation Lab: Presented by Formlabs

Monday, Dec. 2 11:30AM - 11:50AM Room: 3D Printing and Advanced Visualization Theater, North Building, Level 3, Booth 6563

Participants

Gaurav Manchanda, Somerville, MA (*Presenter*) Nothing to Disclose Sarah A. Flora, ARRT, Danville, PA (*Presenter*) Nothing to Disclose

Program Information

Join us to hear trends, observations, and perspectives from Formlabs, the market-leader for professional-grade 3D printers, as well as best practices, common challenges, and lessons learned from Geisinger Health System. Formlabs has deployed over 50,000 SLA printers to date and has a presence in over 80% of the medical schools, medical device companies, and Level I/II trauma centers that have adopted 3D printing. 3D Printing at the Point-of-Care is not new, however, justifying a hospital 3D print program and achieving sustainability without ongoing philanthropy is rare. In this presentation, Sarah Flora, Program Director of the 3D Print Lab at Geisinger Health System, will discuss the route she took to build the business case for fully funding her program as well as discuss use cases and tools she has learned along the way. Geisinger is a 14+ hospital health system spread throughout Pennsylvania and New Jersey that includes two simulation centers, a medical school, and its own health insurance plan. Geisinger uses 3d printed medical models to aid in presurgical planning, patient and learner education, surgical simulation, and surgical aid tools. In the last 4 years, Geisinger's 3D Print lab has provided over 600+ medical models for these purposes at no cost to the patient or physician.







VW19

A Practical Approach to Breast Magnetic Resonance Imaging (MRI) Interpretation: An Interactive Session: Presented by Siemens Healthineers

Monday, Dec. 2 1:05PM - 2:15PM Room: North Building, Booth 8563

Participants

Susan Weinstein, MD, Philadelphia, PA (Presenter) Nothing to Disclose

Program Information

This interactive session will include both didactic and hands-on case review at workstations equipped with *syngo*. MR Brevis. A practical approach to breast MRI interpretation will be discussed as well as utilizing the available sequences and techniques to improve interpretive skills. *RSVP is required; adding this session to your agenda does not secure your seat in this session. Click the link below to RSVP.*

RSVP

https://www.fairorg.de/Siemens-Healthineers/portal/workshop.cfm/rsna19/

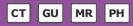




SPPH22

Physics Symposium: Highlights of AAPM Clinical Brachytherapy Physics Summer School

Monday, Dec. 2 1:30PM - 5:45PM Room: S503AB



AMA PRA Category 1 Credits ™: 4.25 ARRT Category A+ Credits: 5.00

FDA Discussions may include off-label uses.

LEARNING OBJECTIVES

1) Explain the role of model-based dose calculation algorithms and their affects for several anatomic site. 2) provide an in-depth understanding on the application of brachytherapy for prostate, gynecological, breast, and skin diseases. 3) Clarify emerging technologies such as electronic brachytherapy, clinical modalities, and intensity-modulated brachytherapy.

ABSTRACT

The Symposium will cover the highlights from the 2017 AAPM Summer School on Clinical Brachytherapy Physics. Presentations by the School Program Directors will include the experiences from experts on eight key aspects of clinical brachytherapy physics: model-based dose calculations, prostate brachytherapy, gynecological brachytherapy, skin brachytherapy, breast brachytherapy, electronic brachytherapy, intensity modulated and anisotropic brachytherapy sources, and early clinical advancements in 3D printing, tracking technologies, and robotic brachytherapy.

Sub-Events

SPPH22A Overview of Commercial Algorithms: Needs and Availability

Participants

Luc Beaulieu, PhD, Quebec, QC (*Presenter*) License agreement, Standard Imaging, Inc; Researcher, Elekta AB; Researcher, Koninklijke Philips NV;

LEARNING OBJECTIVES

1) Understand the need for advanced dose calculation algorithms in brachytherapy. 2) Provide an overview of the basis of the underlying algorithms used in brachytherapy commercial treatment planning systems. 3) Know the key strength and limitations of each algorithm.

ABSTRACT

Brachytherapy is a very efficient cancer treatment modality, essentially due to a best in class dose deposition kernel dominated by 1/r2 spearing tissue at a distance from the source. Furthermore, the energy deposition from the ionizing photons emitted by brachytherapy sources can be calculated, in theory, with very high accuracy. Until recently, the field of brachytherapy relied on a factor-based approach, TG-43, to deal for dose calculation. While TG43 is extremely fast for dose computation and optimization, its accuracy is limited to specific conditions, often not met in clinical situations. This presentation will provide an overview of these different situations and provide ballpark estimates of the expected differences. We will further look at alternatives to solve this issue and briefly described the approaches chosen by the major vendors in providing the next generation of dose calculation engines in their treatment planning system offering. We will finally describe how these new algorithms performed under various scenarios, highlighting both their strength and weakness.

SPPH22B Emphasis on MBDCA Commissioning Infrastructure and Process

Participants

Luc Beaulieu, PhD, Quebec, QC (*Presenter*) License agreement, Standard Imaging, Inc; Researcher, Elekta AB; Researcher, Koninklijke Philips NV;

LEARNING OBJECTIVES

1) Review the commissioning requirements set forth in TG186. 2) Provide an overview of the existing infrastructure and resources available to the clinical medical physicists. 3) Understand the various steps necessary in the commissioning of model-based dose calculation algorithms.

ABSTRACT

With the publication in 2012 of the AAPM/ESTRO/ABG TG-186 report, early adopters were provided with a set of guidelines to help in the integration of advanced dose calculation algorithms in brachytherapy, beyond TG43, and ensuring safe and efficient use of the new features that are enabled by these new algorithms. However, the commissioning aspects were minimal in that report. In the following, the work from a subsequent working group, established to tackle this issue, will be presented. It is intended to provide the clinical users (the clinical medical physicists) with a set of comprehensive commissioning guidelines as well as to provide the necessary information for resources that are available to the community in making the transition from TG43 to TG186.

SPPH22C Prostate Brachytherapy: Real-time Intra-operative

Participants

Luc Beaulieu, PhD, Quebec, QC (*Presenter*) License agreement, Standard Imaging, Inc; Researcher, Elekta AB; Researcher, Koninklijke Philips NV;

LEARNING OBJECTIVES

1) Underline the system components of a real-time prostate brachytherapy program. 2) Understand the possible workflows of realtime ultrasounds based prostate brachytherapy. 3) Understand the difference between real-time LDR and HDR prostate brachytherapy workflows.

ABSTRACT

Prostate brachytherapy is a highly effective treatment option for localized prostate cancer. For low-risk prostate cancer patients, LDR seed implants has proven its long-term efficacy. For intermediate risk and high risk localized prostate cancer, both LDR and HDR brachytherapy boost combined to EBRT (either 3D-CRT or IMRT/VMAT) are providing compelling clinical outcomes. Both approaches deliver very high local dose to the cancerous regions while providing enhanced dose spearing to the organs at risk. The move to real-time intra-operative prostate brachytherapy further enables simplified treatment options to patients, in many cases performed as a single day outpatient procedure while improving the overall treatment accuracy by limiting the uncertainties due to moving the patients from the OR to imaging to finally the treatment room. This presentation will look at the key components of an efficient real-time intra-operative as well as the associated workflows.

SPPH22D Prostate Brachytherapy: Post-implant Evaluation Using CT or MR

Participants

Mark J. Rivard, PhD, Providence, RI (Presenter) Nothing to Disclose

LEARNING OBJECTIVES

1) Learn the importance of post-implant dosimetric analysis. 2) To convey how to evaluate prostate brachytherapy implants using CT or MRI. 3) Be able to utilize modern techniques for post-implant evaluation of prostate brachytherapy implants.

SPPH22E Gynecological Brachytherapy: MRI Guidance and Targeting

Participants

Bruce R. Thomadsen, PhD, Madison, WI (Presenter) Nothing to Disclose

LEARNING OBJECTIVES

1) To understand the rationale for MR targeting in gynecological brachytherapy. 2) To become familiar with techniques and difficulties in MR targeting.

ABSTRACT

Cervical brachytherapy has changed greatly over the last few years. The conventional techniques that served well for the last six decades provided many cures; however, failures still plagued the higher staged disease. The challenges to improving outcomes rested with two issues: 1. Visualizing, localizing and assessing the disease, and 2. Adequately treating the disease once it is demarcated. This presentation will address the first of the challenges, imaging and targeting the disease.

Active Handout:Bruce Robert Thomadsen

http://abstract.rsna.org/uploads/2019/19001779/Active SPPH22E.pdf

SPPH22F Gynecological Brachytherapy: Applicators

Participants

Bruce R. Thomadsen, PhD, Madison, WI (Presenter) Nothing to Disclose

LEARNING OBJECTIVES

1) To understand the evolution of brachytherapy applicators for treatment of cervical cancer. 2) To become familiar with the latest generations of cervical brachytherapy applicators.

ABSTRACT

This presentation continues addressing the challenges for cervical brachytherapy, looking at recent developments in applicator design to facilitate treating the target tissues.

SPPH22G Gynecological Brachytherapy: Comparisons with Conventional

Participants

Bruce R. Thomadsen, PhD, Madison, WI (Presenter) Nothing to Disclose

LEARNING OBJECTIVES

1) To understand the differences in dosimetry between the conventional approach and the MR-guided approach to cervical brachytherapy. 2) To appreciate the benefits to patients of the newer approach.

ABSTRACT

This presentation completes the discussion of cervical brachytherapy by comparison of the newer approaches with the conventional treatments, reviewing the dosimetry and outcomes.

SPPH22H Skin Brachytherapy

Participants

Mark J. Rivard, PhD, Providence, RI (Presenter) Nothing to Disclose

LEARNING OBJECTIVES

1) Develop a sense for the physics concerns surrounding skin brachytherapy. 2) Convey how to dosimetrically evaluate skin brachytherapy treatment plans. 3) Learn several methods for delivering skin brachytherapy.

SPPH22I Breast Brachytherapy: Applications and Applicators

Participants

Bruce R. Thomadsen, PhD, Madison, WI (Presenter) Nothing to Disclose

LEARNING OBJECTIVES

1) To understand the geometry, dosimetry and nature of applicators used in breast brachytherapy.

ABSTRACT

Breast brachytherapy has been shown to be a highly effective treatment with very low toxicity. Many types of applicators have been developed to perform the procedure, each with strength and limitations. This presentation will discuss the various applicators and how they apply to applications.

Active Handout:Bruce Robert Thomadsen

http://abstract.rsna.org/uploads/2019/19001784/09-10 Breast Brachytherapy2019 RSNA.pptx

SPPH22J Breast Brachytherapy: Plan Evaluation

Participants

Bruce R. Thomadsen, PhD, Madison, WI (Presenter) Nothing to Disclose

LEARNING OBJECTIVES

1) To understand what should be checked during a treatment plan review for breast brachytherapy. 2) To understand the quantities used in performing the reviews.

ABSTRACT

Review of a treatment plan serves to help improve quality and prevent errors in treatment. Plan evaluations are crucial for breast brachytherapy. This presentation will discuss the techniques used, and quantities evaluated during a treatment plan review.

SPPH22K Electronic Brachytherapy

Participants Mark J. Rivard, PhD, Providence, RI (*Presenter*) Nothing to Disclose

LEARNING OBJECTIVES

1) Understand the radiological physics differences between electronic brachytherapy and radionuclide-based brachytherapy. 2) Describe several different systems, contrasting and comparing them. 3) Learn how electronic brachytherapy is used clinically.

SPPH22L Intensity Modulated and Anisotropic BT Sources

Participants

Mark J. Rivard, PhD, Providence, RI (Presenter) Nothing to Disclose

LEARNING OBJECTIVES

1) Comprehend the designs and goals for intensity modulated and anisotropic brachytherapy sources. 2) Explain how intensity modulated and anisotropic brachytherapy sources can provide improved dose distributions over conventional brachytherapy sources. 3) Learn how to evaluate and commission intensity modulated and anisotropic brachytherapy sources.

SPPH22M 3D Printing and Tracking Technologies

Participants

Luc Beaulieu, PhD, Quebec, QC (*Presenter*) License agreement, Standard Imaging, Inc; Researcher, Elekta AB; Researcher, Koninklijke Philips NV;

LEARNING OBJECTIVES

1) Understand the potential role of 3D printing in brachytherapy. 2) Have an overview of various tracking technologies that can be integrated into catheters, needles and applicators. 3) Discuss envisioned usage in the brachytherapy clinical workflow.

ABSTRACT

This portion of the AAPM summer school was dedicated to an outlook of the use of novel technologies tot her field of brachytherapy. First, brachytherapy relies heavily on applicators in which one or more sources can travel. As such, custom-made applicators derived from patient-specific 3D imaging or any other relevant information constitute a potential use of 3D printing technology. Second, to proceed with an optimal treatment the location in space of one or more applicators as well as the full 3D path (called channels in brachytherapy) the source will be traveling needs to be known with precision. Tacking technology can simplify the acquisition and validation of this information, thus simplifying the overall clinical workflow. This presentation will look at the various technologies involved with both the steps described above and how they could impact the current clinical workflows. Prerequisites for clinical use will also be discussed.

SPPH22N Robotics and Brachytherapy

Participants Bruce R. Thomadsen, PhD, Madison, WI (*Presenter*) Nothing to Disclose

LEARNING OBJECTIVES

1) To understand some of the principles of robotics in brachytherapy. 2) To learn about some of the robots, their designs and limitations.

ABSTRACT

As with much of medicine, and life in general, automation is improving consistency and ability. Robots have become part of the surgical landscape and are found in most large pharmacies. Robots are just coming into brachytherapy but promise to improve dose distributions and access to procedures. This presentation will review the current, dynamic sate of robotic brachytherapy.

Active Handout:Bruce Robert Thomadsen

http://abstract.rsna.org/uploads/2019/19001789/Active SPPH22N.pdf

Active Handout:Bruce Robert Thomadsen

http://abstract.rsna.org/uploads/2019/19001789/Active SPPH22N.pdf



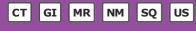




SPSP21

Contrastes y Trazadores: Estado del Art-Sesion del Colegio Interamaricano de Radiologia (CIR) en Espanol/Contrast Agents and Radiopharmaceuticals: State of the Art-Session of Interamerican College of Radiology (CIR) in Spanish

Monday, Dec. 2 1:30PM - 3:30PM Room: E353C



AMA PRA Category 1 Credits ™: 2.00 ARRT Category A+ Credits: 2.25

FDA Discussions may include off-label uses.

Participants

Jose L. Criales, MD, Huixquilucan, Mexico (*Moderator*) Nothing to Disclose Jorge A. Soto, MD, Boston, MA (*Moderator*) Royalties, Reed Elsevier

For information about this presentation, contact:

jorge.soto@bmc.org

jcriales@att.net.mx

LEARNING OBJECTIVES

 Conocer el uso actual, ventajas y desventajas de los medios de contraste en diferentes modalidades y en diversas situaciones clinicas.
 Conocer los diversos trazadores, ademas de FDG, analizando su metabolismo normal y las indicaciones mas frecuentes.
 Understand the current indications, benefits and limitations of the use of contrast agents for various imaging modalities.
 Review the various types of radiotracers available today for PET Imaging, along with their normal metabolism and common indications for their use.

Sub-Events

SPSP21A Bienvenida/Welcome

Participants Jose L. Criales, MD, Huixquilucan, Mexico (*Presenter*) Nothing to Disclose Jorge A. Soto, MD, Boston, MA (*Presenter*) Royalties, Reed Elsevier

For information about this presentation, contact:

jorge.soto@bmc.org

SPSP21B Aplicaciones de Contraste en Ultrasonido/Use of Contrast Agents in Ultrasonography

Participants Alison C. Harris, MBChB, Vancouver, BC (*Presenter*) Nothing to Disclose

LEARNING OBJECTIVES

1) Review the general principles and technique of using CEUS in the abdomen. 2) Discuss the role of CEUS in the diagnosis and characterization of masses in the liver and kidney. 3) Briefly discuss other applications of CEUS including guiding interventional procedures and monitoring of therapy.

ABSTRACT

Contrast-enhanced ultrasound (CEUS) continues to gain traction as a technique that complements traditional B-mode and Doppler ultrasound in the evaluation of the liver and other organs. Because the micro-vasculature can be visualized with CEUS and real-time imaging of tissue perfusion can be performed, imaging with this technique yields supplementary information, including flow and perfusion kinetics. The contrast agent used in CEUS is comprised of microbubbles, which are injected into a peripheral vein. The microbubble composition varies depending on the agent used, but the agent typically consists of an inert gas encased by a stabilizing shell composed of phospholipid, galactose, or albumin. The microbubbles circulate in the bloodstream and oscillate irregularly at low mechanical index settings within the acoustic field, creating nonlinear reflections that resonate at diagnostic ultrasound frequencies (3-5 MHz) and increase the signal produced. Proper technique and optimization of contrast-enhanced ultrasound require a balance between maintaining the integrity of the microbubble contrast agent and preserving the ultrasound signal. Established and emerging applications in the liver include diagnosis and characterization of focal lesions, aiding ultrasound-guided intervention, monitoring of therapy, and aiding surgical management.Read More:

https://www.ajronline.org/doi/10.2214/AJR.17.17843Read More: https://www.ajronline.org/doi/10.2214/AJR.17.17843Read More: https://www.ajronline.org/doi/10.2214/AJR.17.17843

SPSP21C Uso de Agentes Organoespecificos en RM de Higado/Use of Organ-specific Agents in MR of the Liver

Participants Claudio Bonini, MD, Rosario, Argentina (*Presenter*) Speaker, Bayer AG

For information about this presentation, contact:

LEARNING OBJECTIVES

1) Medios de contraste hepatoespecíficos por MR. 2) Estructura molecular y su interacción a nivel celular. 3) Indicaciones actuales. 4) Ventajas y desventajas en comparación con los contrastes convencionales. 5) Contraindicaciones / 1) Hepatospecific contrast by MR. 2) Molecular structure and interaction at the cellular level. 3) Current indications. 4) Advantages and disadvantages compared to conventional contrasts. 5) Contraindications.

SPSP21D PET-CT: Radiotrazadores Mas Alla de FDG/PET-CT: Beyond FDG

Participants

Belen Rivera Bravo, MD, Mexico City, Mexico (Presenter) Nothing to Disclose

For information about this presentation, contact:

brivera@unam.mx

LEARNING OBJECTIVES

1) Identify PET/CT radiopharmaceuticals other than FDG, used in clinical practice. 2) Describe the uptake mechanism of each radiopharmaceutical. 3) Differentiate the normal biodistribution of each radiopharmaceutical by reading the images of the study. 4) Recognize the clinical indication of each radiopharmaceutical based in the uptake mechanism. / 1) Al final de esta actividad, los participantes deberán ser capaces de. 2) Identificar radiofármacos de PET/CT diferentes al FDG utilizados en la práctica clínica. 3) Describir el mecanismo de concentración de cada radiofármaco. 4) Diferenciar la biodistribución habitual de cada radiofármaco al observar las imágenes del estudio. 5) Reconocer la indicación clínica de cada radiofármaco basado en su mecanismo concentración.

SPSP21E Preguntas/Q&A

SPSP21F Presentacion del CIR/CIR Update

Participants

Henrique Carrete Jr, MD, Sao Paulo, Brazil (Presenter) Nothing to Disclose

LEARNING OBJECTIVES

1) Present the Inter-American College of Radiology and its main educational activities. 2) Address the activities of the CIR throughout the year 2019. 3) Outline future directions of CIR.

SPSP21G Contraste Oral en TC: Nunca, Siempre O Algunas Veces?/Oral Contrast for Abdominal CT: Never, Always or Sometimes?

Participants

Antonio Jose B. Madureira, MD, Porto, Portugal (Presenter) Nothing to Disclose

LEARNING OBJECTIVES

1) To understand the rationale for the use of oral contrast agents in CT examinations.2) To become familiar with the major indications of oral contrast use.3) To discuss the benefits and drawbacks of their use.

ABSTRACT

There has been a gradual decline in the last years in the use of oral contrast agents in CT examinations. In spite of these there are some clinical scenarios in which their use is of great benefit as it can clearly establish a diagnosis. In the emergency setting and in patients suspected of high-grade bowel obstruction their use is not warranted and may even be contraindicated. Oral contrast agents administration still has a role in CT imaging and every radiologist should be familiar with their indications and benefits in specific clinical situations.

SPSP21H Daño Renal Agudo por Contraste Iodado: Conceptos Actuales/Iodine Contrast Induced Acute Kidney Injury: Current Concepts

Participants Cristian Varela, MD, Santiago, Chile (*Presenter*) Nothing to Disclose

For information about this presentation, contact:

cvarelaubilla@gmail.com

LEARNING OBJECTIVES

1) Revisar la definición actual de daño renal agudo inducido por medio de contraste iodado/Review the current definition of contrast induced acute renal injury. 2) Conocer las características de los pacientes en riesgo/To know the characteristics of the high risk patients. 3) Definir las medidas de prevención basadas en la evidencia que el radiologo debe conocer y practicar/Define the evidence based prevention that the radiology need to know and apply.

SPSP211 Retencion de Gadolinio/Gadolinium Retention

Participants

Juan E. Gutierrez, MD, Medellin, Colombia (Presenter) Speakers Bureau, Bayer AG

For information about this presentation, contact:

juanes65@gmail.com

LEARNING OBJECTIVES

1) Define the classification of GBCAs based on molecular structure and other physicochemical properties. 2) Discuss current

literature regarding deposition of gadolinium in the brain (Clinical - Pre Clinical). 3) Describe the relationship between the type of contrast agents and gadolinium deposition in brain Describe FDA, ACR, and European Medicines Agency (EMA) guidelines for GBCA usage.

ABSTRACT

Gadolinium Based Contrast Agents (GCBA) had been part of MRI environment for three decades with great benefits on the development of imaging as well as helping radiologists to achieve a better knowledge of the human body and its diseases. So far more than 500 million injections of GCBA's have been applied Worldwide, initially and for many years GBBA's were believed to be a harmless solution, to the point of being used as contrast for DSA and also in double or triple dose for MRI, however, in 2006 evidence of Gadolinium retention in tissues was published proving its link with Nefrogenic Systemic Fibrosis (NSF) in renal impaired patients. This situation triggered multiple academic and regulatory evaluations, involving the pharma industry to define the risk benefit of using GBCA's depending on its safety profile, plus new warning regulations and classification for this agents issued by the FDA, EMA and ACR. New evidence of Gadolinium deposition in the brain, specifically locate at Dentate Nucleus and Globus Pallidus, after multiple GCBA's injections in patients with normal kidney function was recently published (2014), and gives again new evidence of the potential harmful effect of Gadolinium in tissues. This situation brought a new regulatory environment with different approach by the FDA and EMA, as well as a new challenge for the MRI practice worldwide.

SPSP21J Preguntas/Q&A

SPSP21K Clausura/Closing

Participants Jose L. Criales, MD, Huixquilucan, Mexico (*Presenter*) Nothing to Disclose Jorge A. Soto, MD, Boston, MA (*Presenter*) Royalties, Reed Elsevier

For information about this presentation, contact:

jorge.soto@bmc.org





CS24

Advances in MR & CT Imaging: Emphasis on Artificial Intelligence: Presented by the Institute for Advanced Medical Education (IAME), educational grant provided by Canon Medical Systems USA, Inc.

Monday, Dec. 2 2:00PM - 3:00PM Room: S101AB

Participants

Garry E. Gold, MD, Stanford, CA (Presenter) Research support, General Electric Company

Mathias Prokop, PhD, Nijmegen, Netherlands (*Presenter*) Speakers Bureau, Bracco Group Speakers Bureau, Bayer AG Research Grant, Canon Medical Systems Corporation Speakers Bureau, Canon Medical Systems Corporation Research Grant, Siemens AG Speakers Bureau, Siemens AG Departmental spinoff, Thirona Departmental licence agreement, Varian Medical Systems, Inc

PROGRAM INFORMATION

MR and CT imaging are advancing at a rapid rate with new scanner and software technology finding its way into advanced imaging systems each year. Artificial Intelligence (AI) is playing a major role in this expansion. In this one-hour CME accredited symposium, Dr. Gold and Dr. Prokop will provide insight into how they are using new AI tools in their everyday practice and explain how these new tools are providing better patient care and throughput.

СМЕ

Yes, CME credit is available through a third-party provider. Information on claiming credits will be provided at the end of the symposium.

RSVP Link

https://www.appliedradiology.org/RSNA1/default.aspx





SPAI23

RSNA AI Deep Learning Lab: Generative Adversarial Networks (GANs)

Monday, Dec. 2 3:00PM - 4:30PM Room: AI Showcase, North Building, Level 2, Booth 10342



AMA PRA Category 1 Credits ™: 1.50 ARRT Category A+ Credit: 1.75

Participants

Bradley J. Erickson, MD, PhD, Rochester, MN (*Presenter*) Board of Directors and Stockholder, VoiceIt Technologies, LLC; Board of Directors, FlowSigma, LLC; Officer, FlowSigma, LLC; Stockholder, FlowSigma, LLC;

Special Information

In order to get the best experience for this session, it is highly recommended that attendees bring a laptop with a keyboard, a decent-sized screen, and the latest version of Google Chrome. Additionally, it is recommended that attendees have a basic knowledge of deep learning programming and some experience running a Google CoLab notebook. Having a Gmail account is also helpful. Here are instructions for creating and deleting a Gmail account.

ABSTRACT

This course describes a more recent advance in deep learning known as Generative Adversarial Networks (GANs). GANs are a deep learning technology in which a computer is trained to create images that look very 'real' even though they are completely synthetic. Getting 'large enough' data sets is a problem for most deep learning applications, and this is particularly true in medical imaging. This may be one way to address the 'data shortage' problem in medicine. GANs have also been created that can convert MRIs to CTs (e.g. for attenuation correction with MR/PET).





SSE03

Science Session with Keynote: Cardiac (Congenital and Pediatric Imaging)

Monday, Dec. 2 3:00PM - 4:00PM Room: E350



AMA PRA Category 1 Credit ™: 1.00 ARRT Category A+ Credit: 1.00

FDA Discussions may include off-label uses.

Participants

Gautham P. Reddy, MD, Seattle, WA (*Moderator*) Researcher, Koninklijke Philips NV Jean Jeudy JR, MD, Baltimore, MD (*Moderator*) Nothing to Disclose Cylen Javidan, MD, Saint Louis, MO (*Moderator*) Nothing to Disclose

Sub-Events

SSE03-01 Cardiac Keynote Speaker: MRI Evaluation of Function and Physiology in Congenital Heart Disease

Monday, Dec. 2 3:00PM - 3:20PM Room: E350

Participants Gautham P. Reddy, MD, Seattle, WA (*Presenter*) Researcher, Koninklijke Philips NV

SSE03-03 Dual-Venc 4D-Flow MRI For the Follow-Up of Patients with Complex Congenital Heart Disease

Monday, Dec. 2 3:20PM - 3:30PM Room: E350

Participants

Arshid Azarine, MD, MSc, Paris, France (*Presenter*) Advisory Board, Arterys Inc Quentin Alias, Paris, France (*Abstract Co-Author*) Nothing to Disclose Arnaud Fournier, Paris, France (*Abstract Co-Author*) Nothing to Disclose Veronique Marteau-Marty, MD, Paris, France (*Abstract Co-Author*) Nothing to Disclose Charles Roux, Paris, France (*Abstract Co-Author*) Nothing to Disclose Adrien Frison-Roche I, CMD, Clamart, France (*Abstract Co-Author*) Nothing to Disclose Nadia Canepa, Paris, France (*Abstract Co-Author*) Nothing to Disclose Daniel Sidi, Paris, France (*Abstract Co-Author*) Nothing to Disclose Marc Zins, MD, Paris Cedex 14, France (*Abstract Co-Author*) Nothing to Disclose

For information about this presentation, contact:

aazarine@hpsj.fr

PURPOSE

To test the feasibility of dual-velocity encoding (dual-venc) 4D-flow MRI accelerated by katARC for the follow-up of patients with complex congenital heart disease (CHD), to improve dynamic velocity range of 4D-flow MRI and reduce velocity to noise ratio for low velocities measurements.

METHOD AND MATERIALS

A dual-venc 4D flow MRI sequence accelerated by k- & adaptive-t-ARC, assessed vena cava, pulmonary and aortic flows in 10 young adults followed-up after surgery for various complex CHD. Routine cardiac MRI was performed on a 3T magnet followed by a dual-venc 4D-flow MRI sequence (High-Venc/low-venc were set at 300/100cm/s, temporal/spatial resolution=40-45msec/2×2×2.2mm3) after the injection of gadolinium contrast agent (0.15 mmol/kg). The dataset was anonymized and sent on a cloud-based software. After deep learning based phase offsets correction, both high- and low-venc data were analysed separatly and simultaneously for the feasibility and for assessing arterial and venous hemodynamics (flows) at the great vessels. All patients were informed and signed a consent to test dual-venc 4D flow sequence.

RESULTS

All dual-venc 4D flow MRI scans were acquired successfully with an acquisition time of 12±3 minutes. Dual-venc sequence acquisition time was 1.5 times longer than a single venc sequence, the total acquisition time was reduced by 25% compared to two separate scans. Cloud based data analysis enabled 'real-time' simultaneous analysis of both low-venc and high-venc volumes. Concerning vena cavas velocity measurements, Bland-Altman plot showed good agreement within the 95% limits between high- and low- Venc datasets, noise was noted 25% lower on low-venc vs high-venc dataset. Aliasing occurred on most arterial measurements using low-venc volume.

CONCLUSION

Dual-venc 4D flow MRI used for the follow up of patients with complex CHD reliably incorporates low- and high-velocity fields simultaneously, within a reasonable scan time.

CLINICAL RELEVANCE/APPLICATION

Recently, 4-D flow MRI has shown to bring relevant findings in the follow-up of patients with complex CHD. In these patients,

arterial high velocities and venous lower velocities have to be reliably explored but with always a compromise for the choice of the velocity range to explore. Dual-venc sequences enable a new appraoch enabling reliable measurement of these low and high velocity flows within a reasonable scan time, faster than 2 consecutive single Venc 4D flow sequence.

SSE03-04 Rapid Reconstruction of Highly-Accelerated Real-Time Phase Contrast MRI Using Deep Convolutional Network: A Feasibility Study in Patients with Congenital Heart Disease

Monday, Dec. 2 3:30PM - 3:40PM Room: E350

Participants

Hassan Haji-Valizadeh, Evanston, IL (*Presenter*) Nothing to Disclose Daming Shen, Evanston, IL (*Abstract Co-Author*) Nothing to Disclose Joshua D. Robinson, MD, Chicago, IL (*Abstract Co-Author*) Nothing to Disclose Cynthia K. Rigsby, MD, Chicago, IL (*Abstract Co-Author*) Nothing to Disclose Daniel Kim, PhD, Chicago, IL (*Abstract Co-Author*) Nothing to Disclose

For information about this presentation, contact:

hassanhaji-valizadeh2019@u.northwestern.edu

PURPOSE

Standard real-time phase-contrast (rt-PC) MRI produces inadequate spatial and temporal resolution, limiting pediatric applications. Compressed sensing (CS) can be used to highly accelerate real-time phase contrast (rt-PC) MRI for achieving high spatial (1.5x1.5x6mm3) and temporal (40ms) resolution. However, it is challenging to clinically translate CS approaches due to the lengthy image reconstruction time ($\sim 10 min$). We sought to apply a deep learning (DL) framework to rapidly reconstruct rt-PC images and evaluate its performance in patients with CHD.

METHOD AND MATERIALS

We scanned 14 CHD patients (mean age=14.2 \pm 7.1yr; 10 males) on a 1.5T scanner (Aera, Siemens) using our 38.4-fold accelerated, rt-PC sequence employing radial k-space sampling with golden angles. Image reconstruction was performed on a GPU workstation equipped with Pytorch. A convolutional neural network was trained with 9860 (29 valve planes x 85 timeframes per plane x 2 complex components x 2 velocity encodings) zero-filled and the corresponding CS reconstructed images obtained from 9 randomly selected patients as input/output pairs. For validation, we reconstructed 6460 zero-filled images from the remaining 5 patients using our trained network, and the resulting images representing a single heartbeat were compared with the corresponding CS reconstructed images. Our proposed DL network was composed of 10 hidden layers with 16 features each, two concatenation connections, and convolution kernel size of 1x1x3 (Figure 1A).

RESULTS

The reconstruction time for DL ($5.9\pm0.5s$) was significantly lower (p<0.05) than CS ($551.4\pm27.6s$). Figure 1B shows representative images reconstructed with CS and DL as well as their corresponding forward flow and peak velocity curves. Compared to CS, DL produced negligible error in valvular velocities (NRMSE = $4.8\pm1.9\%$). Flow and velocity curves produced by CS and DL reconstruction were strongly correlated (R2>0.94) with small mean differences (<5.9% of means, Figure 1C).

CONCLUSION

This study demonstrates a DL framework to significantly decrease the reconstruction time (93 times) compared with CS for 38.4-fold accelerated rt-PC MRI.

CLINICAL RELEVANCE/APPLICATION

Patients with CHD may benefit from a rapid rt-PC MRI pulse sequence which enables free-breathing imaging.

SSE03-05 Evaluation of Pulmonary Pressure After Glenn Shunts by CT-Based Machine Learning Model

Monday, Dec. 2 3:40PM - 3:50PM Room: E350

Participants

Yuhao Dong, Guangzhou, China (Presenter) Nothing to Disclose

PURPOSE

To develop and validate non-invasive machine-learning classifiers for the separation of post-Glenn shunt patients with mean pulmonary arterial pressure (mPAP) >15 mmHg from those <=15 mmHg based on preoperative cardiac computed tomography (CT).

METHOD AND MATERIALS

This retrospective study included 96 patients with functional single ventricle who had undergone a bidirectional Glenn procedure (BDG) between November 1, 2019 and July, 31, 2017. All underwent post-procedure CT examination, followed by cardiac catheterization within six months. In all, 23 morphologic parameters were manually extracted from cardiac CT images for each patient. The Mann-Whitney U test or Chi-square test was applied to select the predictors associated with the outcome of interest. Six machine-learning algorithms including logistic regression (LR), Naive Bayes (NB), Random Forest (RF), Linear Discriminant Analysis (LDA), Support Vector Machine (SVM), and K-Nearest Neighbor (KNN) were used for modeling. The algorithms were independently trained on the 100 train-validation random splits with a 3:1 ratio. The average performance of algorithms were evaluated by area under ROC curve (AUC), accuracy, sensitivity, and specificity.

RESULTS

Seven CT morphologic parameters were selected for modeling. RF method obtained the best predictive performance compared with other methods, with mean AUC of 0.840 (confidence interval [CI]: 0.832-0.850), 0.787 (95%CI: 0.780-0.794) ; sensitivity of 0.815 (95%CI: 0.797-0.833), 0.778 (95%CI: 0.767-0.788), specificity of 0.766 (95%CI: 0.748-0.785), 0.746 (95%CI: 0.735-0.757), accuracy of 0.782 (95%CI: 0.771-0.793), 0.756 (95%CI: 0.748-0.764) in the training and validation cohorts, respectively.

CONCLUSION

The CI-based RF model demonstrates good performance in the classification of mPAP.

CLINICAL RELEVANCE/APPLICATION

The CT-based RF model may reduce the need for right heart catheterization in post-Glenn shunts patients with suspected mPAP >15 mmHg.

SSE03-06 Dynamic Fetal Cardiac Magnetic Resonance Imaging Using Doppler Ultrasound Gating in the Assessment of the Fetal Aortic Arch: A Feasibility Study and Comparison to Fetal Echocardiography

Monday, Dec. 2 3:50PM - 4:00PM Room: E350

Participants

Bjoern Schoennagel, MD, Hamburg, Germany (*Presenter*) Co-founder and Stakeholder, Northh-Medical GmbH Jin Yamamura, MD, Hamburg, Germany (*Abstract Co-Author*) Nothing to Disclose Fabian Kording, Hamburg, Germany (*Abstract Co-Author*) Co-founder and Stakeholder, Northh Medical GmbH Christian Ruprecht, Hamburg, Germany (*Abstract Co-Author*) Co-founder and Stakeholder, Northh Medical GmbH Kai Fehrs, Hamburg, Germany (*Abstract Co-Author*) Co-founder and Stakeholder, Northh Medical GmbH Kai Fehrs, Hamburg, Germany (*Abstract Co-Author*) Co-founder and Stakeholder, Northh Medical Gerhard B. Adam, MD, Hamburg, Germany (*Abstract Co-Author*) Nothing to Disclose Manuela Tavares de Sousa, Hamburg, Germany (*Abstract Co-Author*) Co-founder and Stakeholder, Northh Medical GmbH

PURPOSE

To investigate the feasibility of dynamic fetal cardiac MRI using a newly developed MR compatible Doppler Ultrasound (DUS) device for fetal cardiac gating for evaluation of the fetal aortic arch in comparison to fetal echocardiography.

METHOD AND MATERIALS

This was a prospective study including 19 fetuses, with 17 of them having a normal aortic arch and two a suspicion of coarctation of the aorta (CoA) at initial fetal echocardiography. Median fetal age was 33 weeks (range 26-38). Dynamic fetal cardiac MRI was performed using a newly developed DUS device for direct fetal cardiac gating at a 1.5 T scanner. The aortic arch was evaluated in para-sagittal planes using a cine steady state free precision (SSFP) sequence. The visualization of the aortic arch and left subclavian artery was studied. MR image quality was assessed by two observers using a 4-point grading scale (increasing image quality from 1-4). Postnatal fetal echocardiography was considered as the standard of reference.

RESULTS

Direct fetal cardiac gating using the DUS device allowed continuous gating of the fetal heart beat. In four cases the DUS device had to be repositioned during examination due to fetal movement. Examination of one fetus was not possible due to severe fetal movement and loss of the cardiac gating signal. Both, fetal cardiac MRI and echocardiography detected the CoA and enabled visualization of the aortic arch in 16/18 cases (89%). Overall MR image quality according to the 4-point scale grading was high with no or only few artifacts and a resulting mean value of 3.1 (\pm 1.1). Agreement in overall image quality between the two observers was good (kappa = 0.75 \pm 0.13).

CONCLUSION

This study shows that dynamic fetal cardiac MRI using the newly developed DUS device for direct cardiac gating allows reliable evaluation of the fetal aortic arch and in agreement to fetal echocardiography.

CLINICAL RELEVANCE/APPLICATION

Dynamic fetal cardiac MRI may be useful in addition to fetal echocardiography for the evaluation of CoA, especially in cases where echocardiography is inconclusive.





SSE15

Musculoskeletal (Accelerated Imaging)

Monday, Dec. 2 3:00PM - 4:00PM Room: N228



AMA PRA Category 1 Credit ™: 1.00 ARRT Category A+ Credit: 1.00

FDA Discussions may include off-label uses.

Participants

Christian W. Pfirrmann, MD, MBA, Forch, Switzerland (*Moderator*) Nothing to Disclose Naveen Subhas, MD, Shaker Heights, OH (*Moderator*) Research support, Siemens AG

Sub-Events

SSE15-01 Acceleration in Knee MRI: Compressed Sensing for 2D and 3D Applications

Monday, Dec. 2 3:00PM - 3:10PM Room: N228

Participants

Grischa Bratke, MD, Cologne, Germany (*Presenter*) Nothing to Disclose Stefan Haneder, MD, Cologne, Germany (*Abstract Co-Author*) Nothing to Disclose Robert Rau, Cologne, Germany (*Abstract Co-Author*) Nothing to Disclose Nuran Abdullayev, MD, Cologne, Germany (*Abstract Co-Author*) Nothing to Disclose Lisa Brueggemann, Bergisch-Gladbach, Germany (*Abstract Co-Author*) Nothing to Disclose David C. Maintz, MD, Koln, Germany (*Abstract Co-Author*) Nothing to Disclose Kilian Weiss, PhD, Hamburg, Germany (*Abstract Co-Author*) Employee, Koninklijke Philips NV

For information about this presentation, contact:

grischa.bratke@uk-koeln.de

PURPOSE

Compressed sensing (CS) allows to accelerate 2D and 3D scans promising higher acceleration factors than previous parallel imaging techniques. This study evaluated potential clinical acceleration factors of SENSE and Compressed SENSE (combination of Compressed Sensing and SENSE) for a fat saturated 2D sagittal and 3D PD sequence in the knee.

METHOD AND MATERIALS

Twenty-one healthy volunteers were scanned with a 3T scanner (Ingenia, Philips, Best, Netherland). All received a standard, commercially available sagittal, fat saturated 2D PD (SENSE 1.4) and three CS (CS2, CS3, CS5) and the time-equivalent SENSE accelerations. The 3D sequence (SENSE 2.0) was acquired with four CS (CS6, CS8, CS10 and CS15) and the equivalent SENSE factors. The images were rated by three independent readers (two radiologists and one orthopedic surgeon) with at least 5 years of experience in MRI imaging regarding diagnostic certainty and overall image impression on a 5-Point-Likert-scale. The non-parametric subjective scoring was analyzed with the Friedmann test for statistical significance and the Dunn's test for post-hoc analysis.

RESULTS

The standard sequences lasted for 221 seconds (2D) and 384 s (3D). The scan time decreased with increasing CS factor (2D CS2: 145 s, 2D CS3: 95 s, 2D CS5: 57 s, 3D CS6: 293 s, 3D CS8: 220 s, 3D CS10: 176 s, 3D CS15: 119 s). The 2D standard sequence was rated best for diagnostic certainty and overall image impression with an average of 4.95 ± 0.21 and 4.78 ± 0.42 , statistical superior in both parameters for all sequences (all p<0.05) except for 2D CS2, 2D S2 and 3D standard. The 3D standard performed only better than 3D CS15 rearding the 3D CS sequences but better than all 3D SENSE accelerations except for the lowest (SENSE 2.2). The post-hoc analysis showed only significant differences for the fast 3D accelerations of CS10 vs. S2.9 (p<0.0001) and CS15 vs. S3.5 (p=0.0002).

CONCLUSION

Compressed Sensing can significantly decrease (34% for 2D and 54% for 3D) the scan time for PD sequences of a knee MRI with unchanged diagnostic certainty and overall image impression compared to the clinical reference. The new technique proved especially valuable for fast 3D accelerations.

CLINICAL RELEVANCE/APPLICATION

The application of Compressed Sensing can increase the patient compliance and can reduce healthcare cost for MR imaging due to significant decreased scan times.

SSE15-02 Next-Generation 5-Min Knee MRI with Combined Simultaneous Multislice and Parallel Imaging Acceleration: Ready for Prime Time?

Monday, Dec. 2 3:10PM - 3:20PM Room: N228

Filippo del Grande, MD, Lugano, Switzerland (*Presenter*) Speaker, Siemens AG; Speaker, Bayer AG; Institutional research collaboration and reference center, Siemens AG;

Ali Rashidi, Baltimore, MD (Abstract Co-Author) Nothing to Disclose

Miho Tanaka, Baltimore, MD (Abstract Co-Author) Nothing to Disclose

Jan Fritz, MD, Baltimore, MD (*Abstract Co-Author*) Institutional research support, Siemens AG; Institutional research support, Johnson & Johnson; Institutional research support, Zimmer Biomet Holdings, Inc; Institutional research support, Microsoft Corporation; Institutional research support, BTG International Ltd; Scientific Advisor, Siemens AG; Scientific Advisor, General Electric Company; Scientific Advisor, BTG International Ltd; Speaker, Siemens AG; Patent agreement, Siemens AG

PURPOSE

2-fold parallel imaging (PI) acceleration can realize 5-min 2D FSE MRI of the knee, but the associated signal loss may require compromises in image quality and anatomical coverage. In contrast, 2-fold simultaneous multi-slice (SMS) acceleration is near signal neutral. Advances in pulse sequence design now allow for the combined use of PI and SMS to enable 4-fold-accelerated 2D FSE, which can achieve fast MRI with higher image quality and improved coverage. We compared traditional 2-fold PI- and novel 4-fold SMS-PI-accelerated 2D FSE MRI of the knee for the detection of internal derangement.

METHOD AND MATERIALS

Following IRB approval and informed consent, 25 symptomatic patients [12 women, 13 men; age 44 (18-64) years] prospectively underwent 1.5T MRI of the knee, including a 2-fold PI-accelerated 5-min 2D FSE MRI protocol, and a 4-fold SMS-PI-accelerated 5min 2D FSE MRI protocol with higher spatial resolution, higher anatomic coverage, smaller inter-slicer gaps, improved suppression of vascular flow artifacts, and stronger and more homogenous fat suppression. Both protocols included sagittal PD, sagittal PDFS, coronal T1, coronal T2FS, axial PDFS sequences. Two MSK radiologists independently assessed image contrast, noise, artifacts, structural visibility, and abnormalities. Non-parametric comparison, kappa agreement, and interchangeability tests were applied.

RESULTS

The inter-reader reliability (kappa=0.681) was good. 5-min SMS-PI MRI of the knee had better image contrast (p<0.001), less noise, (p<0.001), better structural visibility (p<0.001), and no flow or aliasing artifacts (p=0.657). There was unidirectional interchangeability in favor of SMS-PI MRI for the diagnosis of meniscal tears and cartilage defects, and bidirectional interchangeability for anterior cruciate and collateral ligament tears, tendon tears, bone marrow edema pattern, and fractures.

CONCLUSION

Combined, 4-fold-accelerated SMS-PI 2D FSE enables artifact-free 5-min MRI of the knee with higher image quality, better visibility of anatomic structures, and possibly better detectability of cartilage defects and meniscal tears than 2-fold PI-accelerated 5-min 2D FSE MRI of the knee.

CLINICAL RELEVANCE/APPLICATION

The validation of short knee MRI protocols without image degradation are essential to increase MR efficiency in clinical practice.

SSE15-03 Comparison of Modulated Flip Angle in Refocused Imaging with Extended Echo Trains with Compressed Sensing (CS-MATRIX) and Conventional Two-Dimensional Sequences on Knee Imaging

Monday, Dec. 2 3:20PM - 3:30PM Room: N228

Participants

Zhanhao Mo, Changchun, China (*Presenter*) Nothing to Disclose Lin Liu, Changchun, China (*Abstract Co-Author*) Nothing to Disclose Zhongwen Lv, Chang Chun, China (*Abstract Co-Author*) Nothing to Disclose He Sui, MD, MD, Changchun, China (*Abstract Co-Author*) Nothing to Disclose Yongming Dai, Shanghai, China (*Abstract Co-Author*) Nothing to Disclose Xuanyi Zhou, Shanghai, China (*Abstract Co-Author*) Nothing to Disclose

PURPOSE

To evaluate and compare the image quality and diagnostic agreement of an isotropic 3D fast spin echo (FSE) sequence, which employs modulated flip angle technique in refocused imaging with extended echo trains with compressed sensing (CS-MATRIX), to conventional 2D sequences for knee at 3T.

METHOD AND MATERIALS

Forty-four knees from 42 symptomatic patients (mean age: 43.5±14.9 years) were examined on a 3T MR scanner (uMR780, United Imaging Healthcare, Shanghai, China) with 2D T2-weighted fat suppressed (T2-fs) sequence, proton density-weighted (PD) sequence and isotropic 3D CS-MATRIX sequence. A four-point scale (4=Excellent, 3=Good, 2=Acceptable, 1=Poor; based on clarity of anatomical structures, noise and artifacts) was employed to assess image quality subjectively, then the scores of 2D and 3D CS-MATRIX sequences were compared utilizing Wilcoxon signed-rank test. Furthermore, Kappa statistics were used to evaluate diagnostic agreement between 2D and 3D CS-MATRIX sequences for detecting multiple types of knee joint pathologies.

RESULTS

For image quality, no significant difference in scoring was found between 3D CS-MATRIX T2-fs and 2D T2-fs sequences (mean score= 3.29 ± 0.63 and 3.34 ± 0.68 , p=0.715), however, the scores of images obtained from 2D PD was significantly higher than those of 3D CS-MATRIX PD sequence (mean score= 3.84 ± 0.37 and 3.57 ± 0.50 , p<0.05). In diagnostic agreement evaluation, there was a very good agreement between 3D CS-MATRIX and 2D sequences for detecting cartilage lesions (κ =1.000), and bone marrow edemas (κ =0.955). Moreover, the diagnostic agreement was good to very good in grading evaluation of medial and lateral menisci tears (κ =0.748, κ =0.936), as well as of anterior and posterior cruciate ligaments tears (κ =0.725, κ =1.000).

CONCLUSION

The 3D CS-MATRIX sequences allow for faster knee imaging over conventional 2D sequences, while yielding much the same image quality as 2D T2-fs sequences. In addition, 3D CS-MATRIX sequences could present similar diagnostic value in evaluating lesions in cartilage, bone marrow, menisci and cruciate ligaments as 2D sequences.

CLINICAL RELEVANCE/APPLICATION

3D CS-MATRIX sequence has become a non-invasive technique for evaluating knee joint lesions, while providing higher timeefficiency than 2D sequences in magnetic resonance imaging.

SSE15-04 Highly Accelerated 2D Spine Imaging Using Compressed Sensing: Evaluation of Scan Time and Subjective Image Quality

Monday, Dec. 2 3:30PM - 3:40PM Room: N228

Participants Grischa Bratke, MD, Cologne, Germany (*Presenter*) Nothing to Disclose Christoph Kabbasch, Cologne, Germany (*Abstract Co-Author*) Nothing to Disclose Robert Rau, Cologne, Germany (*Abstract Co-Author*) Nothing to Disclose Stefan Haneder, MD, Cologne, Germany (*Abstract Co-Author*) Nothing to Disclose David C. Maintz, MD, Koln, Germany (*Abstract Co-Author*) Nothing to Disclose Kilian Weiss, PhD, Hamburg, Germany (*Abstract Co-Author*) Employee, Koninklijke Philips NV

For information about this presentation, contact:

grischa.bratke@uk-koeln.de

PURPOSE

Imaging of the spine, with 2D as the clinical standard, is the most common examination for MRI and it 's duration has a large impact on the clinical scan schedule and healthcare costs. Due to susceptibility to field inhomogeneities and motion artifacts of the bowel and aorta acceleration techniques remain challenging for sagittal sequences, resulting in comparable low net acceleration factors. The new acceleration technique Compressed Sensing promises higher acceleration factors. In this study Compressed SENSE (combination of Compressed Sensing and SENSE) was evaluated for accelerated sagittal T2 imaging of the lumbar spine using gradient echo (GE) and turbo spin echo (TSE) based prescans.

METHOD AND MATERIALS

All scans were performed on a 3T scanner (Ingenia, Philips, Best, Netherland). Sixteen patients received the standard spine protocol including a sagittal T2 sequence (SENSE factor 1.4, 266 seconds) and three different CS acceleration factors (CS2: 172s, CS3: 109s and CS4: 78s). An additional TSE prescan (35s) was acquired to compare the reconstructions based on the common GE and the TSE prescan. The images were rated by two independent readers (experts in musculoskeletal and neuroradioloyg) regarding diagnostic certainty and overall image impression on a 5-Point-Likert-scale. The non-parametric subjective scoring was analyzed with the Friedmann test for statistical significance and the Dunn's test for post-hoc analysis.

RESULTS

The diagnostic certainty (4.75±0.41) and overall image impression (4,63±0.50) were rated highest for the CS2 with a TSE prescan (TSE CS2) although not with a statistically significant difference to the standard T2 (4.72±0.41 and 4.56±0.51). The standard T2 showed significant better overall image impression compared to the CS3 (p<0.0001) and CS4 (p<0.0001) accelerations with GE prescan while none of the TSE prescan sequences or the CS2 with GE prescan was significant worse.

CONCLUSION

The combination of the standard T2 with the GE prescan (266s) offered unchanged diagnostic certainty and overall image impression than CS2 with the GE prescan (172s) or CS4 with the TSE prescan (112s).

CLINICAL RELEVANCE/APPLICATION

Compressed Sense with the GE prescan (-35%) and especially with a TSE prescan (-58%) drastically reduces the scan time for the sagittal T2 sequence with unchanged subjective scoring. Similar reductions for additional sagittal scans (T1, T2 fat saturated) within the protocol should feasible.

SSE15-05 Compressed Sensing-Sensitivity Encoding (CS-SENSE) Accelerated MR Brachial Plexus Imaging: Reduced Scan Time without Reduced Image Quality

Monday, Dec. 2 3:40PM - 3:50PM Room: N228

Participants

Xiangchuang Kong, Wuhan, China (*Presenter*) Nothing to Disclose Tianjing Zhang, MS, Guangzhou , China (*Abstract Co-Author*) Nothing to Disclose Zhuang Nie, Wuhan , China (*Abstract Co-Author*) Nothing to Disclose Wenliang Fan, BMedSc,PhD, Wuhan, China (*Abstract Co-Author*) Nothing to Disclose Qing Fu, MS,MS, Wuhan , China (*Abstract Co-Author*) Nothing to Disclose

For information about this presentation, contact:

hongke80@163.com

PURPOSE

3D Contrast-enhanced nerve-view Imaging provides has very high clinical value for brachial plexus nerve trauma,tumor etc. However, relatively long acquisition time(above 10min)limits its clinical application. The aim of this study was to reduce the scan time of 3D Nerve-view using Compressed Sensing-Sensitivity Encoding (CS), and evaluate the image quality and capability of diagnosis of accelerated 3D Nerve-view sequences.

METHOD AND MATERIALS

In a consecutive cohort of 15 patients with suspected disease of brachial plexus underwent MR studies. 3D Nerve-view sequences with 6 different CS accelerating factors (4,6,8,10,15,20), and a traditional 3D Nerve-view with 2-fold parallel imaging (sense) as a clinical reference were obtained on a 3T scanner (Ingenia CX, Best, Philips Healthcare). Images were graded by 2 experienced radiologists in MR neurography for image quality (scale of 1 to 5). An Objective quantification analysis of SNR and CNR were also

performed. Beyond that, the similarity between images of the 3D standard sequence and the accelerated sequences was evaluated using the pixelwise root mean square error (RMSE) and structural similarity index (SSIM). The scan time of each sequence were measured. An analysis of variance with repeated measurements and the Friedman test was used to test for potential difference between the sequences.

RESULTS

The mean values of the RMSE ranged from 73.38 \pm 15.91 for CS 8 to 234.66 \pm 43.56 for CS 10, while SSIM was highest for CS 4 with 95.11% \pm 2.23% and lowest for CS 20 with 87.90% \pm 5.32%. The scan time using sense2,CS2,4,6,8,10,15,20 is 11min09s,5min50s,3min55s,2min56s,2min23s,1min35s,1min13s respectively. The two radiologists evaluated all images and mean scored 4.1 \pm 0.3 with CS factor below 8. There is no statistical difference in the contrast between the brachial plexus and the surrounding tissue between CS factor 4-8, and the lesion display of the brachial plexus has no statistical difference. The images of CS factor above 8 have no diagnosis value.

CONCLUSION

In conclusion, CS-3D Nerve-view with factor 8 offer equilibrium between comparable clinical diagnostic quality with less scan time (2min56s)

CLINICAL RELEVANCE/APPLICATION

CS-3D Nerve-view with factor 8 offer equilibrium between comparable clinical diagnostic quality with less scan time , which potentially increasing the productivity of MR scanners.

SSE15-06 Compressed Sensing SEMAC MRI of Hip and Knee Arthroplasty Implants at 1.5T and 3T Field Strengths: An Intra-Subject Comparison Study

Monday, Dec. 2 3:50PM - 4:00PM Room: N228

Participants

Iman Khodarahmi, MD, PhD, New York, NY (Presenter) Nothing to Disclose

John A. Carrino, MD, MPH, New York, NY (*Abstract Co-Author*) Research Consultant, Pfizer Inc; Research Consultant, Image Analysis Group (IAG); Research Consultant, Image Biopsy Lab; Research Consultant, Simplify Medical; ; ; ; Jan Fritz, MD, Baltimore, MD (*Abstract Co-Author*) Institutional research support, Siemens AG; Institutional research support, Johnson & Johnson; Institutional research support, Zimmer Biomet Holdings, Inc; Institutional research support, Microsoft Corporation; Institutional research support, BTG International Ltd; Scientific Advisor, Siemens AG; Scientific Advisor, General Electric Company; Scientific Advisor, BTG International Ltd; Speaker, Siemens AG; Patent agreement, Siemens AG

For information about this presentation, contact:

iman.khodarahmi@nyumc.org

PURPOSE

Metal artifact reduction MRI of metallic arthroplasty implants at 1.5T field strength has inherently lower susceptibility artifacts than at 3T field strength. However, 3T MRI offers higher signal-to-noise and contrast-to-noise ratios, and allows for higher spatial resolution. In this study, we tested the hypothesis that compressed-sensing (CS) accelerated slice-encoding-for-metal-artifactcorrection (SEMAC) MRI of hip and knee arthroplasty implants can generate similar image quality and visibility of periprosthetic abnormalities at 1.5 and 3T field strengths.

METHOD AND MATERIALS

Thirty patients with symptomatic hip (15) and knee (15) arthroplasty implants were included in this IRB-approved study after giving informed written consent. Each patient underwent consecutive 1.5 and 3T MRI using previously optimized protocols consisting of PD-weighted and STIR CS-SEMAC turbo spin echo pulse sequences in coronal (hip) or sagittal (knee) planes. The 3T protocols utilized 25 SEMAC encoding steps while the 1.5 T protocols used 19 SEMAC encoding steps. The 3T protocols had higher spatial resolution. Each pulse sequence took 4-5 min. Paired PD-weighted and STIR image datasets were separated, anonymized and randomly reassigned. Two musculoskeletal radiologists qualitatively evaluated image quality and the presence of six periprosthetic abnormalities independently. Wilcoxon test, Kendall W agreement, and substitutability testing were applied.

RESULTS

Image quality of hip and knee studies were over all good with slight non-significant (hip, p=0.21 / knee, p=0.33) dominance of 1.5T over 3T. Reader agreements were moderate to very good (W range, 0.53-0.81). Inter-method agreement was overall good (W, 0.67/0.71). For each joint, substitution analysis demonstrated that the higher resolution but slightly longer 3T CS-SEMAC could replace the lower spatial resolution, but faster 1.5T CS-SEMAC technique (p-value range, 0.41-0.94) in diagnosing the six abnormalities, including periprosthetic osteolysis, synovitis, bone marrow edema, fractures, tendon tears, and extra-capsular collections.

CONCLUSION

With the use of optimized pulse sequence parameters, 3T CS-SEMAC can generate high-resolution MR images with similar degrees of metal artifact reduction and detection of periprosthetic abnormalities compared to 1.5T CS-SEMAC.

CLINICAL RELEVANCE/APPLICATION

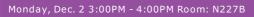
3T CS-SEMAC has the potential to generate high-resolution MR images without diagnostic compromise.





SSE16

Musculoskeletal (Arthritis and Cartilage)





AMA PRA Category 1 Credit ™: 1.00 ARRT Category A+ Credit: 1.00

Participants

Andrew J. Grainger, MD, Leeds, United Kingdom (*Moderator*) Consultant, Levicept Ltd; Director, The LivingCare Group; Kambiz Motamedi, MD, Los Angeles, CA (*Moderator*) Nothing to Disclose

Sub-Events

SSE16-01 Spondyloarthropathy: Improved Sensitivity by Combining UTE with Conventional MRI

Monday, Dec. 2 3:00PM - 3:10PM Room: N227B

Participants

Yeong Sang Hong, Gwangju, Korea, Republic Of (*Presenter*) Nothing to Disclose Eun Hae Park, MD, Jeonju-si, Korea, Republic Of (*Abstract Co-Author*) Nothing to Disclose Donghun Kim, Kwangju, Korea, Republic Of (*Abstract Co-Author*) Nothing to Disclose Young Kwang Lee, MD, Jeonju, Korea, Republic Of (*Abstract Co-Author*) Nothing to Disclose Gong Yong Jin, MD, PhD, Jeonju, Korea, Republic Of (*Abstract Co-Author*) Nothing to Disclose Jin Hee You, MD, Jeonju, Korea, Republic Of (*Abstract Co-Author*) Nothing to Disclose Donghan Shin, Jeonju-si , Korea, Republic Of (*Abstract Co-Author*) Nothing to Disclose

For information about this presentation, contact:

h01096308827@gmail.com

PURPOSE

To evaluate whether the combination of ultrashort TE (UTE) sequences and conventional magnetic resonance imaging (MRI) helps to increase diagnostic performance in the diagnosis of spondyloarthropathy compared with those achieved by using each MRI technique alone.

METHOD AND MATERIALS

The study included 22 sacroiliac joint (SIJ) MRI from 11 spondyloarthropathy (SpA) patients and 52 SIJ MRI from 27 patients without SpA. Three sets of images (UTE only, conventional MR only, combined UTE and conventional MRI) were analyzed independently by 3 reviewers (2 musculoskeletal radiologists, 1 unexperienced radiologist) to diagnose SpA based on bone marrow edema (BME), erosion, sclerosis, and ankyloses. For SpA patients, patient grouping was subdivided to those with BME and those without BME. Diagnostic accuracy, sensitivity, specificity, and positive and negative predictive values were calculated. In those 16 patients with CT, the Pearson correlation test was performed.

RESULTS

The overall sensitivity was significantly higher for the combined set (92.3%) in the group without BME than those for the conventional MRI-only (89.5%) or UTE-only (81.7%) sets (P<0.05). However, in the group with BME, the UTE-only set showed lower sensitivity (83.8%) compared with the combined (93.3%) and conventional MRI (93.4%) sets (P=0.62). All reviewers did not show a significant difference in specificity for the 3 sets in both groups. The Pearson coefficient of correlation between erosion in UTE and erosion in CT was 0.71 (p<0.001).

CONCLUSION

UTE provides CT-like images, allowing good depiction of erosion; a combination set of UTE and conventional MRI showed better sensitivity in the diagnosis of SpA, especially in those without BME.

CLINICAL RELEVANCE/APPLICATION

Recently, BME of the SIJ are reported to be nonspecific findings in SIJ MRI, leaving osseous erosion to be important finding. With UTE providing CT-like imaging, this will help detect early erosion, resulting better diagnosis of SpA.

SSE16-02 Are Undifferentiated Arthritis and Pre-Rheumatoid Arthritis Associated with the Longitudinal MRI Features of Knee Osteoarthritis Structural Damage?

Monday, Dec. 2 3:10PM - 3:20PM Room: N227B

Participants

Arya Haj-Mirzaian, MD, MPH, Baltimore, MD (Presenter) Nothing to Disclose

Bahram Mohajer, Tehran, Iran (Abstract Co-Author) Nothing to Disclose

Ali Guermazi, MD,PhD, Boston, MA (*Abstract Co-Author*) Shareholder, Boston Imaging Core Lab, LLC; Research Consultant, Merck KGaA; Research Consultant, Roche, Inc; Research Consultant, TissueGene, Inc; Research Consultant, Galapagos, Inc; Research Consultant, AstraZeneca PLC; Research Consultant, Pfizer Inc

Frank W. Roemer, MD, Erlangen, Germany (Abstract Co-Author) Officer, Boston Imaging Core Lab, LLC; Research Director, Boston

Imaging Core Lab, LLC; Shareholder, Boston Imaging Core Lab, LLC Shadpour Demehri, MD, Baltimore, MD (*Abstract Co-Author*) Research support, General Electric Company; Research Grant, Carestream Health, Inc; Consultant, Toshiba Corporation

For information about this presentation, contact:

sdemehr1@jhmi.edu

PURPOSE

Shared inflammatory pathophysiology of osteoarthritis (OA) and inflammatory joint diseases such as Rheumatoid Arthritis (RA) have been suggested previously. Undifferentiated arthritis (UA) and Pre-RA are considered as early stage inflammatory arthropathy before the diagnosis of RA based on clinical criteria; However, UA may persist without ultimate progression to RA. We aimed to investigate the association between knee OA structural damage worsening and clinically defined UA/Pre-RA using 3T-MRI measurements.

METHOD AND MATERIALS

This was an IRB-approved and HIPAA-compliant study of 600 subjects from the FNIH project. At the baseline visit, subjects with physician-diagnosed RA were excluded. Participants with any signs of arthritis, but not diagnosed RA, were assessed by connective tissue disease RA screening questionnaire and knee radiography. After exclusions of possible RA subjects (using questionnaire/radiography), the remaining were regarded as UA. Any of the UA-(control) or UA+ subjects who have developed RA in follow-up visits were categorized as Pre-RA. Baseline and 24-month semi-quantitative MRI OA Knee Score (MOAKS) measures of study groups were extracted and analyzed. Logistic regression model, adjusted for age, sex, BMI, and smoking status was used to assess the association between UA/pre-RA and baseline/worsening of MRI-based OA-related structural damages including cartilage thickness/surface scores, Hoffa-synovitis, and effusion-synovitis.

RESULTS

Presence of UA was associated with nearly significant structural damage in cartilage surface/thickness scores of whole knee (OR (95%CI): 1.73(0.94-3.1) and 1.73(1.0-3.04)), especially in patellofemoral joint (OR: 2.05(1.16-3.62) and 1.76(0.99-3.07)). In longitudinal assessment, presence of UA was significantly associated with 24-month worsening of lateral tibiofemoral cartilage damage (OR: 2.46(1.1-5.07). Pre-RA was not significantly related to cartilage damage after adjustments. There was also no association between UA/pre-RA and knee Hoffa-synovitis/effusion-synovitis.

CONCLUSION

Positive history of UA is associated with the concurrent knee joint cartilage defects at baseline, and its worsening over 24-months.

CLINICAL RELEVANCE/APPLICATION

Knee OA characteristic cartilage defects are probable in UA subjects despite absence of knee effusion/synovitis. This finding warrant further investigations for altered OA outcomes in subjects with UA but not definitive RA diagnosis.

SSE16-03 Diagnostic Performance of Texture Analysis for Differentiation of Inflammation versus Degeneration in the Sacroiliac Joints

Monday, Dec. 2 3:20PM - 3:30PM Room: N227B

Participants

Felix Kepp, Zurich, Switzerland (*Abstract Co-Author*) Nothing to Disclose Florian A. Huber, Zurich, Switzerland (*Presenter*) Nothing to Disclose Urs J. Muhlematter, MD, Zurich, Switzerland (*Abstract Co-Author*) Nothing to Disclose Moritz Wurnig, Zurich, Switzerland (*Abstract Co-Author*) Nothing to Disclose Malwina Kaniewska, MD, Baden, Switzerland (*Abstract Co-Author*) Nothing to Disclose Filippo del Grande, MD, Lugano , Switzerland (*Abstract Co-Author*) Speaker, Siemens AG; Speaker, Bayer AG; Institutional research collaboration and reference center, Siemens AG; Roman Guggenberger, Zurich, Switzerland (*Abstract Co-Author*) Nothing to Disclose

For information about this presentation, contact:

florian.huber@usz.ch

PURPOSE

to investigate the performance of texture analysis (TA) for differentiation of inflammation from degeneration in sacroiliac joints (SIJ).

METHOD AND MATERIALS

MR images of SIJ from patients with clinically established ankylosing spondyloarthritis (AS), degenerative changes and healthy individuals (30 patients each) were analyzed retrospectively. Two residents blinded to each other rated typical structural and inflammatory changes on a four-point Likert scale and categorized patients into different groups, using paracoronal sets of TIRM, T1w and T1w fat-sat contrast enhanced (T1wCE) images. Additionally, same-sized regions of interest were placed into pathologic (where applicable) or random healthy spots of SIJ. TA was performed with opensource software (MaZda). Logistic regression with ten-fold cross validation was applied to detect relations with clinical labels. Standard statistical testing was applied for interreader agreements (IA) and regarding distribution of qualitative and TA findings among the clinical categories.

RESULTS

Moderate IA was present for categorization into different groups (k=.40). Qualitative ratings showed weak to moderate IA, but cumulative qualitative scores differed significantly among patient categories (p<.001). TA showed perfect IA (k>.80) for 203, 194 and 210 features in TIRM, T1w & T1wCE, respectively. TA outperformed qualitative evaluation for differentiation between AS vs. non-AS (AUC=.89 vs. .75 for TA vs. qualitative) and between AS vs. degeneration (AUC=.91 vs. .66). MR sets showed different impact on TA based differentiation of AS vs. non-AS with AUCs of .74, .76 and .81 for TIRM, T1w and T1wCE.

CONCLUSION

TA improves accuracy in differentiation of AS from degeneration in the SIJ. Its performance is predominantly determined by T1wCE images.

CLINICAL RELEVANCE/APPLICATION

Determining the aetiology of chronic and acute changes in the sacroiliac joints is an everlasting difficulty in clinical and radiological routine. This work presents a quantitative approach that may help in valid identification of patients with axial spondylarthritis from the remainders, which would imply an impact on further patient management and conservative treatment.

SSE16-04 Quantitative MR Blood Perfusion Patterns of Infrapatellar Fat Pad T2 Hyperintense Lesions on Unenhanced MR in Patients with and without Knee Osteoarthritis

Monday, Dec. 2 3:30PM - 3:40PM Room: N227B

Participants

Bas A. de Vries, MSc, Rotterdam, Netherlands (*Abstract Co-Author*) Nothing to Disclose Rianne A. van der Heijden, MD,PhD, Schiedam, Netherlands (*Presenter*) Nothing to Disclose Dirk Poot, PhD, Rotterdam, Netherlands (*Abstract Co-Author*) Nothing to Disclose Marienke van Middelkoop, Rotterdam, Netherlands (*Abstract Co-Author*) Nothing to Disclose Gabriel P. Krestin, MD, PhD, Rotterdam, Netherlands (*Abstract Co-Author*) Nothing to Disclose Edwin H. Oei, MD, PhD, Rotterdam, Netherlands (*Abstract Co-Author*) Research support, General Electric Company

For information about this presentation, contact:

r.a.vanderheijden@erasmusmc.nl

PURPOSE

Infrapatellar fat pad (IPFP) T2 hyperintense lesions on unenhanced MR are an important imaging feature of knee osteoarthritis (OA) and are thought to represent inflammation. These lesions are very common, though, also in non-OA subjects, and may not always be linked to inflammation. This leads to the hypothesis that IPFP lesions may have different pathophysiological subtypes. The aim of this study was to evaluate quantitative blood perfusion parameters within T2 hyperintense lesions in patients with knee OA, with patellofemoral pain (PFP) (supposed precursor of OA), and in control subjects.

METHOD AND MATERIALS

43 healthy controls, 35 patients with PFP and 22 patients with knee OA were included. All underwent MRI including T2-mapping and dynamic contrast enhanced (DCE)-MRI. Image registration was used to correct for motion. If present, hyperintense T2 lesions in the IPFP were delineated on T2 maps using Horos software (Horosproject.org, USA). A second region was drawn in an adjacent area without T2 signal intensity alteration. Quantitative perfusion parameters (Ktrans, Ve, Vp) were extracted by fitting the extended Tofts' pharmacokinetic model where Ktrans represents the inflow, Ve the extravascular extracellular space and Vp vascular fraction of the region. A paired Wilcoxon-signed-rank test was used to compare regions with and without T2 lesions within subjects for each subgroup.

RESULTS

IPFP T2 hyperintense lesions were present in 14 controls, 13 PFP patients and 16 knee OA patients. Perfusion parameters were not statistically significantly different between areas with and without a T2 lesion within controls and PFP patients. In knee OA patients, the lesions demonstrated statistically significantly higher values of Ktrans and Ve compared to an area without a lesion. Remarkably, all regions drawn in knee OA demonstrated higher perfusion parameters, including Vp, compared to the other groups.

CONCLUSION

IPFP T2 hyperintense lesions are non-specific. In contrast to morphologically similar lesions in PFP patients and controls in knee OA patients IPFP hyperintense lesions are associated with higher perfusion, suggesting inflammation and neo-angiogenesis.

CLINICAL RELEVANCE/APPLICATION

OA has a tremendous societal burden, but the pathophysiology remains unknown. Quantitative DCE-MRI can serve as a method to unravel certain aspects of the pathophysiology of OA.

SSE16-05 Radiographic Hand Osteoarthritis and Its Association with Worsening of MRI-Based Tibiofemoral Osteoarthritis-Related Structural Damage

Monday, Dec. 2 3:40PM - 3:50PM Room: N227B

Participants

Arya Haj-Mirzaian, MD,MPH, Baltimore, MD (*Presenter*) Nothing to Disclose Robert M. Kwee, Heerlen, Netherlands (*Abstract Co-Author*) Nothing to Disclose Farhad Pishgar, Tehran, Iran (*Abstract Co-Author*) Nothing to Disclose Ali Guermazi, MD,PhD, Boston, MA (*Abstract Co-Author*) Shareholder, Boston Imaging Core Lab, LLC; Research Consultant, Merck KGaA; Research Consultant, Roche, Inc; Research Consultant, TissueGene, Inc; Research Consultant, Galapagos, Inc; Research Consultant, AstraZeneca PLC; Research Consultant, Pfizer Inc Frank W. Roemer, MD, Erlangen, Germany (*Abstract Co-Author*) Officer, Boston Imaging Core Lab, LLC; Research Director, Boston Imaging Core Lab, LLC; Shareholder, Boston Imaging Core Lab, LLC Shadpour Demehri, MD, Baltimore, MD (*Abstract Co-Author*) Research support, General Electric Company: Research Grant.

Shadpour Demehri, MD, Baltimore, MD (*Abstract Co-Author*) Research support, General Electric Company; Research Grant, Carestream Health, Inc; Consultant, Toshiba Corporation

For information about this presentation, contact:

sdemehr1@jhmi.edu

PURPOSE

To determine whether the presence of hand osteoarthritis (OA) is associated with radiographic knee OA progression (over 48months) and MRI-based knee OA structural damage worsening (over 24-months).

METHOD AND MATERIALS

600 subjects from the Foundation for the National Institute of Health (FNIH) project which is an IRB approved HIPAA compliant study were included (one index knee and hand in each subject). Baseline hand radiography of all subjects was measured for the presence of hand OA (modified Kellgren and Lawrence (mKL) grade >2 in each hand joints). Baseline and follow-up knee radiographic measurements and MRI OA Knee Score (MOAKS) variables for cartilage damage, bone marrow lesions, osteophytes, effusion, and Hoffa-synovitis as well as MRI-based knee periarticular bone area measurements were extracted. The association between the presence of hand OA (presence vs. absence of hand OA in each hand joint) and 48-months radiographic knee OA progression (>0.7mm reduction in medial tibiofemoral joint space width) as well as 24-months change in knee MOAKS and periarticular bone measurements were analyzed using regression model (adjusted for age and sex).

RESULTS

Presence of any carpometacarpal (CMC) OA (OR 95%CI: 1.58(0.96-2.62)) and overall hand OA (prsence of any mKL>2 in all hand joints) (OR 95%CI: 1.44(0.97-2.07)) was associated with 48-month radiographic knee OA progression (approached but not reached significance). In comparison with controls, subjects with hand OA showed higher odds of worsening tibial/femoral cartilage damage (OR 95%CI: 1.38(0.95-2.01) and 1.79(1.24-2.58)) and femoral periarticular bone area expansion (Beta 95%CI: 10.54(1.40-19.69)) over 24-months. CMC OA and 24-months worsening of MRI-based tibiofemoral cartilage damage and periarticular bone area expansion were also showed approached significant associations.

CONCLUSION

Presence of hand OA, especially in CMC joint, is associated with longitudinal MRI-based knee OA-related structural damage worsening including tibial/femoral cartilage damage and periarticular bone area expansion.

CLINICAL RELEVANCE/APPLICATION

Hand OA (specifically CMC OA), as a marker of generalized OA, may be considered a predictor of more rapid progression of knee OA compared to patients without hand OA, which might be of relevance for inclusion in clinical trials of disease modifying OA drug development.

SSE16-06 Assessment of the Angular Dependence of Multicomponent Driven Equilibrium Single Pulse Observation of T1 and T2 (mcDESPOT) in Patellar Cartilage Samples

Monday, Dec. 2 3:50PM - 4:00PM Room: N227B

Participants

Mei Wu, MD, PhD, Guangzhou, China (*Abstract Co-Author*) Nothing to Disclose Hyungseok Jang, La Jolla, CA (*Abstract Co-Author*) Nothing to Disclose Akhil Kasibhatla, San Diego, CA (*Abstract Co-Author*) Nothing to Disclose Fang Liu, PhD, Madison, WI (*Abstract Co-Author*) Nothing to Disclose Saeed Jerban, PhD, San Diego, CA (*Presenter*) Nothing to Disclose Yajun Ma, San Diego, CA (*Abstract Co-Author*) Nothing to Disclose Eric Y. Chang, MD, San Diego, CA (*Abstract Co-Author*) Nothing to Disclose Richard Kijowski, MD, Verona, WI (*Abstract Co-Author*) Research support, General Electric Company; Consultant, Boston Imaging Core Lab, LLC

Jiang Du, PhD, San Diego, CA (Abstract Co-Author) Nothing to Disclose

For information about this presentation, contact:

may9@sina.com

PURPOSE

To evaluate the magic angle sensitivity of Multicomponent and Single-component parameters of Multicomponent Driven Equilibrium Single Pulse Observation of T1 and T2 (mcDESPOT) in imaging the cadaveric human patellar cartilage samples on a clinical 3T scanner.

METHOD AND MATERIALS

mcDESPOT was prospectively performed on 3 human patellar cartilage samples. Imaging parameters were: FOV=4cm, slice thickness=0.5mm, rBW=125kHz, SPGR TR/TE=11.6ms/3.1ms, IR-SPGR TR/TE=9ms/3.1ms, TI=450ms, SSFP TR/TE=12.2ms/6.1ms, SPGR FA=3,4,5,6,7,9,13,18°, SSFP FA=2,5,10,15,20,30,40,50°; IR-SPGR FA=5°, matrix=160×160×26, and total scan time=~21min. The imaging was performed three times, each with a different orientation (0°, 55°, and 90° relative to B0). Regional analysis (superficial/middle/deep layer and global) was applied. Single-component T1/T2 relaxation time (T1/T2 Single) and the corresponding T1/T2 proton density (T1/T2 PD), multicomponent T1/T2 relaxation times of the fast relaxing water component (T1s/T2s), and fraction of the fast relaxing water component (Ff) were measured, and their angular dependence were analyzed.

RESULTS

Figure 1 shows T1 single values which show the smallest magic angle effect with 5.1% decrease from 1644.5 ms at 0° to 1562.3 ms at 55°. Ff values show a decreased magic angle effect with 48.4% decrease from 15.5 % at 0° to 8.0% at 55°. T2f values show the largest magic angle effect with 200.0% increase from 9.5 ms at 0° to 27.3 ms at 55°. Different degrees of magic angle effect were also observed for T1s, T1f, T1PD, T2PD, T2s and T2 single with a decrease of 19.5%, 26.3%, and increased of 38.4%, 42.2%, 79.3%, 181.8% respectively, by rotating the cartilage samples from 0 to 55 degrees relative to the B0 field. The values of Ff decrease from the deep layer to the superficial layer for all angular orientations. T2f and Ff maps show increased T2f and decreased Ff in patellar cartilage by rotating the cartilage samples from 0 to 55 degrees relative to the B0 field, and the changes in T2f are more obvious than those in Ff.

CONCLUSION

T1, T1s, T1f, T1PD, T2PD, and Ff show much reduced magic angle effect as compared to T2, T2s and T2f. Ff provides reduced magic angle sensitivity in the evaluation of cartilages as compared to T2, T2s and T2f.

CLINICAL RELEVANCE/APPLICATION

Ff is less sensitive to the magic angle effect than T2, T2s and T2f, and may provide more accurate diagnosis for early OA. Printed on: 01/07/20







SSE18

Neuroradiology (Epilepsy/Metabolism/Infection)

Monday, Dec. 2 3:00PM - 4:00PM Room: S401CD



AMA PRA Category 1 Credit ™: 1.00 ARRT Category A+ Credit: 1.00

Participants

Diana M. Gomez-Hassan, MD, PhD, Ann Arbor, MI (*Moderator*) Nothing to Disclose Christopher T. Whitlow, MD, PhD, Winston-Salem, NC (*Moderator*) Nothing to Disclose

Sub-Events

SSE18-01 Functional Brain Connectivity in Periventricular Nodular Heterotopia

Monday, Dec. 2 3:00PM - 3:10PM Room: S401CD

Participants

Sidney Krystal, MD, Paris, France (*Presenter*) Nothing to Disclose Seokjun Hong, Montreal, QC (*Abstract Co-Author*) Nothing to Disclose Julien Savatovsky, MD, Saint Mande, France (*Abstract Co-Author*) Nothing to Disclose Neda Bernasconi, Montreal, QC (*Abstract Co-Author*) Nothing to Disclose Andrea Bernasconi, Montreal, QC (*Abstract Co-Author*) Nothing to Disclose

For information about this presentation, contact:

sidney-krystal@hotmail.fr

PURPOSE

Periventricular nodular heterotopia (PNH) consists of ectopic grey matter nodules accumulation, corresponding to small epileptogenic foci. Network analysis have been widely used to characterize brain network organization and changes in epileptic brains. Our objectives were to analyse network alterations in PNH.

METHOD AND MATERIALS

16 PNH patients and 32 healthy controls matched to age and gender underwent a resting-state functional 3T-MRI. We first assessed the relevance of heterotopic nodules' signal by computing the amplitudes of low-frequency fluctuations (ALFF). Then, we analysed the nodular-cortical connectivity with respect to cortico-cortical connectivity. We analysed the relationships between nodular connectivity and geodesic distance to nodule as well as resting-state networks. Finally, from cortico-cortical functional connectivity matrices, network features such as clustering coefficient (CC) and path length (PL) were computed and compared between PNH patients and controls, based on graph theory.

RESULTS

In heterotopic nodules, ALFF was significantly higher than in white matter: 0.30 vs 0.01 (p<0.001), and lower than in grey matter: 0.30 vs 0.54 (p<0.001). Functional connectivity between heterotopic nodules and grey matter was significantly lower with respect to cortico-cortical connectivity. Nodular-cortical connectivity was significantly anti-correlated to geodesic distance to nodule (p=0.01), and heterotopic nodules were mostly connected to the visual, the dorsal attention and the ventral attention networks. When comparing to controls, functional connectivity was significantly decreased in PNH patients (p=0.02), with a decreased smallworld organization: decrease in CC (p=0,03) and increase in PL (p=0,01).

CONCLUSION

We found for the first time whole-brain network changes in PNH, such as decrease in small-world organization, which could explain decrease in information processing speed encountered in those patients. We also analysed functional connectivity between heterotopic nodules and neocortex, that could explain the functional impact of nodules' surgical resection. Our results are consistent with studies in other focal seizures etiologies, and allow a better understanding of epileptogenicity in PNH.

CLINICAL RELEVANCE/APPLICATION

Resting-state functional MRI and graph theory are useful to explain epileptogenicity and should be more widely used to understand pathophysiological mechanisms in focal epilepsy.

SSE18-02 Cortical Thickness Changes in Newly Diagnosed MRI Negative Pediatric Generalized Epilepsy Patients

Monday, Dec. 2 3:10PM - 3:20PM Room: S401CD

Participants

Mohamed H. Elgendy, MD, Stony Brook, NY (*Presenter*) Nothing to Disclose David Ouellette, MS, Stony Brook, NY (*Abstract Co-Author*) Nothing to Disclose Emilio Garrido Sanabria, MD,PhD, Stony Brook, NY (*Abstract Co-Author*) Nothing to Disclose Lev Bangiyev, DO, Stony Brook, NY (*Abstract Co-Author*) Nothing to Disclose Tim Duong, PhD, Stony Brook, NY (*Abstract Co-Author*) Nothing to Disclose

For information about this presentation, contact:

mohamed.elgendy@stonybrookmedicine.edu

PURPOSE

Patients with generalized epilepsy undergo neuroanatomical changes along their disease course. Previous studies have shown cortical thickness changes in this disease population but with a longer disease duration. The goal of our study was to detect cortical thickness changes in newly-diagnosed pediatric generalized epilepsy patients.

METHOD AND MATERIALS

Generalized epilepsy patients (N=14) and controls (N=14) were studied. Our patient population included: 14 magnetic resonance (MR) negative patients diagnosed with generalized epilepsy and a mean duration of 1 year. The mean age was 16.5 years and the mean age of seizure onset was 15.5 years. EEG was collected and showed generalized pattern with clear background in most of our patient population. FreeSurfer was used to analyze cortical thickness in both patients and age-matched controls.

RESULTS

Pediatric generalized epilepsy patients showed decreased cortical thickness in both hemispheres in the anterior cingulate cortex and medial superior frontal regions.

CONCLUSION

Morphometric analysis in epileptic patients with negative MR showed thinner cortices in both hemispheres in the anterior cingulate cortex and medial superior frontal regions when compared to control group. To the best of our knowledge, this is the first study reporting that a decrease in cortical thickness decreases can be detected within about one year of seizure onset.

CLINICAL RELEVANCE/APPLICATION

Understanding the early changes in generalized epilepsy may prove useful in drug selection, improvement of clinical outcome and in the prediction of long-term cognitive impairments. The role of anterior cingulate cortex and medial superior frontal regions in the pathogenesis of generalized epilepsy or in resulting neurological disturbances remains to be investigated.

SSE18-03 Comparison of the Diagnostic Accuracy of FDG-PET/MR to that of FDG-PET/CT for Epileptogenic Zone Detection

Monday, Dec. 2 3:20PM - 3:30PM Room: S401CD

Participants

Kazufumi Kikuchi, MD,PhD, Fukuoka, Japan (*Presenter*) Nothing to Disclose Akio Hiwatashi, MD, Fukuoka, Japan (*Abstract Co-Author*) Nothing to Disclose Osamu Togao, MD, PhD, Fukuoka, Japan (*Abstract Co-Author*) Nothing to Disclose Daichi Momosaka, MD, Higashi-ku, Japan (*Abstract Co-Author*) Nothing to Disclose Tomohiro Nakayama, MD, PhD, Fukuoka, Japan (*Abstract Co-Author*) Nothing to Disclose Yoshiyuki Kitamura, Fukuoka, Japan (*Abstract Co-Author*) Nothing to Disclose Shingo Baba, Fukuoka, Japan (*Abstract Co-Author*) Nothing to Disclose

PURPOSE

To compare the diagnostic accuracy of FDG-PET/MR and that of FDG-PET/CT with respect to identifying epileptogenic zone (EZ) in patients with localization-related epilepsy

METHOD AND MATERIALS

This prospective study was approved by our institutional review boards, and written informed consent was obtained from each participant. Between November 2014 and April 2018, thirty-one patients (17 males, 14 females; 8-58 years; median 31 years) were evaluated. All patients were firstly scanned by FDG-PET/CT system for a diagnosis of localization-related epilepsy, then followed by FDG-PET/MR system immediately after. Two series of FDG-PET images acquired using PET/CT and PET/MR were interpreted independently by five board-certified radiologists. All readers were blinded to clinical data including the laterality of seizure as well as electroencephalogram. A Likert scale scoring system was used to assess image quality. The epileptogenic zone was histopathologically proven after surgery. Diagnostic sensitivities and Likert scale scores derived from both PET/MR and PET/CT were compared using the paired t-test. A P < 0.05 was considered significant.

RESULTS

Diagnostic sensitivity derived from PET/MR was higher than that from PET/CT ($83.2\pm5.3\%$ vs. $61.9\pm2.7\%$, P = 0.0006). Image quality score derived from PET/MR was higher than that from PET/CT (2.66 ± 1.45 vs. 1.66 ± 1.49 , P < 0.0001).

CONCLUSION

The diagnostic accuracy of FDG-PET/MR was superior to that of PET/CT for detection of EZ in patients with localization-related epilepsy.

CLINICAL RELEVANCE/APPLICATION

FDG-PET/MR provides the accurate information of epileptogenic zone, which improves outcome of patient with localization-related epilepsy.

SSE18-04 Metabolic Connectivity Can Help Predict Seizure Outcomes in Temporal Lobe Epilepsy Surgery

Monday, Dec. 2 3:30PM - 3:40PM Room: S401CD

Participants

Mohamed Tantawi, MBBCh, Philadelphia, PA (*Presenter*) Nothing to Disclose Mahdi Alizadeh, Philadelphia , PA (*Abstract Co-Author*) Nothing to Disclose Caio Matias, Philadelphia, PA (*Abstract Co-Author*) Nothing to Disclose Chengyuan Wu, Philadelphia, PA (Abstract Co-Author) Nothing to Disclose

PURPOSE

The understanding of epilepsy as a network disorder introduced the idea of using the brain connectome as a prognostic indicator. The objective of this study is to assess the potential of metabolic connectivity as a predictive factor of outcome in epilepsy surgery by examining preoperative metabolic connectivity in patients who underwent Laser interstitial Thermal Therapy (LITT) for medically resistant temporal lobe epilepsy (TLE).

METHOD AND MATERIALS

In this study, we collected positron emission tomography (PET) scans from 24 TLE patients who had unilateral mesial temporal sclerosis. At 1 year follow up after surgery 13 patients were seizure free (Engel class IA), but 11 patients had recurrent seizures and were classified as not seizure free (non-IA class). Initially, PET scans were preprocessed using SPM12. Next, connectivity matrices were constructed based on the correlation of interregional glucose metabolic values within subjects. Finally, graph theoretical analysis was performed using Brain Analysis using Graph Theory (BRAPH) software.

RESULTS

Metabolic network organization in the seizure free group differed substantially compared with the not seizure-free group. Compared with seizure free patients, the temporal pole and cingulate regions had higher connectivity with the surrounding areas in the not seizure free group, while multiple regions including cingulate, precentral gyri, postcentral gyri, and superior parietal gyrus were highly clustered with surrounding nodes indicating greater functional segregation.

CONCLUSION

Our study demonstrated a relationship between presurgical metabolic connectivity and post-surgical seizure outcome of the patients who had LITT surgery and the potential role as an imaging biomarker to predict surgical outcomes in this patient cohort. Extension of the disease to extratemporal networks, specifically the limbic network, plays a role in seizure recurrence after surgery. Although MTS typically involves sclerosis of the hippocampus, we can conclude that this pathology will involve other medial structures in the temporal lobes of the brain as well as neuronal connections projecting to other structures involving the limbic system, such as the temporal pole and cingulate.

CLINICAL RELEVANCE/APPLICATION

Combined with the current tests used in clinical practice, metabolic connectivity may be used as an additional prognostic/diagnostic factor during pre-surgical evaluation for refractory TLE patients.

SSE18-05 Resting-State Functional Network Topology Correlates with Surgical Outcome in Temporal Lobe Epilepsy

Monday, Dec. 2 3:40PM - 3:50PM Room: S401CD

Participants

Matthew N. Desalvo, MD, Boston , MA (*Abstract Co-Author*) Nothing to Disclose Linda Douw, Amsterdam, Netherlands (*Abstract Co-Author*) Nothing to Disclose Naoro Tanaka, MD, PhD, Boston, MA (*Abstract Co-Author*) Nothing to Disclose Andrew J. Cole, Boston, MA (*Abstract Co-Author*) Nothing to Disclose Steven M. Stufflebeam, MD, Charlestown, MA (*Presenter*) Nothing to Disclose

For information about this presentation, contact:

mndesalvo@partners.org

PURPOSE

To correlate resting-state functional network topology and surgical outcome in patients with medically refractory temporal lobe epilepsy (TLE).

METHOD AND MATERIALS

Data from forty patients with medically intractable temporal lobe epilepsy were retrospectively analyzed. All (40/40) patients underwent pre-operative resting-state functional magnetic resonance imaging (fMRI) and subsequent unilateral anterior temporal lobectomy. Postoperative seizure-free status was categorized using the Engel Epilepsy Surgery Outcome Scale. Resting-state functional connectivity networks were analyzed for each subject using a minimum spanning tree (MST) approach, and global and regional network properties were calculated and statistically compared between subjects who experienced complete postoperative seizure freedom (Engel IA) and all others (Engel IB-IV).

RESULTS

Global network properties related to network integration were statistically significantly (p<0.05) different between subjects who had Engel IA surgical outcomes and all others, with 9% decreased leaf fraction and 10% decreased tree hierarchy in subjects with ongoing seizures. The regional properties of a cluster of anatomic regions in the contralateral temporoinsular region were statistically significantly (p<0.05) different between subjects in these two groups. Specifically, the group-level leaf proportion was 59% decreased in the contralateral entorhinal cortex, 73% decreased in the contralateral inferior temporal gyrus, 43% decreased in the contralateral temporal pole, and 69% decreased in the contralateral insula in subjects with ongoing seizures.

CONCLUSION

Resting-state network topology correlates with surgical outcome in temporal lobe epilepsy, with decreased network integration globally and involving the contralateral temporoinsular region associated with ongoing postoperative seizures.

CLINICAL RELEVANCE/APPLICATION

Resting-state fMRI may be a useful non-invasive tool to determine whether patients being evaluated for resective epilepsy surgery are more likely to experience postoperative seizure freedom.

SSE18-06 Evaluation of Integrity of White Matter Fibers in Patients with Anti-NMDAR Encephalitis Based on Automated Fiber Quantification

Monday, Dec. 2 3:50PM - 4:00PM Room: S401CD

Participants Chun Zeng, Chongqing, China (*Presenter*) Nothing to Disclose Tianyou Luo, Chongqing, China (*Abstract Co-Author*) Nothing to Disclose Yongmei Li, MD, PhD, Chongqing, China (*Abstract Co-Author*) Nothing to Disclose Yayun Xiang, Chongqing, China (*Abstract Co-Author*) Nothing to Disclose

For information about this presentation, contact:

zengchun19840305@163.com

PURPOSE

To show the changes in integrity of white matters in patients with anti-NMDAR encephalitis based on automated fiber quantification (AFQ).

METHOD AND MATERIALS

Forty-eight patients with anti-NMDA receptor encephalitis diagnosed in our hospital and 40 matching gender, age and education level healthy controls were recruited in this study. All subjects underwent conventional head MRI, diffusion tensor imaging (DTI) scanning, mRS and mini-mental state examination (MMSE) scores. Fractional anisotropy (FA) and mean diffusivity (MD) quantitative analyses were conducted on 100 nodes of 20 white matter fibers in all subjects' brains using AFQ to compare whether there were statistical differences, and to analysis correlations between these two parameters and mRS and MMSE scores, respectively.

RESULTS

(1) Conventional MRI showed that lesions in bilateral corticospinal tracts (CST) and hippocampi in one patients and in left frontal cortex in another patients. (2) Diffuse increase of FA values and reduction of MD values were measured on the bilateral CST, cingulum cingulate, cingulum hippocampus, and arcuat, showing significantly statistical differences from the healthy controls (P < 0.01). Diffusion indexes of the other fibers showed segmental changes, and there was no statistical difference between the two groups (P > 0.05). (3) FA values of the bilateral CST, cingulum cingulate, cingulum hippocampus, and arcuat engatively correlated with mRS score (r = -0.81, -0.77, -0.86, -0.85, respectively; P < 0.01), and positively correlated with MMSE score (r = 0.90, 0.83, 0.92, 0.89, respectively; P < 0.01). MD values of the bilateral CST, cingulum cingulate, cingulum cingulate, cingulum hippocampus, and arcuatand were positively correlated with mRS score (r = 0.84, 0.77, 0.88, 0.77, 0.88, 0.77, respectively; P < 0.01), and negatively correlated with MMSE score (r = -0.92, -0.86, -0.92, -0.89, respectively; P < 0.01).

CONCLUSION

In patients with anti-NMDA receptor encephalitis, extensive microstructural damage is found in the fiberes dominated by CST, cingulum cingulate, cingulum hippocampus, and arcuat, which is closely related to the mRS scores and MMSE scores of patients and is helpful for the diagnosis of occult lesions and explanation of the clinical symptoms.

CLINICAL RELEVANCE/APPLICATION

(Dealing with AFQ and white matter) "Automated fiber quantification can demonstrated white matter changes and this exam is recommended when the underlying cause of such a lesion is unclear"





SSE20

Neuroradiology (Structural Imaging)

Monday, Dec. 2 3:00PM - 4:00PM Room: S504CD



AMA PRA Category 1 Credit ™: 1.00 ARRT Category A+ Credit: 1.00

FDA Discussions may include off-label uses.

Participants

James M. Provenzale, MD, Durham, NC (*Moderator*) Research Grant, Bayer AG; Research funded, sanofi-aventis Group; ; Elizabeth Tong, MD, Stanford, CA (*Moderator*) Nothing to Disclose

Sub-Events

SSE20-01 Substantial Dose Reduction for Sinus CT with Maintenance of High Resolution: A Prospective Clinical Reader Study Utilizing Photon-Counting-Detector CT Substantial Dose Reduction for Sinus CT with Maintenance of High Resolution: A Prospective Clinic

Monday, Dec. 2 3:00PM - 3:10PM Room: S504CD

Participants

Benjamin Voss, MD, Milwaukee, WI (*Presenter*) Nothing to Disclose David R. De Lone, MD, Rochester, MN (*Abstract Co-Author*) Nothing to Disclose Kishore Rajendran, PhD, Rochester, MN (*Abstract Co-Author*) Nothing to Disclose Tammy A. Drees, Rochester, MN (*Abstract Co-Author*) Nothing to Disclose Shuai Leng, PHD, Rochester, MN (*Abstract Co-Author*) License agreement, Bayer AG Joel G. Fletcher, MD, Rochester, MN (*Abstract Co-Author*) Grant, Siemens AG; Consultant, Medtronic plc; Consultant, Takeda Pharmaceutical Company Limited; Grant, Takeda Pharmaceutical Company Limited; ; Cynthia H. McCollough, PhD, Rochester, MN (*Abstract Co-Author*) Research Grant, Siemens AG

For information about this presentation, contact:

fletcher.joel@mayo.edu

PURPOSE

To examine the ability of photon-counting detector (PCD) CT to improve spatial resolution and reduce radiation dose for sinus CT compared to routine energy-integrating detector (EID) CT.

METHOD AND MATERIALS

After informed consent, twenty-eight patients underwent sinus imaging on a PCD CT system following a clinically indicated scan on the same day. EID images were reconstructed using 512 & 1024 matrices (CTDIvol = 13.5-14.5 mGy). Ultra high resolution PCD exams (Sn100kV) acquired at 10, 8, 7 & 6 CTDIvol, corresponding to 28%, 43%, 50%, and 57% dose reduction, were reconstructed using a 1024 matrix (7 patients/dose level). Images were anonymized, randomized and reviewed by a neuroradiologist. Visualization of key anatomic structures [sphenoid ostia (SO), lesser palatine foramen (LPF), nasomaxillary sutures (NS), anterior ethmoid artery canal (AEA)] was rated for each panel on a Likert scale (1=worse visualization and confidence than routine; 2=worse, no confidence change, 3=similar/routine, 4=preferred, no confidence change, 5=Improved detection & confidence). Image quality scores were provided (noise, sharpness, artifacts, overall quality). Wilcoxon signed-rank (p <0.05) was used to test significance.

RESULTS

At 10 and 8 mGy, PCD was significantly superior to EID 512 for all critical anatomy (SO p=0.016, mean difference (MD) 0.56; LPF p=0.0007,MD 1.5; NS p=0.0002,MD 1.2; AEA p=0.0005,MD 1.4). At these dose levels, PCD was also significantly superior to EID 1024 for visualizing the LPF (p<0.05;MD 0.64), the NS(p=0.008; MD 0.64), and the AEA (p=0.009;MD 0.86). At 7 and 6 mGy, PCD was superior to EID 512 for LPF (p=0.03) and AEA (p=0.02), but not significantly different for any anatomic structure compared to EID 1024. Noise, sharpness, and overall image quality was similar between PCD and EID 1024 across dose levels.

CONCLUSION

PCD CT imaging of the sinus demonstrates superior visualization of anatomy with no significant noise increase even at dose reductions of up to 57% when compared to routine imaging, enabling a significant dose reduction in a frequently imaged population.

CLINICAL RELEVANCE/APPLICATION

PCD CT shows potential to improve routine imaging in a variety of clinical scenarios where spatial resolution and image fidelity improve confidence and accuracy while offering lower dose acquisition.

SSE20-02 Spiral T1-SE for Routine Post-Contrast Brain MRI: Multi-Center/Reader Study Results

Monday, Dec. 2 3:10PM - 3:20PM Room: S504CD

Zhiqiang Li, PhD, Phoenix, AZ (Abstract Co-Author) Research support, Koninklijke Philips NV Rvan Robison, PhD, Phoenix, AZ (Abstract Co-Author) Master Enterprise Agreement, Philips Koninklijke NV Dinghui Wang, PhD, Rochester, MN (Abstract Co-Author) Research support, Koninklijke Philips NV Ashley G. Anderson, Rochester, MN (Abstract Co-Author) Employee, Koninklijke Philips NV Nicholas R. Zwart, Phoenix, AZ (Abstract Co-Author) Employee, Hyperfine Research Akshay Bakhru, Bangalore, India (Abstract Co-Author) Nothing to Disclose Suthambhara Nagaraj, Bangalore, India (Abstract Co-Author) Employee, Koninklijke Philips NV Tanya Mathews, Bangalore, India (Abstract Co-Author) Employee, Koninklijke Philips NV Silke Hey, Best, Netherlands (Abstract Co-Author) Employee, Koninklijke Philips NV Jos Koonen, Best, Netherlands (Abstract Co-Author) Employee, Koninklijke Philips NV Ivan Dimitrov, PhD, Dallas, TX (Abstract Co-Author) Researcher, Koninklijke Philips NV Harry Friel, Cleveland, OH (Abstract Co-Author) Employee, Koninklijke Philips NV Quin Lu, Gainesville, FL (Abstract Co-Author) Employee, Koninklijke Philips NV Makoto Obara, Tokyo, Japan (Abstract Co-Author) Employee, Koninklijke Philips NV Indrajit Saha, PhD, Gurgaon, India (Abstract Co-Author) Employee, Koninklijke Philips NV Hui Wang, Louisville, KY (Abstract Co-Author) Employee, Koninklijke Philips NV Yi Wang, Gainesville, FL (Abstract Co-Author) Employee, Koninklijke Philips NV Yansong Zhao, Boston, MA (Abstract Co-Author) Employee, Koninklijke Philips NV Houchun H. Hu, PhD, Columbus, OH (Abstract Co-Author) Nothing to Disclose Thomas L. Chenevert, PhD, Ann Arbor, MI (Abstract Co-Author) Consultant, Koninklijke Philips NV Osamu Togao, MD, PhD, Fukuoka, Japan (Abstract Co-Author) Nothing to Disclose Jean A. Tkach, PhD, Cincinnati, OH (Abstract Co-Author) Nothing to Disclose Usha D. Nagaraj, MD, Cincinnati, OH (Abstract Co-Author) Author with royalties, Reed Elsevier Marco C. Pinho, MD, Dallas, TX (Abstract Co-Author) Nothing to Disclose Rakesh K. Gupta, MD, MBBS, Gurgaon, India (Abstract Co-Author) Nothing to Disclose Juan E. Small, MD, Brookline, MA (Abstract Co-Author) Nothing to Disclose Mara M. Kunst, MD, Burlington, MA (Abstract Co-Author) Nothing to Disclose John P. Karis, MD, Phoenix, AZ (Abstract Co-Author) Nothing to Disclose Jalal B. Andre, MD, Seattle, WA (Abstract Co-Author) Research Grant, Koninklijke Philips NV Consultant, Hobbitview, Inc Research Grant, Toshiba Corporation Jeffrey H. Miller, MD, Phoenix, AZ (Abstract Co-Author) Nothing to Disclose Nandor K. Pinter, MD, Amherst, NY (Abstract Co-Author) Speaker, Koninklijke Philips NV; James G. Pipe, PhD, Rochester, MN (Abstract Co-Author) Research Grant, Koninklijke Philips NV

PURPOSE

Spiral MRI provides several advantages over routine (Cartesian) MRI, including scan efficiency, and robustness to flow, aliasing, and geometric distortions. Nevertheless, spiral MRI has not gained widespread clinical adoption due to its greater demand on system fidelity. We present here the results of a multi-center clinical study to investigate spiral MRI as an added value alternative to routine post-contrast brain MRI.

METHOD AND MATERIALS

A spiral consortium of 7 clinical sites acquired 88 patient cases on Philips 3.0/1.5T Ingenia scanners with standard hardware configurations. For each patient, two post-contrast scans were acquired: a spiral 2DT1SE, and a routine Cartesian 2DT1SE/fast-SE. The spiral was matched to each Cartesian for scan time, FOV/resolution, and a/TR. The spiral-out readout is fully sampled ~10/20 ms for 3.0/1.5T. Crusher gradients around the 180°-pulse provide added flow signal suppression and black blood contrast. Online reconstruction (~1 sec/slice) uses a B0 prescan in a conjugate-gradient algorithm for joint off-resonance deblurring and Dixon water/fat separation. Nine neuroradiologists reviewed all 88 patient cases. For each patient, the matching pair of spiral vs. Cartesian scans were compared side-by-side, and scored on 10 image quality (IQ) metrics using a 5-point Likert scale.

RESULTS

Summary statistics over all patient cases for the 10 metrics (Wilcoxon signed-rank test, p < 0.01) show: Spiral performs better than Cartesian in 7/10 metrics: flow artifact reduction, SNR, GM/WM contrast, image sharpness, lesion conspicuity, preference for diagnosing abnormal enhancement, and overall intracranial IQ. Spirals perform poorer than Cartesian in 2/10 metrics related to magnetic susceptibility: susceptibility artifact, and overall extracranial IQ. Spirals are comparable to Cartesian in 1/10 metrics: motion artifact.

CONCLUSION

Spiral 2DT1SE was superior or comparable to standard-of-care Cartesian 2DT1SE/FSE in 8 of 10 assessed metrics, and was preferred by neuroradiologists for post-contrast intracranial evaluation. Future work to improve IQ in areas of magnetic susceptibility will explore advanced B0 mapping, deblurring, and system characterization methods.

CLINICAL RELEVANCE/APPLICATION

Spiral MRI enables increased scan efficiency (higher SNR, faster scans) and robustness to certain artifacts, providing a compelling alternative to Cartesian MRI that is the current clinical workhorse.

SSE20-03 Neuropathologic Correlates of Enlarged Perivascular Spaces and Contribution to Cognitive Decline in a Community Cohort of Older Adults

Monday, Dec. 2 3:20PM - 3:30PM Room: S504CD

Participants

Carles Javierre Petit, Chicago, IL (*Presenter*) Nothing to Disclose Julie A. Schneider, MD, Chicago, IL (*Abstract Co-Author*) Nothing to Disclose Nazanin Makkinejad, Chicago, IL (*Abstract Co-Author*) Nothing to Disclose Ashish A. Tamhane, MS, Chicago, IL (*Abstract Co-Author*) Nothing to Disclose David A. Bennett, MD, Chicago, IL (*Abstract Co-Author*) Nothing to Disclose Konstantinos Arfanakis, PhD, Chicago, IL (*Abstract Co-Author*) Nothing to Disclose

cjavierr@hawk.iit.edu

PURPOSE

Enlarged perivascular spaces (EPVS) have been associated with aging, increased stroke risk, decreased cognitive function and vascular dementia. However, the relationship of EPVS with age-related neuropathologies is not well understood. Therefore, the purpose of this study was two-fold: to assess the neuropathologic correlates of EPVS, and to determine the contribution of EPVS burden to cognitive decline by combining ex-vivo brain magnetic resonance images (MRI) and pathology in a community cohort of older adults.

METHOD AND MATERIALS

Cerebral hemispheres were obtained from 662 participants of two longitudinal, epidemiologic clinical-pathologic cohort studies of aging. Experienced observers blinded to all pathologic and clinical data rated EPVS burden using a semiquantitative four-level scale (See Figure). Neuropathologic assessment was performed by a board-certified neuropathologist blinded to all clinical and imaging findings. Univariate and multivariate logistic regression was used to investigate the association of EPVS burden with the following age-related neuropathologies: gross and microscopic infarcts, atherosclerosis, arteriolosclerosis, cerebral amyloid angiopathy, amyloid plaques, neurofibrillary tangles, hippocampal sclerosis, Lewy bodies, and TDP-43. Finally, mixed-effects models were used to evaluate EPVS burden contribution to cognitive decline in 6 domains: global, episodic, semantic, working, perceptual, and visuospatial.

RESULTS

Univariate analyses showed significant association of EPVS burden with gross (OR=1.59, p-value=0.002) and microscopic infarcts (OR=1.40, p-value=0.025). Multivariate logistic regression showed a significant association of EPVS burden with gross infarcts (OR=1.60, p=0.004). EPVS burden was significantly contributing to cognitive decline for all cognitive domains except working memory; and the interaction between EPVS burden and time also showed significant for global, episodic and visuospatial cognitive domains.

CONCLUSION

The results suggest: that EPVS and gross infarcts may share similar neurobiological pathways, which is in fair agreement with the literature and proposed etiologies driving these two processes, and that EPVS burden significantly contributes to cognitive decline independently from demographics and neuropathologies.

CLINICAL RELEVANCE/APPLICATION

This is the biggest clinical-pathologic study up to date, and the only one to include cognitive decline in combination with EPVS.

SSE20-04 Visualization of the Morphology and Pathology of the Peripheral Branches of the Cranial Nerves Using 3-Dimensional High Contrast Magnetic Resonance Neurography

Monday, Dec. 2 3:30PM - 3:40PM Room: S504CD

Participants

Lixia Wang, Wuhan, China (*Abstract Co-Author*) Nothing to Disclose Wenjun Wu, Wuhan, China (*Abstract Co-Author*) Nothing to Disclose Feihong Wu, Wuhan, China (*Presenter*) Nothing to Disclose Dingxi Liu, Wuhan, China (*Abstract Co-Author*) Nothing to Disclose Chuansheng Zheng, Wuhan, China (*Abstract Co-Author*) Nothing to Disclose Xiangquan Kong, Wuhan, China (*Abstract Co-Author*) Nothing to Disclose

For information about this presentation, contact:

lisa2003627@163.com

PURPOSE

Aims to assess the feasibility and advantages of a contrast-enhanced three-dimensional (3D) flip-angle evolution (SPACE) shorttau inversion (STIR) T2-weighted (T2W) magnetic resonance neurography (MRN) sequence (ceMRN) for visualizing the morphology and pathology of peripheral branches of the cranial nerves.

METHOD AND MATERIALS

35 volunteers with no relevant cranial nerve symptoms and 12 patients with maxillofacial tumors were enrolled. Conventional MRN (cMRN) and ceMRN were performed with 3T MRI system. The continuity of 10 major branches of the cranial nerves on ceMRN was evaluated based on the 5-score evaluation of 3 readers and their interobserver variability was tested. The image quality was compared between cMRN and ceMRN. The relationship between maxillofacial tumors and adjacent peripheral nerves was classified and analyzed in ceMRN of these patients.

RESULTS

The interobserver consistency of all nerves across the 3 readers was excellent, with an average κ value > 0.83. Visualization of the inferior alveolar nerve, hypoglossal nerve and lingual nerve were excellent, with scores of 3.95, 3.77, and 3.63 respectively. Detection of the facial nerve, infraorbital nerve, masseteric nerve, and glossopharyngeal/vagus nerve were relatively good, with scores of 3.25, 3.15, 3.04 and 3.04 respectively. Depiction of the supraorbital nerve and auriculotemporal nerve were moderate, with scores of 2.87 and 2.79 respectively. Delineation of the buccal nerve was fair, with a score of 1.88. The contrast signal-to-noise ratios of nerve to bone marrow, nerve to muscle and nerve to fat on ceMRN were significantly lower than those on cMRN, and the contrast ratios of nerve to bone marrow, nerve to muscle, and nerve to gland on ceMRN were significantly higher than those on cMRN (all P < 0.05). The relationship between the extracranial branches of the cranial nerves and tumors were classified as isolated, compressed, embodied, invaded or spread perineurally based on the imaging features on ceMRN.

CONCLUSION

The ceMRN demonstrates excellent visualization the peripheral branches of cranial nerves in a 3D pattern and appears to be a promising method for diagnosis and pretreatment assessment of the pathologies of cranial nerves.

CLINICAL RELEVANCE/APPLICATION

(dealing with 3D ceMRN) 'ceMRN can be used as a preoperative method to evaluate the relationship between peripheral branches of the cranial nerves and maxillofacial tumor.'

SSE20-05 Simultaneous Multi-Angular-Relaxometry of Tissue (SMART) MRI Identifies Myelin-Related Tissue Damage in Multiple Sclerosis

Monday, Dec. 2 3:40PM - 3:50PM Room: S504CD

Participants

Biao Xiang, MA, Saint Louis, MO (*Presenter*) Nothing to Disclose Jie Wen, PhD, Saint Louis, MO (*Abstract Co-Author*) Nothing to Disclose Anne H. Cross, Saint Louis, MO (*Abstract Co-Author*) Consultant, Biogen Idec Inc; Consultant, Celgene Corporation; Consultant, Novartis AG; Consultant, Merck KGaA; Consultant, F. Hoffmann-La Roche Ltd; Consultant, TG Therapeutics Dmitriy A. Yablonskiy, PhD, Saint Louis, MO (*Abstract Co-Author*) Nothing to Disclose

PURPOSE

Rapid, pathologically specific and quantitative MRI techniques are needed to assess tissue damage in multiple sclerosis (MS), particularly in progressive MS. The purpose of this study was to demonstrate that SMART MRI metrics can distinguish non-relapsing progressive MS from relapsing-remitting MS (RRMS) and to examine correlations with clinical assessments.

METHOD AND MATERIALS

22 non-relapsing progressive MS and 11 RRMS subjects were scanned at 3T. SMART data with isotropic 1 mm3 resolution were acquired using a three dimensional multi-gradient-echo sequence with five flip angles a (5°, 10°, 20°, 40°, 60°) and three gradient echoes (TE: 2.3, 6.2, 10.1ms) for each a. A phase-based technique was implemented for a-mapping. MS tissue damage, assessed by SMART metrics of macromolecule proton fraction (MPF) and R1 (1/T1) in normal-appearing cortical gray matter (NAGM) and subcortical normal-appearing white matter (NAWM), were correlated with Expanded Disability Status Scale (EDSS), 25-foot timed walk, nine-hole peg test (9HPT), paced auditory serial addition test (PASAT) and Symbol Digit Modality tests. Spearman rank test was used to compute rho values.

RESULTS

MPF was higher in NAWM than in NAGM, consistent with the high macromolecular content in myelin (Fig. 1). MPF measurement demonstrated relatively stronger correlations with the motor related clinical assessments EDSS and 9HPT (p<0.001), while a higher quantitative R1 metric showed significant correlations with better cognitive related PASAT scores (p=0.004). Interestingly, the left hemisphere showed stronger correlations than right hemisphere when assessing correlations between MPF and motor related clinical tests. Additionally, MPF in NAWM had significantly stronger correlation with clinical assessments than MPF of cortical NAGM. Higher MPF measurements in both GM and WM readily differentiated the relapsing-remitting group from the group with non-relapsing progressive MS (p<0.01).

CONCLUSION

Results from this study suggest that SMART MRI has high potential for assessing myelin content and MS-related damage.

CLINICAL RELEVANCE/APPLICATION

Without applying either MT or 180° radiofrequency pulses, SMART MRI generates high resolution quantitative images and is safe for high-field MRI, making it a useful outcome measure in clinical trials.

SSE20-06 Magnetic Resonance Elastography of Brain: Tumor Adherence and Stiffness

Monday, Dec. 2 3:50PM - 4:00PM Room: S504CD

Participants

Sandeep Juvvadi, Hyderabad, India (*Presenter*) Nothing to Disclose Prateek Kalra, Columbus, OH (*Abstract Co-Author*) Nothing to Disclose Arunark Kolipaka, PhD, Columbus, OH (*Abstract Co-Author*) Benzer Pharmacy; Tenet Healthcare Corporation; Lonwin Healthcare

PURPOSE

To determine brain tumor adherence as well as stiffness in patients using magnetic resonance elastography (MRE) and compare to histopathology.

METHOD AND MATERIALS

In vivo brain MRE was performed on 7 patients using a 3T MRI scanner (Skyra, Siemens Healthcare, Germany). Mechanical waves were introduced into the brain using a pneumatic driver system with a pillow driver at 60Hz and a SE EPI-MRE sequence was used to acquire all axial slices of the brain. Imaging parameters included: TR=3333ms, TE=44ms, slice thickness=3, matrix=128x64, FOV=260cm, GRAPPA acceleration factor R=2; mechanical vibration frequency=60Hz; 4 MRE time offsets; and motion-encoding gradient of 16.67ms duration (60Hz) to encode in-plane and through-plane motion of propagating waves in the brain. Wave images were processed using an in-house local frequency estimation algorithm with curl processing to obtain stiffness as well as octahedral shear strain (OSS) to determine mechanical and adherence properties of the brain tumor respectively. Mean stiffness of the tumor and normal brain are reported along with the OSS values around the tumor boundary. Furthermore, the histopathology measurements obtained post surgery were also recorded for comparison.

RESULTS

Figure shows a T2- weighted magnitude image (a), snap shot of wave propagation (b) and the corresponding stiffness map (c) with a mean stiffness value of 1.2kPa in the tumor region (green contour) and 2.3kPa non-tumor (red contour); OSS map (d) also confirms soft tumor and non-adherent along with histopathology (e) confirming soft tumor glioma grade 4 and easily resectable. The stiffness measurements of other tumors ranged from 0.8 to 1.9kPa for meningioma or gliomas or metastasis. Similarly, histopathology results in other patients with varying tumors also confirmed the findings of MRE.

CONCLUSION

This study has demonstrated that stiffness and adherence patterns of different brain tumors can be quantitated using MRE. This study for the first time compared material properties of the brain tumors noninvasively to histopathology observations. However, more studies are further warranted.

CLINICAL RELEVANCE/APPLICATION

Brain MRE is a noninvasive technique, which can potentially differentiate benign vs malignant tumors and provide information on tumor adherence that can enable better guidance for surgical resection.





SPSI23

Special Interest Session: Value MR Imaging-Paradigm Shift from Generic to Targeted-Why and How

Monday, Dec. 2 4:30PM - 6:00PM Room: E353C

MR

AMA PRA Category 1 Credits ™: 1.50 ARRT Category A+ Credit: 1.75

Participants

Clare M. Tempany-Afdhal, MD, Charlestown, MA (*Moderator*) Research Grant, InSightec Ltd; Research Grant, Gilead Sciences, Inc; Advisory Board, Profound Medical Inc; Spouse, Employee, Spring Bank Pharmaceuticals, Inc; Spouse, Director, Trio Healthcare; Spouse, Consultant, Gilead Sciences, Inc; Spouse, Consultant, Merck & Co, Inc; Spouse, Consultant, Echosens SA; Spouse, Consultant, Shinogi; Spouse, Consultant, Ligand Pharmaceuticals, Inc; Spouse, Stock options, Spring Bank Pharmaceuticals, Inc; Spouse, Stock options, Allurion; Spouse, Stock options, Trio Healthcare; ;

LEARNING OBJECTIVES

1) To understand innovative approaches to improving MR efficiency. 2) To understand a novel framework for focused MR interpretations.

Sub-Events

SPSI23A Why We Need to Challenge Status Quo

Participants

Yoshimi Anzai, MD, MPH, Salt Lake City, UT (Presenter) Nothing to Disclose

For information about this presentation, contact:

yoshimi.anzai@hsc.utah.edu

SPSI23B Designing Technology for Optimized MRI

Participants James G. Pipe, PhD, Rochester, MN (*Presenter*) Research Grant, Koninklijke Philips NV

For information about this presentation, contact:

pipe.james@mayo.edu

LEARNING OBJECTIVES

1) List technologies appropriate for increasing MR Value. 2) Describe examples of high-value exams. 3) Debate the metrics involved in optimizing MR use.

SPSI23C 'Fit for Purpose' Approach to MRI

Participants

Mitchell D. Schnall, MD, PhD, Philadelphia, PA (Presenter) Research Grant, Siemens AG

SPSI23D MRgFUS is there Value in Disruption?

Participants

Clare M. Tempany-Afdhal, MD, Charlestown, MA (*Presenter*) Research Grant, InSightec Ltd; Research Grant, Gilead Sciences, Inc; Advisory Board, Profound Medical Inc; Spouse, Employee, Spring Bank Pharmaceuticals, Inc; Spouse, Director, Trio Healthcare; Spouse, Consultant, Gilead Sciences, Inc; Spouse, Consultant, Merck & Co, Inc; Spouse, Consultant, Echosens SA; Spouse, Consultant, Shinogi; Spouse, Consultant, Ligand Pharmaceuticals, Inc; Spouse, Stock options, Spring Bank Pharmaceuticals, Inc; Spouse, Stock options, Allurion; Spouse, Stock options, Trio Healthcare; ;





SPSC30

Controversy Session: MR Elastography versus US Elastography of Liver

Tuesday, Dec. 3 7:15AM - 8:15AM Room: E350



AMA PRA Category 1 Credit ™: 1.00 ARRT Category A+ Credit: 1.00

Participants

Bachir Taouli, MD, New York, NY (Moderator) Research Grant, Bayer AG

Anthony E. Samir, MD, Boston, MA (*Moderator*) Consultant, Pfizer Inc; Consultant, General Electric Company; Consultant, PAREXEL International Corporation; Research Grant, Koninklijke Philips NV; Research Grant, Siemens AG; Research Grant, Canon Medical Systems Corporation; Research Grant, General Electric Company; Research Grant, Samsung Electronics Co, Ltd; Research Grant, Analogic Corporation; Research support, SuperSonic Imagine; Research support, Hitachi, Ltd; Research contract, Koninklijke Philips NV

Laura Kulik, MD, Chicago, IL (*Presenter*) Speaker, Eisai Co, Ltd; Speaker, Dova; Speaker, Gilead Sciences, Inc; Consultant, Bristol-Myers Squibb Company; Consultant, Bayer AG; Consultant, Exelixis, Inc; Consultant, Eisai Co, Ltd; Consultant, CE Outcomes Paul S. Sidhu, MRCP, FRCR, London, United Kingdom (*Presenter*) Speaker, Koninklijke Philips NV; Speaker, Bracco Group; Speaker, Hitachi, Ltd; Speaker, Siemens AG; Speaker, Samsung Electronics Co, Ltd; Advisory Board, Samsung Electronics Co, Ltd; Advisory Board, Itreas Ltd

Scott B. Reeder, MD, PhD, Madison, WI (Presenter) Nothing to Disclose

For information about this presentation, contact:

paulsidhu@nhs.net

LEARNING OBJECTIVES

1) Review the current uses and diagnostic performance of ultrasound and MR elastography of the liver. 2) Review and compare advantages, pitfalls and limitations of ultrasound and MR elastography of the liver.

ABSTRACT

The use of elastography has altered the management of chronic liver disease, and modified the patient pathway. The ability to assess the degree of fibrosis within the accepted classification, either the METAVIR or Ishak scoring systems, allows for clinical diease management. The establishment of elastography in both MR imaging and US imaging has become established, with standrads measured against liver biopsy. The number of liver biopsies for assessment of liver fibrosis has predictably declines as a result. Both imaging techniques have advantages and disadvantages. Advocates of MR imaging indicate the global nature of the measurement, speed of aquisition, whereas the proponents of US based elastograppy suggest the rapid, cost effective methodology is superior. However the need to image an increasing patient population will require a rapid, portable and acceptable method. This debate will highlight the two techniques, the accuracy, acceptance and reproducibility and allow the audience to come to a conclusion of the usefullnees of each technique.





RC303

Cardiac Series: Emerging Cardiovascular MR and CT Imaging

Tuesday, Dec. 3 8:30AM - 12:00PM Room: E350



AMA PRA Category 1 Credits ™: 3.25 ARRT Category A+ Credits: 4.00

FDA Discussions may include off-label uses.

Participants

Karen G. Ordovas, MD, San Francisco, CA (*Moderator*) Advisor, Arterys Inc; Research Grant, General Electric Company Gautham P. Reddy, MD, Seattle, WA (*Moderator*) Researcher, Koninklijke Philips NV Albert Hsiao, MD,PhD, La Jolla, CA (*Moderator*) Founder, Arterys, Inc; Consultant, Arterys, Inc; Shareholder, Arterys, Inc; Speaker, Bayer AG; Research Grant, Bayer AG; Speaker, General Electric Company; Research Grant, General Electric Company; Michael K. Atalay, MD, PhD, Providence, RI (*Moderator*) Nothing to Disclose

Sub-Events

RC303-01 Applications of AI for Cardiovascular Imaging

Tuesday, Dec. 3 8:30AM - 9:00AM Room: E350

Participants

Albert Hsiao, MD,PhD, La Jolla, CA (*Presenter*) Founder, Arterys, Inc; Consultant, Arterys, Inc; Shareholder, Arterys, Inc; Speaker, Bayer AG; Research Grant, Bayer AG; Speaker, General Electric Company; Research Grant, General Electric Company;

LEARNING OBJECTIVES

1) Identify the recent innovations that have enabled a resurgence of interest in applying artificial intelligence (AI) in medical practice. 2) Identify potential applications for AI in the acquisition, analysis and interpretation of cardiovascular CT and MRI. 3) Apply concepts of analytical validity, clinical applicability, to become knowledgeable consumers of AI.

RC303-02 Deep-Learning Quantification of Coronary Calcium on CT and Mortality in the National Lung Screening Trial (NLST)

Tuesday, Dec. 3 9:00AM - 9:10AM Room: E350

Participants

Roman Zeleznik, Boston, MA (Presenter) Nothing to Disclose Borek Foldyna, MD, Boston, MA (Abstract Co-Author) Nothing to Disclose Parastou Eslami, PhD, Boston, MA (Abstract Co-Author) Nothing to Disclose Jakob Weiss, MD, Tubingen, Germany (Abstract Co-Author) Nothing to Disclose Alexander Ivanov, BS, Boston, MA (Abstract Co-Author) Nothing to Disclose Chintan Parmar, Allston, MA (Abstract Co-Author) Nothing to Disclose Jana Taron, MD, Tuebigen, Germany (Abstract Co-Author) Nothing to Disclose Julia Karady, MD, Budapest, Hungary (Abstract Co-Author) Nothing to Disclose Lili Zhang, MD, Boston, MA (Abstract Co-Author) Nothing to Disclose Raza Alvi, Boston, MA (Abstract Co-Author) Nothing to Disclose Yasuka Kikuchi, MD, Boston, MA (Abstract Co-Author) Nothing to Disclose Dahlia Banerji, MD, Boston, MA (Abstract Co-Author) Nothing to Disclose Mio Uno, MD, Tsu-city , Japan (Abstract Co-Author) Nothing to Disclose Jan-Erik Scholtz, MD, Frankfurt, Germany (Abstract Co-Author) Nothing to Disclose Udo Hoffmann, MD, Boston, MA (Abstract Co-Author) Research Grant, Kowa Company, Ltd ; Research Grant, Abbott Laboratories; Research Grant, HeartFlow, Inc; Research Grant, AstraZeneca PLC; Michael T. Lu, MD, Boston, MA (Abstract Co-Author) Grant, NVIDIA Corporation; Institutional Research Grant, Kowa Company, Ltd; Institutional Research Grant, AstraZeneca PLC Hugo Aerts, PhD, Boston, MA (Abstract Co-Author) Stockholder, Sphera Inc

For information about this presentation, contact:

roman_zeleznik@dfci.harvard.edu

PURPOSE

Coronary artery calcification (CAC) is quantifiable on low-dose chest CT and can guide statin therapy. Quantification is not routinely performed due to time and equipment limitations. We developed a deep-learning algorithm that automatically quantifies coronary calcium on standard lung screening CT and evaluated prognostic value in 14,959 National Lung Screening Trial (NLST) participants.

METHOD AND MATERIALS

The deep learning algorithm was developed in 1,600 cardiac CTs from with manual CAC measurement as the reference. The deep learning calcium score was categorized as: High (CAC>300), Moderate (CAC: 101-300), Low (CAC: 1-100), and Very Low (CAC: 0). The association of the deep learning calcium score with all-cause and cardiovascular mortality was then tested in 14,959 heavy

smokers aged 55-74 having lung cancer screening chest CT at 33 US sites in NLST. The intraclass correlation coefficient (ICC) between automated and human manual CAC was assessed in 396 NLST chest CTs.

RESULTS

All-cause (7.3% (1,092/14,959)) and cardiovascular (1.9% (288/14,959)) mortality was assessed over median follow-up of 6.5 years. There was a significant association between deep learning calcium score and all cause mortality: High: HR 2.9 (95%CI: 2.4-3.5), Moderate: 1.9 (1.5-2.3), Low: 1.3 (1.1-1.6), all p<0.01 compared to Very Low; as well as for cardiovascular mortality: High: HR 6.6 (4.3-10.3), Moderate: 3.8 (2.3-6.1), Low: 2.2 (1.4-3.6), all p<0.001 compared to Very Low. The ICC between manual and automatic calcium classes was 0.858 (95%CI: 0.830-0.882).

CONCLUSION

The automated deep learning algorithm quantified CAC on lung screening CT. Automated CAC corresponded closely to human readers and was strongly associated with all-cause and cardiovascular mortality in a large multicenter cohort of NLST participants having lung screening.

CLINICAL RELEVANCE/APPLICATION

Automated quantification of coronary calcium using existing lung screening CTs identifies persons at high and low risk to guide cardiovascular prevention.

RC303-03 Estimation of Agatston Calcium Scores on Chest Radiographs Using Machine Learning

Tuesday, Dec. 3 9:10AM - 9:20AM Room: E350

Participants Peter Kamel, MD, Ellicott City, MD (*Presenter*) Nothing to Disclose Paul H. Yi, MD, Baltimore, MD (*Abstract Co-Author*) Nothing to Disclose Haris I. Sair, MD, Baltimore, MD (*Abstract Co-Author*) Research Grant, Tocagen Cheng Ting Lin, MD, Baltimore, MD (*Abstract Co-Author*) Nothing to Disclose

For information about this presentation, contact:

pkamel1@jhmi.edu

PURPOSE

The Agatston calcium score quantifies the severity of coronary artery disease (CAD) and is typically measured on an EKG-gated cardiac CT. The purpose of this study was to assess the ability of deep convolutional neural networks (DCNNs) to estimate Agatston scores on chest radiographs (CXRs).

METHOD AND MATERIALS

Our dataset was comprised of 471 patients who had undergone a cardiac CT and a PA and lateral CXR in the same year. CT-derived Agatston scores were considered ground truth and used as labels for DCNN training on radiographs. Radiographs were split into 70% training and 30% testing, balancing the distribution of Agatston scores. Weighted augmentation was performed on images to increase data size and balance class distribution. An attention-based network architecture was built on a variety of standard DCNNs such as VGG-16, pretrained with ImageNet weights, and used for (1) binary classification of Agatston scores at variable thresholds and (2) linear regression prediction of absolute calcium scores. Classifier performance was measured using area under the curve (AUC) and regression assessed with the mean absolute error. Attention maps were produced to highlight areas of decision-making and results were additionally compared to radiologist mention of CAD on CXR reports.

RESULTS

Binary classification performed best for discrimination of Agatston scores greater than 75 with AUC of 0.73 (Fig. 1a). Best performing regression algorithms predicted Agatston scores with a mean absolute error of 159. DCNNs trained on PA radiographs outperformed those on lateral radiographs. Attention maps primarily localized to the cardiac silhouette (Fig. 1b), with highest performing binary algorithms additionally including the aortic arch and other vessels in predictions. Of the radiographs with calcium scores >75, none of the reports included mention of CAD.

CONCLUSION

DCNNs on CXRs may have utility in estimating calcium scores and predicting clinically-significant CAD, a finding not often reported by radiologists on radiographs. These results provide proof-of-concept in the promise of deep learning to extract additional information that may not typically be noted on human review.

CLINICAL RELEVANCE/APPLICATION

We illustrate the potential for deep learning to estimate Agatston calcium scores and predict the severity of coronary artery disease on chest radiographs.

RC303-04 Spectral Detector CT

Tuesday, Dec. 3 9:20AM - 9:50AM Room: E350

Participants

Suhny Abbara, MD, Dallas, TX (*Presenter*) Royalties, Reed Elsevier; Institutional research agreement, Koninklijke Philips NV; Institutional research agreement, Siemens AG

RC303-05 Advanced Coronary Plaque Characterization Using a Dual-Layer Spectral CT: Quantitative Assessment of Iodine Uptake in Plaques

Tuesday, Dec. 3 9:50AM - 10:00AM Room: E350

Participants Jonathan Nadjiri, MD, Munich, Germany (*Presenter*) Nothing to Disclose Karl-Ludwig Laugwitz, Munich, Germany (*Abstract Co-Author*) Nothing to Disclose Ernst J. Rummeny, MD, Muenchen, Germany (*Abstract Co-Author*) Nothing to Disclose Tareq Ibrahim, Munich, Germany (*Abstract Co-Author*) Nothing to Disclose Michael Rasper, Munich, Germany (*Abstract Co-Author*) Nothing to Disclose Daniela Pfeiffer, MD, Munich, Germany (*Abstract Co-Author*) Nothing to Disclose Alexandra S. Straeter, Munich, Germany (*Abstract Co-Author*) Nothing to Disclose Maximilian Englmaier, MD, Kraiburg, Germany (*Abstract Co-Author*) Nothing to Disclose Florian Weis, Munich, Germany (*Abstract Co-Author*) Nothing to Disclose Andre Kafka, Munich, Germany (*Abstract Co-Author*) Nothing to Disclose Tobias Koppara, Munich, Germany (*Abstract Co-Author*) Nothing to Disclose

For information about this presentation, contact:

Jonathan.nadjiri@tum.de

PURPOSE

Spectral CT-coronary angiography (SCCTA) with a dual-layer detector allows for quantitative determination of iodine uptake with high accuracy with just one scan. In this pilot project we sought to prospectively evaluate this quantitative method to measure iodine uptake in coronary plaques as a possible surrogate for inflammation.

METHOD AND MATERIALS

We investigated 46 consecutive patients. 50ml of Iodine 400mg/ml was administered 2min before standard contrast-enhanced SCCTA with a regular contrast bolus. Hounsfield Units (HU) as well as iodine content (mg/ml) in each detectable non-calcified plaque were determined. In patients with indication for invasive coronary angiography (ICA) additionally Optical Coherence Tomography (OCT) was performed.

RESULTS

In the study population 18 non-calcified plaques were found in SCCTA. Mean density was 70 ± 56 HU. Mean Iodine uptake was 2.4 \pm 2.1mg/ml, respectively. There was significant correlation between iodine uptake and density of coronary plaques; r = 0.9, p < 0.001. 11 patients underwent ICA; in these group 11 non-calcified plaques were found by SCCTA. For all of those plaque formations a correlate in OCT was found. For low-attenuation plaques (<90HU) there was no significant correlation between density and iodine uptake. In these plaques variance of iodine uptake was very high (standard deviation was 155% of mean) while in plaques with higher density (>=90 HU) variance was small (standard deviation was 33% of mean).

CONCLUSION

In our pilot study we found that in general in non-calcified plaques iodine uptake corresponds to the density of the plaques and we found a correlate of every non-calcified plaque detected by SCCTA in OCT. However, there is relevant difference in iodine uptake of coronary plaques with similar HU in very low attenuation plaques (HU < 90) indicating additional information through determination of quantitative iodine uptake.

CLINICAL RELEVANCE/APPLICATION

Coronary plaque characterization in CT is known to stratify a patient's individual risk for cardiovascular events beyond clinical risk scores, calcification and stenosis. However, a gap in predicting outcomes remains. This gap might be closed by more information about the plaque and its composition. Measuring iodine content as proposed in this abstract might be one of the missing parts to further close the prognostic gap of cardiac CT which has to be evaluated in further outcome studies.

RC303-06 Can Spectral Imaging Technique Reduce Agents Dosage in "One-Stop" Coronary and Aortic CT Angiography?

Tuesday, Dec. 3 10:00AM - 10:10AM Room: E350

Participants

Li Wei, MD,PhD, Liaocheng, China (*Presenter*) Nothing to Disclose Huijuan Jia, Liaocheng, China (*Abstract Co-Author*) Nothing to Disclose Kunpeng Wu, Liaocheng, China (*Abstract Co-Author*) Nothing to Disclose Dawei Wang, Beijing, China (*Abstract Co-Author*) Employee, InferVision Yun Shen, PhD, Beijing, China (*Abstract Co-Author*) Employee, General Electric Company Researcher, General Electric Company Xiaotong Yang, Shenyang, China (*Abstract Co-Author*) Nothing to Disclose

For information about this presentation, contact:

weili286@163.com

PURPOSE

To assess the feasibility of 'one-stop' coronary and aortic examination with low contrast agentss by using spectral imaging technique .

METHOD AND MATERIALS

From Oct. 2017 to Apr. 2018, 96 consecutive patients undergoing both coronary and aortic CT angiography(CTA) examination in hospital were randomly divided into two groups. Conventional group (group A):Single-beat prospective electrocardiogram(ECG)-gated coronary CTA examination was followed by aortic CTA.The coronary artery axial scanning was performed before the spiral scanning. The whole scanning process was completed altogether with one-time injection of contrast agent, and the contrast agents was used for 0.85ml/kg. The Spectral group (group B): Single-beat prospective ECG-gated coronary CTA examination was followed by aortic spectral CTA. The contrast agents used 0.55ml/kg. The routine axial CCTA scanning was performed, and the spectrum of aorta was scanned after CCTA. All data were transferred to AW workstation for post-processing and measurement. The coronary artery and the best monochromatic images were processed by workstation. The contrast agent used 0.55ml/kg and recorded the CT values of descending aortic root in both 120kV and 50keV images were calculated. The radiation dose and the contrast agents dosage was recorded. The image quality of the two groups were evaluated by two radiologists by using 5-point scale. The student t test was used to evaluate continuous variables and the Manny-Whitney U test for image quality evaluation.

RESULTS

There was no significant difference in the image quality and radiation dose between the two groups(p>0.5). (Aotic4.6 \pm 0.5:4.4 \pm 0.6,RCA4.7 \pm 0.5:4.8 \pm 0.4,LAD4.6 \pm 0.4:4.5 \pm 0.5 LCX4.7 \pm 0.5:4.6 \pm 0.5,z=1.76,1.38,0.77,0.97) .Compared with the conventional group, the contrast agent was compared: (38.0 \pm 4.3:57.6 \pm 8.3) ml, and the use of contrast agent was reduced in group B. The ED in Group A was not different from the combined ED in Group B and C (2.1 \pm 0.6:1.9 \pm 0.5) mSv.

CONCLUSION

The"one-stop" coronary CTA and aortic spectral CTA is the feasible examination with low contrast agents dosage.

CLINICAL RELEVANCE/APPLICATION

"One-stop" CTA examination with low contrast agents dosage, is a suitable method for the patients with renal function impairment.

RC303-07 Valvular Flow Quantification with Phase Contrast Imaging

Tuesday, Dec. 3 10:20AM - 10:50AM Room: E350

Participants

Michael Markl, PhD, Chicago, IL (*Presenter*) Institutional research support, Siemens AG; Consultant, Circle Cardiovascular Imaging Inc;

LEARNING OBJECTIVES

1) Understand principles and techniques for cardiovascular flow quantification using 2D phase contrast MRI and 4D flow MRI. 2) Describe advantages of 4D flow MRI for the comprehensive assessment of valvular flow characteristics. 3) Identify possible applications of 2D and 4D flow MRI in clinical cardiovascular imaging.

RC303-08 4D Flow MRI Before and After Bicuspid Aortic Valve Sparing Surgery: Assessment of Aortic Flow Patterns for Monitoring of Successful Repair

Tuesday, Dec. 3 10:50AM - 11:00AM Room: E350

Participants

Alexander Lenz, MD, Hamburg, Germany (*Presenter*) Nothing to Disclose Johannes Petersen, MD, Innsbruck, Austria (*Abstract Co-Author*) Nothing to Disclose Martin Sinn, Hamburg, Germany (*Abstract Co-Author*) Nothing to Disclose Christoph Riedel, MD, Hamburg, Germany (*Abstract Co-Author*) Nothing to Disclose Hendrik Kooijmann, PhD, Hamburg, Germany (*Abstract Co-Author*) Employee, Koninklijke Philips NV Gerhard B. Adam, MD, Hamburg, Germany (*Abstract Co-Author*) Nothing to Disclose Hermann Reichenspurner, MD, Hamburg, Germany (*Abstract Co-Author*) Nothing to Disclose Evaldas Girdauskas, MD, Hamburg, Germany (*Abstract Co-Author*) Nothing to Disclose Peter Bannas, MD, Hamburg, Germany (*Abstract Co-Author*) Nothing to Disclose

For information about this presentation, contact:

a.lenz@uke.de

PURPOSE

To assess the feasibility of 4D flow MRI for evaluation of aortic flow patterns in patients with congenital aortic valve disease before and after aortic valve sparing surgical repair.

METHOD AND MATERIALS

20 patients (median age 34.5 years, IQR 29-47; 16 male) with severe aortic regurgitation [15 bicuspid aortic valves (BAV) and 5 unicuspid aortic valves (UAV)] underwent 4D flow MRI at 3T before and after valve sparing aortic repair. Analysis planes were placed at the aortic valve, sinotubular junction, mid-ascending aorta, and proximal arch. The aortic regurgitant fraction (%) was estimated. The degree of helical and vortical flow was evaluated according to a 3-point scale. Relative flow displacement (FD) as a measure of flow eccentricity and wall shear stress (WSS) were estimated. Results before and after surgery were statistically compared using a paired t-test or a Wilcoxon matched-pairs test.

RESULTS

All patients underwent successful aortic valve surgery (17 isolated aortic valve repairs, 3 aortic root procedures with a significant reduction of the aortic regurgitant fraction ($27\pm13\%$ vs. 6 ± 3 , P=0.001). The degree of both helical (1.6 ± 0.6 vs. 0.9 ± 0.5 , P<0.0001) and vortical flow (1.2 ± 0.8 vs. 0.5 ± 0.6 , P=0.002) in the ascending aorta was significantly reduced after valve sparing surgery. Both FD (0.3 ± 0.1 vs. 0.1 ± 0.1 , P=0.003) and WSS (0.6 ± 0.2 vs. 0.4 ± 0.2 , P=0.007) were significantly reduced after surgery at the level of the mid-ascending aorta.

CONCLUSION

4D flow MRI-based assessment of aortic flow patterns allows to monitor the success of valve sparing surgery in patients with bicuspid aortic valve disease.

CLINICAL RELEVANCE/APPLICATION

4D flow MRI allows to evaluate the success of valve repair surgery and may optimize surgical procedures in the future.

RC303-09 Cardiac Magnetic Resonance with 4D Flow Imaging for Mitral Regurgitation Severity Assessment

Tuesday, Dec. 3 11:00AM - 11:10AM Room: E350

Andrea Baggiano, Milan, Italy (Abstract Co-Author) Nothing to Disclose Andrea Guaricci, MD, Foggia, Italy (Abstract Co-Author) Nothing to Disclose Antonella Loffreno, Varese, Italy (Abstract Co-Author) Nothing to Disclose Francesca Baessato, Verona, Italy (Abstract Co-Author) Nothing to Disclose Gloria Cicala, Parma, Italy (Abstract Co-Author) Nothing to Disclose Francesca Ricci, Rome, Italy (Abstract Co-Author) Nothing to Disclose Patrizia Vivona, Milan, Italy (Abstract Co-Author) Nothing to Disclose Alberico del Torto, Milan , Italy (Abstract Co-Author) Nothing to Disclose Laura Fusini, Milan, Italy (Abstract Co-Author) Nothing to Disclose Ilaria Viscone, Milan, Italy (Abstract Co-Author) Nothing to Disclose Giorgia Bonalumi, Milan, Italy (Abstract Co-Author) Nothing to Disclose Marco Zanobini, Milan, Italy (Abstract Co-Author) Nothing to Disclose Francesco Alamanni, Milan, Italy (Abstract Co-Author) Nothing to Disclose Gianluca Pontone, MD, Milan, Italy (Abstract Co-Author) Speakers Bureau, General Electric Company Consultant, General Electric Company Research Consultant, HeartFlow, Inc Speakers Bureau, HeartFlow, Inc Speakers Bureau, Medtronic plc Speakers Bureau, Baver AG

For information about this presentation, contact:

g.muscogiuri@gmail.com

PURPOSE

Cardiac Magnetic Resonance (CMR) has recently emerged as a technique more accurate than echocardiography in assessing the severity of mitral regurgitation (MR). Standard method for mitral regurgitation determination with CMR is measuring the regurgitant volume (RV) as the difference between the LV stroke volume obtained with SSFP (Steady state free precession) cine imaging and the forward flow obtained with phase contrast (PC) imaging. It has already been demostrated that there is a strong correlation between post-surgical left ventricle (LV) remodeling and MR severity as assessed by CMR SSFP - PC. More recently, time-resolved phase contrast CMR with velocity encoding along all three flow directions and three-dimensional (3D) anatomic coverage (also termed '4D flow') has been developed. The purpose of this study was to compare CMR 4D flow and SSFP imaging for the assessment of MR severity using the degree of left ventricular (LV) remodeling after surgery as the reference standard.

METHOD AND MATERIALS

10 consecutive patients (age: 59 ± 10) with indication to mitral valve plasty for severe mitral regurgitation were enrolled. MR severity was assessed using both CMR SSFP - PC imaging and CMR 4D flo imaging without the use of contrast agents. The pre-surgical estimate of regurgitant severity was correlated with the postoperative decrease in LV end-diastolic volume.

RESULTS

Agreement between CMR SSFP-PC imaging and CMR 4D flow imaging for MR regurgitant volume (RV) was excellent for both pre (r = 0.8, p<0.05, mean difference 5.1 mL) and post surgery (r= 0.9, p<0.05) evaluations. There was a strong correlation between post-surgical LV remodeling and MR severity as assessed by CMR 4D flow imaging (r=0.81, p<0.005) that was comparable to CMR SSFP-PC (r=0.78, p<0.005). The average time for MR assessment with CMR SSFP and PC imaging evaluation was 10 minutes, 2 minutes with CMR 4D flow imaging.

CONCLUSION

CMR 4D flow imaging without contrast agents allows an accurate and quick evaluation of MR regurgitant volume. There is a strong correlation between MR severity assessed with CMR 4D flow imaging and post-surgical LV remodeling. Indeed, CMR 4D flow imaging may represent an alternative method for MR severity assessment.

CLINICAL RELEVANCE/APPLICATION

4D flow approach can be extremely helpful for the management of patients with mitral regurgitation.

RC303-10 Multi-parametric Myocardial MR Mapping (T1, T2, T2*)

Tuesday, Dec. 3 11:10AM - 11:40AM Room: E350

Participants

Kate Hanneman, MD, FRCPC, Toronto, ON (Presenter) Nothing to Disclose

LEARNING OBJECTIVES

1) Describe analysis approaches for $T1/T2/T2^*$ parametric maps. 2) Discuss clinical role of $T1/T2/T2^*$ parametric mapping. 3) Identify findings of common diseases on $T1/T2/T2^*$ parametric maps.

RC303-11 Tissue Heterogeneity in Native MR T1/T2 Map Helps Diagnose Cardiac Involvement in Neuromuscular Diseases

Tuesday, Dec. 3 11:40AM - 11:50AM Room: E350

Participants

Lu Huang, MD, Wuhan, China (*Presenter*) Nothing to Disclose Qian Tao, Leiden, Netherlands (*Abstract Co-Author*) Nothing to Disclose Peijun Zhao, Wuhan, China (*Abstract Co-Author*) Nothing to Disclose Baiyun Liu, PhD, Shanghai, China (*Abstract Co-Author*) Employee, Infervision Liming Xia, MD, Wuhan, China (*Abstract Co-Author*) Nothing to Disclose

PURPOSE

Cardiac involvement is common in neuromuscular diseases (NMDs), and is a major cause of progressive heart failure. Subclinical cardiac involvement in NMDs is however difficult to detect. The aim of this study was to investigate the diagnostic value of native MR T1/T2 mapping parameters to detect cardiac involvement in NMDs.

METHOD AND MATERIALS

Sixty subjects (41±16y) diagnosed as NMDs, including 40 idiopathic inflammatory myopathy, 20 non-inflammatory myopathies, and 20 age and gender-matched healthy controls were enrolled in this study. NMDs patients with abnormal ECG or LGE or reduced LVEF/ RVEF were categorized as the cardiac involvement subgroup. All subjects underwent a CMR exam on a 3T MR scanner (Skyra, Siemens Healthineers, Erlangen, Germany), including short-axis SSFP cine, LGE, native T1 and T2 mapping, covering the whole heart. Endocardial and epicardial contours of the left ventricle were manually drawn on short-axis T1 and T2 maps. Six parameters, including mean, median, minimum, maximum and entropy, were calculated from the T1 and T2 map.

RESULTS

Forty-one NMDs patients were categorized as the cardiac involvement subgroup, and the remaining 19 were categorized as the non-involvement subgroup. Compared to the controls, T1 mean, median, SD and entropy, as well as T2 mean, median, and entropy of the cardiac involvement subgroup all elevated significantly (P<0.05 for all 8 parameters), while in the non-involvement subgroup, only native T1 mean and median increased (P<0.05 for both). The heterogeneity parameters, namely, the native T1/T2 SD and entropy, were all significantly higher in the cardiac involvement subgroup compared to then non-involvement subgroup (P <0.05 for all). A multi-variate regression model including all heterogeneous parameters exhibited a diagnostic accuracy of 83% (AUC 0.81, 95%CI: 0.67-0.94) to detect cardiac involvement in NMDs patients.

CONCLUSION

Tissue heterogeneity in the native MR T1/T2 map showed high diagnostic value in identifying cardiac involvement in NMDs patients. The heterogeneity parameter may substitute LGE acquisition which requires contrast agent.

CLINICAL RELEVANCE/APPLICATION

Early detection of cardiac involvement in NMDs can help prevent overt heart failure. Tissue heterogeneity in the native MR T1/T2 map showed high diagnostic value, without use of contrast agent.

RC303-12 Role of Cardiac MRI in Diagnosis in Patients of Cardiac Sarcoidosis Using T1 Mapping, T2 Mapping and Late Gadolinium Enhancement (LGE)

Tuesday, Dec. 3 11:50AM - 12:00PM Room: E350

Participants

Amarinder Singh SR, MBBS, MD, New Delhi, India (*Abstract Co-Author*) Nothing to Disclose Manish Shaw JR, MD, MBBS, Kolkata, India (*Presenter*) Nothing to Disclose Gurpreet S. Gulati, New Delhi, India (*Abstract Co-Author*) Nothing to Disclose Sanjeev Kumar, MBBS, MD, Delhi, India (*Abstract Co-Author*) Nothing to Disclose Arun Sharma SR, MBBS, MD, New Delhi, India (*Abstract Co-Author*) Nothing to Disclose Rishabh Khurana, MBBS, DMD, New Delhi, India (*Abstract Co-Author*) Nothing to Disclose Sheragaru H. Chandrashekhara, MD, New Delhi, India (*Abstract Co-Author*) Nothing to Disclose Dinkar Bhasin SR, MD, New Delhi, India (*Abstract Co-Author*) Nothing to Disclose

For information about this presentation, contact:

drasmalhi@gmail.com

PURPOSE

To determine whether quantitative tissue characterization with T1 mapping, T2 mapping and late gadolinium enhancement supports recognition of myocardial involvement in patients of cardiac sarcoidosis. To correlate cardiac MRI with PET and echocardiography findings.

METHOD AND MATERIALS

Prospective study with size of 19, Patients with biopsy proven extracardiac sarcoidosis presenting to us with suspicion of cardiac involvement were included. MRI was done on 1.5 Tesla scanner (Aera; Siemens, Erlangen, Germany). Cardiac MRI protocol- localizer sequences->cine images in short axis/vertical long axis/4 chamber view->T1W, T2W F - perfusion imaging in short axis/ vertical long axis/4 chamber view->T1W, T2W F - perfusion imaging in short axis/ vertical long axis/4 chamber view->T1W, T2W F - perfusion imaging in short axis/ vertical long axis/4 chamber view->T1W, T2W F - perfusion imaging in short axis/ vertical long axis/4 chamber view->T1W, T2W F - perfusion imaging in short axis/ vertical long axis/4 chamber view->T1 scout, PSIR sequences after 5 and 15 minutes and Post contrast T1W sequence. T1 (using modified Look-Locker imaging-MOLLI T1 maps) and T2 mapping (using hybrid gradient and spin-echo sequence) were performed in a single midventricular short-axis section.

RESULTS

The mean age was 38 years, F:M=10:9. Most common presenting symptom was palpitations. Presence of characteristic midmyocardial LGE was seen in 11/12 patients with confirmed sarcoidosis. T1 mapping is a technique that helps in tissue characterization without contrast. In our study, we did segment wise analysis of T1 mapping values. We compared T1 mapping values in the involved segments in patients with cardiac sarcoidosis with the values from normal segments in healthy controls. We used ROC curve analysis to establish an optimal cut-off value of 1029 sec's with a sensitivity of 87.5% and high specificity of 96.9%. Using this cut-off value we observed that T1 mapping abnormalities were observed in patients with pulmonary sarcoidosis who were suspected to have cardiac involvement but did not show any LGE. Hence, T1 mapping may add incremental value to LGE in patients with suspected cardiac involvement and allow detection of patients who may be LGE negative. Similar to T1 mapping, T2 mapping (tissue water content and are indicative of myocardial edema. can be used to quantify myocardial tissue characteristics. T2 values represent Elevated T2 map values reflect tissue inflammation and are suggestive of disease activity. In the present study we compared T2 values in the LGE positive segments with the T2 values in normal controls and observed statistically significant difference between the two groups. ROC curve analysis yielded a cut-off value of 46.3 milli seconds.with a sensitivity and specificity of 75% and 71.1% respectively.

CONCLUSION

Quantitative tissue characterization in the myocardium with native T1 and T2 mapping helps in the detection of cardiac involvement in patients with systemic sarcoidosis, in relation to inflammation of the myocardium and disease recognition. Cardiac MRI with T1, T2 mapping and LGE have excellent performance in detecting myocardial involvement in patients suspected to have cardiac sarcoidosis.

CLINICAL RELEVANCE/APPLICATION

T1 and T2 mapping values can be used to diagnose the cardiac sarcoidosis (T1 mapping for fibrosis, T2 mapping for edema/inflammation) without giving contrast.

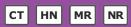




RC306

How Do I Image That? Tips for Improving Challenging Head and Neck Protocols

Tuesday, Dec. 3 8:30AM - 10:00AM Room: E353C



AMA PRA Category 1 Credits ™: 1.50 ARRT Category A+ Credit: 1.75

LEARNING OBJECTIVES

1) Appraise the adequacy of CT and MR protocols for temporal bone imaging. 2) Appropriately modify temporal bone CT and MR protocols based on specific clinical indications. 3) To understand the anatomic challenges faced in imaging structures at the thoracic inlet. 4) To appreciate the importance of adequate dose in parathyroid CT imaging. 5) To be familiar with positioning techniques that will help reduce artifacts and improve visualization of parathyroid adenomas. 6) To simplify the complex imaging anatomy of the brachial plexus using clear anatomical landmarks. 7) To outline the different MR protocols that could be used to image the brachial plexus at 1.5T and 3T. 8) To illustrate the benefits of an adequate MRI technique with some examples. 9) List the MRI pulse sequences used for cranial nerve imaging. 10) Compare the imaging requirements for extracranial versus intracranial cranial nerves. 11) Describe the impact of high resolution cranial nerve imaging on clinical decision making.

Sub-Events

RC306A Optimizing Temporal Bone CT and MRI

Participants

Joseph M. Hoxworth, MD, Scottsdale, AZ (Presenter) Nothing to Disclose

LEARNING OBJECTIVES

1) Appraise the adequacy of CT and MR protocols for temporal bone imaging. 2) Appropriately modify temporal bone CT and MR protocols based on specific clinical indications.

RC306B Optimizing Pituitary MRI

Participants Joshua Lantos, MD, New York, NY (*Presenter*) Nothing to Disclose

For information about this presentation, contact:

jol9057@med.cornell.edu

LEARNING OBJECTIVES

1) Review current techniques in pituitary MRI 2) Briefly review some evidence behind which sequences provide highest yeild imaging 3) Discuss potential future directions of pituitary MRI including sequences to consider adding to our protocols

Active Handout:Joshua Lantos

http://abstract.rsna.org/uploads/2019/19000229/Active RC306B.pdf

RC306C Optimizing TMJ MRI

Participants Bidyut K. Pramanik, MD, Short Hills, NJ (*Presenter*) Nothing to Disclose

For information about this presentation, contact:

bpramanik@northwell.edu

LEARNING OBJECTIVES

1. Optimize TMJ imaging techniques a) Image acquisition b) Review sequences 2. Evaluate normal TMJ anatomy 3. Briefly review MRI findings of internal derangement

RC306D Optimizing Parathyroid 4D CT

Participants Deborah R. Shatzkes, MD, New York, NY (*Presenter*) Nothing to Disclose

For information about this presentation, contact:

shatzkes@hotmail.com

LEARNING OBJECTIVES

1) To understand the anatomic challenges faced in imaging structures at the thoracic inlet. 2) To appreciate the importance of adequate dose in parathyroid CT imaging. 3) To be familiar with positioning techniques that will help reduce artifacts and improve visualization of parathyroid adenomas.

Active Handout:Deborah Rachelle Shatzkes

http://abstract.rsna.org/uploads/2019/19000231/Active RC306D.pdf

RC306E Optimizing Brachial Plexus MRI

Participants Carlos H. Torres, MD,FRCPC, Ottawa, ON (*Presenter*) Nothing to Disclose

For information about this presentation, contact:

catorres@toh.ca

LEARNING OBJECTIVES

1) To simplify the complex imaging anatomy of the brachial plexus using clear anatomical landmarks. 2) To outline the different MR protocols that could be used to image the brachial plexus at 1.5T and 3T. 3) To illustrate the benefits of an adequate MRI technique with some examples.

RC306F Optimizing Cranial Nerve MRI

Participants

Nafi Aygun, MD, Baltimore, MD (Presenter) Nothing to Disclose

LEARNING OBJECTIVES

1) List the MRI pulse sequences used for cranial nerve imaging. 2) Compare the imaging requirements for extracranial versus intracranial cranial nerves. 3) Describe the impact of high resolution cranial nerve imaging on clinical decision making.





RC312

Body MR Angiography: 2019 Update

Tuesday, Dec. 3 8:30AM - 10:00AM Room: N229



AMA PRA Category 1 Credits ™: 1.50 ARRT Category A+ Credit: 1.75

FDA Discussions may include off-label uses.

Participants

Maureen N. Hood, PhD,RN, Bethesda, MD (*Moderator*) In-kind support, General Electric Company Scott B. Reeder, MD,PhD, Madison, WI (*Moderator*) Nothing to Disclose

Sub-Events

RC312A MRA Techniques

Participants Scott B. Reeder, MD,PhD, Madison, WI (*Presenter*) Nothing to Disclose

LEARNING OBJECTIVES

1) Understand the fundamental principles of contrast enhanced MRA. 2) Understand the fundamental principles of non-contrast enhanced MRA. 3) Understand the fundamental principles of phase velocity MRA.

RC312B Thoracic MRA: Clinical Applications

Participants

Robert A. Liotta, MD, Kensington, MD (Presenter) Nothing to Disclose

For information about this presentation, contact:

robert.liotta@usuhs.edu

LEARNING OBJECTIVES

1) Identify common clinical applications for thoracic MRA. 2) Describe the role for non-contrast versus contrast-enhanced thoracic MRA.

RC312C Abdominal/Pelvic MRA: Clinical Applications

Participants Pamela J. Lombardi, MD, Chicago, IL (*Presenter*) Nothing to Disclose

LEARNING OBJECTIVES

1) Describe current contrast enhanced and non contrast MR angiography techniques. 2) Present clinical applications of MR angiography. 3) Introduce future perspectives for MRA.

RC312D MR Safety Concerns in Cardiovascular Patients

Participants Maureen N. Hood, PhD,RN, Bethesda, MD (*Presenter*) In-kind support, General Electric Company

For information about this presentation, contact:

maureen.hood@usuhs.edu

LEARNING OBJECTIVES

1) Discuss the importance of an MR Safety Program in your institution. 2) Describe safety concerns related passive and active cardiovascular devices. 3) Explain the evaluation MR safety procedures for electronic devices. 4) Discuss contrast agent concerns and safety recommendations in MRA.

ABSTRACT

MR safety is a team effort. Cardiovascular patients often need special care and the use of contrast agents. MRI settings that perform cardiac MR and MRA regularly should have advanced education in MR safety. Staff should be trained annually on MR safety, especially with the growth in the number of patients with implanted active cardiovascular devices. Training and proper selection of staff are required for certain active devices. The off-label use of contrast agent use, both gadolinium and iron will be presented along with adverse events the MR team needs to be prepared for. Teamwork is critical for optimal patient care.

Active Handout: Maureen Nanette Hood

http://abstract.rsna.org/uploads/2019/18002591/RC312D Hood MR Safety Concerns 2019_Handout.pdf



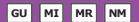




RC317

Emerging Technologies: Prostate Cancer Imaging & Management - Update 2019

Tuesday, Dec. 3 8:30AM - 10:00AM Room: S505AB



AMA PRA Category 1 Credits ™: 1.50 ARRT Category A+ Credit: 1.75

FDA Discussions may include off-label uses.

Participants

Peter L. Choyke, MD, Rockville, MD (Moderator) Nothing to Disclose

For information about this presentation, contact:

pchoyke@mail.nih.gov

LEARNING OBJECTIVES

1) Understand current issues in prostate cancer relevant to imaging. 2) Understand the role of emerging technologies in the imaging and management of prostate cancer.

ABSTRACT

Prostate cancer is a major health issue. Imaging has made great strides in the last decade including the use of multiparametric MRI, MR-ultrasound fusion biopsies and most recently PET scanning. This refresher course explores emerging technolgies in prostate cancer imaging and management.

Sub-Events

RC317A Introduction to Imaging in Prostate Cancer

Participants

Peter L. Choyke, MD, Rockville, MD (Presenter) Nothing to Disclose

For information about this presentation, contact:

pchoyke@mail.nih.gov

LEARNING OBJECTIVES

1) Understand the impact of new screening guidelines on imaging of prostate cancer. 2) Understand the issues facing clinicians treating prostate cancer.

ABSTRACT

This talk will provide an overview regarding the major issues of imaging in prostate cancer including screening and detection, initial staging, biochemical recurrence and metastatic disease. Recent trends in the management of prostate cancer from active surveillance to first and second line androgen deprivation, radium and chemotherapy/immunotherapy will be briefly discussed. The role of imaging in prostate cancer is becoming much more central than it was a decade ago and this talk will set the stage for other talks in the session that will provide new details regarding novel imaging methods.

RC317B Next Generation Prostate MRI

Participants

Baris Turkbey, MD, Bethesda, MD (*Presenter*) Research support, Koninklijke Philips NV; Royalties, Invivo Corporation; Investigator, NVIDIA Corporation

For information about this presentation, contact:

turkbeyi@mail.nih.gov

LEARNING OBJECTIVES

1) Understand current status and uses of multi-parametric MRI. 2) Understand role of MRI in assessment of prostate cancer aggressiveness and tumor heterogeneity. 3) Understand role of computer aided diagnosis systems in evaluation of prostate cancer aggressiveness and tumor heterogeneity.

RC317C Molecular Prostate Imaging: Chemistry to Clinic

Participants

Martin G. Pomper, MD, PhD, Baltimore, MD (*Presenter*) Research Grant, Progenics Pharmaceuticals, Inc; Royalties, Progenics Pharmaceuticals, Inc

For information about this presentation, contact:

mpomper@jhmi.edu

LEARNING OBJECTIVES

1) To compare and contrast the imaging characteristics of present and emerging molecular imaging agents for prostate cancer. 2) To describe how emerging molecular imaging agents for prostate cancer are being integrated into clinical practice. 3) To focus on PET agents targeting the prostate-specific membrane antigen (PSMA) with respect to a new structured reporting system proposed to enhance clinical management.

ABSTRACT

n/a

RC317D Hyperpolarized C-13 MR Molecular Imaging of Prostate Cancer

Participants

Daniel B. Vigneron, PhD, San Francisco, CA (Presenter) Research Grant, General Electric Company;

LEARNING OBJECTIVES

1) To describe the basic principles and techniques used in hyperpolarized carbon-13 MRI. 2) Understand the cellular metabolic reprogramming that occurs in prostate cancer. 3) Demonstrate the changes in pyruvate to lactate conversion that are observed in prostate cancer and differences with cancer aggressiveness and response to therapy.

RC317E Radionuclide Therapy for Prostate Cancer

Participants

Frank I. Lin, MD, Bethesda, MD (Presenter) Nothing to Disclose

For information about this presentation, contact:

Frank.lin2@nih.gov





RC321

Innovations in MR

Tuesday, Dec. 3 8:30AM - 10:00AM Room: S102CD



AMA PRA Category 1 Credits ™: 1.50 ARRT Category A+ Credit: 1.75

FDA Discussions may include off-label uses.

Participants

Matthew A. Bernstein, PhD, Rochester, MN (Coordinator) Former Employee, General Electric Company

LEARNING OBJECTIVES

1) Review newer techniques that can be used to accelerate MR including simultaneous multislice (SMS), compressed sensing, and MR fingerprinting. 2) Review the basic principles of chemical exchange saturating transfer, and discuss its emerging applications. 3) Review recent advances in novel MR systems, including low cryogen magnets, dedicated and compact systems.

Sub-Events

RC321A New Directions in Fast MR

Participants

Kawin Setsompop, Charlestown, MA (*Presenter*) Research Grant, Siemens AG; Royalties, General Electric Company; Royalties, Koninklijke Philips NV; Scientific Advisory Board, Kineticor;

LEARNING OBJECTIVES

1) Describe emerging MR acquisition approaches and their ability to provide faster and higher quality imaging. 2) Identify the most suitable acquisition approach for improving the quality of various imaging sequences/clinical applications.

RC321B New Directions in CEST

Participants

Peter C. van Zijl, PhD, Baltimore, MD (*Presenter*) Research support, Koninklijke Philips NV; Patent agreement, Koninklijke Philips NV; Speakers Bureau, Koninklijke Philips NV

LEARNING OBJECTIVES

1) Understand the basics of CEST, endogenous and exogenous contrast. 2) Be aware of latest applications of CEST in the clinic. 3) Understand interpretation of Amide Proton Transfer weighted (APTw) MRI for assessing brain tumors, including for separating high/low grade, separating progression/pseudoprogression, relationship to IDH status. 4) Be aware of possible contrast agents for CEST MRI.

ABSTRACT

Chemical Exchange Saturation Transfer (CEST) is a relatively new field of magnetic resonance (MR) that combines principles of MR spectroscopy (MRS, chemical selectivity of proton pools) and MRI (imaging of water protons with high sensitivity). It is based on magnetization transfer, especially exploiting the interaction of the exchangeable protons of probe molecules with the water protons to achieve large sensitivity enhancements (several orders of magnitude) for the imaging of molecular information with MRI sensitivity. CEST MRI can be done both using paramagnetic and diamagnetic probes, but the ultimate strength and hope for fast clinical translation lies in the presence of endogenous contrast (e.g. cellular proteins and tissue metabolites, such as glutamate) and in the use of diamagnetic agents, expected to have lower toxicity and to be more applicable for regulatory approval and patient acceptance. After an introduction of the basic principles of CEST MRI to provide insight into the type of molecules that can be studied and the sensitivity of this approach, I will explain the main contributions to the in vivo saturation spectrum (Z-spectrum) and its relationship to the proton MR spectrum. Several application examples will be presented to illustrate the potential of using these signals for clinical diagnosis and prognosis.1) imaging of endogenous proteins, especially the use of amide proton transfer weighted (APTw) MRI for brain tumor diagnosis, including separation of high and low grade, judging progression versus pseudoprogression and the effect of IDH status. 2) Imaging of glutamate.3) Use of simple diamagnetic probes such as D-Glucose and its polymers for imaging tissue perfusion, membrane permeability and metabolism.4) Novel approaches for the future. These examples are only early illustrations of this relatively new field, which has great potential due to the presence of exchangeable protons in most molecular agents.Literature:1) van Zijl PC, Yadav NN. Chemical exchange saturation transfer (CEST): what is in a name and what isn't? Magn Reson Med. 2011 Apr;65(4):927-48. 2) Zhou J, Heo HY, Knutsson L, van Zijl PCM, Jiang S. APTweighted MRI: Techniques, current neuro applications, and challenging issues. J Magn Reson Imaging. 2019 Jan 20. doi: 10.1002/jmri.26645. [Epub ahead of print] Review. 3) Jones KM, Pollard AC, Pagel MD. Clinical applications of chemical exchange saturation transfer (CEST) MRI. J Magn Reson Imaging. 2018 Jan;47(1):11-27

RC321C New Directions in MR Scanners

Participants

Yunhong Shu, PhD, Rochester, MN (Presenter) Nothing to Disclose

For information about this presentation, contact:

LEARNING OBJECTIVES

1) List a variety of emerging technologies for MRI scanner design. 2) Understand major driving forces for these technology advancements. 3) Identify the advantages and suitable applications for specific MR scanners.

Active Handout:Yunhong Shu

http://abstract.rsna.org/uploads/2019/19001802/Active RC321C.pdf





RC329

Liver MRI Essentials (Interactive Session)

Tuesday, Dec. 3 8:30AM - 10:00AM Room: N227B



AMA PRA Category 1 Credits ™: 1.50 ARRT Category A+ Credit: 1.75

Sub-Events

RC329A HCC: Typical and Atypical Appearances

Participants

Kathryn J. Fowler, MD, San Diego, CA (*Presenter*) Consultant, 12 Sigma Technologies; Researcher, Nuance Communications, Inc; Contractor, Midamerica Transplant Services; ;

For information about this presentation, contact:

k1fowler@ucsd.edu

LEARNING OBJECTIVES

1) Review pathological sub-types of HCC. 2) Gain knowledge of the imaging appearance of atypical HCC. 3) Understand impact on management.

RC329B Intrahepatic Cholangiocarcinoma

Participants

Sara Lewis, MD, New York, NY (Presenter) Nothing to Disclose

LEARNING OBJECTIVES

1) Identify the risk factors and clinical features of intrahepatic cholangiocarcinoma (ICC). 2) Examine the cross-sectional typical and atypical imaging characteristics of ICC, with emphasis on CT and MRI. 3) Identify imaging and clinical features that aid in accurate diagnosis of ICC compared to other malignant and benign hepatic lesions.

RC329C Hilar/Perihilar Cholangiocarcinoma

Participants

Koenraad J. Mortele, MD, Boston, MA (Presenter) Nothing to Disclose

RC329D FNH and Hepatocellular Adenomas

Participants

Maxime Ronot, MD, Clichy, France (Presenter) Nothing to Disclose

For information about this presentation, contact:

maxime.ronot@aphp.fr

LEARNING OBJECTIVES

1) To be able to recognize and non-invasively diagnose typical forms of FNH. 2) To understand the pathomolecular classification of hepatic adenomas. 3) To know how to differentiate FNH from adenomas on imaging. 4) To understand the value and pitfalls of liver-specific contrast agents.

RC329E Liver Metastases

Participants Frank H. Miller, MD, Chicago, IL (*Presenter*) Nothing to Disclose

LEARNING OBJECTIVES

1) To be able to identify findings to identify and characterize liver lesions as metastases. 2) To use a variety of MR sequences to detect and distinguish metastases from other benign lesions such as hemangiomas.



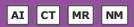




SPAI31

RSNA AI Deep Learning Lab: Generative Adversarial Networks (GANs)

Tuesday, Dec. 3 10:30AM - 12:00PM Room: AI Showcase, North Building, Level 2, Booth 10342



AMA PRA Category 1 Credits ™: 1.50 ARRT Category A+ Credit: 1.75

Participants

Bradley J. Erickson, MD, PhD, Rochester, MN (*Presenter*) Board of Directors and Stockholder, VoiceIt Technologies, LLC; Board of Directors, FlowSigma, LLC; Officer, FlowSigma, LLC; Stockholder, FlowSigma, LLC;

Special Information

In order to get the best experience for this session, it is highly recommended that attendees bring a laptop with a keyboard, a decent-sized screen, and the latest version of Google Chrome. Additionally, it is recommended that attendees have a basic knowledge of deep learning programming and some experience running a Google CoLab notebook. Having a Gmail account is also helpful. Here are instructions for creating and deleting a Gmail account.

ABSTRACT

This course describes a more recent advance in deep learning known as Generative Adversarial Networks (GANs). GANs are a deep learning technology in which a computer is trained to create images that look very 'real' even though they are completely synthetic. Getting 'large enough' data sets is a problem for most deep learning applications, and this is particularly true in medical imaging. This may be one way to address the 'data shortage' problem in medicine. GANs have also been created that can convert MRIs to CTs (e.g. for attenuation correction with MR/PET).



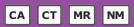




SSG02

Cardiac (CT, MRI, and Nuclear Medicine: General Topics)

Tuesday, Dec. 3 10:30AM - 12:00PM Room: S104A



AMA PRA Category 1 Credits ™: 1.50 ARRT Category A+ Credit: 1.75

Participants

Tarun Pandey, MD, FRCR, Little Rock, AR (*Moderator*) Nothing to Disclose Scott R. Akers, MD, PhD, Philadelphia, PA (*Moderator*) Nothing to Disclose

Sub-Events

SSG02-02 Imaging Findings after Aortic Valve Implantation on 18F-Fluorodeoxyglucose Positron Emission Tomography with Computed Tomography

Tuesday, Dec. 3 10:40AM - 10:50AM Room: S104A

Participants

Ali R. Wahadat, MD,MSc, Rotterdam, Netherlands (*Abstract Co-Author*) Nothing to Disclose Wilco Tanis, The Hague, Netherlands (*Abstract Co-Author*) Nothing to Disclose Asbjorn Scholtens, MD, Utrecht, Netherlands (*Abstract Co-Author*) Nothing to Disclose Margreet Bekker, Rotterdam, Netherlands (*Abstract Co-Author*) Nothing to Disclose Laura H. Graven, MD, Rotterdam, Netherlands (*Abstract Co-Author*) Nothing to Disclose Laurens E. Swart, MD, Rotterdam, Netherlands (*Abstract Co-Author*) Nothing to Disclose Annemarie M. Den Harder, MD, Utrecht, Netherlands (*Abstract Co-Author*) Nothing to Disclose Marnix G. Lam, MD, Utrecht, Netherlands (*Abstract Co-Author*) Nothing to Disclose Linda M. de Heer, MD, Utrecht, Netherlands (*Abstract Co-Author*) Nothing to Disclose Jolien Roos - Hesselink, Rotterdam, Netherlands (*Abstract Co-Author*) Nothing to Disclose Ricardo P. Budde, MD,PhD, Rotterdam, Netherlands (*Presenter*) Nothing to Disclose

PURPOSE

Although 18F-Fluorodeoxyglucose (18F-FDG) Positron Emission Tomography (PET) with computed tomography (CT) is an essential tool in diagnosing prosthetic heart valve (PHV) endocarditis, the normal uptake patterns after PHV implantation have not been studied prospectively. We prospectively assessed perivalvular FDG uptake at different time points after aortic PHV implantation.

METHOD AND MATERIALS

Patients who had undergone uncomplicated aortic PHV implantation were included and underwent 18F-FDG PET/CT at $5(\pm 1)$ weeks (group 1), $12(\pm 2)$ weeks (group 2) or $52(\pm 8)$ weeks (group 3) after implantation. After a preparatory diet to suppress normal myocardial glucose uptake, FDG uptake in the myocardium as well as around the PHV was scored using the Qualification Visual Score for Hypermetabolism (QVSH) as 'none' (< mediastinum), 'mild' (> mediastinum but < liver), 'moderate' (> liver), or 'severe' (intense uptake) and quantitative analysis was performed with maximum Standardized Uptake Value (SUVmax) and target to background ratio (SUVratio) on standardized European Association of Nuclear Medicine Research Ltd. (EARL) reconstructions by an experienced nuclear medicine physician.

RESULTS

In total 37 patients (group 1: n=12, group 2: n=12, group 3: n=13) (age 66±8 years) were included. Myocardial FDG uptake was moderate or less in 29/37 scans (78%). QVSH around the PHV was in 8/12 (67%) mild and 4/12 (33%) moderate in group 1, 7/12 (58%) mild and 5/12 (42%) moderate in group 2 and 8/13 (62%) mild and 5/13 (38%) moderate in group 3 (p=0.91). No scan was scored as 'none' or 'severe'. EARL SUVmax was 3.48 ± 0.57 , 3.50 ± 0.59 and 3.34 ± 0.55 (mean±SD, p=0.77) and EARL SUVratio was 2.00 ± 0.29 , 1.96 ± 0.41 and 1.71 ± 0.26 (mean±SD, p=0.07) for groups 1, 2 and 3, respectively.

CONCLUSION

Baseline FDG uptake around aortic PHV at 5, 12 and 52 weeks after implantation is similar and mild in the majority of cases with an overall mean SUVmax and SUVratio of 3.44±0.56 and 1.89±0.34 respectively.

CLINICAL RELEVANCE/APPLICATION

Knowing the normal baseline FDG uptake around prosthetic heart valves on 18F-FDG-PET-CT is essential to discriminate between normal and infected valves in patients suspected of endocarditis.

SSG02-03 Accuracy of Absolute Myocardial Blood Flow Quantification with Dual-Source CT: Validation in Human Using 150-Water PET

Tuesday, Dec. 3 10:50AM - 11:00AM Room: S104A

Participants Masafumi Takafuji, Tsu, Japan (*Presenter*) Nothing to Disclose Kakuya Kitagawa, MD, PhD, Tsu, Japan (*Abstract Co-Author*) Nothing to Disclose Masaki Ishida, MD, PhD, Tsu, Japan (*Abstract Co-Author*) Nothing to Disclose Yasutaka Ichikawa, MD, Tsu, Japan (*Abstract Co-Author*) Nothing to Disclose Satoshi Nakamura, MD, Tsu, Japan (*Abstract Co-Author*) Nothing to Disclose Yoshitaka Goto, MD, Tsu-city, Japan (*Abstract Co-Author*) Nothing to Disclose Hajime Sakuma, MD, Tsu, Japan (*Abstract Co-Author*) Research Grant, EIZAI; Research Grant, DAIICHI SANKYO Group; Research Grant, FUJIFILM Holdings Corporation; Research Grant, Guerbet SA; Research Grant, Nihon Medi-Physics Co, Ltd;

PURPOSE

15O-water PET is the most accurate method in quantifying myocardial blood flow (MBF). Model-based analysis of perfusion CT with correction of flow-dependent alteration in extraction fraction(E) of iodine contrast medium may permit quantification of absolute MBF. The purpose of this study was to determine the accuracy of CT measurements of stress MBF by CT using 15O-water PET as a reference.

METHOD AND MATERIALS

Thirty-four patients (70±8 years, 27 male) with known or suspected coronary artery disease(CAD) underwent dynamic stress CT perfusion and stress 150-water PET. Perfusion index (PI) was quantified in 16 myocardial segments with a dual-source CT and its dedicated software (Force/VPCT body, Siemens) based on maximal upslope method. Since PI is mathematically equivalent to unidirectional influx constant in compartment model analysis, PI can be expressed as a product of MBF and E. For the quantification of stress MBF using 150-water PET, non-commercial software (Carimas) was used. The E of iopamidol was determined using CT-derived PI and PET-derived MBF (PET-MBF) in 17 subjects (pilot group). For validation, CT-derived MBF (CT-MBF) was calculated using the relation between E and CT-derived PI for the remaining 17 patients (validation group) and compared with PET-MBF. The segments with myocardial infarction were excluded from the analysis.

RESULTS

In the pilot group, CT-derived PI was 1.33 ± 0.27 ml/min/g and PET-MBF value was 2.80 ± 0.84 ml/min/g, respectively. From these data, the relationship between E and MBF was E = $1-\exp[-(0.11\times MBF+1.58)/MBF]$. In the validation group, CT-MBF was 2.40 ± 2.03 ml/min/g, while PET-MBF was 2.54 ± 2.03 ml/min/g. CT-MBF showed a good linear correlation with PET-MBF (r= 0.93, P<000.1). The measurement bias in measuring MBF between CT and PET was 0.14 ± 0.73 ml/min/g.

CONCLUSION

The relationship between E of iodine contrast medium and MBF was determined in this study. By using the relationship, stress MBF can be accurately quantified from the perfusion index obtained from dual-source CT and its dedicated analysis software.

CLINICAL RELEVANCE/APPLICATION

CT-MBF quantification has potential to provide detection of perfusion abnormality and risk stratification in patients with known or suspected CAD with high accuracy comparable to 150-water PET.

SSG02-04 Development of an Automated Software for 3D Quantification of Extracellular Volume in Cardiac CT: Comparison with Cardiac MRI

Tuesday, Dec. 3 11:00AM - 11:10AM Room: S104A

Participants

Mohamed Refaat Nouri, MD, Paris, France (*Abstract Co-Author*) Nothing to Disclose Virgile Chevance, Creteil , France (*Presenter*) Nothing to Disclose Islem Sifaoui, Angers, France (*Abstract Co-Author*) Nothing to Disclose Haytham Derbel, MD, Maisons-Alfort, France (*Abstract Co-Author*) Nothing to Disclose Daphne Gerbaud, Creteil, France (*Abstract Co-Author*) Employee, General Electric Company Vania Tacher, MD, Baltimore, MD (*Abstract Co-Author*) Nothing to Disclose Alain Luciani, MD,PhD, Creteil Cedex, France (*Abstract Co-Author*) Research Consultant, Bracco Group Research Grant, Bracco Group Research Consultant, General Electric Company Research Consultant, Siemens AG Hicham H. Kobeiter, MD, Creteil, France (*Abstract Co-Author*) Nothing to Disclose Jean-Francois Deux, Paris, France (*Abstract Co-Author*) Nothing to Disclose

For information about this presentation, contact:

refaat.nouri@gmail.com

PURPOSE

The objective of our study is to develop and validate a software for automatic three-dimensional (3D) measurement of myocardial extracellular volume (ECV) in cardiac CT compared to CMR in patients with cardiac amyloidosis (CA)

METHOD AND MATERIALS

Twenty patients with a proven diagnosis of CA and 20 control patients free of cardiac pathology were included. Unenhanced and late enhanced (5 minutes) cardiac CT images were analyzed automatically by the software. Duration of processing was recorded. Manual measurements of myocardial attenuation were performed on both sets of images by one operator within the interventricular septum (IVS) as usually performed in clinical practice. Automatic and manual values of ECV were calculated using biological hematocrit and synthetic hematocrit (derived from blood pool attenuation values). Measurements were correlated together and with MR measurements for all patients.

RESULTS

3D automatic segmentation of unenhanced and late enhanced cardiac CT images was successfully performed by the software for all patients. The duration of myocardial segmentation was 20 +/- 5 seconds. The software was able to provide 3D ECV values for all patients. Automated (30+/-20%) and manual (32+/-18%) measurements of ECV were well correlated each other (r2=0.8; p<0.005), and significantly correlated (r2>0.7; p<0.05) with the ECV measured by CMR (34+/-21%). Automatic and manual ECV values calculated with synthetic hematocrit did not significantly differ from biological ones.

CONCLUSION

Automated 3D measurement of ECV in cardiac CT is feasible and well correlated with manual measurements and CMR values. These

results have to be confirmed on a wider range of patients (work in progress)

CLINICAL RELEVANCE/APPLICATION

Myocardial extracellular volume (ECV) is a good diagnostic and prognostic marker in cardiac diseases. ECV measurement is traditionally performed with cardiac magnetic resonance (CMR). Assessment of ECV in cardiac CT may help to use it more often in clinical practice.

SSG02-05 Assessment of Myocardial Extracellular Volume on Routine Body Computed Tomography in Breast Cancer Patients Treated with Anthracyclines

Tuesday, Dec. 3 11:10AM - 11:20AM Room: S104A

Participants

Caterina B. Monti, MD, Milano, Italy (*Presenter*) Nothing to Disclose Tommaso Bosetti, Milan, Italy (*Abstract Co-Author*) Nothing to Disclose Marco Ali, Milan, Italy (*Abstract Co-Author*) Nothing to Disclose Moreno Zanardo, MSc, San Donato Milanese, Italy (*Abstract Co-Author*) Nothing to Disclose Elena De Benedictis, Milan , Italy (*Abstract Co-Author*) Nothing to Disclose Francesco Secchi, MD,PhD, Milano, Italy (*Abstract Co-Author*) Nothing to Disclose Alberto Luporini, Milan, Italy (*Abstract Co-Author*) Nothing to Disclose Francesco Sardanelli, MD, San Donato Milanese, Italy (*Abstract Co-Author*) Speakers Bureau, Bracco Group Advisory Board, Bracco Group Research Grant, Bayer AG Advisory Board, General Electric Company Reserach Grant, General Electric Company Speakers Bureau, Siemens AG Reserach Grant, Real Imaging Ltd

For information about this presentation, contact:

francesco.secchi@unimi.it

PURPOSE

To evaluate the feasibility of estimating myocardial extracellular volume (ECV) on routine thoracic contrast-enhanced CT in breast cancer patients, and, if feasible, to assess if a rise in ECV is associated with anthracyclines administration even in absence of clinical symptoms or echocardiographic changes.

METHOD AND MATERIALS

After Ethics Committee approval, female patients with breast cancer who had undergone routine CT examinations at our institution before and shortly after the end of chemotherapy including anthracyclines were retrospectively evaluated. Patients without available haematocrit, with CT images with artefacts, or who had undergone radiation therapy of the left breast were excluded. Follow-up CT examinations were also analysed, when available. ECV was calculated on scans obtained at about 1, 3, and 7 min after contrast injection.

RESULTS

Thirty-two female patients (aged 57±13 years, mean±standard deviation) with pre-treatment haematocrit 38±4%, and ejection fraction 64±6% were analysed. Pre-treatment ECV was 27.0±2.9% at 1 min, 27.4±3.8% at 3 min, and 26.4±3.8% at 7 min, similar to normal values reported for normal subjects in the literature. Post-treatment ECV (median interval: 89 days after treatment) was $31.1\pm4.9\%$, $32.5\pm5.0\%$, and $30.0\pm5.1\%$, respectively, values significantly higher than pre-treatment values at all times (p < 0.005). ECV at follow-up (median interval: 135 days after post-treatment CT) was $31.0\pm4.5\%$, $30.0\pm3.4\%$, and $27.7\pm3.7\%$, respectively, without significant differences (p > 0.548) when compared to post-treatment values.

CONCLUSION

After anthracyclines treatment, ECV was significantly higher than pre-treatment values. In the follow-up ECV remains higher than pre-treatment values.

CLINICAL RELEVANCE/APPLICATION

Myocardial ECV values from routine contrast-enhanced CT scans could play a role in the assessment of myocardial condition in breast cancer patients undergoing anthracycline-based chemotherapy.

SSG02-06 Cardiac Energetics Alteration in Chronic Hypoxia Rat Model: A Non-Invasive In Vivo 31P Magnetic Resonance Spectroscopy Experimental Study

Tuesday, Dec. 3 11:20AM - 11:30AM Room: S104A

Participants Yinsu Zhu, Nanjing, China (Presenter) Nothing to Disclose

For information about this presentation, contact:

zhuyinsu@njmu.edu.cn

PURPOSE

Energetics alteration plays a key role in the process of myocardial injury in chronic hypoxic diseases (CHD).31P magnetic resonance spectroscopy (MRS) can investigate alterations in cardiac energetic in vivo. This study was aimed to characterize the potential of 31P MRS in evaluating cardiac energetics alteration of chronic hypoxia rats (CHR).

METHOD AND MATERIALS

Thirty CHR were induced by SU5416 combined with hypoxia. 31P MRS (Bruker BioSpec 7.0T) was performed weekly (0-5 week) to follow-up the ratio of concentrations of phosphocreatine (PCr) to adenosine triphosphate (ATP) (PCr/ATP). The index of myocardial structure and systolic function, including the left ventricular function (LVEF) and the right ventricular function (RVEF), were also measured by magnetic resonance imaging (MRI) in each rat. The myocardial injury was shown based on hematoxylin and eosin (H&E) staining and Masson's trichrome staining.

RESULTS

Along weeks, the resting cardiac PCr/ATP ratio decreased from 0 to 5 weeks of modeling. The ratio dropped more markedly after injection of isoproterenol and recovered slowly thereafter. The declension of resting cardiac PCr/ATP ratio in CHR can be observed at the first week, compared with the healthy ones((3.92±0.43vs.4.48±0.56, P<0.05). While the LVEF and RVEF in CHR was similar to healthy rats. Also, the myocardial injury cannot be observed in the first week.

CONCLUSION

31P MRS can sensitivily reveal the cardiac energetics alteration in CHD before the onset of myocardial injury and ventricular dysfunction.

CLINICAL RELEVANCE/APPLICATION

31P MRS at 7.0 T can investigate cardiac energetics alteration in chronic hypoxia rat. Of note, defects in energy regulation were present before detectable myocardial injury and ventricular dysfunction.

SSG02-07 Complete Free-Breathing Adenosine Stress Cardiac MRI Using Compressed Sensing and Motion Correction: Comparison of Functional Parameters, Perfusion and Late Enhancement with the Standard Examination in Breathhold

Tuesday, Dec. 3 11:30AM - 11:40AM Room: S104A

Participants

Wolfgang Wust, MD, Erlangen, Germany (Presenter) Speakers Bureau, Siemens AG Matthias S. May, MD, Erlangen, Germany (Abstract Co-Author) Speakers Bureau, Siemens AG Rafael Heiss, Erlangen, Germany (Abstract Co-Author) Speakers Bureau, Siemens AG Michael Uder, MD, Erlangen, Germany (Abstract Co-Author) Nothing to Disclose Christoph Treutlein, Erlangen, Germany (Abstract Co-Author) Nothing to Disclose

For information about this presentation, contact:

wolfgang.wuest@uk-erlangen.de

PURPOSE

Stress cardiac MRI (CMR) is a demanding examination with multiple breathholds (BH) and long scan times. Aim of this study was to compare free breathing (FB) examinations with the gold standard acquired in BH.

METHOD AND MATERIALS

40 consecutive patients were enrolled prospectively and examined on a 3T MRI. Functional imaging, perfusion and late gadolinium enhancement (LGE) were performed in BH and in FB using compressed sensing and inline motion correction. Left (LV) and right ventricle (RV) functional parameters in BH and FB were compared using Bland-Altman plots and subjective image quality was assessed on a 5-point scale (1=non diagnostic to 5=very good). For perfusion and LGE imaging diagnostic confidence was rated on a 3-point scale (1=low up to 3=high) and image quality on a 5-point scale (1=non diagnostic to 5=very good). Wilcoxon test was used to compare image quality and diagnostic confidence.

RESULTS

Bland-Altman plots showed good agreement for LV and RV functional parameters in BH and FB. Subjective image quality was significantly better with BH for LV (p<0.01) but comparable for RV (p=1.0). Scan time for cine BH was 218s (range 130s-385s), for cine FB 16s (range 11-27s). Extent of perfusion defects, LGE and diagnostic confidence was comparable between both groups. Scan time for LGE BH was 371s (range 239-502s), for LGE FB 189s (range 122-286s).

CONCLUSION

FB adenosine stress CMR examination delivers diagnostic image quality and could represent an alternative for patients who are unable to meet the demands of multiple BH and long examination times.

CLINICAL RELEVANCE/APPLICATION

Free breathing stress cardiac MRI can be performed in significantly shorter time than the gold standard in breathhold.

SSG02-08 Image Quality and Reliability of a Novel Dark Blood Late Gadolinium Enhancement Sequence in Ischemic Cardiomyopathy

Tuesday, Dec. 3 11:40AM - 11:50AM Room: S104A

Participants

Giuseppe Muscogiuri, MD, Milano, Italy (Presenter) Nothing to Disclose Marco Gatti, MD, Turin, Italy (Abstract Co-Author) Nothing to Disclose Serena Dell'Aversana, MD, San Marcellino , Italy (Abstract Co-Author) Nothing to Disclose Marco Guglielmo, Milan, Italy (Abstract Co-Author) Nothing to Disclose Andrea Baggiano, Milan, Italy (Abstract Co-Author) Nothing to Disclose Andrea Guaricci, MD, Foggia, Italy (Abstract Co-Author) Nothing to Disclose Gloria Cicala, Parma, Italy (Abstract Co-Author) Nothing to Disclose Francesca Ricci, Rome, Italy (Abstract Co-Author) Nothing to Disclose Antonella Loffreno, Varese, Italy (Abstract Co-Author) Nothing to Disclose Francesca Baessato, Verona, Italy (Abstract Co-Author) Nothing to Disclose Alberico del Torto, Milan, Italy (Abstract Co-Author) Nothing to Disclose Batrizia Vivona, Milan, Italy (Abstract Co-Author) Nothing to Disclose Gianluca Pontone, MD, Milan, Italy (Abstract Co-Author) Nothing to Disclose Patrizia Vivona, Milan, Italy (Abstract Co-Author) Nothing to Disclose Batrizia Vivona, Milan, Italy (Abstract Co-Author) Nothing to Disclose Batrizia Vivona, Milan, Italy (Abstract Co-Author) Speakers Bureau, General Electric Company Consultant, General Electric Company Research Consultant, HeartFlow, Inc Speakers Bureau, HeartFlow, Inc Speakers Bureau, Medtronic plc Speakers Bureau, Bayer AG

For information about this presentation, contact:

g.muscogiuri@gmail.com

PURPOSE

To assess the reliability of a novel dark-blood LGE (DBLGE) technique compared to standard bright-blood LGE (SBBLGE) sequence in patients with ischemic cardiomyopathy

METHOD AND MATERIALS

This prospective study included 78 patients (63.1 ± 12.6 years, 62 males) with clinical history of ischemic cardiomyopathy who underwent CMR at 1.5T (Discovery MR450w, GE Healthcare, Waukesha, WI) with postcontrast SBBLGE and DBLGE acquisition. Two observers performed the imaging analysis in a double blinded fashion. The endpoints were: a) qualitative and quantitative analysis of signal intensity ratio (SIR) b) n° segments involved; c) transmurality index (i.e. 0-25%; 25-50%, 50-75% and 75-100%) d) papillary muscle enhancement e) microvascular occlusion (MVO). Statistical analysis was performed with non-parametric test.

RESULTS

There were no interobserver variability (all p > 0.05). Subjective image quality in DBLGE compared to SBBLGE was higher for the discrimination between LGE and blood signal (p < 0.001), inferior (p < 0.001) between LGE and myocardium and similar between blood and myocardium (p=0.56). DBLGE provided higher SIR between LGE and blood signal ($1.18\pm1.15vs0.18\pm0.42;p < 0.001$), lower SIR between LGE and myocardium ($0.91\pm4.95vs1.96\pm1.64;p < 0.001$) and between blood and myocardium ($-0.26\pm0.71vs1.57\pm1.26;p < 0.001$). The n° segments involved was similar (p = 0.08). The transmurality index was inferior for DBLGE ($3.09\pm1.02vs3.30\pm1.11;p=0.007$). DBLGE was superior in identifying papillary muscle hyperenhancement (25vs17 cases;p < 0.001)

and inferior in MVO detection (7vs12 cases;p<0.001).

CONCLUSION

The DBLGE sequences when compared to SBBLGE provided better contrast between LGE and blood-pool, seemed to be superior in identifying papillary muscle hyperenancement, whereas underestimated the trasmurality extension of LGE and the presence of MVO.

CLINICAL RELEVANCE/APPLICATION

Black blood LGE can be extremely useful for evaluation of patients with ischemic cardiomyopathy, however it would be carefully evaluated in patients with acute myocardial infarction.

SSG02-09 Transfer Learning has Potential to Produce Better Reconstruction of Highly-Accelerated, Single-Shot LGE Images than Conventional Deep Learning

Tuesday, Dec. 3 11:50AM - 12:00PM Room: S104A

Participants

Daming Shen, Evanston, IL (Presenter) Nothing to Disclose Hassan Haji-Valizadeh, Evanston, IL (Abstract Co-Author) Nothing to Disclose Sushobhan Ghosh, MSc, Evanston, IL (Abstract Co-Author) Nothing to Disclose Daniel Kim, PhD, Chicago, IL (Abstract Co-Author) Nothing to Disclose

For information about this presentation, contact:

damingshen2017@u.northwestern.edu

PURPOSE

Compressed sensing (CS) is capable of highly accelerating single-shot late gadolinium enhanced (LGE) MRI for achieving relatively high spatial resolution (1.6mmx1.6mm), but the lengthy image reconstruction time (~50s per image) and inconsistent performance hinder its clinical translation. Given limited training data, we propose a transfer learning (TL) approach to leverage our access to a large database of real-time cine images having similar image content as single-shot LGE, for developing a rapid image reconstruction framework for single-shot LGE.

METHOD AND MATERIALS

Image reconstruction was performed on a GPU workstation equipped with Pytorch. As shown in Figure 1, we pre-trained two deep learning (DL) networks (one for real and another for imaginary data, layer depth = 3, 64 features on the first layer) using existing 5811 (42 rays per frame) zero-filled and the corresponding CS reconstructed (total variation as constraint) real-time cine images from 19 patients (mean age = 66.1 ± 12.0 years; 8 females) as input/output pairs. For TL, we prospectively obtained 2-shot (42 radial spokes per shot), breath-held LGE data sets from 12 patients (mean age = 51.1 ± 20.3 years; 6 females) on 1.5T scanners (Aera and Avanto, Siemens), retrospectively undersampled the 2-shot data (101 images) by a factor of 2 (42 rays per image), and trained the U-Nets using single-shot, zero-filled (input) and the corresponding 2-shot, CS reconstructed images (output). For validation, we obtained 1-shot LGE (42 rays per image) data sets from 10 other patients (mean age = 56.5 ± 16.2 years; 6 females) and compared TL to CS and DL reconstructed images.

RESULTS

As shown in Figure 1, TL produced sharper images and fewer residual artifacts than DL and CS. Both edge sharpness (1.8 ± 0.4 mm) and CNR for TL (33.5 ± 18.8) were significantly (p<0.05) different from DL (2.3 ± 0.4 mm and 27.0 ± 15.7) and CS (1.9 ± 0.4 mm and 15.9 ± 7.6). The reconstruction time for DL and TL (0.7 ± 0.0 s) was significantly (p<0.05) lower than CS (49.6 ± 1.1 s).

CONCLUSION

This study demonstrates a TL approach to rapidly reconstruct 1-shot LGE with better image quality than a conventional DL approach.

CLINICAL RELEVANCE/APPLICATION

While CS is capable of highly accelerating data acquisition, the lengthy image reconstruction hinders its clinical translation.

Transfer learning enables rapid image reconstruction without requiring a large database of training data.





SSG04

Gastrointestinal (Liver Fibrosis)

Tuesday, Dec. 3 10:30AM - 12:00PM Room: E353A



AMA PRA Category 1 Credits ™: 1.50 ARRT Category A+ Credit: 1.75

Participants

Utaroh Motosugi, MD, Chuo, Japan (Moderator) Nothing to Disclose

Claude B. Sirlin, MD, San Diego, CA (*Moderator*) Research Grant, Gilead Sciences, Inc; Research Grant, General Electric Company; Research Grant, Siemens AG; Research Grant, Bayer AG; Research Grant, Koninklijke Philips NV; Consultant, AMRA AB; Consultant, Fulcrum; Consultant, IBM Corporation; Consultant, Exact Sciences Corporation; Consultant, Boehringer Ingelheim GmbH; Consultant, Arterys Inc; Consultant, Epigenomics; Author, Medscape, LLC; Lab service agreement, Gilead Sciences, Inc; Lab service agreement, ICON plc; Lab service agreement, Intercept Pharmaceuticals, Inc; Lab service agreement, Shire plc; Lab service agreement, Enanta; Lab service agreement, Takeda Pharmaceutical Company Limited; Lab service agreement, Alexion Pharmaceuticals, Inc; Lab service agreement, NuSirt Biopharma, Inc Aoife Kilcoyne, MBBCh, Boston, MA (*Moderator*) Author, Wolters Kluwer nv

Sub-Events

SSG04-01 Assessing Liver Tumor Stiffness by Diffusion-Weighted MR Imaging-Based Virtual Elastography

Tuesday, Dec. 3 10:30AM - 10:40AM Room: E353A

Participants

Takashi Ota, MD,PhD, Suita, Japan (*Presenter*) Nothing to Disclose Masatoshi Hori, MD, Muko, Japan (*Abstract Co-Author*) Nothing to Disclose Hiromitsu Onishi, MD, Suita, Japan (*Abstract Co-Author*) Research Grant, Canon Medical Systems Corporation Atsushi Nakamoto, MD, Suita, Japan (*Abstract Co-Author*) Nothing to Disclose Hideyuki Fukui, Suita, Japan (*Abstract Co-Author*) Nothing to Disclose Noriyuki Tomiyama, MD,PhD, Suita, Japan (*Abstract Co-Author*) Nothing to Disclose Kazuya Ogawa, Suita, Japan (*Abstract Co-Author*) Nothing to Disclose Mitsuaki Tatsumi, MD, PhD, Suita, Japan (*Abstract Co-Author*) Nothing to Disclose

PURPOSE

Recent study showed that there was a significant strong correlation between MR elastographic shear modulus (μ MRE) and a shifted apparent diffusion coefficient (sADC200-1500) calculated from diffusion MR signals acquired with *b* values of 200 and 1500 sec/mm2 in the liver parenchyma. The purpose of our study was to retrospectively estimate the liver tumor stiffness by calculating sADC200-1500, comparing with MR elastography (MRE). We also compared tumor standard ADC values (ADC0-800: *b* values of 0 and 800 sec/mm2) with MRE.

METHOD AND MATERIALS

Eighty-seven patients with hepatic tumors underwent liver MR imaging at 3T (hepatocellular carcinoma [HCC], 32; metastasis, 26; hemangioma, 29). Of these, forty-five patients underwent diffusion-weighted imaging (*b* values of 200, 1500 and *b* values of 0, 800 sec/mm2) and MRE. Of forty-five patients, we measured tumor stiffness in fifteen patients (HCC, 9; metastasis, 6) who had tumors larger than 3cm by calculating μ MRE, sADC200-1500 and ADC0-800 values. We also measured liver stiffness in forty-five patients by calculating μ MRE, sADC200-1500 and ADC0-800 values. Finally, we measured sADC200-1500 values of hepatic tumors in eighty-seven patients. The correlation between μ MRE and ADC values was evaluated using Pearson's correlation test. Receiver operating characteristic (ROC) analysis was used to evaluate the diagnostic performance of sADC200-1500 values for differentiating between benign and malignant tumors.

RESULTS

 μ MRE and sADC200-1500 exhibited strong correlations both for liver tumor (r=0.80; p<.001), and for liver parenchyma (r=0.87; p<.001). Meanwhile, μ MRE and ADC0-800 exhibited no correlation for liver tumor (r=0.32; p=.24), and weak correlation for liver parenchyma (r=0.45; p=.002). The mean sADC200-1500 value of hemangioma was significantly higher than that of HCC and metastasis (1.69, 0.88, and 0.92×10-3mm2/sec; p<.001). A cut-off value of 1.27×10-3mm2/sec for sADC200-1500 detected with ROC analysis yielded 96.6% sensitivity and 89.5% specificity for the differentiation between benign and malignant tumors.

CONCLUSION

There was a significant strong correlation in the liver tumor between μ MRE and sADC200-1500. Mean sADC200-1500 value of benign tumors was significantly higher than that of malignant tumors.

CLINICAL RELEVANCE/APPLICATION

Liver tumor stiffness estimation could be performed with DWI, and liver tumor stiffness assessment by virtual elastography facilitates the differentiation of malignant and benign liver tumors.

SSG04-02 Intravoxel Incoherent Motion Diffusion-Weighted MRI for Characterization of Diffuse Liver Disease

Participants Thierry Lefebvre, Montreal, QC (*Presenter*) Nothing to Disclose Melanie Hebert, Montreal, QC (*Abstract Co-Author*) Nothing to Disclose Laurent Bilodeau, Montreal, QC (*Abstract Co-Author*) Nothing to Disclose Claire Wartelle-Bladou, MD, Montreal, QC (*Abstract Co-Author*) Nothing to Disclose Giada Sebastiani, MD, Montreal, QC (*Abstract Co-Author*) Speaker, Merck & Co, Inc; Speaker, Bristol-Myers Squibb Company; Speaker, Gilead Sciences, Inc; Speaker, AbbVie Inc; Research funded, Merck & Co, Inc; Research funded, Echosens SA Helene Castel, MD, Montreal, QC (*Abstract Co-Author*) Nothing to Disclose Damien Olivie, MD, MS, Qutremont, QC (*Abstract Co-Author*) Nothing to Disclose Bich Nguyen, Montreal, QC (*Abstract Co-Author*) Nothing to Disclose Guillaume Gilbert, PhD, Montreal, QC (*Abstract Co-Author*) Employee, Koninklijke Philips NV An Tang, MD, Montreal, QC (*Abstract Co-Author*) Research Consultant, Imagia Cybernetics Inc Speaker, Siemens AG Speaker, Eli Lilly and Company

For information about this presentation, contact:

an.tang@umontreal.ca

PURPOSE

To evaluate the diagnostic performance of diffusion-weighted imaging (DWI) intravoxel incoherent motion (IVIM) parameters and stretched exponential model parameters for assessing histological features in patients with chronic liver disease (CLD).

METHOD AND MATERIALS

This prospective, cross-sectional multi-center study was approved by the Institutional Review Board of the two participating institutions. Ninety patients with suspected or known CLD who underwent clinically indicated liver biopsies were recruited between January 2014 and July 2018. IVIM parameters (perfusion fraction *f*, diffusion coefficient *D*, and pseudo-diffusion coefficient D^*) and stretched exponential model parameters (intravoxel water diffusion heterogeneity *a* and distributed diffusion coefficient *DDC*) were estimated using a least-squares, non-linear regression on DWI series (10 *b* values up to 800 s/mm2). Inflammation, fibrosis, and steatosis were scored by an expert liver pathologist. Spearman's rho, Kruskal-Wallis test, Mann-Whitney U test, and receiver operating characteristic (ROC) analyses were performed. Multiple regression analysis was used to assess the effects of histological features on diffusion parameters.

RESULTS

Among all parameters and histological features, *f* and *a* showed the strongest correlation with inflammation grades ($\rho = -0.57$ and $\rho = 0.40$, respectively; P < 0.001). Both *f* and *a* were significantly different between all inflammation grades (P < 0.001) and between pairs of inflammation grades <= A1 vs >= A2 (P < 0.001 and P = 0.007, respectively). Areas under the ROC curve for distinguishing <= A1 vs >= A2 were 0.84 (95% confidence interval: 0.74-0.91) with *f* and 0.72 (0.60-0.81) with *a*. In multiple regression analysis, fibrosis had a significant impact on *f* (P = 0.03), but not on *a* (P = 0.18), while steatosis had a significant impact on *a* (P = 0.01), but not on *f* (P = 0.08). Association between inflammation and parameters *f* and *a* remained significant when including fibrosis and steatosis in the regression model (P < 0.001 and P < 0.05, respectively).

CONCLUSION

Perfusion fraction and intravoxel water diffusion heterogeneity show promise as surrogate biomarkers of liver inflammation using IVIM-DWI.

CLINICAL RELEVANCE/APPLICATION

DWI sequence with multiple b values should be performed on abdominal MR examination in patients with chronic liver disease as it could provide supplemental information on inflammatory activity within the liver.

SSG04-03 Can Single-Section, Machine Learning-Based Radiomics Differentiate Normal Liver from Diffuse Liver Diseases?

Tuesday, Dec. 3 10:50AM - 11:00AM Room: E353A

Participants

Ruhani Doda Khera, MD, Cambridge, MA (Abstract Co-Author) Nothing to Disclose

Fatemeh Homayounieh, MD, Boston, MA (Presenter) Nothing to Disclose

Ramandeep Singh, MBBS, Boston, MA (Abstract Co-Author) Nothing to Disclose

Felix Lades, Forchheim, Germany (Abstract Co-Author) Employee, Siemens AG

Andrew Primak, PhD, Cleveland, OH (Abstract Co-Author) Employee, Siemens AG

Subba R. Digumarthy, MD, Boston, MA (*Abstract Co-Author*) Researcher, Siemens AG; Contract, Merck & Co, Inc; Contract, Pfizer Inc; Contract, Bristol-Myers Squibb Company; Contract, Novartis AG; Contract, F. Hoffmann-La Roche Ltd; Contract, Polaris; Contract, Cascadian; Contract, AbbVie Inc; Contract, Consulting Medical Associates, Inc; Contract, Bayer AG; Contract, Zai Laboratries; ;

Mannudeep K. Kalra, MD, Lexington, MA (*Abstract Co-Author*) Research Grant, Siemens AG; Research Grant, Riverain Technologies, LLC;

For information about this presentation, contact:

ruhanidoda@gmail.com

PURPOSE

We hypothesized that machine learning (ML)-based segmentation and radiomic features of liver from a single section of dual-energy CT can differentiate between normal, fatty and cirrhotic liver.

METHOD AND MATERIALS

Our IRB-approved study included 75 patients (mean age 54 ± 16 years; 44 females, 31 males) who underwent clinically-indicated, contrast-enhanced, portal venous phase, dual-energy abdomen-pelvis CT (SOMATOM Flash, Siemens). Low and high tube potential

(80 and 140 kV) image datasets were de-identified and exported to a DECT segmentation and radiomic features analyses prototype (Radiomics, Siemens). The prototype enabled automatic segmentation of liver on a single CT section at the level of the porta hepatis. DECT iodine quantification and radiomics features were derived for the segmented portion of the liver in XML file format. The XML files were imported into a separate ML-based statistical analysis prototype (Radiomics, Siemens) for univariate and multivariate logistic regression and random forest classification.

RESULTS

Both iodine quantification (best AUC 0.95) and radiomic features (best AUC 0.95) differ significantly between normal, fatty and cirrhotic livers (p<0.0001). Normalized iodine concentration was superior than the iodine concentration and mean iodine uptake (p<0.0004) for differentiating the normal from fatty and cirrhotic liver. Amongst the radiomic features, the first order statistics demonstrated the highest accuracy (AUC 0.90-0.95, P< 0.0001). Machine learning based random forest classification yielded an AUC of 0.91 for differentiating normal from cirrhotic liver, 0.95 (AUC) for differentiating fatty and normal liver and 0.93 (AUC) for differentiating fatty and cirrhotic liver.

CONCLUSION

Single-section, DECT iodine quantification and radiomics features enable near-perfect differentiation (AUC up to 0.954) of normal, fatty, and cirrhotic liver from single-section analyses. The most accurate features were iodine concentration and first order statistics from radiomic analyses.

CLINICAL RELEVANCE/APPLICATION

Machine learning-enabled radiomics from single-section DECT can enable automatic distinction of normal liver from fatty and cirrhotic liver.

SSG04-04 Assessment of Liver Fibrosis with Quantitative Analysis of Tc-99m Diethylenetriamine-pentaacetic Acid-galactosyl Human Serum Albumin (GSA) SPECT/CT: Comparison with Histopathological Fibrosis in Hepatectomy Specimen

Tuesday, Dec. 3 11:00AM - 11:10AM Room: E353A

Participants

Yasutaka Ichikawa, MD, Tsu, Japan (*Presenter*) Nothing to Disclose Motonori Nagata, MD, PhD, Tsu, Japan (*Abstract Co-Author*) Nothing to Disclose Hiroki Ikuma, MD, Tsu, Japan (*Abstract Co-Author*) Nothing to Disclose Masaki Ishida, MD, PhD, Tsu, Japan (*Abstract Co-Author*) Nothing to Disclose Hajime Sakuma, MD, Tsu, Japan (*Abstract Co-Author*) Research Grant, EIZAI; Research Grant, DAIICHI SANKYO Group; Research Grant, FUJIFILM Holdings Corporation; Research Grant, Guerbet SA; Research Grant, Nihon Medi-Physics Co, Ltd;

PURPOSE

Assessment of liver fibrosis severity is essential in optimizing treatment in patients with chronic liver disease. Tc-99m GSA scintigraphy has been shown to be useful in assessing regional liver functional reserve, because its liver uptake and blood clearance have strong association with several hepatic function tests such as ICG15. However, the relationship between liver fibrosis and quantitative indices by Tc-99m GSA imaging has not been fully elucidated. The purpose of this study was to evaluate the value of quantitative assessment of Tc-99m GSA SPECT/CT to estimate the extent of liver fibrosis determined by hepatectomy specimen.

METHOD AND MATERIALS

Fifty-five patients who underwent Tc-99m GSA imaging before hepatectomy were studied. Following bolus injection of 185MBq Tc-99m GSA, planar dynamic scintigraphy was performed for 20 minutes. Immediately after the planar acquisition, SPECT data was acquired for 8 minutes (60 steps of 6 s/step and 128x128 matrix). SPECT images were reconstructed with CT attenuation correction and scatter correction. Liver uptake ratio (LUR) defined as radioactivity in whole liver divided by injected radioactivity was calculated. LHL15, a conventional index used for Tc-99m GSA planar scintigram, was also measured. LUR and LHL15 measurements were compared with the histopathological grade of liver fibrosis (F0-F4: F0, absence of fibrosis; F4, severe fibrosis).

RESULTS

LUR measured by SPECT/CT had significant negative correlation with the liver fibrosis stage (p<0.0001, r=-0.60). LUR in patients with severe liver fibrosis (F4) ($30.7\pm12.8\%$) were significantly lower than those with absence/mild liver fibrosis (F0-1) ($49.8\pm6.6\%$, p<0.0001) and intermediate liver fibrosis (F2-3) ($46.0\pm9.3\%$, p=0.017) (Figure 1A). The areas under ROC curve of LUR for the prediction of severe liver fibrosis (F4) was 0.90 (Figure 1B). With an optimal LUR threshold of 40.4%, the sensitivity and specificity of LUR in detecting severe liver fibrosis was 90.9%(10/11) and 90.9%(40/44). The sensitivity and specificity of LHL15 to diagnose severe liver fibrosis was 72.7%(8/11) and 81.8%(36/44), respectively.

CONCLUSION

Quantitative assessment of Tc-99m GSA SPECT permits accurate prediction of severe liver fibrosis with the sensitivity and specificity of > 90%.

CLINICAL RELEVANCE/APPLICATION

Liver uptake ratio quantified with Tc-99m GSA SPECT/CT is a promising biomarker to estimate the severity of liver fibrosis.

SSG04-06 Breath-Hold Look-Locker Inversion Recovery T1 Map on Gd-EOB-DTPA-Enhanced Liver MRI to Estimate Liver Function: Calibration, Reproducibility, and Diagnostic Value

Tuesday, Dec. 3 11:20AM - 11:30AM Room: E353A

Participants

Jimi Huh, MD, Suwon, Korea, Republic Of (*Presenter*) Nothing to Disclose Tae Young Lee, MD, Seoul, Korea, Republic Of (*Abstract Co-Author*) Nothing to Disclose Gyeong Min Park, MD, Ulsan, Korea, Republic Of (*Abstract Co-Author*) Nothing to Disclose Soon Chan Park, BS, Ulsan, Korea, Republic Of (*Abstract Co-Author*) Nothing to Disclose Munyoung Paek, Seoul, Korea, Republic Of (*Abstract Co-Author*) Nothing to Disclose Dominik Nickel, Erlangen, Germany (*Abstract Co-Author*) Employee, Siemens AG Bohyun Kim, MD, Suwon, Korea, Republic Of (*Abstract Co-Author*) Nothing to Disclose Hye Jin Kim, MD, Seoul, Korea, Republic Of (*Abstract Co-Author*) Nothing to Disclose Jei Hee Lee, MD, Suwon, Korea, Republic Of (*Abstract Co-Author*) Nothing to Disclose Jai Keun Kim, MD, PhD, Suwon-si, Korea, Republic Of (*Abstract Co-Author*) Nothing to Disclose Kyung Won Kim, MD, Seoul, Korea, Republic Of (*Abstract Co-Author*) Nothing to Disclose

For information about this presentation, contact:

jimihuh.rad@gmail.com

PURPOSE

To validate Look-Locker T1 map on EOB-MRI for the calibration performance, reproducibility, and diagnostic value to estimate liver function.

METHOD AND MATERIALS

Look-Locker T1 map was established to scan a slice in 13 seconds. For calibration, a quantitative T1-phantom was generated using Gd-EOB-DTPA solutions of various concentrations and was scanned to evaluate T1 linearity. In total 466 consecutive patients with chronic liver disease or liver cirrhosis, MRIs were scanned with a T1-phantom attached. In the liver, T1 values on precontrast and 20-min postcontrast T1 maps were measured and its difference (Δ T1 = T1post - T1pre) and relative change ($\%\Delta$ T1 = Δ T1 / T1pre) were calculated. Relative liver enhancement at 20-min postcontrast T1-WI was calculated [%RLE = (SIpost - SIpre)/SIpre]. Correlation between MRI indices and Child-Pugh score was calculated. Accuracy of Δ T1, $\%\Delta$ T1, and RLE to diagnose decompensated cirrhosis was evaluated by receiver-operating-characteristics (ROC) analysis. Reproducibility of T1 value of attached phantom across all patients (n=466) and test-retest repeatability of T1 map of the liver in the same patients (n=52) were evaluated using repeatability coefficient (RC).

RESULTS

Phantom study showed excellent T1 linearity (coefficient of determination R2, 0.9737). In patients, the correlation coefficients between MRI indices and Child-Pugh score was high in $\Delta\Delta$ T1 (r=0.584), but low in Δ T1 (r=0.339) and \otimes RLE (r=0.241). Accuracy to diagnose Child-Pugh class B and C differentiating from class A was high in both $\otimes\Delta$ T1 and RLE (AUC 0.798 and 0.838, respectively), but low in Δ T1 (AUC 0.683). Accuracy to diagnose Child-Pugh class C differentiating from class A and B was excellent in both $\otimes\Delta$ T1, RLE and Δ T1 (AUC 0.993, 0.976, and 0.976, respectively). Reproducibility across all patients (RC 68.16) and test-retest repeatability in the same patients (RCs, 74.7 in T1pre and 79.4 in T1post) were good.

CONCLUSION

T1 map using Look-Locker sequence on EOB-MRI showed promise for evaluating liver function in patients, especially diagnosing decompensated liver cirrhosis. Of MRI indices, $\&\Delta$ T1 might be the best index for liver function assessment.

CLINICAL RELEVANCE/APPLICATION

Breath-hold Look-Locker T1 map on EOB-MRI can overcome the conventional T1 map's limitation, a long scan time, thus can be easily incorporated in the routine liver MRI for chronic liver disease.

SSG04-07 Diuretic Use Associated with Discordant Estimation of Liver Fibrosis between Magnetic Resonance Elastography (MRE) and Transient Elastography (TE)

Tuesday, Dec. 3 11:30AM - 11:40AM Room: E353A

Participants

Brian Horwich, MD,MS, Los Angeles, CA (*Presenter*) Nothing to Disclose Shida Haghighat, MD,MPH, Los Angeles, CA (*Abstract Co-Author*) Nothing to Disclose Patrick Chang, Los Angeles, CA (*Abstract Co-Author*) Nothing to Disclose Suzanne L. Palmer, MD, Los Angeles, CA (*Abstract Co-Author*) Nothing to Disclose Hyosun Han, Los Angeles, CA (*Abstract Co-Author*) Nothing to Disclose

For information about this presentation, contact:

bhorwich@usc.edu

PURPOSE

Magnetic resonance elastography (MRE) and transient elastography (TE) are preferred surveillance tools for low-risk individuals with liver disease. However, the estimated METAVIR fibrosis stage of these two studies are frequently discordant, obfuscating clinical decision-making. This study aims to identify factors that may contribute to this discordance.

METHOD AND MATERIALS

The radiology database was queried for patients with a TE within 18 months of MRE study from January 1, 2015 to September 30, 2018. Relevant clinical data were collected and analyzed from identified subjects.

RESULTS

The subjects (N=35) had a mean age of 57.6 years and 51.4% were obese (BMI >= 30 kg/m2). The most represented liver disease was nonalcoholic fatty liver disease (62.9%). The most represented comorbidities were hypertension (40.0%) and diabetes (34.3%). A Pearson's chi-square test identified factors associated with discordance in estimated METAVIR fibrosis stage, defined as difference in estimated stage (F0 to F4) greater than 1. Even with the small number of patients on diuretic therapy (n=14), there was a statistically significant discordance associated with diuretic use (p=0.02). There was no significant discordance in individuals with hypertension (p=0.62), or elevated serum creatinine (p=0.79).

CONCLUSION

This small, retrospective cohort study demonstrates a statistically significant discordance in estimated METAVIR fibrosis stage between TE and MRE in patients on diuretic therapy (p=0.02).

CLINICAL RELEVANCE/APPLICATION

Prior studies have demonstrated that venous congestion affects MRE and TE estimation of liver fibrosis. It has also been shown that hepatic venous congestion preferentially accumulates in peripheral liver tissue. As MRE evaluates a larger proportion of the patient's liver, prior research in heart failure patients suggest that MRE more completely characterizes the liver parenchyma. Because TE primary evaluates peripheral tissue, its estimation of liver fibrosis may be more sensitive to changes in volume status. Thus, our observed discordance between MRE and TE in patients on diuretics may be a result of the location of liver tissue assessed. This suggests that MRE may be the preferred initial study for patients on diuretics as its fibrosis estimation may be less affected by fluctuations in volume status. Further study on variability of estimated fibrosis by TE and MRE with concomittant diuretic use is warranted.

SSG04-08 Estimation of Minimal Liver Fibrosis Using Gadoxetic Acid-Enhanced Liver MRI and Machine Learning

Tuesday, Dec. 3 11:40AM - 11:50AM Room: E353A

Participants

Keigo Narita, Hiroshima, Japan (*Presenter*) Nothing to Disclose Yuko Nakamura, MD, Hiroshima, Japan (*Abstract Co-Author*) Nothing to Disclose Motonori Akagi, MD, Hiroshima, Japan (*Abstract Co-Author*) Nothing to Disclose Toru Higaki, PhD, Hiroshima, Japan (*Abstract Co-Author*) Nothing to Disclose Makoto Iida, Hiroshima, Japan (*Abstract Co-Author*) Nothing to Disclose Kazuo Awai, MD, Hiroshima, Japan (*Abstract Co-Author*) Nothing to Disclose Kazuo Awai, MD, Hiroshima, Japan (*Abstract Co-Author*) Research Grant, Canon Medical Systems Corporation; Research Grant, Hitachi, Ltd; Research Grant, Fujitsu Limited; Research Grant, Bayer AG; Research Grant, DAIICHI SANKYO Group; Research Grant, Eisai Co, Ltd;

PURPOSE

The prognosis of patients with chronic hepatitis depends on fibrotic progression. As the transition from minimal to intermediate fibrosis is a major deleterious step, the accurate diagnosis of minimal fibrosis is of clinical importance. Liver biopsy, the reference standard for diagnosing and staging liver fibrosis, is invasive. As MR elastography, an imaging method for diagnosing liver fibrosis, may not be available in many hospitals, we developed a new method for its estimation on gadoxetic acid-enhanced liver MR images using support vector machines (SVM), a traditional application of machine learning. We assessed the diagnostic ability of our SVM analysis using parameters derived from gadoxetic acid-enhanced MR images for identifying minimal liver fibrosis.

METHOD AND MATERIALS

We included 182 patients with pathologically-diagnosed fibrosis stages. The parameters were based on texture analysis of hepatobiliary-phase images. To investigate the significant parameters for the staging of liver fibrosis we performed univariate logistic regression analysis. Parameters with statistical significance were subjected to analysis using multi-class SVMs, and their ability to identify minimal liver fibrosis (F-score >= 2) was determined. The FIB4 index which considers the patient age, the aspartate aminotransferase- and alanine aminotransferase level, and the platelet count was also calculated because it is correlated with the severity of liver fibrosis.

RESULTS

Univariate logistic regression analysis revealed that mean, standard deviation, skewness, kurtosis, the angular second moment, contrast, and entropy were important for the staging of liver fibrosis. The FIB4 index was also significant. The sensitivity, specificity, and accuracy for staging minimal liver fibrosis were 91.5, 55.8, and 81.3% for SVM analysis and 85.4, 60.4, and 78.7% for the FIB4 index based on an optimal cutoff value of 1.90.

CONCLUSION

SVM analysis using parameters derived from gadoxetic acid-enhanced MRI scans was more accurate than the FIB4 index for the staging of minimal liver fibrosis.

CLINICAL RELEVANCE/APPLICATION

SVM analysis using gadoxetic acid-enhanced MRI scans of the liver is a promising method for assessing minimal liver fibrosis.

SSG04-09 Evaluation of Liver Fibrosis by Assessing Hepatic Extracellular Volume Fraction Before and After Direct-Acting Antiviral Therapy in Patients with Chronic Hepatitis C Infection: Comparison with Serum Fibrosis-4 Index

```
Tuesday, Dec. 3 11:50AM - 12:00PM Room: E353A
```

Participants

Akihiko Kanki, MD, Kurasiki, Japan (*Presenter*) Nothing to Disclose Atsushi Higaki, MD, Kurashiki, Japan (*Abstract Co-Author*) Nothing to Disclose Hidemitsu Sotozono, MD, Kurashiki, Japan (*Abstract Co-Author*) Nothing to Disclose Kiyoka Maeba, MD, Kurashiki-City, Japan (*Abstract Co-Author*) Nothing to Disclose Akira Yamamoto, MD, Kurashiki, Japan (*Abstract Co-Author*) Nothing to Disclose Tsutomu Tamada, MD, PhD, Kurashiki, Japan (*Abstract Co-Author*) Nothing to Disclose

PURPOSE

The utility of direct-acting antiviral therapy (DAA) in improving liver fibrosis in patients with chronic hepatitis C virus infection remains unclear. Recent studies demonstrated a strong correlation between hepatic extracellular volume fraction (ECV), assessed using contrast-enhanced CT (CE-CT), and histologic liver fibrosis. Additionally, the fibrosis-4 index (FIB-4) has been proposed as a surrogate marker for hepatic fibrosis in patients with chronic liver disease. This study aimed to evaluate time-dependent changes in ECV using multiphasic contrast-enhanced CT and FIB-4 before and after DAA, and to clarify the difference between both indices.

METHOD AND MATERIALS

Study participants included 41 patients with hepatitis C virus infection who achieved sustained virological response after DAA. All patients underwent multiphasic CE-CT and biochemical examination of blood before and after DAA (pre-treatment, time point 1 (T1); less than 6 months after DAA, T2; 6 to 12 months, T3; 12 to 24 months, T4; greater than 24 months, T5). Absolute

enhancements (in Hounsfield units) of the liver parenchyma (Eliver) and aorta (Eaorta) were measured on precontrast and equilibrium phase scans. ECV was calculated using the following equation: ECV (%) = Δ HUliver/ Δ HUaorta × (100 - Hematocrit [%]). FIB-4 was simultaneously calculated using age, AST, ALT and platelet count.

RESULTS

ECV and FIB-4 after DAA showed a significant decrease at the end of the study period as compared to their values at T1 (ECV: 27.49 \pm 3.72 and 29.45 \pm 4.83, p=0.022; and FIB-4: 3.07 \pm 1.88 and 4.40 \pm 3.47, p=0.001, respectively). ECV showed a significant positive correlation with FIB-4 (r=0.458, p=0.003) at T1, although there was no correlation at the end of the study period (r=0.170, p=0.289). In ECV comparisons between the different time points, a significant difference was seen between T1 and T4, and T1 and T5 (p=0.046 and 0.022, respectively). In FIB-4 comparisons, significant differences were seen between T1 and all other time points (p=0.003 to p<0.001), although no differences in FIB-4 were seen in all comparisons between T2 to T5 (p>0.05).

CONCLUSION

ECV decreased slowly after DAA, suggesting an improvement in hepatic fibrosis. On the other hand, FIB-4 decreased immediately, probably due to an improvement in hepatic inflammation.

CLINICAL RELEVANCE/APPLICATION

ECV has the potential to be a non-invasive biomarker for the assessment of liver fibrosis after DAA.





SSG05

Gastrointestinal (MR Diagnosis)

Tuesday, Dec. <u>3</u> 10:30AM - 12:00PM Room: <u>E351</u>



AMA PRA Category 1 Credits ™: 1.50 ARRT Category A+ Credit: 1.75

FDA Discussions may include off-label uses.

Participants

Janio Szklaruk, MD, PhD, Houston, TX (*Moderator*) Nothing to Disclose Cynthia S. Santillan, MD, San Diego, CA (*Moderator*) Consultant, Robarts Clinical Trials, Inc Alessandro Furlan, MD, Pittsburgh, PA (*Moderator*) Book contract, Reed Elsevier; Royalties, Reed Elsevier

Sub-Events

SSG05-01 Recurrence of HBV-Related Hepatocellular Carcinoma: Diagnostic Algorithms on Gadoxetic Acid-Enhanced MRI

Tuesday, Dec. 3 10:30AM - 10:40AM Room: E351

Participants

Wentao Wang, MD, MD, Shanghai, China (*Presenter*) Nothing to Disclose Li Yang, MD, PhD, Shanghai, China (*Abstract Co-Author*) Nothing to Disclose Mengsu Zeng, MD, PhD, Shanghai, China (*Abstract Co-Author*) Nothing to Disclose Shengxiang Rao, MD, Shanghai, China (*Abstract Co-Author*) Nothing to Disclose

For information about this presentation, contact:

787356268@qq.com

PURPOSE

to better characterize intrahepatic recurrence <20mm after resection of HCC using gadoxetic acid-enhanced MR imaging

METHOD AND MATERIALS

Between March 2012 and January 2017, a total of 373 nodules (median size, 1.4 cm; range, 5.5-19 mm) in 204 HCC patients (median age, 55 years; range, 27-79 years) with chronic hepatitis B virus (HBV) infection after hepatectomy underwent gadoxetic acid-enhanced MR imaging and were included in the retrospective study. Diagnostic performance of the LI-RADS systems were calculated for characterizing recurrence. The modified diagnostic algorithms were proposed by combining significant imaging biomarkers respectively related to subcentimeter and 10-20mm recurrences in multivariate analyses and were compared with the LI-RADS imaging criteria by using McNemar test.

RESULTS

The multivariate analyses showed that nonrim arterial phase hyperenhancement and the three LI-RADS ancillary features (hepatobiliary phase hypointensity, mild-moderate T2 hyperintensity and restricted diffusion) were significantly related with recurrence <20mm. For subcentimeter recurrence, the modified diagnostic algorithm of combining at least two of the three ancillary features achieved better diagnostic performance (sensitivity: 83.3%; specificity: 87.7%) than the LI-RADS 4 criteria (sensitivity: 88.9%, P=0.211; specificity: 70.8%, P=0.006). For 10-19 mm recurrence, combining nonrim arterial phase hyperenhancement and at least one of the three ancillary features achieved significantly enhanced sensitivity of 85.1% and relative high specificity of 86.5% than the LI-RADS 5 criteria (sensitivity: 63.5%, P<0.001; specificity: 94.2%, P=0.134).

CONCLUSION

The diagnostic algorithms for subcentimeter and 10-19mm recurrent HCC should be stratified. For subcentimeter recurrences, the modified diagnostic algorithm on gadoxetic acid-enhanced MRI demonstrated preserved high sensitivity with significantly enhanced specificity than LI-RADS 4 criteria.

CLINICAL RELEVANCE/APPLICATION

The multivariate analyses showed that arterial phase hyperenhancement was the most reliable major feature for characterizing 10-20 mm recurrence while the ancillary features were more valuable for characterizing <10mm recurrence. 3. Our modified diagnostic algorithms demonstrated significantly enhanced sensitivity with preserved high specificity for characterizing recurrent HCC <20mm.

SSG05-02 Exploring Prognostic Risk Factors and Survival Models for T3 Locally Advanced Rectal Cancer: What Can We Learn From the Baseline MRI?

Tuesday, Dec. 3 10:40AM - 10:50AM Room: E351

Participants Qing Zhao, Beijing, China (*Abstract Co-Author*) Nothing to Disclose Hongmei Zhang, MD, Beijing, China (*Abstract Co-Author*) Nothing to Disclose Xinming Zhao, Beijing, China (*Abstract Co-Author*) Nothing to Disclose

For information about this presentation, contact:

zq_pumc@163.com

PURPOSE

To evaluate the baseline MRI characteristics in predicting disease-free survival (DFS) and cancer-specific survival (CSS) in patients with T3 LARC and to explore individualized prognostic risk-stratification models.

METHOD AND MATERIALS

This study retrospectively reviewed 256 T3 LARC patients evaluated from January 2008 to December 2012 in our institution with an average follow-up period of 6.1 years. Two trained radiologists independently evaluated baseline MRI characteristics and reached consensus. Kaplan-Meier survival curves and Cox regression analysis were used to determine the relationship of MRI parameters and other clinicopathological factors to DFS and CSS using SPSS. R software was used to develop individualized risk-stratification nomograms for 3-year and 5-year DFS and CSS. Independent validation was assessed by Harrell concordance (C)-index.

RESULTS

Independent predictors of DFS were found to include baseline MRI-defined T3 substaging (hazard ratio, HR = 3.09, P < 0.001), extramural venous invasion (EMVI) grading (HR = 3.08, P < 0.001), rectal mucinous adenocarcinoma (RMAC) (HR = 2.44, P < 0.001), threatened mesorectal fascia (MRF) (HR = 1.73, P = 0.038), neoadjuvant chemoradiotherapy (NCRT) (HR = 0.44, P < 0.001) and an elevated pretreatment carcinoembryonic antigen (CEA) level (HR = 1.93, P < 0.001). In addition, T3 substaging (HR = 4.09, P < 0.001), EMVI grading (HR = 2.19, P < 0.001) and NCRT (HR = 0.58, P = 0.006) independently affected CSS. The nomograms permitted individualized prediction of 3-year and 5-year DFS and CSS probability with high performance (C-index range, 0.848-0.883).

CONCLUSION

Baseline MRI-defined T3 substaging, EMVI grading, threatened MRF, RMAC, and elevated pretreatment CEA were adverse prognosticators, whereas NCRT promoted positive outcome, in patients with T3 LARC. The models can facilitate individualized pretreatment survival risk-stratification.

CLINICAL RELEVANCE/APPLICATION

This study identified independent prognostic factors and developed nomogram models with high performance for individualized pretreatment prediction of 3-year and 5-year disease-free survival and cancer-specific survival in patients with T3 locally advanced rectal cancer. The models can facilitate individualized pretreatment survival risk-stratification and aid in clinical decision-making.

SSG05-03 Interobserver Variation in the Interpretation of MR Enterography for Crohn's Disease

Tuesday, Dec. 3 10:50AM - 11:00AM Room: E351

Participants

Gauraang Bhatnagar, FRCR, MBBS, London, United Kingdom (Presenter) Nothing to Disclose Laura Quinn, Birmingham, United Kingdom (Abstract Co-Author) Nothing to Disclose Richard A. Beable, MBChB, Portsmouth, United Kingdom (Abstract Co-Author) Nothing to Disclose Helen Bungay, MBBCh, Oxford, United Kingdom (Abstract Co-Author) Nothing to Disclose Gillian Duncan, Dundee, United Kingdom (Abstract Co-Author) Nothing to Disclose Anthony Higginson, Portsmouth, United Kingdom (Abstract Co-Author) Nothing to Disclose Rachel Hyland, MBChB, FRCR, Leeds, United Kingdom (Abstract Co-Author) Nothing to Disclose Rajapandian Ilangovan, MD, FRCR, Northwood, United Kingdom (Abstract Co-Author) Nothing to Disclose Hannah Lambie, Bradford, United Kingdom (Abstract Co-Author) Nothing to Disclose Evgenia Mainta, MD, MMedSc, London, United Kingdom (Abstract Co-Author) Nothing to Disclose Uday B. Patel, MBBS, BSc, Sutton, United Kingdom (Abstract Co-Author) Nothing to Disclose Francois Porte, MBBS, BSc, Tunbridge Wells, United Kingdom (Abstract Co-Author) Nothing to Disclose Andrew Plumb, MBBCh, MRCP, Stockport, United Kingdom (Abstract Co-Author) Nothing to Disclose Andrew Slater, MBBCh, Oxford, United Kingdom (Abstract Co-Author) Nothing to Disclose Mariead Tennent, Dundee, United Kingdom (Abstract Co-Author) Nothing to Disclose Damian J. Tolan, MBBCh, FRCR, Leeds, United Kingdom (Abstract Co-Author) Speaker, Bracco Group Speaker, Merck & Co, Inc Ian A. Zealley, MBChB, Perth, United Kingdom (Abstract Co-Author) Nothing to Disclose Steve Halligan, MD, Herts, United Kingdom (Abstract Co-Author) Research Consultant, iCad, Inc Sue Mallett, DIPLPHYS, MS, Birmingham, United Kingdom (Abstract Co-Author) Nothing to Disclose Stuart A. Taylor, MBBS, Great Missenden, United Kingdom (Abstract Co-Author) Research Consultant, Robarts Clinical Trials, Inc; Shareholder, Motilent

For information about this presentation, contact:

g.bhatnagar@nhs.net

PURPOSE

Quantifying interobserver variability is an important part in evaluating medical imaging. Interpretation of MR enterography (MRE) is complex, and to date there has been little research into interobserver variability across multiple observers.

METHOD AND MATERIALS

The study utilised datasets from a prospective trial comparing the diagnostic accuracy of MRE and US for CD (either newly diagnosed or relapsing disease) recruited from 8 centres. A construct reference standard (multidisciplinary panel diagnosis) was used, incorporating 6 months follow up. 73 (28 new diagnosis, 45 suspected relapse) trial MREs were interpreted 3 times by one of 27 radiologists via an online platform (Biotronics 3Dnet). Radiologists were randomly allocated datasets, blinded to each other's interpretation, patient's symptoms and history, and documented the presence/location of small bowel and colonic disease. Data was analysed separately for new diagnosis and relapse cohorts. Interobserver variability was measured by averaging percentage

agreement with the consensus reference standard across the 3 reads, grouped as disease positive or negative. Prevalence adjusted bias adjusted kappa (PABAK) was reported. Agreement between the radiologists irrespective of agreement with the reference standard was also reported.

RESULTS

For newly diagnosed patients, overall percentage agreement for small bowel disease presence against the consensus reference was 68%, with kappa coefficient(κ) 0.36 (fair agreement). Agreement for colonic disease presence was 61%, κ 0.21(fair agreement). For relapsing cohort, overall percentage agreement for small bowel disease presence against the consensus reference was 76%, κ 0.51(moderate agreement). Agreement for colonic disease presence was 61%, κ 0.21(slight agreement). Agreement was similar when reads were considered without reference to the consensus reference (72% and 60% for small bowel and colonic disease presence respectively).

CONCLUSION

Based on data from a multi-reader, multicenter prospective trial, there is fair to moderate agreement between radiologists for the presence of small bowel and colonic disease against an independent standard of reference

CLINICAL RELEVANCE/APPLICATION

Compared to an independent standard of reference there is fair to moderate agreement between radiologists for the presence of enteric disease on MRE. This indicates the need for standardised training.

SSG05-04 MRI Evaluation of Lateral Pelvic Lymph Node in Locally Advanced Rectal Cancer: Optimized Cutoff Value Chosen and the Relationship to Overall Survival

Tuesday, Dec. 3 11:00AM - 11:10AM Room: E351

Participants

Rui-Jia Sun, Beijing, China (*Presenter*) Nothing to Disclose Qiao-Yuan Lu, Beijing, China (*Abstract Co-Author*) Nothing to Disclose Xiao-Ting Li, Peking City, China (*Abstract Co-Author*) Nothing to Disclose Hui Ci Zhu, Beijing, China (*Abstract Co-Author*) Nothing to Disclose Ying-shi Sun, MD,PhD, Beijing, China (*Abstract Co-Author*) Nothing to Disclose

For information about this presentation, contact:

srj777@163.com

PURPOSE

To study the relationship between MRI-detected pretreatment lateral pelvic lymph node (LPLN) metastasis and prognosis in patients with locally advanced rectal cancer treated with neoadjuvant chemotherapy-radiation therapy (CRT).

METHOD AND MATERIALS

This retrospective study included 517 patients with locally advanced rectal cancer evaluated from August 2008 to December 2014. Baseline and post-CRT MRI and follow-up data were retrieved for all patients. MRI findings of LPLN metastasis were evaluated. Kaplan-Meier curves and ROC analysis were used to determine the relationship of baseline MRI findings to overall survival.

RESULTS

227 patients (43.9%) had visible LPLNs with short axis of at least 5mm on pretreatment MRI. Univariate cox analysis indicated that the short axis (HR=1.12, 95%CI: 1.04-1.21, p<0.01) as well as the long axis of the largest LPLN (HR=1.07, 95%CI:1.02-1.13, P=0.01) were associated with the overall survival (OS). However, there was no significant relation to the metastasis free survival or the local recurrence free survival. A cut-off of 8mm and 12mm were selected for short and long axis respectively by using survival ROC analysis. Kaplan-Meier method showed LPLNs with a short axis greater than 8 mm resulted in a significantly poor OS (3-year OS 92.5% vs 79.7% for less than 8mm vs equal to or greater than 8mm, P<0.01). LPLNs with a long axis greater than 12 mm resulted in a significantly poor OS (3-year OS 92.3% vs 77.3% for less than 12mm vs equal to or greater than 12mm, P<0.01).

CONCLUSION

The presence of lateral pelvic lymph node (LPLN) was associated with overall death in patients with locally advanced rectal cancer. Further research is needed about which pretreatment features of the LPLN predict prognosis and what is needed to prevent these from developing.

CLINICAL RELEVANCE/APPLICATION

The presence of lateral pelvic lymph node at baseline MRI in local advanced rectal cancer is associated with overall survival in patients with locally advanced rectal cancer.

SSG05-05 Visual Grading of Hepatic Steatosis on In and Opposed Phase Imaging: Validation by Reference to Proton Density Fat Fraction

Tuesday, Dec. 3 11:10AM - 11:20AM Room: E351

Participants

Ali B. Syed, MD, Philadelphia, PA (*Presenter*) Research Consultant, IBM Corporation Badar Bin Bilal Shafi, MBBS, MRCP, Liverpool, United Kingdom (*Abstract Co-Author*) Nothing to Disclose Flavius F. Guglielmo, MD, Moorestown, NJ (*Abstract Co-Author*) Nothing to Disclose Jaydev K. Dave, PHD, Philadelphia, PA (*Abstract Co-Author*) Research Grant, Koninklijke Philips NV Equipment support, Lantheus Medical Imaging, Inc Equipment support, General Electric Company Donald G. Mitchell, MD, Philadelphia, PA (*Abstract Co-Author*) Consultant, CMC Contrast AB

For information about this presentation, contact:

PURPOSE

To develop and validate a qualitative, visual scale that can be used to grade severity of hepatic steatosis on in and opposed phase imaging.

METHOD AND MATERIALS

An IRB approved retrospective study was performed. From our institutional PACS, 429 MRI exams were identified that included both quantitative evaluation of proton density fat fraction (PDFF), and dual gradient echo in and opposed phase imaging. PDFF was calculated using the IDEAL-IQ technique (GE Healthcare, Milwaukee, WI). A subset of 113 patients was selected, (44 men and 66 women, ranging from 24-77 years of age), with PDFF ranging from 2% to 43%. Cases with abnormal hepatic iron concentrations (n=4) were excluded. Two readers independently provided visual steatosis score (VSS) according to our proposed 7-point scale based on visual cues, using in and opposed phase imaging only, without reference to clinical history, PDFF or other images. The VSS and PDFF were then compared for each study. ANOVA was performed to identify differences in PDFF as a function of VSS. 95% confidence intervals (CI) were constructed to determine the PDFF values that correlated with each VSS. Interclass correlation coefficient (ICC) was calculated to assess reliability (agreement and correlation).

RESULTS

ANOVA showed a statistically significant difference in PDFF for each VSS (p < 0.05). 95% CI of PDFF for each VSS were as follows. VSS-0: PDFF 4 to 6%; VSS-1: PDFF 7 to 12%; VSS-2: PDFF 15 to 18%; VSS-3: PDFF 26 to 29%; VSS-4: PDFF 31 to 40%; VSS-5: No exams scored; VSS-6: PDFF 35 to 45%. ICC was 0.92, indicating excellent reliability.

CONCLUSION

Specialized sequences for quantitative evaluation of hepatic steatosis are not always included in routine MR abdomen examination. Simple dual-echo technique (matched in and opposed phase) is routinely used as a component of abdominal MRI, including for detecting hepatic steatosis, but severity of steatosis on these sequences is subjective and not standardized. We propose a visual scale that can easily be employed during interpretation which can reliably differentiate various degrees of steatosis in the range commonly seen clinically (0 to 40%).

CLINICAL RELEVANCE/APPLICATION

Simple visual cues can be used to qualitatively grade hepatic steatosis on in and opposed phase imaging, providing greater standardization than currently utilized; these grades are reproducible between readers and demonstrate distinct degrees of steatosis as validated by PDFF.

SSG05-06 The Utility of MR Elastography for Differentiating Non-Cirrhotic Portal Hypertension from Cirrhotic Portal Hypertension

Tuesday, Dec. 3 11:20AM - 11:30AM Room: E351

Participants

Tolga Gidener, MD, Rochester, MN (*Presenter*) Nothing to Disclose Patrick Navin, MBBCh, MRCPI, Rochester, MN (*Abstract Co-Author*) Nothing to Disclose Alina Allen, Rochester, MN (*Abstract Co-Author*) Research support, Gilead Sciences, Inc Meng Yin, PhD, Rochester, MN (*Abstract Co-Author*) Intellectual property, Magnetic Resonance Innovations, Inc; Stockholder, Resoundant, Inc Michael Torbenson, Baltimore, MD (*Abstract Co-Author*) Nothing to Disclose Patrick S. Kamath, MD, Rochester, MN (*Abstract Co-Author*) Nothing to Disclose Richard L. Ehman, MD, Rochester, MN (*Abstract Co-Author*) CEO, Resoundant, Inc; Stockholder, Resoundant, Inc; Sudhakar K. Venkatesh, MD, FRCR, Rochester, MN (*Abstract Co-Author*) Nothing to Disclose

For information about this presentation, contact:

venkatesh.sudhakar@mayo.edu

PURPOSE

In clinical practice, it is difficult to differentiate non cirrhotic portal hypertension (NCPH) from cirrhotic portal hypertension (CPH), based only on clinical and non-invasive objective methods. In this study we evaluated the utility of MR Elastography (MRE) for differentiating NCPH from CPH

METHOD AND MATERIALS

From our database we retrospectively identified 60 patients with NCPH and had MRE. Forty age and sex-matched patients with CPH who had MRE formed the control group. Liver morphologic features, signs of portal hypertension, and overall impression of cirrhosis and PH on MRI images were evaluated. MRE was performed with standard clinical 2D-GRE-MRE sequence. Regions of interest (ROI) were drawn on both liver and spleen on the stiffness map and mean stiffness measurements (kilopascals, kPa) were generated for liver stiffness (LSM) and spleen stiffness (SSM) for each subject. Chi-square analysis for morphologic features and non-parametric analysis for mean LSM, mean SSM, and mean SSM/mean LSM ratio (SSM/LSM) were performed for significant differences. Receiver operating curve (ROC) analysis was also performed when differences were significant.

RESULTS

Mean LSM was significantly higher in CPH group than NCPH [9.7 kPa (95% CI 6.3-13.1) vs. 3.4 kPa (95%CI, 2.0-4.8), p<0.001]. Meanwhile mean SSM was not significantly different between CPH and NCPH [7.8 kPa (95%CI, 6.1-9.5) vs. 8.0 kPa (95%CI, 3.7-12.3), p=0.21]. SSM/LSM ratio was significantly higher in NCPH than CPH [2.6 kPa (95%CI, 1.0-4.2), vs. 0.9 kPa (95%CI, 0.6-1.2), p<0.001]. ROC analysis showed that a mean LSM >5.3 kPa had 100% sensitivity, 99% specificity and 98% accuracy to differentiate NCPH from CPH. SSM/LSM ratio of <1.3 had 88% sensitivity, 84% specificity and 92% accuracy to differentiate NCPH from CPH. Among the MRI morphological features, only the presence of esophageal varices (CPH > NCPH, p<0.018), the presence of perisplenic collaterals (NCPH>CPH, p<0.04) and the overall impression of cirrhosis (CPH> NCPH, p<0.01) were significantly different.

CONCLUSION

MR Elastography is a useful, non-invasive tool that can help differentiate NCPH from CPH.

CLINICAL RELEVANCE/APPLICATION

Non cirrhotic portal hypertension (NCPH) is difficult to differentiate from cirrhotic portal hypertension (CPH). MRE is an accurate non-invasive technique that can help differentiate NCPH from CPH.

SSG05-07 Role of Volumetric Functional MRI in Predicting Histopathologic Grade of Untreated Hepatocellular Carcinoma and Patient Survival

Tuesday, Dec. 3 11:30AM - 11:40AM Room: E351

Participants

Sanaz Ameli, MD, Baltimore, MD (*Presenter*) Nothing to Disclose Mohammadreza Shaghaghi, MD, Baltimore, MD (*Abstract Co-Author*) Nothing to Disclose Mounes Aliyari Ghasabeh, MD, Baltimore, MD (*Abstract Co-Author*) Nothing to Disclose Pallavi Pandey, MD, Baltimore, MD (*Abstract Co-Author*) Nothing to Disclose Pegah Khoshpouri, MD, Baltimore, MD (*Abstract Co-Author*) Nothing to Disclose Bita Hazhirkarzar, MD, Baltimore, MD (*Abstract Co-Author*) Nothing to Disclose Roya Rezvani Habibabadi, Baltimore, MD (*Abstract Co-Author*) Nothing to Disclose Maryam Ghadimi, MD, Baltimore, MD (*Abstract Co-Author*) Nothing to Disclose Ankur Pandey, MD, Baltimore, MD (*Abstract Co-Author*) Nothing to Disclose Robert Grimm, Erlangen, Germany (*Abstract Co-Author*) Nothing to Disclose Robert Anders, Baltimore, MD (*Abstract Co-Author*) Nothing to Disclose Robert Anders, Baltimore, MD (*Abstract Co-Author*) Nothing to Disclose Robert Anders, Baltimore, MD (*Abstract Co-Author*) Nothing to Disclose Robert Anders, Baltimore, MD (*Abstract Co-Author*) Nothing to Disclose Robert Anders, Baltimore, MD (*Abstract Co-Author*) Nothing to Disclose Robert Anders, Baltimore, MD (*Abstract Co-Author*) Nothing to Disclose Robert Anders, Baltimore, MD (*Abstract Co-Author*) Nothing to Disclose

For information about this presentation, contact:

sameli1@jhmi.edu

PURPOSE

To evaluate the role of volumetric ADC (vADC) and volumetric venous enhancement (vVE) in predicting the grade of tumor differentiation in hepatocellular carcinoma (HCC).

METHOD AND MATERIALS

This HIPPA compliant retrospective study was approved by our institutional review board. The study population included 136 HCC patients (188 lesions) who had baseline MR imaging and pathologic report of the HCC either by biopsy or liver transplantation between January 2001 and June 2017. Volumetric measurements of venous enhancement (VE) and apparent diffusion coefficient (ADC) were performed on baseline MRI. The tumors were histologically classified into two groups (low-grade and high-grade). The parameters between the two groups were compared using bivariate and multivariable analysis.

RESULTS

A total of 136 patients, with a median age of 61(56-67) were evaluated. 111 were male and 25 were female. Lesions with higher vADC values and higher absolute vADC-skewness were more likely to be high-grade on histopathology assessment (p=0.001 and p=0.0291, respectively). Also, venous enhancement showed a trend to be lower in high-grade lesions (p=0.079). vADC value of 1218.19 (x10-6 mm2/s) resulted in the highest sensitivity and specificity (77% and 74%, respectively) in distinguishing between the 2 groups. Additionally, vADC-skewness showed association with patient survival (HR=1.64, p=0.035; per increments in skewness).

CONCLUSION

vADC shows the highest accuracy in predicting HCC differentiation. Novel imaging biomarkers depicting tumor heterogeneity (e.g. skewness/kurtosis) could also be used to predict tumor features and patient's survival.

CLINICAL RELEVANCE/APPLICATION

Volumetric functional MRI metrics can be considered as non-invasive measures for determining tumor histopathology in HCC. These metrics can be used for modifying the management approach and reduce the need for tumor biopsy.

SSG05-08 Clinical Validation of Synthetic MRI in Assessing Rectal Cancer and Extramural Fat Invasion: Initial Experience

Tuesday, Dec. 3 11:40AM - 11:50AM Room: E351

Participants

Kexin Zhu, Shenyang , China (*Abstract Co-Author*) Nothing to Disclose Jinli Zhao, Shenyang , China (*Abstract Co-Author*) Nothing to Disclose Fei Bie, Shenyang , China (*Abstract Co-Author*) Nothing to Disclose Yi Liu, MD, PhD, Shenyang, China (*Presenter*) Nothing to Disclose

For information about this presentation, contact:

liuyicmu@sina.cn

PURPOSE

To evaluate the Clinical validation of Synthetic MRI in rectal cancer and extramural fat invasion.

METHOD AND MATERIALS

38 patients pathologically proven rectal cancer were included in the retrospective study, ethical approval and consent forms were obtained. All the patients underwent MR scans with both conventional MR and synthetic MR. Two experienced radiologists independently reviewed the images and identified the regions of normal rectal wall, tumor and extramural fat. The T1/T2/PD values of these different regions were obtained using synthetic MR. T test, Wilcoxon signed-rank test, and Mann-Whitney U test were used to contrast T1/T2/PD values between normal rectal wall and tumor, and that of extramural fat in rectal cancer between T1/2 stage cases and T3/4 stage cases. The diagnostic efficacy was evaluated using the ROC curve. The P<0.05 was used to indicate

RESULTS

Compared with normal rectal wall, the rectal cancer had higher T2 value (P=0.00), however, T1 and PD values had no statistical difference. ROC curve analysis: T2 value (AUC=0.706; 95%CI=0.591-0.822). All of the PD, T1 and T2 values of the extramural fat of T3/4 stage rectal cancer higher than that of T1/2 stage rectal cancer (P=0.00). ROC curve analysis: PD value (AUC=0.808, 95%CI=0.685~0.930), T1 value (AUC=0.997, 95%CI=0.998~1.000), T2 value (AUC= 0.850, 95% CI = 0.699~1.000).

CONCLUSION

Synthetic MRI was useful in accessing rectal cancer and extramural fat invasion. Compare with the normal rectal wall, T2 value of rectal cancer has significantly diagnostic efficiency. T1 value of extramural fat has the highest diagnostic efficiency for invasion of rectal cancer.

CLINICAL RELEVANCE/APPLICATION

The results of this study indicated that Synthetic MRI was useful in evaluating rectal cancer and extramural fat invasion, especially in the diagnosis of extramural fat invasion.

SSG05-09 Comparison of Pre-Operative and Post-Operative MRI after Complex Fistula-In-Ano Surgery -Lessons Learnt in Interpreting Postoperative MRI Scans in an Audit of 1323 MRI

Tuesday, Dec. 3 11:50AM - 12:00PM Room: E351

Participants

Pankaj Garg, MBBS,MS, Mohali, India (*Presenter*) Nothing to Disclose Sundeep Malla, MD, Delhi, India (*Abstract Co-Author*) Nothing to Disclose Anjli Kinariwalla, Mumbai , India (*Abstract Co-Author*) Nothing to Disclose Akhil Monga, MD,MBBS, New Delhi, India (*Abstract Co-Author*) Nothing to Disclose

For information about this presentation, contact:

drgargpankaj@yahoo.com

PURPOSE

The evaluation of MRI after fistula-in-ano surgery has never been done. The aim was to evaluate the utility of MRI in postoperative period after fistula-in-ano surgery.

METHOD AND MATERIALS

Preoperative MRI was done in all the patients and post-operative MRI was done to check radiological healing in clinically healed fistulas or when postoperative complication/ healing problem was seen

RESULTS

1323 MRI were done in 1003 fistula-in-ano patients, out of which, 702 patients underwent surgery. In 702 patients, there were 361-recurrent fistulas,153-associated abscess, 388-multiple tracts, 146-horseshoe and 76-supralevator fistula. 320 postoperative MRI were done in 180/702 patients. There were 189 grade I, 200 grade II, 52 grade III, 205 grade IV and 56 grade V fistula(St James classification). The requirement of postoperative MRI was significantly higher in complex (grade III-V) than simple fistulas (grade I-II) [43.5%(136/313) vs 11.3%(44/389) respectively, p<0.0001]. Lessons learnt in interpreting postoperative MRI scans --MRI was quite accurate to assess healing as well as complications after fistula surgery. --Granulation tissue (healing tissue) and inflammation in tissues (post surgery) looked hyperintense on T2 and STIR and was difficult to differentiate from active fistula tract/ pus. Therefore MRI done in immediate postoperative period (upto 8 weeks post surgery) required care. --After complete healing, the complete tract and internal opening becomes hypointense on T2 and STIR --The complete radiological healing takes at least 10-12 weeks. So getting MRI scan for assessment of healing should be done after 12 weeks. --MRI is very accurate to identify and diagnose postoperative complications like abscess formation, missed tract during surgery or non-healing of a tract. MRI detects such complications even in clinically healed tracts. By early intervention, it helps to prevent delayed recurrence, abscess formation and further spread of tracts. --Closure/healing of internal opening and intersphincteric tract are assessed quite accurately by MRI and they correlate well with the fistula healing.

CONCLUSION

MRI is highly useful to assess healing and detect complications after fistula surgery espesially in higher grades.

CLINICAL RELEVANCE/APPLICATION

MRI is highly useful to assess healing and detect complications after anal fistula surgery. MRI scan for assessment of healing should be done at least after 12 weeks of surgery.





SSG10

Neuroradiology (Stroke 2)

Tuesday, Dec. 3 10:30AM - 12:00PM Room: N229



AMA PRA Category 1 Credits ™: 1.50 ARRT Category A+ Credit: 1.75

FDA Discussions may include off-label uses.

Participants

Greg Zaharchuk, MD, PhD, Stanford, CA (*Moderator*) Research Grant, General Electric Company; Research Grant, Bayer AG; Stockholder, Subtle Medical

Michael H. Lev, MD, Boston, MA (*Moderator*) Consultant, General Electric Company; Research Grant, General Electric Company; Research support, Siemens AG; Consultant, Takeda Pharmaceutical Company Limited;

Sub-Events

SSG10-01 Don't Be Cowed: Bovine Arch and Stroke Laterality

Tuesday, Dec. 3 10:30AM - 10:40AM Room: N229

Participants Jason D. Matakas, MS,BS, The Bronx, NY (*Abstract Co-Author*) Nothing to Disclose Menachem M. Gold, MD, Teaneck, NJ (*Abstract Co-Author*) Nothing to Disclose Jonathan Sterman, MD, Bronx, NY (*Presenter*) Nothing to Disclose Linda B. Haramati, MD, MS, New Rochelle, NY (*Abstract Co-Author*) Spouse, Board Member, Kryon Systems Ltd Daniel Labovitz, Bronx, NY (*Abstract Co-Author*) Nothing to Disclose Michael Allen, Bronx, NY (*Abstract Co-Author*) Nothing to Disclose Shira Slasky, MD, Tenafly, NJ (*Abstract Co-Author*) Nothing to Disclose

For information about this presentation, contact:

sslasky@montefiore.org

PURPOSE

Left-hemispheric strokes are more frequent and often have a worse outcome than their right-hemispheric counterparts. The present study aims to evaluate whether laterality of cardiogenic cerebral embolization is affected by anatomical characteristics of the aortic arch. We hypothesized that laterality varies between patients with a bovine versus standard arch branching.

METHOD AND MATERIALS

We retrospectively identified 1598 acute cardioembolic strokes in patients with atrial fibrillation from our institutional stroke database (2009-2017). Selecting the first event in each patient yielded 1459 infarcts. Inclusion criteria were an acute anterior circulation ischemic infarct and availability of both arch and brain imaging (MR or CT). Alternative causes of stroke (e.g. >50% intra/extracranial stenosis ipsilateral to the stroke, lacunar infarct, dissection) and anomalous arch were excluded. Imaging was reviewed for stroke characterization and laterality and arch branching pattern. Bovine arch denotes a common origin of the brachiocephalic trunk and the left common carotid artery. Strokes were classified as bilateral, left or right hemispheric. Univariate analysis was performed using Chi square tests.

RESULTS

The final cohort comprised 615 patients, mean age 77 (SD 11.8) with 376 women (61%). The majority were ethnic minorities (33% white, 30% black, remainder mixed/Hispanic). Standard arch (n=424) stroke distribution was left 43.6% (185), right 45.1% (191) and bilateral 11.3% (48). Bovine arch (n=191) stroke distribution was left 51.3% (98), right 35.6% (68) and bilateral 13.1% (25). Bovine arches were associated with more left sided strokes compared with standard arches (p=0.035). Of note, 43% of patients with bovine arch were black and there was an association between black race and bovine arch (p=0.0001).

CONCLUSION

Bovine aortic arch configuration is associated with left hemispheric laterality of cardioembolic stroke.

CLINICAL RELEVANCE/APPLICATION

Our study enriches the understanding that arch anatomy influences stroke laterality and highlights the need for further research into the causative hemodynamic factors.

SSG10-02 Reporting Quality and MR Technical Heterogeneity of Intracranial Vessel Wall MR Imaging: A Systematic Review of the Literature

Tuesday, Dec. 3 10:40AM - 10:50AM Room: N229

Participants

Jae W. Song, MD, MS, Philadelphia, PA (*Presenter*) Nothing to Disclose Samantha C. Guiry, BA, Philadelphia, PA (*Abstract Co-Author*) Stockholder, Amgen Inc; Stockholder, CVS Health Corporation; Stockholder, Edwards Lifesciences Corporation; Stockholder, Stryker Corporation Brianna Moon, Philadelphia, PA (*Abstract Co-Author*) Nothing to Disclose Haochang Shou, Philadelphia, PA (*Abstract Co-Author*) Nothing to Disclose Sumei Wang, MD, Philadelphia, PA (*Abstract Co-Author*) Nothing to Disclose David Kung, Philadelphia, PA (*Abstract Co-Author*) Nothing to Disclose Steve Messe, Philadelphia, PA (*Abstract Co-Author*) Nothing to Disclose Scott Kasner, Philadelphia, PA (*Abstract Co-Author*) Nothing to Disclose Zhaoyang Fan, West Hollywood, CA (*Abstract Co-Author*) Nothing to Disclose Walter R. Witschey, Philadelphia, PA (*Abstract Co-Author*) Nothing to Disclose Laurie A. Loevner, MD, Philadelphia, PA (*Abstract Co-Author*) Nothing to Disclose

For information about this presentation, contact:

jae.song@pennmedicine.upenn.edu

PURPOSE

A systematic review of the literature was performed to identify studies using vessel wall MR imaging (VWI) to study intracranial vasculopathies. A qualitative synthesis of each study and an assessment of MR technical heterogeneity and reporting quality was conducted.

METHOD AND MATERIALS

PubMed, MEDLINE and EMBASE databases were searched up to September 2018 using inclusion/exclusion criteria for studies assessing intracranial vasculopathies with VWI. Two independent reviewers screened potential studies and extracted data. Foreign language articles were translated. The 22-point Strengthening the Reporting of Observational Studies in Epidemiology (STROBE) guideline was used to appraise reporting quality of analytic observational studies by calculating a Complete Reporting Score (CRS=yes/[yes+no]) for each study; criteria were scored as 'yes' if reporting was fulfilled. Scores of each manuscript section (introduction, methods, results, discussion) were also assessed. Inter-rater agreement was summarized by a Cohen's kappa (κ). The Preferred Reporting Items for Systematic Reviews and Meta-Analyses guideline was used.

RESULTS

Among 2431 articles, 79 met the inclusion criteria. Work was contributed most frequently from Asia (68%, n=54), received federal funding (62%, n=49), was retrospective (52%, n=42), and designed as analytic observational studies (51%, n=40). Intracranial atherosclerosis (ICAD) was the most commonly studied intracranial vasculopathy (52%, n=41). Considerable MR technical heterogeneity in magnet strength (range: 0.5T to 7T), spatial resolution (in-plane voxel size range: 0.11 to 1.27), and MR protocol was present with postcontrast imaging performed in 62% (n=49) of the exams. Among the 40 analytic observational studies, the overall mean STROBE CRS was 0.64 (range= 0.32-0.82); the introduction section had the strongest mean reporting score (CRSIntro=0.99) compared to the methods section, which emerged as the weakest (CRSMethods=0.53).

CONCLUSION

Assessment of the literature showed considerable MR technical heterogeneity in MR imaging methods. Among the analytic observational studies, the completeness of reporting based on STROBE guidelines, was variable.

CLINICAL RELEVANCE/APPLICATION

Reducing the heterogeneity of MR protocols in VWI studies and more consistent adherence to STROBE guidelines should maximize effective synthesis and clinical translation of findings for intracranial vasculopathies.

SSG10-03 Radiomic Analysis on Symptomatic Intracranial Atherosclerotic Plaque Using High Resolution MRI

Tuesday, Dec. 3 10:50AM - 11:00AM Room: N229

Participants Zhang Shi, Shanghai, China (*Presenter*) Nothing to Disclose Qi Liu, MD, PhD, Shanghai, China (*Abstract Co-Author*) Nothing to Disclose Jianping Lu, MD, Shanghai, China (*Abstract Co-Author*) Nothing to Disclose

For information about this presentation, contact:

shizhangmd@smmu.edu.cn

PURPOSE

This study aims to evaluate a quantitative radiomic approach based on High-resolution magnetic resonance imaging (HR-MRI) to differentiate symptomatic intracranial artery plaque from asymptomatic plaque.

METHOD AND MATERIALS

This study retrospectively analyzed 158 patients with middle cerebral artery (MCA) and basilar artery (BA) stenosis underwent HR-MRI between September 2013 and October 2016. Atherosclerosis plaques from MCA and BA were extracted as the region of interest (ROI) for quantitative evaluation. The stenosis value, plaque area/burden, lumen area, intraplaque hemorrhage (IPH), contrast enhancement ratio and 109 quantitative radiomic features were extracted and compared between symptomatic and asymptomatic patients. Univariate analysis was applied first to find possible variable that was associated with symptoms. Student t-test or twosample Wilcoxon test was used if the variable was/was not normally distributed. P-values <0.05 were considered as statistical significant. Multi-variate logistic analysis and a random forest model were used to evaluate the diagnostic performance.

RESULTS

A total of 158 patients met the inclusion criteria. There were 75 acute, 36 sub-acute symptomatic patients, and 47 asymptomatic patients. Smoking (odds ratio [OR]=2.724; 95%CI,1.200-6.183), IPH (OR=11.340; 95%CI, 1.441-89.221) and enhancement ratio (OR=6.865; 95%CI, 1.052-44.802) were independently associated with symptomatic plaques. The combined smoking, IPH and enhancement ratio had an area under the curve (AUC) of 0.714 for identifying symptomatic plaques. Radiomic features in T2, T1 and CE-T1 images were associated with symptomatic plaques , whose AUC respectively are 0.801,0.835 and 0.846. The combined all radiomic approach had a significantly higher AUC of 0.953. Combination of all features reached an AUC of 0.976, with accuracy

CONCLUSION

Radiomic analysis of intracranial artery plaque on HR-MRI accurately distinguished between plaques in patients who were symptomatic and plaques in patients who were asymptomatic. The highest accuracy was achieved by combining radiomic features with traditional assessment of clinical and morphological features.

CLINICAL RELEVANCE/APPLICATION

The favorable accuracy values in this study over those previously reported by conventional HR-MRI support the use of radiomic analysis to improve identification of acute symptomatic plaque.

SSG10-04 Arterial Transit Artefacts on ASL Perfusion-Weighted MRI in Patients with Carotid Artery Stenosis are a Better Predictor of Recent Symptoms than Degree of Stenosis or Carotid Plaque Morphology

Tuesday, Dec. 3 11:00AM - 11:10AM Room: N229

Participants

Alberto di Napoli, Rome , Italy (*Presenter*) Nothing to Disclose Suk Fun Cheng, MD, London, United Kingdom (*Abstract Co-Author*) Nothing to Disclose John Gregson, London, United Kingdom (*Abstract Co-Author*) Nothing to Disclose David Atkinson, London, United Kingdom (*Abstract Co-Author*) Nothing to Disclose Julia E. Markus, London, United Kingdom (*Abstract Co-Author*) Nothing to Disclose Toby Richards, MD, Perth, Australia (*Abstract Co-Author*) Nothing to Disclose Martin M. Brown, MD, London, United Kingdom (*Abstract Co-Author*) Nothing to Disclose Magdalena Sokolska, PhD, London, United Kingdom (*Abstract Co-Author*) Nothing to Disclose Rolf Jager, MD, London, United Kingdom (*Abstract Co-Author*) Nothing to Disclose

PURPOSE

Using comprehensive advanced MR imaging at 3T, including carotid plaque imaging and ASL perfusion MR, we aim to identify parameters that best distinguish between asymptomatic and symptomatic carotid stenosis, and to gather new evidence regarding the mechanisms causing clinical symptoms.

METHOD AND MATERIALS

We recruited patients with ICA stenosis participating in ongoing trials, who had ASL and carotid plaque imaging in the same sitting. Patients were assessed clinically for recent symptoms of TIA or stroke. MR images were analysed for the degree of stenosis, plaque morphology, presence of intraplaque haemorrhage (IPH), collateral circulation of the circle of Willis, presence and severity of arterial transit artefacts (ATAs). We used t-test and Fisher's exact test to investigate which features were associated with symptomatic status.

RESULTS

44 patients met the inclusion criteria, 22 of these were symptomatic. ATAs were only seen in patients with a >70% stenosis (p for association <0.001), and were associated with the configuration of the circle of Willis (p=0.001), particularly the absence of anterior communicating artery (ACOM) (p=0.003). Associations between symptoms and degree of stenosis, IPH, and plaque surface morphology were non-significant. However, patients with ATAs (n=16) were significantly more likely to be symptomatic than those without ATAs (n=28) (p=0.004). Symptomatic status correlated further with the severity of ATAs (p=0.002).

CONCLUSION

ATA was the only predictor of recent ischaemic symptoms in patients with carotid stenosis.

CLINICAL RELEVANCE/APPLICATION

Haemodynamic factors play a greater role in the mechanism of TIA and stroke associated with carotid stenosis of >70% than currently appreciated.

SSG10-05 Susceptibility-Weighted Imaging in Hyperacute Phase of Ischemic Stroke

Tuesday, Dec. 3 11:10AM - 11:20AM Room: N229

Participants

Niloufar S. Saadat, MD, Chicago, IL (*Presenter*) Nothing to Disclose Yong I. Jeong, Chicago, IL (*Abstract Co-Author*) Nothing to Disclose Mira M. Liu, Chicago, IL (*Abstract Co-Author*) Nothing to Disclose Marek Niekrasz, DVM, Chicago, IL (*Abstract Co-Author*) Nothing to Disclose Steven Roth, MD, Chicago, IL (*Abstract Co-Author*) Nothing to Disclose Timothy J. Carroll, PhD, Chicago, IL (*Abstract Co-Author*) Nothing to Disclose Gregory A. Christoforidis, MD, Chicago, IL (*Abstract Co-Author*) Nothing to Disclose

For information about this presentation, contact:

nsaadat@uchicago.edu

PURPOSE

Using a large animal experimental middle cerebral artery occlusion model, this work sought to determine if there was a significant change in the SWI signal intensity on regions of interest drawn in the penumbra and ischemic core based on perfusion and diffusion-weighted imaging.

METHOD AND MATERIALS

Eight mongrel canines (20-30kg) underwent permanent endovascular occlusion of an M1 segment of the middle cerebral artery (MCA) and acute ischemic stroke MR imaging. Anesthesia was chosen so as not to influence cerebrovascular reactivity. MRI was

acquired on a 3 Tesla unit (Achieva, Philips Healthcare, Best, Netherlands) and included susceptibility- weighted imaging (SWI), diffusion-weighted imaging (DWI) with the corresponding apparent diffusion coefficient (ADC) maps, and perfusion imaging. Susceptibility- weighted imaging was acquired within the first 60 minutes of MCA occlusion. The signal intensity was calculated on SWI images using Image J software (National Institutes of Health, Bethesda, Maryland). Regions of interests (ROI) were drawn manually on the infarct core, penumbra, and deep gray matter and was compared to that of the corresponding contralateral side. The infarct core was selected based on the hypointense areas on the ADC maps, penumbra chosen based on the perfusion imaging and identified by the defect between the ADC abnormality and the perfusion defect. The normality of data was assessed using the Shapiro-Wilk W test.

RESULTS

The median (interquartile range) of signal intensity on the infarct core (374.6 (366.5-393.6), vs. 432.6 (412.3-448.2), P-value<0.0001), and on the penumbra (433.7 (407.6-458.9) vs. 491.6 (467.6-510), P-value<0.0001) was significantly lower than signal intensity on their uninvolved contralateral side. The mean \pm SD of signal intensity was also significantly lower on deep gray matter compared to the uninvolved contralateral side (418.1 \pm 44.89 vs. 464.5 \pm 42.61, P-value<0.0001).

CONCLUSION

Signal intensity significantly drops during the hyperacute phase of MCA occlusion in the infarct core, penumbra, and deep gray matter comparing to the contralateral side. Presumably, this is a result of deoxyhemoglobin effect and venous vasodilation in the early stages of ischemia.

CLINICAL RELEVANCE/APPLICATION

Susceptibility- weighted imaging could possibly be used as a fast and noninvasive imaging to predict cerebral hemodynamic changes.

SSG10-06 Improvement of the Diagnostic Performance for Brain Hemorrhage Using Deep Learning-based Computer-Aided Detection System

Tuesday, Dec. 3 11:20AM - 11:30AM Room: N229

Participants

Yoshiyuki Watanabe, MD, PhD, Suita, Japan (Abstract Co-Author) Research Grant, Canon Medical Systems Corporation; Research Grant, Dai Nippon Printing Co, Ltd; Speakers Bureau, General Electric Company Hiroki Yano, Sakai, Japan (Presenter) Nothing to Disclose Satoshi Umeyama, Tokyo, Japan (Abstract Co-Author) Employee, Dai Nippon Printing Co Ltd Takahiro Tanaka, Tokyo, Japan (Abstract Co-Author) Employee, Dai Nippon Printing Co, Ltd Hiroto Takahashi, MD, Suita, Japan (Abstract Co-Author) Nothing to Disclose Masahiro Fujiwara, MD, Suita , Japan (Abstract Co-Author) Nothing to Disclose Takuya Fujiwara, MD, Suita, Japan (Abstract Co-Author) Nothing to Disclose Hisashi Tanaka, MD, Suita, Japan (Abstract Co-Author) Nothing to Disclose Atsuko Arisawa, MD, Osaka, Japan (Abstract Co-Author) Nothing to Disclose Noriyuki Tomiyama, MD, PhD, Suita, Japan (Abstract Co-Author) Nothing to Disclose Hajime Nakamura, Suita, Japan (Abstract Co-Author) Nothing to Disclose Kazuhisa Yoshiya, Suita, Japan (Abstract Co-Author) Nothing to Disclose Kenichi Todo, Suita, Japan (Abstract Co-Author) Nothing to Disclose Atsushi Nishida, Shinjuku , Japan (Abstract Co-Author) Employee, Dai Nippon Printing Co, Ltd Tsutomu Nakagawa, Tokyo, Japan (Abstract Co-Author) Employee, Dai Nippon Printing Co, Ltd

For information about this presentation, contact:

watanabe@radiol.med.osaka-u.ac.jp

PURPOSE

To elucidate the diagnostic performance with deep learning-based computer-aided detection (CAD) for non-expert and expert doctors in detecting cerebral hemorrhage from head CT.

METHOD AND MATERIALS

40 head CT datasets were evaluated by 15 doctors (5 board certificated radiologists, 5 radiology residents, and 5 interns). The CT datasets have 16 normal and 24 hemorrhagic patients with 48 intracranial hemorrhagic lesions including 5 types of cerebral hemorrhages: extradural hematoma, subdural hematoma, intracerebral hemorrhage, subarachnoid hemorrhage, and intraventricular hemorrhage. The doctors attended 2 reading sessions: diagnosing without and with CAD (more than a week between 2 reading sessions). All doctors annotated the hemorrhagic regions and gave them the degree of confidence on a scale of one to ten. Our CAD system was developed with 522 patients' head CT which consist of 242 normal (5,929 slices) and 280 hemorrhagic patients (2,899 slices), and detection results were displayed as corresponding probability heat maps using U-Net and a machine learning-based false-positive removal method. The normal and hemorrhagic patients were randomly split into training (90%) and validation (10%) datasets and used for constructing CAD. Sensitivity, specificity, and accuracy were evaluated using a paired t test. In addition, a figure of merit (FOM) derived from the jackknife free-response receiver operating characteristic were evaluated.

RESULTS

The mean accuracy of all doctors with patient-based evaluation significantly increased from 83.7% to 89.7% (p<0.01) by using CAD. In addition, the accuracies of board certificated radiologists, radiology residents, and interns showed 92.5%, 82.5%, and 76.0% (without CAD) and 97.5%, 90.5%, and 81.0% (with CAD), respectively. The rate of increase of the mean accuracy for non-expert doctors was 6.5%; it was greater than that for expert doctors (5.0%). The mean FOM of all doctors increased from 0.78 to 0.82 (p<0.05) by using CAD.

CONCLUSION

The diagnostic performance and confidence of intracranial hemorrhage detection improved among all doctors, especially for nonexpert doctors by using CAD.

CLINICAL RELEVANCE/APPLICATION

Our CAD software could improve the diagnostic performance of all doctors in detecting hemorrhage from head CT and reduce the missed reports of faint or small hemorrhage, especially for non-expert doctors.

SSG10-07 Deep Learning Model to Predict Patient Outcome in ICH Using Fluid-Attenuated Inversion Recovery Imaging Data

Tuesday, Dec. 3 11:30AM - 11:40AM Room: N229

Participants

Lili He, Cincinnati, OH (*Presenter*) Nothing to Disclose Ming Chen, Cincinnati, OH (*Abstract Co-Author*) Nothing to Disclose Hailong Li, PhD, Cincinnati, OH (*Abstract Co-Author*) Nothing to Disclose Jinghua Wang, DSc, Cincinnati, OH (*Abstract Co-Author*) Nothing to Disclose Vivek J. Khandwala, PhD, Cincinnati, OH (*Abstract Co-Author*) Nothing to Disclose Daniel Woo, MD, Cincinnati, OH (*Abstract Co-Author*) Nothing to Disclose Achala S. Vagal, MD, Mason, OH (*Abstract Co-Author*) Research Consultant, Nervive; Research Grant, Imaging Core Lab; Research Grant, ENDOLOW Trial; Research Grant, Cerenovus; Research Grant, Johnson & Johnson; Research Grant, General Electric Company

For information about this presentation, contact:

LILI.HE@CCHMC.ORG

PURPOSE

Timely and accurate outcome prediction in intracerebral hemorrhage (ICH) patients is important for optimizing rehabilitation strategy. The objective of this study was to investigate if a deep neural network model can predict recovery outcome in patients with ICH at 3 months using T2-weighted fluid-attenuated inversion recovery (FLAIR) imaging data.

METHOD AND MATERIALS

A convenience sample of 53 left thalamocapsular ICH patients (hemorrhagic volume < 20cc; mean age = 52.4 yrs) were included from the Ethnic/Racial Variation in Intracerebral Hemorrhage (ERICH) study. T2-weighted FLAIR data were acquired using clinical protocols in this multicenter cohort. A deep learning model was trained to identify patients likely to have unfavorable outcomes, defined as 3-month modified rankin scale (mRS) score 3-6. As shown in Figure 1, we employed a pre-trained VGGNet-19 model as a feature generator to learn high-level features from input FLAIR images. We then built a convolutional neural network (CNN) classifier based on the high-level features to identify the patients with unfavorable outcomes. Rotation and shift-based data augmentation strategy was implemented to increase the training samples by 20 times (but not testing samples). Performance was evaluated using 5 fold cross-validation with the metrics of accuracy, sensitivity, specificity, and area under the receiver operating characteristic curve (AUC).

RESULTS

Our model was able to correctly identify patients likely to have unfavorable outcomes with an accuracy of 81.8% (95% confidence interval: 80.7%, 82.9%), AUC of 0.82 (0.80, 0.83), sensitivity of 90.6% (89.6%, 91.6%) and specificity of 72.6% (70.1%, 75.1%).

CONCLUSION

This work demonstrates the feasibility of deep learning approach for predicting outcomes of ICH patients using only FLAIR imaging data with a promising accuracy. Future model improvements will include the incorporation of clinical data. A larger multidimensional study is important to validate our approach.

CLINICAL RELEVANCE/APPLICATION

Deep learning model on FLAIR imaging data can identify ICH patients likely to have unfavorable outcome. Such prognostic model can potentially help with the treatment decision and rehabilitation strategy optimization.

SSG10-08 Microstructural ASYmmetry (MASY) of DTI in Stroke Reveals Interaction Effect of Sex and Clinical Covariates

Tuesday, Dec. 3 11:40AM - 11:50AM Room: N229

Participants

Nagesh Adluru, PhD, Madison, WI (*Abstract Co-Author*) Nothing to Disclose Veena A. Nair, PhD, Madison, WI (*Presenter*) Nothing to Disclose Andrew Alexander, PhD, Madison, WI (*Abstract Co-Author*) Co-founder and Co-owner, Thervoyant, Inc Vivek Prabhakaran, MD, PhD, Fitchburg, WI (*Abstract Co-Author*) Nothing to Disclose

For information about this presentation, contact:

adluru@wisc.edu

PURPOSE

Microstructural investigation of stroke is one of the flagship clinical applications of diffusion tensor imaging (DTI). The purpose of this work was to examine the interaction effect of sex and clinical scores on stroke microstructure measured using DTI. It was hypothesized that using the microstructural *difference* between the contra and ipsilesional regions would be statistically more powerful than using the microstructural measures within the lesion. It was further hypothesized that considering the *distributional difference* of their microstructure, instead of the difference between their averages, would be more sensitive in gleaning this effect.

METHOD AND MATERIALS

Diffusion weighted MR images on n=16 subjects (ages: 52.8+/-14.5(n=6 females), 62.4+/-14.1(n=10 males)) were acquired with a b-value of 2000 s/mm2 along 56 unique non-colinear gradient directions, in addition to 10 non-diffusion weighted (b=0) images. Preprocessing was performed using FSL's eddy to remove distortions from eddy currents and motion. The analysis was performed using the four main (DTI) measures: fractional anisotropy (FA), mean diffusivity (MD), axial diffusivity (AD) and radial diffusivity (RD) and two clinical covariates: the ratio of acute time period to age and normalized verbal fluency (corrected for age and

education) at the time of MRI. The acute time period is the number of days between MRI visit and stroke onset. A linear model that includes the interaction effect of sex and clinical covariates was fit for each of the following dependent variable: (1) average DTI in the acute ipsilesion mask, (2) difference between the average DTI in contra and ipsilesional masks and (3) *microstructural asymmetry (MASY)* computed using symmetrized Kullback-Leibler divergence between DTI distributions of contra and ipsilesional masks. The p-values for the interaction effect from the models were reported.

RESULTS

The main results are summarized in Figure 1. The microstructural features were positively correlated with acute time period ratio and inversely correlated with verbal fluency.

CONCLUSION

The relationships between clinical scores and microstructural asymmetry of DTI in stroke were more pronounced in males compared to females.

CLINICAL RELEVANCE/APPLICATION

(delaing with interaction effects in stroke microstructure) '*Distributional difference approach* is recommended for greater statistical sensitivity to relationships between clinical scores and imaging.'

SSG10-09 High Definition Imaging Reduces Procedure Time Without Impacting Patient Dose in Image-Guided Neuro Interventional Procedures

Tuesday, Dec. 3 11:50AM - 12:00PM Room: N229

Participants

Swetadri Vasan Setlur Nagesh, MS, PhD, Buffalo, NY (*Presenter*) Nothing to Disclose Andrew Kuhls-Gilcrist, PHD, Tustin, CA (*Abstract Co-Author*) Employee, Canon Medical Systems Corporation Kunal Vakharia, Buffalo, NY (*Abstract Co-Author*) Nothing to Disclose Stephan Munich, Buffalo, NY (*Abstract Co-Author*) Nothing to Disclose Muhammad Waqas, MD, MBBS, Buffalo, NY (*Abstract Co-Author*) Nothing to Disclose Yiemeng Hoi, PhD, Tustin, CA (*Abstract Co-Author*) Employee, Canon Medical Systems Corporation Kenneth V. Snyder, Buffalo, NY (*Abstract Co-Author*) Employee, Canon Medical Systems Corporation Kenneth V. Snyder, Buffalo, NY (*Abstract Co-Author*) Nothing to Disclose Jason Davies, Buffalo, NY (*Abstract Co-Author*) Nothing to Disclose Daniel Bednarek, PhD, Buffalo, NY (*Abstract Co-Author*) Research Grant, Canon Medical Systems Corporation Stephen Rudin, PhD, Buffalo, NY (*Abstract Co-Author*) Research Grant, Canon Medical Systems Corporation Elad Levy, MD, Buffalo, NY (*Abstract Co-Author*) Shareholder, Intratech Medical Ltd Shareholder, Blockade Medical LLC Shareholder, NeXtGen Owner, Intratech Medical Ltd Owner, Blockade Medical LLC Owner, NeXtGen Biologics Investigator, Medtronic plc Speaker, Medtronic plc Consultant, Pulsar Vascular Consultant, Blockade Medical LLC Advisory Board, Stryker Corporation Advisory Board, NeXtGen Biologics Advisory Board, MEDX Inc Support, Abbott Laboratories Adnan Siddiqui, MD, PhD, Buffalo, NY (*Abstract Co-Author*) Grant, Canon Medical Systems Corporation

PURPOSE

To quantify the clinical impacts and radiation dose of a novel fluoroscopic x-ray detector that combines high definition (Hi-Def) crystalline-Si imaging modes with 76µm pixels and high efficiency amorphous-Si imaging modes with 194µm pixels.

METHOD AND MATERIALS

DICOM Radiation Dose Structured Report (RDSR) data was collected for all neurointerventional procedures performed before and after installation of the Hi-Def detector at a single center over a 32 month period. There were 1,702 pre- and 2,499 post-Hi-Def cases with over 390k irradiation events in total. A real-time patient skin dose tracking system was used to monitor peak skin dose during the Hi-Def cases. A two-sample student's t-Test analysis was performed to compare various technical parameters included in the RDSR before and after installation of the new Hi-Def technology. To further investigate any potential impacts on radiation dose, cumulative air kerma, dose area product and peak skin dose were plot as a function of Hi-Def utilization as a percentage of the total number of irradiation events.

RESULTS

Hi-Def modes were used in more than 50% of the most complicated cases defined as having procedure times lasting more than 90 minutes. Improved visualization capabilites were demonstrated especially during device deployment and manipulation. Average procedure time and the total number of irradiation events were both significantly reduced by 9% (p<0.01). Average fluoro time, number of CBCT scans and cumulative air kerma were trending lower (5-10% less) but not yet reaching statistical significance (0.05< p<0.16). Peak skin dose data was available for 1,518 cases with 97.7% and 99.5% of cases below 3Gy and 5Gy, respectively. No correlation was observed (R2<0.10) using a best of all fits for all dosimetric indications as a function of Hi-Def utilization.

CONCLUSION

Preliminary results from over 4,000 neurointerventional procedures at a single center demonstrate that the improved spatial resolution of the Hi-Def detector may result in reduced procedure time and number of irradiation events. In addition, there was no observable increase in patient dose with the utilization of the Hi-Def detector.

CLINICAL RELEVANCE/APPLICATION

This is the first study investigating clinical benefits of a new detector that can provide more than 2x the spatial resolution of any other clinically available technology and no patient dose penalty.





SSG14

Physics (MRI - Clinical Applications)

Tuesday, Dec. 3 10:30AM - 12:00PM Room: S504AB



AMA PRA Category 1 Credits ™: 1.50 ARRT Category A+ Credit: 1.75

FDA Discussions may include off-label uses.

Participants

Yi Wang, PhD, New York, NY (*Moderator*) Nothing to Disclose Matthew A. Bernstein, PhD, Rochester, MN (*Moderator*) Former Employee, General Electric Company

Sub-Events

SSG14-01 Development of Respiratory Motion-Resolved Hepatobiliary Phase Cine-MRI Using Compressed SENSE for Stereotactic Body Radiotherapy in Liver Tumor

Tuesday, Dec. 3 10:30AM - 10:40AM Room: S504AB

Participants

Ryuji Shimada, Kobe, Japan (*Presenter*) Nothing to Disclose Keitaro Sofue, MD, Kobe, Japan (*Abstract Co-Author*) Nothing to Disclose Katsusuke Kyotani, RT,MSc, Kobe, Japan (*Abstract Co-Author*) Nothing to Disclose Tianyuan Wang, PhD, Kobe , Japan (*Abstract Co-Author*) Nothing to Disclose Yoshiko Ueno, MD, PhD, Kobe, Japan (*Abstract Co-Author*) Nothing to Disclose Takamichi Murakami, MD, PhD, Osaka, Japan (*Abstract Co-Author*) Nothing to Disclose Takeaki Ishihara, Kobe, Japan (*Abstract Co-Author*) Nothing to Disclose Shintaro Horii, Kobe, Japan (*Abstract Co-Author*) Nothing to Disclose Munenobu Nogami, MD, PhD, Kobe, Japan (*Abstract Co-Author*) Nothing to Disclose Akiko Kusaka, RT, Kobe, Japan (*Abstract Co-Author*) Nothing to Disclose

CONCLUSION

The CS with denoising improved tumor-to-liver contrast and image quality in high temporal resolution HBP cine-MRI, which can be potentially applied for stereotactic body radiotherapy.

Background

For radiotherapy of the liver, cine-MRI has been used to track respiratory-induced motion of the liver and tumor, and to assist accurate delineation of tumor volume. However, tumor boundaries cannot be clearly defined when using balanced SSFP and single-shot T2-weighted sequences because of poor tumor-to-liver contrast. Recent development of Compressed SENSE (CS) enables to accelerate temporal resolution while maintaining contrast resolution. This study aimed to develop and assess hepatobiliary phase (HBP) cine-MRI using CS.

Evaluation

Twenty patients underwent HBP cine-MRI after gadoxetic acid injection, consisted of modified 2D-GRE T1-weighted TFE sequence with saturate recovery prepulse (TR/TE, 3.1/1.46 ms; FA, 30°; FOV, 380 mm; acquisition matrix, 112×201; slice thickness, 3mm) in every 0.5 second for one minute. The images were acquired with SENSE (factor, 4), CS (factor, 4) without denoising (CS-no), and CS with strong denoising level (CS-strong) to assess the capability of CS for image quality improvement. For quantitative analysis, signal noise ratio of the liver and tumor (SNRLiv, SNRTum) and liver-to-tumor contrast ratio (CRLiv/Tum) were measured. For qualitative analysis, two radiologists evaluated lesion conspicuity, contrast enhancement, image noise, motion smoothness, and overall quality on a 4-point scale. The SNRLiv and SNRTum were 6.8 ± 2.7 and 2.8 ± 0.8 for SENSE, 6.7 ± 2.8 and 3.0 ± 1.0 for CS-no, and 14.4 ± 3.9 and 5.7 ± 2.8 for CS-strong, respectively (P<.001, repeated measures ANOVA). The CRLiv/Tum was 0.47 ± 0.13 for SENSE, 0.43 ± 0.12 for CS-no, and 0.49 ± 0.16 for CS-strong (P>.05). The CS-strong showed significantly higher image quality (P<.01, Kruskal-wallis H test) except for motion smoothness (P=.11).

Discussion

The CS can suppress aliasing artifact using random undersampling of k-space trajectory, enabling to apply wavelet transformation and denoising. This algorithm substantially increased SNR, contributed to improvement of contrast ratio and image quality in HBP cine-MRI.

SSG14-02 Multi Band-SWeep Imaging with Fourier Transformation (MB-SWIFT) MRI Can Quantify Bone Mineral Density while Concurrently Characterizing Material-Level and Biochemical Changes in Bone In Vivo

Tuesday, Dec. 3 10:40AM - 10:50AM Room: S504AB

Participants

Rachel K. Surowiec, MSc, Ann Arbor, MI (*Presenter*) Nothing to Disclose Sundaresh Ram, DPhil, Ann Arbor, MI (*Abstract Co-Author*) Nothing to Disclose Djaudat Idiyatullin, PhD, Minneapolis, MN (*Abstract Co-Author*) Nothing to Disclose Robert Goulet, DPhil, Ann Arbor, MI (*Abstract Co-Author*) Nothing to Disclose Craig J. Galban, PhD, Ann Arbor, MI (*Abstract Co-Author*) License agreement, Imbio, LLC Kenneth M. Kozloff, Ann Arbor, MI (*Abstract Co-Author*) Nothing to Disclose

For information about this presentation, contact:

rachelks@umich.edu

PURPOSE

Multi-Band SWeep Imaging with Fourier Transformation (MB-SWIFT) MRI could have novel and specific application in bone where capturing mineral and remaining 40% of the composite tissue that confers to bone quality and strength is desired. We describe a comprehensive set of biomarkers to characterize material-level and biochemical components that are "missed" when using gold-standard bone imaging approaches (clinical DXA, pre-clinical μ CT). Further, we establish the efficacy of MB-SWIFT to measure bone mineral density (BMD) in comparison to μ CT.

METHOD AND MATERIALS

In vivo μ CT (Bruker SkyScan1176, 35 μ m3) and MB-SWIFT MRI (Agilent 9.4T, 156 μ m3) of the proximal tibiae were obtained at baseline and 2, 4, 10 and 12 wks post ovariectomy (OVX) in 7 rats (F, 6 wks old). μ CTs were registered to corresponding MRIs per timepoint and resulting transforms were applied to μ CT-derived cortical and trabecular VOIs guiding analysis across modalities. Cortical water fraction, marrow fat fraction and cortical matrix volumetric T1 relaxation using the variable flip angle method were quantified from MB-SWIFT images. Sensitivity to cortical water loss during sequential drying was confirmed in excised tibia. μ CT and MRI images were converted to Hounsfield units and BMD was calculated using a concurrently imaged calcium hydroxyapatite standard. Pearson's correlation coefficients, simple linear regressions and RM-ANOVAs were employed and significant at p <= 0.05.

RESULTS

MB-SWIFT cortical and trabecular BMD correlated significantly with μ CT BMD (cortical: R=0.67, p<0.0001; trabecular: R=0.62, p<0.0001) which significantly increased longitudinally. Growth appeared to overcome estrogen-deficient changes in bone mass yet MB-SWIFT distinguished significant decreases in cortical water, increases in marrow fat and increases cortical matrix volumetric T1 relaxation consistent with OVX by 10 weeks. MB-SWIFT cortical water fraction significantly correlated to cortical water loss (% by volume) during sequential drying (R=-0.98, p=0.01).

CONCLUSION

MB-SWIFT MRI could have a novel and specific application in bone where capturing information on both mineral and matrix properties that confer quality and strength is highly desired.

CLINICAL RELEVANCE/APPLICATION

MB-SWIFT can quantify biomarkers of bone quality and mineral phase of bone without the use of harmful ionizng radiation holding promise for clinical adaptation allowing for safe longitudinal analysis of bone.

SSG14-03 Quantitative Biliary Tree Imaging by MRI: A Novel Method of Assessing Change Over Time in Hepatobiliary Disease via MRCP

Tuesday, Dec. 3 10:50AM - 11:00AM Room: S504AB

Participants

Marc H. Goldfinger, Msc, PhD, Oxford, United Kingdom (Presenter) Researcher, Perspectum Diagnostics Ltd

Katherine Arndtz, MBChB, Birmingham, United Kingdom (Abstract Co-Author) Nothing to Disclose

Ged Ridgway, Oxford, United Kingdom (Abstract Co-Author) Employee, Perspectum Diagnostics Ltd; Stockholder, Perspectum Diagnostics Ltd

Daniel Halliday, Oxford, United Kingdom (Abstract Co-Author) Employee, Perspectum Diagnostics Ltd

Maria Mavar, Oxford, United Kingdom (Abstract Co-Author) Employee, Perspectum Diagnostics Ltd

Andrea Borghetto, Oxford, United Kingdom (Abstract Co-Author) Employee, Perspectum Diagnostics Ltd

Matt Kelly, PhD, Oxford, United Kingdom (Abstract Co-Author) Employee, Perspectum Diagnostics Ltd

Peter Eddowes, Nottingham, United Kingdom (Abstract Co-Author) Nothing to Disclose

Michael Brady, Oxford, United Kingdom (*Abstract Co-Author*) Founder and Chairman, Perspectum Diagnostics Ltd Founder and Chairman, Volpara Health Technologies Limited Founder, ScreenPoint Medical BV Chairman, Acuitas Medical Ltd Chairman, IRISS Medical Chairman, Colwiz

Rajarshi Banerjee, MD,DPhil, Oxford, United Kingdom (*Abstract Co-Author*) CEO, Perspectum Diagnostics Ltd Gideon Hirschfield, Toronto, ON (*Abstract Co-Author*) Nothing to Disclose

For information about this presentation, contact:

marc.goldfinger@perspectum.com

marc.goldfinger@perspectum.com

CONCLUSION

We demonstrate that state-of-the-art quantitative MRCP enables the extraction of quantitative biomarkers of biliary anatomy able to objectively identify changes in ducts over time, which correlates with biliary disease that were not identified via biochemical markers. Quantitative biliary tree imaging warrants ongoing investigation prospectively as a means of a potential standardised application for disease and therapy monitoring in PSC.

Background

Magnetic resonance cholangiopancreatography (MRCP) is a non-invasive imaging technique for the evaluation of hepatobiliary disease. Despite widespread use there remains a lack of objective assessment of biliary duct changes, and detecting changes in scans can be difficult, hindering monitoring of disease progression. Furthermore, serum biomarkers for hepatobiliary disease lack sensitivity to longitudinal changes biliary disease status. Here we evaluate the utility of novel quantitative biomarkers of biliary anatomy, extracted from 3D MRCP scans, to assess changes in biliary ducts over 1 year in patients with autoimmune liver diseases.

Evaluation

 Patients with primary sclerosing cholangitis (PSC, n=44), autoimmune hepatitis (AIH, n=35) and primary biliary cholangitis (PBC, n=59) were recruited for heavily T2-weighted MRCP imaging at base-line and 1-year follow-up. A total of 284 scans were processed with quantitative image analysis to enhance and quantify the tubular structures. The underlying algorithms combine multi-scale Hessian analysis, gradient vector flow analysis, intelligent path search algorithm and novel duct modelling algorithms.

Discussion

Quantitative imaging, evaluating MR-apparent biliary duct size and length distinguished PSC from AIH and PBC patients (p<0.001). At baseline, the number of strictures was a better classifier of PSC and AIH patients (AUC=0.72) than bilirubin (AUC=0.65). At 1 year follow up PSC patients contained significantly more strictures (p<0.01) and greater stricture severity (p<0.01) compared to AIH and PBC, whilst alkaline phosphatase (ALP) and bilirubin were found to exhibit no significant changes from baseline across the 3 cohorts. High risk PSC patients (ALP>1.5xULN) were found to have more dilatations (p<0.01) and greater stricture severity (p<0.01) than low risk at baseline. Abnormal length sum, stricture length sum (AUC=0.74, 0.73 respectively) were found to accurately classify high and low risk patients. Interestingly, metrics in high risk patients did not change from baseline at follow up, whilst low risk PSC patients were found have an enlarged tree volume (p<0.01), duct length (p<0.01) and stricture severity (p<0.01) at follow up.

SSG14-04 Validation of Highly Accelerated Wave-CAIPI 3D-T1 Sampling Perfection With Application Optimized Contrast Using Different Flip-Angle Evolutions (Wave-3D-T1 SPACE) with Conventional 3D-T1 SPACE for Post-Contrast Brain Imaging

Tuesday, Dec. 3 11:00AM - 11:10AM Room: S504AB

Participants

Maria Gabriela Longo, MD, Boston, MA (*Abstract Co-Author*) Scholarship, Siemens AG John Conklin, MD, MSc, Boston, MA (*Abstract Co-Author*) Nothing to Disclose Steve Cauley, PhD, Charlestown, MA (*Abstract Co-Author*) Nothing to Disclose Daniel Polak, Charlestown, MA (*Abstract Co-Author*) Nothing to Disclose John Kirsch, PhD, Boston, MA (*Abstract Co-Author*) Nothing to Disclose Kawin Setsompop, Charlestown, MA (*Abstract Co-Author*) Research Grant, Siemens AG; Royalties, General Electric Company; Royalties, Koninklijke Philips NV; Scientific Advisory Board, Kineticor; Ramon G. Gonzalez, MD, PhD, Boston, MA (*Abstract Co-Author*) Nothing to Disclose Pamela W. Schaefer, MD, Boston, MA (*Abstract Co-Author*) Nothing to Disclose Otto Rapalino, MD, Boston, MA (*Abstract Co-Author*) Nothing to Disclose Susie Y. Huang, MD,PhD, Boston, MA (*Presenter*) Research Grant, Siemens AG

For information about this presentation, contact:

mfigueirolongo@mgh.harvard.edu

PURPOSE

To evaluate the image quality and diagnostic performance of highly-accelerated Wave-CAIPI 3D-T1 Sampling Perfection with Application-optimized Contrasts by using flip angle Evolution (Wave-T1 SPACE) compared to conventional 3D-T1 SPACE for the detection of intracranial enhancing lesions on post-contrast brain MRI.

METHOD AND MATERIALS

Consecutive patients (N=38) undergoing 3T clinical brain MRI with contrast were prospectively enrolled. The most common indications for MRI were screening for brain metastases (N=21), and evaluation of primary brain tumors (N=8). All MRI scans included a conventional post-contrast T1 SPACE (R=4, acquisition time TA=4min 19s) and resolution-matched (slice thickness = 0.9mm) post-contrast Wave-T1 SPACE sequence (R=9, TA=1min 40s). Studies were performed on a clinical 3T MRI scanners (MAGNETOM Prisma; Siemens, Erlangen). Two neuroradiologists evaluated the images head-to-head for the visualization of enhancing lesions and nonenhancing pathology, grading of motion artifacts and noise, and diagnostic quality using a predefined 5-point scale. Discrepancies were adjudicated by a third reader. Wave-T1 SPACE was tested for non-inferiority compared to conventional T1 SPACE using a 10% non-inferiority margin.

RESULTS

Compared to conventional post-contrast T1 SPACE, Wave-T1 SPACE showed no difference in the visualization of enhancing lesions (P<0.001) and non-enhancing pathology (P=0.003), and no difference in diagnostic quality (P<0.001). Wave-T1 SPACE images demonstrated comparable or reduced motion artifact in the majority of cases and slightly greater image noise, with no impact on overall diagnostic quality. The figure shows representative examples demonstrating the comparable image quality of the post-contrast Wave- and conventional T1 SPACE sequences in delineating leptomeningeal disease and brain tumor.

CONCLUSION

A 1.6-minute Wave-T1 SPACE acquisition demonstrates comparable performance to a 4.3-minute resolution-matched conventional T1 SPACE sequence in identifying enhancing lesions, with an approximate 3-fold reduction in acquisition time. The findings support clinical application of Wave-T1 SPACE over conventional T1 SPACE for routine post-contrast clinical brain imaging.

CLINICAL RELEVANCE/APPLICATION

Wave-T1 SPACE is comparable to conventional T1 SPACE in detecting enhancing lesions with up to 3-fold reduced scan time and less motion, supporting its clinical application in routine brain imaging.

SSG14-05 Application of Magnetic Resonance Imaging with Free-Breathing T1-Weighted Star-VIBE for Improving Image Quality in Chest: A Study Compared with T1-Weighted Conventional Breath-Hold VIBE

Tuesday, Dec. 3 11:10AM - 11:20AM Room: S504AB

Yong Yu, Xianyang City, China (*Abstract Co-Author*) Nothing to Disclose Nan Yu, MD, Xianyang, China (*Abstract Co-Author*) Nothing to Disclose Haifeng Duan, Xianyang City, China (*Abstract Co-Author*) Nothing to Disclose Yun Shen, PhD, Beijing, China (*Abstract Co-Author*) Employee, General Electric Company Researcher, General Electric Company Shan Dang, Xianyang, China (*Abstract Co-Author*) Nothing to Disclose Xiaoxia Chen, MMed, Xianyang City, China (*Abstract Co-Author*) Nothing to Disclose Dong Han, MD, Xianyang, China (*Abstract Co-Author*) Nothing to Disclose Qi Yang, Xianyang, China (*Abstract Co-Author*) Nothing to Disclose Shaoyu Wang, Shanghai, China (*Abstract Co-Author*) Nothing to Disclose Zhang Yanzi, Xianyang City , China (*Abstract Co-Author*) Nothing to Disclose

For information about this presentation, contact:

395654582@qq.COM

PURPOSE

To explore the application of free-breathing T1-weighted Star-VIBE sequence for improving image quality in chest compared with T1-weighted conventional breath-hold VIBE sequence in magnetic resonance(MR) imaging.

METHOD AND MATERIALS

Twenty patients underwent MR chest examination on a 3.0T scanner (MAGNETOM Skyra, Siemens Healthcare, Erlangen, Germany). The scan sequences included T1-weighted conventional breath-hold VIBE(group A: TE 1.29 ms, TR 3.97 ms) and free-breathing T1-weighted Star-VIBE (group B: TE 1.39 ms, TR 2.79 ms). The signal intensity (SI) and standard deviation (SD) of ascending aorta, main pulmonary artery and descending aorta were measured at the level of main pulmonary artery. The signal-to-noise ratio (SNR=SI/SD) and coefficient of variation (CV=SD/SI) of signal intensity were calculated. The image quality was subjectively scored double-blindly using a 5-point scoring system by two radiologists who had five or more years of working experience (5 point, the image quality is best; 4 point, the image quality is better; 3 point, the image quality is general; 2 point, the image quality is poor; 1 point, the image can not be evaluated).

RESULTS

There was no significant difference in population characteristics between the two groups (P>0.05). The signal-to-noise ratio (SNR) of ascending aorta, main pulmonary artery and descending aorta in group B were significantly higher than those of group A(P<0.05), while the coefficient of variation of signal intensity about group B were significantly lower than those of group A(P<0.05). The subjective scores of image quality by the two MR radiologists had excellent consistence (kappa value>0.80, P<0.05), the subjective score of group B were significantly higher thangroup A (P < 0.05).

CONCLUSION

Magnetic resonance imaging with free-breathing T1-weighted Star-VIBE sequence can significantly improve image quality in chest compared with T1-weighted conventional breath-hold VIBE sequence.

CLINICAL RELEVANCE/APPLICATION

In thoracic magnetic resonance imaging, free-breathing T1-weighted Star-VIBE sequence can be used to improve image quality, which can obtain better image quality compared with T1-weighted conventional breath-hold VIBE sequence.

SSG14-06 Design Your MSK MRI: It Needs to be Planned by Radiologist

Tuesday, Dec. 3 11:20AM - 11:30AM Room: S504AB

Participants

Young Kwang Lee, MD, Jeonju, Korea, Republic Of (*Abstract Co-Author*) Nothing to Disclose Eun Hae Park, MD, Jeonju-si, Korea, Republic Of (*Presenter*) Nothing to Disclose Myungjin Seol, MD, Iksan-si, Korea, Republic Of (*Abstract Co-Author*) Nothing to Disclose Donghan Shin, Jeonju-si, Korea, Republic Of (*Abstract Co-Author*) Nothing to Disclose Yeong Sang Hong, Gwangju, Korea, Republic Of (*Abstract Co-Author*) Nothing to Disclose Jin Hee You, MD, Jeonju, Korea, Republic Of (*Abstract Co-Author*) Nothing to Disclose Gong Yong Jin, MD, PhD, Jeonju, Korea, Republic Of (*Abstract Co-Author*) Nothing to Disclose You Seon Song, Busan, Korea, Republic Of (*Abstract Co-Author*) Nothing to Disclose

For information about this presentation, contact:

jiml0826@gmail.com

PURPOSE

To evaluation the recall rate and causes of musculoskeletal MRI scanned at a tertiary center

METHOD AND MATERIALS

From January to July 2018, 1639 musculoskeletal MRI were performed in our institution. Two musculoskeletal radiologists reviewed, recalled, and rescanned cases. Evaluation for reasons of recalled cases by consensus were in the following categories: resolution issue, field of view issue, coil issue, artifact issue, missed sequence issue, newly detected lesion issue, and miscellaneous. Then radiologists reviewed the rescanned images and assessed a 4-point confidence level before and after an additional scan. Finally, they were asked if a rescan could have been avoidable if they were asked to designed the protocol before scanning (yes, not sure, no).

RESULTS

The total recalled cases were 47 out of 1639 (2.8%). The causes of recall were FOV issue (14), adding the sequence (9), resolution issue (8), coil issue (3), metal artifact control (3), incidental lesion (2), changing position (2), and miscellaneous (5). The confidence score significantly increased after a rescan compared with the initial image (3.2 vs. 2.7, respectively, P<0.05). Two radiologists reported 33 out of 47 cases would not need a rescan if the radiologist were able to design the protocol prior to the scan.

CONCLUSION

Musculoskeletal MRI can offer insufficient information at an initial scan for various reasons; and for a better diagnosis, a rescan is necessary. However, the number of rescans may decrease when radiologists design the protocol prior to the scan

CLINICAL RELEVANCE/APPLICATION

Musculoskeletal MRI is complex when designing the protocol compared to other MRI (e.g., brain, breast, liver, etc.). Hence, musculoskeletal MRI needs planning well before scanning, and this is best done by a radiologist.

SSG14-07 Dynamic Contrast-Enhanced Magnetic Resonance Imaging during Free Breathing for Hepatic Lesions: Clinical Applicably and Limitations

Tuesday, Dec. 3 11:30AM - 11:40AM Room: S504AB

Participants

Marcel C. Langenbach, MD, Cologne, Germany (*Presenter*) Research Grant, Guerbet SA Thomas J. Vogl, MD, PhD, Frankfurt, Germany (*Abstract Co-Author*) Nothing to Disclose Tatjana Gruber-Rouh, Frankfurt am Main, Germany (*Abstract Co-Author*) Nothing to Disclose Lajos M. Basten, Frankfurt am Main, Germany (*Abstract Co-Author*) Nothing to Disclose Dominik Nickel, Erlangen, Germany (*Abstract Co-Author*) Employee, Siemens AG Benjamin Kaltenbach, MD, Kelkheim, Germany (*Abstract Co-Author*) Nothing to Disclose

For information about this presentation, contact:

marcel.langenbach@me.com

PURPOSE

To evaluate the clinical applicability and limitations of this new prototype volume-interpolated breath-hold examination (VIBE) with compressed sensing (VIBEcs) for rapid multiphase MRI with free selectable variable temporal resolution for hypervascularized hepatic lesions.

METHOD AND MATERIALS

Twenty patients with hypervascularized hepatic lesions were included in this study and underwent contrast-enhanced liver MRI at 3 T. In all patients, VIBEcs was used for rapid arterial multiphase imaging. Results were analyzed regarding image quality and clinical applicability of the dynamic lesion evaluation. Evaluation of image quality, visibility and conspicuity was performed by three independent radiologist, each with more than 5 years of experience in oncology imaging, based on a 5-point Likert scale (5=excellent). Results were correlated with the lesion entity. Limitations for the use of VIBEcs in image acquisition were defined. Time curves of dynamic contrast enhancement were plotted for each patient and quantification of attenuation performed to isolate the optimal time-point for image acquisition.

RESULTS

All patients were successfully evaluated. Individual setting of acquisition time point (best point 8 seconds) instead of fixed delay allowed high reading scores for image quality, visibility and conspicuity for all lesions (mean score >4). Lesion entity showed no significant impact on the reading performance (p=0.765). Limitation were defined as following: small lesion size (<8 mm), subdiaphragmatic localization, large necrotic area (>80% of lesion).

CONCLUSION

Free-breathing MRI with VIBEcs allows image acquisition with high temporal and spatial resolution using individual acquisition time points during contrast phase to gain optimal results with a robust acquisition protocol.

CLINICAL RELEVANCE/APPLICATION

VIBEcs allows image acquisition with high temporal and spatial resolution for variable time points with a robust acquisition protocol and is recommended quantitavie measurements of hypervascularized liver lesions.

SSG14-08 Myocardial Extracellular Volume from T1 Mapping Measurements by Magnetic Resonance Imaging in Healthy Volunteers

Tuesday, Dec. 3 11:40AM - 11:50AM Room: S504AB

Participants

Xiaohu Li, MD, Hefei, China (*Presenter*) Nothing to Disclose Jianying Li, Beijing, China (*Abstract Co-Author*) Employee, General Electric Company Huayang Liu, MD, Beijing, China (*Abstract Co-Author*) Employee, General Electric Company Yongqiang Yu, MD, Hefei, China (*Abstract Co-Author*) Nothing to Disclose

PURPOSE

To investigate the characteristics of myocardial extracellular volume fraction (ECV) derived from pre- and post-contrast T1 measurements among healthy volunteers.

METHOD AND MATERIALS

A total of 57 healthy volunteers underwent standard CMR imaging with administration of gadolinium. T1 measurements were performed with a Look-Locker sequence followed by gradient-echo acquisition (GRE). We tested the segmental, interslice, inter-, intra-, and test-retest characteristics of the ECV , as well as the association of the ECV with other variables.

RESULTS

57 healthy volunteers were recruited and were included in the analysis. There were 26 men (46%) and 31 women. The mean age of volunteers was 47 ± 17 years(range 21 to 78 years). The average body mass index was 27 ± 4 kg/m2,systolic blood pressure was 119 ± 11 mmHg,diastolic blood pressure was 74 ± 4 mmHg,heart rate was 67 ± 6 beats/min, and hematocrit was 43 ± 2 %. The ECV

averaged 0.27 ± 0.04 (range 0.21 to 0.34). The intraclass coefficients for the intraobserver, interobserver and test-retest absolute agreements of the ECV were 0.95 (95% confidence interval: 0.85 to 0.98), 0.87 (95% confidence interval: 0.64 to 0.96), and 0.97(95% confidence interval: 0.84 to 0.99), respectively. In volunteers, the ECV was associate with age (r=0.81, P<0.001), maximal left atrial volume index (r=0.38, P=0.00036(P<0.01)), and indexed left ventricular mass. There were no differences in the ECV between segments in a slice or between slices.

CONCLUSION

In summary, the ECV is a novel and potentially useful index for quantification of the myocardial extracellular volume fraction. The findings suggest that in healthy volunteers, the myocardial ECV ranges from 0.21 to 0.34, In humans, the myocardial ECV increases with age, is associated with left ventricular mass and left atrial volume, and has reliable test characteristics. Further work will need to be done to test the application of this technique to patients with cardiovascular disease associated with the development of myocardial fibrosis.

CLINICAL RELEVANCE/APPLICATION

In cardiac magnetic resonance (CMR) imaging, the T1 relaxation time for the 1H magnetization in myocardial tissue may represent a valuable biomarker for a variety of pathological conditions

SSG14-09 CAIPIRINHA-Dixon-TWIST (CDT)-Volume-Interpolated Breath-Hold Examination (VIBE) Imaging of the Abdomen at 3.0 Tesla: Optimization and Comparison of Time Resolution and Image Quality

Tuesday, Dec. 3 11:50AM - 12:00PM Room: S504AB

Participants

Yu-Fei Lian, Beijing, China (*Presenter*) Nothing to Disclose Zhen-yu Pan, MD, Beijing, China (*Abstract Co-Author*) Nothing to Disclose Xiao-Jiao Pei, MD, Beijing, China (*Abstract Co-Author*) Nothing to Disclose Qinglei Shi, Beijing, China (*Abstract Co-Author*) Nothing to Disclose Shu-Ye Wang, Beijing, China (*Abstract Co-Author*) Nothing to Disclose Chuan Zhao, Beijing, China (*Abstract Co-Author*) Nothing to Disclose Chen-Peng Liu, Beijing, China (*Abstract Co-Author*) Nothing to Disclose Xue-chao Du, Beijing, China (*Abstract Co-Author*) Nothing to Disclose

PURPOSE

In order to get a higher time resolution or spatial resolution of CAIPIRINHA-Dixon-TWIST (CDT)-Volume-Interpolated Breath-Hold Examination (VIBE) imaging of abdomen at 3.0 Tesla, we optimized the scanning parameters at three conditions and evaluated the time resolution and image's quality of them.

METHOD AND MATERIALS

Twelve patients (8 males, age 42±3.52; 4 females, 39±2.35) with focal liver lesions and eight healthy volunteers (5 males, age36±4.23; 3 females, 40±3.89) were enrolled and underwent abdomen CDT-VIBE imaging MR exam with breath-hold mode before and after contrast-enhancement. The scanning sequences, which included 4 phases within a breath hold, include three optimized sequence with time resolution of 0.4s/phase, 0.6s/phase and 1.5s/phase. The quantitative evaluation index included the signal-to-noise ratio (SNR) of spleen, left and right liver lobe, and the contrast to noise ratio (CNR) of left and right liver lobe. All quantitative indexes were measured in in-phase, opp-phase and water-phase images before and after contrast enhancement. Finally, the homogeneity, the sharpness and the artifacts of whole image was scored by two radiologists independently on the basis of a three-point scale, and the average of data was used as the final scores. All the quantitative and quality parameters were analyzed with One-way ANOVA and Kruskal-Wallis One-way ANOVA were applied for group comparison with Bonferroni correction.

RESULTS

After optimization of the parameters of CDT-VIBE, the highest time resolution can reach 0.4s/phase, and when compared with the optimized protocols with time resolution of 0.6s/phase and 1.5s/phase, no significant difference was found for CNR and SNR at spleen, left and right liver lobe (p>0.05) (Table 2-7). About subject evaluation scores, the average scores of image quality for sharpness in sequence with time resolution of 1.5s/phase was significantly higher than the other two optimized sequence (p<0.001). No significant difference was found for the homogeneity and the artifacts of image quality among three optimized conditions

CONCLUSION

Through optimization of the parameters of CDT-VIBE in abdomen imaging, a higher time resolution (0.4s/phase) or a higher spatial resolution can be acquired, which means a wider clinical application in abdomen imaging of the CDT-VIBE sequence.

CLINICAL RELEVANCE/APPLICATION

CDT-VIBE sequence will be a wider clinical application in abdomen imaging







AI32

AI Theater: AI in Clinical Cardiac MRI: Presented by Circle Cardiovascular Imaging

Tuesday, Dec. 3 11:00AM - 11:20AM Room: AI Showcase, North Building, Level 2, Booth 10724

Participants

Matthias Gutberlet, MD, PhD, Leipzig, Germany (*Presenter*) Speaker, Siemens AG Speaker, Koninklijke Philips NV Speaker, Bayer AG Speaker, Bracco Group Author, Thieme Medical Publishers, Inc





3D33

3D + AV Theater: Next Generation of Advanced Visualization for Surgical Planning and Optimizing Analysis Utilizing Immersive Reality with Haptic Feedback and Air Models: Presented by ImmersiveTouch, Inc.

Tuesday, Dec. 3 12:00PM - 12:20PM Room: 3D Printing and Advanced Visualization Theater, North Building, Level 3, Booth 6563

Participants

Pravin K. Patel, MD, Chicago, IL (*Presenter*) Nothing to Disclose Farid F. Shafaie, MD, Chicago, IL (*Presenter*) Nothing to Disclose

Program Information

Next generation of advanced visualization for surgical planning and optimizing analysis utilizing immersive reality with haptic feedback and air models.







AI34

AI Theater: ScanDiags-AI-driven Decision Support from Musculoskeletal MRI: Presented by Balzano AI Engineers

Tuesday, Dec. 3 12:00PM - 12:20PM Room: AI Showcase, North Building, Level 2, Booth 10724

Participants

Rene Balzano, MSc, Zurich, Switzerland (*Presenter*) Nothing to Disclose Stefan Voser, Zurich, Switzerland (*Presenter*) Nothing to Disclose





SPAI32

RSNA AI Deep Learning Lab: Segmentation

Tuesday, Dec. 3 1:00PM - 2:30PM Room: AI Showcase, North Building, Level 2, Booth 10342



AMA PRA Category 1 Credits ™: 1.50 ARRT Category A+ Credit: 1.75

Participants

George L. Shih, MD, New York, NY (*Presenter*) Consultant, Image Safely, Inc; Stockholder, Image Safely, Inc; Consultant, MD.ai, Inc; Stockholder, MD.ai, Inc;

Special Information

In order to get the best experience for this session, it is highly recommended that attendees bring a laptop with a keyboard, a decent-sized screen, and the latest version of Google Chrome. Additionally, it is recommended that attendees have a basic knowledge of deep learning programming and some experience running a Google CoLab notebook. Having a Gmail account is also helpful. Here are instructions for creating and deleting a Gmail account.

ABSTRACT

This session will focus on the use of deep learning methods for image segmentation, applied to the challenge of CT or MR brain segmentation. While focused on this particular problem, the concepts should generalize to other organs and image types.







SPAI33

RSNA AI Deep Learning Lab: Beginner Class: Classification Task (Intro)

Tuesday, Dec. 3 3:00PM - 4:30PM Room: AI Showcase, North Building, Level 2, Booth 10342



Participants

Bradley J. Erickson, MD, PhD, Rochester, MN (Presenter) Board of Directors and Stockholder, VoiceIt Technologies, LLC; Board of Directors, FlowSigma, LLC; Officer, FlowSigma, LLC; Stockholder, FlowSigma, LLC;

Special Information

In order to get the best experience for this session, it is highly recommended that attendees bring a laptop with a keyboard and decent-sized screen. Having a Gmail account will be helpful. Here are instructions for creating and deleting a Gmail account.

ABSTRACT

This class will focus on basic concepts of convolutional neural networks (CNNs) and walk the attendee through a working example. A popular training example is the MNIST data set which consists of hand-written digits. This course will use a data set we created, that we call 'MedNIST', and consists of images of 6 different classes: Chest X-ray, Chest CT, Abdomen CT, Head CT, Head MR and Breast MRI. The task is to identify the image class. This will be used to train attendees on the basic principles and some pitfalls in training a CNN. • Intro to CNNs • Data preparation: DICOM to jpeg, intensity normalization, train vs test • How do we choose the labels? Inconsistencies... Use Fast.AI routines to classify; Validation of results: Are the performance metrics reliable? 'Extra Credit': if there is time, explore data augmentation options, effect of batch size, training set size.





SSJ04

Cardiac (MRI: General Topics)

Tuesday, Dec. 3 3:00PM - 4:00PM Room: N230B



AMA PRA Category 1 Credit ™: 1.00 ARRT Category A+ Credit: 1.00

FDA Discussions may include off-label uses.

Participants

Seth J. Kligerman, MD, Denver, CO (*Moderator*) Nothing to Disclose Diana Litmanovich, MD, Haifa, Israel (*Moderator*) Nothing to Disclose Robert M. Steiner, MD, Wynnewood, PA (*Moderator*) Nothing to Disclose

Sub-Events

SSJ04-01 Prevalence and Pattern of Cardiac Injury Identified by Late Gadolinium-Enhancement of Cardiac Magnetic Resonance Image in Acute Moderate to Severe CO Poisoning with Elevated High-Sensitivity Troponin I: Prospective Observational Study

Tuesday, Dec. 3 3:00PM - 3:10PM Room: N230B

Participants

Jong Sun Lee, Wonju, Korea, Republic Of (*Presenter*) Nothing to Disclose Woocheol Kwon, Wonju, Korea, Republic Of (*Abstract Co-Author*) Nothing to Disclose Yong Sung Cha, Wonju, Korea, Republic Of (*Abstract Co-Author*) Nothing to Disclose

PURPOSE

Myocardial injury is a frequent consequence of moderate to severe carbon monoxide (CO) poisoning. In addition, long-term mortality is significantly higher in patients who experienced myocardial injury than patients without myocardial injury. No studies have investigated myocardial injury due to carbon monoxide poisoning through cardiac magnetic resonance image (CMR). We want to know whether there are actually cardiac muscle changes identified by late gadolinium-enhancement (LGE) in CMR in acute phase after acute CO poisoning

METHOD AND MATERIALS

This prospective observational study collected data from consecutive patients who were diagnosed with acute CO poisoning and myocardial injury, defined as elevated high-sensitivity TnI (hs-TnI) level above the upper limit, at the ED between August 2017 and February 2019. CMR was performed to evaluate cardiac muscle changes identified by LGE. Patients with coronary artery disease were excluded. We classified the location of myocardial injury into 4 categories (subepicardium, mesocardium, subendocardium, and transmural) and examined the distribution of injured myocardium

RESULTS

Seventy-five patients were included. Fifteen patients (20.0%) had cardiac injury identified by LGE in CMR. The territory of left anterior descending artery (LAD) (7 patients, 46.7%) was the most common distribution in patients with positive LGE. Patients with LAD territory pattern all showed damage to the subendocardial area. In addition, mesocardium (6 patients, 40.0%) was second common site in patients with positive LGE and there was no transmural damage. Two patients with damage to the subepicardial area also showed in the RCA territory pattern. One patient had global damage distribution, defined as including distribution of all three coronary artery (LAD, left circumflex artery, and right coronary artery). Male sex was significantly more in the positive LGE group than in the negative LGE group (p=0.011). Decreased initial mental status was significantly more in the positive LGE group than in the negative LGE group (p=0.006).

CONCLUSION

Cardiac injury identified by LGE of cardiac MRI was found in 15 patients (20.0%) in acute moderate to severe CO poisoning with elevated hs-TnI.

CLINICAL RELEVANCE/APPLICATION

This is the first report about CMR results of CO poisoning. This prospective observational study collected data from consecutive patients who were diagnosed with acute CO poisoning and myocardial injury

SSJ04-02 Feature Tracking Cardiac Magnetic Resonance Imaging: A Supplementary Parameter to Improve the Risk Stratification in Patients with Ischemic Cardiomyopathy

Tuesday, Dec. 3 3:10PM - 3:20PM Room: N230B

Participants Daniel Overhoff, MD, Mannheim, Germany (*Presenter*) Nothing to Disclose Johannes Budjan, MD, Mannheim, Germany (*Abstract Co-Author*) Speaker, Siemens AG; Speaker, Ferring Group Michael Behnes, 68167 Mannheim, Germany (*Abstract Co-Author*) Nothing to Disclose Erol Tueluemen, Mannheim, Germany (*Abstract Co-Author*) Nothing to Disclose Boris Rudic, 68167 Mannheim, Germany (*Abstract Co-Author*) Nothing to Disclose Ibrahim El-Battrawy, 68167 Mannheim, Germany (*Abstract Co-Author*) Nothing to Disclose Holger Haubenreisser, Stuttgart, Germany (*Abstract Co-Author*) Speaker, Siemens AG Speaker, Bayer AG Speaker, Bracco Group Ibrahim Akin, MD, Mannheim, Germany (*Abstract Co-Author*) Nothing to Disclose Martin Borggrefe, Mannheim, Germany (*Abstract Co-Author*) Nothing to Disclose Stefan O. Schoenberg, MD, PhD, Mannheim, Germany (*Abstract Co-Author*) Nothing to Disclose Theano Papavassiliu, Mannheim, Germany (*Abstract Co-Author*) Nothing to Disclose

For information about this presentation, contact:

daniel.overhoff@umm.de

PURPOSE

The aim of this study was to evaluate retrospectively the prognostic value of feature tracking (FT) derived cardiac magnetic resonance imaging (CMR) strain parameters such as Global Circumferential Strain (GCS), Global Longitudinal Strain (GLS) and Global Radial Strain (GRS) for cardiovascular mortality and appropriate therapy in a cohort of patients with severe ischemic cardiomyopathy (ICM).

METHOD AND MATERIALS

ICM patients (n=246) who underwent CMR imaging prior to primary or secondary ICD implantation were retrospectively included. The following CMR parameters were assessed: GCS, GLS and GRS, calculated for both left and right ventricles, cardiac mass, ventricular and atrial volumes, atrial and ventricular functions, scar characteristics, such as ratios between left ventricular mass, infarct core mass and peri-infarction mass. FT parameters were generated from short-axis and two long axis (4-chamber; left 2chamber) cine (SSFP- sequences) views with dedicated software (cvi42, Circle Cardiovascular Imaging Inc., Calgary, Canada). The primary endpoint was a composite of cardiovascular mortality and appropriate ICD therapies (defined as antitachycardia pacing (ATP) and adequate shock).

RESULTS

A total of 246 patients with ICM were followed up to a median of 3.7 years (1336 days; interquartile range (IQR) 460-2.062 days). 11 patients were excluded due to lack of image quality or lack of sequence acquisition resulting in 235 patients. Cardiovascular mortality occurred in 22 patients, while appropriate ICD therapies occurred in 49 patients. Those patients affected by the primary endpoint were associated with significantly reduced GRS (13.44 ± 5.23 vs 15.20 ± 7.63 ; p=0.04) and GLS (-5.99 ± 1.75 vs -6.60 ± 2.44 ; p=0.037) compared to patients without. In multivariable Cox regression analysis, peri-infarction scar (HR 1.11, 95%CI: 1.04-1.22, p=0.005) and GRS (HR 0,94, 95%CI: 0.90-0.98, p=0.003) were independently and significantly associated with the primary endpoint, whereas LVEF and core scar and GLS were not.

CONCLUSION

Reduced GRS seems to be an independent predictor of cardiovascular mortality and/or appropriate ICD therapy. Additionally GRS can identify a subgroup of ICM patients with an increased risk of life-threatening VA and hence could help in clinical decision making.

CLINICAL RELEVANCE/APPLICATION

Feature Tracking derived Global Radial Strain can identify a subgroup of ICM patients with an increased risk of life-threatening VA.

SSJ04-03 Cardiac Magnetic Resonance for Asymptomatic Type 2 Diabetics with Cardiovascular High Risk (CATCH) - Pilot Study

Tuesday, Dec. 3 3:20PM - 3:30PM Room: N230B

Participants

Ming-Yen Ng, MBBS, Toronto, ON (*Presenter*) Nothing to Disclose Varut V. Vardhanabhuti, MBBS, FRCR, Hong Kong, Hong Kong (*Abstract Co-Author*) Nothing to Disclose Wenli Zhou, Hong Kong, Hong Kong (*Abstract Co-Author*) Nothing to Disclose Yee Tak Yu, Hong Kong, Hong Kong (*Abstract Co-Author*) Nothing to Disclose Kit Chan, Shenzhen, China (*Abstract Co-Author*) Nothing to Disclose Paul Chi-Ho Lee, MBBS,MRCP, Hong Kong, Hong Kong (*Abstract Co-Author*) Nothing to Disclose Tai-Pang Ip, Hong Kong, Hong Kong (*Abstract Co-Author*) Nothing to Disclose Kai-Hang Yiu, Hong Kong, Hong Kong (*Abstract Co-Author*) Nothing to Disclose Bernd J. Wintersperger, MD, Toronto, ON (*Abstract Co-Author*) Speaker, Siemens AG Research support, Siemens AG Institutional research agreement, Siemens AG Speaker, Bayer AG

For information about this presentation, contact:

myng2@hku.hk

PURPOSE

Stress cardiac magnetic resonance (CMR) for silent myocardial ischaemia in asymptomatic high risk type 2 diabetics has never been performed and the effectiveness of a screening programme is unknown. To assess feasibility of a screening programme we aimed to (i) determine the prevalence of silent myocardial ischaemia (ii) determine the number of false positive cases.

METHOD AND MATERIALS

We prospectively recruited patients with a Framingham risk score >=20% from 3 sites from August 2017 to January 2019. Adenosine stress CMR was performed in all patients. Positive stress CMR cases were referred for catheter coronary angiography with fractional flow reserve (FFR) measurements. Positive catheter coronary angiography was an FFR<=0.8 or coronary artery narrowing >=70% if FFR was not performed. Myocardial perfusion reserve index (MPRI) was measured in all cases.

RESULTS

63 patients were recruited (mean age 66yrs +/- 4.4; 77.8% male). There were 25 positive stress CMR scans. 3 patients refused catheter coronary angiography (CCA). 9 positive stress CMR patients were shown to have FFR positive (14.3% of patient

population). 13 patients had false positive stress CMRs. 3 negative stress CMR patients had CCA outside the study protocol and were confirmed as true negatives at catheter coronary angiography. 5 patients (7.9%) had infarcts detected of which 2 patients had no evidence of stress perfusion defects. Patients with false positive stress CMR had lower MPRI than true positive patients and patients without perfusion defects (1.32+/-0.29 vs 1.42+/-0.25 vs 1.45+/-0.29 respectively) although this was not statistically significant (p>=0.05). After a median follow-up of 382 days, there was no deaths, myocardial infarcts, heart failure or stroke.

CONCLUSION

14.3% of asymptomatic patients with type 2 diabetes and a Framingham risk >=20% had silent obstructive coronary artery disease which were confirmed by FFR. A false positive rate of 20.6% was demonstrated using stress CMR.

CLINICAL RELEVANCE/APPLICATION

Stress CMR screening of asymptomatic diabetic patients with Framingham risk score >20% found that \sim 14% of patients have obstructive coronary artery disease but there is a high false positive rate probably due to microvascular disease.

SSJ04-04 Decreased Left Atrial Longitudinal Strain is Significantly Associated with All-Cause Mortality in Restrictive Cardiomyopathy

Tuesday, Dec. 3 3:30PM - 3:40PM Room: N230B

Participants

Jadranka Stojanovska, MD, Ann Arbor, MI (*Presenter*) Nothing to Disclose El-Sayed H. Ibrahim, PhD, Milwaukee, WI (*Abstract Co-Author*) Nothing to Disclose Paul P. Cronin, MD, Ann Arbor, MI (*Abstract Co-Author*) Nothing to Disclose Thomas L. Chenevert, PhD, Ann Arbor, MI (*Abstract Co-Author*) Consultant, Koninklijke Philips NV Maryam Ghadimi Mahani, MD, Ann Arbor, MI (*Abstract Co-Author*) Nothing to Disclose Mohamed M. Sayyouh, MBBCh, MSc, Ann Arbor, MI (*Abstract Co-Author*) Nothing to Disclose

PURPOSE

Restrictive cardiomyopathy (RCM) represents a spectrum of disorders with a common physiology but divergent etiologies. The overall prognosis of RCM is poor with progression to heart failure and increased mortality. In this single institution retrospective cohort study, we aim to evaluate the association between cardiac magnetic resonance (CMR) variables and all-cause mortality. The secondary aim is to assess the difference of CMR imaging variables in RCM between women and men.

METHOD AND MATERIALS

98 patients with RCM (30 women and 68 men); age 61 ± 13 years referred to CMR from 2007 to 2015 were included in the study. All patients were followed to date to evaluate all-cause mortality. The CMR exam consisted of late gadolinium enhancement (LGE) images and cine images which were used for measuring indexed left ventricular (LV) mass, ventricular volume, ejection fraction (EF), and ventricular and left atrial (LA) strain. Logistic regression analysis adjusted for cardiovascular disease risk factors were performed to identify CMR variables associated with all-cause mortality.

RESULTS

50 patients (51%) had multiple myeloma and 39 (40%) had amyloidosis. 46 (47%) patients demonstrated signal enhancement on the LGE images and 35 (36%) experienced death. While mortality in patients with RCM was significantly associated with lower body mass index (p=0.03) and higher indexed LV mass (p=0.05), only LA longitudinal strain (p= 0.001) (Figure 1), older age (p=0.05), and presence of amyloid and diabetes (p=0.02 and 0.05) remained significantly associated after adjustment in the regression analysis (table 1). The presence of LGE was not associated with mortality (p=0.29). Women with RCM demonstrated higher LV circumferential strain peak (mean ± SD = 7.4 ± 1.7 versus 6.5 ± 1.6, p=0.03) smaller indexed ventricular end-diastolic volumes (p=0.005 and 0.01 for LV and RV respectively) and smaller LA volume (0.05). Mortality in women was not significantly different than in men (p=0.36).

CONCLUSION

Decreased LA longitudinal strain is independently associated with all-cause mortality in patients with RCM beyond the need for gadolinium administration. Women with RCM demonstrated higher LV circumferential strain peak.

CLINICAL RELEVANCE/APPLICATION

Left atrial longitudinal strain is associated with mortality in patients with restrictive cardiomyopathy and can play role in patients' prognosis.

SSJ04-05 Diastolic Dysfunction in Competitive Male Triathletes with Myocardial Fibrosis following a Strenuous Endurance Exercise

Tuesday, Dec. 3 3:40PM - 3:50PM Room: N230B

Participants

Enver G. Tahir, MD, Hamburg, Germany (*Presenter*) Nothing to Disclose Benedikt Scherz, Hamburg, Germany (*Abstract Co-Author*) Nothing to Disclose Jitka Starekova, MD, Hamburg, Germany (*Abstract Co-Author*) Nothing to Disclose Sebastian Bohnen, Hamburg, Germany (*Abstract Co-Author*) Nothing to Disclose Ulf K. Radunski, Hamburg, Germany (*Abstract Co-Author*) Nothing to Disclose Maxim Avanesov, MD, Hamburg, Germany (*Abstract Co-Author*) Nothing to Disclose Julius M. Weinrich, Hamburg, Germany (*Abstract Co-Author*) Nothing to Disclose Kai Muellerleile, Hamburg, Germany (*Abstract Co-Author*) Nothing to Disclose Gerhard B. Adam, MD, Hamburg, Germany (*Abstract Co-Author*) Nothing to Disclose Gunnar K. Lund, MD, Hamburg, Germany (*Abstract Co-Author*) Nothing to Disclose

For information about this presentation, contact:

e.tahir@uke.de

PURPOSE

The purpose of this study was to analyse left ventricular (LV) diastolic function by cardiac magnetic resonance (CMR) following an endurance competition in triathletes with (LGE+) and without myocardial fibrosis (LGE-).

METHOD AND MATERIALS

30 asymptomatic male triathletes (45 ±10 years) underwent CMR (Philips, Achieva) before and 2.1 ±1.1 hours after an official endurance competition. To detect focal and diffuse myocardial fibrosis late gadolinium enhancement (LGE) imaging and native and post-contrast T1 Mapping were part of the baseline CMR protocol. The modified Look-Locker inversion recovery (MOLLI) sequence was used for T1 Mapping. Diastolic LV function was determined by time-volume analysis using cine SSFP sequences (25 phases of the cardiac cycle). Early peak-filling rates (EPFR) and atrial peak-filling rates (APFR) as well as peak-filling rate ratio (PFRR=EPFR/APFR) were determined at baseline and post-competition.

RESULTS

LGE+ triathletes demonstrated higher LV mass (89 \pm 7 vs. 78 \pm 10 g/mSquared, P<0.01) and ECV (26.2 \pm 1.4 vs. 24.5 \pm 1.3 %, P<0.01) than their LGE- counterparts. At baseline, APFR was higher in LGE+ compared to the LGE- triathletes (161 \pm 34 vs. 121 \pm 30 ml/s/mSquared, P<0.01). While APFR in LGE- triathletes showed a significant increase (121 \pm 30 vs. 163 \pm 57 ml/s/mSquared, P<0.001), it remained unchanged in LGE+ triathletes before and after the competition (161 \pm 34 vs. 169 \pm 50 ml/s/mSquared, P=0.75). EPFR and PFRR remained unchanged in both groups. There were no significant post-competition differences regarding LVEF. However, LGE+ triathletes had higher post-competition left atrial volumes than LGE- triathletes (43 \pm 9 vs. 34 \pm 7 ml/mSquared, P<0.01) and decreased LAEF (53 \pm 6 vs. 59 \pm 6 %, P<0.05).

CONCLUSION

Post-competition diastolic function in LGE- triathletes was characterized by a significant compensatory increase of APFR. In contrast, the LGE+ group did not show any relevant changes coming from already increased baseline values and had decreased post-competition LAEF compared to LGE- triathletes. This suggests exhaustion of left atrial compensatory mechanisms most likely related to impairment of diastolic function in LGE+ triathletes.

CLINICAL RELEVANCE/APPLICATION

Triathletes with focal non-ischemic LGE and increased ECV in the remote myocardium might be in danger of developing subclinical diastolic dysfunction.

SSJ04-06 Myocardial Microvascular Dysfunction in Type 2 Diabetes Mellitus Patients Accompanied with Obesity: Assessment Using 3.0T Cardiovascular Magnetic Resonance Imaging

Tuesday, Dec. 3 3:50PM - 4:00PM Room: N230B

Participants

Li Jiang, Chengdu, China (*Presenter*) Nothing to Disclose Zhigang Yang, MD, Chengdu, China (*Abstract Co-Author*) Nothing to Disclose Yingkun Guo, Chengdu, China (*Abstract Co-Author*) Nothing to Disclose

For information about this presentation, contact:

jianglifs@163.com

PURPOSE

To determine the effect of obesity and type 2 diabetes mellitus (T2DM) on myocardial microvascular function referred for cardiovascular magnetic resonance (CMR) first-pass perfusion imaging, and to clarify the important risk factors contributing to microvascular dysfunction in T2DM patients.

METHOD AND MATERIALS

A total of 79 healthy controls and 120 clinically diagnosed T2DM patients underwent CMR examination. All clinical data and image parameter were recorded and analyzed. Univariable analysis was performed to identify the predictors of myocardial microvascular dysfunction. Variables with a probability value of <0.1 in the univariable analysis were included in a backward multivariable analysis that was based on a linear regression model.

RESULTS

All perfusion parameters showed a trend that the microvascular function decreased in T2DM patients when compared with controls on the same weight scale. For the T2DM subgroup and controls subgroup, the perfusion function gradually reduced as BMI increased, which was confirmed by all perfusion parameters, except TTM (all P < 0.01). In univariable analysis, multiple variables were associated with microvascular perfusion dysfunction, such as gender, BMI, high-density lipoprotein (HDL) levels, smoking history, diabetes duration, HbA1c, heart rate. With further multivariable analysis, the perfusion parameter models demonstrated that different risk factors have varying influences on microvascular function. The microvascular wash-in function and blood flow were mainly related to BMI, and perfusion time was mainly related to heart rate.

CONCLUSION

multiple variables contribute to myocardial microvascular dysfunction and have varying influences on different pathways of microvessels in T2DM patients. Obesity is one of the important risk factors for myocardial microvascular dysfunction, and myocardial microvascular function gradually reduced as BMI increased.

CLINICAL RELEVANCE/APPLICATION

It is well established that obesity is consistently associated with a high incidence of T2DM in the general population, and the underlying cardiovascular diseases are a principal cause of morbidity and mortality in both of them. Microvascular dysfunction, which has emerged as an important role of myocardial impairment, enables the early assessment of patient status and the prediction of prognosis.

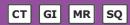




SSJ08

Gastrointestinal (CT Dose and Abbreviated MR Screening Techniques)

Tuesday, Dec. 3 3:00PM - 4:00PM Room: S401CD



AMA PRA Category 1 Credit ™: 1.00 ARRT Category A+ Credit: 1.00

Participants

Jessica B. Robbins, MD, Madison, WI (*Moderator*) Nothing to Disclose Jeong Hee Yoon, MD, Seoul, Korea, Republic Of (*Moderator*) Research Grant, Bayer AG Speaker, Koninklijke Philips NV Speaker, Bayer AG

Sub-Events

SSJ08-01 Diagnostic Performance and Image Quality of Low-Tube Voltage and Low-Contrast Agent Dose Protocol for Hepatic Dynamic Computed Tomography

Tuesday, Dec. 3 3:00PM - 3:10PM Room: S401CD

Participants

Shintaro Ichikawa, MD, PhD, Chuo, Japan (*Presenter*) Nothing to Disclose Utaroh Motosugi, MD, Chuo, Japan (*Abstract Co-Author*) Nothing to Disclose Tatsuya Shimizu, MD, Yamanashi, Japan (*Abstract Co-Author*) Nothing to Disclose Marie-Luise Kromrey, MD, Greifswald, Germany (*Abstract Co-Author*) Nothing to Disclose Yoshihito Aikawa, RT, Chuo, Japan (*Abstract Co-Author*) Nothing to Disclose Hiroshi Onishi, MD, Yamanashi, Japan (*Abstract Co-Author*) Nothing to Disclose

PURPOSE

To evaluate diagnostic performance and image quality of low-tube voltage and low-contrast agent dose protocol for hepatic dynamic computed tomography (CT).

METHOD AND MATERIALS

This retrospective study, held between January and May 2018, included 424 patients (mean age, 70.5±10.1 years; 289 men, 135 women). They underwent hepatic dynamic CT using one of two protocols: tube voltage, 80 kVp; contrast dose, 360 mgI/kg, and iterative reconstraction (n=180) and tube voltage, 120 kVp; contrast dose, 600 mgI/kg, and filtered back projection (n=224). Two radiologists independently scored lesion conspicuity and image quality using 5- and 3-point scales, respectively. Another radiologist measured CT number of abdominal organs, musclues, and hepatocellular carcinoma (HCC) in each phase. Lesion detectability, diagnostic ability for HCC, image quality of the arterial phase, CT number including lesion-to-liver ratio, and radiation dose were compared between protocols.

RESULTS

Both protocols showed high lesion detectability (sensitivity, 86.1%-92.5%; specificity, 94.6%-97.3%; accuracy, 92.8%-95.0%) and diagnostic ability for HCC (sensitivity, 85.7%-93.3%; specificity, 93.6%-98.6%; accuracy, 93.3%-96.6%). The 120-kVp protocol showed better image quality for the arterial phase than the 80-kVp protocol (P<0.0001 for both); however, the ratio of fair image quality was not significantly different (P=0.3161 and 0.4084). CT number of abdominal organs and muscles was higher in the 80-kVp protocol than in the 120-kVp protocol in each phase (P<0.0001-0.0357) for all structures, except portal vein in the arterial phase and renal medulla in the portal venous phase (P=0.1760 and 0.1280). Lesion-to-liver ratio was not significantly different for all phases (P=0.2108-0.8653). Volume CT dose index and dose-length product in the arterial phase were significantly lower for the 80-kVp protocol than for 120-kVp protocol (15.2±3.6 vs 32.1±9.3 mGy and 397.3 ± 122.2 vs 880.2 ± 312.7 mGy·cm, respectively, P<0.0001 for both).

CONCLUSION

The 80-kVp protocol has diagnostic performance and image quality, equivalent to the 120-kVp protocol, with lower radiation and contrast agent doses.

CLINICAL RELEVANCE/APPLICATION

Low-tube voltage with iterative reconstruction for hepatic dynamic CT may decrease radiation and contrast agent doses, with equivalent diagnostic performance and image quality than the 120-kVp protocol.

SSJ08-02 Pilot Study to Assess Feasibility of Fast Whole Body MRI Imaging in Oncologic Screening

Tuesday, Dec. 3 3:10PM - 3:20PM Room: S401CD

Participants Maryam Ghadimi, MD, Baltimore, MD (*Presenter*) Nothing to Disclose Pallavi Pandey, MD, Baltimore, MD (*Abstract Co-Author*) Nothing to Disclose Ankur Pandey, MD, Baltimore, MD (*Abstract Co-Author*) Nothing to Disclose Bita Hazhirkarzar, MD, Baltimore, MD (*Abstract Co-Author*) Nothing to Disclose Mounes Aliyari Ghasabeh, MD, Baltimore, MD (*Abstract Co-Author*) Nothing to Disclose Pegah Khoshpouri, MD, Baltimore, MD (*Abstract Co-Author*) Nothing to Disclose Sanaz Ameli, MD, Baltimore, MD (*Abstract Co-Author*) Nothing to Disclose Roya Rezvani Habibabadi, Baltimore, MD (*Abstract Co-Author*) Nothing to Disclose Mohammadreza Shaghaghi, MD, Baltimore, MD (*Abstract Co-Author*) Nothing to Disclose Li Pan, Baltimore, MD (*Abstract Co-Author*) Nothing to Disclose Vikash Gupta, MD, Baltimore, MD (*Abstract Co-Author*) Nothing to Disclose Ihab R. Kamel, MD, PhD, Baltimore, MD (*Abstract Co-Author*) Research Grant, Siemens AG

For information about this presentation, contact:

mghadim1@jhu.edu

PURPOSE

Assess the feasibility of whole-body MRI imaging in 30 minutes in oncologic applications.

METHOD AND MATERIALS

Our IRB approved this HIPPA-compliant prospective study. Twenty-six adult patients assessed for metastatic diseases were scanned with WB-DWI methods using a 3T MRI scanner. Axial fat-suppressed T2-weighted (T2WI), DWI, precontrast TS T1-weighted (T1WI) followed by post contrast FS T1WI in the arterial, portal venous and delayed phases were acquired (gradient time of 30 minutes). A single reader utilizing a five-point-scale recorded image quality of each WB-MRI study. Findings on whole-body MRI were recorded. The number of lesions was compared to those detected on CT or PET-CT studies, performed with 12 months of whole-body MRI if available. The WB-MRI, CT, and PET-CT were divided into standard anatomical location including chest, abdomen, and pelvis. The number of lesions within each anatomic location was compared in all three modalities.

RESULTS

Our study included 14 males and 12 females with the mean (±standard deviation) age of 55(±14) years. All whole-body MRI examinations were successfully obtained in the median time of 35 (IQR, 29-39) minutes. There were 17,21 and 8 lesions detected from chest, abdomen and pelvis, respectively in CT studies (N=19). Additionally, total of 0, 3, 2 lesions were detected in the chest, abdomen and pelvis respectively by assessing PET-CT studies (N=5). The WB-MRI detected 15 Lesions in chest, 38 Lesions in abdomen and 8 lesions in pelvis. All lesions detected on PET-CT were also detected on WB-MRI. Four lesions (16%) detected on WB-MRI in abdomen parts were missed on CT, while WB-MRI missed 2 lesions (11%) detected by CT in the chest parts; all were less than 10 mm. These two studies are comparable in detecting lesions in the pelvis. The overall image quality of whole-body MRI was 4/5.

CONCLUSION

We have demonstrated that fast multiparametric WB-MRI may be preformed in approximately 30 minutes, with relatively high image quality. Lung lesions <10mm may not be readily detected by WB-MRI.

CLINICAL RELEVANCE/APPLICATION

Whole-body MRI might be an acceptable alternative for CT or PET, in staging, assessment and monitoring of treatment response in oncologic applications.

SSJ08-03 Assessment of Noise Reduction Potential and Image Quality Improvement of a Deep Learning-Based Image Reconstruction Algorithm in Abdomen CT

Tuesday, Dec. 3 3:20PM - 3:30PM Room: S401CD

Participants

Xiaohu Li, MD, Hefei, China (*Presenter*) Nothing to Disclose Jianying Li, Beijing, China (*Abstract Co-Author*) Employee, General Electric Company Huayang Liu, MD, Beijing, China (*Abstract Co-Author*) Employee, General Electric Company Yongqiang Yu, MD, Hefei, China (*Abstract Co-Author*) Nothing to Disclose

PURPOSE

To evaluate the image quality improvement and noise reduction in routine dose, non-enhanced abdomen CT imaging by using a deep learning-based image reconstruction algorithm in comparison with ASIR-V.

METHOD AND MATERIALS

9 patients who underwent routine dose, abdomen CT using GE Revolution CT (GE Healthcare, Waukesha, WI) were included . After scanning, all scans were reconstructed with the recommended level of 40% ASIR-V and for comparison purpose and deep learningbased image reconstruction algorithm (TrueFidelityTM, GE Healthcare).DLIR-L, DLIR-M, DLIR-H. The CT attenuation values and SD of the subcutaneous fat, back muscle and descending aorta were measured at the level of tracheal carina of all reconstructed images. The signal-to-noise ratio (SNR) was calculated with SD representing image noise. The subjective image quality was independently evaluated by two experienced radiologists.

RESULTS

For all DLIR images, the objective image noise (SD) of fat, muscle and aorta decreased and SNR increased along with DLIR-L, DLIR-M, DLIR-H. The SD of DLIR images were significantly lower than that of 40% ASIR-V. In terms of subjective image evaluation, all DLIR reconstructions and 40% ASIR-V had good diagnostic acceptability. However, DLIR-M, DLIR-H showed significantly superior visibility of small structures when compared with the 40% ASIR-V and DLIR-L, and DLIR-H was the best series of TrueFidelity images, with a highest subjective image quality, at the same time the image sharpness was not significantly decreased in DLIR-H images.

CONCLUSION

In routine dose, non-enhanced abdomen CT, DLIR show greater potential in reducing image noise and artefacts and maintaining image sharpness when compared to the recommended level of 40%ASIR-V algorithm. Combining both the objective and subjective evaluation of images, non-enhanced abdomen CT images reconstructed with DLIR-H have the highest image quality.

CLINICAL RELEVANCE/APPLICATION

Recently a deep learning-based image reconstruction algorithm has been introduced. This image reconstruction technique employs deep CNN-based models, including millions of trained parameters, to improve the image quality with natural image texture, lower image noise, and high-resolution

SSJ08-04 Deep-Learning-Based Abdominal CT Denoising: Impact of Changes in Reconstruction Parameters Relative to Training Data

Tuesday, Dec. 3 3:30PM - 3:40PM Room: S401CD

Participants

Nathan Huber, Rochester, MN (*Presenter*) Nothing to Disclose Andrew Missert, PHD, Rochester, MN (*Abstract Co-Author*) Nothing to Disclose Shuai Leng, PHD, Rochester, MN (*Abstract Co-Author*) License agreement, Bayer AG Lifeng Yu, PhD, Rochester, MN (*Abstract Co-Author*) Nothing to Disclose Cynthia H. McCollough, PhD, Rochester, MN (*Abstract Co-Author*) Research Grant, Siemens AG

For information about this presentation, contact:

mccollough.cynthia@mayo.edu

PURPOSE

Deep-learning-based CT denoising methods are typically trained on images using a single set of reconstruction parameters. However, reconstruction parameters vary considerably between abdominal CT exam types and practices. This work aimed to quantify the performance of a convolutional neural network (CNN) denoising algorithm when applied to abdominal CT images with reconstruction parameters different from the training data.

METHOD AND MATERIALS

A CNN with 36 convolutional layers was trained on 250,000 image patches clipped from ten contrast-enhanced abdominal CT scans reconstructed with a Siemens' D30 kernel, 3 mm image thickness, and 275 mm field of view (FOV). Supervised learning was used for training, with simulated quarter dose images used as inputs, full dose images as the ground truth, and a mean-squared-error loss function. Six patients were reserved for testing the network. Baseline performance was evaluated with test data that had the same reconstruction parameters as the training data. Without retraining, the network was then applied to data with a range of reconstruction settings: FOV from 100 mm to 450 mm, kernel strength from D10 to D50, and image thickness from 1 to 5 mm. Performance was evaluated by visual assessment, root mean square error, noise level, and spatial resolution. Percent noise reduction was calculated as the difference in noise level from quarter dose to CNN output divided by quarter dose noise level.

RESULTS

The CNN demonstrated 73±6 % noise reduction relative to quarter dose at baseline, with no degradation of spatial resolution (i.e., when test data reconstruction = training data reconstruction). CNN denoising efficacy was decreased, to only 47±5 % noise reduction, when FOV was decreased by 50 mm (p = 0.0004), or to only 60±7 % noise reduction, when a smoother (D20) kernel was used (p = 0.001). Resolution loss was noted (visual and line profile inspection) when the network was applied to larger FOVs or sharper kernels. CNN performance was largely maintained when applied to test data with different image thicknesses.

CONCLUSION

Performance of the evaluated CNN-based CT denoising method varied significantly with FOV and kernel strength, but not with image thickness.

CLINICAL RELEVANCE/APPLICATION

While impressive noise reduction can be obtained using CNNs, reconstruction parameters must be carefully considered. Improvements in generalizability are therefore necessary.

SSJ08-05 Hepatocellular Carcinoma Screening with Abbreviated MRI: Comparison of Noncontrast, Dynamic-Contrast Enhanced and Hepatobiliary Phase Protocols Post Gadoxetic Acid

Tuesday, Dec. 3 3:40PM - 3:50PM Room: S401CD

Participants

Naik Vietti Violi, Lausanne, Switzerland (Presenter) Nothing to Disclose Sara Lewis, MD, New York, NY (Abstract Co-Author) Nothing to Disclose Joseph H. Liao, MD, New York, NY (Abstract Co-Author) Nothing to Disclose Miriam Hulkower, MD, Bronx, NY (Abstract Co-Author) Nothing to Disclose Gabriela Herandez-Meza, New York, NY (Abstract Co-Author) Nothing to Disclose Katherine Smith, New York, NY (Abstract Co-Author) Nothing to Disclose Xing Chin, MD, New York, NY (Abstract Co-Author) Nothing to Disclose Joseph W. Song, MD, New York, NY (Abstract Co-Author) Nothing to Disclose Eitan Novogrodsky, MD, New York, NY (Abstract Co-Author) Nothing to Disclose Daniela Said, MD, New York, NY (Abstract Co-Author) Nothing to Disclose Shingo Kihira, MD, New York, NY (Abstract Co-Author) Nothing to Disclose Mark Berger, New York, NY (Abstract Co-Author) Nothing to Disclose Maxwell Segall, New York, NY (Abstract Co-Author) Nothing to Disclose Jonathan Rosenblatt, New York, NY (Abstract Co-Author) Nothing to Disclose Mary Sun, New York, NY (Abstract Co-Author) Nothing to Disclose Dillan Villavisanis, New York, NY (Abstract Co-Author) Nothing to Disclose Raphael Golaz, Lausanne, Switzerland (Abstract Co-Author) Nothing to Disclose Keith Sigel, New York, NY (Abstract Co-Author) Nothing to Disclose Bachir Taouli, MD, New York, NY (Abstract Co-Author) Research Grant, Bayer AG

For information about this presentation, contact:

PURPOSE

To compare the performance of reconstructed abbreviated MRI (AMRI) protocols derived from a full gadoxetic acid-enhanced MRI for HCC screening in an at risk population.

METHOD AND MATERIALS

This retrospective study included 237 consecutive eligible patients (M/F 146/91, mean age 58y) with chronic liver disease (cirrhosis or HBV without cirrhosis) who underwent gadoxetic acid MRI in 2017 for HCC screening. Patients with history of HCC/other malignancies, liver transplantation and acute liver disease were excluded. Three reconstructed AMRI sets were assessed separately by 3 independent radiologists: non contrast (NC-AMRI: T2WI HASTE+diffusion weighted imaging (DWI)), Dynamic-AMRI (Dyn-AMRI: T2WI+Dynamic T1WI) and EOB-AMRI (T2WI+DWI +T1WI hepatobiliary phase). Lesions were characterized using a composite scoring system for NC-AMRI and EOB-AMRI [negative, subthreshold (<10mm), positive] and LI-RADS v2018 algorithm was used for Dyn-AMRI. Only LI-RADS5 lesions were considered HCC. A preliminary cost-effectiveness analysis was performed comparing each AMRI set to published ultrasound (US) sensitivity in USA (60%).

RESULTS

The reference standard demonstrated 13/237 patients with HCC (incidence 5.5%, mean size 33.7±30mm, range:10-120mm). Interreader agreement was substantial for NC-AMRI and EOB-AMRI (k=0.76 and 0.75) and excellent for Dyn-AMRI (k=0.86). Pooled perpatient sensitivities were 61.5% for NC-AMRI [CIs: 34.4-83%], 84.6% for Dyn-AMRI [60.8-95.1%] and 80.8% for EOB-AMRI [53.6-93.9%], without significant difference between sets (p-values range:0.06-0.16). Pooled per-patient specificities were 95.5% [92.4-97.4%], 99.8% [98.4-100%] and 94.9% [91.6-96.9%], respectively, with a significant difference between Dyn-AMRI and the other sets (p<0.01). All AMRI methods were cost-effective compared to US. Dyn-AMRI was the most cost-effective with incremental cost-effectiveness ratios (ICER) of \$11,253 and life-year gain of 11months compared to US.

CONCLUSION

We observed limited sensitivity of NC-AMRI protocol for HCC detection. EOB-AMRI and Dyn-AMRI showed a similar sensitivity with a slightly better specificity and cost-effectiveness for Dyn-AMRI. Further confirmation in a larger study is needed.

CLINICAL RELEVANCE/APPLICATION

Non contrast abbreviated MRI (AMRI) showed low diagnostic performance for HCC screening. AMRI with dynamic T1 (Dyn-AMRI) showed higher specificity and better cost effectiveness compared to AMRI with hepatobiliary phase.

SSJ08-06 Accuracy of an Abbreviated Screening MRI Protocol without Contrast Media for Patients at Risk for Hepatocellular Carcinoma

Tuesday, Dec. 3 3:50PM - 4:00PM Room: S401CD

Participants

Julia Noschang, MD, Sao Paulo, Brazil (*Presenter*) Nothing to Disclose Fernando I. Yamauchi, MD, Sao Paulo, Brazil (*Abstract Co-Author*) Nothing to Disclose Thais Mussi, MD,PhD, Sao Paulo, Brazil (*Abstract Co-Author*) Nothing to Disclose Cassia F. Tridente, MD, Sao Paulo, Brazil (*Abstract Co-Author*) Nothing to Disclose Ronaldo H. Baroni, MD, Sao Paulo, Brazil (*Abstract Co-Author*) Nothing to Disclose

For information about this presentation, contact:

julia_noschang@hotmail.com

PURPOSE

To evaluate the accuracy of an abbreviated screening MRI protocol without contrast media for patients at risk for hepatocellular carcinoma (HCC).

METHOD AND MATERIALS

This retrospective study was approved by our institutional review board. Four-hundred and twenty eight MRI exams were performed at our institution in patients with increased risk for hepatocellular carcinoma , from January 2015 to December 2015. Exclusion criteria were: history of treated HCC (166 cases) and subsequent studies of the same patient (123 cases). A total of 139 MRI cases were anonymized without post-contrast series (abbreviated protocol) and retrospectively analysed by three radiologists with different levels of experience (10, 8 and 1 year of experience with abdominal MRI). Later, one senior radiologist re-evaluated the full protocol as the reference standard, using LI-RADS v.2018. The abbreviated protocol included T2 weighted, fat-saturated T2 weighted, diffusion-weighted and GRE in/out-of-phase sequences. The following criteria were evaluated: presence of nodule suspicious for HCC, lesion size, lesion location and presence of nodule on each MRI sequences of the abbreviated protocol.

RESULTS

One-hundred and thirty nine patients were included, 38 women and 101 men, with an average age of 54.1 years. Sensitivity, specificity, positive predictive value, negative predictive value and accuracy of abbreviated protocol for detection of nodules categorized as LI-RADS 4 and 5 (reference standard) were: 88.3%, 77.2%, 74.6%, 89.7% and 82.0% (most experienced reader), 85.0%, 78.5%, 75.0%, 87.3% and 81.3% (intermediate experienced reader) and 85.0%, 73.4%, 70.8%, 86.6% and 78.4% (less experienced reader), respectively. Interobserver agreement was moderate for lesion detection (weighted K= 0.57, CI=0.41-0.78). The sensitivity of each MRI sequence was 71.7%, 73.3% and 76.7% on T2-weighted, 68.3%, 75.0% and 73.3% in fat-saturated T2-weighted, 76.7%, 75.0% and 73.3% in in/out-of-phase and 63.3%, 70.0% and 68.3% in DWI for most experienced, intermediate experienced and less experienced readers, respectively.

CONCLUSION

The abbreviated MRI protocol demonstrated high sensitivity for hepatocellular carcinoma screening in risk patients.

CLINICAL RELEVANCE/APPLICATION

HCC is the most common primary malignancy of the liver and a common cause of death from cancer worldwide. Abbreviated MRI protocol possibly allows more cost-effective, high sensitivity imaging for HCC screening.





SSJ10

Science Session with Keynote: Genitourinary (Quantitative Prostate MRI)

Tuesday, Dec. 3 3:00PM - 4:00PM Room: S502AB



AMA PRA Category 1 Credit ™: 1.00 ARRT Category A+ Credit: 1.00

FDA Discussions may include off-label uses.

Participants

Hebert Alberto Vargas, MD, Cambridge, United Kingdom (*Moderator*) Nothing to Disclose Antonio C. Westphalen, MD, Mill Valley, CA (*Moderator*) Research Grant, General Electric Company; Scientific Advisory Board, 3D

Antonio C. Westphalen, MD, Mill Valley, CA (*Moderator*) Research Grant, General Electric Company; Scientific Advisory Board, 3 Biopsy LLC

Sub-Events

SSJ10-01 Genitourinary Keynote Speaker: Update on Quantitative Prostate MRI - Challenges and Opportunities for Translation Into Clinical Practice

Tuesday, Dec. 3 3:00PM - 3:10PM Room: S502AB

Participants

Nicola Schieda, MD, Ottawa, ON (Presenter) Nothing to Disclose

SSJ10-02 Application of a Novel High-Resolution, Accelerated Quantitative T2 Mapping Sequence at 3T for the Detection of Prostate Cancer

Tuesday, Dec. 3 3:10PM - 3:20PM Room: S502AB

Participants

Andreas Bucher, MD, Frankfurt am Main , Germany (*Presenter*) Travel support, Guerbet SA; Benjamin Kaltenbach, MD, Kelkheim, Germany (*Abstract Co-Author*) Nothing to Disclose Ralph Strecker, Sao Paulo, Brazil (*Abstract Co-Author*) Employee, Siemens AG Elisabeth Weiland, Erlangen, Germany (*Abstract Co-Author*) Nothing to Disclose Tom Hilbert, Lausanne, Switzerland (*Abstract Co-Author*) Employee, Siemens AG Thomas J. Vogl, MD, PhD, Frankfurt , Germany (*Abstract Co-Author*) Nothing to Disclose Boris Bodelle, MD, Frankfurt am Main, Germany (*Abstract Co-Author*) Research support, General Electric Company; Research support, Siemens AG

PURPOSE

Quantitative measurements of the prostate have been shown to produce reliable differentiation of malignant prostate lesions in the peripheral zone in several small scale studies with previous generation T2 mapping sequences. We tested the reliability of a novel, fast, high-resolution T2 mapping prototype sequence with parallel imaging and model-based reconstruction (T2M) in the detection of malignant prostate lesions.

METHOD AND MATERIALS

A total of 46 multiparametric MRI datasets for suspected prostate cancer (pCA) at 3T were included. All examinations included T2M in addition to a standard multiparametric prostate protocol. Confirmed pCA were present in 22 cases. Quantitative T2 mapping was acquired axially (0.7x0.7x3.0 mm3, 16 echoes with delta TE 10.8 ms, TR 5000 ms). Region-of-interest measurements (ROI) were performed on the T2 maps in 3 slices for healthy prostate tissue of the peripheral and transitional zone (apex, midbase, base) with a minimum area of 10 mm2. Confirmed malignant lesions were traced in a separate ROI on the most representative slice. Average and minimum values of T2M relaxation time (T2) were recorded per ROI.

RESULTS

Diagnostic image quality was obtained in all patients. Average acquisition time for T2M was 4:37 mins. Mean T2 was 153.7 ± 45.1 ms for healthy tissue in the peripheral zone, 96.2 ± 22.7 ms in the transitional zone. Mean T2 was significantly reduced for pCA in the peripheral zone (71.6 ± 13.3 ms, p=0.001). Differences of mean T2 of pCA and average tissue of the transitional zone were suffcient to differentiate between tumor infiltration and average healthy tissue of the transitional zone (p=0.001). Minimal values of T2 showed good differentiation between healthy tissue and pCA (healthy: 99.4 ± 19.9 ms, malignant: 52.0 ± 10.6 ms; p=0.001).

CONCLUSION

Quantitative measurements from T2 mapping sequences provide good differentiation between healthy and malignant prostate tissue and are feasible in an expanded standard porstate protocol at high-resolution in acceptable acquisition time.

CLINICAL RELEVANCE/APPLICATION

Accelerated T2 mapping sequences could be a feasible addition to standard multiparametric prostate MRI for detection of prostate cancer.

Transition Zone Prostate Cancer Lesions from Benign Prostatic Hyperplasia Nodules with Wholemount Histopathology as Reference

Tuesday, Dec. 3 3:20PM - 3:30PM Room: S502AB

Participants Sohrab Afshari Mirak, MD, Los Angeles, CA (*Presenter*) Nothing to Disclose Alibek Danyalov, Los Angeles, CA (*Abstract Co-Author*) Nothing to Disclose Kyunghyun Sung, PhD, Los Angeles, CA (*Abstract Co-Author*) Research support, Siemens AG Matthew Ponzini, Los Angeles, CA (*Abstract Co-Author*) Nothing to Disclose Amirhossein Mohammadian Bajgiran, MD, Los Angeles, CA (*Abstract Co-Author*) Nothing to Disclose Melina Hosseiny, MD, Los Angeles, CA (*Abstract Co-Author*) Nothing to Disclose Afshin Azadikhah, MD, Los Angeles, CA (*Abstract Co-Author*) Nothing to Disclose Steven S. Raman, MD, Santa Monica, CA (*Abstract Co-Author*) Consultant, Johnson & Johnson; Consultant, Bayer AG; Consultant, Merck & Co, Inc; Consultant, Amgen Inc; Consultant, Profound Medical Inc

For information about this presentation, contact:

safsharimirak@mednet.ucla.edu

PURPOSE

To investigate the performance of different quantitative texture parameters of 3T multiparametric magnetic resonance imaging (3TmpMRI) for the differentiation of transition zone (TZ) prostate cancer (PCa) lesions from benign prostatic hyperplasia (BPH) nodules with wholemount histopathology as reference standard.

METHOD AND MATERIALS

This IRB approved, HIPAA compliant case-control study, included 77 patients. Regions of interest (ROI) for true positive TZ PCa lesions as well as the BPH nodules were contoured on 3TmpMRI axial T2-weighted images (T2WI), apparent diffusion coefficient (ADC) map of the diffusion weighted images (DWI) and dynamic contrast enhancement (DCE) MRI and the quantitative image analysis was performed. We generated 10 parameters including normalized T2WI signal intensity (SI) (calculated as mean T2WI signal intensity/ROI of obturator muscle), the shape of the histogram of T2WI SI (skewness and kurtosis), ADC minimum, ADC maximum, ADC skewness, ADC kurtosis, Ktrans (influx volume transfer coefficient), kep (efflux reflux rate constant) and Ve (the fractional volume of extracellular extravascular space). The quantitative parameters were compared between the TZ PCa and BPH nodules using paired sample t-test in SPSSv24. P-value<0.05 was considered as significant. The performance of the significant parameters were assessed using AUC for the ROC curves.

RESULTS

Mean patient age was 62.9 ± 7.6 years with mean prostate specific antigen (PSA) 7.6 ± 8.3 ng/ml. Compared to the BPH nodules, TZ PCa lesions had significantly higher T2WI SI (p=0.004), ADC skewness (p<0.001), Kep (p-value=0.026) and significantly lower ADC minimum (p<0.001) and ADC maximum (p=0.001). T2WI skewness, T2WI kurtosis, ADC kurtosis, Ktrans and Ve were not significantly different between cancerous and benign lesions (p>0.05). The highest AUC for the differentiation of TZ PCa from BPH was resulted from ADC skewness (0.998) followed by ADC minimum (0.891), ADC maximum (0.790), T2WI SI (0.625) and Kep (0.403) (figure 1).

CONCLUSION

3T mpMRI quantitative texture parameters, with higher performance of the parameters generated based on ADC maps, can be of significant value for the differentiation of TZ PCa from BPH nodules.

CLINICAL RELEVANCE/APPLICATION

Differentiation of transition zone prostate cancer from benign prostatic hyperplasia on 3T mpMRI can be difficult due to overlapping features, however mpMRI quantitative parameters may increase the performance.

SSJ10-04 PI-RADS-Based 3D Prostate Cancer Detection Using Residual Convolutional Neural Networks

Tuesday, Dec. 3 3:30PM - 3:40PM Room: S502AB

Participants

Helen Xu, Toronto, ON (*Presenter*) Researcher, Ezra Alon Hazan, Toronto, ON (*Abstract Co-Author*) Researcher, IBM Corporation; Researcher, Ezra; Spouse, Regulatory Affairs Manager, Venus Concept Oguz Akin, MD, New York, NY (*Abstract Co-Author*) Research Consultant, Ezra AI Ismail Caymaz, New York, NY (*Abstract Co-Author*) Nothing to Disclose Fuad Nurili, MD, New York, NY (*Abstract Co-Author*) Nothing to Disclose Diego Cantor-Rivera, Toronto, ON (*Abstract Co-Author*) Chief Technical Officer, Ezra

For information about this presentation, contact:

helen.xu@ezra.com

PURPOSE

Multi-parametric magnetic resonance imaging (mp-MRI) is playing an increasing role in prostate cancer assessment. Automated cancer localization as part of clinical decision support system can reduce inter-observer variability and time spent on image interpretation. This study evaluates the performance of a residual convolutional neural network (ResCNN) in the identification of potential areas of prostate cancer.

METHOD AND MATERIALS

A total of 337 cancer patients from the PROSTATEX dataset were analyzed in this study. Three radiologists segmented lesions that were PI-RADS v2 category three or higher using T2-weighted, ADC, and high b-value images. A 2D patch-based ResCNN was trained based on segmentations from the most senior radiologist. Volumetric predictions were generated using an adaptive threshold that controls the number of false positives. Sensitivity was measured by comparing network predictions to biopsy locations with

clinically significant cancer using a distance criterion of 10 mm or less.

RESULTS

The network's sensitivity for detecting clinically significant cancer was 97% for all PI-RADS categories, whereas radiologists' sensitivities were 79±0.06%, 94±0.04%, and 99±0.02% for category 3, 4, and 5 lesions, respectively. The trade-offs for an increased network sensitivity were lesion volume overestimation (radiologists: 1.5cc, network: 3.2cc) and an increased number of false positives (PI-RADS 3: 29%, PI-RADS 4,5: 2%).

CONCLUSION

The proposed ResCNN was able to obtain similar sensitivity for detecting clinically significant cancer as the radiologists. This demonstrates the network's potential to assist radiologists in prostate cancer detection, especially for PI-RADS 3 lesions where the presence of clinically significant cancer is equivocal (sensitivity: network 97% vs radiologists 79%).

CLINICAL RELEVANCE/APPLICATION

We have demonstrated that a residual convolutional neural network trained on PI-RADS v2 protocol has the potential to assist radiologists in detecting clinically significant prostate cancers.

SSJ10-05 Radiomic Features from Prostate Bi-Parametric MRI Differentiate MRI-Invisible Lesions from Non-Tumor Region in the Peripheral Zone: A Preliminary Multi-Site Study

Tuesday, Dec. 3 3:40PM - 3:50PM Room: S502AB

Participants

Lin Li, MS, Cleveland, OH (*Presenter*) Stockholder, Elucid Bioimaging Inc; Stockholder, Inspirata Inc; Scientific Advisor, Inspirata Inc; Scientific Advisory Board, AstraZeneca PLC; Scientific Advisory Board, Merck & Co, Inc; Researcher, Koninklijke Philips NV; Researcher, Inspirata Inc; License agreement, Elucid Bioimaging Inc; License agreement, Inspirata Inc; Grant, PathCore; Grant, Inspirata Inc Andrei S. Purysko, MD, Westlake, OH (*Abstract Co-Author*) Nothing to Disclose

Rakesh Shiradkar, PhD, Cleveland, OH (Abstract Co-Author) Nothing to Disclose

Cristina Magi-Galluzzi, MD, PhD, Cleveland, OH (Abstract Co-Author) Nothing to Disclose

Ivan Jambor, MD, PhD, New York, NY (Abstract Co-Author) Nothing to Disclose

Eric Klein, Cleveland, OH (Abstract Co-Author) Nothing to Disclose

Anant Madabhushi, PhD, Cleveland, OH (*Abstract Co-Author*) Stockholder, Elucid Bioimaging Inc; Stockholder, Inspirata Inc; Consultant, Inspirata Inc; Scientific Advisory Board, Inspirata Inc; Scientific Advisory Board, AstraZeneca PLC; Scientific Advisory Board, Merck & Co, Inc; Researcher, Koninklijke Philips NV; Researcher, Inspirata Inc; License agreement, Elucid Bioimaging Inc; License agreement, Inspirata Inc; Grant, PathCore Inc; Grant, Inspirata Inc

For information about this presentation, contact:

lxl477@case.edu

PURPOSE

Approximately 12% of biopsy-confirmed prostate cancer (PCa) lesions cannot be detected on MRI, which are referred to as 'MRIinvisible' lesions (PI-RADS < 3 and Gleason Grade Group (GGG) >= 1). Radiomics derived from prostate multi-parametric MRI (mpMRI) have been shown to complement imaging in characterizing PCa. In this work, we explore radiomics from bi-parametric MRI (bpMRI) including T2-weighted MRI (T2WI) and apparent diffusion coefficient (ADC) maps to differentiate MRI-invisible lesions from nontumor prostate tissue in the peripheral zone (PZ).

METHOD AND MATERIALS

In this study, a set of N = 100 PCa patients was included from 4 different institutions. Of these, 64 patients (N1) underwent 3T mpMRI prior to radical prostatectomy (RP) and 36 patients (N2) underwent 3T mpMRI with no abnormal signs followed by systematic biopsy that was negative. For N1, delineation of lesion regions of interest (ROIs) on bpMRI were obtained by mapping ROIs from corresponding RP surgical specimens and verified by an experienced radiologist. N = 39 visible lesions (VL) and N=25 invisible lesions (IL) were identified by the radiologist. Patients from N2 were used to obtain non-tumor (NR) ROIs within the PZ on T2WI and ADC maps. Training set (D1) consists of 15 NR, 15 IL and 18 VL, and the testing set (D2) consists of 21 NR, 10 IL and 21 VL. In D1, we identified stable radiomic features (test-retest and cross-site stability) that distinguished NR and IL, as well as NR and VL (to ensure their association with PCa). A logistic regression model (CL) was trained to separate NR and PCa lesions (IL + VL) in D1 and was then validated on D2 in terms of receiver operating characteristic (ROC).

RESULTS

Radiomic features including Co-occurrence of Local Anisotropic Gradient Orientations (CoLIAGe), Haralick features from T2WI; CoLIAGe and Laws features from ADC maps were found to distinguish NR and IL, VL. The area under the ROC curve (AUC) of CL on D2 is 0.93 (NR vs lesions), 0.97 (NR vs IL) and 0.91 (NR vs VL).

CONCLUSION

Radiomic features derived from prostate bpMRI were able to differentiate MRI-invisible lesions from non-tumor regions within the PZ.

CLINICAL RELEVANCE/APPLICATION

Radiomic based approaches might allow for non-invasive identification of PI-RADS invisible tumors and improve the lesion detection sensitivity of prostate MRI.

SSJ10-06 A Machine Learning-Assisted Decision Support Model with MRI Can Better Spare the Extended Pelvic Lymph Node Dissection at Cost of Less Missing in Prostate Cancer

Tuesday, Dec. 3 3:50PM - 4:00PM Room: S502AB

Yu-Dong Zhang, Nanjing, China (Abstract Co-Author) Nothing to Disclose

For information about this presentation, contact:

njmu_hy@163.com

PURPOSE

To develop a machine learning (ML)-assisted model for identifying the candidates for extended pelvic lymph node dissection (ePLND) in prostate cancer by integrating clinical, biopsy and precisely defined MRI findings.

METHOD AND MATERIALS

248 patients treated with radical prostatectomy and ePLND or PLND were included. ML-based models were developed from 18 integrated features using a logistic regression (LR), support vector machine (SVM) and random forests (RFs) algorithm, respectively. The models were compared to a MSKCC nomogram using the receiver operating characteristic-derived area under the curve (AUC), calibration plot and decision-curve analysis (DCA).

RESULTS

Total 59/248 (23.8%) lymph node invasion (LNIs) were identified at surgery. After cross validation, the predictive accuracy of these ML-based predictors yielded similar AUCs (RFs: 0.906; 95% confidence interval [CI], 0.856-0.928; SVM: 0.891; 95% CI, 0.840-0.917; LR+: 0.886; 95% CI, 0.834-0.913), while higher than MSKCC nomogram (0.816, 95% CI, 0.762-0.862). The calibration of MSKCC tended to underestimate LNI risk across the entire range of predicted probabilities compared to RFs and SVM. The DCA demonstrated three ML-based models significantly improved risk prediction at risk threshold <= 80% compared to MSKCC. If ePLNDs missed was controlled < 3%, RFs resulted in higher positive predictive value (55/107 [51.4%] vs 56/139 [40.3%]), similar negative predictive value (137/141 [97.2%] vs 106/109 [97.2%]), and higher No. of ePLNDs spared (141/248 [56.9%] vs 109/248 [43.9]) compared to MSKCC.

CONCLUSION

Our ML-based model below 15% cutoff, superior to MSKCC nomogram, allows to 57% ePLNDs spared at the cost of missing < 3% LNIs.

CLINICAL RELEVANCE/APPLICATION

Preoperative identification of LNI is critical for appropriate treatment selection and planning. As precisely defining nodal stage is to allow surgeons to define which patients may benefit from ePLND or PLND during radical prostatectomy and which patients may safely avoid it.





SSJ16

Musculoskeletal (Knee)

Tuesday, Dec. 3 3:00PM - 4:00PM Room: E353A



AMA PRA Category 1 Credit ™: 1.00 ARRT Category A+ Credit: 1.00

FDA Discussions may include off-label uses.

Participants

Donna G. Blankenbaker, MD, Fitchburg, WI (*Moderator*) Consultant, Reed Elsevier; Royalties, Reed Elsevier Adam D. Singer, MD, Atlanta, GA (*Moderator*) Nothing to Disclose

Sub-Events

SSJ16-01 Comparing Clinical and Semi-Quantitative Cartilage Grading in Predicting Outcomes After Arthroscopic Partial Meniscectomy

Tuesday, Dec. 3 3:00PM - 3:10PM Room: E353A

Participants

Naveen Subhas, MD, Shaker Heights, OH (*Abstract Co-Author*) Research support, Siemens AG Ceylan Colak, MD, Cleveland, OH (*Presenter*) Nothing to Disclose Joshua M. Polster, MD, Shaker Heights, OH (*Abstract Co-Author*) Nothing to Disclose Nancy A. Obuchowski, PhD, Cleveland, OH (*Abstract Co-Author*) Research Consultant, Siemens AG; Research Consultant, IBM Corporation; Research Consultant, Elucid Bioimaging Inc; Research Consultant, FUJIFILM Holdings Corporation Morgan Jones, MD, Cleveland, OH (*Abstract Co-Author*) Nothing to Disclose Greg Strnad, Cleveland, OH (*Abstract Co-Author*) Royalties, nPhase Soterios Gyftopoulos, MD, Scarsdale, NY (*Abstract Co-Author*) Nothing to Disclose Kurt Spindler, MD, Nashville, TN (*Abstract Co-Author*) Nothing to Disclose

PURPOSE

Cartilage loss on preoperative knee MRI is a predictor of poor outcomes after arthroscopic partial meniscectomy (APM). Previous studies have used time-intensive MRI grading systems which are not amenable for routine clinical use. The ability to predict outcomes with a clinically used grading system has not been studied. This study's purpose was to compare the ability to predict outcomes after APM with cartilage loss graded using a clinically used modified Outerbridge system and a semi-quantitative MOAKS (MRI Osteoarthritis Knee Score) system.

METHOD AND MATERIALS

Cases were randomly selected meeting the following criteria: 1. Preoperative knee MRI performed within 6 months of APM surgery 2. Outcomes measured at the time of surgery and 1 year after surgery. Surgical failure was defined as a less than 10 point improvement in the Knee Osteoarthritis Pain Score (KOOSpain). Cases were independently evaluated by 2 musculoskeletal (MSK) radiologists and 1 radiology fellow using both grading systems. Accuracy of each system in discriminating success and failure was estimated using area under the ROC (AUC) with 95% confidence intervals. A Wald test was used to test non-inferiority of the clinical grading system to MOAKs. Inter-reader agreement of two grading systems in predicting outcomes was also compared.

RESULTS

80 cases from 78 patients (38 females and 40 males) with mean age of 56.6 years (range of 45-77) were studied. 21 patients (27%) were surgical failures. At least Grade 2 (< 50% cartilage thickness loss) ranged from 23.3% (lateral tibial plateau) to 52.5% (medial femoral condyle) of the observations. Prediction model using clinical grading (AUC = 0.695 [0.566, 0.824]) was non-inferior (p = 0.047) to MOAKS grading (AUC = 0.683 [0.539, 0.812]). Both MRI prediction models performed better than a model with only demographics (AUC = 0.667 [0.522, 0.812]. Inter-reader agreement with clinical grading (80.8%) was significantly higher (P = 0.012) than with MOAKS (65%).

CONCLUSION

Cartilage loss graded on MRI with a clinically used system has similar ability in predicting outcomes after APM compared to a semiquantitative system with significantly better inter-reader agreement.

CLINICAL RELEVANCE/APPLICATION

The ability to use a clinical MRI cartilage grading system to predict outcomes after APM allows for the development of point of care prediction tools from routine MRI readings.

SSJ16-02 Deep Convolutional Neural Network-Based Detection of Meniscus Tears: Comparison with Radiologists and Surgery as Standard of Reference

Tuesday, Dec. 3 3:10PM - 3:20PM Room: E353A

Giuseppe Marbach, Zurich, Switzerland (*Abstract Co-Author*) Employee, Balzano Informatik AG Francesco Civardi, Zurich, Switzerland (*Abstract Co-Author*) Employee, Balzano Informatik AG Sandro F. Fucentese, MD, Zurich, Switzerland (*Abstract Co-Author*) Consultant, MEDACTA International SA Christian W. Pfirrmann, MD, MBA, Forch, Switzerland (*Abstract Co-Author*) Nothing to Disclose

PURPOSE

To evaluate a novel fully automated deep convolutional neural network (DCNN) for detection of meniscus tears.

METHOD AND MATERIALS

This retrospective study was approved by the local ethics committee. We included 100 patients, who had undergone MRI and arthroscopy of the knee in our institution. All MRI studies were evaluated for medial and lateral meniscus tears by two musculoskeletal radiologists independently and by the DCNN. The surgical reports served as the standard of reference. Statistics included sensitivity, specificity, accuracy and ROC curve analysis as well as kappa-statistics.

RESULTS

Fifty-seven percent (57/100) of patients had a tear of the medial and 24% (24/100) of the lateral meniscus, including 12% (12/100) of patients with a tear of both menisci. For medial meniscus tear detection, the sensitivity, specificity and accuracy were for reader 1: 93%, 91%, and 92%, for reader 2: 96%, 86% and 92%, and for the DCNN: 84%, 88% and 86%. For lateral meniscus tear detection, the sensitivity, specificity, and accuracy were for reader 1: 71%, 95% and 89%, for reader: 2 67%, 99% and 91%, and for the DCNN: 58%, 92% and 84%. Sensitivity for medial meniscus tear detection was significantly different between reader 2 and the DCNN (p=0.039), no significant differences existed for all other comparisons (all p >= 0.092). The AUC-ROC of the DCNN was 0.882, 0.781 and 0.961 for detection of medial, lateral and overall meniscus tear. Inter-reader reliability was very good for the medial (kappa 0.876) and good for the lateral meniscus (kappa 0.741).

CONCLUSION

Our DCNN has the capability to detect tears of the medial and lateral meniscus in a fully automated fashion and with similar performances than radiologists.

CLINICAL RELEVANCE/APPLICATION

Fully automated detection of meniscus tears may decrease workload for radiologists and reduce health care costs.

SSJ16-03 ACL Graft Remodeling Revealed by Serial UTE-T2* MRI

Tuesday, Dec. 3 3:20PM - 3:30PM Room: E353A

Participants

Scott Tashman, PhD, Houston, TX (*Abstract Co-Author*) Nothing to Disclose Payam Zandiyeh, PhD, Houston, TX (*Abstract Co-Author*) Nothing to Disclose Michael Kutzler, MD, Houston, TX (*Abstract Co-Author*) Nothing to Disclose Blake Purtle, Houston, TX (*Abstract Co-Author*) Nothing to Disclose Travis Alford, Houston, TX (*Abstract Co-Author*) Nothing to Disclose Colton Wayne, Houston, TX (*Abstract Co-Author*) Nothing to Disclose Ryan J. Warth, Houston, TX (*Presenter*) Nothing to Disclose James McDermott, MD, Houston, TX (*Abstract Co-Author*) Nothing to Disclose Ahmed Taher, MD, Houston, TX (*Abstract Co-Author*) Nothing to Disclose Ponnada A. Narayana, PhD, Houston, TX (*Abstract Co-Author*) Nothing to Disclose Refaat E. Gabr, PhD, Houston, TX (*Abstract Co-Author*) Nothing to Disclose Manickam Kumaravel, MD, FRCR, Houston, TX (*Abstract Co-Author*) Nothing to Disclose Walter Lowe, MD, Houston, TX (*Abstract Co-Author*) Nothing to Disclose

For information about this presentation, contact:

ahmedramadantawfik@gmail.com

PURPOSE

Evaluate changes over time in UTE T2* MRI relaxation times of implanted ACL grafts during graft healing/remodeling over the first year after ACL reconstruction.

METHOD AND MATERIALS

10 patients (ages 14-45 years) who underwent primary ACL reconstruction (ACLR) with or without meniscal injury. UTE-MRI evaluation at 1, 3, 6, 9, and 12 months after surgery. High-resolution 3D T2 scan (slice thickness: 0.6mm, TR: 18.7ms; TE: 11.5ms); Quad-echo UTE-T2 sequence (slice thickness: 1mm, TR: 20ms; TE: 0.3, 3, 6, and 9ms). The ACL-reconstructed knee was scanned at all 5 time points (1, 3, 6, 9, and 12 months), and the contralateral knee was imaged at 1 month. The region of interest (ROIs) for the ACL-reconstructed knee include the central 2/3 of the intra-articular portion of the ACL graft The region of interest for the contralateral uninjured knee included the ACL, patellar tendon (PT), and semitendinosus tendon (SemiT). At the 1-month time point for both injured and uninjured knees, each ROI was manually segmented from the surrounding tissues on the 3D T2 images using Mimics software (Materialise, Inc.; Belgium) (Figure 1). The 1-month segmentation masks were co-registered with the 4-echo UTE images obtained at each subsequent time point to ensure voxel-to-voxel anatomic matching of each segmentation mask. T2* relaxation times were calculated by fitting an exponential curve to the signal intensity data from the 4-echo UTE sequences. Mean T2* values for each ROI were calculated from all voxels within each ROI. Custom software was created using Python to extract average UTE-T2* values underlying each segmented ROI.

RESULTS

Mean T2* relaxation times for the ACL graft (Figure 2) increased over time, from 3.5 ms at 1 month to 5.4 ms at 6 months, with a statistically significant increase between 1 and 3 months (p < 0.05). Qualitatively, T2* relaxation times increased from near the values of the native SemiT tendon (2.2 ms) to approach that of the intact (contralateral) ACL (4.9 ms). Serial changes in T2* were not uniform throughout the graft substance (Figure 3). Remodeling appears to have begun near the tibial insertion site and

progressed proximally towards the femoral insertion.

CONCLUSION

T2* values progressively increased over time, followed by regression towards the values of the intact native ACL.

CLINICAL RELEVANCE/APPLICATION

Early results show promise of UTE-T2 MRI for assessing ACL graft state.

SSJ16-04 Collagen Proton Fraction Estimated with Ultrashort Echo Time Magnetization Transfer (UTE-MT) MRI Modeling Correlates Well with Mechanical Properties of Cortical Bone

Tuesday, Dec. 3 3:30PM - 3:40PM Room: E353A

Participants

Saeed Jerban, PhD, San Diego, CA (*Presenter*) Nothing to Disclose Yajun Ma, San Diego, CA (*Abstract Co-Author*) Nothing to Disclose Erik W. Dorthe, La Jolla, CA (*Abstract Co-Author*) Nothing to Disclose Lena Kakos, San Diego, CA (*Abstract Co-Author*) Nothing to Disclose Nicole Le, La Jolla, CA (*Abstract Co-Author*) Nothing to Disclose Salem Alenezi, Riyadh, Saudi Arabia (*Abstract Co-Author*) Nothing to Disclose Robert Sah, La Jolla, CA (*Abstract Co-Author*) Nothing to Disclose Eric Y. Chang, MD, San Diego, CA (*Abstract Co-Author*) Nothing to Disclose Darryl D'Lima, MD, PhD, La Jolla, CA (*Abstract Co-Author*) Research funded, Stryker Corporation; Consultant, Advanced Mechanical Technology, Inc; Research funded, ConforMIS, Inc; Consultant, Ossur HF; Officer and Stockholder, XpandOrtho, Inc Jiang Du, PhD, San Diego, CA (*Abstract Co-Author*) Nothing to Disclose

For information about this presentation, contact:

sjerban@ucsd.edu

PURPOSE

To investigate the relationship between human cortical bone mechanics and the macromolecular proton fraction (MMF) obtained from ultrashort echo time magnetization transfer (UTE-MT) MRI modeling.

METHOD AND MATERIALS

156 cortical bone strips (\sim 4×2×40 mm3) were harvested from the tibial and femoral midshafts of 43 donors (62±22 yo). Specimens were scanned using a 1-inch diameter T/R birdcage coil on a 3T clinical scanner (MR750, GE). The UTE-MRI scans involved: a) an actual flip angle imaging variable TR (AFI-VTR) sequence (AFI: TE=0.032; TRs=20, 100 ms; VTR: TE=0.032; TRs=20, 40, 100, and 150 ms; FA=45°) for T1 measurement (1), which is the prerequisite for the two-pool MT modeling, and b) a set of 3D-UTE-Cones-MT sequences (pulse power=400°, 600°, and 800°; frequency offset=2, 5, 10, 20, and 50kHz; FA=10°) for MT modeling (2-4). Other imaging parameters included: field of view=40×40mm2, matrix=160×160, slice-thickness=2mm. Afterwards, specimens were scanned using a Skyscan 1076 (Kontich, Belgium) μ CT at 9 μ m3 voxel size to measure bone porosity and bone mineral density (BMD). Finally, mechanical properties of the specimens were measured using 4-point bending tests. Pearson's correlation coefficients were calculated between MRI and μ CT and mechanical properties.

RESULTS

Fig.1a shows the UTE-MRI image in axial plane at the middle of 20 bone strips with 4mm×2mm approximate cross-sections. Two representative specimens harvested from a 47-year-old male (I) and a 57-year-old female (II), respectively, are indicated with yellow rectangles. Fig.1b shows the corresponding μ CT images. Figs.1c,d show corresponding MT modeling analyses. Figs. 1e-h show the scatterplots of Young's modulus, yield stress, ultimate stress, and failure energy on MMF, respectively. Young's modulus, yield stress, and ultimate stress demonstrated significant moderate correlations with MMF (R=0.60-0.61, p<0.01). MMF showed significant strong correlations with porosity (R=0.72) and BMD (R=0.71).

CONCLUSION

Significant correlations between bone MMF, mechanical properties, and microstructure suggest that the UTE-MT model can potentially serve as a novel tool to detect the variations of bone mechanics and microstructure.

CLINICAL RELEVANCE/APPLICATION

A UTE-MRI-based technique that correlates with bone mechanics and miscrostructure may be useful in future clinical studies for fracture risk estimation.

SSJ16-05 Reliability of a Novel Scoring System for Intraarticular Calcification of the Knee: BUCKS (Boston University Calcium Knee Score)

Tuesday, Dec. 3 3:40PM - 3:50PM Room: E353A

Participants

Mohamed Jarraya, MD, Philadelphia, PA (*Presenter*) Nothing to Disclose Tuhina Neogi, Boston, MA (*Abstract Co-Author*) Nothing to Disclose John A. Lynch, PhD, San Francisco, CA (*Abstract Co-Author*) Nothing to Disclose David T. Felson, MD, MPH, Boston, MA (*Abstract Co-Author*) Consultant, Zimmer Biomet Holdings, Inc Michael C. Nevitt, PhD, San Francisco, CA (*Abstract Co-Author*) Nothing to Disclose Ali Guermazi, MD,PhD, Boston, MA (*Abstract Co-Author*) Shareholder, Boston Imaging Core Lab, LLC; Research Consultant, Merck KGaA; Research Consultant, Roche, Inc; Research Consultant, TissueGene, Inc; Research Consultant, Galapagos, Inc; Research Consultant, AstraZeneca PLC; Research Consultant, Pfizer Inc

For information about this presentation, contact:

PURPOSE

Describe and assess the reliability of a novel computed tomography (CT)-based scoring system, the BUCKS (Boston University Calcium Knee Score) method, for assessing the burden and determining the localization of intra-articular mineralization.

METHOD AND MATERIALS

We included both knees from subjects of the most recent visit of the Multicenter Osteoarthritis Study (MOST), an NIH-funded longitudinal cohort of community-dwelling older adults with or at risk of knee osteoarthritis (OA). All subjects underwent CT scans of bilateral knees. For each knee, a musculoskeletal radiologist assessed the presence and severity of mineralization in cartilage, menisci, capsule and ligaments. Readings of a sample of 31 participants by the same reader and a second reader were repeated 12 later. The BUCKS method assesses 14 cartilaginous subregions and 6 meniscal segments (each meniscus was subdivided into 3 segments: anterior horn, body and posterior horn), similar to WORMS system. Cartilaginous subregions and meniscal segments were assigned a score ranging from 0-3 (figure). The joint capsule, bilateral posterior meniscal roots, 2 cruciate (ACL/PCL) and 2 collateral ligaments (MCL/LCL) were each scored 0 or 1 for absence or presence of mineralization. Vascular calcifications were scored 0-3.

RESULTS

Thirty one subjects (61 knees) were included. Mean age was 72.3 years (SD= 6.7, range=63-86). Mean BMI was 31.0 kg/m2 (SD 5.2). Sixty one percent (n=19) were female. Intra-articular calcium crystals were present on CT images of 50 knees, with 38 having articular cartilage calcifications and 35 having meniscal calcifications. Of the 61 knees, tibio-femoral Kellgren and Lawrence Grades were K&L=0 in 18 knees, K&L=1 in 13 knees, K&L=2 in 14 knees, K&L=3 in 12 knees and K&L=4 in 3 knees. The intra-reader reliability (weighted-kappa) ranged from 0.93 for ligaments to 0.94 for cartilage, 0.97 for vessels, 0.98 for meniscus, and 1.0 for joint capsule. The inter-reader reliability (weighted-kappa) ranged from 0.92 for cartilage to 0.95 for meniscus and vessels, and 1.0 for joint capsule and ligaments.

CONCLUSION

We have designed and described a novel scoring system for intraarticular mineralization of the knee, BUCKS, which shows excellent intra- and inter-reader reliability.

CLINICAL RELEVANCE/APPLICATION

BUCKS is a potentially useful tool for the understanding of the role of calcium crystals in knee OA.

SSJ16-06 Efficacy of Knee Unloader Bracing Evaluated with Quantitative MRI

Tuesday, Dec. 3 3:50PM - 4:00PM Room: E353A

Participants

Won C. Bae, PhD, La Jolla, CA (*Abstract Co-Author*) Nothing to Disclose
Asako Yamamoto, MD, Tokyo, Japan (*Abstract Co-Author*) Nothing to Disclose
Mitsue Miyazaki, PhD, La Jolla, CA (*Abstract Co-Author*) Employee, Canon Medical Systems Corporation
Aditi Vaidya, La Jolla, CA (*Abstract Co-Author*) Nothing to Disclose
Yordanos Tesfai, La Jolla, CA (*Abstract Co-Author*) Nothing to Disclose
Torrance Teng, La Jolla, CA (*Abstract Co-Author*) Nothing to Disclose
Elizabeth M. Bird, La Jolla, CA (*Abstract Co-Author*) Nothing to Disclose
Sheronda Statum, San Diego, CA (*Abstract Co-Author*) Nothing to Disclose
John Lane, San Diego, CA (*Abstract Co-Author*) DonJoy Global
Christine B. Chung, MD, Solana Beach, CA (*Presenter*) Nothing to Disclose

For information about this presentation, contact:

wbae@ucsd.edu

PURPOSE

Unloader knee braces aim to shift the weight off the damaged compartment of the knee, and may offer pain reduction and delay time to surgery. Despite perceived benefits, the efficacy of bracing to reduce pain and preserve integrity of joint tissues, is under debate. The purpose of this study was to investigate if quantitative magnetic resonance imaging (qMRI) measures of bone marrow edema (BME; a pain correlate), cartilage, and meniscus are preserved after 9 months of unloader brace use in patients with osteoarthritis (OA).

METHOD AND MATERIALS

Patients with medial knee OA (n=4; 4 male; 50+/-13.4 yrs, mean+/-standard deviation) were imaged at 3T, before and 9 months after brace use. To evaluate BME, proton density fat suppressed images were processed to quantify the volume of high signal intensity within subchondral bone (Figure AB). To evaluate cartilage and meniscus, spin echo T2 map was acquired in sagittal plane, in the weight-bearing regions of lateral and medial tibiofemoral compartments. T2 values in tibial/femoral cartilage, and anterior/posterior meniscus, were determined (Figure C). Using repeated measures ANOVA, effects of brace use and knee compartment on BME and T2 values were assessed.

RESULTS

Initially, BME was found in 2 medial femoral condyles and all 4 medial tibial plateaus, with a mean volume of 1027+/-1103 mm3. After bracing, BME volume decreased by 82+9 % (p = 0.081). Changes in cartilage and meniscus T2 values are shown in Figure D. Femoral and tibial pooled cartilage T2 values (32.8+8 ms before, 32.6+5 ms after bracing) did not vary significantly with compartment (p=0.14) or bracing (p=0.9). Meniscus T2 values were initially higher (p=0.01) in the medial (17.4+5.4 ms) than lateral (12.8+3.5 ms) compartment but did not change after bracing (p=0.24).

CONCLUSION

In all patients, there was a decrease in BME volume without any new lesion development after 9 months of brace use. Despite small number of subjects, this data is promising, considering that without intervention, BME size may either decrease or increase.

Combined with stable cartilage and meniscus T2 values, these results demonstrate the feasibility of using unloader brace to manage knee OA.





HW 33

AI Hands-on Workshop: Deep Learning for MRI Interpretation on the Microsoft Azure ML Platform: Presented by Balzano AI Engineers

Tuesday, Dec. 3 3:30PM - 5:00PM Room: AI Showcase, North Building, Level 2, Booth 11536

Participants

Rene Balzano, MSc, Zurich, Switzerland (*Presenter*) Nothing to Disclose Stefan Voser, Zurich, Switzerland (*Presenter*) Nothing to Disclose

Program Description

During this session, the attendees will be walked through the end-to-end process of preprocessing MRI studies, extracting labels from reports and facilitating deep learning with both in a Microsoft Azure ML environment. Each attendee will receive access to an individual workspace on the platform that will continue to be available for a week after the workshop. In order to get the best experience for this workshop, it is highly recommended that attendees bring a laptop with a keyboard and decent-sized screen. *RSVP is required; adding this session to your agenda does not secure your seat in this session. Click the link below to RSVP.*

RSVP Link

https://www.eventbrite.com/e/deep-learning-with-microsoft-azure-ml-for-mri-interpretation-tickets-64334393904







VW 26

A Practical Approach to Breast Magnetic Resonance Imaging (MRI) Interpretation: An Interactive Session: Presented by Siemens Healthineers

Tuesday, Dec. 3 3:50PM - 5:00PM Room: North Building, Booth 8563

Participants

Susan Weinstein, MD, Philadelphia, PA (Presenter) Nothing to Disclose

Program Information

This interactive session will include both didactic and hands-on case review at workstations equipped with *syngo*. MR Brevis. A practical approach to breast MRI interpretation will be discussed as well as utilizing the available sequences and techniques to improve interpretive skills. *RSVP is required; adding this session to your agenda does not secure your seat in this session. Click the link below to RSVP.*

RSVP

https://www.fairorg.de/Siemens-Healthineers/portal/workshop.cfm/rsna19/





Articular Discs, Menisci, and Labra: Structure, Function, and Dysfunction Using MRI with Emphasis on the Knee Meniscus, Triangular Fibrocartilage, and Glenoid and Acetabular Labrum

Tuesday, Dec. 3 4:30PM - 6:00PM Room: E451B

MR MK

AMA PRA Category 1 Credits ™: 1.50 ARRT Category A+ Credit: 1.75

Participants

Donald L. Resnick, MD, San Diego, CA (Director) Nothing to Disclose

LEARNING OBJECTIVES

1) To detail the anatomy, composition, and function of several intraarticular structures including the menisci of the knee, the triangular fibrocartilage of the wrist, and the labra of the hip and glenohumeral joint. 2) To correlate the anatomic framework of these structures with their patterns of failure, emphasizing MR imaging. 3) To detail the morphology of the human knee meniscus with particular emphasis on its collagen composition. 4) To illustrate the basic patterns of meniscal failure as displayed on MR imaging. 5) To correlate these patterns of failure with an understanding of meniscal morphology. 6) Compare and contrast the normal anatomy and function of the labrum in two main main-ball-socket joints, the hip and shoulder. 7) Identify common labral disorders in the shoulder and hip and recognize imaging findings that distinguish them from normal variants.

Sub-Events

RC404A Meniscus of the Knee

Participants

Donald L. Resnick, MD, San Diego, CA (Presenter) Nothing to Disclose

LEARNING OBJECTIVES

1) To detail the morphology of the human knee meniscus with particular emphasis on its collagen composition. 2) To illustrate the basic patterns of meniscal failure as displayed on MR imaging. 3) To correlate these patterns of failure with an understanding of meniscal morphology.

ABSTRACT

The morphology of the knee meniscus will be explored, particularly its collagen framework, in an effort to elucidate the basic patterns of meniscal failure as viewed in MR images and during arthroscopy. Particular attention will be given to those structures that influence meniscal function and dysfunction, structures that include the meniscal root ligaments, the popliteomeniscal ligaments, and the capsular ligaments.

RC404B Triangular Fibrocartilage Complex (TFCC) of the Wrist

Participants

Christine B. Chung, MD, Solana Beach, CA (Presenter) Nothing to Disclose

RC404C Labrum of the Glenohumeral Joint and of the Hip

Participants David A. Rubin, MD, Saint Louis, MO (*Presenter*) Nothing to Disclose

For information about this presentation, contact:

drubin001@gmail.com

LEARNING OBJECTIVES

Compare and contrast the normal anatomy and function of the labrum in two main main-ball-socket joints, the hip and shoulder.
 Identify common labral disorders in the shoulder and hip and recognize imaging findings that distinguish them from normal variants.





Chronic Pelvic Pain: Added Value of MRI in Endometriosis, Fibroids, and Pelvic Floor Relaxation

Tuesday, Dec. 3 4:30PM - 6:00PM Room: N226



AMA PRA Category 1 Credits ™: 1.50 ARRT Category A+ Credit: 1.75

LEARNING OBJECTIVES

1) Improve knowledge of the economic and psychosocial impact of chronic pelvic pain. 2) Review the indications and MRI imaging protocols for endometriosis. 3) Recognize the MRI appearance of endometriosis. 4) Review the epidemiology and clinical presentations of leiomyomas. 5) Review current treatment options for symptomatic leiomyomas. 6) Recognize the MRI appearance of leiomyomas to include differentiating them from other myometrial masses. 7) Review common surgical interventions for stress urinary incontinence and pelvic organ prolapse. 8) Describe the MRI technique for imaging synthetic material in the pelvic floor. 9) Recognize normal and abnormal MRI appearances of synthetic materials used in pelvic floor dysfunction. 10) Understand the pathophysiology of endometriosis. 11) Recognize MRI finding of endometriosis. 12) Avoid the pitfalls of endometriosis imaging. 13) Review common surgical interventions for stress urinary incontinence and pelvic organ prolapse. 14) Describe the MRI technique for imaging synthetic materials used in pelvic floor. 15) Recognize normal and abnormal MRI appearances of stress urinary incontinence and pelvic organ prolapse. 14) Describe the MRI technique for imaging synthetic material in the pelvic floor. 15) Recognize normal and abnormal MRI appearances of synthetic materials used in pelvic organ prolapse. 14) Describe the MRI technique for imaging synthetic material in the pelvic floor. 15) Recognize normal and abnormal MRI appearances of synthetic materials used in pelvic floor dysfunction.

Sub-Events

RC407A Overview: Why is this Subject Important?

Participants

Susan M. Ascher, MD, Washington, DC (Presenter) Nothing to Disclose

RC407B Endometriosis and Adenomyosis: MR Imaging Pearls and Pitfalls

Participants

Elizabeth A. Sadowski, MD, Madison, WI (Presenter) Nothing to Disclose

LEARNING OBJECTIVES

1) Understand the pathophysiology of endometriosis. 2) Recognize MRI finding of endometriosis. 3) Avoid the pitfalls of endometriosis imaging.

RC407C Leiomyomas: Pre- and Post-procedural Imaging-More Than a Roadmap

Participants

Yuliya Lakhman, MD, New York, NY (Presenter) Nothing to Disclose

RC407D Slings and Meshes: Guide to MR Imaging of Pelvic Floor Following Surgical Repair

Participants Gaurav Khatri, MD, Irving, TX (*Presenter*) Nothing to Disclose

LEARNING OBJECTIVES

1) Review common surgical interventions for stress urinary incontinence and pelvic organ prolapse. 2) Describe the MRI technique for imaging synthetic material in the pelvic floor. 3) Recognize normal and abnormal MRI appearances of synthetic materials used in pelvic floor dysfunction.

Active Handout:Gaurav Khatri

http://abstract.rsna.org/uploads/2019/18000692/Active RC407D.pdf







The Newly Diagnosed Cancer: Different Viewpoints

Tuesday, Dec. 3 4:30PM - 6:00PM Room: E451A



AMA PRA Category 1 Credits ™: 1.50 ARRT Category A+ Credit: 1.75

Participants

Margarita L. Zuley, MD, Pittsburgh, PA (Moderator) Investigator, Hologic, Inc

For information about this presentation, contact:

zuleyml@upmc.edu

LEARNING OBJECTIVES

1) Review the role of ultrasound, MRI, and contrast enhanced mammography in the evaluation of disease extent in the newly diagnosed breast cancer patient. 2) Recognize the advantages and limitations of these three imaging modalities in the assessment of patients' response to neoadjuvant chemotherapy. 3) Be familiar with the evolving management of the axilla.

Sub-Events

RC415A Role of MRI

Participants Constance D. Lehman, MD,PhD, Boston, MA (*Presenter*) Research Grant, General Electric Company Medical Advisory Board, General Electric Company

RC415B The Newly Diagnosed Cancer: Different Viewpoints: The Role of Ultrasound

Participants Regina J. Hooley, MD, Weston, CT (*Presenter*) Consultant, Hologic, Inc

For information about this presentation, contact:

regina.hooley@yale.edu

RC415C Role of CEM

Participants Margarita L. Zuley, MD, Pittsburgh, PA (*Presenter*) Investigator, Hologic, Inc

For information about this presentation, contact:

zuleyml@upmc.edu





Anatomical MR Imaging for Radiotherapy Planning and Guidance

Tuesday, Dec. 3 4:30PM - 6:00PM Room: S501ABC



AMA PRA Category 1 Credits ™: 1.50 ARRT Category A+ Credit: 1.75

Participants

Kristy K. Brock, PhD, Houston, TX (*Moderator*) License agreement, RaySearch Laboratories AB; Grant support, RaySearch Laboratories AB; Research support, Mirada Medical Ltd; ;

Sub-Events

RC422A State of the Art in Anatomical MR Imaging

Participants

Aradhana M. Venkatesan, MD, Houston, TX (Presenter) Research Grant, Canon Medical Systems Corporation

For information about this presentation, contact:

avenkatesan@mdanderson.org

LEARNING OBJECTIVES

1) Review opportunities and unmet needs for state of the art imaging techniques to inform radiotherapy strategies. 2) Summarize the current state of the art role for contemporary MRI in radiotherapy, with an emphasis on gynecologic and prostate cancer therapy. 3) Describe emerging solutions enabled by MR imaging guidance and their potential gains for patients.

RC422B Clinical Need for Anatomical MR Imaging in Radiation Therapy

Participants

Cynthia Menard, MD, Montreal, QC (Presenter) Nothing to Disclose

For information about this presentation, contact:

Cynthia.Menard@umontreal.ca

LEARNING OBJECTIVES

1) Understand the various roles of MRI in radiotherapy practice. 2) Identify pitfalls in integrating MRI in radiotherapy planning. 3) Describe anatomical sites where the integration of MRI is established as standard-care.

RC422C Technical Challenges in the Integration of Anatomical MR Imaging into Radiotherapy

Participants

Carri Glide-Hurst, PHD, Detroit, MI (*Presenter*) Researcher, ViewRay, Inc; Research Consultant, Koninklijke Philips NV; Researcher, Koninklijke Philips NV; Researcher, Modus Medical Devices Inc; Equipment support, Medspira, LLC; Equipment support, QFix

LEARNING OBJECTIVES

To understand the unique imaging challenges and benefits for incorporating MRI into radiation therapy treatment planning.
 To describe the magnetic resonance simulation (MR-SIM) process to yield images that are more robust for radiation therapy planning.
 To describe emerging technologies in MR-only treatment planning and MR-guided radiation therapy and opportunities for collaboration between imaging and radiation therapy colleagues.





MRI Safety Course (Gadolinium and Pacemakers) (Interactive Session) (The In-Person Session is Supported in part by an Unrestricted Educational Grant from Bayer)

Tuesday, Dec. 3 4:30PM - 6:00PM Room: E350



AMA PRA Category 1 Credits ™: 1.50 ARRT Category A+ Credit: 1.75

FDA Discussions may include off-label uses.

Sub-Events

RC429A MRI in Patients with Pacemakers/Cardiac Devices

Participants

Robert J. Russo, MD, PhD, La Jolla, CA (Presenter) Nothing to Disclose

LEARNING OBJECTIVES

1) Differentiate an MRI-conditional pacing system from a non-MRI-conditional system. 2) Assess the risks associated with MRI for patients with non-MRI-conditional pacemakers and defibrillators. 3) Integrate the performance of clinically indicated MRI in patients with pacemakers and defibrillators into the practice of radiology, cardiology, neurology, neurosurgery, and orthopedics. 4) Understand the current 2017 Heart Rhythm Society (HRS) Guidelines for performing MRI with an implanted cardiac device, as well as the Centers for Medicare and Medicaid Services (CMS) Decision Memo for Magnetic Resonance Imaging (MRI) (CAG-00399R4). 5) Utilize the current research results and clinical guidelines regarding MRI in patients with pacemakers and defibrillators for the establishment of a cardiology collaboration with the purpose of improving patient access to MRI.

RC429B Gadolinium Deposition: What Do I Tell Patients, Referring Physicians, Other Radiologists, and Attorneys?

Participants

Emanuel Kanal, MD, Pittsburgh, PA (*Presenter*) Consultant, Medtronic plc; Consultant, Bracco Group; Consultant, General Electric Company;

For information about this presentation, contact:

ekanal@pitt.edu

LEARNING OBJECTIVES

1) Provide an overview of the history of the long term safety effects of gadolinium based contrast agents regarding both nephrogenic systemic fibrosis (NSF) as well as gadolinium retention, and specify similarities as well as significant clinical differences between these two concerns. 2) Explain mechanisms how gadolinium based contrast agents, which do not cross the blood brain barrier, is believed today to be successfully transported from the vascular lumen to the parenchyma of the brain. 3) List similarities as well as differences among the various types of gadolinium based contrast agents relative to gadolinium retention/deposition as well as NSF. 4) Describe how the FDA's response to gadolinium retention concerns differs from that the European regulatory agencies. 5) Identify what we definitively know today - and what we still don't know - about the safety of retained gadolinium in the brain.

ABSTRACT

2006 was accompanied by the discovery of a relationship between the intravenous administration of at least some gadolinium based contrast agents (GBCA) and the development of nephrogenic systemic fibrosis (NSF) in patients with significant renal disease. Roughly 8 years later GBCAs were found to deposit or leave a very small amount of their administered intravenous dose in the brain as well as other tissues/organs of its recipients that can be found months or even year following its initial administration. This time, however, this finding was present even in those with normal renal function, although it did seem more pronounced in patients with renal disease. In the more than 5 years that have passed since this discovery was first publicized, there is much that we have learned - and a great deal that we still have not determined - about gadolinium retention. Still being investigated are such issues as similarities versus differences between individual GBCAs with respect to gadolinium retention and potential high risk patients or populations for gadolinium retention. Perhaps the single main question that remains, however, is whether there is any significant clinical consequence or harm as a result of such deposition, and if that potential consequence is the same in type and incidence for all GBCA. This presentation will attempt to provide a succinct summary of the more salient issues and facts that we know regarding retained gadolinium, and will at the same time stress what we still do NOT confidently know or understand regarding the safety of gadolinium retention in humans today.

RC429C Establishing an Efficient Workflow for MRI Safety

Participants

Bradley N. Delman, MD, New York, NY (Presenter) Consultant, Bayer AG Speaker, Bayer AG

For information about this presentation, contact:

bradley.delman@mountsinai.org

LEARNING OBJECTIVES

1) Assess current MRI environment in critical aspects of safety. 2) Understand key structures of MRI safety oversight, including current consensus models for management. 3) Define potential risks in MRI suites to patients, personnel and visitors. 4) Explain considerations in special populations. 5) Establish a reliable method of response in emergent situations. 6) Identify resources for optimizing the safety program.

RC429D Q&A

Participants Robert J. Russo, MD, PhD, La Jolla, CA (*Presenter*) Nothing to Disclose Emanuel Kanal, MD, Pittsburgh, PA (*Presenter*) Consultant, Medtronic plc; Consultant, Bracco Group; Consultant, General Electric Company; Bradley N. Delman, MD, New York, NY (*Presenter*) Consultant, Bayer AG Speaker, Bayer AG

For information about this presentation, contact:

bradley.delman@mountsinai.org





PI-RADS Hands-on Workshop (Interactive Session)

Wednesday, Dec. 4 8:00AM - 10:00AM Room: E450A



AMA PRA Category 1 Credits ™: 2.00 ARRT Category A+ Credits: 2.25

Participants

Jelle O. Barentsz, MD, PhD, Nijmegen, Netherlands (*Moderator*) Nothing to Disclose
Jelle O. Barentsz, MD, PhD, Nijmegen, Netherlands (*Coordinator*) Nothing to Disclose
Baris Turkbey, MD, Bethesda, MD (*Presenter*) Research support, Koninklijke Philips NV; Royalties, Invivo Corporation; Investigator, NVIDIA Corporation
Roel D. Mus, MD, Nijmegen, Netherlands (*Presenter*) Nothing to Disclose
Antonio C. Westphalen, MD, Mill Valley, CA (*Presenter*) Research Grant, General Electric Company; Scientific Advisory Board, 3D
Biopsy LLC
Daniel J. Margolis, MD, New York, NY (*Presenter*) Consultant, Blue Earth Diagnostics Ltd
Geert M. Villeirs, MD, PhD, Gent, Belgium (*Presenter*) Nothing to Disclose
Joseph J. Busch, MD, Chattanooga, TN (*Presenter*) Nothing to Disclose
Leonardo K. Bittencourt, MD, PhD, Rio de Janeiro, Brazil (*Presenter*) Nothing to Disclose
Vibeke B. Logager, MD, Herlev, Denmark (*Presenter*) Nothing to Disclose
Silvia D. Chang, MD, Vancouver, BC (*Presenter*) Nothing to Disclose
William J. Weadock, MD, Ann Arbor, MI (*Presenter*) Owner, Weadock Software, LLC

For information about this presentation, contact:

Vibeke.Loegager@regionh.dk

Roel.Mus@radboudumc.nl

djm9016@med.cornell.edu

turkbeyi@mail.nih.gov

LKAYAT@gmail.com

pshankar@med.umich.edu

jelle.barentsz@radboudumc.nl

Special Information

Participants will review cases on their own devices and answer questions. The cases will then be reviewed by the presenters. Note: this activity is best done on a laptop or tablet. Although phones will work, their small size limits optimal image view.

LEARNING OBJECTIVES

1) Understand and how to use the PI-RADS v2.1 Category Assessment to detect and localize significant prostate cancer for both peripheral and transitional zone. 2) Recognize benign pathology like prostatitis and BPH and to differentiate these from significant prostate cancers.

ABSTRACT

You need to bring your own laptops or tablets, as in this 'Hands-on Workshop' you will review multi-parametric MRI cases with various prostatic pathology using your own laptop or tablet. Though a Cloud-connection (RadPix) your device will serve as a dedicated prostate-MRI workstation through which you can analyse 20 cases. This activity is best done on a laptop or tablet. Although phones and small tablets will work, their small size limits optimal image viewing. Focus will be on the overall assessment of PI-RADS v2.1 category. You will be interactively teached how to score the probability of the presence of a significant prostate in patients with elevated PSA or other suspicion to have prostate cancer. All 20 cases are from daily practice, and have various levels of difficulty. They include easy and difficult significant cancers, inflammation, BPH, and most common pitfalls. Internationally renowned teachers will guide you during your PI-RADS v2.1 scoring process. You will be able to ask them all question you have on prostate mp-MRI, from acquisition to diagnosis to MR-biopsy. Prior to this course you need to download a digital course book at http://bit.ly/prostate2019. This digital pdf-course book includes all the cases and will guide you during the course through the various cases.

Active Handout:Roel Dirk Mus

http://abstract.rsna.org/uploads/2019/16002001/Active RC507.pdf







Musculoskeletal Series: MRI of Elbow, Wrist, and Hand

Wednesday, Dec. 4 8:30AM - 12:00PM Room: S406A



AMA PRA Category 1 Credits ™: 3.00 ARRT Category A+ Credits: 3.50

FDA Discussions may include off-label uses.

Participants

Bruce B. Forster, MD, Vancouver, BC (*Moderator*) Stockholder, Canada Diagnostic Centres Bethany U. Casagranda, DO, Pittsburgh, PA (*Moderator*) Nothing to Disclose Linda Probyn, MD, Toronto, ON (*Moderator*) Nothing to Disclose Tetyana A. Gorbachova, MD, Huntingdon Valley, PA (*Moderator*) Nothing to Disclose

For information about this presentation, contact:

bethany.casagranda@ahn.org

LEARNING OBJECTIVES

1) To familiarize the audience with imaging diagnosis of common pathologies involving the elbow, wrist and hand, including abnormalities affecting tendons and ligaments in the setting of trauma.

Sub-Events

RC504-01 MRI of Elbow Ligament Injuries

Wednesday, Dec. 4 8:30AM - 8:50AM Room: S406A

Participants

Kirkland W. Davis, MD, Madison, WI (Presenter) Author with royalties, Reed Elsevier; Editor with royalties, Reed Elsevier

For information about this presentation, contact:

kdavis@uwhealth.org

LEARNING OBJECTIVES

1) Demonstrate normal anatomy of the principle ligaments of the elbow. 2) Understand imaging options when assessing for elbow ligament injury. 3) Identify partial and complete tears of the principle ligaments of the elbow.

RC504-02 MRI of Elbow Tendon Injuries

Wednesday, Dec. 4 8:50AM - 9:10AM Room: S406A

Participants

Soterios Gyftopoulos, MD, Scarsdale, NY (Presenter) Nothing to Disclose

For information about this presentation, contact:

Soterios.Gyftopoulos@nyumc.org

LEARNING OBJECTIVES

1) Review the important elbow tendon anatomy. 2) Review the imaging options available to evaluate elbow tendon pathology. 3) Describe the imaging appearances of the clinically relevant tendon pathology that occurs at the elbow.

RC504-03 Associated Radiological Findings in Patients with Ulnar Collateral Ligament Injuries of the First Metacarpophalangeal Joint

Wednesday, Dec. 4 9:10AM - 9:20AM Room: S406A

Participants

Sebastian Manneck, MD, Basel, Switzerland (*Presenter*) Nothing to Disclose Anna Hirschmann, MD, Basel, Switzerland (*Abstract Co-Author*) Nothing to Disclose

PURPOSE

To evaluate the frequency of concomitant volar plate avulsion in patients with ulnar collateral ligament (UCL) tear of the first metacarpophalangeal (MCP) joint indicating extensive injury.

METHOD AND MATERIALS

Patients with radiographs and MR images of the thumb obtained between January 2014 and November 2018 were selected through a retrospective search of our PACS database for the keywords "UCL injury" and "thumb" in the radiological report. Twenty-five

patients with an injury at the UCL of the first MCP joint on radiographs and MRI were then retrospectively assessed for a concomitant injury at the palmar structures by two musculoskeletal radiologists independently. Descriptive statistics were used to report the imaging interpretation. Wilcoxon and kappa statistics were calculated (P-value < 0.05).

RESULTS

24% [6]/16% [4](Reader1/Reader2) partial tears and 48% [12]/60% [15] (R1/R2) complete tears of the UCL were evident on MRI. UCL avulsion fractures were seen more frequently on MRI (28% [7]/16% [4]; R1/R2) compared to radiographs 12% [3]; (P=0.046; 0.317). Volar plate injuries were evident in 12% [3]/ 8% [2] on radiographs and in 80% [20]/76% [19] (R1/R2) on MRI (P =0.0001). Dislocation of the UCL >= 3 mm, as an indication for surgery, was evident in 8% [2] on radiographs and 40% [10] /56% [14] (R1/R2) on MRI (P=0.005). Ten/11 patients (R1/R2) with a dislocated UCL tear showed a concomitant volar plate injury (100 %/ 79%) as opposed to 10/8 patients (R1/R2) with non-displaced UCL-tears (66 %/ 72%). No injury to the dorsal ligament complex was seen. Interrater-agreement was 1.0/0.444 for UCL and 0.783/0.566 for palmar plate injuries on radiographs/MRI.

CONCLUSION

UCL and palmar plate injuries commonly coexist and radiographs underestimate the severity of injury. MR images show more subtle abnormalities.

CLINICAL RELEVANCE/APPLICATION

MRI is advocated in patients with suspected UCL tears to assess concomitant volar capsulo-ligamentous injuries. Accurate diagnosis of first MCP-joint injury can significantly impact treatment strategy and clinical outcome to prevent from developing persistent pain and chronic instability.

RC504-04 High-Resolution 3D Cone-Beam CT with a New Prototype of a Twin Robotic X-Ray System in Wrist Imaging: Comparison of Image Quality to Third-Generation Dual-Source CT

Wednesday, Dec. 4 9:20AM - 9:30AM Room: S406A

Participants

Tobias Gassenmaier, MD, Wurzburg, Germany (*Presenter*) Nothing to Disclose Andreas Kunz, MD, Wurzburg, Germany (*Abstract Co-Author*) Nothing to Disclose Carsten H. Gietzen, MD, Wuerzburg, Germany (*Abstract Co-Author*) Research Grant, Siemens AG Andreas M. Weng, Wuerzburg, Germany (*Abstract Co-Author*) Nothing to Disclose Thorsten A. Bley, MD, Wuerzburg, Germany (*Abstract Co-Author*) Nothing to Disclose Jan P. Grunz, MD, Wuerzburg, Germany (*Abstract Co-Author*) Research Grant, Siemens AG

PURPOSE

To evaluate image quality of a prototype version for cone-beam computed tomography (CBCT) of a twin robotic X-ray system in wrist imaging compared to a 3rd gen. dual-source CT (DSCT).

METHOD AND MATERIALS

16 cadaveric human wrists were examined with a not commercially available prototype version for CBCT of the above mentioned Xray system and a conventional 3rd gen. DSCT. Images were acquired with a standard-dose (SD) and low-dose (LD) protocol with matched radiation doses between systems (16 cm CTDIvol = 13.8 mGy in SD and 3.3 mGy in LD protocol). Two independent, blinded radiologists assessed overall image quality (IQ) in axial, coronal and sagittal MPRs utilizing a seven-point Likert scale (1 - very poor, [...], 7 - excellent IQ). Interrater reliability was assessed with the intraclass correlation coefficient (ICC; absolute agreement, 2way random-effects model). For objective analysis of IQ, the number of pixels within the highest (representing trabecula) and lowest (representing fatty bone marrow) 20% of grey values were quantified within a region of interest measurement in cancellous bone. High pixel numbers within the defined ranges were considered to indicate higher spatial resolution with good trabecular contrast.

RESULTS

In general, subjective IQ in CBCT was superior to dose-equivalent DSCT scans (all p<=0.030 for SD and p<0.001 for LD). For instance, median subjective IQ values for coronal MPRs were 7/7 (Reader 1 / Reader 2) in CBCT vs. 6/6 in DSCT with the SD protocol and 5/6 in CBCT vs. 3/3 in DSCT with the LD protocol. Single measure ICC was 0.936 (95% confidence interval, 0.897-0.961; p<0.001), indicating good to excellent reliability. Objective image analysis revealed higher pixel counts within the defined ranges when comparing CBCT to DSCT in both the SD (median 1744 pixels [IQR 1345 - 2237] vs. 1240 [657 - 1762]; p=0.001) and LD protocol (904 [577 - 1533] vs. 697 [486 - 1110]; p=0.013), indicating better delineation of trabecula in CBCT.

CONCLUSION

The new prototype version of the twin robotic X-ray system's CBCT mode provides superior image quality regarding delineation of trabecula at standard and low dose levels compared to dose-equivalent scan protocols on 3rd gen. DSCT.

CLINICAL RELEVANCE/APPLICATION

With improved image quality compared to 3rd gen. DSCT the new CBCT mode of the multifunctional X-ray system appears highly promising for 3D wrist imaging in vivo and may well hold potential for dose reduction.

RC504-05 Evaluation of the Ulnar Nerve with Shear-Wave Elastography: A Potential Sonographic Method for the Diagnosis of Ulnar Neuropathy

Wednesday, Dec. 4 9:30AM - 9:40AM Room: S406A

Participants

Sujin Kim, MD, Seoul, Korea, Republic Of (*Presenter*) Nothing to Disclose Guen Young Lee, Seongnam, Korea, Republic Of (*Abstract Co-Author*) Nothing to Disclose Ara Ko, MD, Seoul, Korea, Republic Of (*Abstract Co-Author*) Nothing to Disclose Jiyun Oh, Seoul, Korea, Republic Of (*Abstract Co-Author*) Nothing to Disclose Seok-min Jeong, Seoul, Korea, Republic Of (*Abstract Co-Author*) Nothing to Disclose

For information about this presentation, contact:

jaywony@gmail.com

PURPOSE

The aim of this study was to verify if shear-wave elastography (SWE) can be used to differentiate ulnar neuropathy at the cubital tunnel from asymptomatic ulnar nerve or medial epicondylitis and to determine a cut-off value for this parameter accurately identifying patient with ulnar neuropathy

METHOD AND MATERIALS

This study included 10 patients with ulnar neuropathy at the cubital tunnel, which was confirmed with electromyography (3 women, 7 men; mean age, 51.9 years), 10 patients with medial epicondylitis (5 women, 5 men; mean age, 56.1 years), and 37 patients with asymptomatic ulnar nerve and lateral epicondylitis (21 women, 16 men; 54.0 years). Each patient was subjected to SWE of the ulnar nerve at three levels: in the cubital tunnel and at the distal upper arm, and proximal forearm.

RESULTS

Patients with ulnar neuropathy in the cubital tunnel (mean, 66.8kPa) presented with significantly greater ulnar nerve stiffness in the cubital tunnel than the controls with medial epicondylitis (mean, 21.2kPa, P=0.015) or lateral epicondylitis (mean, 33.9kPa, P=0.040). There are no statistically significant differences of ulnar nerve stiffness at the distal upper arm and the proximal forearm between patients and controls. Ulnar nerve stiffness of 31kPA provide 100% specificity, 80.0% sensitivity, 100% positive predictive value and 83.3% negative predictive value for the differentiation between ulnar neuropathy and medial epicondylitis.

CONCLUSION

SWE seems to be a reliable and simple quantitative adjunct test to support the diagnosis of ulnar neuropathy at the cubital tunnel, especially to differentiate ulnar neuropathy at the cubital tunnel from medial epicondylitis.

CLINICAL RELEVANCE/APPLICATION

SWE seems to be a reliable and simple quantitative adjunct test to differentiate ulnar neuropathy at the cubital tunnel from medial epicondylitis.

RC504-06 MRI of Ulnar-sided Wrist Pain

Wednesday, Dec. 4 9:40AM - 10:00AM Room: S406A

Participants

Bruce B. Forster, MD, Vancouver, BC (Presenter) Stockholder, Canada Diagnostic Centres

For information about this presentation, contact:

bruce.forster@vch.ca

LEARNING OBJECTIVES

1) Understand the anatomy relevant to wrist/hand, with respect to ulnar sided wrist pain (USWP). 2) Appreciate the advantages and disadvantages of imaging modalities in workup of USWP. 3) List the common imaging features of causative pathologies of USWP, including Kienbock's disease, ulnocarpal abutment, TFCC pathology, hook of hamate fracture, and ECU pathology.

RC504-07 MRI of Radial-sided Wrist Pain

Wednesday, Dec. 4 10:30AM - 10:50AM Room: S406A

Participants Bethany U. Casagranda, DO, Pittsburgh, PA (*Presenter*) Nothing to Disclose

For information about this presentation, contact:

bethany.casagranda@ahn.org

LEARNING OBJECTIVES

1) Identify relevant wrist anatomy. 2) Describe physical exam tactics. 3) Develop differential diagnosis. 4) Identify imaging findings of each differential including osseous and soft tissue trauma, arthritis, Wartenberg's syndrome, De Quervain's tenosynovitis, lateral antebrachial cutaneous nerve neuritis and intersection syndrome.

RC504-08 Direct Visualization of Finger Pulley Injuries at 7T MRI: An Ex Vivo Feasibility Study

Wednesday, Dec. 4 10:50AM - 11:00AM Room: S406A

Participants

Rafael Heiss, Erlangen, Germany (*Presenter*) Speakers Bureau, Siemens AG Alexander Librimir, Erlangen, Germany (*Abstract Co-Author*) Nothing to Disclose Christoph Lutter, Bamberg, Germany (*Abstract Co-Author*) Nothing to Disclose Frank W. Roemer, MD, Erlangen, Germany (*Abstract Co-Author*) Officer, Boston Imaging Core Lab, LLC; Research Director, Boston Imaging Core Lab, LLC; Shareholder, Boston Imaging Core Lab, LLC Michael Uder, MD, Erlangen, Germany (*Abstract Co-Author*) Nothing to Disclose Rolf Janka, MD, PhD, Erlangen, Germany (*Abstract Co-Author*) Nothing to Disclose Volker Schoffl, Bamberg, Germany (*Abstract Co-Author*) Nothing to Disclose Armin Nagel, DiplPhys, Heidelberg, Germany (*Abstract Co-Author*) Nothing to Disclose Thomas Bayer, MD, Bamberg, Germany (*Abstract Co-Author*) Nothing to Disclose

PURPOSE

To evaluate feasibility of 7T magnetic resonance imaging (MRI) for direct visualization of the finger flexor pulleys A2, A3 and A4

before and after artificial pulley injury in an ex-vivo model and to correlate results with anatomical preparations.

METHOD AND MATERIALS

30 fingers from 10 human cadavers were examined before and after iatrogenic pulley disruption with a 7T imaging protocol, which is comparable to a clinical protocol lasting 15 minutes. Images were assessed by two experienced radiologists for the presence and location of finger pulley lesions. Image quality was evaluated according a 4-point Likert scale from not evaluable to excellent. Macroscopic and histopathological preparation was used as gold standard for comparing findings with MRI. Diagnostic performance was assessed using sensitivity and specificity.

RESULTS

Mechanically induced finger flexor pulley lesions were detected with a sensitivity of 100% and a specificity of 98%. Finger flexor A2, A3 and A4 pulley lesions were detected at the radial and ulnar, as well as in the middle parts of the finger pulley in 33.3% each. In 62.5% of all pulley lesions a dislocation and intercalation of the pulley stump in between the flexor tendon and finger phalanges was observed. The average Likert score for direct visualization of pulleys before rupture was 2.67 and after rupture creation 2.79, meaning a very good image quality in average.

CONCLUSION

7T MRI enables direct visualization and characterization of traumatic pulley lesions with definition of rupture morphology, detection of complicated lesions and evaluation of small pulleys such as A3 and A4.

CLINICAL RELEVANCE/APPLICATION

Direct 7T visualization allows pre-surgical evaluation of pulley injuries and is able to characterize complex pulley injuries including those exhibiting stump dislocations, even for small pulleys.

RC504-09 A Multimodality Census of Carpal Coalitions

Wednesday, Dec. 4 11:00AM - 11:10AM Room: S406A

Participants

Alessandra J. Sax, MD, Philadelphia, PA (*Presenter*) Nothing to Disclose William B. Morrison, MD, Philadelphia, PA (*Abstract Co-Author*) Consultant, AprioMed AB Patent agreement, AprioMed AB Consultant, Zimmer Biomet Holdings, Inc Consultant, Samsung Electronics Co, Ltd Consultant, Medical Metrics, Inc Aleksandr Rozenberg, MD, Philadelphia, PA (*Abstract Co-Author*) Nothing to Disclose Adam C. Zoga, MD, Philadelphia, PA (*Abstract Co-Author*) Nothing to Disclose

For information about this presentation, contact:

alisax87@gmail.com

PURPOSE

Coalition in the wrist is less common than the foot, but still encountered routinely. Although frequently incidental, they can also be a primary or secondary source of pain. To date, few series have been conducted to establish the prevalence and morphology of carpal coalitions. We endeavored to create the largest known study to date detailing the configurations and imaging features of carpal coalitions across multiple imaging modalities.

METHOD AND MATERIALS

A report database from upper extremity x-ray, CT, and MRI exams was retrospectively mined for the word 'coalition'. Studies were reviewed by 2 MSK radiologists. Configurations, ordering indication, and pathology across the coalition were logged. Pathology potentially related to the coalition was observed and the relative risks were calculated.

RESULTS

Of the 430 x-rays, lunotriquetral coalition was most prevalent in 88%, capitohamate in 7%, scapholunate in 2%, hamate-pisiform in 1%, trapezoid-capitate in 1%, with single occurrences in other locations. 71% of x-rays were ordered for recent injury (within 1 month), 29% for non-traumatic pain. Of the 114 MRIs, lunotriquetral coalition was most common in 83%, capitohamate in 2%, hamate-pisiform in 3%, trapezoid-capitate in 6%, and 6% at an os styloideum or os trapezoideum secundareum. 35% of MRIs were ordered for recent injury, 65% for non-traumatic pain. Degenerative changes across the coalition occurred in 33% of MRIs. There was a significant increased risk of triscaphe arthritis, (23% of MRIs, relative risk (RR) 3.09, 95% confidence interval (CI) 1.36-7.04). 43% of exams involved extensor tendons (RR 1.23, 95% CI .79-1.93). Extensor tears (13%, RR 10.11, 95% CI 1.61-63.49), specifically the extensor carpi ulnaris (10%, RR 7.58, 95% CI 1.17-48.94) were the most significant. A scapholunate tear was present in 24% (RR 1.61, 95% CI .85-3.07). Flexor compartment tendinosis was present in 24% (RR 1.61, 95% CI .85-3.07).

CONCLUSION

While carpal coalitions are relatively infrequent, some cause variations in biomechanical stability and can be symptomatic. Radiologists should be familiar with the most common coalitions including lunotriquetral and capitohamate as well as less common locations, morphologic variations, and imaging findings associated with carpal coalitions.

CLINICAL RELEVANCE/APPLICATION

Recognizing carpal coalition and associated pathology is important as it may be directly or indirectly responsible for patients' symptoms.

RC504-10 Clinical and Cost-Effectiveness Implications of Utilizing Immediate Acute Magnetic Resonance Imaging (MRI) in the Management of Patients with Suspected Scaphoid Fracture and Negative Initial Radiographs: Results From a Randomized Clinical Trial

Wednesday, Dec. 4 11:10AM - 11:20AM Room: S406A

Sanjay Vijayanathan, MBBS, Harrow, United Kingdom (*Abstract Co-Author*) Nothing to Disclose Davina Mak, MBBS, BSC, Middlesex, United Kingdom (*Presenter*) Nothing to Disclose Alireza Zavareh, MD, FRCR, Bristol, United Kingdom (*Abstract Co-Author*) Nothing to Disclose Amanda Isaac, MBChB, FRCR, Rickmansworth, United Kingdom (*Abstract Co-Author*) Nothing to Disclose Bharti Malhotra, MBA, London, United Kingdom (*Abstract Co-Author*) Nothing to Disclose Laura Hunter, London, United Kingdom (*Abstract Co-Author*) Nothing to Disclose Janet Peacock, PhD, London, United Kingdom (*Abstract Co-Author*) Nothing to Disclose James Shearer, PhD, London, United Kingdom (*Abstract Co-Author*) Nothing to Disclose Vicky J. Goh, MBBCh, Chalfont St Giles, United Kingdom (*Abstract Co-Author*) Nothing to Disclose Paul McCrone, London, United Kingdom (*Abstract Co-Author*) Nothing to Disclose

Sam Gidwani, London, United Kingdom (Abstract Co-Author) Nothing to Disclose

For information about this presentation, contact:

tiago.rua@kcl.ac.uk

PURPOSE

Given the limited accuracy of radiographs on presentation to the Emergency Department (ED), the management of suspected scaphoid fractures remains clinically challenging and an economic burden to healthcare systems. This trial evaluated the clinical and cost-effectiveness implications of using immediate Magnetic Resonance Imaging (MRI) as an add-on test during the ED attendance for patients with negative findings on the initial radiographs.

METHOD AND MATERIALS

A pragmatic, randomized, single-center trial compared the use of immediate MRI for patients presenting to the ED with suspected scaphoid fractures against standard care with radiographs only. Participants' use of health services was estimated from primary care and secondary care databases and questionnaires at baseline, 3 and 6 months post-recruitment. Costs were compared using generalized linear models and combined with quality-adjusted life years (QALYs) to estimate cost-effectiveness.

RESULTS

A total of 136 participants were recruited based on 1:1 ratio, block randomization methods (mean age 37 years; 57% male; 79% full-time employed). 6.2% (4/65, control group) and 10% (7/67, intervention group) of participants sustained scaphoid fractures (p=0.37). 7.7% (5/65, control group) and 22% (15/67, intervention group) of participants had other fractures diagnosed (p=0.019). The use of MRI increased the diagnostic accuracy both in the diagnosis of scaphoid fracture (100.0% vs 93.8%) and any other fracture (98.5% vs 84.6%). Mean (SD) cost per participant up to 3 months post-recruitment was £542.4 (£855.2) for the control group and £368.4 (£338.6) for the intervention, leading to a cost difference of £174 (95% CI -£30 to £378, p=0.094). The cost difference per participant at 6 months increased to £266 (95% CI £3.3 to £528, p=0.047). The MRI intervention dominated standard care costing less and achieving more QALY gains, presenting a probability of 96% and 100% of being cost-effective at month 3 and 6 considering traditional willingness-to-pay thresholds.

CONCLUSION

The use of immediate MRI in the management of participants with suspected scaphoid fracture and negative radiographs led to significant cost-savings whilst improving and expediting the pathway's diagnostic accuracy.

CLINICAL RELEVANCE/APPLICATION

The immediate use of MRI in the management of suspected scaphoid fractures should be included as part of standard of care as an add-on test for patients with negative radiographs.

RC504-11 MRI of Thumb Injuries

Wednesday, Dec. 4 11:20AM - 11:40AM Room: S406A

Participants

Linda Probyn, MD, Toronto, ON (Presenter) Nothing to Disclose

For information about this presentation, contact:

linda.probyn@sunnybrook.ca

LEARNING OBJECTIVES

1) Describe relevant normal anatomy of the thumb including tendons, ligaments and pulleys. 2) Explain common pathologies related to thumb injuries, including tendon, ligament and osseous injuries. 3) Compare other imaging modalities and how they can be complimentary to assist in diagnosing injuries of the thumb.

RC504-12 MRI of Finger Injuries

Wednesday, Dec. 4 11:40AM - 12:00PM Room: S406A

Participants Tetyana A. Gorbachova, MD, Huntingdon Valley, PA (*Presenter*) Nothing to Disclose

For information about this presentation, contact:

gorbacht@einstein.edu

LEARNING OBJECTIVES

1) Recognize normal osseous and soft tissue anatomy of the fingers on MRI. 2) Describe various types of finger injuries and their clinical and treatment implications. 3) Identify common pitfalls in diagnosis of finger injuries on MRI.





Vascular Series: MR Angiography-New Techniques and Their Application

Wednesday, Dec. 4 8:30AM - 12:00PM Room: S503AB



AMA PRA Category 1 Credits ™: 3.00 ARRT Category A+ Credits: 3.50

FDA Discussions may include off-label uses.

Participants

Thomas K. Foo, PhD, Niskayuna, NY (Moderator) Employee, General Electric Company

Martin R. Prince, MD,PhD, New York, NY (*Moderator*) Patent agreement, General Electric Company; Patent agreement, Hitachi, Ltd; Patent agreement, Siemens AG; Patent agreement, Koninklijke Philips NV; Patent agreement, Nemoto Kyorindo Co, Ltd; Patent agreement, Bayer AG; Patent agreement, Lantheus Medical Imaging, Inc; Patent agreement, Bracco Group; Patent agreement, Mallinckrodt plc; Patent agreement, Guerbet SA; Patent agreement, Toshiba Corporation

Tim Leiner, MD, PhD, Utrecht, Netherlands (Moderator) Speakers Bureau, Koninklijke Philips NV Research Grant, Bayer AG

For information about this presentation, contact:

map2008@med.cornell.edu

thomas.foo@ge.com

LEARNING OBJECTIVES

1) Understand the latest MR Angiography methods. 2) Identify optimal approaches to using MR Angiography techniques throughout the body. 3) Appraise the strengths and weaknesses of various MR approaches to vascular imaging.

Sub-Events

RC512-01 K-Space Options for Improving MRA

Wednesday, Dec. 4 8:30AM - 9:00AM Room: S503AB

Participants

Walter F. Block, PhD, Madison, WI (*Presenter*) Stockholder and Co-founder, TherVoyant; Research support, General Electric Company;

For information about this presentation, contact:

wfblock@wisc.edu

LEARNING OBJECTIVES

1) Understand basic strategies used in MR Angiography to subsample the MR raw data space (k-space) to improve the temporal and spatial performance parameters of MRA. 2) Learn how spatial resolution, temporal resolution, and SNR performance are linked. 3) Learn the difference between an acquisition method's temporal footprint and temporal frame rate.

ABSTRACT

MR Angiography is hampered by MR's need to acquire data in an alternative domain (k-space) with a relative lack of sensors (receivers) relative to CT and US, where thousands of detectors can be active at once. To capture the human vascular system at the temporal and spatial resolution necessary to answer important diagnostic questions, clinical MRA pulse sequences sub-sample the k-space acquisition space in a myriad of ways that tradeoff performance in spatial resolution, temporal resolution, and SNR. The presentation will highlight the general classes of these methodologies, which usually acquire lower spatial frequency data more often than higher spatial frequencies (variable k-space density). Often these k-space acquisition strategies are paired with a reconstruction methodology that iteratively works to generate the mostly likely image reconstruction possible for the given subsampled k-space data. The presentation will discuss the assumptions that all these methodologies make and ways physicians can assess the effects these assumptions may make on clinical decision-making.

RC512-02 Added Value of MRI-Based Vascular Calcification Visualization for the Assessment of Arterial Stenosis in Patients with Lower-Extremity Peripheral Artery Disease Undergoing Non-Contrast Quiescent Interval Slice-Selective (QISS) MRA

Wednesday, Dec. 4 9:00AM - 9:10AM Room: S503AB

Participants

Akos Varga-Szemes, MD, PhD, Charleston, SC (*Presenter*) Research Grant and Travel Support, Siemens AG Research Consultant, Elucid Bioimaging

Megha Penmetsa, Charleston, SC (Abstract Co-Author) Nothing to Disclose

Thomas M. Todoran, MD, Charleston, SC (*Abstract Co-Author*) Research Consultant, Medtronic plc; Research Consultant, General Electric Company

Pal Suranyi, MD, PhD, Charleston, SC (*Abstract Co-Author*) Nothing to Disclose Stephen R. Fuller, Charleston, SC (*Abstract Co-Author*) Nothing to Disclose Andreas Fischer, MD, Charleston, SC (*Abstract Co-Author*) Nothing to Disclose Robert R. Edelman, MD, Evanston, IL (*Abstract Co-Author*) Research support, Siemens AG; Royalties, Siemens AG Ioannis Koktzoglou, PhD, Evanston, IL (*Abstract Co-Author*) Research support, Siemens AG U. Joseph Schoepf, MD, Charleston, SC (*Abstract Co-Author*) Research Grant, Astellas Group; Research Grant, Bayer AG; Research Grant, Bracco Group; Research Grant, Siemens AG; Research Grant, Heartflow, Inc; Research support, Bayer AG; Consultant, Elucid BioImaging Inc; Research Grant, Guerbet SA; Consultant, HeartFlow, Inc; Consultant, Bayer AG; Consultant, Siemens AG; ; ;

For information about this presentation, contact:

schoepf@musc.edu

PURPOSE

This study sought to investigate the added value of prototype proton density weighted, in-phase 3D stack-of-stars (PDIP-SOS) MRI-based calcification visualization on the diagnostic accuracy of detecting peripheral artery disease (PAD) using non-contrast quiescent interval slice-selective (QISS) MRA.

METHOD AND MATERIALS

Twenty-six patients (70±8 years) with suspected PAD, referred for lower extremity CTA prior to digital subtraction angiography (DSA), were prospectively enrolled for a same-day 1.5T or 3T MRI. PDIP-SOS MRI and QISS MRA were acquired covering the iliofemoral run-off. Two readers rated image quality (4-point scale) and graded stenosis (>=50%) on QISS-MRA without and with the visualization of calcification. Sensitivity and specificity were calculated using DSA as reference. Intra-arterial calcium was quantified using ImageJ (NIH) and compared between MRI and non-contrast CT (NCCT) using paired t-test, Pearson's correlation and Bland-Altman analysis.

RESULTS

Overall subjective image quality ratings were significantly higher for CTA compared to MRA (4.0 [3.0-4.0] and 3.0 [3.0-4.0]; p=0.0369) with good to excellent inter-reader agreement (all ICCs >0.746). The sensitivity and specificity of QISS MRA, QISS MRA with PDIP-SOS, and CTA for the detection of >=50% stenosis were 85.4%, 92.2%, 90.2% and 90.3%, 93.2%, 94.2%, respectively. Calcification was visualized by PDIP-SOS and NCCT in 123 (59.4%) and 126 (60.8%) vascular segments, respectively (p=0.2500). Quantification of calcification showed statistically significant differences between PDIP-SOS and NCCT (80.6±31.2mm3 vs 88.0±29.8mm3; p=0.0002) with high correlation (r=0.77, p<0.0001) and moderate mean of differences (-7.4mm3) between the techniques.

CONCLUSION

PDIP-SOS MRI increases the accuracy of non-contrast QISS MRA in patients evaluated for PAD. This combined protocol may prove especially useful for the comprehensive assessment of vascular anatomy prior to interventional procedure planning.

CLINICAL RELEVANCE/APPLICATION

The visualization and quantification of vascular calcification by MRI may prove especially useful for the comprehensive assessment of vascular anatomy prior to interventional procedure planning.

RC512-03 Radial Self-Navigated Native MRA in Comparison to Conventional Navigator-Gated Contrast-Enhanced MRA of the Thoracic Aorta in an Aortic Patient Collective

Wednesday, Dec. 4 9:10AM - 9:20AM Room: S503AB

Participants

Martina Roxane Correa Londono, MD, Bern, Switzerland (*Presenter*) Nothing to Disclose Verena Obmann, MD, Cleveland Heights, OH (*Abstract Co-Author*) Nothing to Disclose Nino Trussardi, Bern, Switzerland (*Abstract Co-Author*) Nothing to Disclose Davide Piccini, Erlangen, Germany (*Abstract Co-Author*) Employee, Siemens AG Michael Ith, Bern, Switzerland (*Abstract Co-Author*) Nothing to Disclose Hendrik von Tengg-Kobligk, MD, Bern, Switzerland (*Abstract Co-Author*) Research Grant, W. L. Gore & Associates, Inc Bernd Jung, Freiburg, Germany (*Abstract Co-Author*) Nothing to Disclose

For information about this presentation, contact:

martina.correa-londono@insel.ch

PURPOSE

The non-enhanced balanced steady state with free precession MRA technique has been shown to provide high diagnostic image quality of thoracic aortic disease.

METHOD AND MATERIALS

In this retrospective study, 92 patients were enrolled, 31 patients received a native MRA (mean age 63.9 years) and 61 patients a CE-MRA (mean age 63.1 years). Scan time was recorded and image quality with respect to vessel contrast, vessel sharpness and artifact level was assessed in three thoracic aortic segments: aortic root/ascending aorta, aortic arch and descending aorta. Imaging protocol: Native MRA based on an ECG-triggered self-navigated prototype 3D radial bSSFP sequence (TE=1.83 ms; TR=3.6 ms) was acquired with an inherent isotropic FOV of 250 mm and spatial resolution of 1.3 mm. A ECG-triggered first-pass CE-MRA (TE=1.33 ms; TR=3.4 ms) with navigator respiration control was acquired with a FOV of $340 \times 255 \times 83$ mm and a spatial resolution of $1.4 \times 1.3 \times 1.3$ mm with 0.1 ml/kg body weight gadobenate dimeglumine at a flow rate of 0.4 ml/s. To measure the inter-rater agreement the weighted Cohen's kappa coefficient (κ) was calculated. To assess statistical differences between the two MRA sequences, first the Fisher's Exact test and than the Mann-Whitney-U test were applied.

RESULTS

The overall diagnostic image quality of native MRA was superior at all areas analyzed, compared to the CE-MRA (p<0.001, p<0.001, p=0.005, respectively). A detailed analysis of how the presence of foreign materials like sternal cerclage or artificial heart valves deteriorates image quality for different MRA methods is of interest for future analysis. Scan time of the non CE-MRA was significantly reduced, mean 05:56 ±01:32 min vs. 08:51± 02:57 min in the CE-MRA (p<0.001).

CONCLUSION

In conclusion diagnostic image quality of the entire thoracic aorta including the aortic root can be obtained without administration of contrast media offering a benefit in potential side effects of contrast media, especially in patients with impaired renal function or by avoiding deposition of Gd in the body in general. In addition this superior image quality is gained within a faster scan time, a valuable feature in daily radiological routine.

CLINICAL RELEVANCE/APPLICATION

Superior diagnostic image quality of the entire thoracic aorta can be obtained without contrast media and within a faster scan time, a highly valuable feature in daily routine.

RC512-04 Reproducibility of High-Resolution DANTE-Prepared 3D FLASH MRI in Serial Studies of Atherosclerotic Femoral Arteries

Wednesday, Dec. 4 9:20AM - 9:30AM Room: S503AB

Participants

Yuting Wang, Chengdu, China (*Presenter*) Nothing to Disclose Xinke Liu, Beijing, China (*Abstract Co-Author*) Nothing to Disclose Henrik Haraldsson, PhD, San Francisco, CA (*Abstract Co-Author*) Nothing to Disclose Chengcheng Zhu, San Francisco, CA (*Abstract Co-Author*) Nothing to Disclose Megan Ballweber, San Francisco, CA (*Abstract Co-Author*) Nothing to Disclose Warren J. Gasper, San Francisco, CA (*Abstract Co-Author*) Nothing to Disclose David A. Saloner, PhD, San Francisco, CA (*Abstract Co-Author*) Nothing to Disclose

For information about this presentation, contact:

wangyuting_330@163.com

PURPOSE

To evaluate the reproducibility of high-resolution MR imaging of atherosclerotic femoral arteries in serial follow-up scans, and calculate the sample size needed for future longitudinal studies.

METHOD AND MATERIALS

Ten patients with known femoral artery atherosclerosis were imaged with a 3D isotropic FLASH sequence with DANTE-prepared black blood contrast. Studies were acquired at baseline, within 1 week and 1 month. Five of these patients were also scanned at 6 months. Using internal fiducials strict registration of arterial segment levels was obtained. Total vessel area, lumen area, wall area and wall volume were measured to assess atheroma in the wall. Measurements were compared among the scans repeated at different timepoints. Agreement was measured by the intraclass correlation coefficient (ICC). Measurement error was quantified by pairwise slice-based/ patient-based coefficient of variance (CV) as defined by pooled variance/mean. Sample sizes needed to detect 5% and 10% changes in vessel area/volume were calculated using 80% power and 5% significance level.

RESULTS

The measurement of vessel area, lumen area, wall area and wall volume showed excellent agreement among repeated scans, with ICCs ranging from 0.97 to 0.99 for 3 scans, and 0.96 to 0.99 for 4 scans. Relatively small interscan measurement errors were observed. The slice-based CVs for the vessel area, lumen area and wall area were 5.0%, 6.8%, 8.4%, and the patient-based CV for volume measurement was 5.9% among 3 scans. Similar results were observed for patients who had 4 scans, with above-mentioned CVs of 5.5%, 6.6%, 9.4% and 7.2% respectively. These results indicate to compare treatment efficacy for two strategies for treatment of femoral artery atherosclerosis, it would be necessary to recruit 89 subjects if differences in wall area/volume changes were 5%, and 22 subjects if the differences were 10%.

CONCLUSION

High resolution DANTE-FLASH MRI is useful for quantifying atherosclerotic vessel area and volume of femoral arteries with low variability among serial repeated scans. Volume measurement tends to be more reproducible than vessel wall area measurements.

CLINICAL RELEVANCE/APPLICATION

High resolution DANTE-FLASH MRI is useful for quantifying atherosclerotic vessel area and volume of femoral arteries, and measuring the corresponding changes due to therapeutic effects.

RC512-05 4D Flow MRA

Wednesday, Dec. 4 9:30AM - 10:00AM Room: S503AB

Participants

Shreyas S. Vasanawala, MD, PhD, Palo Alto, CA (*Presenter*) Research collaboration, General Electric Company; Consultant, Arterys Inc; Consultant, Inkspace; Research Grant, Bayer AG;

LEARNING OBJECTIVES

1) To know components required to implement clinically 4D flow. 2) To know types of clinically relevant data that can be extracted from 4D flow. 3) Become familiar with applications of 4D flow for MRA.

ABSTRACT

4D flow is a time resolved volumetric phase contrast MRI technique. This presentation will cover essential components required to implement 4D flow in a clinical setting, review types of clinically relevant data that can be extracted from 4D flow, and present several approaches to integrating 4D flow into clinical MRI protocols. Essential components include a pulse sequence and postprocessing software. Data that can be extracted includes blood flow, cardiovascular function, and anatomy. Protocols can be greatly simplified with 4D flow, enabling a decoupling of image acquisition and interpretation, thereby enhancing efficiency of patient, technologist, and radiologist time. Representative thoracic and abdominal applications will be presented.

RC512-06 Non-Contrast MRA

Wednesday, Dec. 4 10:30AM - 11:00AM Room: S503AB

Participants

Robert R. Edelman, MD, Evanston, IL (Presenter) Research support, Siemens AG; Royalties, Siemens AG

For information about this presentation, contact:

redelman999@gmail.com

LEARNING OBJECTIVES

1) Explore rationale for non-contrast MR angiography. 2) Discuss techniques for optimized non-contrast MR-based vascular imaging in clinical practice, including advantages and limitations. 3) Review current evidence for clinical utility in comparison to contrast-enhanced MRA and CT angiography.

ABSTRACT

Non-contrast MRA techniques offer a viable alternative to CTA and contrast-enhanced MRA (CEMRA) for cross-sectional vascular imaging without the risks or costs associated with contrast agent administration. They can evaluate the renal and peripheral arteries with image quality and accuracy that is competitive with CTA. Recently developed non-contrast neurovascular imaging techniques can substantially outperform legacy 2D and 3D time-of-flight MRA, providing image quality that approaches that of CEMRA. In addition to the use of non-contrast MRA for depiction of the vascular lumen, high-resolution non-Cartesian 3D MRI can now show vessel wall calcifications comparably to CT. This information (hitherto unavailable using MRI) can be critical to the planning of interventional vascular procedures. The anatomic information provided by non-contrast MRA can also be efficiently complemented with hemodynamic information that is not available from CTA using phase contrast and ASL-based approaches.

RC512-07 Free-Breathing Fast Low-Angle Shot Quiescent-Interval Slice-Selective MR Angiography for Improved Detection of Vascular Stenoses in the Pelvis and Abdomen

Wednesday, Dec. 4 11:00AM - 11:10AM Room: S503AB

Participants

Akos Varga-Szemes, MD, PhD, Charleston, SC (*Presenter*) Research Grant and Travel Support, Siemens AG Research Consultant, Elucid Bioimaging

Emily A. Aherne, MBBCh, FFR(RCSI), New York, NY (Abstract Co-Author) Nothing to Disclose

U. Joseph Schoepf, MD, Charleston, SC (*Abstract Co-Author*) Research Grant, Astellas Group; Research Grant, Bayer AG; Research Grant, Bracco Group; Research Grant, Siemens AG; Research Grant, Heartflow, Inc; Research support, Bayer AG; Consultant, Elucid BioImaging Inc; Research Grant, Guerbet SA; Consultant, HeartFlow, Inc; Consultant, Bayer AG; Consultant, Siemens AG; ; ; Thomas M. Todoran, MD, Charleston, SC (*Abstract Co-Author*) Research Consultant, Medtronic plc; Research Consultant, General Electric Company

Ioannis Koktzoglou, PhD, Evanston, IL (Abstract Co-Author) Research support, Siemens AG

Robert R. Edelman, MD, Evanston, IL (Abstract Co-Author) Research support, Siemens AG; Royalties, Siemens AG

For information about this presentation, contact:

redelman999@gmail.com

PURPOSE

Balanced steady-state free precession (bSSFP)-based quiescent-interval slice-selective (QISS) magnetic resonance angiography (MRA) is accurate for the non-contrast evaluation of peripheral artery disease (PAD); however, drawbacks include the need for breath-holding and sensitivity to off-resonance artifacts. The purpose of this study was to evaluate the image quality and diagnostic accuracy in the pelvis and abdomen of free-breathing fast low-angle shot (FLASH)-based QISS techniques in comparison to standard QISS in patients with PAD, using computed tomographic angiography (CTA) as the reference.

METHOD AND MATERIALS

Twenty-seven patients (69±10 years, 17 men) with PAD were enrolled in this IRB approved, HIPAA compliant prospective study between April and December 2018. Patients underwent non-contrast MRA using standard bSSFP-based QISS and prototype free-breathing radial-FLASH and Cartesian-FLASH-based QISS at 3T. A subset of patients (n=22) also underwent CTA as the reference standard. Nine arterial segments per patient were evaluated spanning the abdomen, pelvis, and upper thigh regions. Objective (signal intensity ratio (SIR) and relative standard deviation (SD)) and subjective image quality (4-point scale) and stenosis (>50%) were evaluated by two readers and compared using one-way analysis of variance, Wilcoxon and McNemar tests, respectively.

RESULTS

A total of 179 vascular segments were available for analysis by all QISS techniques. No significant difference was observed among bSSFP, radial-FLASH, and Cartesian-FLASH-based techniques in SIR (p=0.428) and relative SD (p=0.220). Radial-FLASH-based QISS demonstrated the best image quality (p<0.0001) and the highest inter-reader agreement ($\kappa=0.721$). The sensitivity values of bSSFP, radial-FLASH, and Cartesian-FLASH-based QISS for the detection of >50% stenosis were 76.0%, 84.0%, and 80.0%, respectively, while specificity values were 97.6%, 94.0%, and 92.8%, respectively. Moreover, FLASH-based QISS consistently reduced off-resonance artifacts compared to the bSSFP-based approach.

CONCLUSION

Free-breathing FLASH-based QISS MRA techniques provide improved image quality and sensitivity, high specificity, and reduced offresonance artifacts for vascular stenosis detection in the abdomen and pelvis.

CLINICAL RELEVANCE/APPLICATION

FLASH-based QISS MRA provides improved image quality, accuracy and reduced off-resonance artifacts, thereby enhancing the utility of QISS for the non-contrast evaluation of PAD.

RC512-08 Advanced Fresh Blood Imaging (FBI) Using Centric ky-kz Trajectory with a New Exponential

Refocusing Flop Angle

Wednesday, Dec. 4 11:10AM - 11:20AM Room: S503AB

Participants

Mitsue Miyazaki, PhD, La Jolla, CA (*Presenter*) Employee, Canon Medical Systems Corporation Masaaki Umeda, Otawara, Japan (*Abstract Co-Author*) Employee, Canon Medical Systems Corporation Yoshimori Kassai, MS, Otawara, Japan (*Abstract Co-Author*) Employee, Canon Medical Systems Corporation Lijun Zhang, Beijing, China (*Abstract Co-Author*) Employee, Canon Medical Systems Corporation Cheng Ouyang, La Jolla, CA (*Abstract Co-Author*) Nothing to Disclose Sheronda Statum, La Jolla, CA (*Abstract Co-Author*) Nothing to Disclose Won C. Bae, PhD, La Jolla, CA (*Abstract Co-Author*) Nothing to Disclose Katsumi Nakamura, MD, Kitakyushu, Japan (*Abstract Co-Author*) Nothing to Disclose Christine B. Chung, MD, Solana Beach, CA (*Abstract Co-Author*) Nothing to Disclose

For information about this presentation, contact:

mimiyazaki@ucsd.edu

PURPOSE

To advance fresh blood imaging (FBI) in peripheral non-contrast MR angiography (NC-MRA) using a new centric ky-kz trajectory with an exponential flop angle to reduce specific absorption rate (SAR) and tremendous reduction in scan time.

METHOD AND MATERIALS

FBI utilizes a physiological signal difference between systolic and diastolic triggered images. The centric ky-kz trajectory is implemented in FBI (cFBI), acquiring multiple slice-encodings (SEs) and phase-encodings (PEs) per TR; whereas, standard FBI acquires one SE per TR. By applying exponential flop angle (eFA), cFBI enables reduction of SAR. The design of eFA has high flop angles (Hflop) at the center of k space (about 36 lines or more) for bright blood imaging and exponentially decreasing flop angles at periphery of k space to reduce SAR. Having about 36-line Hflop of 180 deg is required to ensure depiction of bright blood; imaging of cFBI was performed maintaining Hflop and varying low flop angles (Lflop), Hflop/Lflop of 180/180, 180/90, 180/60, 180/30 and 180/1 deg. Parameters are: for all lower flop <180 (TR of 2RR intervals) and constant (180/180) flop (TR of 3RR intervals due to SAR), TEeff of 60 ms, 1NAQ, 320x320 matrix, 100 1.4-mm slices, FOV of 40x40 cm, parallel imaging of 3, and resolution of 0.63(PE)x0.63(RO)x 0.7(SE) mm after interpolation. All exteriments were performed using a 3T clinical system on healthy volunteers (5 males, 24-68 yo).

RESULTS

The scan time of cFBI was reduced to about 1/2 to 1/3 (1:30-2:00 min) by acquiring multiple SEs and PEs data compared to standard FBI. The Hflop/Lflop of 180/180 deg. causes lengthen of TR due to high SAR and longer scan time. Regarding artifacts, standard FBI often causes N/2 artifacts in the PE direction that degrade image quality; whereas, cFBI minimizes N/2 artifacts. As shown in Fig. 1, image quality of all 5 images was evaluated all 'excellent' without any N/2 artifacts.

CONCLUSION

Advanced cFBI with eFA enables high resolution quality NC-MRA images with fast acquisition without major artifacts like N/2 artifacts. Compared to standard FBI, cFBI reduces the scan time to 1/3 to 1/2, opening a possibility of scanning entire peripheral vasculature in 5 to 6 mins.

CLINICAL RELEVANCE/APPLICATION

This study demonstrates tremendous scan time reduction in centric ky-kz FBI (cFBI) with eFA compared to standard FBI. This advanced cFBI enables obtaining quality NC-MRA images without N/2 artifacts seen in standard FBI.

RC512-09 Low-Dose Contrast-Enhanced MR Angiography of the Lower Extremities at 3T with Dynamic 3 Station Imaging

Wednesday, Dec. 4 11:20AM - 11:30AM Room: S503AB

Participants

Guenther K. Schneider, MD, PhD, Homburg, Germany (*Abstract Co-Author*) Research Grant, Siemens AG; Speakers Bureau, Siemens AG; Speakers Bureau, Bracco Group; Research Grant, Bracco Group;

Tobias Woerner, MD, Homburg, Germany (Presenter) Nothing to Disclose

Arno Buecker, MD, Homburg, Germany (*Abstract Co-Author*) Consultant, Bracco Group Speaker, Bracco Group Consultant, Medtronic plc Speaker, Medtronic plc Research Grant, Novartis AG Research Grant, GlaxoSmithKline plc Research Grant, Biotest AG Research Grant, OncoGenex Pharmaceuticals, Inc Research Grant, Bristol-Myers Squibb Company Research Grant, Eli Lilly & Company Research Grant, Pfizer Inc Research Grant, F. Hoffmann-La Roche Ltd Research Grant, sanofi-aventis Group Research Grant, Merrimack Pharmaceuticals, Inc Research Grant, Sirtex Medical Ltd Research Grant, Concordia Healthcare Corp Research Grant, AbbVie Inc Research Grant, Takeda Pharmaceutical Company Limited Research Grant, Merck & Co, Inc Research Grant, Affimed NV Research Grant, Bayer AG Research Grant, Johnson & Johnson Research Grant, Seattle Genetics, Inc Research Grant, Onyx Pharmaceuticals, Inc Research Grant, Synta Pharmaceuticals Corp Research Grant, Siemens AG Research Grant, iSYMED GmbH Research Grant, Abbott Laboratories Co-founder, Aachen Resonance GmbH

Paul S. Raczeck, MD, Homburg, Germany (Abstract Co-Author) Nothing to Disclose

For information about this presentation, contact:

dr.guenther.schneider@uks.eu

PURPOSE

In our study we evaluated the diagnostic performance of lower extremity MR Angiography in patients with suspected lower limb atherosclerotic disease using a three-station dynamic MRA approach.

METHOD AND MATERIALS

10 consecutive adult nations perceptating diagnostic imaging of the lower limb arteries for suspected athemscleratic disease

underwent MRA at 3 T. Imaging was performed by acquiring a three-station dynamic MRA using a TWIST-sequence. For each station a 3ml contrast medium bolus (Gd-HP-DO3A / Prohance) was injected (1.5ml/sec) each followed by a 20 ml saline flush. Images were retrospectively reviewed and evaluated with regard to image quality and visualization of arterial segments; severity of stenosis; and presence of venous contamination. 16 patients underwent subsequent DSA yielding 256 artery segments for correlation between MRI and DSA.

RESULTS

Dynamic three station low dose CE-MRA at 3T allows for diagnostic, dynamic imaging in every vessel territory of the lower limb even in patients with advanced arteriosclerotic disease. Diagnostic performance based on the vessel segments both evaluated by CE MRA and DSA for > 50 % stenosis demonstrated a sensitivity of 93.55% [84.3 -98.2% (95%-CI)] and specifity of 98.51% [95.7-99.8%(95%-CI)] for CE-MRA; For vessel occlusion sensitivity was 93.1% [77.23 -99.15 % (95%-CI] and specifity of 99.13% [96.91 - 99.89%](95%-CI)]. No studies were rated non-diagnostic due to venous overlay, since always an optimal 3D-dataset from dynamic imaging could be chosen.

CONCLUSION

With a total of only 9 ml ProHance (corresponding to 0.05 mmol/kg BW in a 90 kg patient resp. 0.06 mmol/kg in a 75 kg patient) three station dynamic CE MRA of the lower extremity is possible.Advantages of this approach include the possibility to look at the optimal time of arterial enhancement of each leg separately and the possibility of avoiding venous contamination of images. Time for each dataset typically is approximately 5 sec. to allow for a high enough spatial resolution, nevertheless this temporal resolution is enough to achieve a solely arterial image.

CLINICAL RELEVANCE/APPLICATION

Regarding the discussion on safety of Gd-based contrast agents the lowest possible dose should be used in any indication for CE MRI. Our study shows the feasibility of low dose CE MRA with a macrocyclic contrast agent only using a total of 9 ml of a 0.5 M contrast agent for the evaluation of the complete run-off vessels.

RC512-10 Phase Contrast MRA: Technology Advances and Impact of High Performance Gradients

Wednesday, Dec. 4 11:30AM - 12:00PM Room: S503AB

Participants

Thomas K. Foo, PhD, Niskayuna, NY (Presenter) Employee, General Electric Company

For information about this presentation, contact:

thomas.foo@ge.com

LEARNING OBJECTIVES

1) To know the impact on gradient performance on phase-contrast velocity imaging 2) To know how phase-velocity noise, vascular signal-to-noise ratio, and sequence echo time (TE) impacts the measurement of flow volume 3) To know how high-performance gradients with 3-4x the maximum gradient amplitude and 2.5-4.0x the maximum slew rate impacts phase-contrast MRA and 4D Flow.

ABSTRACT

With increasing capability in gradient amplitude to 80 mT/m, the echo time (TE) can be reduced. However, in whole-body systems, there is still a limitation of peripheral nerve stimulation as to how fast the gradient amplitudes can be switched. With the development of new high-performance head-only gradient systems, maximum gradient amplitudes of 3-4x and maximum slew rates of 2.5-4.0x can be achieved. This benefits phase-contrast MRA, especially for low-velocity encoding values (VENC) for slow flow, as in the CSF.







BI-RADS Interactive Challenge (Interactive Session)

Wednesday, Dec. 4 8:30AM - 10:00AM Room: E451A



AMA PRA Category 1 Credits ™: 1.50 ARRT Category A+ Credit: 1.75

Participants

Carol H. Lee, MD, Guilford, CT (Moderator) Nothing to Disclose

For information about this presentation, contact:

zuleyml@upmc.edu

Special Information

This interactive session will use RSNA Diagnosis Live™. Please bring your charged mobile wireless device (phone, tablet or laptop) to participate.

LEARNING OBJECTIVES

1) Identify cases for which the BI-RADS assessment may be unclear. 2) Apply the appropriate BI-RADS descriptors and categories to breast imaging studies.

Sub-Events

RC515A Mammography

Participants Carol H. Lee, MD, Guilford, CT (*Presenter*) Nothing to Disclose

LEARNING OBJECTIVES

1) Identify areas of confusion in applying BI-RADS to mammograms. 2) Assess instances of inappropriate BI-RADS assessment to mammograms. 3) Apply appropriate descriptors and assessment categories to mammograms.

RC515B Ultrasound

Participants

Paula B. Gordon, MD, Vancouver, BC (*Presenter*) Stockholder, OncoGenex Pharmaceuticals, Inc ; Stockholder, Volpara Health Technologies Limited; Scientific Advisory Board, Real Imaging Ltd; Scientific Advisory Board, DenseBreast-info, Inc; Scientific Advisor, Dense Breasts Canada

LEARNING OBJECTIVES

1) Show interesting cases that include ultrasound images will be shown; audience participation will be invited.

RC515C MRI

Participants Wendy B. Demartini, MD, Stanford, CA (*Presenter*) Nothing to Disclose

LEARNING OBJECTIVES

1) Recognize and describe clinically relevant findings. 2) Apply appropriate assessment categories. 3) Use interpretation strategies that improve diagnostic performance.







Metabolic Tumor Imaging: Current and Beyond

Wednesday, Dec. 4 8:30AM - 10:00AM Room: S501ABC



AMA PRA Category 1 Credits ™: 1.50 ARRT Category A+ Credit: 1.75

FDA Discussions may include off-label uses.

Participants

Marius E. Mayerhoefer, MD, PhD, Vienna, Austria (Moderator) Speaker, Siemens AG; Research support, Siemens AG

For information about this presentation, contact:

marius.mayerhoefer@meduniwien.ac.at

LEARNING OBJECTIVES

Learn about he new PET tracers and they new potential clinical applications.
 Review the added value of PET/MRI in oncology.
 Learn about the current and future applications of hyperpolarised MRI.

Sub-Events

RC518A PET Tracers: Which Ones Will Be Next to Make it to Clinical Practice?

Participants

Jan Grimm, MD, PhD, New York, NY (Presenter) Nothing to Disclose

LEARNING OBJECTIVES

1) To have an appreciation for some of the latest PET tracers in clinical research in oncology. 2) Understand the PET and radiotherapy agents currently FDA approved and those undergoing the approval process. 3) Understand the next generation of PET tracers and molecular imaging agents that could be the next standard-of-care imaging probes.

RC518B PET/MRI: The Added Value in Oncology

Participants

Hebert Alberto Vargas, MD, Cambridge, United Kingdom (Presenter) Nothing to Disclose

LEARNING OBJECTIVES

1) To understand the concept of value in imaging and how it relates to PET/MR technology. 2) To discuss the need for research specifically geared toward assessing the value of PET/MRI in oncology.

RC518C Hyperpolarized MRI: Current and Future Applications

Participants

Ferdia A. Gallagher, PhD, FRCR, Cambridge, United Kingdom (*Presenter*) Research support, General Electric Company; Research support, GlaxoSmithKline plc

For information about this presentation, contact:

fag1000@cam.ac.uk

LEARNING OBJECTIVES

1) To explore the role of metabolism in cancer development. 2) To understand how these changes in metabolism can be exploited using hyperpolarized 13C-pyruvate. 3) To review the current evidence for hyperpolarized carbon-13 imaging in oncology. 4) To understand potential clinical applications for hyperpolarized carbon-13 imaging. 5) To consider the role of new hyperpolarized molecules in oncology.

ABSTRACT

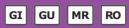
There is increasing evidence to support a role for metabolism in tumor development; for example, deregulation of cellular energetics is now considered to be one of the key hallmarks of cancer. Changes in tumor metabolism over time are now known to be early biomarkers of successful response to chemotherapy and radiotherapy. There are a number of imaging methods that have been used to probe cancer metabolism: the most widely available is 18F-fluorodeoxyglucose (FDG), an analogue of glucose, used in PET. Hyperpolarized carbon-13 MRI (13C-MRI) is an emerging molecular imaging technique for studying cellular metabolism, particularly in the field of oncology. This method allows non-invasive measurements of tissue metabolism in real-time. To date, the most promising probe used in conjunction with hyperpolarized MRI has been 13C-labelled pyruvate: pyruvate is metabolized into lactate in normal tissue in the absence of oxygen, but in tumors this occurs very rapidly even in the presence of oxygen. Results from many animal models have shown that there is a reduction in the metabolism of pyruvate following successful treatment with chemotherapy. Tumor lactate labelling has also been shown to correlate with the grade of some tumor types. There are now a small number of sites performing human hyperpolarized carbon-13 MRI imaging. This talk will discuss the progress that has been made in this field within the area of oncology and potential clinical applications.





MR Image Guidance Radiotherapy

Wednesday, Dec. 4 8:30AM - 10:00AM Room: E353A



AMA PRA Category 1 Credits ™: 1.50 ARRT Category A+ Credit: 1.75

FDA Discussions may include off-label uses.

Participants

Kathryn J. Fowler, MD, San Diego, CA (*Moderator*) Consultant, 12 Sigma Technologies; Researcher, Nuance Communications, Inc; Contractor, Midamerica Transplant Services; ;

For information about this presentation, contact:

k1fowler@ucsd.edu

LEARNING OBJECTIVES

1) Review MR imaging staging for gynecological cancers. 2) Discuss acquisition parameters and recommended sequences for evaluation. 3) Evaluate techniques for evaluating treatment response. 4) Emerging techniques. 5) Recognize the role of MR guided SBRT for borderline resectable and locally advanced pancreas tumors. 6) Recognize the role of MR guided SBRT for intra-abdominal oligometastatic tumors. 7) Identify adaptive workflow strategies to increase physician utilization and clinic efficiency. 8) Identify why MRI-guided radiation therapy has the potential to improve treatment outcomes in the management of pelvic malignancies. 9) Differentiate between rules for safe dose escalation during non-adaptive stereotactic body radiation therapy (SBRT) versus adaptive MRI-guided SBRT. 10) Develop an MRI-guided adaptive treatment flow for the management of cervical cancer. 11) recognize the unique challenges of implementing MRI-guided radiation therapy workflows. 12) develop procedures for safe and efficient delivery of online adaptive radiation therapy. 13) understand the common sources of dosimetric errors in MRI-guided radiation therapy.

Sub-Events

RC520A MR Imaging Requirements for Gastrointestinal/Gynecological Tumors

Participants

Rebecca Rakow-Penner, MD, PhD, San Diego, CA (Presenter) Research Grant, General Electric Company

For information about this presentation, contact:

rrakowpenner@ucsd.edu

LEARNING OBJECTIVES

1) Review MR imaging staging for gynecological cancers. 2) Discuss acquisition parameters and recommended sequences for evaluation. 3) Evaluate techniques for evaluating treatment response. 4) Emerging techniques.

RC520B Role of MR-guided RT for Abdominal Tumors

Participants

Hyun Kim, MD, Saint Louis, MO (*Presenter*) Research Grant and Speakers Bureau, Varian Medical Systems, Inc; Research Grant and Speakers Bureau, ViewRay, Inc

For information about this presentation, contact:

kim.hyun@wustl.edu

LEARNING OBJECTIVES

1) Recognize the role of MR guided SBRT for borderline resectable and locally advanced pancreas tumors. 2) Recognize the role of MR guided SBRT for intra-abdominal oligometastatic tumors. 3) Identify adaptive workflow strategies to increase physician utilization and clinic efficiency.

RC520C Role of MR-guided RT for Pelvic Tumors

Participants

Lorraine Portelance, MD, Miami, FL (*Presenter*) Advisory Committee, Sirtex Medical Ltd; Advisory Board, BTG International Ltd; Moderator, ViewRay, Inc

For information about this presentation, contact:

lportelance@med.miami.edu

LEARNING OBJECTIVES

1) Identify why MRI-guided radiation therapy has the potential to improve treatment outcomes in the management of pelvic malignancies. 2) Differentiate between rules for safe dose escalation during non-adaptive stereotactic body radiation therapy

(SBRT) versus adaptive MRI-guided SBRT. 3) Develop an MRI-guided adaptive treatment flow for the management of cervical cancer.

RC520D Practical Aspects and Workflow for MR-guided Radiotherapy

Participants

Olga Green, PhD, St. Louis, MO (Presenter) Speaker, ViewRay, Inc

For information about this presentation, contact:

ogreen@wustl.edu

LEARNING OBJECTIVES

1) recognize the unique challenges of implementing MRI-guided radiation therapy workflows. 2) develop procedures for safe and efficient delivery of online adaptive radiation therapy. 3) understand the common sources of dosimetric errors in MRI-guided radiation therapy.





Practical Aspects of MR

Wednesday, Dec. 4 8:30AM - 10:00AM Room: E351



AMA PRA Category 1 Credits ™: 1.50 ARRT Category A+ Credit: 1.75

FDA Discussions may include off-label uses.

Participants

Matthew A. Bernstein, PhD, Rochester, MN (Coordinator) Former Employee, General Electric Company

LEARNING OBJECTIVES

1) Understand basic aspects of MR Safety in the clinical environment, including how to avoid projectile incidents and manage patients with implanted devices. Understand the differences between MR Safe, MR Conditional, and MR Unsafe. 2) Understand the origin of MR artifacts that commonly occur in clinical practice. Acquire techniques to reduce or eliminate these artifacts. 3) Understand the basics of MR Siting and Acceptance testing. Review environmental factors such as vibration and moving metal. Review tests that can be performed after the MRI system is installed to verify its proper operation.

Sub-Events

RC521A MR Safety

Participants Robert E. Watson JR, MD, PhD, Rochester, MN (*Presenter*) Nothing to Disclose

For information about this presentation, contact:

Watson.robert16@mayo.edu

LEARNING OBJECTIVES

1) Provide a general framework about essential elements of MR safety, to include a) risks associated with the main magnetic field, radiofrequency field, and time varying gradient fields; b) MRI zones I, II, III, IV; c) MRI safe, MRI conditional, and MRI unsafe device labeling; d) Quenches; e) Patient screening and ferromagnetic detection; and f) management of patients with implanted devices.

RC521B MR Artifacts and How to Solve Them

Participants

Xiaohong J. Zhou, PhD, Chicago, IL (*Presenter*) Owner, Medical Physics Services; Consultant, Horizon Medical Physics Services; Consultant, General Electric Company; Consultant, Rush University; Advisor, Chinese Academy of Sciences; Consultant, Chinese Academy of Sciences; Reviewer, American College of Radiology; Royalties, Reed Elsevier

For information about this presentation, contact:

xjzhou@uic.edu

LEARNING OBJECTIVES

1) Recognize common artifacts in MR images. 2) Understand the root cause of the artifacts. 3) Describe the strategies to reduce or remove the artifacts.

RC521C MR Site Planning and Acceptance Testing

Participants

Lisa C. Lemen, PhD, Cincinnati, OH (Presenter) Consultant, General Electric Company; Consultant, Johnson & Johnson

LEARNING OBJECTIVES

1) Describe environmental factors which may impact the site selection or planning, including potential sources of vibration and moving metal. 2) Review a preliminary site layout for potential problems, including necessary support areas and access routes. 3) List environmental and system tests that can be performed after the MRI system is installed to verify its proper operation.





Protocol Optimization and Artifacts in MRI (Interactive Session)

Wednesday, Dec. 4 8:30AM - 10:00AM Room: N227B

MR

AMA PRA Category 1 Credits ™: 1.50 ARRT Category A+ Credit: 1.75

Sub-Events

RC529A How to Build an Efficient MRI Workflow

Participants

Steven S. Raman, MD, Santa Monica, CA (*Presenter*) Consultant, Johnson & Johnson; Consultant, Bayer AG; Consultant, Merck & Co, Inc; Consultant, Amgen Inc; Consultant, Profound Medical Inc

LEARNING OBJECTIVES

1) Understand the components of an MRI workflow Understand customer needs. 2) Develop a culture of quality. 3) Develop a culture of ongoing disruption. 4) Develop feedback loops to improve quality of key personnel. 5) Develop ongoing PQI metrics.

ABSTRACT

In this talk, we will discuss how to develop an innovative, efficient and flexible MRI workflow that maximizes image quality, mimizes imaging time, improves technologist performance, develops a culture of quality and innovation, and improves the patient and referring physician experience.

RC529B Optimized Abdominal MRI Protocol

Participants

Scott B. Reeder, MD, PhD, Madison, WI (Presenter) Nothing to Disclose

LEARNING OBJECTIVES

1) Understand emerging strategies for optimized liver MRI protocols.2) Describe at least three examples of optimized liver MRI protocols.3) Be familiar with the challenges with implementing liver MRI protocols.

RC529C Optimized Prostate MRI Protocol

Participants

Aytekin Oto, MD, Chicago, IL (*Presenter*) Research Grant, Koninklijke Philips NV; Research Grant, Guerbet SA; Research Grant, Profound Medical Inc; Medical Advisory Board, Profound Medical Inc; Consultant, AbbVie Inc; ; ;

For information about this presentation, contact:

oto@uchicago.edu

LEARNING OBJECTIVES

1) Review the critical sequences of multi-parametric prostate MR protocol and their added values to the interpretation. 2) Illustrate the impact of different technical approaches on image quality of different sequences. 3) Provide different options for optimized prostate MR protocol.

RC529D Optimized Female Pelvis MRI Protocol

Participants

Stephanie Nougaret, MD, Montpellier, France (Presenter) Nothing to Disclose

LEARNING OBJECTIVES

1) To discuss the technical and practical requirements for optimizing female pelvis MRI. 2) To become familiar with the optimal female pelvis MRI protocols. 3) To discuss the recent technological innovations in MR female pelvis imaging.

RC529E Top 10 MRI Artifacts

Participants

Mustafa R. Bashir, MD, Cary, NC (*Presenter*) Research Grant, Siemens AG; Research Grant, General Electric Company; Research Grant, NGM Biopharmaceuticals; Research Grant, Madrigal Pharmaceuticals, Inc; Research Grant, Metacrine, Inc; Research Grant, Pinnacle Clinical Research; Research Grant, ProSciento Inc; Research Consultant, RadMD

LEARNING OBJECTIVES

1) To describe common artifacts in body MRI and strategies to mitigate them.

ABSTRACT

Artifacts are unavoidable in abdominal MRI. As pressure mounts to use shorter, more time-efficient protocols, fewer redundant sequences are available in a typical MRI protocol, and the diagnostic impact of artifacts may be increased. This discussion will

focus on common artifacts encountered in clinical practice and methods to minimize their effects on diagnostic interpretation. Printed on: 01/07/20







VW 27

A Practical Approach to Breast Magnetic Resonance Imaging (MRI) Interpretation: An Interactive Session: Presented by Siemens Healthineers

Wednesday, Dec. 4 10:15AM - 11:25AM Room: North Building, Booth 8563

Participants

Susan Weinstein, MD, Philadelphia, PA (Presenter) Nothing to Disclose

Program Information

This interactive session will include both didactic and hands-on case review at workstations equipped with *syngo*. MR Brevis. A practical approach to breast MRI interpretation will be discussed as well as utilizing the available sequences and techniques to improve interpretive skills. *RSVP is required; adding this session to your agenda does not secure your seat in this session. Click the link below to RSVP.*

RSVP

https://www.fairorg.de/Siemens-Healthineers/portal/workshop.cfm/rsna19/







MSRO42

BOOST: Lymphoma-Case-based Multidisciplinary Review (Interactive Session)

Wednesday, Dec. 4 10:30AM - 12:00PM Room: S103CD



AMA PRA Category 1 Credits ™: 1.50 ARRT Category A+ Credit: 1.75

Participants

Chelsea C. Pinnix, MD, PhD, Houston, TX (*Moderator*) Research Grant, Merck & Co, Inc; Consultant, Global One Inc; Speaker, International Journal of Radiation Oncology, Biology & Physics Jurgen Rademaker, MD, New York, NY (*Presenter*) Nothing to Disclose Yolanda D. Tseng, MD, Seattle, WA (*Presenter*) Nothing to Disclose

LEARNING OBJECTIVES

1) Case-based review of staging and treatment response in lymphoma. 2) Discuss imaging findings in lymphoma and their clinical significance (PET, CT, MRI). 3) Describe the management of patients with lymphoma, including the role of imaging and radiation treatment options.

ABSTRACT

Management of lymphoma continues to evolve in the setting of improved imaging, pathologic understanding of this heterogeneous disease, systemic therapy, and radiotherapy techniques. This interactive, multi-disciplinary session is geared to general radiologists and radiation oncologists with the goal to provide clinically relevant, up-to-date knowledge and skills in evaluating and treating these patients. Through cases, we will review common manifestations of Hodgkin and non-Hodgkin lymphoma and imaging features of these lymphomas that are important for workup, staging, and assessment of treatment response. Cases will be used to walk participants through the management of common lymphomas with a focus on the role of radiotherapy.





SPAI41

RSNA AI Deep Learning Lab: Segmentation

Wednesday, Dec. 4 10:30AM - 12:00PM Room: AI Showcase, North Building, Level 2, Booth 10342



AMA PRA Category 1 Credits ™: 1.50 ARRT Category A+ Credit: 1.75

Participants

George L. Shih, MD, New York, NY (*Presenter*) Consultant, Image Safely, Inc; Stockholder, Image Safely, Inc; Consultant, MD.ai, Inc; Stockholder, MD.ai, Inc;

Special Information

In order to get the best experience for this session, it is highly recommended that attendees bring a laptop with a keyboard, a decent-sized screen, and the latest version of Google Chrome. Additionally, it is recommended that attendees have a basic knowledge of deep learning programming and some experience running a Google CoLab notebook. Having a Gmail account is also helpful. Here are instructions for creating and deleting a Gmail account.

ABSTRACT

This session will focus on the use of deep learning methods for image segmentation, applied to the challenge of CT or MR brain segmentation. While focused on this particular problem, the concepts should generalize to other organs and image types.





SSK16

Neuroradiology (Movement Disorders)

Wednesday, Dec. 4 10:30AM - 12:00PM Room: S401CD



AMA PRA Category 1 Credits ™: 1.50 ARRT Category A+ Credit: 1.75

FDA Discussions may include off-label uses.

Participants

Seung-Koo Lee, MD, PhD, Seoul, Korea, Republic Of (*Moderator*) Nothing to Disclose Jody L. Tanabe, MD, Aurora, CO (*Moderator*) Invited participant, GE Signa Masters 2019 Neuro Summit, General Electric Company Michael M. Zeineh, PhD, MD, Stanford, CA (*Moderator*) Research funded, General Electric Company;

Sub-Events

SSK16-01 Bi-Modality MRI Radiomics Features in Identifying Parkinson's Disease and Its Clinical Subtypes

Wednesday, Dec. 4 10:30AM - 10:40AM Room: S401CD

Participants

Xiaojun Guan, Hangzhou, China (Presenter) Nothing to Disclose Tao Guo, Hangzhou, China (Abstract Co-Author) Nothing to Disclose Cheng Zhou, Hangzhou, China (Abstract Co-Author) Nothing to Disclose Ting Gao, Hangzhou , China (Abstract Co-Author) Nothing to Disclose Victor Han, Berkeley, CA (Abstract Co-Author) Nothing to Disclose Steven Cao, Berkeley, CA (Abstract Co-Author) Nothing to Disclose Chunlei Liu, Berkeley, CA (Abstract Co-Author) Nothing to Disclose Hongjiang Wei, Shanghai, China (Abstract Co-Author) Nothing to Disclose Yuyao Zhang, Shanghai, China (Abstract Co-Author) Nothing to Disclose Min Xuan, Hangzhou, China (Abstract Co-Author) Nothing to Disclose Quanquan Gu, MD, PhD, Hangzhou, China (Abstract Co-Author) Nothing to Disclose Jingjing Wu, Hangzhou, China (Abstract Co-Author) Nothing to Disclose Peiyu Huang, Hangzhou, China (Abstract Co-Author) Nothing to Disclose Jia L. Pu, Hangzhou, China (Abstract Co-Author) Nothing to Disclose Baorong Zhang, Hangzhou, China (Abstract Co-Author) Nothing to Disclose Xiaojun Xu, Hangzhou, China (Abstract Co-Author) Nothing to Disclose Minming Zhang, Hangzhou, China (Abstract Co-Author) Nothing to Disclose

For information about this presentation, contact:

xiaojunguan1102@zju.edu.cn

PURPOSE

Due to lacking of objective biomarkers, it remains a big challenge to reach a good diagnosis for Parkinson's disease (PD). Thus, we hypothesized that, in combination with radiomics and machine-learning methods, MRI-based iron quantification and structure measurement might contribute to constructing imaging biomarker.

METHOD AND MATERIALS

245 PD patients and 170 normal controls were finally included in data analysis. All of them underwent ESWAN and high-resolution 3D T1-weighted imaging scanning. Quantitative susceptibility mapping (QSM) and R2* were processed from ESWAN data. Based on newly created age-specific QSM template, symmetrical registration technology (ANTs) was used to obtain subcortex segmentations in the individual QSM and R2* space. FSL-FIRST and ANTs-CorticalThickness methods were used to segment subcortical and cortical regions respectively. Radiomics features including histogram and GLCM features in QSM, R2* and T1 images were obtained from the segmented subcortical regions. Normalized cortical features including thickness, volume, mass and surface area were calculated. In summary, 1408 radiomics features were obtained. Random Forest (RF) algorithm was used to perform feature selection with 1000 permutation and top-20 features were selected.By inputting these top-20 features, RF classifier was constructed to classify different PD subtypes and normal controls with 1000 iterations for each test.

RESULTS

We observed that the obtained 20 features, where the mean QSM signal of bilateral substantia nigra (SN) occupied the top 2 features (the impotence were 100% for left SN and 84% for right SN), had good generalization. In the classification between PD patients and normal controls, the accuracy was 81.3%, while it was 77.4% for early PD and 81.2% for late PD. The performance to identify different motor subtypes were both 79.9%. Besides, we identically subdivided PD patients into 4 classes according to an ascending rank of UPDRS scores, and the diagnostic accuracies were 79.3%, 80.2%, 80.1% and 85% from early to late stages.

CONCLUSION

Radiomics features calculated from iron and structure images could reach a good performance of PD diagnosis. By feature selection, we confirmed that nigral iron content (mean signal) is the most important feature for PD.

CLINICAL RELEVANCE/APPLICATION

Radiomics features calculated on brain iron and structural images have good generalization ability to diagnose PD with acceptable accuracy.

SSK16-02 Diagnostic Accuracy of the Magnetic Resonance Parkinsonism Index and Midbrain-to-Pons Ratio in Differentiating Progressive Supranuclear Palsy from Parkinson's Disease and Controls

Wednesday, Dec. 4 10:40AM - 10:50AM Room: S401CD

Participants

Aman Snehil, MBBS, Mumbai, India (*Abstract Co-Author*) Nothing to Disclose Ritu M. Kakkar, MBBS, DMRD, Mumbai, India (*Abstract Co-Author*) Nothing to Disclose Shrinivas B. Desai, MD, Mumbai, India (*Presenter*) Nothing to Disclose

For information about this presentation, contact:

riturupesh@gmail.com

PURPOSE

To compare the efficacy of MRPI and M/P ratio in the diagnosis and differentiation of Progressive Supranuclear Palsy from Parkinson's disease and Controls.

METHOD AND MATERIALS

40 consecutive patients were enrolled in this study, satisfying the diagnostic criteria by the National Institute for Neurological Disorders and Stroke, and the Society for PSP (NINDS SPSP), along with 40 PD and 40 control patients. All patients were assessed using standard MR imaging protocol.Standard MPrage sequence was included .The area of midbrain ,pons was calculated on midsagittal images while diameter of MCP and SCP on parasagittal and coronal images respectively .MRPI was calculated by multiplying the pons area/midbrain area ratio by MCP width/SCP width ratio. The midbrain/pons (M/P) ratio was measured as the ratio of midbrain area to pons area.

RESULTS

Mean MRPI in PSP patients (19.1 ± 4.87) was significantly higher than that in PD patients (9.11 ± 1.6) and controls (9.21 ± 2.11). In this study, MRPI was 100% sensitive, specific, and accurate in differentiating PSP from PD and was 100% sensitive, 100% specific, and 100% accurate in differentiating PSP from controls. Positive correlation was found between the duration of disease, and MRPI in the present study. MRPI was superior to the M/P ratio in differentiating between PSP and PD patients on an individual basis. No overlapping values were observed in the PSP and PD patients.There was moderate association between outcome of NINDS SPSP Criteria for PSP cases and MRPI (Eta squared=0.03). Also, moderate association between the MRPI values of possible and probable cases of PSP (t=6.46, p>0.001).

CONCLUSION

Magnetic Resonance Parkinsonism Index is more sensitive, specific, and accurate than M/P ratio in differentiating PSP from PD in the early stages on an individual basis

CLINICAL RELEVANCE/APPLICATION

MR Parkisnons Index is a simple MRI based calculation that should routinely be included in patients with atypical Parkinsons disease and can significantly impact management and prognosis

SSK16-03 Twelve-Year Diffusion Changes in the Deep Gray Nuclei on Serial MRI in Parkinson's Disease

Wednesday, Dec. 4 10:50AM - 11:00AM Room: S401CD

Participants

Leon Q. Ooi, MENG, Singapore, Singapore (*Abstract Co-Author*) Nothing to Disclose Isabel H. Chew, BA, Singapore, Singapore (*Abstract Co-Author*) Nothing to Disclose Huihua Li, Singapore, Singapore (*Abstract Co-Author*) Nothing to Disclose Septian Hartono, Singapore, Singapore (*Abstract Co-Author*) Nothing to Disclose Chu-Ning Ann, Singapore, Singapore (*Abstract Co-Author*) Nothing to Disclose Soo Lee Lim, MS, Singapore, Singapore (*Abstract Co-Author*) Nothing to Disclose Eng King Tan, Singapore, Singapore (*Abstract Co-Author*) Nothing to Disclose Ling Ling Chan, MBBS, FRCR, Singapore, Singapore (*Presenter*) Nothing to Disclose

PURPOSE

Basal ganglia pathology has been linked to motor deterioration in Parkinson's disease (PD). Diffusion tensor imaging (DTI) interrogates deep gray nuclei (DGN) microstructure in vivo, but results from cross-sectional studies in PD have been inconsistent. We investigated temporal DTI profiles in the DGN (caudate, putamen and thalamus) over a 12-year study in relation to their clinical progression.

METHOD AND MATERIALS

PD patients and HC underwent 3 scans 6 years apart (157 subjects in total at baseline), on the same 1.5T scanner. Patients were clinically evaluated using the UPDRS and H&Y staging. The standardized protocol included DTI and structural MPRAGE sequences. The DGN were segmented through FSL FIRST. Structures were individually screened and corrected during quality assessment. The segmentation masks were resampled to the DTI space and used to sample DTI indices (FA, MD, AD, RD) from each nucleus. Statistical analysis was carried out using a generalized estimating equation (GEE) to investigate differences between HC and PD at baseline, along with their longitudinal progression, adjusting for age and sex. Additionally, the GEE was used to predict H&Y and UPDRS motor scores. Statistical significance was accepted at p < 0.05.

Longitudinal analysis revealed a more severe increase in caudal diffusivity as compared to other DGN. DGN DTI indices were significantly different between HC and PD at the 3rd timepoint. Increasing diffusivity in the caudate correlated with worsening UPDRS and H&Y scores. Putaminal diffusivity correlated with worsening H&Y scores only.

CONCLUSION

Neuronal degeneration is accompanied by decrease in FA and increase in diffusivity. However, significant nucleic DTI differences only manifest in the later stages of PD. This may be secondary to known effects of iron on DTI indices, which artifactually reverse and thence blunt expected DTI changes. The correlation between increased diffusivity and worsening motor performance suggests neuronal degeneration related to PD. This degeneration likely linked to a loss of dopaminergal neurons characteristic to PD in the caudate and putamen throughout the progression of the disease.

CLINICAL RELEVANCE/APPLICATION

Temporal changes to diffusivity suggest artefactual effects from iron deposition during early stages in PD patients. Caudate diffusivity was shown to be an effective biomarker for motor performance.

SSK16-04 Response to Deep Brain Stimulation Correlates with L-DOPA Responsiveness

Wednesday, Dec. 4 11:00AM - 11:10AM Room: S401CD

Participants

Anup K. Bhattacharya, Springfield, PA (*Presenter*) Nothing to Disclose John Pearce, Philadelphia, PA (*Abstract Co-Author*) Nothing to Disclose Mahdi Alizadeh, Philadelphia, PA (*Abstract Co-Author*) Nothing to Disclose Jennifer Muller, MS,BS, Philadelphia, PA (*Abstract Co-Author*) Nothing to Disclose Daniel Kremens, Philadelphia, PA (*Abstract Co-Author*) Nothing to Disclose Tsao Wei Liang, MD, Philadelphia, PA (*Abstract Co-Author*) Nothing to Disclose Victor Romo, MD, Philadelphia, PA (*Abstract Co-Author*) Nothing to Disclose Ashwini Sharan, MD, Philadelphia, PA (*Abstract Co-Author*) Nothing to Disclose Feroze B. Mohamed, PhD, Philadelphia, PA (*Abstract Co-Author*) Nothing to Disclose Chengyuan Wu, Philadelphia, PA (*Abstract Co-Author*) Nothing to Disclose

For information about this presentation, contact:

anupb792@gmail.com

PURPOSE

Deep brain stimulation (DBS) of the subthalamic nucleus (STN) or globus pallidus pars interna (GPi) is indicated in patients with refractory Parkinson's disease (PD) with significant motor fluctuations. While clinical characteristics facilitate patient selection, currently no objective tool to predict response to DBS exists. We examined resting state functional magnetic resonance imaging (rsfMRI) to determine the feasibility of this modality to identify early responders to DBS with minimal programming.

METHOD AND MATERIALS

Ten patients with advanced PD underwent preoperative rsfMRI under anesthesia in preparation for DBS surgery. Motor scores (UPDRS-III) were collected before and after DBS. Scans were performed on a 3T MR scanner, and images were preprocessed to correct for spatial and temporal artifacts. Regions of interest (ROIs) were defined using the Harvard-Oxford and ATAG-MNI04 basal ganglia (BG) atlases. Functional connectivity (FC) was calculated using the MATLAB®-based CONN toolbox via two-tailed bivariate correlations. Significant FC differences between patients who were good responders (> 30% improvement) following DBS versus those who were poor responders (< 30% improvement) were evaluated with an ROI-to-voxel analysis (FDR-corrected p < 0.05).

RESULTS

Patients who responded more favorably to DBS had desynchronization between the putamen and supplementary motor area (SMA) and synchronization between the lentiform nucleus with the superior frontal gyrus (SFG) (Figure 1), similar to characteristic changes seen following L-DOPA administration (p=0.0001).

CONCLUSION

Our findings show promise in the ability of rsfMRI to potentially improve patient selection and provide better pre-surgical consultation for patients regarding early prognosis from DBS.

CLINICAL RELEVANCE/APPLICATION

Resting state functional MRI (rsfMRI) can be used as an objective biomarker to identify those patients who are most likely to benefit from deep brain stimulation surgery.

SSK16-05 Functional Connectivity Patterns Predictive of Treatment Response in Deep Brain Stimulation for Dystonia

Wednesday, Dec. 4 11:10AM - 11:20AM Room: S401CD

Participants

Lela Okromelidze, MD, Jacksonville, FL (*Presenter*) Nothing to Disclose Tsuboi Takashi, MD,PhD, Gainesville, FL (*Abstract Co-Author*) Nothing to Disclose Robert Eisinger, Gainesville, FL (*Abstract Co-Author*) Nothing to Disclose Leonardo Almeida, MD, Gainesville, FL (*Abstract Co-Author*) Nothing to Disclose Matthew Burns, MD, Gainesville, FL (*Abstract Co-Author*) Nothing to Disclose Kelly Foote, MD, Gainesville, FL (*Abstract Co-Author*) Nothing to Disclose Michael Okun, MD, Gainesville, FL (*Abstract Co-Author*) Nothing to Disclose Erik H. Middlebrooks, MD, Ponte Vedra Beach, FL (*Abstract Co-Author*) Research Consultant, Varian Medical Systems, Inc; Research Support, Varian Medical Systems, Inc; Research Support, Boston Scientific Corporation

PURPOSE

Globus pallidus interna (GPi) deep brain stimulation (DBS) is an effective method of treatment for medication-refractory primary generalized and cervical dystonia. However, up to 25% of patients do not respond to DBS, mainly attributed to factors such as: variation in stimulation parameters, target selection, and lack of objective biomarker. Moreover, DBS treatment in dystonia is further complicated due to delayed improvement of dystonic symptoms after stimulation, making optimal device programming challenging. An understanding of the brain connectivity patterns that underpin positive treatment response may prove to be a valuable biomarker to improve outcomes and reduce side effects by improved DBS targeting and programming.

METHOD AND MATERIALS

Group-level analysis of 39 patients with optimized DBS of GPi for primary dystonia was performed. UDRS score percentage change from pre-surgery and six months post-surgery was the primary end point. After co-registration and normalization of post-operative CT/MRI images into standard MNI atlas space, electrode contacts were reconstructed along the lead trajectories using the PaCER algorithm with manual refinement. Volume of tissue activated (VTA) was estimated based on the final DBS programming settings. The VTA was used for seed-based connectivity analysis in each subject using a group-averaged resting-state fMRI dataset of 1000 patients from the Human Connectome Project. Group-level analysis was performed using subjects' first level rs-fMRI t-score maps correlated with percentage change in UDRS score. Controlling for family-wise error rate, statistical significance was considered as p<.001.

RESULTS

Stimulation volumes with greater connectivity to the motor network correlated with improvement in UDRS score. In particular, the primary motor cortex, supplementary motor cortex, and ventral thalamus correlated strongly with UDRS improvement. Expected regions in the motor cerebellum (including lobules IV, V, VI, and VIII) also strongly correlated with UDRS improvement.

CONCLUSION

Functional imaging is a promising tool for medication-refractory primary dystonia patients' DBS treatment planning and outcome prediction.

CLINICAL RELEVANCE/APPLICATION

Functional MRI connectivity patterns may serve as a valuable biomarker for DBS targeting and programming in patients with primary dystonia.

SSK16-06 A Deeper Impact - Using MR Guided Focused Ultrasound for the Treatment of Essential Tremor Targeting Both Thalamic Ventralis Intermidius Nucleus and the Subthalamic Zona Incerta

Wednesday, Dec. 4 11:20AM - 11:30AM Room: S401CD

Participants

Ayesha Jameel, MBBS, London, United Kingdom (*Presenter*) Research Grant, InsighTec Peter Bain, London, United Kingdom (*Abstract Co-Author*) Nothing to Disclose Dipkander Nandi, London, United Kingdom (*Abstract Co-Author*) Nothing to Disclose Brynmor Jones, MRCP, FRCR, London, United Kingdom (*Abstract Co-Author*) Nothing to Disclose Olga Kirmi, MBBS, London, United Kingdom (*Abstract Co-Author*) Nothing to Disclose Wladyslaw M. Gedroyc, MBBS, MRCP, London, United Kingdom (*Abstract Co-Author*) Research Grant, InsighTec

For information about this presentation, contact:

ayesha.jameel@nhs.net;w.gedroyc@imperial.ac.uk

PURPOSE

Essential Tremor (ET) is estimated to affect 10 million people in the United States. Magnetic Resonance guided focused ultrasound (MRgFUS) is a non-invasive treatment for ET that allows targeted thermal ablation of brain tissue under real time image guidance. Previous studies have demonstrated successful targeting of the thalamic Ventral Intermedius Nucleus (Vim) to be an effective treatment in ET; this paper describes the world's first trial using MRgFUS to target both the thalamic Vim and the subthalamic Zona Incerta (ZI).

METHOD AND MATERIALS

This prospective study enrolled 13 patients with medication refractory ET for unilateral MRgFUS procedure. Tremor severity and functional impairment were assessed at baseline and regular intervals post-treatment for 24 months, using the Clinical Rating Scale for Tremor (CRST), Quality of Life in Essential Tremor (QUEST) and Bain-Findley Spirals (BFS) scores. BFS Spirals were also collated intraoperatively: immediately pre-procedure, after targeting the Vim and after targeting the ZI. All spirals were scored by 3 blinded movement disorder Neurologists. The percentage improvement in the spiral scores after Vim ablation and after ZI ablation were compared and analysed.

RESULTS

In all patients there was successful thermal ablation of the target tissue at both Vim and ZI, with improvement in all parameters over the 24months: CRST tremor score of the treated arm 73.5% and the non-treated arm 38.4%, QUEST 38%, BFS 46.9%. The intraoperative BFS scores demonstrated the additional benefit of targeting the ZI was 21.8% - improvement after Vim lesioning 27.9% but after both Vim and ZI lesioning was 49.7%. One patient (7.69%) experienced a significant adverse event; post-treatment unilateral hemi-chorea persistent at 2 years.

CONCLUSION

Our study provides further evidence that MRgFUS is an effective curative treatment for ET and demonstrates the additional benefit of targeting the subthalamic ZI with the thalamic Vim. Furthermore improvement in the tremor scores of non-treated arm shows the positive bilateral effects of targeting the ZI.

CLINICAL RELEVANCE/APPLICATION

MRgFUS has the potential to revolutionise the treatment of movement disorders such as ET It provides an non-invasive alternative

SSK16-07 Cerebellar Atrophy and Cognitive Impairment in Friedreich Ataxia

Wednesday, Dec. 4 11:30AM - 11:40AM Room: S401CD

Participants Elena A. Vola, MD, Naples, Italy (*Presenter*) Nothing to Disclose Sirio Cocozza, MD, Naples, Italy (*Abstract Co-Author*) Speaker, sanofi-aventis Group; Speaker, Genzyme Corporation; Advisory Board, Amicus Therapeutics, Inc Teresa Costabile, Naples, Italy (*Abstract Co-Author*) Nothing to Disclose Giuseppe Pontillo, MD, Capodrise, Italy (*Abstract Co-Author*) Nothing to Disclose Maria Lieto, MD, Naples, Italy (*Abstract Co-Author*) Nothing to Disclose Camilla Russo, Napoli, Italy (*Abstract Co-Author*) Nothing to Disclose Chiara Pane, Napoli, Italy (*Abstract Co-Author*) Nothing to Disclose Francesco Sacca, Naples, Italy (*Abstract Co-Author*) Nothing to Disclose Arturo Brunetti, MD, Naples, Italy (*Abstract Co-Author*) Nothing to Disclose

For information about this presentation, contact:

elena.a.vola@gmail.com

PURPOSE

Recent studies have suggested the presence of a significant atrophy affecting the cerebellar cortex in Friedreich ataxia (FRDA) patients, an area of the brain long considered to be relatively spared by the neurodegenerative phenomena occurring in this condition. Cognitive deficits, which occurs in FRDA patients, have been associated to cerebellar volume loss in other conditions. Aim of this study was to investigate the correlation between cerebellar volume and cognition in FRDA.

METHOD AND MATERIALS

19 patients with genetically confirmed FRDA (M/F:13/6; 28.4±14.1y), along with a group of 20 healthy controls (HC) of comparable age and sex (M/F:11/9; 29.4±9.7y) were included in this study. All subjects underwent an MRI scan including a 3D-T1-weighted sequence and a neuropsychological examination mainly oriented at cognitive domain that are related to cerebellar function (i.e. visuo-perception and visuo-spatial functions, visuospatial memory and working memory). Cerebellar global and lobular volumes were computed using the Spatially Unbiased Infratentorial Toolbox (SUIT v3.2), implemented in SPM12. Furthermore, a cerebellar Voxel Based Morphometry (VBM) analysis was also carried out. Correlations between MRI metrics and clinical data were tested via partial correlation analysis, correcting for age and sex.

RESULTS

FRDA patients showed a significant reduction of the total cerebellar volume (p=0.004), significantly affecting the Lobule IX (p=0.001). At the VBM analysis, a cluster of significant reduced GM density encompassing the entire lobule IX was found (p=0.003). When correlations were probed, a direct correlation between Lobule IX volume and impaired visuo-spatial functions was found (r=0.580, p=0.02), with a similar correlation between the same altered function and results obtained at the VBM (r=0.520; p=0.03).

CONCLUSION

With two different and complementary image analysis techniques, we confirmed the presence of cerebellar volume loss in FRDA, mainly affecting the posterior lobe. In particular, Lobule IX atrophy correlate with worst performances at visuo-spatial functions, further expanding our knowledge about the physiopathology of cognitive damage in FRDA.

CLINICAL RELEVANCE/APPLICATION

In FRDA patients, a significant cerebellar atrophy is present, mainly affecting the posterior lobe and Lobule IX in particular, which also correlate with cognitive performance in the domain of visuo-spatial abilities

SSK16-08 Functional and Structural Integrity Following Focused Ultrasound Thalamotomy and Its Correlation With Tremor Relief

Wednesday, Dec. 4 11:40AM - 11:50AM Room: S401CD

Participants

Gil Zur, Haifa, Israel (*Presenter*) Nothing to Disclose Orit Lesman, MD, Haifa, Israel (*Abstract Co-Author*) Nothing to Disclose Itamar Kahn, PhD, Haifa, Israel (*Abstract Co-Author*) Nothing to Disclose Ayelet Eran, MD, Haifa, Israel (*Abstract Co-Author*) Nothing to Disclose

For information about this presentation, contact:

g_zur@rambam.health.gov.il

PURPOSE

We aim to explore the impact of MRgFUS treatment functional connectivity nd white matter integrity in tremor-related circuits and test whether tremor improvement is correlated to specific pre- or post-treatment functional responsese.

METHOD AND MATERIALS

60 patients with either essential tremor or Parkinson's disease underwent tremor and quality-of-life assessments prior to and at one and six months following focused ultrasound ablation. 21 patients underwent MRI including T1, T2-Flair and resting-state fMRI before treatment and at one day, 7-10 days, 1-3 months, and 4-12 months following it. 39 patients underwent MRI including T1, T2-Flair and diffusion tensor weighted imaging before treatment and at similiar time points to the fMRI group. Diffusivity parameters were calculated and fiber tractography measures were extracted. Changes in functional connectivity and in diffusivity parameters were assessed in different brain areas that are related to tremor.

RESULTS

Decreased functional connectivity was found between the dentate nucleus and the motor thalamus following ablation. Long term damage, was found in the ablated core and in the tract connecting the thalamus and red-nucleus. Inverse correlation was found between fractional anisotropy in the motor thalamus one day following ablation and tremor improvement in both patient groups, with lower values before treatment associated with better outcome (tremor relief) in essential tremor patients.

CONCLUSION

long-term changes in functional connectivity and white matter integrity are present following focused ultrasound thalamotomy. Regions demonstrating long-term white matter changes may be responsible for the tremor relief seen in patients, implicating these regions in the disorder's pathogenesis.

CLINICAL RELEVANCE/APPLICATION

The expected findings of this project would ultimately aid in more accurate patient selection for thalamotomy, as well as assist in further development of ET tremor treatments.

SSK16-09 Correlation between Fractional Anisotropy (FA) and Apparent Diffusion Coefficient (ADC) Changes in the Targeted Ventral Intermediate Nucleus (VIM) after MRgFUS Thalamotomy and Clinical Outcome: Preliminary Results in a Single Center

Wednesday, Dec. 4 11:50AM - 12:00PM Room: S401CD

Participants

Silvia Torlone, L'Aquila, Italy (*Presenter*) Nothing to Disclose Antonella Corridore, L'Aquila, Italy (*Abstract Co-Author*) Nothing to Disclose Milvia Martino, MS, Laquila , Italy (*Abstract Co-Author*) Nothing to Disclose Maria Valeria Marcella Micelli, Laquila , Italy (*Abstract Co-Author*) Nothing to Disclose Emanuele Tommasino, MD,MSc, Laquila , Italy (*Abstract Co-Author*) Nothing to Disclose Federico Bruno, MD, L'Aquila, Italy (*Abstract Co-Author*) Nothing to Disclose Alessia Catalucci, MD, L'Aquila, Italy (*Abstract Co-Author*) Nothing to Disclose Marco Varrassi, L'Aquila, Italy (*Abstract Co-Author*) Nothing to Disclose Francesco Arrigoni, L'Aquila , Italy (*Abstract Co-Author*) Nothing to Disclose Alessandra Splendiani, MD, L'Aquila , Italy (*Abstract Co-Author*) Nothing to Disclose Carlo Masciocchi, MD, L'Aquila, Italy (*Abstract Co-Author*) Nothing to Disclose

For information about this presentation, contact:

Torlone.silvia@gmail.com

PURPOSE

The aim of the study was to evaluate changes of Fractional Anisotropy (FA) and Apparent Diffusion Coefficient (ADC) in the Ventral Intermediate Nucleus (VIM) of the thalamus after MR-guided focused ultrasound (MRgFUS) thalamotomy and the correlation with clinical outcome.

METHOD AND MATERIALS

In the period February 2018-March 2019 we enrolled 39 patients with disabling and refractory tremor (18 Essential Tremor (ET), 21 Parkinson Disease (PD) tremor, mean age 64,6 years) who underwent to unilateral VIM ablation using MRgFUS. The MRgFUS sonications were performed using a 3-Tesla MRI (GE) and a focused ultrasound system (ExAblate Neuro, Insightec). Measurements of the FA and ADC values were performed before thalamotomy, and 1 day, 1 month and 6 months thereafter using Avantage Workstation AW4.7 (GE Healthcare). Clinical evaluation was performed using the Fahn-Tolosa-Marin Scale (FTM) for tremor before treatment, 1 day, 1 month and 6 months thereafter.

RESULTS

Treatment was effective (considerable and immediate reduction of tremor) in 38 out of 39 patients (97,4%). Changes in FA and ADC values after treatment were statistically significant. There was a statistically significant (p<0,005) positive correlation between FA values in the targeted VIM at 1 day after thalamotomy and FTM score at 6 months after treatment. There were not a statistically significant association between ADC values and clinical outcomes.

CONCLUSION

Our data have demonstrated that MRgFUS thalamotomy for treatment of ET and PD tremor results in a significant change of FA and ADC values in the target VIM. Particularly, FA values at 1 day after thalamotomy showed significant associations with clinical outcome. The limitations of this report are the small number of patients and the short follow-up period. Large randomized studies are needed to assess if FA value may be considered a possible imaging marker for early prediction of clinical outcome after MRgFUS thalamotomy for ET and PD tremor.

CLINICAL RELEVANCE/APPLICATION

MRgFUS thalamotomy for treatment of ET and PD tremor results in a significant change of FA and ADC values in the target VIM: these changes may be considered a possible imaging marker for clinical outcome and provided an important prognostic value.







AI Theater: Hitting the Bull's AI in Neuroradiology: Unlocking Value from Workflow to Patient: Presented by icometrix

Wednesday, Dec. 4 11:30AM - 11:50AM Room: AI Showcase, North Building, Level 2, Booth 10724

Participants

Wim van Hecke, PhD, Edegem, Belgium (*Presenter*) Officer, icometrix Co-founder, icometrix Dirk Smeets, PhD, Leuven, Belgium (*Presenter*) Officer, icoMetrix NV

Program Information

The future based on AI is already here. icobrain combines the power of the Cloud and AI to bring brain quantification for MR and CT to daily clinical practice for (neuro)radiologists. Find out how cloud-based AI tools can change your patient care and can impact the speed, accuracy, and consistency of your radiological reading.



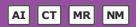




SPAI42

RSNA AI Deep Learning Lab: Generative Adversarial Networks (GANs)

Wednesday, Dec. 4 1:00PM - 2:30PM Room: AI Showcase, North Building, Level 2, Booth 10342



AMA PRA Category 1 Credits ™: 1.50 ARRT Category A+ Credit: 1.75

Participants

Bradley J. Erickson, MD, PhD, Rochester, MN (*Presenter*) Board of Directors and Stockholder, VoiceIt Technologies, LLC; Board of Directors, FlowSigma, LLC; Officer, FlowSigma, LLC; Stockholder, FlowSigma, LLC;

Special Information

In order to get the best experience for this session, it is highly recommended that attendees bring a laptop with a keyboard, a decent-sized screen, and the latest version of Google Chrome. Additionally, it is recommended that attendees have a basic knowledge of deep learning programming and some experience running a Google CoLab notebook. Having a Gmail account is also helpful. Here are instructions for creating and deleting a Gmail account.

ABSTRACT

This course describes a more recent advance in deep learning known as Generative Adversarial Networks (GANs). GANs are a deep learning technology in which a computer is trained to create images that look very 'real' even though they are completely synthetic. Getting 'large enough' data sets is a problem for most deep learning applications, and this is particularly true in medical imaging. This may be one way to address the 'data shortage' problem in medicine. GANs have also been created that can convert MRIs to CTs (e.g. for attenuation correction with MR/PET).





MSRO44

BOOST: Advanced Techniques in Image-guided Therapy (Interactive Session)

Wednesday, Dec. 4 3:00PM - 4:15PM Room: S103CD



AMA PRA Category 1 Credits ™: 1.25 ARRT Category A+ Credits: 1.50

Participants

Florence K. Keane, MD, Boston, MA (*Presenter*) Advisory Board, AstraZeneca PLC Susanna I. Lee, MD, PhD, Boston, MA (*Presenter*) Royalties, Wolters Kluwer nv; Royalties, Springer Nature Homer A. Macapinlac, MD, Houston, TX (*Presenter*) Nothing to Disclose Peter Balter, PhD, Houston, TX (*Presenter*) Research Grant, Varian Medical Systems, Inc; Research Grant, RaySearch Laboratories AB

For information about this presentation, contact:

slee0@mgh.harvard.edu

LEARNING OBJECTIVES

1) Explain and apply modern CT, MR, and PET technologies for treatment planning of solid malignancies in the chest, abdomen and pelvis. 2) Explain and apply the modern techniques in radiotherapy safely and effectively in the chest, abdomen and pelvis.

ABSTRACT

The last decade has seen emergence of important advances in locoregional cancer therapy. Use of functional imaging and advanced radiotherapy often integrated with targeted chemotherapy have improved patient outcomes. This course will present the underlying principles in diffusion MRI, novel MR contrast agents, ultrasound contrast agents and dual energy CT. PET tracers to be discussed are F-18 FDG, widely used for most solid tumors, C-11 choline/F-18 Fluciclovine for prostate cancer and Ga-68-DOTATATE for neuroendocrine tumors. Advances in PET detector instrumentation will be presented. Advanced radiotherapy techniques such as Image Guided Radiotherapy (IGRT), Intensity Modulated Radiation Therapy (IMRT), and Stereotactic Body Radiation Therapy (SBRT) using image guidance with X-ray, CT, MRI and PET will be described.







SPAI43

RSNA AI Deep Learning Lab: Beginner Class: Classification Task (Intro)

Wednesday, Dec. 4 3:00PM - 4:30PM Room: AI Showcase, North Building, Level 2, Booth 10342



Participants Bradley J. Erickson, MD, PhD, Rochester, MN (*Presenter*) Board of Directors and Stockholder, VoiceIt Technologies, LLC; Board of Directors, FlowSigma, LLC; Officer, FlowSigma, LLC; Stockholder, FlowSigma, LLC;

Special Information

In order to get the best experience for this session, it is highly recommended that attendees bring a laptop with a keyboard, a decent-sized screen. Having a Gmail account will be helpful. Here are instructions for creating and deleting a Gmail account.

ABSTRACT

This class will focus on basic concepts of convolutional neural networks (CNNs) and walk the attendee through a working example. A popular training example is the MNIST data set which consists of hand-written digits. This course will use a data set we created, that we call 'MedNIST', and consists of images of 6 different classes: Chest X-ray, Chest CT, Abdomen CT, Head CT, Head MR and Breast MRI. The task is to identify the image class. This will be used to train attendees on the basic principles and some pitfalls in training a CNN. • Intro to CNNs • Data preparation: DICOM to jpeg, intensity normalization, train vs test • How do we choose the labels? Inconsistencies... Use Fast.AI routines to classify; Validation of results: Are the performance metrics reliable? 'Extra Credit': if there is time, explore data augmentation options, effect of batch size, training set size.





SSM03

Cardiac (Myocardial Disease)

Wednesday, Dec. 4 3:00PM - 4:00PM Room: S401CD



AMA PRA Category 1 Credit ™: 1.00 ARRT Category A+ Credit: 1.00

FDA Discussions may include off-label uses.

Participants

Hajime Sakuma, MD, Tsu, Japan (*Moderator*) Research Grant, EIZAI; Research Grant, DAIICHI SANKYO Group; Research Grant, FUJIFILM Holdings Corporation; Research Grant, Guerbet SA; Research Grant, Nihon Medi-Physics Co, Ltd; Borek Foldyna, MD, Boston, MA (*Moderator*) Nothing to Disclose Friedrich D. Knollmann, MD, PhD, Wynnewood, PA (*Moderator*) Nothing to Disclose

Sub-Events

SSM03-01 Role of Cardiac Magnetic Resonance (CMR) Imaging for Early Detection of Myocardial Involvement in Patients Affected by Anderson- Fabry Disease (AFD)

Wednesday, Dec. 4 3:00PM - 3:10PM Room: S401CD

Participants

Simona Coco, MD, Roma, Italy (*Presenter*) Nothing to Disclose Angelica Bracci, Rome, Italy (*Abstract Co-Author*) Nothing to Disclose Gianluca de Rubeis, Rome, Italy (*Abstract Co-Author*) Nothing to Disclose Nicola Galea, MD, Rome, Italy (*Abstract Co-Author*) Spouse, Employee, Merck & Co, Inc Marco Francone, MD,PhD, Rome, Italy (*Abstract Co-Author*) Nothing to Disclose Carlo Catalano, MD, Rome, Italy (*Abstract Co-Author*) Nothing to Disclose Francesco Cilia, MD, Rome, Italy (*Abstract Co-Author*) Nothing to Disclose Rosa Maria Ammendola, Rome, Italy (*Abstract Co-Author*) Nothing to Disclose

For information about this presentation, contact:

simona.coco@uniroma1.it

PURPOSE

Cardiomyopathy is a complication of Anderson-Fabry Disease (AFD) with dramatic impact on morbidity and mortality; medical therapy is recommended in patients with evidence of cardiac involvement. However, early identification of cardiac involvement in AFD patients may be arduous at pre-hypertrophic stage. Our aim was to evaluate the role of Cardiac Magnetic Resonance (CMR) in early detection of cardiac involvement in AFD at pre-hypertrophic stage.

METHOD AND MATERIALS

16 biopsyproven AFD patients with normal maximal wall thickness at echocardiography (<11mm) underwent to CMR (1.5 T, Avanto, Siemens, Erlangen, Germany) with following sequence protocol: STIR T2w, cineMR, late enhancement and T1 mapping with MOLLI technique before and 15 minutes after injection of 0.15 mmol/Kg gadolinium (GdDOTA, Guerbet, Paris, France). Indexed LV volumes and mass, native T1 (nT1), extracellular volume fraction (ECV) and tissue tracking parameters were analyzed. Results were compared with 16 healthy age and gendermatched volunteers.

RESULTS

No significative differences were found in myocardial mass (Mass/BSA:45,61vs51,24 g/m2,p:0,27), ventricular volumes (EF:58,9vs60,62%,p:0,62) and left ventricular myocardial strain (Global radial strain:46,11vs42,75,p:0,65; global circumferential strain:-20,4vs-18,8,p:0,26; global longitudinal strain:-20,9 vs-18,7,p:0,09) between AFD and healthy subjects. No subjects had shown edema or LGE; nT1 was significantly lower (p=0,01) in AFD patients (988+/-58 ms) than healthy volunteer cohort (1024+/-63 ms); no significative differences was noted between the two groups in ECV values (23%vs24,2%,p:0,23).

CONCLUSION

Native T1 value appears the only marker of early myocardial involvement in pre-hypertrophic AFD patients.

CLINICAL RELEVANCE/APPLICATION

AFD patients should be treated as soon as early signs of organ injury occur (kidney, heart and/or neurological signs). Enzyme replacement therapy is the only specific treatment for AFD but is very expensive and limited to patients with demonstrated organ involvement. Native T1 mapping appear to be reliable and accurate to detect early cardiac involvement before hypertrophic phenotype expression.

SSM03-02 Impact of Myocardial Fibrosis on Left Ventricular Function Evaluated by Feature Tracking Myocardial Strain CMR in Competitive Male Triathletes with Normal Ejection Fraction

Wednesday, Dec. 4 3:10PM - 3:20PM Room: S401CD

Participants

Enver G. Tahir, MD, Hamburg, Germany (*Presenter*) Nothing to Disclose Jitka Starekova, MD, Hamburg, Germany (*Abstract Co-Author*) Nothing to Disclose Kai Muellerleile, Hamburg, Germany (*Abstract Co-Author*) Nothing to Disclose Maxim Avanesov, MD, Hamburg, Germany (*Abstract Co-Author*) Nothing to Disclose Julius M. Weinrich, Hamburg, Germany (*Abstract Co-Author*) Nothing to Disclose Christian Stehning, Hamburg, Germany (*Abstract Co-Author*) Nothing to Disclose Christian Bohnen, Hamburg, Germany (*Abstract Co-Author*) Nothing to Disclose Ulf K. Radunski, Hamburg, Germany (*Abstract Co-Author*) Nothing to Disclose Gerhard B. Adam, MD, Hamburg, Germany (*Abstract Co-Author*) Nothing to Disclose Gunnar K. Lund, MD, Hamburg, Germany (*Abstract Co-Author*) Nothing to Disclose

For information about this presentation, contact:

e.tahir@uke.de

PURPOSE

To analyze the impact of myocardial fibrosis on left ventricular (LV) function evaluated by feature-tracking strain analysis using cine cardiac magnetic resonance (CMR) in competitive male triathletes with normal ejection fraction.

METHOD AND MATERIALS

78 asymptomatic male triathletes with >10 weekly training hours (43 ± 11 years) and 28 male age-matched controls were studied by late gadolinium enhancement (LGE) and cine CMR. Global and segmental radial, longitudinal and circumferential strains were analyzed using feature-tracking cine CMR. Focal non-ischemic LGE was observed in 15 of 78 triathletes (19%, LGE+) with predominance in basal inferolateral segments. LV ejection fraction was normal in LGE+ ($62\pm6\%$) and in LGE- triathletes ($62\pm5\%$, P=0.958). In contrast, global radial strain was lower in LGE+ triathletes with 40 $\pm7\%$ compared to LGE- triathletes ($45\pm7\%$, P<0.05). Reduced segmental radial strain occurred either in LGE+ segments or in directly adjacent segments. Strain analysis revealed regional differences in controls with highest radial and longitudinal strain in the inferolateral segments, which were typically affected by fibrosis in LGE+ triathletes.

RESULTS

Focal non-ischemic LGE was observed in 15 of 78 triathletes (19%, LGE+) with predominance of the basal inferolateral segments. LV ejection fraction was normal in LGE+ ($62 \pm 6\%$) and in LGE- triathletes ($62 \pm 5\%$, P=0.958). In contrast, global radial strain was lower in LGE+ triathletes with 40 $\pm 7\%$ compared to LGE- triathletes ($45 \pm 7\%$, P<0.05). Reduced segmental radial strain occurred either in LGE+ segments or in directly adjacent segments. Strain analysis revealed regional differences in controls with highest radial and longitudinal strain in the inferolateral segments, which were typically affected by fibrosis in LGE+ triathletes.

CONCLUSION

Reduced global and regional radial strain suggests a negative effect of myocardial fibrosis on LV function in LGE+ triathletes with normal ejection fraction. The observed regional differences in controls with highest radial and longitudinal strains in the inferolateral segments may explain the typical occurrence of fibrosis in this myocardial region in triathletes.

CLINICAL RELEVANCE/APPLICATION

Non-ischemic myocardial fibrosis might cause subclinical impairment of LV systolic function in athletes.

SSM03-03 Multiparametric Cardiac Magnetic Resonance Detects Extensive Subclinical Myocardial Disease in Patients with Advanced Liver Cirrhosis

Wednesday, Dec. 4 3:20PM - 3:30PM Room: S401CD

Participants

Alexander Isaak, Bonn, Germany (*Presenter*) Nothing to Disclose Michael Praktiknjo, Bonn, Germany (*Abstract Co-Author*) Nothing to Disclose Darius Dabir, Bonn, Germany (*Abstract Co-Author*) Nothing to Disclose Anton Faron, MD, Bonn, Germany (*Abstract Co-Author*) Nothing to Disclose Christian Jansen, Bonn, Germany (*Abstract Co-Author*) Nothing to Disclose Daniel Kuetting, MD, Bonn, Germany (*Abstract Co-Author*) Nothing to Disclose Daniel K. Thomas, MD, PhD, Bonn, Germany (*Abstract Co-Author*) Nothing to Disclose Julian A. Luetkens, MD, Bonn, Germany (*Abstract Co-Author*) Nothing to Disclose

For information about this presentation, contact:

alexander.isaak@ukbonn.de

PURPOSE

Liver cirrhosis is the end-stage of different chronic liver diseases and causes multi-systemic pathologies, leading to a high mortality level, especially in mid-age people. Cirrhotic cardiomyopathy (CCM) was defined as a cardiac involvement in patients suffering from cirrhosis, which can increase the risk for cardiac dysfunction and induce poor prognosis, especially in the context of other invasive procedures such as surgery, transjugular intrahepatic portosystemic shunt (TIPS) or liver transplantation. We aimed to determine the extent of cardiovascular involvement in patients with liver cirrhosis by a comprehensive cardiac magnetic resonance (CMR) approach.

METHOD AND MATERIALS

Patients with advanced cirrhosis (n=15; mean MELD-Score: 15±5), without known cardiac disease and preserved ejection fraction

as well as matched control subjects (n=15) underwent CMR. In the setting of a multiparamteric CMR protocol, cardiac function, T1 relaxation times, T2 relaxation times, visible myocardial edema, extracellular volume fraction (ECV) and late gadolinium enhancement (LGE) were determined.

RESULTS

Patients suffering from cirrhosis showed significant changes in myocardial tissue composition (native T1 relaxation times: 1018 ± 48 ms vs. 953 ± 32 ms, P<0.001; T2 relaxation times: 59 ± 3 ms vs. 53 ± 3 ms, P<0.001; ECV: 36.7 ± 6.4 % vs. 29.2 ± 5.7 %, P=0.002). Non-ischemic LGE indicating fibrosis was found in 6/15 (40%) patients (P<0.001). No differences in left ventricular ejection fraction were present between both groups ($65\pm6\%$ vs. 64 ± 3 %, P=0.100).

CONCLUSION

Comprehensive CMR showed extensive myocardial alterations in patients with cirrhosis without history for cardiac disease or symptoms. The elevated markers for focal and diffuse myocardial fibrosis and inflammation indicate a high prevalence of subclinical myocardial disease in cirrhotic patients. Subclinical myocardial disease might be a precursor of CCM in patients with advanced liver cirrhosis.

CLINICAL RELEVANCE/APPLICATION

Comprehensive CMR revealed a high burden of cardiovascular disease in patients with advanced liver cirrhosis and might serve as a potential new screening parameter for CCM.

SSM03-04 Circulating microRNAs as Biomarkers for Myocardial Fibrosis in Hypertrophic Cardiomyopathy

Wednesday, Dec. 4 3:30PM - 3:40PM Room: S401CD

Participants

Kate Hanneman, MD, FRCPC, Toronto, ON (*Presenter*) Nothing to Disclose Filio Billia, Toronto, ON (*Abstract Co-Author*) Nothing to Disclose Shanna Stanley Hasnain, Toronto, ON (*Abstract Co-Author*) Nothing to Disclose Daniela Grothe, Toronto, ON (*Abstract Co-Author*) Nothing to Disclose Harry Rakowski, Toronto, ON (*Abstract Co-Author*) Nothing to Disclose Andrew M. Crean, MD, Cincinnati, OH (*Abstract Co-Author*) Research support, sanofi-aventis Group

PURPOSE

Circulating microRNAs (miRNAs) are important regulators of a range of cellular processes and may represent novel biomarkers for myocardial disease. The purpose of this study was to evaluate whether miRNAs are differentially expressed in the blood of patients with hypertrophic cardiomyopathy (HCM) and whether they correlate with cardiac magnetic resonance imaging (MRI) findings.

METHOD AND MATERIALS

Thirty HCM patients (51.4±11.6 years, 80.0% male) and 10 healthy controls (38.9±12.6 years, 70.0% male) were prospectively recruited. Peripheral plasma levels of 11 miRNAs were assessed by quantitative real-time polymerase chain reaction and compared between HCM patients and controls. Cardiac MRI was performed at 3T including late gadolinium enhancement (LGE) and T1 mapping using a modified inversion recovery Look-Locker (MOLLI) sequence.

RESULTS

Sixteen HCM patients demonstrated LGE (53.3%), quantified at $9.5\pm7.3\%$ of left ventricular (LV) mass. Native T1 values were significantly higher in HCM patients with LGE compared to those without (1281.5±62.4 ms vs. 1234.9±62.4 ms, p=0.017). Four miRNAs were significantly downregulated in all HCM patients (miRNA-10b, -17, -133, and -18a). Two miRNAs were significantly downregulated in HCM patients with LGE but not in those without LGE (miRNA-192, fold change -2.15, p=0.024 and miRNA-133, fold change -1.84, p=0.028) and one miRNA was significantly upregulated only in patients with extensive fibrosis (defined as LGE >15% of LV mass; miRNA-146, fold change 8.36, p=0.046), suggesting that these miRNAs may play a role in fibrotic HCM. miRNA-192 correlated significantly with quantitative LGE (r=0.328, p=0.047), whereas miRNA-146 and miRNA-193 correlated significantly with native T1 (r=-0.456, p=0.008 and r=-0.423, p=0.007, respectively).

CONCLUSION

Our data suggest that circulating levels of miRNAs are differentially expressed in the blood of patients with HCM. miRNA-192 is downregulated and miRNA-146 is upregulated in HCM patients with LGE. These miRNAs correlate with cardiac MRI markers of fibrosis, identifying them as potential non-invasive biomarkers for myocardial remodelling assessment in HCM.

CLINICAL RELEVANCE/APPLICATION

Circulating miRNAs are potential non-invasive biomarkers for myocardial fibrosis in HCM. These results support the necessity for future larger studies to confirm these findings and evaluate their prognostic significance.

SSM03-05 The Application Value of Multi-Modal MRI in Assessment of Myocardial Edema in Patients with End-Stage Renal Disease

Wednesday, Dec. 4 3:40PM - 3:50PM Room: S401CD

Participants

Wanlin Peng, MS, Chengdu, China (*Abstract Co-Author*) Nothing to Disclose Huayan Xu, Chengdu, China (*Abstract Co-Author*) Nothing to Disclose Chunchao Xia, Chengdu, China (*Abstract Co-Author*) Nothing to Disclose Zhenlin Li, MD, Chengdu, China (*Abstract Co-Author*) Nothing to Disclose Keling Liu, Chengdu, China (*Presenter*) Nothing to Disclose

PURPOSE

ESRD patients are highly prevalent cardiovascular risk. ME occurred in various cardiovascular disease and precipitate myocardial fibrosis and arrhythmia in ESRD patients, and ultimately lead to heart failure or cardiac death. The study is to compare the

effectiveness of native T1 mapping,T2 mapping and conventional T2-weighted imaging (T2WI) in the detection of myocardial edema in patients with end stage renal disease, and further explore clinical value of ME in early diagnosis of myocardial injury.

METHOD AND MATERIALS

Seventy hemodialysis ESRD patients and 16 age- gender-matched healthy volunteers were prospectively enrolled and underwent CMR. All the parameters from CMR, including native T1 values,T2 values, T2 SI ratio, were measured (cmr42; Circle Cardiovascular Imaging Inc.; Calgary; Canada) and compared. Receiver operating characteristic analysis was performed to determine whether T2 values could be used in discriminating myocardial edema between ESRD patients and normal subjects.

RESULTS

The global T2 and native T1 values of ERSD patients were higher than normal controls (all P<0.05). But there was nosignificant difference in T2 SI ratios between two groups (p=0.146). The myocardial native T1 and T2 values of ESRD patients with preserved and decreased LVEF were both higher than those of normal controls (p<0.05), but there was no significant difference between the two groups in native T1 and T2 values. There was no significant difference between the three groups in T2 SI values (p=0.366). Moreover, the global T2 values of patients with MF and without MF were higher than normal controls (43.69 \pm 3.62, 41.82 \pm 3.43 v.s 38.79 \pm 3.69ms, respectively, all P<0.05). The global T1 values of ERSD patients with MF was highest among three groups (1286.12 \pm 52.60 v.s 1321.02 \pm 56.65, 1356.79 \pm 40.08ms, respectively, all P<0.05),but no statistical difference were found between normals and patients without MF. There were no significant difference in T2 SI ratios among three groups (p=0.311). In ESRD with MF is the proportion of left ventricular dysfunction (19, 52.8%) was higher than that in the ESRD without MF (8, 23.5%). By ROC analysis, T2 values exhibited a higher diagnostic accuracy for detecting ME than did native T1 or T2 SI values (0.83 vs. 0.67 and 0.63, all p<0.05). A cutoff value for global myocardial T2 of >= 41.94ms provided a sensitivity and specificity of 73.5% (52.0-85.8%) and 87.5% (61.7-98.4%) for ME in ESRD patients, respectively.

CONCLUSION

The myocardial pathological changes in patients with end stage renal disease were complex. The multiple cardiac magnetic resonance sequence demonstrated that myocardial edema exited in patients with ESRD patients. The CMR T2 mapping technique has a higher accuracy in quantifying the myocardial edema in patients with end stage renal disease compared with native T1 mapping and conventional T2WI.

CLINICAL RELEVANCE/APPLICATION

Early and accurate evaluation of ME in ESRD patients to evaluate the extent and scope of left ventricular myocardial tissue injury is greatly important for adjustment of clinical dialysis and medication intervention programs timely, combination of multiple sequence (includingT2 mapping, native T1 mapping, T2WI) will contribute to detection of diffused ME in ESRD patients.

SSM03-06 Multiparametric Cardiac Magnetic Resonance Imaging in Fabry's Disease Improves Diagnostic Accuracy Compared to T1 Mapping

Wednesday, Dec. 4 3:50PM - 4:00PM Room: S401CD

Participants

Tilman S. Emrich, MD, Mainz, Germany (*Presenter*) Nothing to Disclose Sebastian Benz, Mainz, Germany (*Abstract Co-Author*) Nothing to Disclose Moritz Halfmann, Mainz, Germany (*Abstract Co-Author*) Nothing to Disclose Sarah Lyschik, Mainz, Germany (*Abstract Co-Author*) Nothing to Disclose Christoph Dueber, MD, Mainz, Germany (*Abstract Co-Author*) Nothing to Disclose Julia B. Hennermann, PhD,MD, Mainz, Germany (*Abstract Co-Author*) Nothing to Disclose Christoph Kampmann, MD, Mainz, Germany (*Abstract Co-Author*) Nothing to Disclose Karl F. Kreitner, MD, Mainz, Germany (*Abstract Co-Author*) Nothing to Disclose

For information about this presentation, contact:

tilman.emrich@gmail.com

PURPOSE

Fabry's Disease (FD) is a hereditary, x-chromosomal linked storage disease that lead to accumulation of sphingolipids. Recently published work highlight the diagnostic potential of T1 Mapping in the detection of Fabry's disease. The aim of this study was to evaluate a combined diagnostic approach using basic cardiac parameters, T1 and T2 Mapping as well as left and right ventricular strain values.

METHOD AND MATERIALS

In this retrospective study, 61 patients in all phenotypic stages of Fabry's disease and 57 healthy volunteers were included. CMR was performed at 3T and incorporated CINE imaging, T1 and T2 Mapping as well as Late Gadolinium Enhancement imaging. In a post-processing manner, cvi42 (Circle, Calgary, Canada) was used to calculate global and septal T1 and T2 times as well as left and right ventricular function and Feature-tracking based strain parameters.

RESULTS

In univariate analysis, longitudinal strain parameters outperform conventional and mapping parameters in detection of Fabry's disease. Nevertheless, the combination of left and right ventricular global longitudinal strain (GLS) with T1 Mapping yielded the highest diagnostic accuracy with a sensitivity and specificity of 83.3 and 82.4% (Figure). The combined approach results in significant improvement of diagnostic accuracy compared to a univariate approach, demonstrated by increasing Youden's indexes (YI): YI (T1 Mapping) 0.468 vs YI (LV GLS) 0.623 vs YI (combination) 0.657.

CONCLUSION

A multi-parametric imaging approach incorporating FT strain parameters and T1 Mapping improved the diagnostic accuracy of CMR for detection of Fabry's disease in all stages of disease. Further research is needed to establish Strain imaging as a surrogate for prognosis and therapy.

CLINICAL RELEVANCE/APPLICATION

CMR with T1 Mapping is an important diagnostic method for diagnosis, initiation of therapy and estimation of prognosis in FD. Our work demonstrates the additive value of LV and RV FT strain imaging in FD.







SSM04

Cardiac (Anatomy and Function)

Wednesday, Dec. 4 3:00PM - 4:00PM Room: S404AB



AMA PRA Category 1 Credit ™: 1.00 ARRT Category A+ Credit: 1.00

Participants

Hildo J. Lamb, MD, PhD, Leiden, Netherlands (*Moderator*) Nothing to Disclose Pamela K. Woodard, MD, Saint Louis, MO (*Moderator*) Researcher, Siemens AG; Research Grant, F. Hoffmann-La Roche Ltd; Consultant, Medtronic plc; ; ; ; ; ; Frandics P. Chan, MD, PhD, San Francisco, CA (*Moderator*) Nothing to Disclose

Sub-Events

SSM04-01 Overdiagnosis of Late Gadolinium Enhancement by Cardiovascular Magnetic Resonance

Wednesday, Dec. 4 3:00PM - 3:10PM Room: S404AB

Participants

Hui Zhou, MD, Changsha, China (*Presenter*) Nothing to Disclose Ping Hu, Changsha, China (*Abstract Co-Author*) Nothing to Disclose Zhenhua Chen, Changsha, China (*Abstract Co-Author*) Nothing to Disclose Moling Zhou, Changsha, China (*Abstract Co-Author*) Nothing to Disclose Yihua Huang, Shenzhen, China (*Abstract Co-Author*) Nothing to Disclose Rong Chen, Changsha, China (*Abstract Co-Author*) Nothing to Disclose

PURPOSE

To evaluate the rate of overdiagnosis of late gadolinium enhancement (LGE) by cardiac magnetic resonance (CMR) in a large-scale comprehensive university hospital.

METHOD AND MATERIALS

This study is a retrospective review of all cardiac magnetic resonance examinations performed in a comprehensive university hospital over a 18-month period. Studies originally reported as positive for myocardial LGE were retrospectively reinterpreted by three subspecialty cardiovascular radiologists with more than 5 years' experience. A CMR was considered negative for LGE when all three cardiovascular radiologists were in agreement that the CMR study was negative for LGE. The location and potential causes for LGE overdiagnosis were recorded.

RESULTS

A total of 523 CMR studies were performed over the study period. LGE was diagnosed in the initial report in 126 of these cases (24.1%). There was discordance between the cardiovascular radiologists and the original radiologist in 32 of 126 (25.4%) cases. Discordance occurred more often where there were partial volume effects (46.9%, 15/32): in interventricular septum caused by RV deep intertrabecular recesses were mistaken for stria LGE (40.0%, 6/15); in lateral wall caused by non-compacted myocardium were mistaken for subendocardial LGE (33.3%, 5/15); in RV insertion point caused by RV cavity were mistaken for patchy LGE (26.7%, 4/15). Crypt and diverticulum (18.8%, 6/32) were mistaken for indramyocardial (50.0%, 3/6) or subendocardial LGE (50.0%, 3/6). Pericardial fat were mistaken for epicardial LGE (15.6%, 5/32); False positive LGE (12.5%, 4/32) as detected by original observers due to a wrong inversion time (TI). Lipomatous metaplasia were mistaken for LGE (3.1%, 1/32). Congenital aneurysm in apical wall were mistaken for transmural LGE (3.1%, 1/32).

CONCLUSION

When compared with the consensus opinion of expert cardiovascular radiologists, we found a high rate of overdiagnosis of LGE by CMR In routine clinical practice. Improvements in the quality of CMR examination and increased recognition of potential diagnostic pitfalls in CMR are recommended to minimize misdiagnosis of LGE.

CLINICAL RELEVANCE/APPLICATION

LGEs diagnosed by CMR are frequently overdiagnosed, which appeared to be due to a lack of recognition of the false positive LGEs. Increased education among radiography technologists, radiologists, and clinicians regarding these imaging pitfalls should be encouraged.

SSM04-02 Single and Multiframe Super-Resolution: Feasibility for Cardiac MRI

Wednesday, Dec. 4 3:10PM - 3:20PM Room: S404AB

Awards

Trainee Research Prize - Medical Student

Participants

Evan Masutani, La Jolla, CA (*Presenter*) Nothing to Disclose Naeim Bahrami, PhD, MSc, San Diego, CA (*Abstract Co-Author*) Nothing to Disclose Albert Hsiao, MD,PhD, La Jolla, CA (*Abstract Co-Author*) Founder, Arterys, Inc; Consultant, Arterys, Inc; Shareholder, Arterys, Inc; Speaker, Bayer AG; Research Grant, Bayer AG; Speaker, General Electric Company; Research Grant, General Electric Company;

For information about this presentation, contact:

emasutan@ucsd.edu

PURPOSE

Cardiac MRI (cMRI) is the clinical reference standard for visual and quantitative assessment of heart function. However, MRI suffers from long acquisition times, averaging over multiple heart beats, and a tradeoff between spatial and temporal resolution. We investigated the use of convolutional neural networks (CNN) to recover spatial resolution of subsampled MR images with the goal of accelerating cMRI.

METHOD AND MATERIALS

With HIPAA compliance and IRB waiver of informed consent, we retrospectively collected 200 short axis (SAX) cine SSFP from cMRI examinations performed at our institution. Spatial-subsampling was simulated by zeroing outer k-space. We simulated downsampling factors ranging from 2-32x. We employed CNNs to perform single-frame and multi-frame superresolution, called k-SRNet and kt-SRNet respectively, to predict full-sampling from subsampled images. We used 70% of cases for training, 20% for validation, and 10% for testing. We compared SRNet and traditional methods of bicubic interpolation and Fourier-based zero-padding (Z-pad) by calculating the Structural Similarity Index (SSIM) between fully-sampled ground truth and each method of upscaling. We report the mean and standard deviation of SSIM and determine statistical significance using paired Student's t-test with type I error threshold of 0.05.

RESULTS

For single frame spatial superresolution (k-SRNet), mean SSIM was 0.943±0.022 for 8x, 0.878±0.036 for 16x, and 0.810±0.052 for 32x upsampling. For multiframe spatiotemporal superresolution (kt-SRNet), mean SSIM was 0.941±0.021 for 8x, 0.886±0.035 for 16x, and 0.816±0.052 for 32x upsampling. In comparison, bicubic interpolation yielded mean SSIM of 0.827±0.054 for 8x and 0.723±0.076 for 16x upsampling. Z-pad yielded mean SSIM of 0.924±0.029 for 8x and 0.857±0.047 for 16x upsampling. SRNet significantly outperformed traditional methods at all upscaling factors.

CONCLUSION

CNNs can recover spatial resolution from spatially subsampled MR images. Multiframe kt-SRNet yielded comparable results to k-SRNet in recovering image quality from spatial undersampling. Both k-SRNet and kt-SRNet appear to be superior to traditional methods of image upsampling, especially for higher upsampling factors.

CLINICAL RELEVANCE/APPLICATION

Convolutional neural networks have potential to reduce the sampling requirements for resolving cardiac structures in cardiac MRI, and may complement other techniques used to accelerate MRI.

SSM04-03 Biventricular and Left Atrial Myocardial Strain Assessment by MRI Feature Tracking in T2DM Patients with and without Hypertension

Wednesday, Dec. 4 3:20PM - 3:30PM Room: S404AB

Participants

Yukun Cao, Wuhan, China (*Presenter*) Nothing to Disclose Guozhu Shao, Wuhan, China (*Abstract Co-Author*) Nothing to Disclose Heshui Shi, MD, Wuhan, China (*Abstract Co-Author*) Nothing to Disclose

PURPOSE

The purpose of this study was to assess left atrium (LA), right ventricle (RV) and left ventricle(LV) strain in type 2 diabetes mellitus (T2DM) patients with and without hypertension using CMR feature tracking (FT) and their underlying relationships with clinical parameters.

METHOD AND MATERIALS

We recruited 20 T2DM patients without hypertension(T2DM-NHT) (mean age: 53 ± 7 years; 11 males), 20 T2DM patients with hypertension(T2DM-HT) and 40 controls matched for gender, age, and BMI to undergo CMR examinations. The LA , LV and RV myocardial strains were evaluated with using routine cine images based on feature-tracking software. The clinical baseline parameters were collected before the CMR examination.

RESULTS

The T2DM-NHT patients had significantly reduced LA global longitudinal (GLS), circumferential (GCS), radial strain (GRS), and RVGLS compared with those in the controls(LAGCS: 27.6 \pm 3.6% vs 33.9 \pm 8.7%; LAGRS: -29.2 \pm 4.7% vs -32.9 \pm 3.9%; LAGLS: 23.8 \pm 5.5% vs 30.9 \pm 6.0%; RVGLS: -22.1 \pm 3.3% vs -26.0 \pm 7.4%, p<0.05 for all). The T2DM-HT patients had significantly greater LAGCS, LAGRS and LAGLS compared with those in T2DM-NHT patients (LAGCS: 39.4 \pm 12.7% vs 27.6 \pm 3.6%; LAGRS: -34.8 \pm 7.3% vs -29.3 \pm 4.7%; LAGLS: 36.7 \pm 17.6% vs 23.8 \pm 5.5%, p<0.05 for all). However, the LA volume, the LV global systolic strain and routine cardiac function were similar between three groups. Moreover, in the diabetic patients, the LA GCS was independently associated with the microalbuminuria levels (standardized β =-0.56, p=0.023), and the LA GLS was independently correlated with diuretic treatment (standardized β =0.313, p=0.027).

CONCLUSION

T2DM-NHT patients with preserved LV function demonstrated impaired LAGRS, LAGLS, LAGCS and RVGLS compared with controls. Hypertension may compensatorily improve LA strain in T2DM patients, as opposed to the microalbuminuria levels. Diuretic treatment can help ameliorate LA function.

CLINICAL RELEVANCE/APPLICATION

In T2DM patients, the impact of hypertension, microalbuminuria levels and diuretic treatment on LA strain deserves further study.

SSM04-04 Association B-Type Natriuretic Peptide (BNP) of and Dialysis Vintage with CMRI- Derived Cardiac Indices in Stable Hemodialysis Patients with Preserved Left Ventricular Ejection Fraction

Wednesday, Dec. 4 3:30PM - 3:40PM Room: S404AB

Participants Xiaoyu Han, Wuhan, China (*Presenter*) Nothing to Disclose Heshui Shi, MD, Wuhan, China (*Abstract Co-Author*) Nothing to Disclose Yukun Cao, Wuhan, China (*Abstract Co-Author*) Nothing to Disclose

For information about this presentation, contact:

xiaoyuhan1123@163.com

PURPOSE

Cardiovascular disease (CVD) is a major cause of morbidity and mortality in (HD) patients. Native T1/T2 mapping and tissuetracking strain analysis by cardiac magnetic resonance imaging (CMRI) are proved to be useful as early quantitative techniques for evaluating myocardial tissue and mechanical alterations in HD patients. We aim to assess the left ventricular myocardial native T1/T2 values and systolic strains and the associations with B-type natriuretic peptide (BNP) and dialysis vintage in HD patients with a preserved left ventricular ejection fraction (LVEF).

METHOD AND MATERIALS

Forty-three stable HD patients (mean age: 59 ± 11 years; 28 males)with end-stage renal disease with a preserved LVEF (>=50%) and 28 healthy volunteers (mean age: 61 ± 7 years; 14 males)matched for sex, age, and body mass index. The native T1/T2 values of the left ventricular myocardium were measured on the T1 and T2 maps. The left ventricular global systolic strain was evaluated on routine cine images using prototype postprocessing software. BNP was measured at the time of CMR measurements.

RESULTS

Compared with controls, the global native T1 and T2 values were significantly higher in the HD patients than in the controls (native T1: $1056\pm32 \text{ ms vs.} 1006\pm25 \text{ ms}$, p<0.001; T2: $50\pm3 \text{ ms vs.} 46\pm2 \text{ ms}$, p<0.001). The mean peak global circumferential strain (GCS) and global longitudinal strain (GLS) were both significantly reduced in the HD patients compared with the controls (GCS: $-13\pm3 \text{ vs.} -16\pm3$, p<0.001; GLS: $-12\pm4 \text{ vs.} -15\pm3$, p=0.001). However, no significant difference was found between two groups regarding LVEF($61\pm8 \text{ vs } 64\pm8$, p=0.057). In HD patients, a significant positive correlation was found between T2 value and BNP levels (r=0.402,p<0.001). The GLS was independently correlated with the dialysis vintage in HD patients (standardized β =-0.321, p=0.044).

CONCLUSION

The HD patients with preserved LVEF have increased native T1/T2 value and decreased strain, while increased T2 values relates to high BNP. GLS may be improved in long-term HD patients.

CLINICAL RELEVANCE/APPLICATION

Multiple advanced CMR technologies, including native T1/T2 mapping and tissue-tracking analysis could detected early cardiomyopathy in HD patients without gadolinium-based contrast agents. The correlation of CMRI-derived cardiac indices with heart failure index BNP and dialysis vintage could help timely prevent cardiovascular disease and assess prognosis in HD patients.

SSM04-05 Preliminary Validation of Turbulent Kinetic Energy Measurement of HOCM by Using Multi-VENC 4D Flow MRI

Wednesday, Dec. 4 3:40PM - 3:50PM Room: S404AB

Participants

Kotomi Iwata, Tokyo, Japan (*Presenter*) Nothing to Disclose Tetsuro Sekine, MD, PhD, Tokyo, Japan (*Abstract Co-Author*) Nothing to Disclose Masaki Tachi, MD, PhD, Tokyo, Japan (*Abstract Co-Author*) Nothing to Disclose Yoichi Imori, Tokyo, Japan (*Abstract Co-Author*) Nothing to Disclose Junya Matsuda, Tokyo, Japan (*Abstract Co-Author*) Nothing to Disclose Yasuo Amano, MD, Tokyo, Japan (*Abstract Co-Author*) Nothing to Disclose Takahiro Ando, Tokyo, Japan (*Abstract Co-Author*) Nothing to Disclose Makoto Obara, Tokyo, Japan (*Abstract Co-Author*) Nothing to Disclose Makoto Obara, Tokyo, Japan (*Abstract Co-Author*) Nothing to Disclose Hitoshi Takano, Tokyo, Japan (*Abstract Co-Author*) Nothing to Disclose Shinichiro Kumita, MD, Tokyo, Japan (*Abstract Co-Author*) Nothing to Disclose

For information about this presentation, contact:

kotomi-iwata@nms.ac.jp

PURPOSE

In the patients with hypertrophic cardiomyopathy (HCM), the impairment of cardiac ejection efficiency due to the obstruction of left ventricle outflow tract (LVOT) relates to the HCM-related death. Recently, the turbulent kinetic energy (TKE) estimation based on 4D Flow MRI has been developed. Previous studies revealed that 4D Flow-based TKE measurement well correlates to the pressure drop at LVOT in the patients with aortic stenosis which has a similar physiological entity as HCM. The purpose of this study was to validate the clinical value of 4D Flow-based TKE measurement in the patients with HCM.

METHOD AND MATERIALS

From April 2018 to March 2019, we recruited consecutive 17 HCM patients. Based on echocardiography, they were assigned into obstructive HCM (HOCM) (9 patients, 67.0 ± 9.9 years old, 4 males) or non-obstructive HCM (HNCM) (8 patients, 68.9 ± 12.8 years old, 5 males). We also recruited 9 normal volunteers(30.9 ± 3.0 years old, 6 males). The parameters of 4D Flow MRI were as follows; resplution=1.7*1.7*2.0mm; Triple VENC acquisition = 50-150-450 cm/s; k-t PCA (acceleration factor, 5-7), free breath acquisition;

and acquisition time 8-15 min.). GT Flow (Gyrotools, Zurich, Switzerland) was used for analysis. The VOI from left ventricular to aortic arch was drawn semi-automatically. We defined TKEphase as the sum of entire VOI at each cardiac phase, and TKEpeak as the highest TKEphase in the all cardiac phase.

RESULTS

TKEpeak of HOCM is significantly higher than HNCM (p=0.008) or volunteers (p=0.002). TKEpeak correlated to max velocity (p=0.007, r=0.631) and maximum short dimeter of the valve orifice (p=0.006, r=-0.658). TKEpeak in the patients with systolic anterior movement (SAM) were significantly higher than without SAM (p=0.008). TKEpeak correlated to LV mass (p=0.035, r=0.514).

CONCLUSION

TKE measurement based on 4D Flow MRI can noninvasively detect the flow alteration induced not only by systolic flow jet but also by LVOT geometry such as SAM in the patients with HOCM. The elevated TKE correlates increasing LV mass. It may indicate that increasing cardiac load by the pressure loss due to turbulence induced the progression of LV mass. This physiology reaction is considered as the worse outcome.

CLINICAL RELEVANCE/APPLICATION

TKE measurement based on 4D Flow MRI can noninvasively detect the flow alteration in the patients with HOCM.

SSM04-06 T2 Mapping and Cardiac Stress Test to Detect and Monitor Myocardial Edema and Ischemia in Female Patients after Left-Sided Breast Cancer Radiation Therapy

Wednesday, Dec. 4 3:50PM - 4:00PM Room: S404AB

Participants

Enver G. Tahir, MD, Hamburg, Germany (Presenter) Nothing to Disclose Sahar Shihada, Hamburg, Germany (Abstract Co-Author) Nothing to Disclose Manuella Azar, Hamburg, Germany (Abstract Co-Author) Nothing to Disclose Jitka Starekova, Hamburg, Germany (Abstract Co-Author) Nothing to Disclose Malte L. Warncke, MD, Hamburg, Germany (Abstract Co-Author) Nothing to Disclose Yvonne Goy, Hamburg, Germany (Abstract Co-Author) Nothing to Disclose Cordula L. Petersen, Dresden, Germany (Abstract Co-Author) Nothing to Disclose Katharina Seiffert, Hamburg, Germany (Abstract Co-Author) Nothing to Disclose Volkmer Muller, Hamburg, Germany (Abstract Co-Author) Nothing to Disclose Isabell Witzel, Hamburg, Germany (Abstract Co-Author) Nothing to Disclose Ulf K. Radunski, Hamburg, Germany (Abstract Co-Author) Nothing to Disclose Sebastian Bohnen, Hamburg, Germany (Abstract Co-Author) Nothing to Disclose Jan Schneider, Hamburg, Germany (Abstract Co-Author) Nothing to Disclose Kai Muellerleile, Hamburg, Germany (Abstract Co-Author) Nothing to Disclose Gerhard B. Adam, MD, Hamburg, Germany (Abstract Co-Author) Nothing to Disclose Gunnar K. Lund, MD, Hamburg, Germany (Abstract Co-Author) Nothing to Disclose

For information about this presentation, contact:

e.tahir@uke.de

PURPOSE

To detect and monitor subclinical cardiomyopathy by cardiac magnetic resonance (CMR) in female patients with first-time diagnosis of left-sided breast cancer following radiation therapy.

METHOD AND MATERIALS

27 female patients (56 ±14 years) with newly diagnosed breast cancer underwent serial 3 Tesla CMR (Ingenia, Philips Medical Systems). Baseline (BL) CMR was performed 18 ±16 days before the start of a left-sided radiation. None of the patients received chemotherapy. First follow-up (FU1) CMR was 7 ±12 days and second follow-up (FU2) 12 ±1 months after completion of radiotherapy. A free-breathing, navigator-gated multi-echo sequence was used for short-axis T2 mapping. Cardiac stress test was performed at 400 μ g regadenoson stress on 3 representative short axis slices (basal, midventricular and apical) using an ultrafast gradient echo sequence.

RESULTS

A mean radiation dose of 47 ±4 Gy was applied with a calculated mean cardiac dose of 2.4 ±2.3 Gy. High sensitive Troponin T increased immediately after radiation therapy (5 ±2 vs. 6 ±3 pg/ml, P<0.05) and declined to baseline values on FU2 (6 ±3 vs. 5 ±2 pg/ml, P<0.05). NT-proBNP and creatine kinase remained unchanged throughout the observation period. LVEF was constant between BL and FU1 (62 ±5 vs. 64 ±6%, P=0.218) and FU1 and FU2 (64 ±6 vs. 62 ±5%, P=0.171). LVEDV declined on FU1 (78 ±10 vs. 75 ±11 ml/m2, P<0.05) and remained decreased on FU2 (72 ±11 ml/m2, P<0.05). RVEDV declined between BL and FU2 (81 ±12 vs. 75 ±13 ml/m2, P<0.05). T2 relaxation times increased on FU1 (47 ±2 vs. 48 ±4 ms, P<0.05) and declined on FU2 (47 ±2 ms, P=0.092). On visual evaluation cardiac stress test did not detect any myocardial ischemia after radiation therapy.

CONCLUSION

Radiation treatment of female left-sided breast cancer can lead to development of myocardial edema and troponin increase in the early phase following therapy, which subside within the first 12 months. Both ventricular volumes decrease after radiation therapy. There is no evidence of myocardial ischemia development within the first 12 months post-radiation.

CLINICAL RELEVANCE/APPLICATION

Development of myocardial edema and decreased of ventricular volumes might be used as indicators for subclinical cardiomyopathy in patients with left-sided breast cancer undergoing radiation therapy.





SSM12

Genitourinary (Bi-Parametric versus Multi-Parametric Prostate MRI)

Wednesday, Dec. 4 3:00PM - 4:00PM Room: N229



AMA PRA Category 1 Credit ™: 1.00 ARRT Category A+ Credit: 1.00

FDA Discussions may include off-label uses.

Participants

Valeria Panebianco, MD, Rome, Italy (*Moderator*) Nothing to Disclose Temel Tirkes, MD, Indianapolis, IN (*Moderator*) Nothing to Disclose

Sub-Events

SSM12-01 The Added Value of Dynamic Contrast Enhanced Sequences for Detection of Clinically Significant Prostate Cancer: Results from the PROMIS Study

Wednesday, Dec. 4 3:00PM - 3:10PM Room: N229

Participants

Ahmed El-Shater Bosaily, PhD,MSc,MBBCh, London, United Kingdom (*Presenter*) Nothing to Disclose Elena Frangou, London, United Kingdom (*Abstract Co-Author*) Nothing to Disclose Hashim Ahmed, London, United Kingdom (*Abstract Co-Author*) Nothing to Disclose Mark Emberton, London, United Kingdom (*Abstract Co-Author*) Nothing to Disclose Richard Kaplan, London, United Kingdom (*Abstract Co-Author*) Nothing to Disclose Louise Brown, London, United Kingdom (*Abstract Co-Author*) Nothing to Disclose Alex P. Kirkham, MBChB, MD, London, United Kingdom (*Abstract Co-Author*) Nothing to Disclose

For information about this presentation, contact:

ashater@nhs.net

PURPOSE

Multiparametric MRI(MP-MRI) is now a well-established tool in the prostate cancer diagnostic pathway. Recently, the optimal combination of sequences has come into question with opposing views on the added value of dynamic contrast enhanced sequences (DCE). The main phase of the PROMIS (Prostate MRI Imaging Study) trial was adapted to provide a prospective analysis of the incremental value of diffusion (DWI) and DCE sequences in detection of significant cancer.

METHOD AND MATERIALS

497 biopsy naïve men underwent standardized MP-MRIs using T2, DWI (including a dedicated long b sequence) and DCE, followed by a detailed transperineal prostate mapping biopsy covering the whole prostate in 0.5cm intervals. In one sitting, the radiologist assigned a Likert score of 1-5 for the presence of significant tumour, in sequence, for the T2 images, then T2+DWI images , and finally T2+DWI+DCE images. For the primary analysis, a score of >/= 3 was considered positive for clinically significant cancer. Each combination was assessed against the primary PROMIS outcome measure of significance (>/= Gleason 4+3 tumour or >/=6mm maximum cancer core length) on biopsy.

RESULTS

The addition of DCE to T2+DWI resulted in a sensitivity of 95% vs 94%, specificity of 38% vs 37%, positive predictive value of 51% vs 51% and negative predictive value of 90% vs 91% respectively. Marginally more patients could avoid biopsy (score of 2/5 or less) with DCE (123/497 vs 121/497 patients). There was some evidence that contrast reduced the number of equivocal scores: 36% of positive patients were classified as equivocal (3/5) with addition of DCE compared to 42% on T2+DWI alone. The proportion of equivocal (3/5) and positive (4-5/5) cases showing significant tumour were similar (20% and 69 % with DCE, 23% and 71% with T2+DWI alone). None of these differences were statistically significant. No dominant Gleason pattern 4 disease or higher was missed with T2+DWI+DCE, compared to a single case with T2+DWI.

CONCLUSION

DCE did not significantly improve sensitivity or specificity. One dominant Gleason 4 tumour was missed using T2+DWI and none missed with DCE. Though not statistically significant, fewer cases were scored equivocal with the addition of DCE.

CLINICAL RELEVANCE/APPLICATION

The addition of DCE to T2+DWI in a prospective, multi centre study of prostate MRI did not result in convincing improvements in accuracy or a reduction in the number of men recommended for biopsy.

SSM12-02 Comparison of Biparametric and Multiparametric MRI in the Diagnosis of Prostate Cancer

Wednesday, Dec. 4 3:10PM - 3:20PM Room: N229

Gu Mu Yang Zhang, MD, Beijing, China (*Abstract Co-Author*) Nothing to Disclose Zhengyu Jin, Beijing, China (*Abstract Co-Author*) Nothing to Disclose Hao Sun, MD, Beijing, China (*Abstract Co-Author*) Nothing to Disclose

PURPOSE

To compare the diagnostic accuracy of biparametric MRI (bpMRI) and multiparametric MRI (mpMRI) for prostate cancer (PCa) and clinically significant prostate cancer (csPCa), and to explore the application value of dynamic contrast-enhanced (DCE) MRI in prostate imaging.

METHOD AND MATERIALS

This study retrospectively enrolled 235 patients with suspected PCa in our hospital from 2016 to 2017. The lesions were scored according to the Prostate Imaging Reporting and Data System version 2 (PI-RADS V2). The bpMRI and mpMRI scores were recorded to plot the receiver operating characteristic curve (ROC). Area under the curve (AUC), accuracy, sensitivity, specificity, negative predictive value (NPV), and positive predictive value (PPV) for each method were calculated and compared. The patients were further stratified according to bpMRI scores for the application value of DCE MRI.

RESULTS

The AUC values of bpMRI and mpMRI for PCa were comparable (0.790 and 0.791, respectively). The accuracy, sensitivity, specificity, PPV and NPV of bpMRI for PCa were 76.2%, 79.5%, 72.6%, 75.8%, and 76.6%; and the values for mpMRI were 77.4%, 84.4%, 69.9%, 75.2%, and 80.6%, respectively. For the diagnosis of csPCa, the AUC values of bpMRI and mpMRI were similar (0.781 and 0.779, respectively). The accuracy, sensitivity, specificity, PPV and NPV of bpMRI for csPCa were 74.0%, 83.8%, 66.9%, 64.8%, and 85.0%; and 73.6%, 87.9%, 63.2%, 63.2%, and 87.8% for mpMRI. For patients with bpMRI score >= 3, the difference in DCE between PCa and non-PCa, and between csPCa and non-csPCa were both statistically significant (both P = 0.001). Further stratification analysis showed that for patients with bpMRI score = 4, DCE had statistically significant difference between PCa and non-PCa, and between csPCa (P = 0.003, and P < 0.001, respectively).

CONCLUSION

The diagnostic accuracy of bpMRI is comparable with that of mpMRI in the detection of PCa and identification of csPCa. DCE is helpful in further identifying PCa and csPCa lesions in patients with bpMRI >= 3, especially bpMRI = 4, which may be conductive to achieve more accurate PCa risk stratification.

CLINICAL RELEVANCE/APPLICATION

For patients with suspected PCa, DCE may improve the tumor detection and aggressiveness classification. Rather than omitting DCE, we think further comprehensive studies are required for prostate MRI.

SSM12-03 Comparison of Bi-Parametric MRI Based Artificial Intelligence and Multi-Parametric MRI in Detection of Intraprostatic Lesions: A Multi-Reader Study

Wednesday, Dec. 4 3:20PM - 3:30PM Room: N229

Participants

Sherif Mehralivand, MD, Bethesda, MD (Presenter) Nothing to Disclose Stephanie A. Harmon, PhD , Bethesda, MD (Abstract Co-Author) Research funded, NCI Nathan S. Lay, PhD, Bethesda, MD (Abstract Co-Author) Nothing to Disclose Clayton P. Smith, BA, Bethesda, MD (Abstract Co-Author) Nothing to Disclose Thomas H. Sanford, Bethesda, MD (Abstract Co-Author) Research collaboration, NVIDIA Corporation Sonia Gaur, MD, Philadelphia, PA (Abstract Co-Author) Nothing to Disclose Jonathan J. Sackett, BS, Bethesda, MD (Abstract Co-Author) Research collaboration, NVIDIA Corporation Ronaldo H. Baroni, MD, Sao Paulo, Brazil (Abstract Co-Author) Nothing to Disclose Karabekir Ercan, Ankara, Turkey (Abstract Co-Author) Nothing to Disclose Peter Pinto, Bethesda, MD (Abstract Co-Author) Nothing to Disclose Andrei S. Purysko, MD, Westlake, OH (Abstract Co-Author) Nothing to Disclose Soroush Rais-Bahrami, MD, Birmingham, AL (Abstract Co-Author) Consultant, Koninklijke Philips NV; Consultant, Blue Earth Diagnostics Ltd; Consultant, Genomic Health, Inc Victor M. Tonso, MD, Sao Paulo, Brazil (Abstract Co-Author) Nothing to Disclose Bradford J. Wood, MD, Bethesda, MD (Abstract Co-Author) Researcher, Koninklijke Philips NV; Researcher, Celsion Corporation; Researcher, BTG International Ltd; Researcher, Siemens AG; Researcher, XAct Robotics; Researcher, NVIDIA Corporation; Intellectual property, Koninklijke Philips NV; Intellectual property, BTG International Ltd; Royalties, Invivo Corporation; Royalties, Koninklijke Philips NV; Equipment support, AngioDynamics, Inc; Researcher, Profound Medical Inc; Researcher, Canon Medical Systems Corporation; Researcher, AstraZeneca PLC; Researcher, Exact Imaging Inc Jennifer Gordetsky, MD, Birmingham, AL (Abstract Co-Author) Nothing to Disclose Maria Merino, MD, Bethesda, MD (Abstract Co-Author) Nothing to Disclose Tristan Barrett, MBBS, Cambridge, United Kingdom (Abstract Co-Author) Nothing to Disclose Leonardo K. Bittencourt, MD, PhD, Rio de Janeiro, Brazil (Abstract Co-Author) Nothing to Disclose Mehmet Coskun, MD, Ankara, Turkey (Abstract Co-Author) Nothing to Disclose Christopher M. Knaus, MD, Bethesda, MD (Abstract Co-Author) Nothing to Disclose Yan Mee Law, MBBS, Singapore, Singapore (Abstract Co-Author) Nothing to Disclose Ashkan A. Malayeri, MD, Andover, MA (Abstract Co-Author) Nothing to Disclose Daniel J. Margolis, MD, New York, NY (Abstract Co-Author) Consultant, Blue Earth Diagnostics Ltd Jamie Marko, MD, Bethesda, MD (Abstract Co-Author) Nothing to Disclose Derya Yakar, MD, PhD, Groningen, Netherlands (Abstract Co-Author) Nothing to Disclose Peter L. Choyke, MD, Rockville, MD (Abstract Co-Author) Nothing to Disclose Ronald M. Summers, MD, PhD, Bethesda, MD (Abstract Co-Author) Royalties, iCAD, Inc; Royalties, Koninklijke Philips NV; Royalties, ScanMed, LLC; Royalties, Ping An Insurance Company of China, Ltd; Research support, Ping An Insurance Company of China, Ltd; Research support, NVIDIA Corporation; ;;;

Baris Turkbey, MD, Bethesda, MD (*Abstract Co-Author*) Research support, Koninklijke Philips NV; Royalties, Invivo Corporation; Investigator, NVIDIA Corporation

turkbeyi.mail.nih.gov

PURPOSE

To compare a bi-parametric magnetic resonance imaging (bMRI) based artificial intelligence (AI) system which provides proposed regions of interests (ROI) overlaid on T2 weighted (T2W) with multi-parametric MRI (mpMRI) using PI-RADSv2 guided interpretation.

METHOD AND MATERIALS

Case and control patients were collected from 5 institutions and 9 radiologists from 9 different institutions participated as readers: 3 highly, 3 moderately, 3 less-experienced in reading prostate MRI. Patients were consecutive at each institution and underwent 3T mpMRI (T2W, ADC map, b-1500, DCE MRI). Case patients had subsequent radical prostatectomy with pathology mapping available, control patients had negative MRI and negative systematic biopsy. Two interpretation arms were executed with readers blinded to pathology: an mpMRI-alone arm utilizing PI-RADSv2 guidelines, then after 4-week washout, a first-reader AI-assisted arm. Lesion detection sensitivity was calculated for whole prostate. Per-lesion specificity was calculated on the AI-assisted arm on a per-ROI level.

RESULTS

153 case and 84 control patients were included across 5 institutions. For mpMRI-alone interpretation, lesion-based sensitivity was 62.2%, 63%, 65.3% and 58.2% for overall, high, moderate and low-experienced readers, respectively. For bMRI based AI system assisted interpretation, lesion-based sensitivity was 66.5%, 67.8%, 71.7% and 59.9% for overall, high, moderate and low-experienced readers, respectively. At threshold of PI-RADS >=3, specificity of AI assisted bMRI were 81.1%, 86.3%, 70.2% and 86.8% for overall, high, moderate and low-experienced readers, respectively.

CONCLUSION

AI-assisted bi-parametric MRI reads demonstrated higher sensitivities compared to multiparametric MRI reads at all experience categories for radiologists.

CLINICAL RELEVANCE/APPLICATION

AI-assisted MRI reads can standardize and improve prostate MRI reporting.

SSM12-04 Value of Dynamic Contrast Enhanced (DCE) MR Imaging for Patients in PI-RADS 4 Category

Wednesday, Dec. 4 3:30PM - 3:40PM Room: N229

Participants

Tim Ulirich, Duesseldorf, Germany (*Abstract Co-Author*) Nothing to Disclose Lars Schimmoeller, MD, Dusseldorf, Germany (*Abstract Co-Author*) Nothing to Disclose Farid Ziayee, Dusseldorf, Germany (*Presenter*) Nothing to Disclose Michael Quentin, MD, Duesseldorf, Germany (*Abstract Co-Author*) Nothing to Disclose Christian Arsov, MD, Duesseldorf, Germany (*Abstract Co-Author*) Nothing to Disclose Gerald Antoch, MD, Dusseldorf, Germany (*Abstract Co-Author*) Nothing to Disclose

PURPOSE

To assess the impact of dynamic contrast-enhanced imaging (DCE) in mp-MRI on prostate cancer (PCa) detection in a large patient cohort assigned to PI-RADS category 4.

METHOD AND MATERIALS

This prospective, single center cohort study includes 193 consecutive patients with PI-RADS assessment category 4 after mp-MRI (T2WI, DWI, DCE) at 3T with combined targeted plus systematic biopsy as reference standard. Prostate cancer detection with DCE and without inclusion of DCE upgraded lesions was compared.

RESULTS

Overall PCa detection rate in PI-RADS-4-patients was 62% (119/193) with DCE and 52% (101/193) without inclusion of DCE upgraded lesions; 48% (92/193) had clinically significant PCa (csPCa; Gleason score >=3+4=7) and 40% (78/193) without use of DCE. 38 of the 193 patients (20%) had peripheral lesions upgraded from PI-RADS category 3 to an overall PI-RADS category 4 due to focal positive DCE findings. Of these 38 patients 18 had PCa including 14 with a csPCa. Thus, 15% (18/119) of the patients with any prostate cancer and 15% (14/92) of the patients with csPCa were detected only based on additional DCE information.

CONCLUSION

DCE allows detection of a significant number of mostly csPCa in PI-RADS-4-patients and thus improves detection rates. The current PI-RADS decision rules regarding upgrading PI-RADS-3-lesions to overall category 4 due to positive DCE imaging are useful for PCa detection.

CLINICAL RELEVANCE/APPLICATION

Patients assigned to PI-RADS category 3 benefit from DCE for primary (early) tumor detection.

SSM12-05 Comparison of Standard Multiparametric and Unenhanced Biparametric MRI in Men with Elevated Prostate-Specific Antigen

Wednesday, Dec. 4 3:40PM - 3:50PM Room: N229

Participants

Filippo Pesapane, MD, Milan, Italy (*Presenter*) Nothing to Disclose Giorgio Maria Agazzi, Brescia, Italy (*Abstract Co-Author*) Nothing to Disclose Marzia Acquasanta, Milan, Italy (*Abstract Co-Author*) Nothing to Disclose Priyan Tantrige, London, United Kingdom (*Abstract Co-Author*) Nothing to Disclose Chiara A. Mattiuz, MD, Milan, Italy (*Abstract Co-Author*) Nothing to Disclose Francesco Sardanelli, MD, San Donato Milanese, Italy (*Abstract Co-Author*) Speakers Bureau, Bracco Group Advisory Board, Bracco Group Research Grant, Bayer AG Advisory Board, General Electric Company Reserach Grant, General Electric Company Speakers Bureau, Siemens AG Reserach Grant, Real Imaging Ltd Marina Codari, MENG,PhD, San Donato Milanese, Italy (*Abstract Co-Author*) Nothing to Disclose

Anastasia Esseridou, MD, San Donato Milanese, Italy (Abstract Co-Author) Nothing to Disclose

For information about this presentation, contact:

filippo.pesapane@unimi.it

PURPOSE

Multiparametric MRI (mpMRI) for prostate cancer (PCa) is usually composed of diffusion-weighted (DW), T2W and dynamic contrast enhancement (DCE) sequences. We compared biparametric MRI (bpMRI) composed of T2W and DW against mpMRI in patients with elevated prostate-specific antigen (PSA).

METHOD AND MATERIALS

1.5-T prostate MR was performed in 431 men (61.5+/-8.3 years) with PSA>4.0 ng/mL and included in a retrospective analysis. bpMRI and mpMRI were independently assessed in separate sessions >1 month apart in a random order by 2 readers with 5 (R1) and 3 years (R2) experience, using the PI-RADS2 criteria. Histopathology or >=2 years of follow-up served as a reference standard. PI-RADS score 3 was the threshold for a positive exam. Sensitivity and specificity were calculated with their 95% confidence interval (CI); McNemar and Cohen's K statistics were also used.

RESULTS

Population consisted in 195/431 (45,3%) histopathologically proven PCa, with 62/195 (31.8%) high-grade- (GS>=7b) and 133/195 (68.2%) low-grade-PCa. PCa could be excluded by histopathology in 58/431 (13.5%) patients and by follow-up in 178/431 (41.3%) patients. For bpMRI, sensitivity was 164/195 (84%, 95%CI 79-89%) for R1 and 156/195 (80%, 95%CI 74-86%) for R2; specificity was 182/236 (77%, 95%CI 72-82%) for R1 and 175/236 (74%, 95%CI 68-80%) for R2. For mpMRI, the sensitivity was 168/195 (86%, 95%CI 81-91%) for R1 and 160/195 (82%, 95%CI 77-87%) for R2; the specificity was 184/236 (78%, 95%CI 73-83%) for R1 and 177/236 (75%, 95%CI 69-81%) for R2. Omitting the DCE sequences (namely, using bpMRI) changed the PIRADS2 scores in 25/431 (5.8%) patients for R1 and in 35/431 (8.1%) patients for R2, when compared to mpMRI. PI-RADS score 3 increased by 5.3% for R1 and 7.4% for R2. bpMRI resulted in 4 more false negatives, compared to mpMRI, for both R1 and R2 and all of these were low-grade PCa. No high-grade PCa was missed with bpMRI. Not significant differences in accuracy were observed with both approaches by each readers (p>0.08). Interobserver agreement was substantial for both bpMRI (κ =0.802) and mpMRI (κ =0.787).

CONCLUSION

Diagnostic performance of bpMRI and mpMRI were similar, with no change in the detection of high-grade PCa

CLINICAL RELEVANCE/APPLICATION

bpMRI for PCa's detection could eliminate the adverse events and the retention of gadolinium, shorten time and reduce costs, possibly resulting in increased accessibility of MRI for men with elevated PSA

SSM12-06 Comparison of Measured Ultra-High b-Value ADC to Quantitative DCE for Enhancing Bi-Parametric (T2w and DWI) MRI Assessment of Clinically Significant Prostate Cancer

Wednesday, Dec. 4 3:50PM - 4:00PM Room: N229

Participants

Anoshirwan A. Tavakoli, MD, Heidelberg, Germany (*Presenter*) Nothing to Disclose Tristan A. Kuder, PhD, Heidelberg, Germany (*Abstract Co-Author*) Nothing to Disclose Jan P. Radtke, Heidelberg, Germany (*Abstract Co-Author*) Nothing to Disclose Viktoria Schutz, Heidelberg, Germany (*Abstract Co-Author*) Nothing to Disclose Magdalena Gortz, Heidelberg, Germany (*Abstract Co-Author*) Nothing to Disclose Markus Hohenfellner, MD, PhD, Heidelberg, Germany (*Abstract Co-Author*) Nothing to Disclose Heinz-Peter W. Schlemmer, MD, Heidelberg, Germany (*Abstract Co-Author*) Nothing to Disclose David Bonekamp, MD, PhD, Heidelberg, Germany (*Abstract Co-Author*) Speaker, Profound Medical Inc

For information about this presentation, contact:

s.tavakoli@gmx.de

PURPOSE

To compare the added diagnostic value of measured ultra-high b-value (UHB) - derived apparent diffusion coefficient (ADC) to quantitative normalized DCE assessment for the enhancement of bi-parametric (T2w and ADC) MRI for the prediction of clinically significant prostate cancer (sPC).

METHOD AND MATERIALS

73 consecutive patients (67.2 \pm 7.7 years, PSA 10.7 \pm 18.1 ng/dl) underwent prostate MRI at 3T (Magnetom Prisma) with EPI-DWI images acquired at b=50/500/1000/1500 s/mm2 as well as at b=100/500/1000/2250/3000/4000 s/mm2. Extended systematic and targeted MRI/TRUS fusion biopsies based on prospective clinical reads were matched to a second, retrospective blinded read and MR lesions segmented manually. ADC, UHB-ADC100,4000, early arterial DCE lesion contrast to surrounding parenchyma (nDCE) and T2w intensity normalized to pectineus muscle (nT2w) were extracted from each lesion. Three logistic regression models were created for prediction of sPC defined as Gleason Grade Group (GGG) >= 2: Model A (nT2w, ADC), model B (nT2w, ADC, nDCE) and model C (nT2w, ADC, UHB-ADC). For evaluation of the models AUC was calculated from ROC curves and Chi-square analysis of deviance or Vuong's test were used to compare the models.

RESULTS

In 73 patients 55 MRI-detected retrospectively validated MR-lesions revealed no cancer in 23 lesions (42%), GGG=1 in 10 lesions (18%), GGG=2 in 12 lesions (22%), GGG=3 in 4 lesions (7%), GGG=4 in 4 lesions (7%) and GGG=5 in 2 lesions (4%). Model A yielded an AUC of 0.810 (sensitivity 80%, specificity 73%), model B yielded an AUC of 0.840 (sensitivity 80%, specificity 79%) and model C

yielded an AUC of 0.806 (sensitivity 80%, specificity 73%), indicating a slightly higher AUC for model B when compared to model A and C (p=0.04 and p=0.13) and a comparable AUC between model A and C (p=0.76).

CONCLUSION

Measured UHB-ADC achieved no improvement in predictive performance over bi-parametric assessment with ADC and T2w, whereas added quantitative normalized DCE did improve predictive performance.

CLINICAL RELEVANCE/APPLICATION

Measured UHB-ADC does not provide a contrast-free alternative to DCE for the enhancement of bi-parametric prostate MRI.







MSSR44

RSNA/ESR Sports Imaging Symposium: Postoperative Imaging of Sports Injuries (Interactive Session)

Wednesday, Dec. 4 3:30PM - 5:00PM Room: E350



AMA PRA Category 1 Credits ™: 1.50 ARRT Category A+ Credit: 1.75

Participants

Andrew J. Grainger, MD, Leeds, United Kingdom (*Moderator*) Consultant, Levicept Ltd; Director, The LivingCare Group; Laura W. Bancroft, MD, Venice, FL (*Moderator*) Author with royalties, Wolters Kluwer nv; Editor, Thieme Medical Publishers, Inc; Travel support, Thieme Medical Publishers, Inc;;

For information about this presentation, contact:

laurabancroftmd@gmail.com

LEARNING OBJECTIVES

1) To review MRI findings of ACL reconstruction and cartilage repair. 2) To review the expected and abnormal MR imaging findings after labral repair, capsular shift/capsulorrhaphy and Laterjet/Bristow procedures. 3) To consolidate the knowledge gained from the session with interactive cases of postoperative sports imaging.

Sub-Events

MSSR44A Postoperative Shoulder MRI after Instability Surgery

Participants

Laura W. Bancroft, MD, Venice, FL (*Presenter*) Author with royalties, Wolters Kluwer nv; Editor, Thieme Medical Publishers, Inc; Travel support, Thieme Medical Publishers, Inc;

For information about this presentation, contact:

laurabancroftmd@gmail.com

LEARNING OBJECTIVES

1) To become familiar with the expected and abnormal MR imaging findings after labral repair. 2) To learn about the postoperative imaging features after capsular shift/capsulorrhaphy. 3) To appreciate normal imaging and complications after remplissage and Laterjet/Bristow procedures.

ABSTRACT

Purpose: To become familiar with the expected and abnormal MR imaging findings after labral repair, capsular shift/capsulorrhaphy, remplissage and Latarjet/Bristow procedures. Methods and Materials: MR imaging will be used to demonstrate the various normal and abnormal imaging appearances after shoulder instability surgery. Results/Conclusion: Labral re-tear will be evident as contrast or joint fluid extension into linear or complex tear cleft, absent/truncated/fragmented labrum, or labral displacement from anatomic location. Capsular shift results in smaller capacity joint and sometimes irregular capsular nodularity. Complications of capsulorrhaphy include capsular tears and subluxation of humeral head. Postoperative MR imaging can evaluate healing after combined remplissage and Bankart repair for moderate size, engaging Hill-Sachs lesions. Laterjet and Bristow procedures may be performed in patients with recurrent dislocations and glenoid deficiency. Incorporated bone will yield non-anatomic glenoid configuration, and complications include non-union, fatty degeneration of subscapularis muscle, and osteoarthrosis.

MSSR44B ACL Reconstruction and Cartilage Repair

Participants

Claudia Weidekamm, MD, Auckland, New Zealand (Presenter) Nothing to Disclose

For information about this presentation, contact:

claudia.weidekamm@meduniwien.ac.at

LEARNING OBJECTIVES

1) To review the common and uncommon ACL reconstruction techniques. 2) To appreciate the expected and abnormal MR imaging findings after ACL reconstruction. 3) To understand common cartilage repair techniques, and corresponding normal and abnormal postoperative MRIs.

ABSTRACT

The aim of ACL reconstruction is to stabilize the knee and prevent chondral and meniscal injuries, which are sequelae of anteroposterior translation and are associated with early osteoarthritis. The idea of the double-bundle ACL graft was to restore normal joint kinematics by anatomic reconstruction of the anteromedial and the posterolateral bundle of the original ACL. This was expected to improve clinical outcomes and restore anterior and rotational knee stability. The single-bundle technique, however, causes less osseous defects and is still a popular technique. Complications, such as ACL graft failure, impingement, cyclops lesion, arthrofibrosis, and patellar inferior syndrome, are discussed. The second part of this presentation will illustrate cartilage repair techniques and imaging findings. The radiologist must be familiar with the different cartilage repair procedures and characteristics in

cartilage imaging to evaluate long-term progression or failure. Abnormal postoperative findings include hypertrophic filling, incomplete integration of the transplant into the surrounding cartilage, or subchondral defects, osteophytes, cysts, and persistent bone marrow edema and joint effusion.

MSSR44C Interactive Case Discussion

Participants

Laura W. Bancroft, MD, Venice, FL (*Presenter*) Author with royalties, Wolters Kluwer nv; Editor, Thieme Medical Publishers, Inc; Travel support, Thieme Medical Publishers, Inc;

Claudia Weidekamm, MD, Auckland, New Zealand (Presenter) Nothing to Disclose

For information about this presentation, contact:

laurabancroftmd@gmail.com

LEARNING OBJECTIVES

1) To review the expected and abnormal MR imaging findings after labral repair, capsular shift/capsulorrhaphy and Laterjet/Bristow procedures in a case-based format. 2) To become familiar with the diagnosis features of failed ACL reconstructions, intact and failed cartilage repair. 3) To consolidate the knowledge gained from the session with interactive cases of postoperative sports imaging.

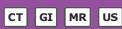




SPSC42

Controversy Session: Hepatocellular Carcinoma: Should We Use CT, MR, or US?

Wednesday, Dec. 4 4:30PM - 6:00PM Room: N227B



AMA PRA Category 1 Credits ™: 1.50 ARRT Category A+ Credit: 1.75

Participants

Claude B. Sirlin, MD, San Diego, CA (*Moderator*) Research Grant, Gilead Sciences, Inc; Research Grant, General Electric Company; Research Grant, Siemens AG; Research Grant, Bayer AG; Research Grant, Koninklijke Philips NV; Consultant, AMRA AB; Consultant, Fulcrum; Consultant, IBM Corporation; Consultant, Exact Sciences Corporation; Consultant, Boehringer Ingelheim GmbH; Consultant, Arterys Inc; Consultant, Epigenomics; Author, Medscape, LLC; Lab service agreement, Gilead Sciences, Inc; Lab service agreement, ICON plc; Lab service agreement, Intercept Pharmaceuticals, Inc; Lab service agreement, Shire plc; Lab service agreement, Enanta; Lab service agreement, Takeda Pharmaceutical Company Limited; Lab service agreement, Alexion Pharmaceuticals, Inc; Lab service agreement, NuSirt Biopharma, Inc

R. Brooke Jeffrey Jr, MD, Stanford, CA (Moderator) Nothing to Disclose

LEARNING OBJECTIVES

1) To understand the need for screening and surveillance for HCC in cirrhosis. 2) To understand that ultrasound is currently recommended as the primary modality for this purpose by all national and international guidelines. 3) To understand the advantages and disadvantages of ultrasound, CT, and MRI for HCC screening and surveillance in cirrhosis.

Sub-Events

SPSC42A Overview of HCC Screening and Surveillance: Definitions, Rationale, Basic Concepts, Current Guidelines, USA Landscape, Worldwide Landscape

Participants

Aya Kamaya, MD, Stanford, CA (Presenter) Royalties, Reed Elsevier; Researcher, Koninklijke Philips NV; Researcher, Siemens AG

SPSC42B Why Ultrasound Should Be Used for HCC Screening/Surveillance

Participants

Shuchi K. Rodgers, MD, Philadelphia, PA (Presenter) Nothing to Disclose

SPSC42C Why CT Should Be Used for HCC Screening/Surveillance

Participants

Avinash R. Kambadakone, MD, Boston, MA (*Presenter*) Research Grant, General Electric Company; Research Grant, Koninklijke Philips NV

For information about this presentation, contact:

akambadakone@mgh.harvard.edu

LEARNING OBJECTIVES

1) Understand the role of CT in the diagnosis of HCC. 2) Learn the limitations of CT in HCC screening including radiation dose and strategies to diminish the risk. 3) Review innovations in CT and its impact on screening of HCC.

SPSC42D Why MRI Should Be Used for HCC Screening/Surveillance

Participants Takeshi Yokoo, MD, PhD, Dallas, TX (*Presenter*) Nothing to Disclose

For information about this presentation, contact:

Takeshi.Yokoo@UTSouthwestern.EDU





MSCM51

Case-based Review of Magnetic Resonance (Interactive Session)

Thursday, Dec. 5 8:30AM - 10:00AM Room: S100AB



AMA PRA Category 1 Credits ™: 1.50 ARRT Category A+ Credit: 1.75

FDA Discussions may include off-label uses.

Participants

Jorge A. Soto, MD, Boston, MA (Director) Royalties, Reed Elsevier

For information about this presentation, contact:

jorge.soto@bmc.org

LEARNING OBJECTIVES

1) Review key MR imaging findings of common and infrequent conditions of various organs in adult and pediatric patients. 2) Highlight key MR imaging features that are useful to narrow the differential diagnosis. 3) Increase confidence in the interpretation of complex MR studies.

Sub-Events

MSCM51A MRI of the Brain

Participants Carlos H. Torres, MD,FRCPC, Ottawa, ON (*Presenter*) Nothing to Disclose

For information about this presentation, contact:

catorres@toh.ca

LEARNING OBJECTIVES

1) Review key MR imaging findings of common and infrequent conditions in the adult brain. 2) Highlight key features that are useful to narrow the differential diagnosis. 3) Increase confidence in the interpretation of complex MR studies of the brain.

MSCM51B MRI of the Spine

Participants Pia C. Maly Sundgren, MD, PhD, Lund, Sweden (*Presenter*) Nothing to Disclose

LEARNING OBJECTIVES

1) Review key MR imaging findings of common and infrequent conditions in the pediatric and adult spine. 2) Highlight key features that are useful to narrow the differential diagnosis. 3) Increase confidence in the interpretation of MR studies of the spine.

MSCM51C Synovial Linings Playbook

Participants

Bruce B. Forster, MD, Vancouver, BC (Presenter) Stockholder, Canada Diagnostic Centres

For information about this presentation, contact:

bruce.forster@vch.ca

LEARNING OBJECTIVES

1) Appreciate a range of synovial pathologies imaged on various imaging modalities. 2) Understand when additional diagnostic information is gained with the use of intra-articular and intravenous contrast. 3) Identify features typical of aggressive and malignant synovial lesions.

MSCM51D MRI of the Pelvis and Hips

Participants

Donna G. Blankenbaker, MD, Fitchburg, WI (Presenter) Consultant, Reed Elsevier; Royalties, Reed Elsevier

LEARNING OBJECTIVES

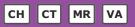
1) Review the MR imaging appearance of specific hip conditions. 2) Develop the differential diagnosis for common and uncommon hip/pelvis pathology. 3) Understand characteristic imaging patterns in diagnosis.





Pulmonary Vascular Imaging

Thursday, Dec. 5 8:30AM - 10:00AM Room: S103CD



AMA PRA Category 1 Credits ™: 1.50 ARRT Category A+ Credit: 1.75

FDA Discussions may include off-label uses.

Participants

Ioannis Vlahos, MRCP, FRCR, Houston, TX (Moderator) Nothing to Disclose

LEARNING OBJECTIVES

1) Highlight practical applications, best current practice, and state of the art multimodality CT and MRI practice with regards to pulmonary vascular imaging. 2) Review acute and chronic pulmonary embolism, pulmonary hypertension, and pulmonary arteriovenous malformations.

Sub-Events

RC601A Imaging of Acute Pulmonary Embolism

Participants

Ioannis Vlahos, MRCP, FRCR, Houston, TX (Presenter) Nothing to Disclose

LEARNING OBJECTIVES

1) Overview current imaging strategies and key facts in acute pulmonary embolism imaging. 2) Provide an update on current issues and challenges in acute pulmonary embolism imaging.

RC601B Imaging of Chronic Pulmonary Embolism and Pulmonary Hypertension

Participants

Elsie Nguyen, MD, Toronto, ON (Presenter) Nothing to Disclose

LEARNING OBJECTIVES

1) Review the classification of pulmonary hypertension. 2) List CT and MRI features of PH. 3) Describe imaging characteristics of chronic pulmonary embolism.

RC601C Imaging of Pulmonary Arteriovenous Malformations

Participants Kristopher W. Cummings, MD, Scottsdale, AZ (*Presenter*) Nothing to Disclose

LEARNING OBJECTIVES

1) Explain the role MDCT plays in the evaluation of suspected hereditary hemorrhagic telangiectasia. 2) List the most important information provided by MDCT for management of pulmonary arteriovenous malformations.

RC601D Pulmonary MRA: Practical Applications

Participants

Christopher J. Francois, MD, Madison, WI (Presenter) Departmental research support, General Electric Company;

For information about this presentation, contact:

cfrancois@uwhealth.org

LEARNING OBJECTIVES

1) Identify roles for magnetic resonance angiography (MRA) in imaging patients with pulmonary artery disease, particularly on the use of MRA in pulmonary embolism. 2) Describe techniques and protocols for robust, clinical pulmonary MRA. 3) Summarize the evidence supporting the use of pulmonary MRA for pulmonary embolism.

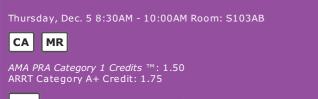
ABSTRACT

1) Pulmonary MRA is appropriate for imaging patients suspected of having pulmonary embolism who have contra-indications to CTA, particularly those in whom avoiding iodinated contrast (due to allergy or decreased renal function) or minimizing radiation exposure (younger patients) would be beneficial. 2) Current, commercially available MRA sequences that take advantage of newer parallel imaging techniques help ensure consistent pulmonary MRA in a clinical setting in under ten minutes. 3) Although older, multi-center studies using MRA techniques and protocols suggested pulmonary MRA may not be accurate enough for routine clinical use, more recent studies using commercially available accelerated image acquisition techniques indicate that pulmonary MRA is effective in identifying clinically significant pulmonary embolism.





Nonischemic Cardiomyopathies: Role of Cardiac MRI



FDA Discussions may include off-label uses.

Participants

Phillip M. Young, MD, Rochester, MN (Moderator) Consultant, Arterys Inc

LEARNING OBJECTIVES

1) To recognize MRI appearance of the most common right ventricular cardiomyopathies. 2) To describe the phenotypic spectrum of morpho-functional and tissue abnormalities of hypertrophic cardiomyopathy. 3) To review different faces and phases of the disease reflecting its natural history. 4) To analyze critical role of CMR tissue characterization of the differential diagnoses of hypertrophic CMPs, from phenotype to genotype. 5) To review T1 and T2 tissue mapping variations in different clinical scenarios. 6) To analyze prognostic implications of CMR in HCM. 7) Describe the relevant clinical findings of patients with restrictive cardiomyopathy. 8) Define the role of cardiac MR (CMR) in the evaluation of patients with restrictive cardiomyopathy. 9) Discuss the different patterns of myocardial enhancement and other ancillary imaging findings as they relate to narrowing the differential diagnosis in patients with restrictive cardiomyopathy. 10) Identify the different forms of Dilated Cardiomyopathies (DCM). 11) Apply the most common Cardiac Magnetic Resonance (CMR) techniques to differentiate between the various DCM etiologies. 12) Assess the Pros & Cons of different CMR techniques for the DCM evaluation.

Sub-Events

RC603A Arrhythmogenic Right Ventricular Cardiomyopathies

Participants

Karen G. Ordovas, MD, San Francisco, CA (Presenter) Advisor, Arterys Inc; Research Grant, General Electric Company

LEARNING OBJECTIVES

1) To recognize MRI appearance of the most common right ventricular cardiomyopathies.

RC603B Role of MRI in Hypertrophic Cardiomyopathy

Participants

Marco Francone, MD, PhD, Rome, Italy (Presenter) Nothing to Disclose

LEARNING OBJECTIVES

1) To describe the phenotypic spectrum of morpho-functional and tissue abnormalities of hypertrophic cardiomyopathy. 2) To review different faces and phases of the disease reflecting its natural history. 3) To analyze critical role of CMR tissue characterization of the differential diagnoses of hypertrophic CMPs, from phenotype to genotype. 4) To review T1 and T2 tissue mapping variations in different clinical scenarios. 5) To analyze prognostic implications of CMR in HCM.

RC603C Restrictive Cardiomyopathy and Amyloidosis

Participants

Daniel Vargas, MD, Aurora, CO (Presenter) Nothing to Disclose

For information about this presentation, contact:

Daniel.vargas@ucdenver.edu

LEARNING OBJECTIVES

1) Describe the relevant clinical findings of patients with restrictive cardiomyopathy. 2) Define the role of cardiac MR (CMR) in the evaluation of patients with restrictive cardiomyopathy. 3) Discuss the different patterns of myocardial enhancement and other ancillary imaging findings as they relate to narrowing the differential diagnosis in patients with restrictive cardiomyopathy.

RC603D Role of MRI in Dilated Cardiomyopathies

Participants

Matthias Gutberlet, MD, PhD, Leipzig, Germany (*Presenter*) Speaker, Siemens AG Speaker, Koninklijke Philips NV Speaker, Bayer AG Speaker, Bracco Group Author, Thieme Medical Publishers, Inc

LEARNING OBJECTIVES

1) Identify the different forms of Dilated Cardiomyopathies (DCM). 2) Apply the most common Cardiac Magnetic Resonance (CMR) techniques to differentiate between the various DCM etiologies. 3) Assess the Pros & Cons of different CMR techniques for the DCM evaluation.







Case Review: Rectal MRI (Interactive Session)

Thursday, Dec. 5 8:30AM - 10:00AM Room: E451B

GI MR

AMA PRA Category 1 Credits ™: 1.50 ARRT Category A+ Credit: 1.75

Special Information

Participants will review cases on their own devices and answer questions. The cases will then be reviewed by the presenters. Note: this activity is best done on a laptop or tablet. Although phones will work, their small size limits optimal image view.

Sub-Events

RC609A Rectal MR Cases - Set 1

Participants

David H. Kim, MD, Middleton, WI (Presenter) Shareholder, Cellectar Biosciences, Inc; Shareholder, Elucent Medical;

LEARNING OBJECTIVES

1) Identify key anatomic landmarks that are helpful in rectal cancer staging at MR. 2) Critically evaluate whether tumor is contained or extends past the muscularis propria of the rectum. 3) State the criteria for regional lymph node positivity at MR.

RC609B Rectal MR Cases - Set 2

Participants

Elena K. Korngold, MD, Portland, OR (Presenter) Nothing to Disclose

For information about this presentation, contact:

korngold@ohsu.edu

LEARNING OBJECTIVES

1) To interactively view rectal MRI cases and incorporate salient teaching points, with self and group evaluation during the process, building towards an understanding of practical rectal MRI for rectal cancer staging. 2) To gain working knowledge of anatomy and MRI findings to optimally interpret and report on rectal cancer staging and features.

RC609C Rectal MR Cases - Set 3

Participants Zahra Kassam, MD, London, ON (*Presenter*) Nothing to Disclose

For information about this presentation, contact:

zahra.kassam@sjhc.london.on.ca

LEARNING OBJECTIVES

1) Provide overview of MR imaging in rectal cancer staging. 2) Highlight pearls and pitfalls in technique and interpretation, to increase staging accuracy. 3) Review reporting guidelines pertinent to rectal MR staging.

RC609D Rectal MR Cases - Set 4

Participants

Mukesh G. Harisinghani, MD, Boston, MA (Presenter) Nothing to Disclose

For information about this presentation, contact:

MHARISINGHANI@MGH.HARVARD.EDU

LEARNING OBJECTIVES

1) Provide overview of MR imaging in rectal cancer staging. 2) Highlight important technical pointers for accurate staging.





Head and Neck PET/CT: Clinical Approach

Thursday, Dec. 5 8:30AM - 10:00AM Room: S504CD

CT HN MR NR NM

AMA PRA Category 1 Credits ™: 1.50 ARRT Category A+ Credit: 1.75

Sub-Events

RC611A Oropharyngeal Cancer: Evolving Challenges-Clinician's Perspective

Participants

Colette J. Shen, MD, PhD, Chapel Hill, NC (Presenter) Speaker, Nanobiotix

LEARNING OBJECTIVES

1) To understand how radiological interpretation of pre-treatment and post-treatment imaging studies influences the management of patients with head and neck cancer. 2) Using PET to delineate the radiation target. 3) Can we OMIT treatment of the PET negative neck? 4) 3 month Post-Treatment PET/CT response assessment.

RC611B CT and MRI Anatomy and Interpretation

Participants

Valerie L. Jewells, DO, Chapel Hill, NC (Presenter) Nothing to Disclose

LEARNING OBJECTIVES

1) Provide radiologists with the tools to access CT and MRI imaging for head and neck cancer. 2) Teach attendees how to address the images in a manner that will assist the ENT surgeon for staging and surgical planning. 3) Address the principles for critical thinking and analysis as well as preparation and skill development for a head and neck tumor board.

ABSTRACT

A successful multidisciplinary head and neck tumor board requires coordination and imaging review on the part of radiology to assist the surgeon, radiation oncolcogist and medical oncologist. The goal is to reach the best option for each individual patient depending upon tumor type, staging and underlying medical conditions. Appropriate imaging and interpretation is key to this endeavor. These topics will be addressed through discussion of selective CT and MRI cases from our weekly tumor board. References: 1. Heineman T, St John MA, Wein RO and Weber RS. It takes a village: The importance of multidisciplinary care. Otoloaryngol Clin North Am 2017 Aug;50(4):679-687. 2. Liao CT, Kang CJ, Lee LY et al. Association between multidisciplinary team care approach and survival rates in patients with oral cavity squamous cell carcinoma. Head Neck 2016 Apr;38 Suppl 1:E5444-53. 3. Shah BA, Qureshi MM, Jalisi et al. Analysis of decision making at a multidisciplinary head and neck tumor board incorporating evidence-based National Cancer Comprehensive Network (NCCN) guidelines. Pract Radiat Oncol 2016 Jul-Aug;6(4):248-54.

RC611C FDG-PET/CT: Applications and Interpretation

Participants

Terence Z. Wong, MD, PhD, Chapel Hill, NC (Presenter) Consultant, Lucerno Dynamics, LLC;

LEARNING OBJECTIVES

1) Describe applications for FDG-PET/CT for initial evaluation and follow up of patients with head and neck cancer. 2) Learn the value of combining metabolic findings on FDG-PET findings with morphology on CT and endoscopic appearance. 3) Understand potential etiologies of false positive and false negative studies.

ABSTRACT

Optimal evaluation of patients with head and neck malignancies requires a multidisciplinary approach. Correlation of FDG-PET, CT, direct visualization, and clinical examination is important to provide the best management of these patients.

RC611D Panel Discussion: Q&A

Participants Terence Z. Wong, MD, PhD, Chapel Hill, NC (*Presenter*) Consultant, Lucerno Dynamics, LLC; Valerie L. Jewells, DO, Chapel Hill, NC (*Presenter*) Nothing to Disclose Colette J. Shen, MD,PhD, Chapel Hill, NC (*Presenter*) Speaker, Nanobiotix

LEARNING OBJECTIVES

1) To discuss case examples which highlight the value of multidisciplinary approaches for managing patients with head and neck cancer.







Pediatric Series: Pediatric Safety and Quality

Thursday, Dec. 5 8:30AM - 12:00PM Room: S502AB



AMA PRA Category 1 Credits ™: 3.25 ARRT Category A+ Credits: 4.00

Participants

David B. Larson, MD, MBA, Stanford, CA (*Moderator*) Grant, Siemens AG Grant, Koninklijke Philips NV Brian D. Coley, MD, Cincinnati, OH (*Moderator*) Royalties, Reed Elsevier; Travel support, Canon Medical Systems Corporation; Travel support, Koninklijke Philips NV; Board of Directors, NeoView Ltd; Departmental Research support, Canon Medical Systems Corporation; Departmental Research support, Koninklijke Philips NV; Departmental Research Support, Siemens AG Marta Hernanz-Schulman, MD, Nashville, TN (*Moderator*) Nothing to Disclose Lynn A. Fordham, MD, Chapel Hill, NC (*Moderator*) Nothing to Disclose

Sub-Events

RC613-01 MRI Safety: Risks Unique to a Pediatric Environment

Thursday, Dec. 5 8:30AM - 8:50AM Room: S502AB

Participants

Douglas C. Rivard, DO, Kansas City, MO (Presenter) Nothing to Disclose

LEARNING OBJECTIVES

1) Understand unique elements of the pediatric MRI environment. 2) Review fundamentals of MRI safety. 3) Discuss how a ferro free program works and how to implement.

ABSTRACT

no abstract

RC613-02 Impacts of 3.0 Tesla Magnetic Resonance Imaging Noise on Hearing Function in Children with Hearing Protection

Thursday, Dec. 5 8:50AM - 9:00AM Room: S502AB

Participants

Huifang Zhao, Xian, China (*Presenter*) Nothing to Disclose Chao Jin, Xian, China (*Abstract Co-Author*) Nothing to Disclose Yannan Cheng, BS,BS, Xi'an, China (*Abstract Co-Author*) Nothing to Disclose Peiyao Chen, Xian, China (*Abstract Co-Author*) Nothing to Disclose Heng Liu, PhD, Xi'an, China (*Abstract Co-Author*) Nothing to Disclose Jian Yang, Xian, China (*Abstract Co-Author*) Nothing to Disclose

For information about this presentation, contact:

zhaohf810@163.com

PURPOSE

Although 3.0T MRI has been increasingly used for children, the strong noise remains a great concern. By using Distortion product OAE (DPOAE), this study aimed to investigate the effect of MRI noise on children' cochlear function.

METHOD AND MATERIALS

131 ears of 72 patients with no hearing impairment were enrolled and underwent a 3.0T brain MRI examination(Table 1). The subjects were divided into three groups(0-1, 2-5 and 6-12 years old) according to the development of auditory system. Two DPOAE measurements were performed before MRI and the first (test1) was recorded as baseline. The third DPOAE measurement (test3) was performed within 30 minutes after MRI. DPOAE amplitudes at frequency of 1.5~9.0 kHz were recorded. All statistical analysis were performed by SPSS 18.0 (SPSS, Chicago, IL, USA); P<0.05 was considered as statistically significant difference.

RESULTS

As for the paired t test, there was significant increase of 1.06dB at 3kHz in DPOAE amplitude following exposure to MRI noise for 0-1 years old group (P<0.05; Figure 1). The standard deviations (SD) of DPOAE amplitudes change between test2 and test1, between test3 and test1 were calculated. In contrast to those before MRI, the SD of DPOAE amplitudes change at frequencies of 1.5~9.0 kHz remarkably increased after MRI(Figure 2). This effect represented the increase of DPOAE amplitude variability and with a maximum effect in 6-12 age group(Figure 3).

CONCLUSION

Our results found a subtle reaction of cochlear function in children after exposure to 3.0T MRI noise with hearing protection. And we also observed that the younger group is likely to be more sensitive to acoustic noise.

CLINICAL RELEVANCE/APPLICATION

The effect of the MRI noise on children with immature auditory system development has thus prompted the concern of noiseinduced hearing loss after MRI. Thus efficient hearing protection and noise reduction techniques are necessary to improve the safety of MRI examinations.

RC613-03 Finding "Just right": The Goldilocks of MRI Sequences in Pediatric PET/MRI

Thursday, Dec. 5 9:00AM - 9:10AM Room: S502AB

Participants Mary Ellen I. Koran, MD, PhD, Stanford, CA (*Presenter*) Nothing to Disclose Helen R. Nadel, MD, Palo Alto, CA (*Abstract Co-Author*) Nothing to Disclose

For information about this presentation, contact:

hnadel@stanford.edu

PURPOSE

The challenge for pediatric PET/MRI is to optimize MRI sequences and PET acquisition without prolonging sedation and examination time. As yet, there are no standard protocols utilized in pediatric PET/MRI. Utilizing the 'one-stop shop' method as has been done in PET/CT with contrast enhanced CT for attenuation correction and diagnostic evaluation would undervalue the ability of specialized MRI sequences to provide additional important information based on tumor type or disease status. The goal of this study is to correlate lesion identification on multiple MRI sequences with PET imaging, with the hopes of streamlining and optimizing pediatric PET/MRI studies.

METHOD AND MATERIALS

Over 100 known (based off of released report) lesions were categorized as visualized or not visualized on the individual images from FDG/PET, T2-weighted coronal (T2), diffusion weighted (DWI), and T1-post contrast (T1+) MRI series independently. These included staging, response assessment, and surveillance lesions of lymph nodes, lung, bone, soft tissue, and solid organ disease.

RESULTS

Independently, FDG/PET, T1+, DWI, and T2 MRI images were able to identify 86, 73, 68, and 67 percent of the lesions. A total of 3, 4, and 5 lesions were identified on T1+, T2, and DWI MRI, respectively, and not on PET. Conversely, 14, 21, and 20 lesions were identified on PET and not on T1+, T2, and DWI MRI, respectively. T1+, T2, and DWI provided data beyond the other two MRI sequences in 23, 16, and 23 cases respectively. T2 provided information beyond that attained by the T1+ in only 3 cases.

CONCLUSION

After analysis of our first 100 lesions, we believe that the optimal PET/MRI screening sequence would be dependent upon the type of primary tumor, with DWI adding important information for bony disease, and T2 and T1+ adding important information for nodal disease. Interestingly, the added data from T1+ and T2 overlaps, showcasing an area for improvement in MRI protocol.

CLINICAL RELEVANCE/APPLICATION

Optimizing MRI sequences for pediatric PET/MRI acquisition is beneficial for both the child and the imaging center, in order to obtain the best diagnostic information while coupled with minimal exam time and complexity.

RC613-04 Whole-Body Diffusion Weighted MRI Compared to 18F?FDG PET/CT in Initial Staging and Therapy Response Assessment of Hodgkin's Lymphoma in Pediatric Patients

Thursday, Dec. 5 9:10AM - 9:20AM Room: S502AB

Participants

Gali Shapira Zaltsberg, MD, Ottawa, ON (*Presenter*) Nothing to Disclose Nagwa M. Wilson, MD, PhD, Montreal, QC (*Abstract Co-Author*) Nothing to Disclose Maria Esther Perez Trejo, Ottawa, ON (*Abstract Co-Author*) Nothing to Disclose Lesleigh Abbott, Ottawa, ON (*Abstract Co-Author*) Nothing to Disclose Stephen Dinning, MD,FRCPC, Ottawa, ON (*Abstract Co-Author*) Nothing to Disclose Jorge Davila, Ottawa, ON (*Abstract Co-Author*) Nothing to Disclose Cassandra Kapoor, BSC, Ottawa, ON (*Abstract Co-Author*) Nothing to Disclose Barry Smith, Ottawa, ON (*Abstract Co-Author*) Nothing to Disclose Elka Miller, MD, Nepean, ON (*Abstract Co-Author*) Nothing to Disclose

For information about this presentation, contact:

Shapira.gali1979@gmail.com

PURPOSE

Lymphomatous lesions have low ADC values. With treatment, there is a decrease in cellularity and subsequent increased diffusion on DWI. Whole-body diffusion weighted MRI (WB-DWI-MRI) has been shown as a sensitive and specific method for assessing treatment response in adult lymphoma patients; however, numerous small studies in pediatric patients have shown inconsistent results. The aim of our study was to compare the diagnostic performance of WB- DWI-MRI to FDG-PET/CT in the assessment of initial staging and treatment response in pediatric patients with Hodgkin's lymphoma, assessing both nodal and extra-nodal disease.

METHOD AND MATERIALS

This prospective study comprised 11 children with Hodgkin's lymphoma. WB-DWI-MRI and FDG-PET/CT were obtained prior to initiation of treatment and after completion of two cycles of chemotherapy. Two radiologists measured the ADC values of the nodal and extra-nodal sites of involvement agreed upon in consensus and one nuclear medicine physician assessed the PET/CT. Reliability of radiologists' ratings was assessed by intra-class correlation coefficients based on a two-way random model (ICC2,1). ADC ratios (defined as ADCpost/ADCpre) were assessed. The SUVmax at baseline and at follow-up of the nodal and extra-nodal sites considered positive was assessed. The patients were staged (based on the Ann Arbor staging system) according to both

modalities. Therapeutic response for PET/CT was based on the Lugano classification. The same size criteria used in the Lugano classification were used for therapeutic response on MRI. Since no guidelines are available for assessment of therapeutic response based on DWI, for this study, we defined ADC ratio < 1-0.2SD as progressive disease, 1-0.2 SD< ADC ratio <=1+0.5SD as stable disease, 1+0.5SD < ADC ratio <=1+1.5SD as partial response, and ADC ratio > 1+1.5SD as complete response.

RESULTS

There was good agreement between the two raters for both nodal and extra-nodal ADC measurements. DW-MRI determined correct tumor stage in 8/11(72.7%) examinations, underrating three patients (27.3%). Response to treatment based on DWI and PET showed concordance in all patients (100%).

CONCLUSION

Our experience showed that WB-DWI-MRI is inferior to PET/CT for initial staging of Hodgkin lymphoma in pediatric patients, however, it has the potential to be sensitive enough to assess response to treatment in lieu of PET/CT.

CLINICAL RELEVANCE/APPLICATION

WB-DWI-MRI can potentially be a radiation free alternative to PET/CT in assessing response to treatment of Hodgkin lymphoma in pediatric patients.

RC613-05 Reassessing the Risk of Acute Kidney Injury After Intravenous Contrast Media Administration for CT Imaging in Children

Thursday, Dec. 5 9:20AM - 9:30AM Room: S502AB

Participants

Juan Calle Toro, MD, Philadelphia, PA (*Abstract Co-Author*) Nothing to Disclose Bernarda Viteri, MD, Philadelphia, PA (*Abstract Co-Author*) Spouse, Employee, Bristol-Myers Squibb Company Ammie M. White, MD, Flourtown, PA (*Abstract Co-Author*) Nothing to Disclose Madhura Pradhan, MD, Philadelphia, PA (*Abstract Co-Author*) Nothing to Disclose Christian A. Barrera, MD, Philadelphia, PA (*Abstract Co-Author*) Nothing to Disclose Hansel J. Otero, MD, Philadelphia, PA (*Presenter*) Nothing to Disclose Suraj D. Serai, PhD, Philadelphia, PA (*Abstract Co-Author*) Nothing to Disclose

For information about this presentation, contact:

juan53670@gmail.com

PURPOSE

Recently, the concept of post-contrast acute kidney injury (AKI) has been challenged in the adult literature. However, there is no similar data pertaining to children. Hence, we aim to determine whether intravenous iodinated contrast administration for computed tomography (CT) in children is independently associated with increased risk for AKI by comparing the incidence of AKI in patients receiving contrast to the incidence in those that did not.

METHOD AND MATERIALS

This IRB approved HIPAA-compliant retrospective cohort analysis was performed at a large, urban, academic stand-alone children's hospital. From January 2008 to January 2018 all children in whom creatinine levels were available before and within 48 hours after undergoing CT with or without contrast. The primary outcome was the incidence of AKI according to the Acute Kidney Injury Network (AKIN) definition and the "Kidney Disease: Improving Global Outcomes" (KDIGO) guidelines. Patients with history of renal disease or dysfunction prior to CT were excluded. Odds ratios were calculated between groups and within group controlling for gender, age and weight.

RESULTS

Of over 54,000 CT studies during the study period, 19,441 studies were included in the analysis; 8,872 (45.6%) studies used contrast and the remaining 10,569 (54.4%) did not. The incidence of AKI using the AKIN definition was 25% in the contrast group vs. 34% in the non-contrast group (p 0.09). According to the KDIGO guidelines the incidence of AKI was 7% in the contrast group vs. 11% in the non-contrast group (p 0.17). We found no significant difference in the OR when comparing groups (OR 1.3, CI 95% 0.9-1.4, p 0.17) nor when stratified by gender, age and weight.

CONCLUSION

In agreement with recent adult literature, we found that intravenous iodinated contrast was not associated with an increased incidence of AKI in children.

CLINICAL RELEVANCE/APPLICATION

Recently, the concept of post-contrast acute kidney injury (AKI) has been challenged in the adult literature. However, there is no similar data pertaining to children. Here we found no association of contrast with AKI.

RC613-06 Risk Factors of Post-Contrast Acute Kidney Injury: A Retrospective Study in Pediatric Patients

Thursday, Dec. 5 9:30AM - 9:40AM Room: S502AB

Participants

Liya Ma, MD, Wuhan, China (*Presenter*) Nothing to Disclose Zhen Li, MD, PhD, Wuhan, China (*Abstract Co-Author*) Nothing to Disclose Yaqi Shen, PhD, MD, Wuhan, China (*Abstract Co-Author*) Nothing to Disclose Xuemei Hu, MD, Wuhan, China (*Abstract Co-Author*) Nothing to Disclose Daoyu Hu, Wuhan, China (*Abstract Co-Author*) Nothing to Disclose

For information about this presentation, contact:

PURPOSE

To investigate risk factors of post-contrast acute kidney injury (PC-AKI) in pediatric patients and the correlation between PC-AKI and age.

METHOD AND MATERIALS

We performed a retrospectively study of inpatients under 18 years. CT examinations, serum creatinine (SCr) values and clinical information of each subject was searched. Then 1:1 matching of PSM (propensity score matching) was performed on risk factors between enhanced and unenhanced group, and age stratification of PC-AKI was performed. Two kinds of threshold of PC-AKI was used: an increase in SCr by more than 25% or 44 μ mol/L (named CIN, contrast-induced nethropathy), or 50% or 44 μ mol/L (named AKI, acute kindney injury).The incidence of AKI/CIN before and after matching was analyzed between two groups and among different age groups.

RESULTS

A total of 1380 cases were extracted (1081 and 299 cases in unenhanced and enhanced group respectively). 524 cases were obtained by 1:1 PSM, 262 cases in the two group respectively. After matching, the distribution of propensity score between the two groups was more similar (Figure 1). Before matching, risk factors were statistically different between two groups, including age, congenital heart disease, renal tumor, renal surgery, heart surgery, and chemotherapy, and after matching there was no significant difference in all risk factors. The total incidence of CIN and AKI before matching was 1.2% (1.1% in unenhanced group, 1.7% in enhanced group) and 6.8% (7.4% in unenhanced group, 4.7% in enhanced group) respectively, both without significant difference. After matching, the incidence of total CIN was 1.3% (1.1% in the unenhanced group, 1.4% in enhanced group) and AKI was 5.9% (7.3% in unenhanced group), also without significance. Several risk factors, such as congenital heart disease and cardiac surgery was positive correlated with CIN, and urinary calculus was negative correlated with AKI. There was no significant difference in the incidence of PC-AKI among different age groups.

CONCLUSION

For pediatric inpatients, some risk factors (congenital heart disease, cardiac surgery, urinary calculus) may have correlation with PC-AKI. The use of iodinated contrast agent did not have correlation with PC-AKI. There was no significance in the incidence of PC-AKI among age groups.

CLINICAL RELEVANCE/APPLICATION

The use of iodinated contrast agent is safe in CT examination of pediatric patients.

RC613-07 Providing Expert Pediatric Teleradiology Services Around the Globe: The World Federation of Pediatric Imaging Experience

Thursday, Dec. 5 9:40AM - 9:50AM Room: S502AB

Participants

Hansel J. Otero, MD, Philadelphia, PA (*Presenter*) Nothing to Disclose Daphine C. Grassi, MD, Barueri, Brazil (*Abstract Co-Author*) Nothing to Disclose Savvas Andronikou, MBBS, Philadelphia, PA (*Abstract Co-Author*) Nothing to Disclose Cicero J. Silva, MD, New Haven, CT (*Abstract Co-Author*) Nothing to Disclose

For information about this presentation, contact:

oteroh@email.chop.edu

PURPOSE

To descriptively analyze the utilization, case characteristics, and referrers' opinion of a pediatric-specific teleradiology portal for low- and middle income countries.

METHOD AND MATERIALS

This is a retrospective analysis of all cases referred to the WFPI pro-bono second-opinion teleradiology service between October 2014 and October 2018. Basic case and patient characteristics as well as feedback on usefulness and satisfaction from referrers.

RESULTS

A total of 668 cases (352 boys, 316 girls) with a median age 1 year 4 months (range 1 day - 18 years) were reviewed over a period of 4 years by a team of 45 volunteer pediatric radiologists. The majority (n=548) of the cases came from a single referral center (Lao Friends Hospital for Children, 82%); while the remaining 120 cases came from nine additional centers, distributed among Asia (6.7%), Africa (87.5%) and The Americas (5.8%). The median delay between receiving the case and its allocation to a radiologist was 0.73 hours (IQR: 0.26-1.87 hours). The median time delay to the first radiologist response was 5.53 hours (IQR: 2.14- 13.19 hours). The most common imaging modality submitted for interpretation was radiography (n=559, 83.7%), followed by computed tomography (n=78, 11.7%), ultrasound (n=58, 8.7%) and MRI (n=5, 0.7%). Referrers provided feedback on 94 cases (14.1%), which was overwhelmingly positive

CONCLUSION

Teleradiology offers a viable and well received option in centers with access to imaging but limited access to pediatric radiology expertise from around the world with reasonable delays in terms of time to first radiologist's response

CLINICAL RELEVANCE/APPLICATION

The WFPI pediatric teleradiology platform provides pediatric radiology expertise, offering services among a wide range of modalities and from a variety of international referring institutions.

RC613-08 Strategies to Reduce Pediatric MRI Scan Time and Sedation

Thursday, Dec. 5 9:50AM - 10:10AM Room: S502AB

Participants Michael S. Gee, MD, PhD, Boston, MA (*Presenter*) Nothing to Disclose

LEARNING OBJECTIVES

1) Identify strategies to reduce MRI scan time in children. 2) Develop strategies to decrease the use of sedation/anesthesia in pediatric MRI.

ABSTRACT

None.

RC613-09 Tools for Successful and Sustainable Quality Improvement Projects

Thursday, Dec. 5 10:20AM - 10:40AM Room: S502AB

Participants Lane F. Donnelly, MD, Palo Alto , CA (*Presenter*) Nothing to Disclose

For information about this presentation, contact:

lane.donnelly@stanford.edu

LEARNING OBJECTIVES

1) To learn key tools, processes, and key drivers to increase the likelihood of success for improvement projects.

RC613-10 Children are Not Small Adults: Assessment of ACR TI-RADS in Pediatric Thyroid Nodules

Thursday, Dec. 5 10:40AM - 10:50AM Room: S502AB

Participants Danielle M. Richman, MD, MS, Boston, MA (*Abstract Co-Author*) Nothing to Disclose Carol B. Benson, MD, Boston, MA (*Abstract Co-Author*) Nothing to Disclose Peter M. Doubilet, MD, PhD, Boston, MA (*Abstract Co-Author*) Nothing to Disclose Elizabeth Asch, MD, Winchester, MA (*Abstract Co-Author*) Nothing to Disclose Ari Wassner, MD, Boston, MA (*Abstract Co-Author*) Nothing to Disclose Jessica Smith, MD, Boston, MA (*Abstract Co-Author*) Nothing to Disclose Christine Cherella, MD, Boston, MA (*Abstract Co-Author*) Nothing to Disclose Mary C. Frates, MD, Boston, MA (*Presenter*) Nothing to Disclose

For information about this presentation, contact:

DMRichman@partners.org

PURPOSE

To assess the reliability of the American College of Radiology (ACR) Thyroid Imaging, Reporting and Data System (TI-RADS) criteria, designed for use in adults, for guiding decisions whether or not to biopsy thyroid nodules in pediatric patients.

METHOD AND MATERIALS

We determined the ACR TI-RADS score of each thyroid nodule in our database of patients <19 years of age who underwent ultrasound-guided fine needle aspiration (FNA) between January 2004 and July 2017. For each nodule, we determined whether the TI-RADS criteria would have led to a recommendation to biopsy, follow, or not follow the nodule.

RESULTS

There were 404 thyroid nodules in 314 patients in our database, and 77 of the nodules (19.1%) were malignant. The majority of cancers were papillary carcinoma (68/77, 88.3%). Among the 77 cancers, 64 (83.1%) cancers had a TI-RADS score in the moderately suspicious category 4 or highly suspicious category 5. Based on TI-RADS criteria, only 60 of the 77 malignant nodules (77.9%) would have undergone FNA, while 10 of 77 (13.0%) would have been assigned follow-up without FNA, and 7 of 77 (9.1%) would have had neither follow-up or FNA. Of the 7 cancers that would have had no follow up, 2 nodules were scored as benign TI-RADS category 1, 4 as not suspicious category 2, and 1 as mildly suspicious category 3. Of the 10 cancers that would have been followed, 1 scored as mildly suspicious category 3, 4 as moderately suspicious category 4 but too small for FNA, and 5 as highly suspicious category 5 but too small for FNA.

CONCLUSION

The use of ACR TI-RADS criteria in our pediatric thyroid nodules would have resulted in a high percentage (22.1%) of cancers not biopsied at initial visit, including a high percentage (9.1%) of cancers missed entirely (not biopsied or followed up). This suggests that ACR TI-RADS is not reliable for guiding decisions in pediatric patients.

CLINICAL RELEVANCE/APPLICATION

To determine whether management of pediatric thyroid nodules by the ACR TI-RADS criteria would affect the timely diagnosis of cancer.

RC613-11 Potential Cost Implications of a Clinical Decision Support System on Emergency CT Head Examinations at a Quaternary Pediatric Hospital

Thursday, Dec. 5 10:50AM - 11:00AM Room: S502AB

Participants

Shireen Hayatghaibi, MA, MPH, Houston, TX (*Presenter*) Nothing to Disclose Varsha Varghese, Houston, TX (*Abstract Co-Author*) Nothing to Disclose Andrew Sher, MD, Houston, TX (*Abstract Co-Author*) Nothing to Disclose

PURPOSE

To determine the cost implications using time-driven activity-based costing for CT Head examinations ordered from the Emergency Center and graded as 'usually not inappropriate' by a commercially available Clinical Decision Support (CDS) tool.

METHOD AND MATERIALS

CT head without contrast is the most commonly ordered CT examination from our pediatric Emergency Department. Following the implementation of a CDS tool (CareSelect; National Decision Support Co., Madison, WI) into the EHR, all CT examinations from September 18, 2018 through February 28, 2019 received a score based on appropriateness as per the ACR Appropriate Use Criteria. Orders were scored with the following scale: 1-3: usually not appropriate, 4-6: may be appropriate, and 7-9: usually appropriate. The CDS tool was run in silent mode (i.e. without displaying appropriateness grades to ordering providers). A micro-costing assessment was subsequently conducted on CT Head examinations receiving a grade of 1-3 using time-driven activity-based costing (TDABC). Process maps were created through shadowing 20 encounters and EHR time-stamp review of 150 patient records. Capacity cost rates for personnel, equipment, facilities, and supplies were established from institutional accounting data. The cost of each process step was determined by multiplying step-specific capacity cost rates by the mean time required to complete the step. Total pathway cost was computed by summing the costs of all steps through the process pathway.

RESULTS

Of 1877 CT examinations ordered from the EC, 24% (445/1877) were scored 'usually not appropriate'; CT Head without contrast studies accounted for 76% (339/445) of these examinations. Utilizing TDABC, the mean total CT pathway time for a CT Head without contrast was calculated to be 42 minutes and the mean total cost of the examination was \$198 (Figure 1). Based on the 339 CT Head without contrast examinations that were graded as 'usually not appropriate', the potential cost savings extrapolated annually amounts to \$134,244.

CONCLUSION

Implementation of a clinical decision support tool may have significant utilization effects on imaging studies ordered from pediatric emergency departments and result in substantial cost savings.

CLINICAL RELEVANCE/APPLICATION

As reimbursement models transition to value-based health care, implementation of CDS to determine appropriate imaging utilization may assist in deriving high value health care.

RC613-13 Dose Line Integral (DLI) for Tracking Cumulative Dose from Multiple Multi-Sequence CT Exams with Tube Current Modulation in Children

Thursday, Dec. 5 11:10AM - 11:20AM Room: S502AB

Participants Azadeh Tabari, Boston, MA (*Abstract Co-Author*) Nothing to Disclose Xinhua Li, PhD, Boston, MA (*Abstract Co-Author*) Spouse, Employee, Juniper Pharmaceuticals; Employee, Constellation Pharmaceuticals Kai Yang, PhD, Boston, MA (*Abstract Co-Author*) Nothing to Disclose Bob Liu, PhD, Boston, MA (*Abstract Co-Author*) Nothing to Disclose Michael S. Gee, MD, PhD, Boston, MA (*Abstract Co-Author*) Nothing to Disclose Sjirk J. Westra, MD, Boston, MA (*Presenter*) Nothing to Disclose

For information about this presentation, contact:

atabari@mgh.harvard.edu

PURPOSE

We introduce Dose Line Integral (DLI), a new metric that allows adding radiation dose in children undergoing multiple multi-series CT scans obtained with tube current modulation (TCM) with different z-axis coverage

METHOD AND MATERIALS

Our institutional review board approved study included children in four different age categories who underwent multiple CT (3-5) of the abdomen on various scanner platforms within 1 year from 2017-2018. All patients were scanned with fixed kV and TCM. In each series, mA was recorded for each slice to evaluate the cross-sectional average dose along the z-axis. With a multi-series examination, the dose at each z-location was accumulated over all acquisition series. This method was applied to 13 clinical CT examinations (16 acquisition, patient age; 0-1 (n=2), 5-6 (n=2), 10-11 (n=4), 15-16 (n=5) yrs-old). DLI profile of each acquisition was compared with conventional dose parameters CTDIvol, and SSDE, and the sum of all recorded doses as a function of z-axis location was compared with DLP

RESULTS

We generated a graphic display of mA and dose as a function of the z-axis location for each acquisition series and for the whole exam. Differences ranging from 32.4% (23.1 vs 7.5 mGy) and 48.3% (25.1 vs 12.1 mGy) were observed between the maximum value of the accumulated dose profile and the conventional CTDIvol and SSDE, respectively. The sum of all DLIs per patient exceeded the sum of all DLPs by an average of more than 100% (438,94,564,1057 mGy.cm vs 148,39,273 and 545 mGy.cm, respectively)

CONCLUSION

The graphic overall dose profile gives a complete description of z-axis dose distribution for the studied CT examinations under a wide range of patient variables and acquisition conditions, including multiple acquisition series. Visualization of the dose profiles across and beyond the scan ranges provided a more valid tool for CT dose optimization than simple arithmetic summations of CTDIvol, SSDE and DLP

CLINICAL RELEVANCE/APPLICATION

We present a new way to calculate cumulative doses from multiple multi-phase CT scans obtained with tube current modulation, which better satisfies legal requirements and serves as a tool for individual long term dose monitoring in children

RC613-14 Impact of Patient Off-Centering on Organ Radiation Doses in Pediatric CT of the Head and Trunk

Thursday, Dec. 5 11:20AM - 11:30AM Room: S502AB

Participants

Andre Euler, MD, Zurich, Switzerland (*Presenter*) Nothing to Disclose Natalia Saltybaeva, PhD, Zurich, Switzerland (*Abstract Co-Author*) Nothing to Disclose Hatem Alkadhi, MD, Zurich, Switzerland (*Abstract Co-Author*) Nothing to Disclose

PURPOSE

To assess the impact of patient positioning on organ dose of head and trunk CT in a pediatric phantom.

METHOD AND MATERIALS

An anthropomorphic phantom simulating a 5-year-old child was used. Semiconductor dosimeters were placed in various organs of the head and trunk. CT of the head and trunk using automatic tube current modulation (ATCM) and default bowtie filters were performed. The phantom was imaged repeatedly at vertical table positions ranging from -6 to +6 cm from the 0-position. Tube current time products, organ doses, and image noise were recorded. Scatter radiation was measured in the thyroid for head CT. The effect of ATCM and bowtie filters was assessed.

RESULTS

Depending on patient position, organ doses differed up to 22% for the supratentorial brain, 34% for the infratentorial brain, 19% for the eyes, 28% for the lungs, 25% for the stomach, and 22% for the liver compared to the 0-position. The relation between position and dose was linear and mainly affected by the bowtie filter in head CT while it was quadratic and affected by ATCM and bowtie filter in trunk CT. It further depended on the relative position of each organ to the isocenter. Image noise was inversely related to organ dose. Scatter radiation in the thyroid was not significantly related to patient position (P=0.21).

CONCLUSION

In pediatric CT, vertical patient positioning had a substantial impact on radiation dose with differences of up to 34%. This effect depended on the body region and location of each individual organ.

CLINICAL RELEVANCE/APPLICATION

Proper patient positioning is crucial in the pediatric population to avoid unintended irradiation of radiosensitive organs.

RC613-15 Accurate Camera-Based Positioning of Pediatric Patients Undergoing Chest, Abdominal and Pelvic CT Examinations

Thursday, Dec. 5 11:30AM - 11:40AM Room: S502AB

Participants

Marilyn J. Siegel, MD, Saint Louis, MO (*Abstract Co-Author*) Speakers Bureau, Siemens AG Spouse, Consultant, General Electric Company

Juan Carlos Ramirez-Giraldo, PhD, Cary, NC (*Abstract Co-Author*) Employee, Siemens AG Philipp Hoelzer, PhD, DIPLENG, Malvern, PA (*Presenter*) Employee, Siemens AG

PURPOSE

To compare vertical isocenter offsets and its impact on radiation exposure of manually versus automated 3d-camera-based positioning for pediatric body CT exams

METHOD AND MATERIALS

In this retrospective, IRB approved study, vertical isocenter offsets and radiation exposures of pediatric patients undergoing body CT exams (chest, abdomen-pelvis, and chest-abdomen-pelvis) between Nov 2, 2018 and February 20, 2019 were retrospectively analyzed using dose tracking software. The patient cohort included CT exams of a total of 413 patients ranging from 3 years to 24 years. Automatic positioning was achieved with the help of a 3d camera (FAST 3D Camera, Siemens) that captures the depth profile of the patient lying on the patient bed and through an Artificial Intelligence algorithm automatically adjusts the table vertically. Patient's effective diameter (in mm), isocenter offset (in mm) and, CTDIvol (in mGy) were recorded. Patients were categorized as either manually or automatically positioned with the 3d camera. Unpaired statistical comparisons were performed.

RESULTS

A total of 33 patients were automatically positioned with the camera, while the other 380 patients were positioned manually. The isocenter offset was smaller for patients automatically positioned with the camera with a median [25th to 75th quartile] -0.6 [-4.2 to 4.2] mm versus manually positioned patients with -10.9 [-21.9 to -2.2] mm (P? 0.05).

CONCLUSION

The use of the 3d camera significantly reduced patient off-centering in the vertical direction for pediatric CT examinations of the body.

CLINICAL RELEVANCE/APPLICATION

Our results suggest that 3d-camera based positioning can lead to consistent patient centering that is expected to reduce variability in radiation exposure and image quality in pediatric body CT examinations. Future studies with larger sample sizes should look into the impact of the camera on radiation exposure and image quality.

RC613-16 Engaging Patients and Families in Pediatric Radiology

Thursday, Dec. 5 11:40AM - 12:00PM Room: S502AB

Participants Nadja Kadom, MD, Atlanta, GA (*Presenter*) Nothing to Disclose

For information about this presentation, contact:

nkpiano@gmail.com

LEARNING OBJECTIVES

1) Identify opportunities for patient engagement in pediatric radiology. 2) Develop patient-centered initiatives in pediatric radiology.

ABSTRACT

n/a





RC617

Emerging Technology: Elastography of the Liver - Update 2019

Thursday, Dec. 5 8:30AM - 10:00AM Room: S505AB



AMA PRA Category 1 Credits ™: 1.50 ARRT Category A+ Credit: 1.75

Participants

Richard L. Ehman, MD, Rochester, MN (Moderator) CEO, Resoundant, Inc; Stockholder, Resoundant, Inc;

LEARNING OBJECTIVES

1) To understand how elastography measurements are integrated into the management of patients with chronic liver disease. 2) To learn imaging techniques and protocols of ultrasound and MR elastography. 3) To compare US and MR elastography in assessing liver fibrosis. 4) To review emerging clinical indications of US and MR elastography. 5) To understand limitations of current elastography techniques.

Sub-Events

RC617A Elastography of the Liver: Why Clinicians Use It

Participants

Alina Allen, Rochester, MN (Presenter) Research support, Gilead Sciences, Inc

For information about this presentation, contact:

allen.alina@mayo.edu

LEARNING OBJECTIVES

1) Recognize the importance of fibrosis estimation in liver disease. 2) Assess the role of elastography in clinical practice.

RC617B MR Elastography: Update 2019

Participants

Richard L. Ehman, MD, Rochester, MN (Presenter) CEO, Resoundant, Inc; Stockholder, Resoundant, Inc;

LEARNING OBJECTIVES

1) To be able to understand the basic physical principles of MR Elastography (MRE). 2) To be able to describe the clinical indications for MRE in liver disease. 3) To be able to describe published evidence on the diagnostic performance of MRE in assessing liver fibrosis. 4) To be able to compare ultrasound based elastography to MRE. 5) To be able to describe the current limitations of MRE.

RC617C Ultrasound Elastography: Update 2019

Participants

Richard G. Barr, MD, PhD, Campbell, OH (*Presenter*) Consultant, Siemens AG; Consultant, Koninklijke Philips NV; Research Grant, Siemens AG; Research Grant, SuperSonic Imagine; Speakers Bureau, Koninklijke Philips NV; Research Grant, Bracco Group; Speakers Bureau, Siemens AG; Consultant, Canon Medical Systems Corporation; Research Grant, Esaote SpA; Research Grant, BK Ultrasound; Research Grant, Hitachi, Ltd

LEARNING OBJECTIVES

1) Understand the clinical indications of ultrasound elastography (USE). 2) Learn about the various techniques and imaging protocols of USE. 3) Review the diagnostic accuracy of USE in the assessment of elasticity in liver fibrosis and other clinical applications in the body. 4) Compare USE with MR elastography. 5) Understand current limitations of USE.

ABSTRACT

Ultrasound elastography (USE) is a general term for various techniques available for objectively and quantitatively assessing tissue stiffness using ultrasonic techniques, creating noninvasive images of mechanical characteristics of tissues. Elastography is based on the fact that the elasticity of a tissue is changed by pathological or physiological processes. For example, cancer or fibrosis associated with various disease processes including chronic liver disease or chronic pancreatitis result in increased tissue stiffness. Recently, various USE techniques have been cleared by the FDA and all major ultrasound companies offer different approaches of measuring tissue stiffness on their ultrasound machines. The objective of this talk is to familiarize the audience with the clinical indications, imaging techniques and protocols, interpretation, diagnostic accuracy, and limitations of the various USE technique for assessment of tissue stiffness, with special focus on assessment of fibrosis in chronic liver disease.





RC622

Functional MR Imaging for Tumor Targeting in Radiotherapy

Thursday, Dec. 5 8:30AM - 10:00AM Room: E353A



AMA PRA Category 1 Credits ™: 1.50 ARRT Category A+ Credit: 1.75

FDA Discussions may include off-label uses.

Participants

Kristy K. Brock, PhD, Houston, TX (*Moderator*) License agreement, RaySearch Laboratories AB; Grant support, RaySearch Laboratories AB; Research support, Mirada Medical Ltd; ;

Sub-Events

RC622A State of the Art in Functional MR Imaging for Tumor Targeting

Participants

R. Jason Stafford, PhD, Houston, TX (Presenter) Nothing to Disclose

For information about this presentation, contact:

jstafford@mdanderson.org

LEARNING OBJECTIVES

1) Identify some advanced and emerging MRI techniques which inform on tumor physiology and metabolism. 2) Explain the relevance of functional MR observations to basic underlying tumor physiology and biology. 3) Understand key limitations and tradeoffs of functional MR techniques for tumor assessment.

RC622B Clinical Need for Functional MR Imaging for Tumor Targeting in Radiation Therapy

Participants

Michelle M. Kim, MD, Ann Arbor, MI (Presenter) Nothing to Disclose

LEARNING OBJECTIVES

1) Describe the major limitations of anatomic imaging for tumor target delineation in radiation therapy. 2) Identify key physiologic and functional MRI techniques of value in radiation treatment planning. 3) Explain emerging concepts of radiation treatment-individualization using advanced MRI techniques. 4) Discuss the generalizability and application of advanced MRI techniques for radiation treatment planning.

RC622C Technical Challenges in the Integration of Functional MR Imaging for Tumor Targeting into Radiotherapy

Participants

Ning Wen, PHD, Detroit, MI (Presenter) Nothing to Disclose

For information about this presentation, contact:

nwen1@hfhs.org

LEARNING OBJECTIVES

This presentation is going to review the technical challenges to integrate the functional MR Imaging into radiotherapy including the following aspects: 1) tumor characterization among different imaging modalities; 2) reproducibility of functional imaging across different institutions/scanners/protocols; 3) interpretation of imaging features extracted in the deep machine learning algorithms 4) precision to identify the boundary of the targets; 5) reliable imaging biomarkers to predict treatment response.







RC629

Machine Learning and Radiomics in MRI

Thursday, Dec. 5 8:30AM - 10:00AM Room: E451A



AMA PRA Category 1 Credits ™: 1.50 ARRT Category A+ Credit: 1.75

Sub-Events

RC629A Basics of Radiomics Applied to MRI

Participants Olivier Gevaert, PhD, Stanford, CA (*Presenter*) Nothing to Disclose

LEARNING OBJECTIVES

1) How to use radiomics for multi-modal MR imaging with examples using brain MRI. 2) How to develop robust radiomics pipeline from MRI data by using normalization approaches. 3) How to place radiomics in the era of deep learning and convolutional neural networks for MRI data.

RC629B Basics of Machine Learning

Participants

Tarik K. Alkasab, MD, PhD, Boston, MA (Presenter) Consultant, Nuance Communications, Inc

RC629C Applications of Machine Learning for Image Reconstruction

Participants

Hersh Chandarana, MD, New York, NY (Presenter) Equipment support, Siemens AG; Software support, Siemens AG; ;

LEARNING OBJECTIVES

1) Brief review of state-of-art MR acquisition and reconstruction schemes. 2) Examine why deep learning is of interest in MR image reconstruction. 3) Explore some of the novel proposed methods for image reconstruction and discuss potential applications.

ABSTRACT

Machine learning or deep learning is a powerful tool that is already impacting or will impact the entire imaging life cycle. In this talk we will focus on the role of machine learning (specifically deep learning) in MR image generation (reconstruction).

RC629D MRI Applications of Machine Learning for Cancer Diagnosis

Participants

Andrea G. Rockall, FRCR, MRCP, London, United Kingdom (Presenter) Speaker and Chairman, Guerbet SA

LEARNING OBJECTIVES

1) To be familiar with some key examples of clinical development of machine learning tools in MRI in oncology. 2) To know about many of the challenges related to MRI oncology datasets. 3) To be aware of methods of clinical validation of machine learning tools in MRI in oncology.







MSCM52

Case-based Review of Magnetic Resonance (Interactive Session)

Thursday, Dec. <u>5 10:30AM - 12:00PM Room: S100AB</u>

MR

AMA PRA Category 1 Credits ™: 1.50 ARRT Category A+ Credit: 1.75

Participants

Jorge A. Soto, MD, Boston, MA (Director) Royalties, Reed Elsevier

For information about this presentation, contact:

jorge.soto@bmc.org

LEARNING OBJECTIVES

1) Review key MR imaging findings of common and infrequent conditions of various organs in adult and pediatric patients. 2) Highlight key MR imaging features that are useful to narrow the differential diagnosis. 3) Increase confidence in the interpretation of complex MR studies.

Sub-Events

MSCM52A MRI of the Pediatric MSK

Participants Kirsten Ecklund, MD, Boston, MA (*Presenter*) Nothing to Disclose

For information about this presentation, contact:

kirsten.ecklund@childrens.harvard.edu

LEARNING OBJECTIVES

1) Recognize manifestations of normal skeletal development that may be confused with disease. 2) Identify common benign pediatric bone and soft tissue lesions that mimic aggressive neoplasms.

ABSTRACT

Pediatric Musculoskeletal Cases

MSCM52B MRI of the Liver

Participants Jay P. Heiken, MD, Rochester, MN (*Presenter*) Patent agreement, Guerbet SA; Patent agreement, Bayer AG

For information about this presentation, contact:

heiken.jay@mayo.edu

LEARNING OBJECTIVES

1) Identify the MR imaging features of select benign and malignant liver masses. 2) Discuss the indications for MRI hepatobiliary contrast agents. 3) Apply basic principles of LI-RADS categorization of liver observations in patients with cirrhosis.

MSCM52C MRI of the Kidneys, Adrenals, and Retroperitoneum

Participants Avneesh Gupta, MD, Boston, MA (*Presenter*) Nothing to Disclose

For information about this presentation, contact:

avgupta@bmc.org

LEARNING OBJECTIVES

1) Describe the pros and cons of MRI versus other imaging modalities for diagnosis of conditions that affect the kidneys, adrenals and retroperitoneum. 2) Define the MRI sequences that are used in imaging of the kidneys, adrenals and retroperitoneum. 3) Understand the strengths, weaknesses and specific uses of various MRI sequences. 4) Utilize different MRI sequences to accurately diagnose renal, adrenal and retroperitoneal disease processes.

ABSTRACT

This educational session will emphasize MRI as a valuable tool for diagnosis of a variety of conditions that affect the kidneys, adrenals and retroperitoneum. The utility of individual MRI sequences for diagnosis will be discussed, as well as how MRI is used alongside other imaging modalities in the radiologist's armamentarium.

MSCM52D MRI of the Female Pelvis

Participants Marcia C. Javitt, MD, Haifa, Israel (*Presenter*) Nothing to Disclose

LEARNING OBJECTIVES

1) Recognize imaging patterns of benign and malignant disease. 2) Identify, analyze, and interpret key findings that enable an informed evaluation. 3) Be mindful of the need for accurate, safe, and efficient patient management.

ABSTRACT

This case based review of female pelvic imaging will emphasize the process of triage, appropriate selection of diagnostic imaging tools, lesion detection, characterization, and differential diagnosis. The complimentary role of Ultrasound, CT, and MRI will be emphasized with a discussion of the utility of each modality, the clinical impact on medical decision making, and the need for cost minimization.





SSQ03

Cardiac (Coronary Artery Disease: CT and MRI Techniques)

Thursday, Dec. 5 10:30AM - 12:00PM Room: E450B



AMA PRA Category 1 Credits ™: 1.50 ARRT Category A+ Credit: 1.75

FDA Discussions may include off-label uses.

Participants

Evan J. Zucker, MD, Stanford, CA (*Moderator*) Nothing to Disclose Ming-Yen Ng, MBBS, Toronto, ON (*Moderator*) Nothing to Disclose

Sub-Events

SSQ03-01 Iterative Reconstruction in Coronary CT Angiography from Full Coverage Axial Data with Less than 180° of Rotation

Thursday, Dec. 5 10:30AM - 10:40AM Room: E450B

Participants

Wenjing Cao, Shanghai, China (*Abstract Co-Author*) Employee, Shanghai United Imaging Healthcare Co, Ltd Chunfeng Qian, MD, Shanghai, China (*Abstract Co-Author*) Employee, Shanghai United Imaging Healthcare Co, Ltd Xiaoming Wu, Shang Hai, China (*Abstract Co-Author*) Employee, Shanghai United Imaging Healthcare Co, Ltd Yi Wang, Shanghai, China (*Abstract Co-Author*) Employee, Shanghai United Imaging Healthcare Co, Ltd Stanislav Zabic, PhD, Mayfield Village, OH (*Presenter*) Employee, UIH America, Inc

PURPOSE

This abstract reports diagnostic image quality measurements of coronary CT angiography on a 16cm coverage system with high temporal resolution using model-based iterative reconstruction(MBIR).

METHOD AND MATERIALS

Even in the systems with 0.25s rotation time, it is not guaranteed that a quiet cardiac phase is possible to be captured within 240° of axial projections, which equals approximately $180^{\circ} +2 \cdot \gamma \max(\gamma \max \text{ denotes the maximum fan angle})$ and is the amount of data that FBP requires before limited angle artifacts show up in the image. Using an analytic cardiac vessel phantom, mean square error and structural similarity metrics, we have determined that 135° degrees of axial rotation is a threshold for which MBIR still returns images without limited angle artifacts. Evaluated projection range was between 90° and 240°. Then, MBIR was applied to 48 scans from a clinical trial, using only 135° of data centered at the predetermined quiet cardiac phase. Data was acquired on a 320-row, 16cm CT scanner and MBIR images were compared to the standard protocol reconstruction that uses 240° of data. Average heart rate in the trial was 78.6±16.1 bpm and mean effective dose was 1.5 ± 0.75 mSv. Two experienced radiologists evaluated the image quality using a 4-point rating system focusing on motion artifacts. Scores above 3 were considered diagnostic, with 4 being the best.

RESULTS

MBIR cases were rated diagnostic 83.3% of the time, while standard protocol reconstruction was diagnostic only 58.3% of the time. Average rating for MBIR was 3.28 and 3.16 for the two observers and standard cases were rated 2.72 and 2.7 respectively. There was a significant difference in the scores between MBIR and standard cases by both radiologists (p<0.001).

CONCLUSION

MBIR improved the diagnostic image quality significantly by allowing stable reconstructions from a shorter scan, thereby increasing temporal resolution by at least 25%. Other improvements in image quality such as low noise and high resolution were also noted.

CLINICAL RELEVANCE/APPLICATION

Stable MBIR reconstruction with less than 180° of projection data can be used to reduce the motion artifacts in coronary CT angiography, improving the scan success rate of the single beat cardiac scans significantly and thereby reducing the need for repeated scanning.

SSQ03-03 Contrast Media Iodine Concentration in the Left Ventricle Affects the Level of Radiation-Induced DNA Damage during CCTA

Thursday, Dec. 5 10:50AM - 11:00AM Room: E450B

Participants

Toon van Cauteren, MSc, Brussels , Belgium (*Presenter*) Nothing to Disclose Kaoru Tanaka, MD, PhD, Brussels, Belgium (*Abstract Co-Author*) Nothing to Disclose Dries Belsack, MD, Brussels, Belgium (*Abstract Co-Author*) Nothing to Disclose Gert van Gompel, PhD, Brussel , Belgium (*Abstract Co-Author*) Nothing to Disclose Veerle Kersemans, Oxford, United Kingdom (*Abstract Co-Author*) Nothing to Disclose Kristin Jochmans, Brussels, Belgium (*Abstract Co-Author*) Nothing to Disclose Johan de Mey, MD, PhD, Brussels, Belgium (*Abstract Co-Author*) Nothing to Disclose Nico Buls, DSc, PhD, Jette, Belgium (*Abstract Co-Author*) Nothing to Disclose

For information about this presentation, contact:

toon.van.cauteren@vub.be

PURPOSE

To investigate the relationship between iodine concentration in the left ventricle and radiation-induced DNA damage in blood lymphocytes during a coronary CT angiography (CCTA).

METHOD AND MATERIALS

This prospective patient study was approved by the institutional ethical committee and written informed consent was obtained. All scans were performed on a Revolution CT (GE Healthcare) using a one heartbeat scan and a patient-tailored contrast media injection protocol, administering Ultravist 370 mg I/mL (Bayer Healthcare) with a patient specific injection volume, depending on the sex, weight and height of the patient. Blood samples (5 mL) were collected, before and after the CCTA, and radiation-induced DNA double-strand breaks were assessed using γ H2AX immunofluorescent staining of the blood lymphocytes. An average of 3000 lymphocytes was analyzed for each blood sample. The net amount of induced DNA damage was considered as the difference in the amount of γ H2AX foci per cell before and after the CCTA scan, and was normalized to the CTDIvol (mGy). Iodine concentration in the left ventricle was determined by measuring the CT signal (HU) in a 477.5±208.9 mm² ROI and by applying a HU-iodine calibration curve obtained from phantom experiments. Correlation between the iodine concentration in the left ventricle amount of DNA damage per cell was investigated using a Spearman's rank-order test.

RESULTS

We report results of the first 15 patients (median age 66 y, 9M/6F) included in the study. Patients were scanned with a median CTDIvol of 10.8 mGy (95% CI: 8.4-15.8 mGy). Due to differences in patient physiology, the left ventricle iodine concentrations ranged from 13,7 till 25,2 mg I/mL. The CCTA scans caused a net increase in DNA damage ranging from 0.00041 to 0.0074 foci/cell. We observed a significant exponential correlation (r=0.55, p-value=0.035) between dose normalized DNA damage and left ventricle iodine concentration.

CONCLUSION

The amount of iodine contrast concentration in the left ventricle has an impact on the amount of radiation induced DNA double strand breaks.

CLINICAL RELEVANCE/APPLICATION

In CCTA, iodine contrast concentration has an impact on radiation safety. A reduction in iodine concentration reduces radiation induced DNA damage.

SSQ03-04 3D Multiparametric Image Fusion in Coronary Artery Disease

Thursday, Dec. 5 11:00AM - 11:10AM Room: E450B

Participants

Jochen Von Spiczak, MD, Zurich, Switzerland (*Presenter*) Nothing to Disclose Manoj Mannil, Zurich, Switzerland (*Abstract Co-Author*) Nothing to Disclose Hanna Model, Zurich, Switzerland (*Abstract Co-Author*) Nothing to Disclose Chris Schwemmer, Erlangen, Germany (*Abstract Co-Author*) Employee, Siemens AG Sebastian Kozerke, PhD, Zurich, Switzerland (*Abstract Co-Author*) Nothing to Disclose Robert Manka, Zurich, Switzerland (*Abstract Co-Author*) Nothing to Disclose Hatem Alkadhi, MD, Zurich, Switzerland (*Abstract Co-Author*) Nothing to Disclose

PURPOSE

To allow for comprehensive non-invasive diagnostics of coronary artery disease (CAD) by 3D image fusion of CT coronary angiography (CT-CA), CT derived fractional flow reserve (CT-FFR), whole-heart dynamic 3D cardiac MR perfusion (CMR-Perf), and 3D cardiac MR late gadolinium enhancement (CMR-LGE).

METHOD AND MATERIALS

17 patients (54±10 years, one female) who underwent both cardiac CT and CMR imaging due to suspected or known CAD were included. A software facilitating 3D fusion of multimodal, multiparametric cardiac image data was developed. Post processing of CT data included: a) segmentation of the coronary tree and heart contours; b) calculation of CT-FFR values; c) color-coding of the coronary tree according to CT-FFR. Post processing of CMR data included: a) segmentation of the left ventricle (LV) in CMR-Perf and CMR-LGE; b) co-registration of CMR to CT data; c) mathematical projection of CMR-Perf and CMR-LGE values onto the high-resolution LV from CT. Algorithms adopted from the animation movie industry were applied yielding photorealistic rendering. Results from 3D image fusion were compared to separate 2D readouts of CT and CMR.

RESULTS

Image quality of CT-CA, CMR-Perf, and CMR-LGE was rated good to excellent (scores 2.6, 2.6, and 2.5 on four-point Likert scale, 3 = excellent). CT-CA revealed significant stenoses (i.e., >50%) in 7/17 cases (41%). CT-FFR was possible in 16/17 cases (94%) and showed pathologic flow in 7/17 cases (41%). CMR-Perf identified 8/17 patients (47%) with hypoperfusion; average ischemic burden was $17\pm5\%$. CMR-LGE showed myocardial scar in 3/17 cases (18%); average scar burden was $7\pm4\%$. Conventional 2D readout of all imaging modalities resulted in 9/17 cases (53%) with inconsistent findings. Multimodal 3D image fusion was feasible in all patients. Perfusion deficits and myocardial scar could be correlated to culprit coronary lesions where applicable. Most (7/9=78%) of the problems with separate 2D readout could be solved by 3D image fusion, with two cases remaining controversial or incomplete, respectively.

CONCLUSION

Multimodal, multiparametric 3D cardiac image fusion of CT and CMR image data is feasible and helps for comprehensive non-invasive CAD diagnostics.

CLINICAL RELEVANCE/APPLICATION

Comprehensive, non-invasive diagnostic workup of coronary artery disease involves a multitude of pathologic aspects, which are all combined within one 3D visualization approach for the first time.

SSQ03-05 A Randomized Controlled Clinical Trial of Prolonged Stent Deployment Strategy in Primary Percutaneous Coronary Intervention for ST-Segment Elevation Myocardial Infarction

Thursday, Dec. 5 11:10AM - 11:20AM Room: E450B

Participants Min Ma, Chengdu, China (*Presenter*) Nothing to Disclose Ling Wang, Mianyang, China (*Abstract Co-Author*) Nothing to Disclose Yong He, Chengdu, China (*Abstract Co-Author*) Nothing to Disclose

For information about this presentation, contact:

foundhope@foxmail.com

PURPOSE

The aim of this study was to evaluate whether prolonged inflation would decrease the no-reflow phenomenon in primary percutaneous coronary intervention(PPCI) compared with the conventional strategy.

METHOD AND MATERIALS

This was a prospective, single-center, blinded, randomized controlled trial. The primary outcomes were the number of patients with Thrombolysis in myocardial infarction (TIMI) flow grade 3, the incidence of intraoperative no-reflow/slow flow, the corrected TIMI frame count, the myocardial blush grade(MBG), and the number of patients with ST-segment resolution>50%. The procedural time and radiation exposure time were also assessed. A subset of patients was included in a cardiac magnetic resonance (CMR) examination approximately 3 to 5 days after the index procedure to assess extent of microvascular obstruction (MVO).

RESULTS

Sixty patients were randomized into a prolonged inflation strategy group(A group, n=30) and a rapid inflation/deflation strategy group (B group, n=30). TIMI flow grade 3 was found in 96.7% (29/30) of the A group and 63.3% (19/30) of the B group (p=0.005). The A and B group respectively showed the following parameters: 0% (0/30) VS 30% (9/30) no-reflow or slow flow (p=0.002); 90% (29/30) vs 66.7% (20/30) ST-segment resolution >=50% (p=0.028); 35.6 ± 14.5 frames vs 49.18 ± 25.2 frames on corrected TIMI frame count (p=0.014); and 60% (16/30) vs 20% (6/30) MBG 3 (p=0.001). The major cardiovascular adverse event rate was 3.3% (1/30) in both groups (p=1.0) at one month and 3.3% (1/30) for the A group vs 6.7% (2/30) for the B at one year (p=1.0). There were no statistically significant differences in the procedural time, the radiation exposure time and major bleeding events between the two groups. In the CMR substudy, the presence of MVO was detected in 6.7% (1/15) of patients in the A group and in 50% (5/10) of patients in the B group(p=0.023).

CONCLUSION

The effect of the prolonged inflation strategy could prevent the no-reflow phenomenon and reducing the incidence of MVOs and improve myocardial microcirculation perfusion. In addition, long term follow-up and large-sample, randomized controlled clinical trials with a long-term follow-up period are needed to confirm this preliminary result.

CLINICAL RELEVANCE/APPLICATION

The effect of the prolonged inflation strategy may be an effective way to reduce microvascular obstruction.CMR modality is an effective technique to prove this phenomenon.

SSQ03-06 Implementation of Transdermal versus Sublingual Nitroglycerin Administration to Optimize Coronary CT Angiography Scanner Utilization

Thursday, Dec. 5 11:20AM - 11:30AM Room: E450B

Participants

Jan-Erik Scholtz, MD, Frankfurt, Germany (*Presenter*) Nothing to Disclose Vinit Baliyan, MBBS, MD, Boston, MA (*Abstract Co-Author*) Nothing to Disclose Sandeep S. Hedgire, MD, Lexington, MA (*Abstract Co-Author*) Nothing to Disclose Nandini M. Meyersohn, MD, Boston, MA (*Abstract Co-Author*) Nothing to Disclose Frederick R. McNulty JR, RT, Boston, MA (*Abstract Co-Author*) Nothing to Disclose Travis L. Redel, Boston, MA (*Abstract Co-Author*) Nothing to Disclose Katherine Stockton, Boston, MA (*Abstract Co-Author*) Nothing to Disclose Brian B. Ghoshhajra, MD, Boston, MA (*Abstract Co-Author*) Research Grant, Siemens AG

PURPOSE

Coronary CT angiography (CCTA) requires patient preparation including nitroglycerin (NTG) administration, which improves coronary artery assessment. We compared CCTA exam times when using sublingual vs. transdermal NTG administration.

METHOD AND MATERIALS

This retrospective, single center study included outpatients who underwent elective CCTA betweem 4/2016 and 3/2019 and received NTG. Until 5/2018, patients received sublingual NTG tablets (0.6 mg), administered by the supervising physician on the CT scanner table. After 6/2018, patients received transdermal NTG patches (0.8mg/h), placed at least 45 minutes prior to the exam outside the scanner room by a qualified nurse. CCTA time slots were 20 minutes. We compared number of exams exceeding allotted time slots and CCTA exam times subcategorized by room time (patient time inside the scanner suite), preparation time (time from registration to start of room time), and total appointment time (arrival in the radiology department to dismissal) between the two NTG delivery methods by Wilcoxon Rank Sum Test. Severity of coronary artery disease (CAD) burden was also recorded.

The study population included 3,180 patients of whom 2,341 (73.6%) received NTG by tablets and 839 (26.4%) by patches. Mean age was 59.8±13.1 years, 1,388 (43.6%) were females and average BMI was 29.0±6.0 kg/m2. Patient characteristics and CAD burden were not significantly different between NTG delivery methods (>50% luminal coronary stenosis: n=716 [22.5%], p=0.770). Room time was significantly shorter when using NTG patches compared to tablets (18 min [95% confidence interval (CI): 10-37 min], 27 [15-54] min, p<0.001). Preparation time was significantly longer in patients receiving NTG patches compared to tablets (88 [46-135] min, 58 [26-120] min, p<0.001). Total appointment time was significantly longer in patients receiving NTG patches compared to tablets (107 min [68-160] min, 87 [51-151] min, p<0.001). Only 36.6% (n=307) of the exams following patient preparation with NTG patches exceeded the 20-min exam time slot limit compared to 73.0% of exams (n=1,709) using NTG tablets.

CONCLUSION

A workflow using transdermal NTG patches reduce exam times inside the scanner suite and results in less exams exceeding the allotted exam time slot.

CLINICAL RELEVANCE/APPLICATION

Using transdermal NTG patches for patient preparation prior CCTA reduces times in the scanner room and allowed the use of 20minutes time slots.

SSQ03-07 Automatic Coronary Artery Disease Reporting and Data System (CAD-RADSTM) in Cardiac CT **Angiography Using Paired Convolutional Neural Networks**

Thursday, Dec. 5 11:30AM - 11:40AM Room: E450B

Participants

Xiang Wang, Wuhan, China (Presenter) Nothing to Disclose Zengfa Huang, Wuhan, China (Abstract Co-Author) Nothing to Disclose Jianwei Xiao, Wuhan, China (Abstract Co-Author) Nothing to Disclose Yuanliang Xie, Wuhan, China (Abstract Co-Author) Nothing to Disclose Yun Hu, Wuhan, China (Abstract Co-Author) Nothing to Disclose

For information about this presentation, contact:

wangxiang1971@163.com

PURPOSE

The coronary artery disease reporting and data system (CAD-RADSTM) was recently introduced for standard reporting and decision making. We aimed to assess the utility of an automatic post-processing and reporting system based on CAD-RADSTM in suspected coronary artery disease patients.

METHOD AND MATERIALS

A machine learning model was designed for CAD-RADS assessment categories with automatic coronary lumen segmentation algorithm based on convolutional neural networks. The model was trained in a derivation cohort encompassing 2000 patients who underwent coronary computed tomography angiography (CCTA). Patients with bypass grafts, stents were excluded from the training. Then compared to radiologists for classification of CAD-RADS with commercially-available automated segmentation and manual post-processing in a prospective validation cohort.

RESULTS

346 patients were included in the study among 360 patients with three poor CCTA images. Compared with radiologists, the positive predictive value, negative predictive value, sensitivity and specificity of AI for diagnosis of coronary heart disease were 80%, 70%, 80% and 70% respectively. There was no significant difference between the CNN-based CAD-RADS grading and radiologists based CAD-RADS grading in CCTA (P=0.87). The consistency test showed that the Kappa value of the two groups was 0.694 (P<0.05), the consistency was good.

CONCLUSION

The standardized report of CNN-based CAD-RADS in CCTA images can accurately evaluate suspected patients with CAD, and has good consistency with the radiologists.

CLINICAL RELEVANCE/APPLICATION

Report of CNN-based CAD-RADS has good consistency with the radiologists.

SSQ03-08 Use of Salient Features to Optimize a Machine Learning Classifier of Coronary Artery Disease Severity

Thursday, Dec. 5 11:40AM - 11:50AM Room: E450B

Participants

Alexander R. Podgorsak, MS, Buffalo, NY (Presenter) Nothing to Disclose Kelsey N. Sommer, East Amherst, NY (Abstract Co-Author) Nothing to Disclose Vijay Iyer, Buffalo, NY (Abstract Co-Author) Nothing to Disclose Michael F. Wilson, Buffalo, NY (Abstract Co-Author) Nothing to Disclose Umesh Sharmab, Buffalo, NY (Abstract Co-Author) Nothing to Disclose Kanako K. Kumamaru, MD, PhD, Tokyo, Japan (Abstract Co-Author) Nothing to Disclose Frank J. Rybicki III, MD, PhD, Sudbury, MA (Abstract Co-Author) Medical Director, Imagia Cybernetics Inc Dimitrios Mitsouras, PhD, Ottawa, MA (Abstract Co-Author) Research Grant, Canon Medical Systems Corporation; Erin Angel, PhD, Tustin, CA (Abstract Co-Author) Employee, Canon Medical Systems Corporation Ciprian N. Ionita, PhD, Buffalo, NY (Abstract Co-Author) Grant, Canon Medical Systems Corporation; Grant, Stratasys, Ltd; Grant, Medtronic plc;

For information about this presentation, contact:

PURPOSE

Machine learning-based methods have been proposed as an alternative to the current gold standard of determining the hemodynamic significance of coronary artery lesions, invasive Fractional Flow Reserve (FFR) measurements. In this work, we look to optimize the performance of a machine learning classifier that used coronary CT angiography image data to determine coronary artery disease severity.

METHOD AND MATERIALS

50 coronary CT angiographies (CTAs) were collected (Aquilion ONE, Canon Medical Systems) at 70% of the R-R cardiac cycle. Straightened curved planar reformations (SCPRs) of different artery branches were generated (Vitrea, Vital Images) using a slice thickness of 5.0 mm considering four rotational views around the vessel centerline per CTA for a total dataset size of 200. The dataset was split into a training cohort numbering 125 and a testing cohort numbering 75. FFR values were measured to create a labeled dataset. A convolutional neural network was developed to classify input SCPRs by the severity of the coronary lesion. The network synthesized class activation maps (CAMs) such that the most salient features (lesion and aorta) in the SCPRs were visualized. SCPR image data were modified such that the aorta was removed, rendering the lesion as the only salient feature present, and the network was re-trained using the optimized data. Network performance on both original and optimized test data was assessed using area under the receiver operating characteristics curve (AUC), classification accuracy, and a Student's T-Test.

RESULTS

Mean AUC was 0.727 (95% confidence interval, 0.675-0.773) and 0.799 (0.761-0.837) using the original and optimized SCPR data respectively. Mean classification accuracy was 68.1% (63.8%-72.4%) and 79.1% (76.1%-82.1%) using the original and optimized SCPR data respectively. There was a statistically significant advantage to using the optimized SCPR data for classification of coronary disease severity in terms of both AUC (p = 0.001) and classification accuracy (p = 0.0001).

CONCLUSION

This work indicates the potential utility of CAMs for debugging and optimizing a machine learning algorithm to aid in clinical decision making.

CLINICAL RELEVANCE/APPLICATION

Machine learning provides a valuable alternative to invasive FFR measurements for the determination of coronary artery disease severity.

SSQ03-09 Comparison of Post-Surgical Wall Shear Stress Values in Arterial and Venous Coronary Grafts Using Computational Fluid Dynamics Guided by CCTA and 4D Flow MR Imaging

Thursday, Dec. 5 11:50AM - 12:00PM Room: E450B

Participants

Francesca Condemi, PhD, Toronto, ON (*Abstract Co-Author*) Nothing to Disclose Stephen E. Fremes, MD, Toronto, ON (*Abstract Co-Author*) Nothing to Disclose Piero Triverio, PhD, Toronto, ON (*Abstract Co-Author*) Nothing to Disclose Laura Jimenez-Juan, MD, Toronto, ON (*Presenter*) Nothing to Disclose

PURPOSE

Graft failure is a major complication in coronary artery bypass graft (CABG) surgery, whose root causes are still unknown. In coronary arteries, growing evidence indicates that low and oscillatory values of wall shear stress (WSS) contribute to atherosclerosis plaque progression. The role of WSS in graft failure remains still unclear. In a pilot cohort of patients, we developed a computational fluid dynamics model to obtain WSS non-invasively from CCTA images, and compared WSS values in arterial and venous grafts. Differently from previous works, the study is prospective, with a uniform interval between CABG surgery and WSS analysis of one month. Furthermore, 4D flow MRI is used to incorporate patient-specific flow conditions into the computational model.

METHOD AND MATERIALS

Five participants were scanned using CCTA and 4D flow MRI 30±5 days after CABG surgery. Fluid dynamics simulations with appropriate coronaries and graft material properties were performed with Simvascular (Stanford University, Stanford, CA). WSS was spatially and temporally averaged (spatially-averaged TAWSS) for 5 arterial and 6 venous grafts. The oscillatory shear index (OSI) and the ratio between wall area exposed to adverse TAWSS (< 0.4 Pa) and total graft area were also analyzed.

RESULTS

No significant difference was found in spatially-averaged TAWSS between venous and arterial grafts (2.26 ± 2.12 Pa in venous vs. 5.11 ± 3.48 Pa in arterial grafts, p=0.079) and maximum OSI (0.27 ± 0.20 in arterial and 0.25 ± 0.20 in venous grafts, p=0.456). The relative area exposed to low TAWSS was significantly higher in venous grafts ($22.4\pm20.0\%$ in venous vs. $0.77\pm0.98\%$ in arterial grafts, p=0.022).

CONCLUSION

One month after surgery, our study found larger areas of abnormal WSS in venous than in arterial grafts. This observation may be related to the higher failure rate of venous grafts.

CLINICAL RELEVANCE/APPLICATION

This work is a step forward towards understanding the root causes of graft failure in CABG patients, and identifying reliable biomarkers for the early prediction of graft failure.







SSQ05

Science Session with Keynote: Chest (Thoracic MRI)

Thursday, Dec. 5 10:30AM - 12:00PM Room: E350



AMA PRA Category 1 Credits ™: 1.50 ARRT Category A+ Credit: 1.75

FDA Discussions may include off-label uses.

Participants

Jurgen Biederer, MD, Seeheim-Jugenheim, Germany (*Moderator*) Nothing to Disclose Andrew J. Plodkowski, MD, Brookside, NJ (*Moderator*) Nothing to Disclose

Sub-Events

SSQ05-01 Chest Keynote Speaker: MRI of the Thorax - Concepts and Challenges

Thursday, Dec. 5 10:30AM - 10:40AM Room: E350

Participants

Jurgen Biederer, MD, Seeheim-Jugenheim, Germany (Presenter) Nothing to Disclose

SSQ05-02 Distinguishing Cystic Fibrosis Severity Using Dynamic 19F Lung MR Imaging

Thursday, Dec. 5 10:40AM - 10:50AM Room: E350

Participants

Tyler Glass, BEng, Chapel Hill, NC (*Presenter*) Nothing to Disclose Sang H. Chung, Chapel Hill, NC (*Abstract Co-Author*) Nothing to Disclose Jennifer Goralski, Chapel Hill, NC (*Abstract Co-Author*) Nothing to Disclose Scott Donaldson, Chapel Hill, NC (*Abstract Co-Author*) Nothing to Disclose Agathe Ceppe, Chapel Hill, NC (*Abstract Co-Author*) Nothing to Disclose Cecil Charles, PhD, Durham, NC (*Abstract Co-Author*) Nothing to Disclose Brian J. Soher, PhD, Durham, NC (*Abstract Co-Author*) Nothing to Disclose Yueh Z. Lee, MD,PhD, Chapel Hill, NC (*Abstract Co-Author*) License agreement, XinRay Systems Inc

For information about this presentation, contact:

tyler_glass@med.unc.edu

PURPOSE

To investigate dynamic 19F lung MRI gas dynamics to distinguish disease severity in Cystic Fibrosis (CF) patients

METHOD AND MATERIALS

Coronal images of 14 healthy controls and 18 subjects with CF were acquired using a multinuclear capable 3.0 T MRI scanner (PRISMA, Siemens) with a custom 8-channel 19F-tuned chest coil (ScanMed). Subjects inhaled 19F labelled perfluoropropane (PFP) gas mixed with 21% O2 (operating under investigational new drug IND 122,215) during the wash-in phase of the scan. Fifteen second 19F GRE vibe breath hold images were obtained following three breaths of PFP for five cycles of wash in. Gas was then switched to room air for wash-out phase and images were similarly acquired every 3 breaths until wash-out was complete. Semi-automated segmentation was used to identify ventilated voxels and custom software then implemented a previously described biexponential model fit with parameters including wash-in and wash-out time constants, peak signal, delay from origin, and delay to steady state. Upper and lower limits for wash-in and wash-out time constants were then defined to derive fractional lung volumes (FLV) comprising a percent of fitted time constants above upper limit ("slow") or below lower limit ("fast").

RESULTS

For fitted wash-out time constant, one-way ANOVA revealed differences between normal, mild, and moderate CF groups for "fast" FLV (p<0.001), "slow" FLV (p=0.0012), and standard deviation of all fitted wash-out time constant (p<0.001). For fitted wash-in time constant, one-way ANOVA revealed no differences for "fast" FLV (p=0.51), "slow" FLV (p=0.34), or standard deviation of all fitted wash-in time constants (p=0.12). Tukey's HSD revealed differences between mild and moderate CF using wash-out time constant for "fast" FLV (p=0.011) and standard deviation (p=0.015).

CONCLUSION

Dynamic 19F ventilation MRI is able to distinguish cystic fibrosis severity using parameters based on bi-exponential fit model. Washout time constant showed the most differentiating power corresponding to progressive air trapping physiology seen in cystic fibrosis.

CLINICAL RELEVANCE/APPLICATION

This novel imaging technique has advantages over xenon ventilation MRI including cheaper contrast material and inert compound allowing functional imaging with multiple image sets. We anticipate applications for many other lung diseases including pediatric lung malformations, lung resection, COPD monitoring, and bronchiectasis.

SSQ05-03 Automated Quantification of T2 High-Signal-Intensity Volume for Monitoring Lung Inflammation and Response to Treatment in Cystic Fibrosis

Thursday, Dec. 5 10:50AM - 11:00AM Room: E350

Participants

Gael Dournes, MD, PhD, Pessac, France (*Presenter*) Nothing to Disclose Ilyes Benlala, Bordeaux, France (*Abstract Co-Author*) Nothing to Disclose Julie Macey, Bordeaux, France (*Abstract Co-Author*) Nothing to Disclose Stephanie Bui, Bordeaux, France (*Abstract Co-Author*) Nothing to Disclose Francois H. Laurent, MD, Pessac, France (*Abstract Co-Author*) Nothing to Disclose

For information about this presentation, contact:

gael.dournes@chu-bordeaux.fr

PURPOSE

We aim at quantifying the relative high-signal-intensity volume (T2-HSV) using a T2 radial turbo spin echo sequence (T2-RTSE) with black blood contrast, in both healthy volunteers and CF. Secondary objectives were to correlate T2-HSV to pulmonary function test (PFT) in CF, to evaluate T2-HSV changes after treatment, and to evaluate the quantification provided by a composite volume-intensity product (T2-VIP).

METHOD AND MATERIALS

Ten healthy volunteers and twelve CF patients were prospectively enrolled between January 2017 and November 2017. All participants underwent a lung MR protocol including T2-RTSE. CF participants also underwent PFTs the same day. Six CF were under respiratory exacerbation and repeated MRI after treatment. Automated quantification of T2-HSV and T2-VIP were done by two observers. Comparison of means was performed using Mann-Whitney test, correlations were done by using Pearson test, comparison of paired means using paired t-test and reproducibility evaluated using intraclass correlation coefficient.

RESULTS

In healthy volunteers and CF, T2-HSV was equal to $0\% \pm 0$ and $5.9\% \pm 5.0$, respectively and T2-VIP was equal to $0ms \pm 0$ and 464ms \pm 340, respectively (p<0.001). In CF, correlations were found between T2-HSV or T2-VIP with forced expiratory volume in 1 second (r -0.81 and r -0.90, respectively; p<0.001). A significant decrease in both T2-HSV and T2-VIP was observed after treatment (p=0.005 and p<0.001, respectively). The reproducibility of MR metrics were very good.

CONCLUSION

Automated quantification of high-signal-intensity volume is feasible in vivo in CF using MRI. The reproducible method may be a promising MR tool to monitor inflammatory modifications and response to treatment, without radiation nor contrast-product exposure.

CLINICAL RELEVANCE/APPLICATION

Automated quantification of high-signal-intensity volume is feasible in vivo in CF using MRI. The reproducible method may be a promising MR tool to monitor inflammatory modifications and response to treatment, without radiation nor contrast-product exposure.

SSQ05-04 Opportunities for Functional Lung Imaging at Low-Field MRI

Thursday, Dec. 5 11:00AM - 11:10AM Room: E350

Participants

Ipshita Bhattacharya, Bethesda, MD (*Presenter*) Nothing to Disclose Joel Moss, MD,PhD, Bethesda, MD (*Abstract Co-Author*) Nothing to Disclose Kenneth Olivier, Bethesda, MD (*Abstract Co-Author*) Nothing to Disclose Ashkan A. Malayeri, MD, Andover, MA (*Abstract Co-Author*) Nothing to Disclose Elizabeth C. Jones, MD, Bethesda, MD (*Abstract Co-Author*) Nothing to Disclose Robert S. Balaban, PhD, Bethesda, MD (*Abstract Co-Author*) Nothing to Disclose Adrienne Campbell, Bethesda, MD (*Abstract Co-Author*) Nothing to Disclose

For information about this presentation, contact:

adrienne.campbell@nih.gov

PURPOSE

Lung imaging is notoriously difficult with MRI. We show that a high-performance low field MRI system may offer two advantages for lung imaging: 1. Improved field homogeneity resulting in prolonged T2* and improved imaging of the lung parenchyma and 2. Increased oxygen relaxivity for functional assessment of ventilation.

METHOD AND MATERIALS

Lung MRI was performed on a prototype 0.55T system (ramped down MAGNETOM Aera, Siemens Healthcare, Erlangen, Germany). This system is unique because it uses modern magnet design, fast gradient design, modern RF system, custom phased array coils and advanced imaging methods. Images were compared to a commercial 1.5T (MAGNETOM Aera, Siemens Healthcare, Erlangen, Germany). Anatomical lung imaging (T2w turbo spin echo) and 3D oxygen-enhanced ultrashort TE imaging was performed on healthy volunteers and patients with disease (eg. lymphangioleiomyomatosis (LAM) and bronchiectasis) with 100% oxygen (15L/min through, non-rebreather face mask). Room-air and oxygen images were registered and subtracted to estimate regional ventilation.

RESULTS

Images at 0.55T provided superior visualization of the lung parenchyma compared to 1.5T and useful insight into lung pathology, including the assessment of cysts and bronchial wall thickening. This can be attributed to the improved B0 homogeneity, minimized susceptibility gradients at air/tissue interfaces, and the longer T2* of lung tissue. The relaxivity of molecular oxygen was 4.7e-4

mmHg-1s-1 at 0.55T (vs 3.1e-4 mmHg-1s-1 at 1.5T). In healthy volunteers, lung signal increased by 18.2 \pm 6.3% (n = 5) with oxygen inhalation, compared with only 8.6 \pm 2.9% at 1.5T in the same subjects. Patients with LAM (n = 8) had only 6.5 \pm 5.1% signal increase with oxygen inhalation and showed increased heterogeneity in the signal enhancement.

CONCLUSION

This system pairs modern system design with low magnetic field. By comparison, most low field systems are not designed to be high performance and, thus, compromise image quality. We demonstrate the potential of a state-of-the-art low field MRI to enable lung imaging. Moreover, we demonstrate the potential of oxygen as a contrast that performs better at lower field for the assessment of regional lung function.

CLINICAL RELEVANCE/APPLICATION

Low field MRI with modern magnet design may provide a unique opportunity for functional assessment of the lung by virtue of the improved field uniformity and improved oxygen contrast performance.

SSQ05-05 Ferumoxytol-Enhanced MR Venography of the Central Veins of the Thorax to Evaluate Stenoses and Occlusions in Patients with Renal Failure

Thursday, Dec. 5 11:10AM - 11:20AM Room: E350

Participants

Christopher J. Gallo, BS, Durham, NC (*Presenter*) Nothing to Disclose Joseph G. Mammarappallil, MD,PhD, Durham, NC (*Abstract Co-Author*) Nothing to Disclose David Y. Johnson, MD, Durham, NC (*Abstract Co-Author*) Nothing to Disclose Charles Y. Kim, MD, Raleigh, NC (*Abstract Co-Author*) Consultant, Medtronic plc; Consultant, Humacyte; Consultant, Galvani

For information about this presentation, contact:

christopher.gallo@duke.edu

PURPOSE

Hemodialysis patients have a high prevalence of central venous stenosis and frequently need imaging for access planning; however, these individuals cannot receive gadolinium due to concern for NSF. The purpose of this study was to assess the diagnostic performance of ferumoxytol-enhanced MR venography (MRV) for detection of stenoses and occlusions of the central veins of the thorax, with conventional venography as the reference standard.

METHOD AND MATERIALS

This retrospective study was approved by the IRB; a waiver of informed consent was obtained. Analysis was performed on 35 consecutive patients (mean age 48.6 years, 17 male, 18 female) who underwent ferumoxytol-enhanced MRV of the central veins and concurrent conventional venography. The central veins were divided into 7 segments for evaluation. Two radiologists interpreted MRVs in consensus for stenoses and occlusions. Confidence levels were scored on a scale of 1-4, with 4 being completely confident. Quantitative analysis consisted of measurement and calculation of the signal-to-noise ratio (SNR), contrast-to-noise ratio (CNR), and intraluminal signal heterogeneity for all venous segments.

RESULTS

Of the 126 total venous segments with corresponding conventional venography, 80 were stenotic or occluded. The sensitivity and specificity for detection of stenosis or occlusion was 0.98 and 1.0, respectively, whereas the sensitivity and specificity for detecting occlusions alone was 0.98 and 0.99. Mean reader confidence was 3.5. The calculated mean intraluminal SNR, CNR, and heterogeneity was 219.7, 169.2, and 0.07, respectively. There were no adverse events related to contrast administration.

CONCLUSION

Ferumoxytol-enhanced MR venography demonstrated excellent sensitivity and specificity for detection of central venous stenoses and occlusions of the thorax. Given that ferumoxytol is an FDA-approved parenteral iron supplement for hemodialysis patients that does not carry a risk of NSF, this contrast agent is particularly well-suited for noninvasive vascular imaging in this population.

CLINICAL RELEVANCE/APPLICATION

Since gadolinium is contraindicated for hemodialysis patients, ferumoxytol-enhanced MRV is an excellent modality for evaluation of the central veins and avoids the risk of Gd-associated NSF.

SSQ05-06 Quantitative Assessment of Diaphragm Dysfunction Using MRI in COPD

Thursday, Dec. 5 11:20AM - 11:30AM Room: E350

Participants Yifan Wang, PhD, Rotterdam, Netherlands (*Presenter*) Nothing to Disclose Yong Chen, Yinchuan, China (*Abstract Co-Author*) Nothing to Disclose Harm A. Tiddens, MD, Rotterdam, Netherlands (*Abstract Co-Author*) Nothing to Disclose Marleen De Bruijne, PhD, Rotterdam, Netherlands (*Abstract Co-Author*) Research Grant, AstraZeneca PLC Pierluigi Ciet, MD, Rotterdam, Netherlands (*Abstract Co-Author*) Nothing to Disclose

For information about this presentation, contact:

y.wang@erasmusmc.nl

PURPOSE

It is believed that diaphragm dysfunction is related to the airflow limitation resulting in lung hyperinflation in patients with chronic obstructive pulmonary disease (COPD). We applied dynamic MRI to quantitatively evaluate diaphragm dysfunction in COPD.

METHOD AND MATERIALS

The study comprised 80 stable COPD patients with different disease severities (GOLD stages 1-4) and 21 healthy volunteers. Chest

MRI was performed in a 3T scanner with end-inspiratory/expiratory 3D-SPGR sequence and 2D dynamic diaphragmatic sequence. Images were automatically segmented. We measured the area under the diaphragm (ds), the height of the diaphragm (dh), cranialcaudal length (cc), anterior-posterior length (ap) and lung area (ls) at the start and end of inspiration. The anterior and posterior diaphragm angles and the paradoxical diaphragmatic movement ratio were analyzed. These parameters were investigated in correlation with pulmonary function test and emphysema index.

RESULTS

In the severe COPD patients with GOLD 3-4, we observed that insp-exp-ratio of ds and dh decreased significantly, and insp-expratio of the ls, cc and ap reduced, which reflected the change of diaphragmatic position. The anterior and posterior diaphragm angles reduced in patients with GOLD3-4 at the start and end of inspiration, which reflected the change of the diaphragmatic shape.

CONCLUSION

Chest dynamic MRI can provide new imaging biomarkers to assess diaphragm dysfunction in COPD without specialized equipment.

CLINICAL RELEVANCE/APPLICATION

Figure 1: Sagittal dynamic cine-MRI image of the right hemidiaphragm at the end of inspiration (left) and expiration (right), showing the shape of diaphragm in COPD patient get flat and the excursion diaphragm in COPD patient reduced.

SSQ05-07 Non-Invasive MR-Based Characterization of Pleural Effusions and Ascites in Patients with Suspected Lymphatic Leakage Using a 6-Point mDIXON Fat Quantification Method

Thursday, Dec. 5 11:30AM - 11:40AM Room: E350

Participants

Daniel Kuetting, MD, Bonn, Germany (*Presenter*) Nothing to Disclose Anton Faron, MD, Bonn, Germany (*Abstract Co-Author*) Nothing to Disclose Julian A. Luetkens, MD, Bonn, Germany (*Abstract Co-Author*) Nothing to Disclose Daniel K. Thomas, MD, PhD, Bonn, Germany (*Abstract Co-Author*) Nothing to Disclose Claus C. Pieper, MD, Bonn, Germany (*Abstract Co-Author*) Nothing to Disclose

PURPOSE

To assess whether MR-based 6-point mDixon fat quantification (mDIXONquant) allows for non-invasive differentiation of chylous (i.e. rich in triglycerides [TG]; e.g. chylothorax) and non-chylous effusions.

METHOD AND MATERIALS

In-vitro, ex-vivo and in-vivo MR-examinations were performed using the commercially available mDIXONquant on a clinical 1.5T MRscanner. Proton density fat fraction (PDFF) was measured by a ROI-based approach on parameter maps. For in-vitro experiments eight fatty fluid solutions with known TG content (145 to 19000 mg/dl) were examined. For ex-vivo evaluation 14 chylous and 6 non-chylous clinical fluid samples were examined. In-vivo testing was performed in 29 patients with chylous (n=16) and nonchylous (n=13) effusions. All clinical samples underwent laboratory testing for TG, total protein, leucocytes, sodium, potassium, calcium and chloride levels. Laboratory values were correlated with PDFF and receiver operating characteristic analysis was used to determine the optimal PDFF threshold to differentiate chylous and non-chylous fluids.

RESULTS

In-vitro analysis showed that PDFF-values highly correlated with TG-content (r=0.998). Ex-vivo analysis revealed significant differences between PDFF for chylous (2.5% ±1.2) and non-chylous fluids ($0.8\% \pm 0.2$)(p=0.0013). Ex-vivo PDFF highly correlated with TG-content (p<0.0001; r=0.88). In-vivo PDFF also significantly differed between chylous ($6.2\% \pm 4.3$) and non-chylous fluids ($0.6\% \pm 0.6$)(p<0.0001). In-vivo PDFF correlated strongly with TG-content (p<0.0001; r=0.96), and moderately with protein levels (p =0.0054; r=-0.66). Using PDFF cut-off values of either > 1.2% or > 1.8% yielded a sensitivity of 86% or 79% and specificity of 91% or 100%, respectively, for in-vivo differentiation of chylous and non-chylous effusions.

CONCLUSION

Non-invasive differentiation of chylous and non-chylous effusions is feasible using a commercially available MR-based fat quantification method. This can be helpful for pre-interventional work-up of complex cases (e.g combined pleural/pericardial effusions and ascites) in which diagnostic paracentesis may lead to an increased risk of complications

CLINICAL RELEVANCE/APPLICATION

This noninvasive MR technique can be seen as an alternative and reliable diagnostic approach allowing for the differentiation between chylous and non-chylous effusions in cases where paracentesis is not possible.

SSQ05-08 Imaging and Quantitative Evaluation of Pulmonary Blood Flow Using Pseudo-Continuous Arterial Spin Labeling (PCASL) with True-FISP Imaging at 1.5 Tesla: Free-Breathing and Timed Breath-Hold Examinations

Thursday, Dec. 5 11:40AM - 11:50AM Room: E350

Participants

Ferdinand F. Seith, MD, Tubingen, Germany (*Presenter*) Nothing to Disclose Rolf Pohmann, Tubingen, Germany (*Abstract Co-Author*) Nothing to Disclose Thomas Kuestner, DIPLENG, Stuttgart, Germany (*Abstract Co-Author*) Nothing to Disclose Klaus Scheffler, Tuebingen, Germany (*Abstract Co-Author*) Nothing to Disclose Martin Schwartz, Tuebingen, Germany (*Abstract Co-Author*) Nothing to Disclose Marius Horger, MD, Tuebingen, Germany (*Abstract Co-Author*) Nothing to Disclose Konstantin Nikolaou, MD, Tuebingen, Germany (*Abstract Co-Author*) Nothing to Disclose Konstantin Nikolaou, MD, Tuebingen, Germany (*Abstract Co-Author*) Nothing to Disclose Fritz Schick, MD, PhD, Tuebingen, Germany (*Abstract Co-Author*) Nothing to Disclose Petros Martirosian, PhD, Tuebingen, Germany (*Abstract Co-Author*) Nothing to Disclose

PURPOSE

To evaluate PCASL imaging with True-FISP data acquisition to assess lung perfusion at 1.5 Tesla and to evaluate a free-breathing examination scheme.

METHOD AND MATERIALS

Ten volunteers (31±7 y/o, 2f) were examined in a 1.5 Tesla MRI with ECG-triggered PCASL True-FISP imaging of the lung under free-breathing (FB) and timed breath-hold (TBH) by labeling the pulmonary trunk during systole. Four coronal slices were acquired with a post labeling delay of 1000 ms and non-rigidly registered in several steps by a cubic B-spline-based multi-resolution non-rigid registration with mutual information as similarity metric and Quasi-Newton optimization algorithm. To assess the quality of image registration, the mean structural similarity index (MSSIM) and the normalized mean squared error (NMSE) were calculated using TBH data as reference. MSSIM and NMSE were compared using a paired sample t-test. A p-value <0.05 was considered significant. To quantify lung perfusion, parenchyma was segmented using Gaussian mixture model clustering and compared with Bland-Altman plots. In two patients with pulmonary embolism, FB examinations were performed.

RESULTS

High perfusion signal could be assessed in all volunteers and patients. Image registration lead to high image quality even under free breathing. Mean average over cardiac cycle pulmonary perfusion values acquired under FB (slice 1-4, ml/min/ml: 1.34 ± 0.39 , 0.98 ± 0.36 , 0.97 ± 0.38 , 0.94 ± 0.43) were in good accordance to those from TBH (slice 1-4, ml/min/ml: 1.30 ± 0.40 , 0.97 ± 0.35 , 0.95 ± 0.37 , $0.87\pm.38$). In patients, perfusion deficits were in accordance with embolism visible in CT.

CONCLUSION

ECG-triggered PCASL True-FISP imaging of the lung at 1.5 Tesla can provide perfusion images of high image quality by labeling the pulmonary trunk. Using non-rigid image registration, reliable quantitative perfusion maps and good image quality can be assessed, even when acquired under free breathing.

CLINICAL RELEVANCE/APPLICATION

PCASL imaging with True-FISP data acquisition enables perfusion images of the lung of high image quality even under free breathing without contrast agent which can be of clinical singificance for different types of lung diseases.

SSQ05-09 Pulmonary Thin-Section MR Imaging with Ultra-Short Echo Time (UTE) versus Low-Dose CT versus Standard-Dose CT: Capability for Nodule Detection and Lung-RADS Classification

Thursday, Dec. 5 11:50AM - 12:00PM Room: E350

Participants

Yoshiharu Ohno, MD, PhD, Toyoake, Japan (*Presenter*) Research Grant, Canon Medical Systems Corporation; Research Grant, DAIICHI SANKYO Group; ;

Masao Yui, Otawara, Japan (*Abstract Co-Author*) Employee, Canon Medical Systems Corporation Yuji Kishida, MD,PhD, Kobe, Japan (*Abstract Co-Author*) Nothing to Disclose Shinichiro Seki, Kobe, Japan (*Abstract Co-Author*) Research Grant, Canon Medical Systems Corporation Daisuke Takenaka, MD, Akashi, Japan (*Abstract Co-Author*) Nothing to Disclose Takeshi Yoshikawa, MD, Kobe, Japan (*Abstract Co-Author*) Research Grant, Canon Medical Systems Corporation

For information about this presentation, contact:

yohno@fujita-hu.ac.jp

PURPOSE

To compare the capability of pulmonary MR imaging with ultra-short echo time (UTE-MRI) for lung nodule detection and Lung-RADS classification with thin-section low- and standard-dose CTs.

METHOD AND MATERIALS

110 consecutive patients (64 males and 46 females: mean age, 65 years) with suspected pulmonary nodules at near-by hospital were examined with standard- and low-dose CTs (270 mA [SDCT] and 60 mA [LDCT]) and UTE-MRI. According to SDCT findings, all nodules were divided into solid, part-solid and ground glass nodules. In each patient, probability of presence at each pulmonary nodule was assessed on all three methods by means of 5-point visual scoring system by two board certified chest radiologists. In addition, all nodules were classified based on Lung-RADS on each method by same radiologists. To compare nodule detection capability, Jackknife alternative free-response receiver operating characteristic (JAFROC) analysis were performed among all methods. In addition, we assessed the differences among the three methods in terms of figure of merit (FOM) values, sensitivity and false-positive rate by means of one-way ANOVA. To evaluate Lung-RADS classification capability, inter-observer agreement of each method was evaluated by kappa statistics with χ^2 test. In addition, inter-method agreements were also assessed by kappa statistics with χ^2 test were performed.

RESULTS

FOMs of all methods (UTE-MRI: FOM=0.89, LDCT: FOM=0.86, SDCT: FOM=0.89) had no significant difference (p>0.05). Sensitivity (SE) and false-positive rate per case (FP) of UTE-MRI (SE: 92.5[508/549] %, FP: 0.62/case) had no significant difference with those of LDCT (SE: 93.2 [512/549] %, p>0.05; FP: 0.68/case, p>0.05) and SDCT (SE: 93.4 [513/549] %, p>0.05; FP: 0.55/case, p>0.05). Inter-observer agreement of each method for Lung-RADS classification was shown as almost perfect (UTE-MRI: κ =0.92, p<0.0001; LDCT: κ =0.93, p<0.0001; SDCT: κ =0.95, p<0.0001). Inter-method agreements for Lung-RADS classification were also assessed as almost perfect (UTE-MRI vs. LDCT: κ =0.87, p<0.0001; UTE-MRI vs. SDCT: κ =0.89, p<0.0001; LDCT vs. SDCT: κ =0.95, p<0.0001).

CONCLUSION

Pulmonary MR imaging with UTE is considered at least as valuable as low- and standard-dose CTs for lung nodule detection and Lung-RADS classification.

CLINICAL RELEVANCE/APPLICATION

 MR imaging with UTE is considered at least as valuable as low- and standard-dose CTs for lung nodule detection and Lung-RADS classification.







SSQ07

Gastrointestinal (Advanced MRI Techniques)

Thursday, Dec. 5 10:30AM - 12:00PM Room: S103CD



AMA PRA Category 1 Credits ™: 1.50 ARRT Category A+ Credit: 1.75

Participants

Hersh Chandarana, MD, New York, NY (*Moderator*) Equipment support, Siemens AG; Software support, Siemens AG; ; Kelly L. Cox, DO, Jacksonville, FL (*Moderator*) Nothing to Disclose Michael A. Ohliger, MD, PhD, Burlingame, CA (*Moderator*) Nothing to Disclose

Sub-Events

SSQ07-01 Impact of Temporal Resolution and Motion Correction for Dynamic Contrast-Enhanced MR Imaging of the Liver Using an Accelerated Golden-Angle Radial Sequence

Thursday, Dec. 5 10:30AM - 10:40AM Room: S103CD

Participants

Rihab Mansour, Montreal, QC (*Abstract Co-Author*) Nothing to Disclose Alana Thibobeau-Antonacci, Montreal, QC (*Abstract Co-Author*) Nothing to Disclose Laurent Bilodeau, Montreal, QC (*Abstract Co-Author*) Nothing to Disclose Milena Cerny, MD, Montreal, QC (*Abstract Co-Author*) Nothing to Disclose Guillaume Gilbert, PhD, Montreal, QC (*Abstract Co-Author*) Employee, Koninklijke Philips NV An Tang, MD, Montreal, QC (*Abstract Co-Author*) Research Consultant, Imagia Cybernetics Inc Speaker, Siemens AG Speaker, Eli Lilly and Company

Samuel Kadoury, Montreal, QC (Presenter) Nothing to Disclose

PURPOSE

To evaluate the impact on image quality and quantitative dynamic contrast-enhanced (DCE)-MRI perfusion parameters when varying the number of respiratory motion states on DCE-MRI perfusion parameters using eXtraDimensional Golden-Angle Radial Sparse Parallel (XD-GRASP).

METHOD AND MATERIALS

This prospective study was approved by the institutional review board and consent was obtained from patients. Eleven patients, 6 men and 5 women (70 years ± 11 [standard deviation]), underwent DCE-MRI examinations on a 3.0 T MRI (Achieva TX, Philips Healthcare). T1 mapping was performed using the variable flip-angle method with fat-saturated cartesian 3D gradient-echo acquisitions in breath-hold. DCE acquisition was performed in free-breathing using a 3D stack-of-stars gradient-echo golden-angle radial acquisition. Contrast injection was performed 30 s after initiating the DCE acquisition. Nonparametric analysis was conducted on the time-intensity curves. Parametric analysis was performed using a dual-input single-compartment model. Comparison of signal-to-noise ratio (SNR), contrast-to-noise ratio (CNR) and perfusion parameters was made for XD-GRASP with different number of respiratory motion states.

RESULTS

A total of 22 HCCs (size: 11 - 52 mm) were evaluated. XD-GRASP reconstructed with increased motion states improves the SNR (P < 0.05) but reduces temporal resolution (0.04 volume/s vs 0.17 volume/s for one motion state) (P < 0.05). The peak enhancement ratio and normalized maximum intensity time ratio increased with decreasing number of motion states (P < 0.001) while the transfer constant from the portal venous plasma to the surrounding tissue significantly decreased (P < 0.05).

CONCLUSION

Peak enhancement ratio, normalized maximum intensity time ratio and transfer constant from the portal venous plasma to the surrounding tissue were sensitive to the number of motion states and to the temporal resolution. While a higher number of motion states improves SNR, the resulting lower temporal resolution can influence quantitative parameters that capture rapid signal changes.

CLINICAL RELEVANCE/APPLICATION

XD-GRASP can be used to perform quantitative perfusion measures for HCC response assessment, but the number of motion states may significantly alter some quantitative parameters.

SSQ07-02 Clinical Application of Amide Proton Transfer Imaging in the Liver: The Feasibility Study

Thursday, Dec. 5 10:40AM - 10:50AM Room: S103CD

Participants Nieun Seo, MD, Seoul, Korea, Republic Of (*Presenter*) Nothing to Disclose Yong Eun Chung, MD, PhD, Seoul, Korea, Republic Of (*Abstract Co-Author*) Nothing to Disclose Ha-Kyu Jeong, Suwon, Korea, Republic Of (*Abstract Co-Author*) Nothing to Disclose Jin-Young Choi, Seoul, Korea, Republic Of (*Abstract Co-Author*) Nothing to Disclose

For information about this presentation, contact:

neseo.radiology@gmail.com

PURPOSE

To investigate the feasibility of amide proton transfer (APT) magnetic resonance imaging (MRI) in the liver and to evaluate its ability to characterize focal liver lesions (FLL)

METHOD AND MATERIALS

A total of 85 patients with suspected FLLs who underwent APT imaging at 3T were included. APT imaging was obtained at single slice to include FLL through five breath holds with interleaved APT and B0 field map scans. APT signals in the background liver and FLL were analyzed with the asymmetric magnetization transfer ratio (MTRasym). Technical success rate of APT imaging was calculated. MTRasym values were compared between the background liver and FLL, and between different FLLs using paired sample t-test or Wilcoxon signed rank test.

RESULTS

Technical success rate of APT imaging in the liver was 69.4% (59/85), and the reason of failure was too large B0 inhomogeneity. The acquisition time of APT imaging was approximately 1 minute. Among 59 FLLs with analyzable APT images, MTRasym values of 27 patients with liver metastases and 23 patients with hepatocellular carcinomas (HCCs) were compared. MTRasym values of metastases and background liver were significantly different ($0.13 \pm 2.15\%$ vs. $-1.62 \pm 2.12\%$, P = 0.001), while those values of HCCs and background liver were similar ($-1.41 \pm 3.68\%$ vs. $-1.18 \pm 1.60\%$, P = 0.767). MTRasym values of metastases were significantly higher than those of liver metastases (P = 0.027).

CONCLUSION

APT imaging could have a role to differentiate metastasis from HCC, although approximately 30% of cases were failed to obtain acceptable APT images of the liver.

CLINICAL RELEVANCE/APPLICATION

APT imaging might be useful to characterize focal liver lesions, but further technical improvement is required to apply APT imaging in the human liver.

SSQ07-03 Evaluation of Liver MRE Analyzability Criteria Using a Simulation Method Based on Successively and Concentrically Decreasing the Size of Selected Regions-of-Interest: A Proof-of-Concept Study

Thursday, Dec. 5 10:50AM - 11:00AM Room: S103CD

Participants

Michael S. Middleton, MD,PhD, San Diego, CA (*Presenter*) Institutional research contract, Alexion Pharmaceuticals, Inc; Institutional research contract, AstraZeneca PLC; Institutional research contract, BioClinica, Inc; Institutional research contract, Biomedical Systems; Consultant, Bracco Group; Institutional research contract, Bristol-Myers Squibb Company; Institutional research contract, Enanta; Institutional research contract, Galmed Pharmaceuticals Ltd; Institutional consultant contract, F. Hoffmann-La Roche Ltd; Institutional research contract, General Electric Company; Institutional research contract, Gilead Sciences, Inc; Institutional research contract, Guerbet SA; Institutional research contract, ICON plc; Institutional research contract, Intercept Pharmaceuticals, Inc; Consultant, Kowa Company, Ltd; Consultant, MEDIAN Technologies; Consultant, IBM Corporation; Consultant, Novo Nordisk AS; Institutional research contract, Pfizer Inc; Stockholder, Pfizer Inc; Institutional research contract, Prosciento; Consultant, Quantitative Insights, Inc; Institutional research contract, F. Hoffmann-La Roche Ltd; Institutional research contract, Synageva; Institutional research contract, Siemens AG; Institutional research contract, VirtualScopics, Inc

Chetan Potu, La Jolla, CA (Abstract Co-Author) Nothing to Disclose

Walter Henderson, La Jolla, CA (Abstract Co-Author) Nothing to Disclose

Timoteo I. Delgado, BA, San Diego, CA (Abstract Co-Author) Nothing to Disclose

Chuhan Chung, MD, Foster City, CA (Abstract Co-Author) Employee, Gilead Sciences, Inc

Stephen Djedjos, MD, Foster City, CA (Abstract Co-Author) Employee, Gilead Sciences, Inc

Robert Myers, MD, Foster City, CA (Abstract Co-Author) Employee, Gilead Sciences, Inc

Richard L. Ehman, MD, Rochester, MN (Abstract Co-Author) CEO, Resoundant, Inc; Stockholder, Resoundant, Inc;

Claude B. Sirlin, MD, San Diego, CA (*Abstract Co-Author*) Research Grant, Gilead Sciences, Inc; Research Grant, General Electric Company; Research Grant, Siemens AG; Research Grant, Bayer AG; Research Grant, Koninklijke Philips NV; Consultant, AMRA AB; Consultant, Fulcrum; Consultant, IBM Corporation; Consultant, Exact Sciences Corporation; Consultant, Boehringer Ingelheim GmbH; Consultant, Arterys Inc; Consultant, Epigenomics; Author, Medscape, LLC; Lab service agreement, Gilead Sciences, Inc; Lab service agreement, ICON plc; Lab service agreement, Intercept Pharmaceuticals, Inc; Lab service agreement, Shire plc; Lab service agreement, Enanta; Lab service agreement, Takeda Pharmaceutical Company Limited; Lab service agreement, Alexion Pharmaceuticals, Inc; Lab service agreement, NuSirt Biopharma, Inc

For information about this presentation, contact:

msm@ucsd.edu

PURPOSE

An objective method to determine the adequacy of liver magnetic resonance elastography (MRE) exams is to use a cutoff for total region-of-interest (ROI) size, usually either 500 or 700 pixels (Px) over four slices. However, little objective evidence supports either of these cutoffs. We performed a simulation study to evaluate how the mean, and the range of calculated liver stiffness values varies for these, and two higher cutoff values as we concentrically shrink total ROI size, for data from a multi-center drug development clinical trial of adults with nonalcoholic steatohepatitis (NCT02854605).

METHOD AND MATERIALS

Two-hundred and six MR exams were selected from the aforementioned clinical trial, based on availability of elastograms, and ROI

size >= 4000 Px over four slices placed at clinical trial sites during the study. For each exam, stiffness values for all pixels were recorded. Stiffness values were calculated by randomly removing ten concentric Px at a time from the ROI edges, and repeating 100 times. For each simulation of 100 iterations, the stiffness ranges, at 500, 700, 2000, and 4000 Px were captured, and the medians were calculated. An absolute stiffness value difference was recorded for each of the four cutoffs, compared to the stiffness value reported using all pixels, and the means were calculated.

RESULTS

Average absolute differences in mean stiffness values across all simulations at the four cutoff values, compared to those obtained using all pixels, increased as cutoff values decreased (0.073, 0.148, 0.256, and 0.292 kPa for 4000, 2000, 700, and 500 Px, respectively). The median values of the the stiffness ranges across all simulations at the four cutoffs similarly increased as cutoff value decreased (0.014, 0.021, 0.038, 0.043 kPa at 4000, 2000, 700, and 500 Px, respectively).

CONCLUSION

At a proof-of-concept level, and subject to validation in other independent cohorts, this data supports that MRE liver stiffness analyzability cutoffs down to 500 Px over four slices are reasonable. For all four pixel cutoffs, the median values of the stiffness ranges, and the average absolute differences in mean liver stiffness compared to values obtained using all pixels, were small.

CLINICAL RELEVANCE/APPLICATION

These results suggest that MRE analyzability using a cutoff as low as 500 Px is likely to be acceptable for drug development clinical trials, and also for clinical care after further validation.

SSQ07-04 T1 Relaxation Times of the Liver and Spleen to Predict Significant Liver Fibrosis: Is There an Additional Value of Normalization to Blood Pool?

Thursday, Dec. 5 11:00AM - 11:10AM Room: S103CD

Participants

Verena Obmann, MD, Cleveland Heights, OH (*Abstract Co-Author*) Nothing to Disclose Annalisa Berzigotti, Bern, Switzerland (*Abstract Co-Author*) Nothing to Disclose Lukas Ebner, MD, Bern, Switzerland (*Abstract Co-Author*) Nothing to Disclose Andreas Christe, Bern, Switzerland (*Abstract Co-Author*) Nothing to Disclose Adrian T. Huber, MD, Bern, Switzerland (*Presenter*) Nothing to Disclose

For information about this presentation, contact:

adrian.huber@insel.ch

PURPOSE

To analyze liver and spleen native T1 relaxometry values to predict significant fibrosis and their additional value when normalized to the blood pool.

METHOD AND MATERIALS

156 patients without solid liver lesions, prior liver surgery or portal vein thrombosis on routine liver multidetector CT scans underwent liver MRI with gradient-echo based MR elastography (MRE) and Shortened Modified Look-Locker Inversion recovery (shMOLLI) based T1 relaxometry. T1 relaxation times were measured in the right liver lobe and in the spleen, as well as in the aorta and in the vena cava. MRE liver stiffness were compared with T1 relaxation times alone, as well as T1 relaxation times normalized to the blood pool in the vena cava and in the aorta. Pearson correlation, students t-test and receiver operation characteristics (ROC) analysis were used to investigate the usefulness of different T1 relaxometry values to predict significant liver fibrosis, using a cutoff value of 3.5kPa in MRE (corresponding to F2 or higher in histology).

RESULTS

Correlation between T1 relaxometry values and MRE liver stiffness was r=0.49-0.59 (p<0.001) for T1 of the liver and for T1 of the liver normalized to blood pool, while T1 of the spleen was less useful (r=0.11-0.17). Both normalized and not normalized T1 values of the liver allowed to significantly separate patients with significant liver fibrosis from those without significant liver fibrosis (p<0.001). In ROC-analysis, T1 relaxometry values normalized to the blood pool did not perform better than T1 values alone (Figure).

CONCLUSION

Native T1 relaxation times of the liver allowed to predict clinically significant liver fibrosis, while T1 relaxation times of the spleen were less useful. There was no additional value of liver and spleen native T1 relaxometry values to predict significant fibrosis when normalized to the blood pool.

CLINICAL RELEVANCE/APPLICATION

T1 relaxometry is acquired in 9 seconds per slice and may be installed on any MR scanner without the need for additional hardware. It allows to predict significant liver fibrosis without time-consuming image post-processing

SSQ07-05 New Radial Technique for the Calculation of T2 Relaxation Time in Liver MRI

Thursday, Dec. 5 11:10AM - 11:20AM Room: S103CD

Participants

Janio Szklaruk, MD, PhD, Houston, TX (*Presenter*) Nothing to Disclose Jong Bum Son, PhD, Houston, TX (*Abstract Co-Author*) Nothing to Disclose Jia Sun, Houston, TX (*Abstract Co-Author*) Nothing to Disclose Bryce Starr, Durhan, NC (*Abstract Co-Author*) Nothing to Disclose Priya R. Bhosale, MD, Bellaire, TX (*Abstract Co-Author*) Nothing to Disclose Jingfei Ma, PhD, Houston, TX (*Abstract Co-Author*) Royalties, Siemens AG; Royalties, General Electric Company; Consultant, C4 Imaging

For information about this presentation, contact:

jszklaru@mdanderson.org

PURPOSE

The purpose is to investigate the clinical application of 2D radial TSE (2DRTSE) sequencing by evaluating the quantitative T2 relaxation time (msec) of liver lesions and the background liver parenchyma. We also evaluated image quality.

METHOD AND MATERIALS

MRI was performed at 3.0 T in this IRB-approved prospective study. The prototype 2D radial TSE sequence (2DRTSE) generated 22 echo axial images corresponding to 22 different TEs (ranging from 8.6 ms to 188.8 ms) with prospective acquisition correction for free-breathing patient scans. By placing an ROI on the automatically generated T2 map, 2 radiologists obtained relaxation times for various liver lesions and background liver. Radiologists scored image quality. Weighted linear kappa statistics and the Lin concordance correlation coefficient (CCC) were used to assess inter-reader agreement. The differences in paired T2RTs of the two readers were plotted against their mean values using Bland-Altman plots. Multiple lesions within the same patient were considered independently. The Kruskal-Wallis test was used to compare T2RTs among different lesion types.

RESULTS

19 patients were included in the study. There were 36 liver lesions: 2 cysts, 9 hemangiomas, 21 solid lesions, and 4 necrotic metastatic lesions. The solid lesions were 12 metastases, 8 HCC, and 1 FNH. The mean calculated T2RT value for solid lesions (81.5 ms) was significantly lower than that for hemangiomas (153.9 ms; P = 0.0024). The Wilcoxon rank-sum test revealed that the mean calculated T2RT for liver cysts (285.7 ms) was significantly higher than solid lesions (81.5 ms; P = 0.025). For the 2 radiologists, the CCC was 0.996 (95% confidence interval 0.9914-0.9978) for the calculated T2 of each liver lesion, indicating substantial agreement. The mean calculated T2RT for the background liver was 42.2 ms. The Bland-Altman plot of the liver T2RT data showed 95% agreement between readers, allowing for a range of +10 to -13.3 ms. Qualitative analysis of liver margins revealed good liver margin visibility in 100% of the evaluated slices

CONCLUSION

2D radial TSE sequencing is capable of providing good T2W images and a quantitative T2RT map. The quantitative T2 map was useful for the characterization of liver lesions.

CLINICAL RELEVANCE/APPLICATION

2D radial TSE sequence may supplant current T2WI acquisition. The value of lesion detection for T2-weighted imaging will be enhanced by the addition of quantitative T2RTs.

SSQ07-06 Respiratory Motion Artifacts in Gadoterate- and Gadoxetate-Enhanced Dynamic Phase Liver MRI After Intensified and Standard Pre-Scan Preparation: A Bi-Institutional Analysis

Thursday, Dec. 5 11:20AM - 11:30AM Room: S103CD

Participants

Florian Siedek, MD, Stanford, CA (*Presenter*) Nothing to Disclose Christian Wybranski, MD, Magdeburg, Germany (*Abstract Co-Author*) Nothing to Disclose Robert Damm, Magdeburg, Germany (*Abstract Co-Author*) Nothing to Disclose Angelos Gazis, Frankfurt am Main, Germany (*Abstract Co-Author*) Nothing to Disclose Ortrud Kosiek, Magdeburg, Germany (*Abstract Co-Author*) Nothing to Disclose Stefan Haneder, MD, Cologne, Germany (*Abstract Co-Author*) Nothing to Disclose Thorsten Persigehl, MD, Koeln, Germany (*Abstract Co-Author*) Nothing to Disclose Susanne Steinhauser, Cologne, Germany (*Abstract Co-Author*) Nothing to Disclose MacIej Pech, Berlin, Germany (*Abstract Co-Author*) Nothing to Disclose Frank Fischbach, PhD, Magdeburg, Germany (*Abstract Co-Author*) Nothing to Disclose Katharina Fischbach, Magdeburg, Germany (*Abstract Co-Author*) Nothing to Disclose

For information about this presentation, contact:

f.siedek@gmail.com

PURPOSE

Gadoxetate disodium induced transient severe arterial phase respiratory motion (TSM) substantially degrades image quality in liver dynamic contrast-enhanced MRI (DCE-MRI). Extent of liver DCE-MRI procedural information and explanation and/or training of breath-hold commands in standard pre-scan patient preparation (SPPP) might vary between institutions due to missing standardization, contributing to the occurrence of gadoxetate-related TSM. This bi-institutional study investigates the effect of intensified pre-scan patient preparation (IPPP; SPPP + custom-made educational material about liver DCE-MRI + standardized breath-hold training) on gadoxetate-related TSM.

METHOD AND MATERIALS

At site A and B, 50 (site A) and 58 (site B) patients received IPPP and 50 (site A) and 52 (site B) patients received SPPP prior to gadoxetate-enhanced liver DCE-MRI. As control, the effect of IPPP and SPPP was crosschecked in each 101 patients who received gadoterate-enhanced liver DCE-MRI (site B). Respiratory motion (RM) was scored in dynamic phase images using a Likert-scale (1 [none] - 5 [non-diagnostic]) independently by 5 (site A) and 2 (site B) blinded readers.

RESULTS

In the gadoxetate group, IPPP neither significantly mitigated TSM which was observed in 19% of patients (p=0.366) nor RM in any dynamic phase of patients without TSM (all p>0.072). In the gadoterate group, however, IPPP significantly mitigated RM in all dynamic phases (all p<0.031) compared to SPPP. The inter-reader agreement for grading of RM artifacts was excellent in precontrast and all dynamic phase images with all intra-class correlation coefficients (ICCs) >0.92.

CONCLUSION

IPPP failed to reduce gadoxetate-related TSM supporting the hypothesis that gadoxetate disodium acts as a chemo-toxic trigger that evokes breath-hold difficulty which cannot be willingly suppressed or attenuated by education and training. Interestingly, IPPP also did not significantly mitigate RM in any dynamic phase in the non-TSM subgroup of patients who received gadoxetate disodium whereas IPPP very effectively reduced RM in all dynamic phases in the non-TSM subgroup of patients who received gadoterate meglumine. This implies that gadoxetate-related breath-hold difficulty does not only affect the TSM subgroup of patients or exclusively the arterial phase as previously proposed but rather all dynamic phases, albeit to a much lesser extent.

CLINICAL RELEVANCE/APPLICATION

Intensified pre-scan patient preparation seems to be a very effective and cost-neutral strategy to reduce respiratory motion in liver DCE-MRI employing extracellular contrast agents.

SSQ07-07 Clinical Evaluation of Diffusion-Weighted MRI based Virtual Elastography for the Assessment of Liver Fibrosis

Thursday, Dec. 5 11:30AM - 11:40AM Room: S103CD

Participants

Marie-Luise Kromrey, MD, Greifswald, Germany (*Presenter*) Nothing to Disclose Denis J. Le Bihan, MD, PhD, Gif-Sur-Yvette, France (*Abstract Co-Author*) Research Consultant, Olea Medical Shintaro Ichikawa, MD, PhD, Chuo, Japan (*Abstract Co-Author*) Nothing to Disclose Utaroh Motosugi, MD, Chuo, Japan (*Abstract Co-Author*) Nothing to Disclose

For information about this presentation, contact:

marie-luise.kromrey@uni-greifswald.de

PURPOSE

To compare diffusion-weighted MRI (dMRI) based elastography and standard MR elastography (MRE) for the assessment of liver fibrosis in a clinical setting.

METHOD AND MATERIALS

In an IRB approved retrospective study 99 patients underwent 2D MRE and dMRI on a 3T scanner. 25 patients had to be excluded due to insufficient image quality resulting in a final study population of 74 patients (45 men, mean age 68.1±8.7 years). Shear modulus measured by MRE (μ MRE) was obtained in each subject by placing liver ROIs on the stiffness maps by two independent readers. Shifted apparent diffusion coefficient (sADC) was calculated from dMRI acquired without mechanical vibration with b=200 and 1500 s/mm2. dMRI-based virtual shear modulus (μ Diff) was then derived from sADC as previously shown. MRI-based liver fibrosis stages were estimated from μ MRE and μ Diff values using optimal cutoff values according to METAVIR score (F0-F4). Statistical analysis was undertaken using Bland-Altman plots and Bayesian prediction analysis.

RESULTS

Inter-reader agreement was very high (mean difference: 0.04 ± 0.43 kPa; -0.03 ± 0.60 kPa for µDiff and µMRE, respectively, not significant). Correlation between sADC and µDiff was highly significant (r2=0.81, p=6 10-24) with µMRE and µDiff values showing agreement for each patient (mean difference: -0.02 ± 0.88 kPa, not significant). Complete agreement in fibrosis staging was obtained in 55% of the patients and good agreement ($\Delta F=\pm1$) in 36%. Categorizing fibrosis into "insignificant" (F0/F1) and "significant" (F2-F4) agreement between the two methods reached 85% (63/74, Kappa=0.85).

CONCLUSION

dMRI-based virtual shear modulus values and resulting fibrosis stages showed high agreement with those by MRE. dMRI holds great potential for the evaluation of liver fibrosis non-invasively without the need for any mechanical vibration setup as an alternative to MRE and biopsy.

CLINICAL RELEVANCE/APPLICATION

Diffusion MRI based virtual elastography holds great potential as an alternative to MRE to evaluate liver fibrosis non-invasively without the need for any mechanical vibration setup.

SSQ07-08 Diagnostic Accuracy of Liver Imaging Reporting and Data System (LI-RADS) for HCC in Non-Cirrhotic Patients with Chronic Hepatitis

Thursday, Dec. 5 11:40AM - 11:50AM Room: S103CD

Participants

Yu Han, Guangzhou, China (*Abstract Co-Author*) Nothing to Disclose Jingbiao Chen, Guangzhou, China (*Abstract Co-Author*) Nothing to Disclose Linqi Zhang, Guangzhou, China (*Abstract Co-Author*) Nothing to Disclose Sichi Kuang, Guangzhou, China (*Abstract Co-Author*) Nothing to Disclose Sidong Xie, Guangzhou, China (*Abstract Co-Author*) Nothing to Disclose Claude B. Sirlin, MD, San Diego, CA (*Abstract Co-Author*) Nothing to Disclose Claude B. Sirlin, MD, San Diego, CA (*Abstract Co-Author*) Research Grant, Gilead Sciences, Inc; Research Grant, General Electric Company; Research Grant, Siemens AG; Research Grant, Bayer AG; Research Grant, Koninklijke Philips NV; Consultant, AMRA AB; Consultant, Fulcrum; Consultant, IBM Corporation; Consultant, Exact Sciences Corporation; Consultant, Boehringer Ingelheim GmbH; Consultant, Arterys Inc; Consultant, Epigenomics; Author, Medscape, LLC; Lab service agreement, Gilead Sciences, Inc; Lab service agreement, ICON plc; Lab service agreement, Intercept Pharmaceuticals, Inc; Lab service agreement, Shire plc; Lab service agreement, Enanta; Lab service agreement, Takeda Pharmaceutical Company Limited; Lab service agreement, Alexion Pharmaceuticals, Inc; Lab service agreement, NuSirt Biopharma, Inc Jin Wang, MD, Guangzhou, China (*Presenter*) Nothing to Disclose

For information about this presentation, contact:

ysshrine@163.com

PURPOSE

The use of the Liver Imaging Reporting and Data System (LI-RADS) has not been validated in non-cirrhotic patients with chronic hepatitis. This study examines the accuracy of LI-RADS v2018 for hepatocellular carcinoma (HCC) using contrast-enhanced MR imaging in non-cirrhotic patients with chronic hepatitis.

METHOD AND MATERIALS

This retrospective single-center study was approved by our IRB with waived informed consent requirement. Between 2016 and 2018, 160 patients with chronic hepatitis and histology-proven absence of cirrhosis underwent contrast-enhanced MR imaging. In consensus, two radiologists retrospectively assigned LI-RADS v2018 categories to each of a total of 161 observations. The reference standard was histology for malignant lesions and clinical and radiological follow-up for at least one year for benign lesions. Sensitivity, specificity, accuracy, positive predictive value (PPV), negative predictive value (NPV), and false positive rate (FPR) of LR-5 for the diagnosis of HCC were estimated.

RESULTS

The final diagnoses and LI-RADS categories of each observation are summarized in Table. Overall, 71 (44.1%) lesions were HCCs, 23 (14.3%) were non-HCC malignancies, and 67 (41.6%) were benign. LI-RADS categories of LR-1, LR-2, LR-3, LR-4, LR-5, and LR-M were assigned in 6 (3.7%), 43 (26.7%), 15 (9.3%), 12 (7.5%), 70 (43.5%), and 15 (9.3%) observations, respectively. Among LR-5s, 64 (91.4%) were HCCs and 69 (98.6%) were malignant. The sensitivity, specificity, accuracy, PPV, NPV, and FPR of LR-5 for HCC were 90.1%, 93.3%, 91.2%, 91.4%, 92.3%, and 6.7%, respectively. Among LR-Ms, 4 (27%) were HCCs and 15 (100%) were malignant.

CONCLUSION

This single-center, retrospective study suggests that LIRADS v2018 using contrast-enhanced MR imaging has high accuracy for HCC in non-cirrhotic HCC patients with chronic hepatitis. Multicentric, prospective studies are needed to validate this preliminary finding.

CLINICAL RELEVANCE/APPLICATION

This single-center, retrospective study suggests that LI-RADS v2018 using contrast-enhanced MRI may be valid in non-cirrhotic patients with chronic hepatitis. Further studies are warranted.







SSQ09

Genitourinary (Imaging of Pregnancy)

Thursday, Dec. 5 10:30AM - 12:00PM Room: E351



AMA PRA Category 1 Credits ™: 1.50 ARRT Category A+ Credit: 1.75

Participants

Jeanne M. Horowitz, MD, Chicago, IL (*Moderator*) Nothing to Disclose Jin Yamamura, MD, Hamburg, Germany (*Moderator*) Nothing to Disclose Priyanka Jha, MBBS, San Francisco, CA (*Moderator*) Nothing to Disclose

Sub-Events

SSQ09-01 The Placenta Accreta Spectrum (PAS) and MRI: Preliminary Findings in High-Risk Pregnancies and Associated Need for Cesarean Hysterectomy

Thursday, Dec. 5 10:30AM - 10:40AM Room: E351

Participants Ambereen A. Khan, MD, Dallas, TX (*Presenter*) Nothing to Disclose Haley R. Clark, MD, Dallas, TX (*Abstract Co-Author*) Nothing to Disclose Quyen N. Do, PhD, Dallas, TX (*Abstract Co-Author*) Nothing to Disclose Yin Xi, PhD, Dallas, TX (*Abstract Co-Author*) Nothing to Disclose

Diane M. Twickler, MD, Dallas, TX (*Abstract Co-Author*) Nothing to Disclose

For information about this presentation, contact:

diane.twickler@utsouthwestern.edu

PURPOSE

To evaluate MR findings described in PAS and identify those significantly associated with PAS severe enough to result in cesarean hysterectomy. Interobserver agreement was also assessed.

METHOD AND MATERIALS

We performed an IRB approved retrospective review of 56 pregnancies, from our 2006-2019 MR database referred for clinically suspected PAS. After randomization, single shot fast spin echo, balanced steady state free precession and T1-weighted sequences were independently evaluated by two reviewers, one expert and one with 4 years MR experience, after review of 10 test training cases. Evaluation of 11 variables was performed, including bladder-serosal interface interruption, bridging vessels, placental texture near the scar, presence of complete or low-lying previa, radiology impression of presence or absence of invasion and degree, bulge characteristics, dark linear bands or lacunae, and cervical varices. To assess readers agreement, simple kappa and prevalence adjusted bias adjusted kappa(PABAK) were used. Univariate logistic regressions were used to assess the association with cesarean hysterectomy.

RESULTS

From the study, 6 of 11 characteristics assessed by the expert were significantly associated(p<0.05) with the outcome of hysterectomy:interrupted bladder-serosal interface(0.007), serosal bridging vessels(0.005), radiologist prediction of invasion degree(0.002) and presence(0.02), inhomogeneous texture near scar(0.003) and low-lying or placenta previa(0.0005). Dark linear band quantification, cervical varices size, lacunae and bulge presence or size were not significant. The reader agreement was fair to moderate according to PABAK. Simple Kappa was constantly underestimated due to unbalance in the dataset.

CONCLUSION

An expert reader was significantly predictive of presence and degree of invasion with MRI in women whose placental invasion was severe enough to result in cesarean hysterectomy. Other significant findings included bridging vessels, bladder serosal interruption, low-lying or complete previa, and inhomogeneous texture near scar. However, in this small series, interobserver agreement was only fair to moderate, suggesting the need for better-defined variables assessed with more MRI cases and larger training datasets.

CLINICAL RELEVANCE/APPLICATION

Several MR findings were associated with PAS severe enough to result in cesarean hysterectomy, but interobserver agreement between radiologists remains less than optimal.

SSQ09-02 MRI Diagnosis of Placenta Accreta Spectrum Disorder

Thursday, Dec. 5 10:40AM - 10:50AM Room: E351

Participants Sherelle L. Laifer-Narin, MD, Englewood, NJ (*Presenter*) Nothing to Disclose Mirella Mourad, MD, New York, NY (*Abstract Co-Author*) Nothing to Disclose Fady Khoury Collado, MD, New York , NY (*Abstract Co-Author*) Nothing to Disclose Leslie Moroz, New York, NY (*Abstract Co-Author*) Nothing to Disclose Chia-Ling Nhan-Chang, MD, New York, NY (Abstract Co-Author) Nothing to Disclose

For information about this presentation, contact:

sll2122@cumc.columbia.edu

PURPOSE

To evaluate the accuracy of magnetic resonance imaging in diagnosing abnormal placentation.

METHOD AND MATERIALS

A retrospective review of placental MRI exams from December 2004 to January 2019 was performed. MRI reports were reviewed for suspicion of abnormal placentation. Criteria suggesting pathology included the presence of dark intraplacental bands, heterogeneous signal intensity, thick nodular contour along the urinary bladder surface, uterine bulging into the bladder, and loss of the myometrial margin with attention paid to parametrial regions. MRI was considered positive even if only one of these criteria were present. Comparison was made with findings at either delivery, operation, and pathology reports.

RESULTS

478 MRI exams were reviewed. 279 exams were negative both on MRI and delivery/pathology. 13 exams interpreted as normal on MRI underwent hysterectomy with pathology demonstrating placenta accreta. 148 exams were interpreted as positive for abnormal placentation, and were diagnosed as accreta, increta, or percreta on delivery/pathology. 38 cases interpreted as positive on MRI had normal placental delivery and pathology. MR diagnosis of abnormal placentation had a sensitivity of 92%, specificity of 88%, PPV of 80%, NPV of 96%, and an accuracy of 89%.

CONCLUSION

Placental adhesive spectrum disorder is a significant cause of maternal morbidity and mortality. Detailed imaging provides important information critical for the management of patients with this disorder. Prenatal MRI has a high degree of accuracy for the diagnosis of placenta adhesive spectrum disorder, specifically the myoinvasive forms. MRI provides detailed topographic information and is a critical component in the workup of patients at high risk for this condition.

CLINICAL RELEVANCE/APPLICATION

Advance knowledge of the diagnosis of abnormal placentation allows for predelivery operative planning and management. With this information, a multidisciplinary approach to this potentially catastrophic condition can be put into place to prevent significant morbidity and mortality.

SSQ09-03 Abnormal Fetal Placental Vasculature on MRI of Patients at High Risk for Placenta Accreta Spectrum Disorders: Analysis of 130 Cases

Thursday, Dec. 5 10:50AM - 11:00AM Room: E351

Participants

Charis Bourgioti, MD, Athens, Greece (*Presenter*) Nothing to Disclose Anastasia Konstantinidou, Athens, Greece (*Abstract Co-Author*) Nothing to Disclose Konstantina Zafeiropoulou, Athens, Greece (*Abstract Co-Author*) Nothing to Disclose Chara Tzavara, Athens, Greece (*Abstract Co-Author*) Nothing to Disclose Stavros Fotopoulos, Athens, Greece (*Abstract Co-Author*) Nothing to Disclose George Daskalakis, Athens, Greece (*Abstract Co-Author*) Nothing to Disclose Maria Evangelia Nikolaidou, Athens, Greece (*Abstract Co-Author*) Nothing to Disclose Marianna Theodora, Athens, Greece (*Abstract Co-Author*) Nothing to Disclose Lia A. Moulopoulos, MD, Athens, Greece (*Abstract Co-Author*) Nothing to Disclose

For information about this presentation, contact:

charisbourgioti@gmail.com

PURPOSE

To investigate the association of abnormal intraplacental (fetal) vessels on MRI of patients with placenta accreta spectrum (PAS) disorders with extent of invasiveness and poor clinical outcome

METHOD AND MATERIALS

Between 3/2016-2/2019, 130 high-risk gravid patients for abnormal placentation were referred for dedicated prenatal MRI (mean age:34.7 years, mean gestational age: 32.5 weeks); all patients underwent C-section within 6 weeks from MRI. Intraoperative/pathological findings confirmed the presence of PAS in 101/130 patients (percreta: n=58, creta/increta: n=43). 48/101 patients with PAS underwent hysterectomy, whereas in 44/101 patients, bladder repair was performed. All MRIs were reviewed by consensus by two expert radiologists after completion of the study for the presence of at least one long (>2cm), intraplacental flow void structure originating from the chorionic plate, crossing the placental parenchyma and reaching the basal plate, with paucity of branching along its course (stripped fetal vessel). Presence of stripped fetal vessels and their caliper were statistically tested for any association with degree of invasiveness and peripartum events including intraoperative blood loss, operation time, and need for hysterectomy or bladder repair.

RESULTS

There was a significant association (p<0.001) between presence of stripped fetal vessels with number of prior C-sections, presence of placenta percreta, hysterectomy and bladder repair treatment. Subjects with stripped fetal vessels on MRI, had significantly greater blood loss (1514.2.8vs382.8ml, p<0.001) and increased delivery times (145.2vs60.3min, p<0.001). The diameter of stripped fetal vessels was greater in patients with >=2 prior C-sections (5.2vs4.3mm,p<0.001), placenta percreta (5.3vs3.6mm,p<0.001), major bladder repair (6.4vs3.6mm,p<0.001) and caesarian hysterectomy (5.5vs3.5mm,p<0.001); additionally, stripped fetal vessel diameter was positively and significantly associated with intraoperative blood loss and duration of delivery.

CONCLUSION

The presence and extent of appermal fetal intradisental vacculature seems to be related with DAC invasiveness and adverse

The presence and extent of abnormal relating pacental vasculature seens to be related with PAS invasiveness and adverse peripartum events.

CLINICAL RELEVANCE/APPLICATION

Accurate prenatal identification of aggressive forms of PAS may optimize treatment planning, improving patients' clinical outcome.

SSQ09-04 Apparent Diffusion Coefficient Differences in Twins of Monochorionic Diamniotic Pregnancy Complicated by Twin-To-Twin Transfusion Syndrome

Thursday, Dec. 5 11:00AM - 11:10AM Room: E351

Participants

Michael Aertsen, MD, Leuven, Belgium (*Presenter*) Nothing to Disclose Isabel Couck, Leuven, Belgium (*Abstract Co-Author*) Nothing to Disclose Frederik De Keyzer, Leuven, Belgium (*Abstract Co-Author*) Nothing to Disclose Steven Dymarkowski, MD, Leuven, Belgium (*Abstract Co-Author*) Nothing to Disclose Liesbeth Lewi, MD, Leuven, Belgium (*Abstract Co-Author*) Nothing to Disclose

For information about this presentation, contact:

michael.aertsen@uzleuven.be

PURPOSE

To evaluate the difference in apparent diffusion coefficient (ADC) of the placental parenchyma between donor and receptor of monochorionic diamniotic (MCDA) pregnancies complicated by twin-to-twin transfusion syndrome (TTTS) and compare those values with a control group of uncomplicated MCDA pairs.

METHOD AND MATERIALS

Prospective monocentric cohort study. Magnetic resonance (MR) was performed prior to surgery in TTTS and electively planned around 20 weeks (w) of gestation age (GA) for the uncomplicated MCDA cohort. Regions of interest (ROIs) for ADC calculations were placed at the cord insertion of each twin or as close as possible in velamentous insertion. Another ROI was drawn at the border of the placenta away from the presumed vascular equator. Intrapair ADC differences for the different ROIs (central (c) and peripheral (p), resp.) were compared between donor and recipient (Wilcoxon-signed rank test). GA at time of MR and intertwin ADC differences were compared between TTTS and MCDA twins (Mann-Whitney test).

RESULTS

71 pregnancies were included in the analysis. Median GA at the time of MRI was 21 w (range 18-27) in the uncomplicated (N=47) and 21 w (range 18 - 29) in the TTTS cohort (N=24) (p=.9). Intrapair ADC differences for the different placental regions and the difference in mean ADC (=(cADC + pADC)/2) of both regions in TTTS are summarized in the table. Between TTTS and MCDA cohorts, central ADC measurements in the donor (168 x10^-5 mm^2/s; 159 - 182 x10^-5 mm^2/s) and smallest twin (179 x10^-5 mm^2/s; 166-197 x10^-5 mm^2/s), respectively, differed significantly (p=.02), whereas no differences were observed between the receptor and larger twin (p=.6). cADC difference between the donor and receptor in TTTS were also larger than those in uncomplicated MCDA pregnancies (p=0.04).

CONCLUSION

In TTTS, central ADC measurements are helpful to differentiate receptor and donor insertion compared to peripheral ADC calculations. Furthermore, from an ADC point of view, the receptor seems to exhibit normal values, with the donor behaving significantly different.

CLINICAL RELEVANCE/APPLICATION

Diffusion weighted imaging has demonstrated differences in pregnancies with abnormal placental function. We want to analyze the added value of ADC measurements in TTTS twins prior to surgery.

SSQ09-05 The Value of MRI in Predicting Intraoperative Massive Hemorrhage during Hysteroscopic Treatment of Cesarean Scar Pregnancy

Thursday, Dec. 5 11:10AM - 11:20AM Room: E351

Participants

Piaoe Zeng, Beijing, China (*Presenter*) Nothing to Disclose Yan Zhou, Beijing, China (*Abstract Co-Author*) Nothing to Disclose Jianyu Liu, Beijing, China (*Abstract Co-Author*) Nothing to Disclose

PURPOSE

To explore the value of MRI in predicting intraoperative massive hemorrhage during hysteroscopic treatment for cesarean scar pregnancy

METHOD AND MATERIALS

A retrospective analysis of 77 first trimester CSP patients who were diagnosed by MRI and confirmed by operation and pathology from January 20 to December 2018. According to the intraoperative blood loss, CSP patients were divided into two groups. The Inclusion criteria of intraoperative massive bleeding group: intraoperative blood loss >=200ml, by hysteroscopic treatment with or without preoperative bilateral uterine artery embolization or medication; The Inclusion criteria of non-massive bleeding group: intraoperative bilateral uterine artery embolization or medication. The Inclusion criteria data and MRI features were compared between the two groups. The multivariate logistic regression analysis was used to analyze the risk factors of CSP intraoperative massive hemorrhage. The ROC curve was used to evaluate the efficacy and optimal threshold

RESULTS

Between the intraoperative massive hemorrhage group (11 cases) and non-massive hemorrhage group (66 cases), the gestational

age, the maximum diameter of the gestational sac, the depth of the gestational sac, and LUST were significantly different(p < 0.05). There were no significant differences in age, number of cesarean delivery, interval between current CSP and last cesarean, number of abortions, preoperative β -HCG, CSP types, gestational sac or uterine hemorrhage between the two groups (P>0.05). Multivariate logistic regression analysis showed that only the lower uterus scar thickness was significantly different (P=0.034,OR=2.757, 95% CI=1.082-7.028). The ROC curve analysis showed that the AUC of the gestational age, the maximum diameter of the gestational sac, the depth of the gestational sag and LUST were 75.0%, 82.1%, 85.9%, and 91.5%, respectively. The best predictor is the LUST and the optimal cutoff value is 2.2mm, the diagnostic sensitivity, specificity, and the Youden index are 90.9%, 74.2%, and 65.2%, respectively.

CONCLUSION

Preoperative MRI can accurately predict the risk of major bleeding during cesarean section scar pregnancy and guide treatment

CLINICAL RELEVANCE/APPLICATION

To inverstigate risk factors of intraoperative excessive haemorrhage during during hysteroscopic treatment of cesarean scar pregnancy, and to guide treatment.

SSQ09-06 Role of Placental Elastography for Prediction of Preeclampsia in Early Second Trimester

Thursday, Dec. 5 11:20AM - 11:30AM Room: E351

Participants Rajkumar Meena, MBBS, New Delhi, India (*Presenter*) Nothing to Disclose Amita Malik, MD, New Delhi, India (*Abstract Co-Author*) Nothing to Disclose Madhuvendra S. Narwaria, MBBS, New Delhi, India (*Abstract Co-Author*) Nothing to Disclose

For information about this presentation, contact:

rajkumarvmmc@gmail.com

PURPOSE

To evaluate the role of shear wave placental elastography (SWE) in pre-clampsia (PE) and to give a cut off value of elasticity that would help in prediction of pre-eclampsia in early second trimester (14-20 weeks of period of gestation).

METHOD AND MATERIALS

A total of 230 patients who presented in obstetric OPD between 14-20 weeks of gestation and were willing to have delivery in our instituition were enrolled in the study. After taking detailed obstetric history, gray scale obstetric ultrasound with doppler scan SWE was performed. Mean value of elasticity was taken in every patient; and data were analysed to give the best cut-off value that would determine the diagnosis of PE. Sensitivity, specificity, positive predictive value (PPV), negative predictive value (NPV), and diagnostic accuracy for prediction of PE were calculated based on SWE measurements. Statistical analysis was done using Statistical Package for Social Sciences (SPSS) version 21.0. A p value of <0.05 was considered statistically significant.

RESULTS

There was a statically significant difference in the value of elasticity in normal patients and in those who developed PE. The study concluded cut-off value of 2.9667 kPa for prediction of pre-eclampsia, with a sensitivity of 92%, specificity of 91.71%, PPV of 57.5% and NPV of 98.9% in a statistically significant manner with p-value of <0.05.

CONCLUSION

Placental stiffness is higher in patients who develop pre-eclampsia during pregnancy. It can be quantitatively measured by shear wave elastography values for prediction of pre-eclampsia in early second trimester.

CLINICAL RELEVANCE/APPLICATION

Placental elastographic values were statistically significant and higher in the patients developing preeclampsia in later pregnancy. Shear wave elastography can help us to diagnose this life threatening condition in early second trimester before the clinical appearance of preeclampsia, and act to provide early treatment and antenatal care to reduce the devastating maternal as well as fetal outcomes.

SSQ09-07 Differences in Brain Development between Fetuses with Intrauterine Growth Restriction and Normally-Grown Group Assessed by Fetal MRI

Thursday, Dec. 5 11:30AM - 11:40AM Room: E351

Participants

Behnaz Moradi, MD, Tehran, Iran (islamic Rep. Of) (*Abstract Co-Author*) Nothing to Disclose Mahboobeh Shirazi, MD, Tehran, Iran (islamic Rep. Of) (*Abstract Co-Author*) Nothing to Disclose Nazanin Seyed Saadat, MD, Tehran, Iran (islamic Rep. Of) (*Abstract Co-Author*) Nothing to Disclose Zohreh Alibeigi Nezhad, MD, Tehran, Iran (islamic Rep. Of) (*Abstract Co-Author*) Nothing to Disclose Hasan Hashemi, MD, Tehran, Iran (islamic Rep. Of) (*Abstract Co-Author*) Nothing to Disclose Hasoumeh Gity, MD, Tehran, Iran (islamic Rep. Of) (*Abstract Co-Author*) Nothing to Disclose Hossein Ghanaati, MD, Tehran, Iran (islamic Rep. Of) (*Abstract Co-Author*) Nothing to Disclose Mohammad Ali Kazemi, MD, Tehran, Iran (islamic Rep. Of) (*Abstract Co-Author*) Nothing to Disclose Maryam Rahmani, MD, Tehran, Iran (islamic Rep. Of) (*Abstract Co-Author*) Nothing to Disclose Ghazaleh Arabkheradmand, MS, Chicago, CA (*Abstract Co-Author*) Nothing to Disclose Farzaneh Fattahi Masrour, MD, Hartford, CT (*Presenter*) Nothing to Disclose

For information about this presentation, contact:

b.moradi80@gmail.com

To evaluate different features of brain development by Magnetic Resonance Imaging (MRI) in intrauterine growth restricted (IUGR) fetuses compared to normally-grown fetuses.

METHOD AND MATERIALS

3T MRI was performed in 42 IUGR and 28 nearly age-matched normally-grown fetuses using T2-weighted half Fourier acquisition single-shot turbo spin echo (HASTE). Cortical thickness was assessed in 4 brain regions (insula, frontal, occipital and temporal) and corrected by biparietal diameter/2. Also whole brain area (WBA) at the level of cavum septum pellucidum and area of 6 brain regions (frontal, temporal, occipital, cerebellum, midbrain and pons) were evaluated and corrected by WBA and compared between the two groups. Any cases with brain structural anomaly were excluded. All fetuses were followed until birth.

RESULTS

No significant differences were found about maternal characteristic and fetal gestational age between two groups. IUGR fetuses had significantly lower birth weight (2377 g vs 2965 g in control group). Brain signal was normal in all cases. The corrected thickness of cortex was significantly thinner in insula and temporal lobes in IUGR fetuses compared to control group (0.034 vs 0.043 and 0.036 vs 0.047 respectively, P value of < 0.05), but there was no significant different in frontal and occipital lobes. IUGR fetuses has significantly smaller WBA. The assessed corrected area of brain regions was not significantly different between groups except the corrected area of cerebellum which was smaller in normally-grown fetuses (0.147 vs 0.130, P value of < 0.05). During follow up, there was only one still birth in IUGR group.

CONCLUSION

IUGR fetuses had a significantly thinner Insular and temporal lobe cortex and smaller WBA. Among different brain regions, cerebellum was less affected by growth restriction.

CLINICAL RELEVANCE/APPLICATION

Growth restriction significantly affects brain development and the fetal MRI has a potential value to assess the various aspects of this effect.

SSQ09-08 Fetal Anterior Abdominal Wall Thickness (FAAWT): A Promising Parameter to Predict Fetal Macrosomia in Pregnancies with Gestational Diabetes

Thursday, Dec. 5 11:40AM - 11:50AM Room: E351

Participants

Ashish Bansal, MBBS, New Delhi, India (*Presenter*) Nothing to Disclose Brijbhushan Thukral, New Delhi, India (*Abstract Co-Author*) Nothing to Disclose

For information about this presentation, contact:

ashish_bansal1820@yahoo.com

PURPOSE

To evaluate the correlation of fetal anterior abdominal wall thickness and other standard fetal biometric parameters between 36-39 weeks of gestation with neonatal birth weight in pregnancies with gestational diabetes.

METHOD AND MATERIALS

This is a prospective cohort study conducted in a tertiary care Centre with institutional ethics approval. One hundred singleton pregnancies with gestational diabetes mellitus (GDM) between 36-39 weeks of gestation were included after informed written consent. Exclusion criteria comprised of women with diseases known to affect fetal growth, uncertain gestational age, fetuses with congenital anomalies and intrauterine growth restriction. Standard fetal biometry parameters including Biparietal diameter (BPD), head circumference (HC), abdominal circumference (AC), femur length (FL) and estimated fetal weight (EFW) were measured. Fetal anterior abdominal wall thickness (FAAWT) was measured ultrasonographically in AC view. Actual neonatal birth weights were recorded. Birth weight >90th centile (INTERGROWTH-21st charts) was considered as a cut-off for macrosomia. Statistical analysis was done and 95% confidence level was considered significant for all tests.

RESULTS

16 out of 100 neonates were found to be macrosomic (16%). Third trimester mean FAAWT was significantly higher in macrosomic babies (6.36±0.5 mm) as compared to non-macrosomic babies (5.54±0.61 mm) (p-value <0.0001). A FAAWT >6 mm (ROC curve derived) provided sensitivity of 87.5% (95% CI 61.7-98.4), specificity of 75% (95% CI 64.4-83.8), PPV of 40% (95% CI 23.9-57.9) and NPV of 96.9% (95% CI 89.3-99.6) for prediction of macrosomia. While other standard fetal biometric parameters (BPD, HC, AC, FL and EFW) did not correlate well with actual birth weight in neonates with macrosomia in GDM patients, only FAAWT was found to have statistically significant correlation (correlation coefficient of 0.626, p-value 0.009).

CONCLUSION

The FAAWT was the only fetal sonographic parameter to have significant correlation with neonatal birth weight in macrosomic neonates of GDM mothers. We found a high sensitivity (87.5%), specificity (75%) and NPV (96.9%) which suggests that FAAWT <6 mm can quite confidently rule out macrosomia in pregnancies with GDM.

CLINICAL RELEVANCE/APPLICATION

FAAWT is a promising and easily measurable parameter to rule out fetal macrosomia in late third trimester in pregnancies with GDM, thus, allowing proper obstetric management .

SSQ09-09 Three-Dimensional Fetal MRI Visualization of Cerebellar White Matter Tracts

Thursday, Dec. 5 11:50AM - 12:00PM Room: E351

Peter C. Brugger, MD, PhD, Vienna, Austria (*Abstract Co-Author*) Nothing to Disclose Gerlinde Gruber, Vienna, Austria (*Abstract Co-Author*) Nothing to Disclose Daniela Prayer, MD, Vienna, Austria (*Abstract Co-Author*) Nothing to Disclose Gregor Kasprian, MD, Vienna, Austria (*Abstract Co-Author*) Nothing to Disclose

PURPOSE

Cerebellar white matter connectivity plays a crucial role in affective, cognitive and motor processing. Prenatal diffusion tensor imaging (DTI) can non-invasively visualize major white-matter tracts of the fetal forebrain. We retrospectively assessed the success rate of visualizing the superior, middle and inferior cerebellar peduncle (SCP, MCP and ICP) as well as transverse pontine fibers (TPF) in the third trimester.

METHOD AND MATERIALS

Cases with DTI sequences (b-value of 700 s/mm², 16 gradient encoding directions) covering the cerebellum were retrospectively assessed. Deterministic tractography was performed using the Philips IntelliSpace software based on at least two regions of interest. A visibility score was calculated as the fraction of visible tracts divided by the amount of potentially visible tracts.

RESULTS

14 Fetal MRI were assessed (9 with 1.5T and 5 with 3T MRI) with 38.51 ± 1.00 GW (mean±standard deviation) at 1.5 T and 35.80 ± 1.20 at 3T. There was no significant difference (p=.66) between the scores of 1.5T (0.69±0.27) and 3T (0.74±0.17). SCP could be depicted in 71% of cases, MCP in 71%, ICP in 55% and TPF in 93%.

CONCLUSION

Prenatal tractography of cerebellar white matter tracts is feasible in the third trimester and shows excellent correlation with the respective anatomy. Fetal MR based DTI thus may improve the characterization of infratentorial malformations during the third trimester, when ultrasound is limited by acoustic shadowing at the skull base.

CLINICAL RELEVANCE/APPLICATION

Fetal MR tractography with diffusion tensor imaging can demonstrate cerebellar white matter tracts in the third trimester of pregnancy. This could improve the characterization of infratentorial malformations prenatally.

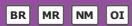




SSQ14

Nuclear Medicine (Breast/General Oncology Nuclear Medicine and PET)

Thursday, Dec. 5 10:30AM - 12:00PM Room: S402AB



AMA PRA Category 1 Credits ™: 1.50 ARRT Category A+ Credit: 1.75

Participants

Amy M. Fowler, MD, PhD, Madison, WI (*Moderator*) Research support, General Electric Company Bital Savir-Baruch, MD, Atlanta, GA (*Moderator*) Research Grant, Blue Earth Diagnostics Ltd; Consultant, Blue Earth Diagnostics Ltd; Speaker, Koninklijke Philips NV

Sub-Events

SSQ14-01 Can We Replace Sentinel Lymph Node Resection in Breast Cancer Patients by Breast MRI, Axillary MRI, Axillary 18F-FDG PET/MRI or Axillary Sonography?

Thursday, Dec. 5 10:30AM - 10:40AM Room: S402AB

Participants

Ole Martin, Duesseldorf, Germany (*Abstract Co-Author*) Nothing to Disclose Julian Kirchner, Dusseldorf, Germany (*Abstract Co-Author*) Nothing to Disclose Nils M. Bruckmann, MD, Duesseldorf, Germany (*Abstract Co-Author*) Nothing to Disclose Benedikt M. Schaarschmidt, MD, Essen, Germany (*Abstract Co-Author*) Nothing to Disclose Johannes Grueneisen, Essen, Germany (*Abstract Co-Author*) Nothing to Disclose Lale Umutlu, MD, Essen, Germany (*Abstract Co-Author*) Nothing to Disclose Gerald Antoch, MD, Dusseldorf, Germany (*Abstract Co-Author*) Nothing to Disclose Lino Sawicki, MD, Dusseldorf, Germany (*Presenter*) Nothing to Disclose

PURPOSE

To compare the diagnostic performance of Mamma-MRI, axillary MRI, axillary 18F-FDG PET/MRI and axillary sonography in the detection of lymph node metastases in patients suffering from breast cancer.

METHOD AND MATERIALS

56 female patients with breast cancer (mean age 53.5±12.2 years) with newly diagnosed, histopathologically proven breast cancer were prospectively enrolled in this two-center trial. All patients underwent dedicated prone 18F-FDG breast PET/MRI and supine whole-body 18F-FDG PET/MRI as well as axillary sonography. Sentinel lymph node biopsy (SLNB) and/or axillary lymph node dissection were performed in all patients and histopathology served as reference standard. Sensitivity, specificity, PPV, NPV and accuracy regarding axillary lymph node assessment were calculated for dedicated breast MRI, axillary MRI, axillary 18F-FDG PET/MRI and axillary sonography.

RESULTS

According to the reference standard, lymph node metastases were present in 25 patients with a total of 78 metastases. On a patient based analysis, dedicated breast MRI identified 14/25 (56%), axillary MRI 15/25 (60%), axillary PET/MRI 19/25 (76%) and axillary sonography 18/25 (72%) of the patients with a positive nodal status. On a lesion-based analysis, sensitivity, specificity, PPV, NPV and accuracy were 54.5%, 88.9%, 88.9%, 54.5% and 67.6% for breast MRI; 55.1%, 90%, 89.3%, 53.2% and 57,5% for axillary MRI; 71.4%, 92.1%, 65.0%, 89.7% and 78.2% for axillary PET/MRI and 60.0%, 86.2%, 84.0%, 61.1% and 71.9% for axillary sonography.

CONCLUSION

18F-FDG PET/MRI and sonography serve equally acceptable diagnostic accuracy for nodal staging in breast cancer patients and are both superior to dedicated breast MRI or supine whole-body MRI. Although PET/MRI provides important information for staging workup breast cancer patients, neither PET/MRI nor axillary sonography do reliably differentiate N-positive from N-negative breast cancer patients.

CLINICAL RELEVANCE/APPLICATION

Sentinel lymph node biopsy cannot be replaced by imaging procedures alone and is still mandatory for staging breast cancer patients.

SSQ14-02 Simultaneous PET/MRI in the Early Prediction of Response to Neoadjuvant Chemotherapy in Patients with Locally-Advanced Breast Cancer

Thursday, Dec. 5 10:40AM - 10:50AM Room: S402AB

Participants Valeria Romeo, Naples, Italy (*Presenter*) Nothing to Disclose Carlo Cavaliere, Naples, Italy (*Abstract Co-Author*) Nothing to Disclose Luca Basso, Naples, Italy (*Abstract Co-Author*) Nothing to Disclose Nunzia Garbino, Naples, Italy (*Abstract Co-Author*) Nothing to Disclose Mario Petretta, 80125, Italy (*Abstract Co-Author*) Nothing to Disclose Emanuele Nicolai, Napoli, Italy (*Abstract Co-Author*) Nothing to Disclose Massimo Imbriaco, MD, Napoli, Italy (*Abstract Co-Author*) Nothing to Disclose Marco Salvatore, MD, Napoli, Italy (*Abstract Co-Author*) Nothing to Disclose

For information about this presentation, contact:

valeria.romeo@unina.it

PURPOSE

Aim of the study was to assess whether simultaneous PET/MRI could be helpful in the early prediction of the response to neoadjuvant chemotherapy (NAC) in patients with locally advanced breast cancer (LABC).

METHOD AND MATERIALS

Between January 2017 and July 2018, 20 consecutive patients (mean age 45 yrs) with LABC who underwent anthracycline- and taxane-based neoadjuvant chemotherapy (NAC) followed by surgical resection were prospectively enrolled. Simultaneous breast PET/MRI examination was performed twice in each patient, one week before NAC and early after the second anthracycline cycle. PET/MRI images were analyzed to extract quantitative diffusion (ADCmin, ADCmean), perfusion (Ktrans, Kep, Ve, IAUC) and metabolic (SUV2d, SUV3d, MTV) parameters. The variation of each parameter (delta, D) after the second anthracycline cycle was then calculated. The normality of the data was tested using the Shapiro-Wilk test. Differences in terms of pre-treatment and D parameters between patients histologically classified as complete response (CR) and partial response (PR) were compared using of the nonparametric Mann-Whitney U test. Logistic regression analysis was performed to identify imaging parameters predictive of the response.

RESULTS

D-Size, D-Ktrans, Kep, D-Kep, MTV and D-MTV resulted significantly different (p<0.03) between patients who showed CR and PR. In detail, pre-treatment Kep and MTV were significantly lower in patients with CR while the variation of each parameter was significantly higher in patients with CR as compared to patients with PR. A cut-off value of 5.09 D-MTV perfectly predicted the response to treatment (Figure 1). MRI parameters significantly associated to the response to treatment were D-Ktrans (p=0.05), Kep (0.04), and D-Kep (0.05).

CONCLUSION

Simultaneous breast PET/MRI could be useful to early predict the response to NAC in patients with LABC. Our preliminary observations show that functional (i.e. perfusion and metabolic) rather than morphological parameters may identify patients who will respond completely, particularly using both pre-treatment and the variation of quantitative parameters early after the second cycle of NAC.

CLINICAL RELEVANCE/APPLICATION

Simultaneous breast PET/MRI may be useful for early identification of LABC patients who would benefit from continuing NAC or for whom surgical excision could be optionally considered.

SSQ14-03 Quantitative 18F-FDG Uptake of Invasive Breast Cancer Using Harmonized Prone PET/CT and Simultaneous Breast PET/MRI with 10 Minute PET Acquisition Time

Thursday, Dec. 5 10:50AM - 11:00AM Room: S402AB

Participants

Amy M. Fowler, MD,PhD, Madison, WI (*Presenter*) Research support, General Electric Company
Manoj Kumar, MS, Madison, WI (*Abstract Co-Author*) Nothing to Disclose
Leah Henze Bancroft, PhD, Madison, WI (*Abstract Co-Author*) Institutional research support, General Electric Company
Jacob Johnson, Madison, WI (*Abstract Co-Author*) Institutional research support, General Electric Company
Jillian A. Karow, MD, Minneapolis, MN (*Abstract Co-Author*) Nothing to Disclose
Kelley Salem, PhD, Madison, WI (*Abstract Co-Author*) Nothing to Disclose
Tyler Bradshaw, Madison, WI (*Abstract Co-Author*) Nothing to Disclose
Alan B. McMillan, PhD, Madison, WI (*Abstract Co-Author*) Nothing to Disclose
Roberta M. Strigel, MD, Madison, WI (*Abstract Co-Author*) Research support, General Electric Company

For information about this presentation, contact:

afowler@uwhealth.org

PURPOSE

To compare tumor 18F-FDG uptake measured with 10 min PET acquisition using breast PET/MRI harmonized with prone PET/CT in patients with newly diagnosed invasive breast cancer.

METHOD AND MATERIALS

This HIPAA-compliant, IRB-approved single-institution, prospective study was performed from 2016 to 2018. Patients with biopsyproven invasive breast cancer undergoing preoperative breast MRI were included. Patients who were pregnant, lactating, had implants, or underwent neoadjuvant therapy were not eligible. Fasting subjects underwent PET/CT (Discovery 710) of the breasts 60 min after injection of 10 mCi 18F-FDG. Patients were scanned at one bed position for 10 min in the prone position using the breast MRI coil housing with metal components removed. A low dose CT scan was obtained for attenuation correction. Subjects then underwent simultaneous breast PET/MRI (Signa 3.0T PET/MR) using an 8-channel breast coil 85 min after 18F-FDG injection. Standard clinical breast MRI sequences and Dixon-based sequences for attenuation correction were obtained simultaneously with the PET acquisition for 30 min. PET reconstruction was harmonized between scanners based on phantom scans. For analysis, the first 10 min of PET/MRI acquisition was compared to PET/CT. Standardized uptake value (SUV) measurements were performed for the tumor and contralateral normal (nl) fibroglandular tissue. Bland-Altman analysis was performed to determine measurement bias and 95% limits of agreement. 23 women (mean 49.6 yrs; 33-70) with 24 biopsy-proven sites of invasive breast carcinoma participated. Mean lesion size was 3.8 cm (1.1-8.8 cm) on MRI. Mean±SEM for tumor SUVmax, tumor SUVmean, and nl breast SUVmean for PET/MRI vs PET/CT, respectively, were 8.6±1.3 vs 7.3±1.1, 4.9±0.76 vs 3.7±0.57, and 1.4±0.083 vs 1.3±0.090. Measurement bias for PET/MRI vs PET/CT was 15.6% [-15.1,46.2] for tumor SUVmax, 28.7% [-7.21,64.6] for tumor SUVmean, 3.74% [-29.3,36.7] for tumor SUVmax/nl breast SUVmean, and 17.1% [-18.2,52.5] for tumor SUVmean/nl breast SUVmean.

CONCLUSION

Quantitative assessment of 18F-FDG uptake of invasive breast cancer is feasible using simultaneous breast PET/MRI with acceptable agreement between PET/MRI and PET/CT.

CLINICAL RELEVANCE/APPLICATION

Establishing the agreement between PET/CT and simultaneous breast PET/MRI for tumor 18F-FDG uptake is important for potential clinical applications such as neoadjuvant therapy response assessment.

SSQ14-04 Comparison of Whole-Body 18F-FDG-PET/MRI and PET/CT in Terms of Lesion Detection in Asymptomatic Subjects: A Retrospective Study

Thursday, Dec. 5 11:00AM - 11:10AM Room: S402AB

Participants

Mingxiang Sun, Shanghai, China (*Abstract Co-Author*) Nothing to Disclose Mu Lin, Shanghai, China (*Abstract Co-Author*) Employee, Siemens AG Liling Peng, Shanghai, China (*Abstract Co-Author*) Nothing to Disclose Xin Gao, MD, Shanghai , China (*Presenter*) Nothing to Disclose Holger Schmidt, Erlangen, Germany (*Abstract Co-Author*) Employee, Siemens AG

PURPOSE

To compare fluorine fluorodeoxyglucose (18F-FDG) combined positron emission tomography and magnetic resonance imaging (PET/MRI) with 18F-FDG combined positron emission tomography and computed tomography (PET/CT) in terms of organ-specific lesion detection in asymptomatic subjects for cancer screening.

METHOD AND MATERIALS

2794 individuals undergoing PET/MRI (Biograph mMR, Siemens Healthcare, Erlangen, Germany) and 4283 individuals undergoing PET/CT examinations (Biograph mCT, Siemens Healthcare, Knoxville, USA), from January 2016 to December 2017 in our center, were enrolled for this retrospective study. The local ethics committee approved this study. Written, informed consent was obtained from all subjects. Besides PET/MRI and PET/CT examinations, the screening methods included ultrasound, CT (for PET/MRI), MRI (for PET/CT) and tumor marker tests of CEA, CA19-9, PSA (for male) and CA125 (for female), dependent on the cancer type. Subjects who had no positive findings in the following 12 months were considered as 'cancer negative'.

RESULTS

In the 2794 subjects, PET/MRI detected 66 suspicious lesions, 54 of them were diagnosed as malignant tumors (true positive) and 12 of them were benign (false positive). 12 malignant tumors were missed but detected by other modalities (false negative). The detection rate, sensitivity, specificity, PPV and NPV of PET/MRI screening were 1.93% (54/2794), 81.8% (54/66), 99.5% (2715/2728), 81.8% (54/66) and 99.5% (2715/2728) respectively. In the 4283 subjects, PET/CT detected 55 suspicious lesions and 48 of them were malignant tumors (true positive) and 7 of them were benign (false positive). 7 malignant tumors were missed but detected by other modalities (false negative). The detection rate, sensitivity, specificity, PPV and NPV of PET/CT screening were 1.12% (48/4283), 87.3% (48/55), 99.8% (4228/4283), 87.3% (48/55) and 99.8% (4228/4283) respectively. The detailed distribution of cancer types is shown in Figure.

CONCLUSION

To our best knowledge, this is the first work to compare the diagnostic values of PET/MRI and PET/CT for cancer screening in asymptomatic subjects. Both methods can detect a wide variety of cancer at early stage.

CLINICAL RELEVANCE/APPLICATION

Compared to PET/CT, PET/MRI has a higher detection rate and a higher sensitivity in solid organs except lung. Considering also the reduced radiation dose, PET/MRI is recommended as part of a cancer screening program for asymptomatic subjects.

SSQ14-05 Whole-Body MRI and 18F-FDG PET/MRI for N and M Staging in Primary Breast Cancer: A Multicenter Trial

Thursday, Dec. 5 11:10AM - 11:20AM Room: S402AB

Participants

Nils M. Bruckmann, MD, Duesseldorf, Germany (*Presenter*) Nothing to Disclose Julian Kirchner, Dusseldorf, Germany (*Abstract Co-Author*) Nothing to Disclose Ole Martin, Duesseldorf, Germany (*Abstract Co-Author*) Nothing to Disclose Benedikt M. Schaarschmidt, MD, Essen, Germany (*Abstract Co-Author*) Nothing to Disclose Lale Umutlu, MD, Essen, Germany (*Abstract Co-Author*) Consultant, Bayer AG Gerald Antoch, MD, Dusseldorf, Germany (*Abstract Co-Author*) Nothing to Disclose Lino Sawicki, MD, Dusseldorf, Germany (*Abstract Co-Author*) Nothing to Disclose

PURPOSE

To evaluate and compare the diagnostic potential of whole-body MRI and 18F-FDG PET/MRI for N and M staging in newly diagnosed, histopathological proven breast cancer.

METHOD AND MATERIALS

A total of 77 patients with newly diagnosed, histopathological proven breast cancer were enrolled in this study prospectively. All

patient underwent a whole-body 18F-FDG PET/MRI in supine position. The MRI protocol included a transverse T2-weighted, a T1weighted and a DWI sequence of the whole body from head to the thigh. The N and M staging was assessed according to the eighth edition of the American Joint Committee on Cancer staging manual in MRI datasets alone and in 18F-FDG PET/MRI datasets, respectively. Histopathology or follow up examination as reference standard were available in all 77 patients for N and M staging. A McNemar chi2 test was performed to investigate whether differences in the evaluation of the correct N and M stage between 18F-FDG PET/MRI and MRI were statistically significant.

RESULTS

MRI and PET/MRI were concordant for N and M staging in 74 of 77 (96.1%) patients. Compared to the reference standard, PET/MRI as well as MRI determined a correct N and M stage in 57/77 (74%) of the patients, respectively. A positive nodal status was present in 33/77 patients (43%). PET/MRI determined the N stage correctly in 62 of 77 (80.5%) patients with a sensitivity of 78.8% and a specificity of 93.2%. MRI determined the N stage correctly in 61 of 77 (79%) with a sensitivity of 75.8% and a specificity of 93.2%. Distant metastases were present in 4/77 patients (5%). PET/MRI detected all of the histopathological proven metastases (100% identification), while one metastasis was missed in MRI (75% identification). Additionally, PET/MRI leads to false-positive findings in 6 patients (8%) and MRI in 5 patients (7%). No statistically significant differences between the modalities were seen.

CONCLUSION

18F-FDG PET/MRI was shown to be slightly superior to MRI in the N and M staging in primary breast cancer patients. However, both modalities bear the risk to overestimate the M-stage.

CLINICAL RELEVANCE/APPLICATION

A whole-body 18F-FDG PET/MRI and MRI are highly accurate for evaluating the M stage in breast cancer patients and therefore could be considered in combination with a dedicated breast 18F-FDG PET/MRI as staging method of choice at time of diagnosis.

SSQ14-06 Correlation of 18F-FDG PET/MRI Imaging Information with Relevant Immunohistochemical Markers in Breast Cancer Patients: Could PET/MRI Identify High-Risk Patients?

Thursday, Dec. 5 11:20AM - 11:30AM Room: S402AB

Participants

Ole Martin, Duesseldorf, Germany (*Abstract Co-Author*) Nothing to Disclose Julian Kirchner, Dusseldorf, Germany (*Abstract Co-Author*) Nothing to Disclose Nils M. Bruckmann, MD, Duesseldorf, Germany (*Abstract Co-Author*) Nothing to Disclose Benedikt M. Schaarschmidt, MD, Essen, Germany (*Abstract Co-Author*) Nothing to Disclose Johannes Grueneisen, Essen, Germany (*Abstract Co-Author*) Nothing to Disclose Yan Li, Essen, Germany (*Abstract Co-Author*) Nothing to Disclose Lale Umutlu, MD, Essen, Germany (*Abstract Co-Author*) Nothing to Disclose Gerald Antoch, MD, Dusseldorf, Germany (*Abstract Co-Author*) Nothing to Disclose Lino Sawicki, MD, Dusseldorf, Germany (*Presenter*) Nothing to Disclose

PURPOSE

To correlate prognostically relevant immunohistochemical parameters of breast cancer with simultaneously acquired standardized uptake values (SUV) and apparent diffusion coefficient (ADC) derived from hybrid PET/MRI.

METHOD AND MATERIALS

56 female patients with therapy naive, histologically proven breast cancer (mean age 54.1±12.0 years) underwent dedicated prone 18F-FDG breast PET/MRI and supine whole-body 18F-FDG PET/MRI. As part of the diagnostic imaging protocol, diffusion-weighted imaging (DWI, b values: 0, 500, 1000 s/mm²) was performed simultaneously with PET acquisition. A region of interest (ROI) encompassing the entire primary tumor was drawn into each patient's breast and prone PET/MR images to determine the glucose metabolism represented by maximum and mean SUV and into ADC maps to assess tumor cellularity represented by mean and minimum ADC values. Histopathological tumor grading as well as additional prognostically relevant immunohistochemical markers, i.e. Ki-67, progesterone, estrogen receptor, and human epidermal growth factor receptor 2 (HER2/neu) were determined.

RESULTS

We found a significant inverse correlation between both SUV- and ADC-values derived from breast PET/MRI (r=-0.49 for SUVmean vs. ADCmean and r=-0.43 for SUVmax vs. ADCmin, both p<0.001). Tumor grading as well as Ki67 showed a significant positive correlation with SUVmean from both whole-body PET/MRI (r=0.42 and r=0.37, p<0.001) and breast PET/MRI (r=0.37 and r=0.32, p<0.01). For immunohistochemical markers, HER2/neu significantly correlates inverse with ADC-values from breast PET/MRI (r=-0.35, p<0.01). In addition, estrogen receptor expression showed significant inverse correlation with SUV-values from whole-body PET/MRI (r=-0.45, p<0.001).

CONCLUSION

The present data show a correlation between increased glucose-metabolism, cellularity, degree of differentiation as well as Ki67 and HER2/neu expression of breast cancer primaries. 18F-FDG-PET and DWI from hybrid PET/MRI may offer complementary information for evaluation of breast cancer aggressiveness in initial staging and treatment response.

CLINICAL RELEVANCE/APPLICATION

Easily applicable information from PET/MRI leads to complementary knowledge in breast cancer staging workup. This could help to identify high-risk patients efficiently.

SSQ14-07 Impact of 18FDG PET/MRI on Therapeutic Management in Breast Cancer Patients - A Prospective Multicenter Comparison Trial to the Guideline Staging Algorithm

Thursday, Dec. 5 11:30AM - 11:40AM Room: S402AB

Ole Martin, Duesseldorf, Germany (Abstract Co-Author) Nothing to Disclose

Lale Umutlu, MD, Essen, Germany (Abstract Co-Author) Consultant, Bayer AG

Ken Herrmann, Essen, Germany (Abstract Co-Author) Co-founder, SurgicEye GmbH Stockholder, SurgicEye GmbH Consultant, Sofie Biosciences Consultant, Ipsen SA Consultant, Siemens AG Research Grant, Advanced Accelerator Applications SA Research Grant, Ipsen SA

Gerald Antoch, MD, Dusseldorf, Germany (*Abstract Co-Author*) Nothing to Disclose Christian Buchbender, Dusseldorf, Germany (*Abstract Co-Author*) Nothing to Disclose

For information about this presentation, contact:

Julian.Kirchner@med.uni-duesseldorf.de

PURPOSE

To investigate whether the differences between the traditional staging imaging algorithm and 18F-FDG PET/MR lead to different therapeutic decisions in patients with breast carcinoma

METHOD AND MATERIALS

A total of 57 female patients with newly diagnosed breast cancer and elevated pre-test probability for distant metastases (initial tumor stage, immunohistochemical receptor expression) from two centers were prospectively included in this study. The traditional staging imaging algorithm was performed in clinical routine at the home institution of the patient. Additionally, each patient underwent a PET/MRI including dedicated diagnostic breast imaging and a whole-body MRI. Tumor stage was determined according to AJCC Staging Manual separately for both, 18F-FDG PET/MR and traditional staging algorithm. To determine the different treatment strategies each patient was discussed two times in separate DMT sessions. In one, the determination of the treatment strategy was based exclusively on the results of the traditional algorithm and in the other on the PET/MR. The primary endpoint was the incidence of differences between the therapy recommendations. The secondary endpoint was the comparison of diagnostic accuracy between the traditional staging algorithm and PET/MR for the TNM classification.

RESULTS

PET/MR and the traditional staging algorithm agreed on TNM-stages in 45 of 57 (78.9%) patients. All deviations between were due to a higher stage in PET/MR. Compared with the reference standard, PET/MR determined correct stage in 53/57 (93.0%) and the traditional staging algorithm in 43/57 (75.4%), respectively and resulting in a significant higher diagnostic accuracy in PET/MR. Different therapeutic decisions between PET/MR and the traditional staging algorithm occurred in 7/57 (12.3%) of the patients.

CONCLUSION

For breast cancer patients with elevated pre-test probability for distant metastases a change of the therapy regime occurs in 12.3% compared to the traditional staging algorithm when staged by 18F-FDG PET/MR. Furthermore the study revealed the diagnostic superiority for determining the exact TNM stage of 18F-FDG PET/MR over the traditional staging algorithm

CLINICAL RELEVANCE/APPLICATION

Current guidelines should consider systemic staging with 18F-FDG-PET/MRI in breast cancer patients with elevated pre-test probability for distant metastases at the time of initial diagnosis.

SSQ14-08 CT-Less Direct Correction of Attenuation and Scatter in Image Space Using Deep Learning for Total-Body PET: A Feasibility Study

Thursday, Dec. 5 11:40AM - 11:50AM Room: S402AB

Participants

Jaewon Yang, San Francisco, CA (*Presenter*) Nothing to Disclose Dookun Park, PhD,DPhil, Seattle, WA (*Abstract Co-Author*) Nothing to Disclose Grant Gullberg, PhD, Berkeley, CA (*Abstract Co-Author*) Nothing to Disclose Youngho Seo, PhD, San Francisco, CA (*Abstract Co-Author*) Nothing to Disclose

PURPOSE

A total-body PET scanner like EXPLORER provides a substantial sensitivity gain of a factor of approximately 40 over current clinical PET scanners. The 40-fold increase in the effective sensitivity can reduce total radiation dose by 1/40th; however, the extra radiation dose of CT for PET attenuation and scatter correction (ASC) will mitigate the merit of the ultralow-dose PET. Therefore, we propose CT-less direct ASC without any intermediate step using deep learning (DL) potentially for total-body PET.

METHOD AND MATERIALS

In an IRB-approved study, we obtained images from 59 whole-body 18F-FDG PET/CT studies that were acquired from March 2016 through August 2017. A deep convolutional neural network (DCNN) was implemented with the 59 pairs of uncorrected PET (without ASC; PETUC) and corrected PET (with ASC; PETASC) as inputs to predict attenuation-scatter corrected PET (PETDCNN) directly from uncorrected PET (50/9 split for training and test data). Quality of the predicted images (PETDCNN) was evaluated using standardized uptake values (SUV) by the normalized root mean square error (NRMSE), peak signal to noise ratio (PSNR), and structural similarity index (SSIM). Statistical analyses were performed using joint and error histograms.

RESULTS

The overall performance of PETDCNN is quantitatively comparable to CT-based ASC (PETASC). Across the test set of 9 subjects, the NRMSE was 0.26 ± 0.05 ; the average PSNR was 14.75 ± 3.22 ; the average SSIM was 0.94 ± 0.03 , demonstrating high image similarity between PETDCNN and reference PETASC. The joint histogram shows the voxel-wise similarity between PETDCNN and reference PETASC. The joint histogram shows the result of the error histogram where most of errors (~ 90%) stay within ± 0.5 SUV differences.

CONCLUSION

We demonstrated the feasibility of CT-less direct ASC using deep learning potentially for total-body PET. The clinical translation of our approach will remove the need of CT scans for PET ASC, which results in significant reduction of radiation dose particularly for pediatric patients or treatment follow-ups.

CLINICAL RELEVANCE/APPLICATION

Our proposed DL method can remove the need of CT for PET ASC, which reduces the radiation dose from a whole-body CT scan, preserving the merit of ultra-low dose imaging in total-body PET.

SSQ14-09 Quantitative Standardized Uptake Value Evaluation of 4x Faster PET Scans Enhanced Using Deep Learning

Thursday, Dec. 5 11:50AM - 12:00PM Room: S402AB

Participants

Akshay Chaudhari, PhD, Menlo Park, CA (*Abstract Co-Author*) Research Consultant and Stockholder, Subtle Medical; Research Consultant, Skope MR; Scientific Advisory Board and Stockholder, Brain Key; Scientific Advisory Board, Chondrometrics GmbH; Stockholder, LVIS Corporation; ;

Praveen Gulaka, PhD, Menlo Park, CA (Presenter) Employee, Subtle Medical

Tao Zhang, Menlo Park, CA (Abstract Co-Author) Employee, Subtle Medical

Shyam Srinivas, MD, PhD, Cleveland, OH (Abstract Co-Author) Nothing to Disclose

Greg Zaharchuk, MD, PhD, Stanford, CA (*Abstract Co-Author*) Research Grant, General Electric Company; Research Grant, Bayer AG; Stockholder, Subtle Medical

Enhao Gong, PhD, Menlo Park, CA (Abstract Co-Author) Stockholder, Subtle Medical

For information about this presentation, contact:

enhao@subtlemedical.com

PURPOSE

The goal of this study was to evaluate the accuracy of quantitative standardized uptake values (SUV) for noisy PET scans acquired 4x faster and subsequently enhanced using deep learning.

METHOD AND MATERIALS

15 subjects (7 male, 8 female; mean age: 67 years, range: 45;85 yrs, average BMI: 30, range: 19-48) referred for clinical wholebody PET/CT exams underwent two separate PET scans - one with the standard acquisition duration followed by one acquired 4 times faster, following IRB approval and informed consent. The 4x faster PET images were enhanced using a deep learning (DL) software (SubtlePET, Subtle Medical, Menlo Park, CA). One nuclear medicine physician reviewed the standard acquisition PET images, identified possible lesions and some normal regions, and drew regions of interest (ROIs) in OsiriX. The same lesions were reviewed on the DL-enhanced 4x faster scan images and the ROIs from the standard acquisition were propagated to the DLenhanced 4x faster scan. Quantitative mean and maximum SUV values per ROI between the standard and DL-enhanced 4x faster acquisitions were visualized using Bland-Altman tests and compared using concordance correlation coefficients (CCC), linear regressions, and Mann-Whitney U-Tests.

RESULTS

A total of 63 ROIs were identified in the standard acquisition PET images. The Bland-Altman plot in Fig.1a-b (dotted line indicating mean, and dashed line indicating 95% limits of agreement) showed minimal differences between SUVs obtained from the two sets of scans, with almost all values contained within the 95% limits of agreement interval. CCC and linear Pearson coefficient values of 0.99 for both SUV-max and SUV-mean indicated very strong agreement between the SUV values from standard acquisition and DL-enhanced scan (Fig.1c-d, where the dotted line indicates the unity line). This was further indicated by the lack of statistical significance of p=0.68 for SUV-max and p=0.77 for SUV-mean values using the Mann-Whitney U-Test. Sample images can also be seen in Fig.1.

CONCLUSION

Deep learning can enhance 4x faster PET acquisitions without compromising quantitative SUV values compared a standard duration acquisition.

CLINICAL RELEVANCE/APPLICATION

Deep learning can enhance image quality of noisy 4x faster PET acquisitions thereby enabling higher comfort for patients, higher throughput of PET scans for hospitals, or reduced radiotracer dosages.





SSQ16

Neuroradiology (White Matter)

Thursday, Dec. 5 10:30AM - 12:00PM Room: S404CD



AMA PRA Category 1 Credits ™: 1.50 ARRT Category A+ Credit: 1.75

FDA Discussions may include off-label uses.

Participants

John Kim, MD, Boston, MA (*Moderator*) Consultant, Tempus Inc Christopher T. Whitlow, MD, PhD, Winston-Salem, NC (*Moderator*) Nothing to Disclose Avner Meoded, MD, Baltimore, MD (*Moderator*) Nothing to Disclose

Sub-Events

SSQ16-01 High-Resolution Myelin Imaging Using Synthetic MRI in 3D

Thursday, Dec. 5 10:30AM - 10:40AM Room: S404CD

Participants

Marcel Warntjes, Linkoping, Sweden (*Presenter*) Consultant, SyntheticMR AB Peter Johansson, Linkoping, Sweden (*Abstract Co-Author*) Employee, SyntheticMR AB Peter Lundberg, PhD, Linkoping, Sweden (*Abstract Co-Author*) Co-owner, AMRA AB Stockholder, AMRA AB Anders Tisell, Linkoping, Sweden (*Abstract Co-Author*) Nothing to Disclose

For information about this presentation, contact:

marcel.warntjes@syntheticmr.com

PURPOSE

Intact myelin is crucial for efficient signal transfer in the central nervous system. Neurodegenerative diseases such as MS and dementia result in myelin damage and the associated impairment of motor and cognitive function. Quantitative assessment of myelination is an important clinical biomarker in the treatment and follow-up of patients. Myelin can be measured using synthetic MRI; the measurement of the R1 and R2 relaxation and proton density PD in conjunction with a myelin model can provide myelin partial volume maps for the entire brain. Recently, a 3D acquisition method was developed for high-resolution, isotropic synthetic MRI. The purpose of this work was to compare myelin detection based on the 3D method with the more established 2D method.

METHOD AND MATERIALS

The 3D QALAS sequence is a segmented spoiled gradient echo sequence with 5 parallel acquisitions, interleaved with a T2 preparation and inversion pulse. The 2D MDME sequence (MAGiC) is a saturation recovery multi-slice TSE sequence with multi-echo read-out. Both sequences had a scan time of 6:10 minutes. The scanner was a patched Philips Ingenia 3T. Post-processing was performed by a prototype version based on SyMRI 11.1 (SyntheticMR, Sweden). A group of 12 volunteers was acquired two times with 3D QALAS and 2 times MDME in SAG orientation, both at 1.5T and 3T, to correlate automatically segmented myelin volume and myelin fraction of the brain.

RESULTS

The mean myelin volume for the entire group was 183 mL and the mean brain volume was 1300 mL (14.1%). A high correlation was found between volumes determined by QALAS and MDME. The Pearson correlation coefficient was 0.94, the mean difference was 0±13 mL. The difference between measurement 1 and 2 was -2 ± 10 mL at 1.5T and 1 ± 13 mL at 3T for QALAS whereas it was 0 ± 4 mL at 1.5T and -3 ± 4 mL at 3T for MDME. In Fig.1 representative images are shown for myelin mapping using MDME SAG, MDME AX and 3D QALAS. The color scale range is 0-40% partial volume.

CONCLUSION

Myelin measurements using 3D QALAS provides very similar values myelin and brain volumes in comparison to 2D MDME. The advantage of 3D QALAS is the ability to view the data in all orientations.

CLINICAL RELEVANCE/APPLICATION

High-resolution 3D myelin imaging can be done in a short scan time using synthetic MRI. The same data also provides conventional T1W, T2W and FLAIR images.

SSQ16-02 Quantitative Susceptibility Weighted Imaging (SWI): A Novel Imaging Biomarker to Predict Disease Activity in Multiple Sclerosis

Thursday, Dec. 5 10:40AM - 10:50AM Room: S404CD

Participants

Vinayagamani S, Trivandrum, India (*Abstract Co-Author*) Nothing to Disclose Sabarish S S JR, MBBS, MD, Madurai, India (*Presenter*) Grant, General Electric Company Bejoy Thomas, Trivandrum, India (*Abstract Co-Author*) Stockholder, WIPRO LIMITED; Grant, General Electric Company Chandrasekharan Kesavadas, MD, Trivandrum, India (*Abstract Co-Author*) Nothing to Disclose Sruthi S Nair, Trivandrum, India (*Abstract Co-Author*) Nothing to Disclose

For information about this presentation, contact:

dr.vinayagamani@gmail.com

PURPOSE

Gadolinium(Gd) enhancement of multiple sclerosis (MS) lesions in T1W imaging (T1W+Gd) is the currently practiced method to differentiate active from inactive lesions. Our primary aim is to study the evaluation of Quantitative SWI in differentiating active from inactive lesions of MS using SWI phase values , there by assessing the variations in the iron content.

METHOD AND MATERIALS

In this prospective study, clinical data and images from patients who underwent MRI from September 2017 to January 2019 were reviewed. Lesions were divided into two groups; active (Group 1) and inactive (Group 2) lesions based on contrast enhancement. Phase values of the lesions (PL) and the contralateral normal white matter (PNWM) were calculated using SPIN software by drawing ROI. Subtracted phase values (PS=PL - PNWM) and iron content (PS /3) of the lesions were calculated in both groups. The means were compared by student T test and statistical significance was determined as p value < 0.05. Using ROC curve , a optimum cut off value with sensitivity and specificity were calculated

RESULTS

48 active lesions from 25 patients (Group 1) and 52 inactive lesions from 27 patients (Group 2) were analysed. Mean subtracted phase values in group 1 and 2 were 3.64 and 15.84 respectively. The iron content (Mean \pm SD) of the inactive lesions was found to be higher (5.39 \pm 1.72 µg/g) than the active lesions (1.21 \pm 0.52 µg/g), which was statistically significant (P value <0.001). A cut off value of >2.5 µg/g will provide a sensitivity and specificity of 96.5% and 96.4% respectively to detect inactive lesion

CONCLUSION

Quantification of iron content using SWI phase values will differentiate active from inactive lesions, which can be a novel imaging biomarker in assessing disease activity.

CLINICAL RELEVANCE/APPLICATION

1.Various studies have concluded that repetitive use of Gd leads to deposition in brain accelerating secondary progression and atrophy inspite of normal renal function 2. Thus it can be a novel imaging biomarker to identify disease activity in patients who undergo routine neuroimaging for MS.

SSQ16-03 White Matter Hyperintensities on Magnetic Resonance Imaging and Aging: Comparison of Three Visual Rating Scales Using Convolutional Neural Networks

Thursday, Dec. 5 10:50AM - 11:00AM Room: S404CD

Participants

Josep Puig, MD, PhD, Winnipeg, MB (*Abstract Co-Author*) Nothing to Disclose Ana Jimenez-Pastor, Valencia, Spain (*Abstract Co-Author*) Nothing to Disclose Eduardo Camacho, Valencia, Spain (*Abstract Co-Author*) Nothing to Disclose Carles Biarnes, Girona, Spain (*Abstract Co-Author*) Nothing to Disclose Joan C. Vilanova, MD, PhD, Girona, Spain (*Abstract Co-Author*) Nothing to Disclose Josep Garre-Olmo, Girona, Spain (*Abstract Co-Author*) Nothing to Disclose Reinald Pamplona, Lleida, Spain (*Abstract Co-Author*) Nothing to Disclose Rafel Ramos, Girona, Spain (*Abstract Co-Author*) Nothing to Disclose Marco Essig, MD, Winnipeg, MB (*Abstract Co-Author*) Nothing to Disclose Salvador Pedraza, MD, PhD, Girona, Spain (*Abstract Co-Author*) Nothing to Disclose Angel Alberich-Bayarri, PhD, Valencia, Spain (*Presenter*) Nothing to Disclose

For information about this presentation, contact:

jpuigmd@gmail.com

PURPOSE

White matter hyperintensities (WMH) on magnetic resonance imaging (MRI) increase with age and are associated with stroke, cognitive decline, and dementia. Although consistent assessment of WMH burden is crucial for epidemiological and clinical studies, little evidence is available about the performance of proposed visual rating scales. We used deep-learning-based models to compare three visual WMH rating scales.

METHOD AND MATERIALS

We studied 418 healthy participants (mean, 66.67±7.96 years [range, 50-96 years]) consecutively recruited in a population-based aging study. All imaging studies were obtained on a 1.5 T MRI system (Vantage Elan, Canon Medical Systems, Japan). WMHs were rated according to Fazekas' scale (FZ), Age-Related White Matter Change (ARWMC) scale, and van Swieten's (VS) scale. For each scale, WMH burden was categorized as none or slight, moderate, or severe. Artifacts, lacunae, and chronic territorial infarcts were excluded. We used convolutional neural networks to assess WMH-metrics, including volume, dissemination, number of lesions, and mean entropy. We used t-tests to compare group means.

RESULTS

The different scales classified WMH burden as none or slight (FZ=331 subjects [mean WMH volume 0.487±0.639 mL]; ARWMC=327 subjects [0.477±0.625 mL]; VS=186 subjects [0.231±0.361 mL]), moderate (FZ=69 subjects [3.529±2.652 mL], ARWMC=70 subjects [3.404±2.604 mL], VS=177 [1.192±1.561 mL]), and severe (FZ=18 subjects [9.568±4.795 mL], ARWMC=21 subjects [8.707±5.068 mL], VS=57 subjects [5.675±4.326 mL]). On FZ and ARWMC, WMH volumes in each category were similar. However, on SV, WMH volumes in all categories were smaller than on FZ and ARWMC (P<0.001). Additionally, on FZ and ARWMC, WMH dissemination, number of lesions and mean entropy in moderate and severe category were also similar.

CONCLUSION

Our results indicate that FZ and ARWMC ratings of WMH CNN-based quantification are similar; SV tends to underrate WMH burden. Therefore, FZ and ARWMC could be applied equally to assess WMH characterization.

CLINICAL RELEVANCE/APPLICATION

FZ and ARWMC scales and volumes provide near-equivalent estimates of WMH burden; therefore, either can be used.

SSQ16-04 Unsupervised Learning Approach for Multiple Sclerosis Lesion Segmentation in Brain MRI: Application of Minimum Distance Estimation with a Cramer-von Mises Type Statistic

Thursday, Dec. 5 11:00AM - 11:10AM Room: S404CD

Participants

Jiwoong Kim, PhD, Seoul, Korea, Republic Of (*Presenter*) Nothing to Disclose Jin Hee Jang, MD, Seoul, Korea, Republic Of (*Abstract Co-Author*) Spouse, Employee, VUNO Inc Yoonho Nam, Seoul, Korea, Republic Of (*Abstract Co-Author*) Nothing to Disclose Wojoon Kim, Seoul, Korea, Republic Of (*Abstract Co-Author*) Nothing to Disclose Yangsean P. Choi, Seoul, Korea, Republic Of (*Abstract Co-Author*) Nothing to Disclose Na-Young Shin, Seoul, Korea, Republic Of (*Abstract Co-Author*) Nothing to Disclose Kookjin Ahn, MD, PhD, Seoul, Korea, Republic Of (*Abstract Co-Author*) Nothing to Disclose Bum-Soo Kim, MD, PhD, Seoul, Korea, Republic Of (*Abstract Co-Author*) Nothing to Disclose

For information about this presentation, contact:

znee@catholic.ac.kr

PURPOSE

While recent advances in machine learning could enable automatic segmentation of multiple sclerosis (MS) lesions in brain MRI, many algorithms were based on the supervised learning. One caveat to this approach is its demand for large volume of labeled data with high quality. Considering difficulty of labeling, an approach of the unsupervised scheme can be an alternative solution to this self-contradictory problem. Here, we developed an algorithm based on the unsupervised learning to segment MS lesions on FLAIR MR image and validated its feasibility through open, clinical datasets.

METHOD AND MATERIALS

To segment MS lesions with using unlabeled data, we estimated their locations in the MR image. To obtain non-parametric and data-driven estimates, we used minimum distance estimation (MDE) with a Cramer-von Mises (CvM) type statistic which is known to be robust against anomalies. Briefly, starting from two randomly-generated regions of the MR image, our algorithm provided two segmented regions - MS lesions and another area - in a fast and stable manner. From pre-processed (brain extracted and bias-corrected) 3D FLAIR images, MS lesions were estimated for each axial image, using small-sized patches for sliding window scheme. After applying the median filtering to combined patches, final lesion maps were acquired. We applied a developed method for two different datasets: our hospital dataset (N=10, confirmed MS) and open dataset (MSSEG challenge, N=10). We calculated a dice coefficient for open dataset which has reference standard lesion segmentation results. Also we assessed visual appropriateness for two datasets.

RESULTS

A developed model was applied successfully to 3D FLAIR images, both in open and our hospital datasets. In general, there was good agreement for segmentation results with visual inspection of MS lesions and reference standard. Median DICE index for reference standards of open dataset was 0.39 (range 0.20-0.58), which was comparable with results of previous challenge winners. Even though some false negative lesions were found, they were small and subtle. Majoirty of false positive were cerebral cortices.

CONCLUSION

We demonstrated that MDE with a CvM type statistic could be a useful unsupervised method to segment MS lesions in FLAIR images.

CLINICAL RELEVANCE/APPLICATION

Unsupervised method for MS lesion segmentation could have clinical potential over supervised learning, when manual labeling data is limited.

SSQ16-05 New Multiple Sclerosis Clinical MR Protocol to Limit the Use of Intravenous Contrast Using CAD Software

Thursday, Dec. 5 11:10AM - 11:20AM Room: S404CD

Participants

Michel Bilello, MD, PhD, Philadelphia, PA (*Presenter*) Nothing to Disclose Jeffrey Rudie, MD, PhD, San Francisco, CA (*Abstract Co-Author*) Nothing to Disclose Raghav Mattay, MD, Philadelphia, PA (*Abstract Co-Author*) Nothing to Disclose Saima Rathore, Philadelphia, PA (*Abstract Co-Author*) Nothing to Disclose Alexander C. Mamourian, MD, Philadelphia, PA (*Abstract Co-Author*) Nothing to Disclose

PURPOSE

The growing concern about deposition of free gadolinium in the brain of patients that undergo serial contrast-enhanced MRI studies demands careful use of IV contrast. We have implemented a new, CAD-assisted clinical MR protocol for the purpose of limiting gadolinium-based contrast injections in our patients with multiple sclerosis (MS).

METHOD AND MATERIALS

Following the results of our recent publication that demonstrated that all MS patients with enhancing lesions on their followup brain MR scan also have new lesions on pregad imaging, the new protocol uses a CAD software to determine in real time which patients

have new brain lesions, and only those patients who do get IV contrast. There are two major components in this clinical decision support system: 1) The CAD program, which detects new brain lesions by comparing 3D T2/FLAIR images from current and prior studies. 2) Our department clinical 3D lab, staffed with technologists, who not only run the program, but also assess the CAD results for new brain lesions. The workflow goes like this: The patient (without IV) gets the 3D FLAIR sequence first. As soon as this is done, the 3D lab runs the CAD program. Then the 3D lab calls the MR tech with the results: If there is no new lesion, only non-contrast imaging gets performed. If there is at least one new lesion, the MR tech places a butterfly in the patient's arm, and proceed with a complete contrast-enhanced scan.

RESULTS

The new clinical protocol has been used for about 2 months, on 360 followup scans, and resulted in 60% reduction in the rate of gadolinium injection. The accuracy of 3D lab assessment of CAD results versus final radiologist interpretation was more than 95%. Our preliminary study predicted a rate of 75% reduction, and the main reason for not achieving this figure in the clinical implementation is the unavailability of the 3D lab after hours. In that case, patients get contrast automatically. There is still room for improvement in CAD sensitivity, and assessment of CAD results by 3D lab techs.

CONCLUSION

We have implemented a new MR clinical protocol to avoid unnecessary gadolinium injections in patients with MS with a real-time decision support system. We believe that this will address the growing concern of our patients, as well as save time and resources.

CLINICAL RELEVANCE/APPLICATION

This protocol is now being used on every MS followup case, and is poised to improve patient experience, and save resources.

SSQ16-07 Comparing Selective Inversion Recovery Quantitative Magnetization Transfer and Diffusion Tensor Imaging to Assess Myelin Integrity in Multiple Sclerosis

Thursday, Dec. 5 11:30AM - 11:40AM Room: S404CD

Participants

Dhairya Lakhani, MD, Nashville , TN (*Presenter*) Nothing to Disclose Giulia Franco, Nashville, TN (*Abstract Co-Author*) Nothing to Disclose Michael Kammer, Nashville, TN (*Abstract Co-Author*) Nothing to Disclose Aneri Balar, Nashville, TN (*Abstract Co-Author*) Nothing to Disclose Fie Ye, Nashville, TN (*Abstract Co-Author*) Nothing to Disclose Run Fan, Nashville, TN (*Abstract Co-Author*) Nothing to Disclose Ipek Oguz, Nashville, TN (*Abstract Co-Author*) Nothing to Disclose Seth A. Smith, PhD, Nashville, TN (*Abstract Co-Author*) Nothing to Disclose Junzhong Xu, Nashville, TN (*Abstract Co-Author*) Nothing to Disclose Richard Dortch, PhD, Nashville, TN (*Abstract Co-Author*) Nothing to Disclose Francesca Bagnato, MD, Nashville, TN (*Abstract Co-Author*) Nothing to Disclose

For information about this presentation, contact:

dhairya.lakhani@gmail.com

PURPOSE

We propose to validate Quantitative Magnetization Transfer (qMT) protocol and its derived myelin-sensitive pool-size-ratio (PSR) by comparing it with conventional radial diffusivity (RD) derived from diffusion tensor imaging (DTI). We hypothesize that i) Both PSR and RD discriminate pathological versus healthy tissue in brain of persons with multiple MS, ii) PSR shows comparatively stronger associations with clinical measures due to its superior specificity to myelin integrity.

METHOD AND MATERIALS

In this prospective case-control study 18 persons with MS and nine age-and-sex-matched healthy controls(HC) underwent conventional scans, DTI and qMT protocol scan on 3T. Disability was measured using Expanded Disability Status Scale (EDSS) and Timed 25-Foot Walk Test (T25-FW). Generalized linear mixed models for binary outcome were used to assess differences in PSR and RD between white-matter-lesions(WMLs), chronic-black-holes(cBHs), normal-appearing-white matter(NAWM), and normal-white-matter(NWM) of HCs. Association between variables were measured using non-parametric Spearman's Rank correlation analyses.

RESULTS

PSR and RD differed (p<0.001) between cBH and WML, WML and NAWM, but not between NAWM and NWM. PSR derived from cBHs (r=-0.83, p<0.001) and WML (r=-0.76, p<0.001) correlated with volume of cBH. No correlation was observed between RD and lesion burden or between both PSR and RD with brain atrophy. PSR derived from cBHs and WML correlated with EDSS (r=-0.44, p=0.005; r=-0.63, p=0.005), T25-FW (r=-0.62, p<0.05; r=-0.63, p=0.005) and disease duration (r=-0.61, p=0.05; r=-0.71, p=0.002) respectively.(Figure 1) On the contrary, no significant associations were seen between RD values and clinical measures.

CONCLUSION

Both PSR and RD can discriminate tissues with different types of pathology, but only PSR is sensitive to clinical measures. The differences can be attributed to the fact that qMT provides an indirect measure of macromolecular content through its communication with surrounding water, whereas DTI only offers information related to the presence or absence of barriers, which in damaged tissue, is complex. Additionally, qMT is not sensitive to fiber orientation as DTI and thus may also have a pivotal role in explaining our results.

CLINICAL RELEVANCE/APPLICATION

SIR-qMT derived metrics add specificity to the assessment of myelin integrity in persons with MS, suggesting a role as biomarker of neurodegeneration and repair.

SSQ16-08 Imaging of Acute Optic Neuritis: Is It Possible to Diagnose Demyelinating Disorders based on Optic Nerve Enhancement Patterns?

Participants

Maximiliano Darakdjian, MD, Buenos Aires City, Argentina (*Presenter*) Nothing to Disclose Hernan Chaves, MD, Vicente Lopez, Argentina (*Abstract Co-Author*) Consultant, ENTELAI Jairo Hernandez, MD, MS, Buenos Aires, Argentina (*Abstract Co-Author*) Nothing to Disclose Claudia P. Cejas, MD, Buenos Aires, Argentina (*Abstract Co-Author*) Nothing to Disclose

For information about this presentation, contact:

maxdarakdjian@gmail.com

PURPOSE

MRI patterns of optic nerve involvement have been described and correlated with underlying optic neuritis (ON) etiologies. Optic nerve enhancement is an accurate biomarker of acute ON. Our purpose is to analyze if there is any difference between patterns of optic nerve enhancement and acute ON etiologies.

METHOD AND MATERIALS

We retrospectively analyzed enhancement patterns on fat-suppressed T1-weighted images of 50 optic nerves (43 patients) with clinical and radiological acute ON, who presented at our institution over a 4-year period. We evaluated location and extension of enhancing optic nerve segments and the presence of perineural enhancement (PE). Images were analyzed in consensus by a third-year radiology resident and a neuroradiologist. The relation between optic nerve enhancement patterns and underlying etiology was evaluated. Fisher's exact test and chi2 were calculated.

RESULTS

Patients mean age was 30.7 years-old (range 6-79) and 28 were females (65.1%). Twenty-three (53.4%) were diagnosed with Multiple Sclerosis (MS), 8 (18.6%) Neuromyelitis Optica (NMO) and 12 (27.9%) anti-MOG. Seven patients had bilateral involvement [14.29% MS, 14.3% NMO, 71.3% anti-MOG (p=0.029)]. Nine nerves had PE (33.3% MS, 33.3% NMO and 33.3% anti-MOG). Thirty-five had intraorbital involvement [34.2% MS, 22.8% NMO, 42.8% anti-MOG (p=0.012)]. Canalicular involvement was seen in 28 patients (46.4% MS, 10.6% NMO, 42.9% anti-MOG), intracranial in 20 (45% MS, 15% NMO, 40% anti-MOG) and chiasmatic in 3 patients (33% MS, 33% NMO, 33% anti-MOG). Twenty-six patients had only 1 involved segment (61.54% MS, 19.23% NMO, 19.23% anti-MOG), 13 patients had 2 segments (38.5% MS, 15.4% NMO, 46.2% anti-MOG), 10 patients had 3 segments (30% MS, 20% NMO, 50% anti-MOG) and only one patient had 4 segments affected (anti-MOG). The median time from symptom onset to MRI was 8.7 days (range 0-33).

CONCLUSION

In acute ON, bilaterality and intraorbital involvement of optic nerves were more frequent in anti-MOG patients compared to MS and NMO groups. There was no statistically significant difference in the presence of PE or number of involved segments between groups.

CLINICAL RELEVANCE/APPLICATION

Despite acute ON treatment is similar in all demyelinating entities, prognosis and further management differs considerably. Patterns of nerve enhancement could differentiate between etiologies.

SSQ16-09 Neuromyelitis Optica Spectrum Disorders (NMOSD) - Is that Possible to Characterize Different Phenotypes by Magnetic Resonance Imaging?

Thursday, Dec. 5 11:50AM - 12:00PM Room: S404CD

Participants

Lucas L. Resende, MD, Sao Paulo, Brazil (*Abstract Co-Author*) Nothing to Disclose Luana M. Salles, Sao Paulo , Brazil (*Abstract Co-Author*) Nothing to Disclose Eduarda L. Dias, MD, Sao Paulo, Brazil (*Presenter*) Nothing to Disclose Eduardo A. Valadares, Sao Paulo, Brazil (*Abstract Co-Author*) Nothing to Disclose Douglas K. Sato, Sao Paulo, Brazil (*Abstract Co-Author*) Nothing to Disclose Samira A. Pereira, Sao Paulo, Brazil (*Abstract Co-Author*) Nothing to Disclose Renata F. Simm, Sao Paulo, Brazil (*Abstract Co-Author*) Nothing to Disclose Frederico M. Jorge, Sao Paulo, Brazil (*Abstract Co-Author*) Nothing to Disclose Leandro T. Lucato, MD, Sao Paulo, Brazil (*Abstract Co-Author*) Nothing to Disclose Dagoberto Callegaro, Sao Paulo, Brazil (*Abstract Co-Author*) Nothing to Disclose Claudia D. Leite, MD,PhD, Sao Paulo, Brazil (*Abstract Co-Author*) Nothing to Disclose Carolina M. Rimkus, MD, Sao Paulo, Brazil (*Abstract Co-Author*) Nothing to Disclose

For information about this presentation, contact:

lucaslresende@gmail.com

PURPOSE

Patients with neuromyelitis optica spectrum disorders (NMOSD) can be positive for antibodies against aquaporin-4 (anti-AQP4), against myelin oligodendrocyte glycoprotein (anti-MOG) or even double negative. Our goal in this study is to compare MRI findings between anti-AQP4 positive, anti-MOG positive and double negative patients.

METHOD AND MATERIALS

Two neuroradiologist blind for the antibody measures results retrospectively analyzed MRI scans from 72 NMOSD patients (29 patients positive for anti-MOG; 26 patients positive for anti-AQP4, and 17 patients negative for both antibodies). We compared the frequency and characteristics of optic neuritis, myelitis and brain lesions, including presence of medullary and area postrema lesions; the number of abnormal optic nerve and medullary segments, and the encephalic regions involved in each condition. We performed chi-square and person test for categorical variables and analysis of median with Mann-Whitney test for continuous variables.

RESULTS

When comparing anti-MOG versus anti-AQP4 patients, we observed significant differences in: presence of medullary lesions, MOG 44% AQP4 88% (p=0.001); presence of area postrema lesions MOG 3.7% AQP4 38% (p=0.002), normal brain MRI MOG 69% AQP4 23% (p=<0.001), optic chiasm lesions MOG 13,3% AQP4 61,1% (p=0.005); longitudinally extensive transverse myelitis (LETM) MOG 7% AQP4 80% (p<0.001); medullary bright spot lesions MOG 0% AQP4 50% (p<0.001). When comparing anti-MOG versus double negative (DN) we observed significant differences in: normal brain MRI MOG 69% DN 29% (p=0.009); optic chiasm lesions MOG 13% DN 53% (p=0.042); median number of medullary segments involved MOG 4 DN 13 (p=0.01); corticospinal tract involvement MOG 3% DN 35% (p=0,048).

CONCLUSION

Anti-MoG related myelitis is less frequent and less extensive, compared to anti-AQP4 and double negative patients, and the bright spotty lesions are absent in anti-MoG patients. The anti-MOG related optic neuritis frequently spares the optic chiasm. These MRI findings might provide surrogate markers to differentiate NMOSD phenotypes.

CLINICAL RELEVANCE/APPLICATION

NMOSD patients showed different MRI patterns depending on the serological evaluation. To recognize specific MRI patterns for each autoantibody-related presentation might help understanding different pathological mechanisms and to guide personalized diagnostic and therapeutic interventions.







AI52

AI Theater: Is AI Enough? From Research to Daily Practice for Better Patient Care in Stroke: Presented by Cercare Medical

Thursday, Dec. 5 11:00AM - 11:20AM Room: AI Showcase, North Building, Level 2, Booth 10724

Participants

Ronald J. Borra, MD, PhD, Turku, Finland (Presenter) Nothing to Disclose

Program Information

Artificial intelligence is a technology that opens up new horizons in many areas of our lives, especially radiology. However, machine learning on its own does not guarantee higher performance or precision. Cercare Medical uses AI as a tool to make the results of years of research available to doctors in their daily practice and support their life-changing decisions in acute ischemic stroke. Cercare Medical is a software company founded in 2013 as a spin-out of the Center of Functionally Integrative Neuroscience at Aarhus University, Denmark. Cercare Medical extends more than 10 years of research, led by Professor Leif Østergaard and Professor Kim Mouridsen, in neuroimaging and artificial intelligence. The Cercare Medical Neurosuite stroke solution provides automated, AI-powered oxygenation analysis, segmentation and quantification of brain tissue status for fast decision making in acute stroke. Note: Cercare Medical products are not commercially available for the U.S.





SPAI52

RSNA AI Deep Learning Lab: Segmentation

Thursday, Dec. 5 1:00PM - 2:30PM Room: AI Showcase, North Building, Level 2, Booth 10342



AMA PRA Category 1 Credits ™: 1.50 ARRT Category A+ Credit: 1.75

Participants

George L. Shih, MD, New York, NY (*Presenter*) Consultant, Image Safely, Inc; Stockholder, Image Safely, Inc; Consultant, MD.ai, Inc; Stockholder, MD.ai, Inc;

Special Information

In order to get the best experience for this session, it is highly recommended that attendees bring a laptop with a keyboard, a decent-sized screen, and the latest version of Google Chrome. Additionally, it is recommended that attendees have a basic knowledge of deep learning programming and some experience running a Google CoLab notebook. Having a Gmail account is also helpful. Here are instructions for creating and deleting a Gmail account.

ABSTRACT

This session will focus on the use of deep learning methods for image segmentation, applied to the challenge of CT or MR brain segmentation. While focused on this particular problem, the concepts should generalize to other organs and image types.





Advanced Imaging of Arthritis

Thursday, Dec. 5 4:30PM - 6:00PM Room: S402AB



AMA PRA Category 1 Credits ™: 1.50 ARRT Category A+ Credit: 1.75

FDA Discussions may include off-label uses.

Participants

Thomas M. Link, MD, PhD, San Francisco, CA (*Director*) Research Grant, General Electric Company; Research Consultant, General Electric Company; Research Consultant, InSightec Ltd; Research Grant, InSightec Ltd; Consultant, Springer Nature; Research Consultant, Pfizer Inc;

For information about this presentation, contact:

thomas.link@ucsf.edu

LEARNING OBJECTIVES

1) Specify a systematic approach to classify inflammatory and degenerative arthropathies. 2) Identify pitfalls in interpreting imaging studies obtained in inflammatory arthropathies. 3) Describe imaging findings in spondylarthropathies with a focus on MRI. 4) Develop cartilage mapping protocols that can be implemented in clinical practice. 5) Apply advanced osteoarthritis imaging techniques clinically.

Sub-Events

RC704A My Approach to Imaging of Arthritis

Participants

Thomas M. Link, MD, PhD, San Francisco, CA (*Presenter*) Research Grant, General Electric Company; Research Consultant, General Electric Company; Research Consultant, InSightec Ltd; Research Grant, InSightec Ltd; Consultant, Springer Nature; Research Consultant, Pfizer Inc;

For information about this presentation, contact:

thomas.link@ucsf.edu

LEARNING OBJECTIVES

1) Differentiate inflammatory and degenerative arthropathies based on the anatomic location of findings. 2) Identify radiographic findings in arthropathies and list their differential diagnoses. 3) Classify MRI findings in inflammatory and degenerative arthropathies.

RC704B Pitfalls of Inflammatory Arthritis Imaging

Participants Connie Y. Chang, MD, Boston, MA (*Presenter*) Nothing to Disclose

For information about this presentation, contact:

cychang@mgh.harvard.edu

LEARNING OBJECTIVES

1) To know the differential diagnosis for inflammatory arthritis in large and small joints. 2) To analyze the distinguishing clinical and imaging features of the inflammatory arthritis pitfalls. 3) To apply this knowledge to formulating recommendations for next steps (imaging, clinical tests).

RC704C Imaging of Spondyloarthritis

Participants Robert G. Lambert, MBBCh, Edmonton, AB (*Presenter*) Nothing to Disclose

For information about this presentation, contact:

rlambert@ualberta.ca

LEARNING OBJECTIVES

1) Describe the imaging findings commonly seen in spondylarthritis with a focus on MRI. 2) Distinguish the patterns of disease that occur in spondyloarthritis from degeneration. 3) Identify pitfalls in interpreting imaging studies obtained in spondylarthritis.

RC704D Implementing Cartilage Mapping in Clinical Practice

Participants

Carl S. Winalski, MD, Rocky River, OH (Presenter) Institutional service agreement, Medical Metrics, Inc Institutional service

agreement, BioClinica, Inc Institutional service agreement, PAREXEL International Corporation Institutional service agreement, CartiHeal Ltd Shareholder, Pfizer Inc Spouse, Shareholder, General Electric Company

For information about this presentation, contact:

winalsc@ccf.org

RC704E Advanced Techniques in Osteoarthritis Imaging

Participants

Shadpour Demehri, MD, Baltimore, MD (*Presenter*) Research support, General Electric Company; Research Grant, Carestream Health, Inc; Consultant, Toshiba Corporation

For information about this presentation, contact:

sdemehr1@jhmi.edu

LEARNING OBJECTIVES

1) To evaluate advanced imaging based biomarkers for diagnosis and risk assessment for OA outcomes. 2)To list the MRI-based anatomical imaging techniques for cartilage imaging. 3) To introduce novel CT imaging techniques for OA imaging and their potential role in routine clinical practice.





What's in the Pipeline for Neuro MRI?

Thursday, Dec. 5 4:30PM - 6:00PM Room: E451B



AMA PRA Category 1 Credits ™: 1.50 ARRT Category A+ Credit: 1.75

FDA Discussions may include off-label uses.

Participants

Michael M. Zeineh, PhD, MD, Stanford, CA (Moderator) Research funded, General Electric Company;

For information about this presentation, contact:

mzeineh@stanford.edu

LEARNING OBJECTIVES

Develop a framework for task-based fMRI for language mapping. 2) Assess what resting state fMRI can accomplish as an alternative. 3) Define clinical applications of quantitative susceptibility mapping (QSM). 4) Identify real-world clinical applications of advanced diffusion imaging beyond DWI and DTI. 5) Identify patient selection and training considerations for fMRI. 6) Develop guidelines for paradigm and sequence decisions. 7) Describe quality control aspects of data processing. 8) Assess activation in key eloquent brain regions. 9) Specify the relevant information concisely. 10) Explain how information about intrinsic brain networks are generated from resting state fMRI. 11) Define common analysis methods for resting state fMRI data. 12) Describe pitfalls in the processing, analysis, and interpretation of resting state fMRI data. 13) Identify potential clinical applications of resting state fMRI.
 14) Describe the benefits of using 7T field strength for imaging susceptibility. 15) Explain the challenges associated with quantification of susceptibility. 16) Assess the benefits of using quantitative susceptibility due to neurodegenerative disease. 17) Identify which brain regions most commonly experience changes in susceptibility due to neurodegenerative diseases.
 18) Examine the role of iron deposition in predicting symptom severity, disease burden, and cognitive impairment. 19) Describe how the diffusion MRI signal is sensitive to brain cellular features. 20) Define the concepts of diffusion tensor imaging (DTI) and tractography. 21) Identify the benefits of higher order methods and how to implement them in clinic. 22) Assess how specificity to cellular pathology is attained through biophysical modeling. 23) Compare popular biophysical models (WMTI, NODDI) and their use in clinical applications.

Sub-Events

RC705A Task-based Language fMRI in 20 Minutes

Participants

Michael M. Zeineh, PhD, MD, Stanford, CA (Presenter) Research funded, General Electric Company;

For information about this presentation, contact:

mzeineh@stanford.edu

LEARNING OBJECTIVES

1) Identify patient selection and training considerations for fMRI. 2) Develop guidelines for paradigm and sequence decisions. 3) Describe quality control aspects of data processing. 4) Assess activation in key eloquent brain regions. 5) Specify the relevant information concisely.

RC705B Resting State fMRI in 20 Minutes

Participants

Haris I. Sair, MD, Baltimore, MD (Presenter) Research Grant, Tocagen

LEARNING OBJECTIVES

1) Explain how information about intrinsic brain networks are generated from resting state fMRI. 2) Define common analysis methods for resting state fMRI data. 3) Describe pitfalls in the processing, analysis, and interpretation of resting state fMRI data. 4) Identify potential clinical applications of resting state fMRI.

RC705C 7T Susceptibility and Neurodegenerative Disorders

Participants

Janine M. Lupo, PhD, San Francisco, CA (Presenter) Grant, General Electric Company

LEARNING OBJECTIVES

1) Describe the benefits of using 7T field strength for imaging susceptibility. 2) Explain the challenges associated with quantification of susceptibility. 3) Assess the benefits of using quantitative susceptibility imaging methods in neurodegenerative disease. 4) Identify which brain regions most commonly experience changes in susceptibility due to neurodegenerative diseases. 5) Examine the role of iron deposition in predicting symptom severity, disease burden, and cognitive impairment.

RC705D Clinical Applications of Advanced Diffusion MRI

Els Fieremans, PhD, New York, NY (*Presenter*) Scientific Advisory Board, Microstructure Imaging, Inc; Stockholder, Microstructure Imaging, Inc; Royalties, General Electric Company

For information about this presentation, contact:

Els.Fieremans@nyulangone.org

LEARNING OBJECTIVES

1) Describe how the diffusion MRI signal is sensitive to brain cellular features. 2) Define the concepts of diffusion tensor imaging (DTI) and tractography. 3) Identify the benefits of higher order methods and how to implement them in clinic. 4) Assess how specificity to cellular pathology is attained through biophysical modeling. 5) Compare popular biophysical models (WMTI, NODDI) and their use in clinical applications.





Emerging Technology: PET/MRI Update 2019

Thursday, Dec. 5 4:30PM - 6:00PM Room: S505AB



AMA PRA Category 1 Credits ™: 1.50 ARRT Category A+ Credit: 1.75

FDA Discussions may include off-label uses.

Participants

Rathan M. Subramaniam, MD, PhD, Dunedin, New Zealand (Moderator) Nothing to Disclose

For information about this presentation, contact:

rathan.subramaniam@utsouthwestern.edu

LEARNING OBJECTIVES

1) To discuss opportunities of PET/MRI in clinical practice and research. 2) To discuss challenges of PET/MRI in clinical practice and research.

Sub-Events

RC717A PET/MRI Update 2019: Clinical Practice Implementation - Pearls

Participants

Geoffrey B. Johnson, MD, PhD, Rochester, MN (Presenter) Research Grant, General Electric Company Research Grant, Pfizer Inc

RC717B PET/MRI Update 2019: Clinical Applications - Brain and Head and Neck

Participants

Alexander Drzezga, MD, Cologne, Germany (*Presenter*) Research support, Siemens AG; Speakers Bureau, Siemens AG; Stockholder, Siemens AG; Research support, General Electric Company; Consultant, General Electric Company; Research support, Life Molecular Imaging; Speakers Bureau, sanofi-aventis Group; Speakers Bureau, General Electric Company; Research support, Eli Lilly and Company;

LEARNING OBJECTIVES

1) Review relevant clinical applications for PET/MR in the diagnostic work-up of disorders of the brain. 2) Review strengths of PET/MR for disorders of the head and neck. 3) Understand the value of different currently available tracers for neuroimaging and oncological applications. 4) Review challenges and limitations of PET/MR in brain/head & neck and expected future developments.

RC717C PET/MRI Update 2019: Clinical Applications - Body

Participants

Spencer C. Behr, MD, San Francisco, CA (*Presenter*) Research Grant, General Electric Company; Consultant, Navidea Biopharmaceuticals, Inc; Grant, Navidea Biopharmaceuticals, Inc

LEARNING OBJECTIVES

1) Review common current applications for abdominopelvic oncologic PET/MRI, including hepatic malignancies, rectal cancer, and cervical cancer. 2) Understand the role of novel tracers in prostate cancer (PSMA PET) and neuroendocrine tumors (somatostatin receptor PET). The presentation will focus on prostate cancer as an application. 3) Present the current limitations and future advances in PET/MRI that will help increase the clinical acceptance and applicability of body PET/MRI.

RC717D PET/MRI Update 2019: Clinical Applications - Cardiac

Participants

Pamela K. Woodard, MD, Saint Louis, MO (*Presenter*) Researcher, Siemens AG; Research Grant, F. Hoffmann-La Roche Ltd; Consultant, Medtronic plc; ; ; ; ; ;

For information about this presentation, contact:

Woodardp@wustl.edu

LEARNING OBJECTIVES

1) Individuals attending this session will understand clinical cardiac PET/MR imaging applications; applications will include a) myocardial perfusion and viability, b) inflammation, c) nonischemic cardiomyopathy, and d) tumor assessment.

RC717E PET/MRI Update 2019: Clinical Applications - Pediatrics

Participants

Lisa J. States, MD, Plymouth Mtng, PA (Presenter) Nothing to Disclose

For information about this presentation, contact:

States@email.chop.edu

LEARNING OBJECTIVES

1) Suggest optimal protocols for pediatric PET/MRI. 2) List indications for pediatric PET/MRI in oncologic and non-oncologic applications. 3) Understand the challenges of these studies in children.

RC717F PET/MRI Update 2019: Physics

Participants

Georges El Fakhri, PhD, Boston, MA (Presenter) Nothing to Disclose

LEARNING OBJECTIVES

1) Understand the challenges and opportunities afforded by simultaneous PET/MR. 2) Understand the role of PET/MR in imaging myocardial membrane potential.





Innovations in MR and CT Perfusion

Thursday, Dec. 5 4:30PM - 6:00PM Room: S103AB



AMA PRA Category 1 Credits ™: 1.50 ARRT Category A+ Credit: 1.75

FDA Discussions may include off-label uses.

Participants

Roland Bammer, PhD, Parkville, Australia (*Coordinator*) Founder, iSchemaView, Inc; Director, iSchemaView, Inc; Stockholder, iSchemaView, Inc; Founder, HobbitView, Inc; Director, HobbitView, Inc; Stockholder, HobbitView, Inc

LEARNING OBJECTIVES

1) A survivors guide for perfusion methodology. 2) Practical considerations of perfusion imaging and leakage measurements in tumors. 3) How to use and interpret perfusion imaging in cerebro-vascular disease.

Sub-Events

RC721A MR and CT Perfusion and Pharmacokinetic Imaging

Participants

Roland Bammer, PhD, Parkville, Australia (*Presenter*) Founder, iSchemaView, Inc; Director, iSchemaView, Inc; Stockholder, iSchemaView, Inc; Founder, HobbitView, Inc; Director, HobbitView, Inc; Stockholder, HobbitView, Inc

RC721B Evidence-Based Best Acquisition Protocols for DSC-MRI in Brain Tumors

Participants

Jerrold L. Boxerman, MD, PhD, Providence, RI (Presenter) Nothing to Disclose

For information about this presentation, contact:

jboxerman@lifespan.org

LEARNING OBJECTIVES

1) Explain the DSC-MRI contrast mechanism and vessel size dependence of gradient-echo and spin-echo signal changes. 2) Identify the major protocol decisions for single-echo, gadolinium-based DSC-MRI. 3) Describe techniques for reducing contrast agent leakage effects in DSC-MRI. 4) Recommend an evidence-based best-practice protocol for DSC-MRI applications in neuro-oncology and clinical trials.

RC721C Perfusion Imaging in Cerebrovascular Disease

Participants

Shalini A. Amukotuwa, BMedSc, MBBS, Melbourne, Australia (Presenter) Spouse, Founder, iSchemaview







Functional MR Imaging for Normal Tissue Response Assessment in Radiotherapy

Thursday, Dec. 5 4:30PM - 6:00PM Room: S503AB



AMA PRA Category 1 Credits ™: 1.50 ARRT Category A+ Credit: 1.75

Participants

Kristy K. Brock, PhD, Houston, TX (*Moderator*) License agreement, RaySearch Laboratories AB; Grant support, RaySearch Laboratories AB; Research support, Mirada Medical Ltd; ;

Sub-Events

RC722A State of the Art in Functional MR Imaging for Normal Tissue Assessment

Participants

Kiaran P. McGee, PhD, Rochester, MN (Presenter) Nothing to Disclose

LEARNING OBJECTIVES

1) Identify underlying biological processes associated with functional magnetic resonance imaging techniques. 2) List most commonly used functional imaging techniques in magnetic resonance imaging. 3) Explain the physics of various functional magnetic resonance imaging technique described in the presentation.

RC722B Clinical Need for Functional MR Imaging for Normal Tissue Assessment in Radiation Therapy

Participants

Clifton D. Fuller, MD, PhD, Houston, TX (Presenter) Research Consultant, Elekta AB Research Grant, Elekta AB Speaker, Elekta AB

For information about this presentation, contact:

cdfuller@mdanderson.org

LEARNING OBJECTIVES

Discuss the relevant needs for normal tissue imaging after radiotherapy, using head and neck radiotherapy as a use case.Define opportunities for enhanced normal tissue imaging procedures for post-therapy toxicity and monitoring.

RC722C Technical Challenges in the Integration of Functional MR Imaging for Normal Tissue Assessment into Radiotherapy

Participants

Martha M. Matuszak, PhD, Ann Arbor, MI (*Presenter*) Research funded, Varian Medical Systems, Inc; Consultant, Varian Medical Systems, Inc

LEARNING OBJECTIVES

1) Discuss the challenges in incorporating functional MR into treatment planning.





Rectal MRI (Interactive Session)

Thursday, Dec. 5 4:30PM - 6:00PM Room: S105AB



AMA PRA Category 1 Credits ™: 1.50 ARRT Category A+ Credit: 1.75

Sub-Events

RC729A Surgeon Point of View

Participants Scott Strong, Chicago, IL (*Presenter*) Consultant, Johnson & Johnson; Instructor, Intuitive

For information about this presentation, contact:

scott.strong@nm.org

LEARNING OBJECTIVES

1) Understand the operative options for radical resection of rectal cancer. 2) Describe the imaging features important to planning radical resection of rectal cancer. 3) Realize the implications of changes in imaging features following neoadjuvant therapy.

RC729B MRI Protocol

Participants Mukesh G. Harisinghani, MD, Boston, MA (*Presenter*) Nothing to Disclose

For information about this presentation, contact:

MHARISINGHANI@MGH.HARVARD.EDU

LEARNING OBJECTIVES

1) Provide an overview of MR protocol for rectal cancer staging. 2) Provide pointers on sequence optimization.

RC729C MRI Staging

Participants Regina G. Beets-Tan, MD, PhD, New York, NY (*Presenter*) Nothing to Disclose

RC729D Response to Neoadjuvant Therapy

Participants

Kartik S. Jhaveri, MD, Mississauga, ON (*Presenter*) Research Grant, General Electric Company; Research Grant, Bayer AG; Speaker, Siemens AG; Speaker, Bayer AG

LEARNING OBJECTIVES

1) Discuss role of MRI in assessing neoadjuvant treatment response in rectal cancer. 2) Review MRI assessment of treatment response. 3) Highlight limitations and pitfalls.

RC729E Case Review

Participants

Mukesh G. Harisinghani, MD, Boston, MA (*Presenter*) Nothing to Disclose Regina G. Beets-Tan, MD, PhD, New York, NY (*Presenter*) Nothing to Disclose Kartik S. Jhaveri, MD, Mississauga, ON (*Presenter*) Research Grant, General Electric Company; Research Grant, Bayer AG; Speaker, Siemens AG; Speaker, Bayer AG

For information about this presentation, contact:

MHARISINGHANI@MGH.HARVARD.EDU

LEARNING OBJECTIVES

1) Provide overview of MR imaging in rectal cancer staging. 2) Highlight important technical pointers for accurate staging.





MR Imaging-guided Breast Biopsy (Hands-on)

Thursday, Dec. 5 4:30PM - 6:00PM Room: E260



AMA PRA Category 1 Credits ™: 1.50 ARRT Category A+ Credit: 1.75

Participants

Roberta M. Strigel, MD, Madison, WI (Presenter) Research support, General Electric Company Rosalind P. Candelaria, MD, Houston, TX (Presenter) Nothing to Disclose Brian Johnston, MD, Queen Creek, AZ (Presenter) Nothing to Disclose Jennifer R. Kohr, MD, Seattle, WA (Presenter) Nothing to Disclose Diana L. Lam, MD, Seattle, WA (Presenter) Nothing to Disclose Santo Maimone IV, MD, Jacksonville Beach, FL (Presenter) Research Consultant, GRAIL Inc Cecilia L. Mercado, MD, New York, NY (Presenter) Nothing to Disclose Jessica H. Porembka, MD, Dallas, TX (Presenter) Nothing to Disclose Gaiane M. Rauch, MD, PhD, Houston, TX (*Presenter*) Nothing to Disclose Jeffrey S. Reiner, MD, New York , NY (*Presenter*) Nothing to Disclose Raman Verma, MD, Ottawa, ON (Presenter) Nothing to Disclose Ryan W. Woods, MD, MPH, Madison, WI (Presenter) Nothing to Disclose Bethany L. Niell, MD, PhD, Tampa, FL (Presenter) Nothing to Disclose Beatriu Reig, MD, New York, NY (Presenter) Nothing to Disclose Anand K. Narayan, MD, PhD, Boston, MA (Presenter) Nothing to Disclose Eren D. Yeh, MD, Belmont, MA (Presenter) Consultant, Statlife SAS Debbie L. Bennett, MD, Saint Louis, MO (Presenter) Advisory Board, Devicor Medical Products, Inc Dana Ataya, MD, Tampa, FL (Presenter) Nothing to Disclose Richard S. Ha, MD, New York, NY (Presenter) Nothing to Disclose Erin I. Neuschler, MD, Chicago, IL (Presenter) Nothing to Disclose Denise M. Thigpen, MD, Washington, DC (Presenter) Nothing to Disclose

For information about this presentation, contact:

gmrauch@mdanderson.org

jessica.porembka @utsouthwestern.edu

rstrigel@uwhealth.org

rcandelaria@mdanderson.org

Debbie.bennett@health.slu.edu

LEARNING OBJECTIVES

1) Explain why MR-guided breast biopsy is needed for patient care. 2) Identify relative and absolute contraindications to MR-guided breast biopsy. 3) Describe criteria for MR-guided breast biopsy patient selection. 4) Debate risks and benefits of pre-biopsy targeted ultrasound for suspicious MRI findings. 5) Understand the basic MR-guided biopsy procedure, protocol and requirements for appropriate coil, needle and approach selection. 6) Manage patients before, during and after MR-guided breast biopsy. 7) Define the benefits and limitations of MR-guided vacuum assisted breast biopsy. 8) Apply positioning and other techniques to challenging combinations of lesion location and patient anatomy for successful MR-guided biopsy.

ABSTRACT

This course is intended to provide basic didactic instruction and hands-on experience for MR-guided breast biopsy. Because of the established role of breast MRI in the evaluation of breast cancer through screening and staging, there is a proven need for MR-guided biopsy of the abnormalities that can only be identified on MRI. This course will be devoted to the understanding and identification of: 1) appropriate patient selection 2) optimal positioning for biopsy 3) target selection and confirmation 4) various biopsy technologies and techniques 5) potential problems and pitfalls and 6) radiology/pathology concordance. Participants will spend 30 minutes in didactic instruction followed by 60 minutes practicing MR-guided biopsy using provided phantoms. Various combinations of full size state-of-the-art breast MRI coils, biopsy localization equipment and needles from multiple different vendors will be available for hands-on practice. Some stations will have monitors loaded with targeting software. Expert breast imagers from around the world will be at each of 10 stations to provide live coaching, tips, techniques and advice.





Practical MR Imaging

Friday, Dec. 6 8:30AM - 10:00AM Room: E353B



AMA PRA Category 1 Credits ™: 1.50 ARRT Category A+ Credit: 1.75

LEARNING OBJECTIVES

1) Discuss application of optimized non-vascular thoracic MR protocols for troubleshooting problematic mediastinal masses. 2) Use case based discussion to highlight which indeterminate mediastinal masses could benefit from further tissue characterization provided by MR. 3) Describe MR imaging appearances of select indeterminate and complex cystic mediastinal masses. 4) Harness the tissue characterization properties of MRI to add diagnostic specificity to assessment of pleural lesions beyond that of CT. 5) Understand how higher soft tissue contrast of MR can make CT-occult lesions visible. 6) Recognize how the higher soft tissue contrast of MR than CT can: a) add precision to lesion compartment localization, narrowing the differential diagnosis b) better show integrity of tissue planes and invasion across them. 7) To give an overview over the diagnostic scope of lung MRI for pathologies of lung parenchyma and airway disease. 8) To review the diagnostic yield of MRI for the detection and characterisation of lung nodules. 9) To introduce MRI as potential first choice modality for imaging pulmonary disease in young or pregnant patients. 10) To discuss the potential role of lung MRI as an alternative or adjunct modality, e.g. in COPD or interstitial lung diseases. 11) List most common benign and malignant cardiac masses. 12) Assemble key magnetic resonance imaging sequences into a protocol to assess cardiac masses.13) Recognize magnetic resonance imaging features of select benign and malignant cardiac masses.

Sub-Events

RC801A Troubleshooting Problematic Mediastinal Masses with MR Imaging

Participants

Rachna Madan, MD, Boston, MA (Presenter) Nothing to Disclose

For information about this presentation, contact:

rmadan@bwh.harvard.edu

LEARNING OBJECTIVES

1) Discuss application of optimized non-vascular thoracic MR protocols for troubleshooting problematic mediastinal masses. 2) Use case based discussion to highlight which indeterminate mediastinal masses could benefit from further tissue characterization provided by MR. 3) Describe MR imaging appearances of select indeterminate and complex cystic mediastinal masses.

RC801B The Value of MRI for Diagnosis of Pleural Disease

Participants

Jeanne B. Ackman, MD, Weston, MA (*Presenter*) Spouse, Stockholder, Everest Digital Medicine; Spouse, Consultant, Everest Digital Medicine; Spouse, Stockholder, Cynvenio Biosystems, Inc; Spouse, Scientific Advisory Board, Cynvenio Biosystems, Inc; Spouse, Consultant, PAREXEL International Corporation

LEARNING OBJECTIVES

1) Harness the tissue characterization properties of MRI to add diagnostic specificity to assessment of pleural lesions beyond that of CT. 2) Understand how higher soft tissue contrast of MR can make CT-occult lesions visible. 3) Recognize how the higher soft tissue contrast of MR than CT can: a) add precision to lesion compartment localization, narrowing the differential diagnosis b) better show integrity of tissue planes and invasion across them.

RC801C MR Imaging of the Lung: Added Value for Your Thoracic Imaging Practice

Participants Juergen Biederer, MD, Heidelberg, Germany (*Presenter*) Nothing to Disclose

For information about this presentation, contact:

juergen.biederer@uni-heidelberg.de

LEARNING OBJECTIVES

1) To give an overview over the diagnostic scope of lung MRI for pathologies of lung parenchyma and airway disease. 2) To review the diagnostic yield of MRI for the detection and characterisation of lung nodules. 3) To introduce MRI as potential first choice modality for imaging pulmonary disease in young or pregnant patients. 4) To discuss the potential role of lung MRI as an alternative or adjunct modality, e.g. in COPD or interstitial lung diseases.

ABSTRACT

MRI of the lung can play an interesting role and be added value to your thoracic imaging practice besides X-ray and CT. The sensitivity of MRI for infiltrates is at least similar to X-ray and CT, lung nodule detection is superior to X-ray and slightly inferior to CT and favorable options for tissue characterization (exclusion of malignancy) and functional imaging capacities (perfusion, ventilation, respiratory motion) are available with standardized protocols. Given this, MRI may serve as a radiation-free alternative in patients who should not be exposed to ionizing radiation (children and young subjects, pregnant patients), e.g. as your first

choice modality in patients with cystic fibrosis. It may well serve as an adjunct to other modalities for comprehensive lung imaging in COPD and some cases of interstitial lung diseases, e.g. sarcoidosis (dark lymph node sign). In young patients, MRI may well be used for the long term follow-up of malignancy (e.g. seminoma) or inflammatory disease (e.g. GPA/Wegener's disease). As an adjunct or alternative to other modalities, MRI can be helpful in lung cancer staging and follow-up (differentiation of atelectasis and lung cancer) or the characterization of lung nodules ('actionable nodules' with contrast uptake, high NPV in nodules with no or low contrast uptake, fatty content in hamartoma). MRI might even be suitable for the early detection of lung cancer, either as the primary screening tool or for the ad-hoc diagnostic work-up of detected lesions on site.

RC801D Magnetic Resonance Imaging of Cardiac Masses

Participants

Nila J. Akhtar, MD, Rochester, MN (Presenter) Nothing to Disclose

LEARNING OBJECTIVES

1) List most common benign and malignant cardiac masses. 2) Assemble key magnetic resonance imaging sequences into a protocol to assess cardiac masses. 3) Recognize magnetic resonance imaging features of select benign and malignant cardiac masses.

RC801E MR Imaging of Aortopathies

Participants

Cristina Fuss, MD, Portland, OR (Presenter) Spouse, Officer, ViewRay, Inc

LEARNING OBJECTIVES

1) To familiarize the learner with the most common familiar aortopathies, their clinical background, imaging appearance on MRI and specific considerations for MR acquisition planning.

ABSTRACT

Familial aortopahties comprise a grounp of inherited disorders of aortic aneurysms and/or dissection including. These include Thoracic Aortic Aneurysms and Aortic Dissections (TAAD), Marfan syndrome, Loeys-Dietz syndrome, and Ehlers-Danlos syndrome, only to name the most common ones.

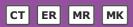






Avulsion Injuries of the Upper and Lower Extremities

Friday, Dec. 6 8:30AM - 10:00AM Room: E451B



AMA PRA Category 1 Credits ™: 1.50 ARRT Category A+ Credit: 1.75

Participants

Zehava S. Rosenberg, MD, Hoboken, NJ (Director) Nothing to Disclose

Sub-Events

RC804A Upper Extremity

Participants Lee F. Rogers, MD, Tucson, AZ (*Presenter*) Nothing to Disclose

For information about this presentation, contact:

lfrogers@comcast.net

LEARNING OBJECTIVES

1) Obtain appropriate radiographs, AP, lateral and obliques; oblique views are essential as certain fractures may be visible only on this projection. 2) Certain fractures and dislocations are notorious for being overlooked; know these injuries and be certain to identify or exclude them. 3) Certain ligamentous avulsion of the digits are associated with characteristic deformities allowing a definitive diagnosis of the underlying abnormality. 4) Be aware of the potential for satisfaction of search and the potential of diagnostic oversights in certain injuries; once such an injury is noted look closely for the commonly associated injury. 5) When the clinical diagnosis is not apparent or uncertain on the initial radiographs, do not hesitate to obtain CT or MRI to confirm or exclude an injury.

RC804B Avulsion Injuries of the Pelvis and Hip

Participants

Omer A. Awan, MD, Baltimore, MD (Presenter) Nothing to Disclose

LEARNING OBJECTIVES

1) Outline the spectrum of avulsive injuries in the pelvis and hip. 2) Delineate imaging characteristics of pelvic and hip avulsive injuries, with emphasis on radiography and MRI. 3) Elucidate practical and clinical applications to pelvic and hip avulsive injuries.

ABSTRACT

n/a

RC804C Knee

Participants Thomas L. Pope, MD, Denver, CO (*Presenter*) Nothing to Disclose

For information about this presentation, contact:

thomaspopemd@gmail.com

LEARNING OBJECTIVES

1) Delineate the most common avulsion injuries in the knee. 2) Outline the most common imaging features of avulsion injuries in the knee. 3) Describe the complimentary role of radiography, CT and MR imaging in the diagnosis of avulsion injuries of the knee. 4) Provide some hints on keys to avoid missing these lesions in your clinical practice.

RC804D Foot and Ankle

Participants

Zehava S. Rosenberg, MD, Hoboken, NJ (Presenter) Nothing to Disclose

LEARNING OBJECTIVES

1) Familiarize the radiologist with radiographic findings of common avulsion injuries of the ankle and foot with emphasis on frequently missed entities. 2) Provide cross sectional imaging correlation for all the described entities. 3) Provide the radiologist with tools for distinguishing radiographic evidence of pathology from mimickers of disease.







The Neoadjuvant Patient

Friday, Dec. 6 8:30AM - 10:00AM Room: E352



AMA PRA Category 1 Credits ™: 1.50 ARRT Category A+ Credit: 1.75

Participants

Eric L. Rosen, MD, Seattle, WA (Moderator) Nothing to Disclose

For information about this presentation, contact:

zuleyml@upmc.edu

LEARNING OBJECTIVES

1) To discuss three clinically significant areas involving care of the breast cancer patient undergoing neoadjuvant therapy. 2) To apply in everyday clinical practice the principles and conclusions learned.

Sub-Events

RC815A State-of-the-Art: An Evidence-based Approach

Participants

Eric L. Rosen, MD, Seattle, WA (Presenter) Nothing to Disclose

RC815B Ongoing Trials and Future Directions

Participants

Jessica W. Leung, MD, Houston, TX (Presenter) Scientific Advisory Board, Subtle Medical

LEARNING OBJECTIVES

1) To learn the design of some of the ongoing clinical trials involving care of the breast cancer patient receiving neoadjuvant therapy. 2) To describe the imaging components of these trials. 3) To understand the role that imaging plays in these trials.

RC815C Ultrasound Evaluation of the Axilla in the Neoadjuvant Patient

Participants

Steven P. Poplack, MD, Saint Louis, MO (Presenter) Nothing to Disclose

LEARNING OBJECTIVES

1) Identify the key US criteria that are predictive of axillary lymph node metastases. 2) Appraise the accuracy of axillary US in the setting of Invasive Breast Cancer. 3) Describe the role of axillary US in the surgical management of the axilla after neoadjuvant treatment.





Abdominal/Pelvic MRI in the Emergent Setting

Friday, Dec. 6 8:30AM - 10:00AM Room: E263



AMA PRA Category 1 Credits ™: 1.50 ARRT Category A+ Credit: 1.75

Participants

John R. Leyendecker, MD, Dallas, TX (Moderator) Nothing to Disclose

LEARNING OBJECTIVES

1) Understand the advantages and disadvantages of MRI in the acute setting for the diagnosis of acute genitourinary disorders. 2) Identify the diagnostic criteria for ovarian torsion and also predict ovarian viability with MRI. 3) Contrast the strengths of different MRI sequences for the diagnosis of pyelonephritis. 4) Apply a rapid, noncontrast MRI protocol for the imaging of acute abdominopelvic pain that is accurate for the diagnosis of acute genitourinary disorders. 5) Discuss clinical and imaging features of a spectrum of entities that present with acute female pelvic pain including complications of fibroids, pelvic inflammatory disease and complicated cysts. 6) Highlight the pathogenesis and pertinent MR imaging features of adnexal (ovarian and tubal) torsion. 7) Assess the relative advantages and disadvantages for MR vs. other imaging modalities for suspected appendicitis in adults. 8) Assess the ability of MR for making alternative diagnoses to acute appendicitis in the setting of non-traumatic abdominal pain. 9) Consider the implications for the potential increased use of MR in the ED for non-traumatic abdominal pain. 10) Identify patients who will benefit from MR enterography in the acute setting. 11) Protocol and perform MR enterography in the acute setting. 12) Identify and report acute findings of Crohn's disease on MR enterography. 13) Discuss the most common indications for abdominal or pelvic MRI in pediatric patients in the emergent setting. 14) Demonstrate and discuss the most frequently encountered MRI imaging manifestations of these conditions. 15) Review the most appropriate MRI protocols for evaluation of pediatric patients presenting to the Emergency Department with acute abdominal or pelvic pain. 16) Discuss available techniques for achieving patient cooperation and limiting exam time in pediatric patients. 17) Understand MRI safety concerns in the setting of pregnancy. 18) Understand indications for emergency MRI during pregnancy. 19) Implement an imaging protocol for emergency MRI during pregnancy. 20) Understand MRI appearance of common acute disease processes during pregnancy.

Sub-Events

RC829A MRI for Acute Genitourinary Disorders

Participants

Bobby T. Kalb, MD, Tucson, AZ (Presenter) Nothing to Disclose

LEARNING OBJECTIVES

1) Understand the advantages and disadvantages of MRI in the acute setting for the diagnosis of acute genitourinary disorders. 2) Identify the diagnostic criteria for ovarian torsion and also predict ovarian viability with MRI. 3) Contrast the strengths of different MRI sequences for the diagnosis of pyelonephritis. 4) Apply a rapid, noncontrast MRI protocol for the imaging of acute abdominopelvic pain that is accurate for the diagnosis of acute genitourinary disorders.

RC829B MRI for Acute Pelvic Pain in Women

Participants Christine O. Menias, MD, Chicago, IL (*Presenter*) Nothing to Disclose

For information about this presentation, contact:

menias.christine@mayo.edu

LEARNING OBJECTIVES

1) Discuss clinical and imaging features of a spectrum of entities that present with acute female pelvic pain including complications of fibroids, pelvic inflammatory disease and complicated cysts. 2) Highlight the pathogenesis and pertinent MR imaging features of adnexal (ovarian and tubal) torsion.

RC829C MRI for Acute Appendicitis and Differential Diagnosis

Participants

Perry J. Pickhardt, MD, Madison, WI (*Presenter*) Stockholder, SHINE Medical Technologies, Inc; Stockholder, Elucent Medical; Advisor, Bracco Group;

LEARNING OBJECTIVES

1) Assess the relative advantages and disadvantages for MR vs. other imaging modalities for suspected appendicitis in adults. 2) Assess the ability of MR for making alternative diagnoses to acute appendicitis in the setting of non-traumatic abdominal pain. 3) Consider the implications for the potential increased use of MR in the ED for non-traumatic abdominal pain.

RC829D MRI for Crohn's Disease in the Acute Setting

For information about this presentation, contact:

dgrand@lifespan.org

LEARNING OBJECTIVES

1) Identify patients who will benefit from MR enterography in the acute setting. 2) Protocol and perform MR enterography in the acute setting. 3) Identify and report acute findings of Crohn's disease on MR enterography.

RC829E MRI for Acute Pediatric Disorders

Participants

Sarah D. Bixby, MD, Boston, MA (Presenter) Nothing to Disclose

For information about this presentation, contact:

sarah.bixby@childrens.harvard.edu

LEARNING OBJECTIVES

1) Discuss the most common indications for abdominal or pelvic MRI in pediatric patients in the emergent setting. 2) Demonstrate and discuss the most frequently encountered MRI imaging manifestations of these conditions. 3) Review the most appropriate MRI protocols for evaluation of pediatric patients presenting to the Emergency Department with acute abdominal or pelvic pain. 4) Discuss available techniques for achieving patient cooperation and limiting exam time in pediatric patients.

RC829F Emergency MRI During Pregnancy

Participants

Gaurav Khatri, MD, Irving, TX (Presenter) Nothing to Disclose

LEARNING OBJECTIVES

1) Understand MRI safety concerns in the setting of pregnancy. 2) Understand indications for emergency MRI during pregnancy. 3) Implement an imaging protocol for emergency MRI during pregnancy. 4) Understand MRI appearance of common acute disease processes during pregnancy.

Active Handout:Gaurav Khatri

http://abstract.rsna.org/uploads/2019/19001016/Active RC829F.pdf